TRANSACTIONS

OF THE

AMERICAN INSTITUTE OF MINING AND METALLURGICAL ENGINEERS

(INCORPORATED)

Volume 150

IRON AND STEEL DIVISION

1942

Notice

This volume is the fifteenth of a series containing papers and discussions presented before the Iron and Steel Division of the American Institute of Mining and Metallurgical Engineers since its organization in 1928; one volume each year, as follows:

1928, Iron and Steel Technology in 1928 (later listed as Volume 80 of the TRANSACTIONS); 1929 (vol. 84), 1930 (vol. 90), 1931 (vol. 95), 1932 (vol. 100), 1933, 1934, 1935, 1936, 1937, 1938, 1939, 1940, 1941 and 1942, TRANSACTIONS of the American Institute of Mining and Metallurgical Engineers, Iron and Steel Division.

This volume contains papers and discussions presented at the meetings at Chicago, April 23–25, 1941; Philadelphia, Oct. 20–22, 1941; New York, Feb. 9–12, 1942.

Papers on iron and steel subjects published by the Institute prior to 1928 are to be found in many volumes of the TRANSACTIONS of the Institute; in Vols. 37 to 45, inclusive; 47, 50 and 51, 53, 56, 58, 62, 67 to 71, inclusive; 73 and 75. Vol. 67 was devoted exclusively to iron and steel.

Iron and steel papers published in the TRANSACTIONS before the year 1936 may be found by consulting the general indexes to Vols. 1 to 35 (1871–1904), Vols. 36 to 55 (1905–1916), Vols. 56 to 72 (1917–1925), and Vols. 73 to 117 (1926–1935).

FOREWORD

This volume of the Transactions is the fifteenth of these annual publications and is devoted exclusively to papers and discussions on iron and steel that were presented at the several meetings of the Iron and Steel Division held during the year ending with the 1942 annual meeting. The 27 papers in this book are of the usual high quality and cover a field that is exceptionally broad; they should contain data that are of interest to metallurgists and operating men throughout the country.

Including Dr. Johnston's Howe Memorial lecture, there are eight papers of interest to blast-furnace and open-hearth men, two of which deal with the physical chemistry of steelmaking.

The eleven papers on constitution and thermal treatment contain the results of important research in practically every phase of physical metallurgy, ranging from a new determination of A_3 in high-purity iron, through decarburization, diffusion, nucleation and growth of pearlite, S-curves and lattice relationships in iron-carbon alloys, to a new and important method of calculating hardenability from chemical composition.

Included among the eight papers on properties are a new approach to our understanding of cohesive strength, a description of tensile testing by the two-load method, and a contribution to the art of creep testing. The other papers in this group contain the results of investigations on iron-rich iron-manganese alloys, iron-nickel-cobalt alloys, medium-carbon and low-alloy steels, and on heat-resistant alloys of the 26 per cent chromium, 12 per cent nickel type.

The Division's Open Hearth and Blast Furnace Committees held their 25th conference at Cincinnati in April, with an attendance of 642. The full transcript of the discussions and the technical papers presented at this joint conference—which was very successful and aroused much interest—is contained in the Open Hearth Proceedings published in July, and in the Blast Furnace Proceedings now on the press.

EARLE C. SMITH, *Chairman*,
Iron and Steel Division.

CLEVELAND, OHIO
September 8, 1942

4

CONTENTS

5

CONTENTS

Properties

IRON AND STEEL DIVISION

Established as a Division February 22, 1928

(Bylaws published in the 1939 TRANSACTIONS Volume of the Division)

Officers and Committees for Year Ending February 1943

Chairman, E. C. Smith, Cleveland, Ohio
Past Chairman, C. H. HERTY, JR., Bethlehem, Pa.
Vice-chairman, WILLIAM A. HAVEN, Cleveland, Ohio
Vice-chairman, H. W. GRAHAM, Pittsburgh, Pa.
Vice-chairman, W. J. REAGAN, Warren, Ohio
Secretary, FRANK T. SISCO, New York, N. Y.
29 West 39th Street,
New York, N. Y.

Executive Committee

1943	1944
R. S. ARCHER, Chicago, Ill.	A. L. BOEGEHOLD, Detroit, Mich.
R. L. BALDWIN, Niagara Falls, N. Y.	W. E. BREWSTER, Chicago, Ill.
T. L. JOSEPH, Minneapolis, Minn.	JOSEPH WINLOCK, Philadelphia, Pa.

1945
C. E. MacQUIGG, Columbus, Ohio
GILBERT SOLER, Canton, Ohio
T. S. WASHBURN, Indiana Harbor, Ind.

Past Chairmen

RALPH H. SWEETSER, 1928	JOHN JOHNSTON, 1933	J. T. MACKENZIE, 1938
G. B. WATERHOUSE, 1929	L. F. REINARTZ, 1934	J. HUNTER NEAD, 1939
W. J. MACKENZIE, 1930	A. B. KINZEL, 1935	FRANK T. SISCO, 1940
F. M. BECKET, 1931	C. E. WILLIAMS, 1936	C. H. HERTY, JR., 1941
F. N. SPELLER, 1932	FRANCIS B. FOLEY, 1937	

Mining and Metallurgy

A. B. KINZEL, *Chairman*

R. H. ABORN	T. S. FULLER	A. D. POTTS
	W. E. JEWELL	

Blast Furnace and Raw Materials

PETER F. DOLAN, *Chairman*		GARNETT M. HARRIS, *Vice-chairman*
B. M. STUBBLEFIELD, *Vice-chairman*		CARL G. HOGBERG, *Secretary*
A. J. BOYNTON	W. A. HAVEN	R. A. LINDGREN
O. E. CLARK	H. W. JOHNSON	H. E. McDONNELL
FORBES B. CRONK	T. L. JOSEPH	G. E. STEUDEL
P. G. HARRISON	C. D. KING	C. L. WYMAN

7

Open-hearth Steel

L. F. REINARTZ, *Chairman*   A. P. MILLER, *Vice-chairman*

FRANK T. SISCO, *Secretary*

GEORGE S. BALDWIN   C. H. HERTY, JR.   E. A. SCHWARTZ
R. L. BOWRON   E. G. HILL   C. E. SIMS
R. K. CLIFFORD   J. L. HYLAND   GILBERT SOLER
J. F. CONNERS   J. W. KINNEAR, JR.   DON N. WATKINS
M. J. DEVANEY   WILLIAM C. KITTO   F. G. WHITE
C. R. FONDERSMITH   E. L. RAMSEY   C. E. WILLIAMS
R. C. GOOD   W. J. REAGAN

Bessemer Steel

H. W. GRAHAM, *Chairman*

JOHN D. GOLD   G. A. REINHARDT   G. B. WATERHOUSE
E. F. KENNEY   E. C. SMITH   GORDON M. YOCOM
C. D. KING   E. B. STORY

Alloy Steel

J. L. GREGG, *Chairman*

R. S. ARCHER   C. D. KING   R. M. PARKE
G. R. BROPHY   A. B. KINZEL   R. W. ROUSH
J. P. GILL   V. N. KRIVOBOK   JEROME STRAUSS
G. F. JENKS   C. H. LORIG   F. M. WASHBURN

Cast Ferrous Metals

E. K. SMITH, *Chairman*

J. W. BOLTON   JOHN HOWE HALL   S. C. MASSARI
H. BORNSTEIN   R. F. HARRINGTON   H. A. SCHWARTZ
ROY A. GEZELIUS   J. T. MacKENZIE

Metallography and Heat Treatment

G. R. BROPHY, *Chairman*

E. C. BAIN   ZAY JEFFRIES   DuRAY SMITH
C. Y. CLAYTON   V. T. MALCOLM   A. M. STEEVER
R. L. DOWDELL   B. R. QUENEAU   W. P. SYKES
A. J. HERZIG   MERRILL A. SCHEIL   A. B. WILDER

Physical Chemistry of Steelmaking

JOHN CHIPMAN, *Chairman*

J. J. EGAN, *Secretary*

R. S. ARCHER   J. H. KELLEY   GILBERT SOLER
H. M. BANTA   R. K. KULP   R. B. SOSMAN
L. S. DARKEN   B. M. LARSEN   H. J. SWEENEY
K. L. FETTERS   A. E. MARTIN   F. M. WASHBURN
J. W. HALLEY   F. G. NORRIS   T. S. WASHBURN
C. H. HERTY, JR.   W. O. PHILBROOK   T. T. WATSON
E. R. JETTE   G. L. PLIMPTON, JR.   H. J. WEIGLE
T. L. JOSEPH   L. F. REINARTZ   H. K. WORK
                           C. E. SIMS

Howe Memorial Lecture

E. C. SMITH, *Chairman*

E. C. BAIN   A. V. DE FOREST   C. H. HERTY, JR.
                           H. W. GILLETT

Robert W. Hunt Medal and Prize

E. C. SMITH, *Chairman*

E. S. DAVENPORT	F. B. FOLEY	C. E. WILLIAMS
	W. C. HAMILTON	

J. E. Johnson, Jr. Award

B. J. HARLAN, *Chairman*

O. E. CLARK	T. L. JOSEPH	F. B. RICH
	P. V. MARTIN	

Membership

R. L. BALDWIN, *Chairman*

W. E. BREWSTER	W. E. JEWELL	R. M. PARKE
J. L. GREGG	T. L. JOSEPH	H. S. RAWDON
E. G. HILL	W. JOHN KING	W. J. REAGAN
J. E. JACOBS	E. C. MILLER	C. E. SIMS

Programs

E. C. SMITH, *Chairman*

LEWIS S. BERGEN	R. C. GOOD	J. S. MARSH
D. EPPELSHEIMER, JR.	JOHN HOWE HALL	W. H. SWANGER
	C. H. LORIG	

Papers

E. C. SMITH, *Chairman*

G. R. BROPHY	H. W. GRAHAM	L. F. REINARTZ
JOHN CHIPMAN	J. L. GREGG	E. K. SMITH
P. F. DOLAN	A. B. KINZEL	

Nominating

C. H. HERTY, JR., *Chairman*

A. B. KINZEL	J. T. MACKENZIE	L. F. REINARTZ
	J. H. NEAD	

The Howe Memorial Lecture

THE Howe Memorial Lecture was authorized in April 1923, in memory of Henry Marion Howe, as an annual address to be delivered by invitation under the auspices of the Institute by an individual of recognized and outstanding attainment in the science and practice of iron and steel metallurgy or metallography, chosen by the Board of Directors upon recommendation of the Iron and Steel Division.

So far, only American metallurgists have been invited to deliver the Howe lecture. It is believed that this lecture would gain in importance and significance were it possible to include metallurgists from other countries, but the Institute has not yet been able to do this on account of lack of special funds to support this lectureship.

The titles of the lectures and the lecturers are as follows:

1924 What is Steel? By Albert Sauveur.
1925 Austenite and Austenitic Steels. By John A. Mathews.
1926 Twenty-five Years of Metallography. By William Campbell.
1927 Alloy Steels. By Bradley Stoughton.
1928 Significance of the Simple Steel Analysis. By Henry D. Hibbard.
1929 Studies of Hadfield's Manganese Steel with the High-power Microscope. By John Howe Hall.
1930 The Future of the American Iron and Steel Industry. By Zay Jeffries.
1931 On the Art of Metallography. By Francis F. Lucas.
1932 On the Rates of Reactions in Solid Steel. By Edgar C. Bain.
1933 Steelmaking Processes. By George B. Waterhouse.
1934 The Corrosion Problem with Respect to Iron and Steel. By Frank N. Speller.
1935 Problems of Steel Melting. By Earl C. Smith.
1936 Correlation between Metallography and Mechanical Testing. By H. F. Moore.
1937 Progress in Improvement of Cast Iron and Use of Alloys in Iron. By Paul D. Merica.
1938 On the Allotropy of Stainless Steels. By Frederick Mark Becket.
1939 Some Things We Don't Know about the Creep of Metals. By H. W. Gillett.
1940 Slag Control. By C. H. Herty, Jr.
1941 Some Complexities of Impact Strength. By Alfred V. de Forest.
1942 Time as a Factor in the Making and Treating of Steel. By John Johnston.

JOHN JOHNSTON

Henry Marion Howe Memorial Lecturer, 1942

Time as a Factor in the Making and Treating of Steel

By John Johnston,* Member A.I.M.E.

(Henry Marion Howe Memorial Lecture†)

When I was honored by being invited to give the Howe Memorial Lecture, I decided to read Howe's book, "The Metallography of Steel and Cast Iron," published in 1916—that is, about 25 years ago—in search of a text. I found the book written in fine, clear, attractive, yet precise style, as I expected, knowing that his father—Dr. Samuel Gridley Howe, his mother—Julia Ward Howe, and all of his four brothers and sisters had lived in a New England literary atmosphere and had written books. This leads me to suggest that many authors of metallurgical papers and books could well study Howe's writings with a view to the improvement of their own. I failed to find a specific text, but did find a subject, for in reading his book I was struck by the few instances in which time is considered explicitly as a factor in the phenomena examined, and by the fact that many of the hottest arguments would have been settled had time been taken properly into account. Indeed, Howe hardly mentions time except in a rather incidental way, as in a few references to lag; for instance:

The lowering of temperature at which the transformation occurs by rapid cooling . . . is a phenomenon of undercooling or lag. It is in part explained by the fact that the transformation itself is a time-consuming reaction which, setting in during a rapid fall of temperature, is naturally protracted till the temperature has sunk far below that at which it is due.

He does discuss, quite fully, the iron-carbon equilibrium diagram, as known at that time, introducing it by stating:

As he is a reasonable man who is not deterred from using a hand truck for moving his trunk by the consideration that he has thus to move a trunk plus a truck, so am I reasonable in putting into your hands this useful, indeed indispensable, tool for mastering the ABC of iron metallurgy.

Somewhat later, in introducing a discussion of the phase rule, which "it would be hardly proper to pass . . . by without an attempt to outline its meaning," for "a clear exposition of its applicability or jurisdiction is needed to restrain the half-initiated from misusing it and the uninitiated from being misled by these misuses," he writes—and I quote his statement because we cannot properly discuss the influence of time on a process until we know the state of equilibrium which would ultimately be reached by the system under consideration:

It is a most remarkable and valuable generalization, its conceptions help greatly toward getting a broad outlook on metallography, but its misconception has brought out a flood of obscuring writings. It tells us about the constitution towards which alloys tend, that which they reach when equilibrium is complete, when all tendencies have corrected themselves and have been complied with completely. Its application, in absence of true equilibrium, is like determining density with a telescope or even with a tuning fork; it is like the mad tea party at which the butter put into the works of the watch was the best butter. If the reader learns no more than to beware of attempts to decipher the conditions of inequilibrium by a law which touches only the conditions of exact

equilibrium, if he rejects summarily all attempts to deduce the constitution of hardened steel by the application of the phase rule unless they show a complete mastery of the subject, he will have learned something of value. To which the busy reader may reply aptly that if that is all he may as well stop at this point in the discussion, and if he does I do not see that I can make any effective rejoinder, inclining to submit that if I were in his place I too might.

But I must resist the temptation to quote further, and proceed to point out that Howe, while recognizing clearly the necessity for learning just what the equilibrium state would be, was somewhat puzzled by the many cases in which equilibrium was not even approached. This, coupled with the circumstance that one still sees, not infrequently, cases of inequilibrium handled as if true equilibrium had been reached, led me to choose, as the subject of this lecture, the influence of time on some of the long sequence of processes and operations from raw materials to finished steel product. That is, I propose to speak of the rate of a number of these processes, preferring, however, for the sake of clarity, to discuss them in terms of time as a parameter, since it is directly measured, rather than in terms of a rate, which is a derived quantity. On this general subject much has been learned in the 25 years since Howe's book was published; we cannot yet "explain" rates, nor predict them, even in the simplest case; but we can measure and describe them and use this knowledge to control our operations and our products far more closely than was practicable on a large scale in Howe's time.

I propose therefore to bring together, from the metallurgy of steel, a number of diverse instances, none of them entirely new, which have been clarified during the last decade, as a means of emphasizing the importance of knowing the time-rate of our processes, and of using this knowledge properly; for we need it both to map out the conditions of real equilibrium and to interpret our practical observations in

terms of the equilibrium state which would, in time, be reached. We shall consider time, not in the historians' sense, but in the sense commonly used by the physical scientist because of his necessary interest in the rate at which something happens or can be made to happen; and we shall find instances of processes that can, in principle at least, be speeded up, and of others that are inherently slower than has been generally supposed. Indeed, time is a factor that influences the degree of success, commercially as well as technically, attained by the steelmaker in keeping his products up to the standards now demanded by the consumer; for this implies that he carry on each step in his production as fast as it can be made to go without impairing the useful quality of the product, and proper recognition of this is particularly important under present circumstances.

THE BLAST FURNACE

The blast furnace, when well run, is a highly efficient unit for its purpose, with a high rate of throughput per unit of volume. Which reaction is slowest, and thereby limits the rate of the whole process, is not quite clear; but everything points to the latest of the series of reactions, down near, or in, the hearth, and particularly to the reduction of residual iron oxide by solid carbon which occurs thereabouts, a reaction which can go on only as fast as its large requirement of heat is supplied to the reaction zone. In this connection it may be remarked that the coke consumption in the blast-furnace process for iron, when carried out well, is determined primarily by the amount of energy needed for chemical reduction of the final iron oxide and not by the total heat requirement of the reactions.

If we attempt to reduce ore completely at a temperature so low that no melting of metal or of gangue occurs, we find that the over-all rate becomes less and less as

reaction proceeds from the surface toward the center of each particle of ore. The reason for this is plain; namely, that the reducing gas must go in, and the gaseous product must come out, through a progressively thicker skin of reduced metal, which sinters, and so becomes less pervious, at a relatively low temperature. This limitation of over-all rate becomes worse and worse as we aim to bring the residual unreduced oxide down to zero, so that this is a case of rapidly diminishing return from equipment of given size as we approach the substantially complete degree of reduction necessary. This inescapable condition —unless someone should find a way of using very finely ground ore at a competitive cost—precludes, in my opinion, the possibility of any low-temperature reduction process as a real competitor of the blast furnace for the production of iron to be made into steel.

CONVERSION OF IRON TO STEEL

In the conversion of blast-furnace iron into steel, there are two main processes, the Bessemer and the open-hearth. Both accomplish the same purpose—the removal by oxidation of silicon, carbon and other oxidizable elements, some of which indeed we would at times prefer to see retained by the steel; yet the Bessemer process is substantially completed in a few minutes, whereas the open-hearth process requires as many hours. In the former, there is thorough mixing and intimate contact of the reagent (air) with the metal; in the latter, the oxygen has to get into the slag and thence to and through the metal. Thus the Bessemer is in principle a better process than the open-hearth and, when properly controlled, undoubtedly yields a product equal in usefulness for a great number of products—for some purposes, even superior.

That Bessemer steel has been regarded as inferior to open-hearth steel is largely, or entirely, due to the circumstance that Bessemer steel has been less uniform from batch to batch; this lack of uniformity has been mainly due to an overemphasis on finishing each batch in the shortest possible time, with the consequent impracticability of stopping each blow at precisely the proper end point. To obtain a reproducible indication of an end point is, however, not the whole story; for, as is well known, the *relative* rate of oxidation of the several elements changes with the temperature of the metal and, therefore, the final composition of the metal leaving the converter depends upon the temperature of the metal throughout the process as well as upon the end point chosen. Within the last few years these questions have received more attention than during the preceding half century, with the result that instruments and methods are being developed to enable the Bessemer operator to furnish a more uniform product. The number of tons of ingots he produces each hour may be smaller, but the number of tons of acceptable product may be expected to increase, with a consequent increase in the proportion of Bessemer to open-hearth steel.

In the open-hearth process, on the contrary, the time a heat of steel remains in the furnace has tended to be longer, perhaps considerably longer, than the absolute minimum which under the very best operating conditions would be required. To discuss this question thoroughly would require a series of lectures and lecturers; I shall limit myself to directing attention to a few specific points. First, the over-all speed of the oxidation reaction is limited, not by the rate of reaction itself, which is clearly very great, but by the rate at which the reacting molecules get to each other —that is, by the rate of effective transfer of oxygen across the slag-metal interface, which in turn may at times be limited by the rate at which oxygen from the furnace atmosphere passes into and through the slag to that interface. The over-all rate therefore will be increased by any means that enlarges the interface per unit

of steel; therefore by anything that causes convection or stirring, or by any procedure that brings slag and metal into more intimate contact. If, on the other hand, we try
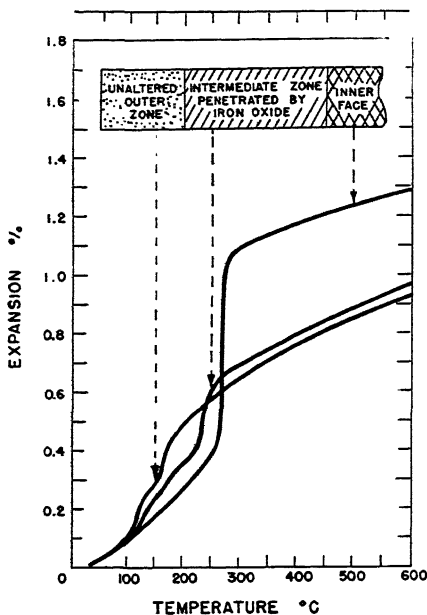
FIG. 1.—THERMAL EXPANSION OF DIFFERENT ZONES IN A USED SILICA BRICK.

to quicken the process by adding ore unduly fast toward the end of a heat, we shall

apparent end point, tend to come to a different real end point; hence the product will differ to that extent. Second, the total furnace time for a heat can be lessened insofar as it is feasible to increase the rate of supply of high-temperature heat until the steel bath is receiving all the heat it can take. This implies, among other things, an efficient, tight regenerative system; a slag that is not a blanket, but a transmitter of heat; and the maintenance of the furnace temperature as high as its roof and bottom will withstand, without undue time out for repairs. One of these limits is set by the refractories we can afford to use; even if price is left out of account, there are very few substances that will withstand the iron oxide fume together with the high temperature, which passes rapidly through a considerable range in the course of each heat. An example of what exposure in an open-hearth roof does to a silica brick is illustrated in Fig. 1, which shows the zones formed in the brick by permeation with iron oxide from the inner hotter surface, and curves representing the thermal expansion of these several zones, each curve being characteristic of the dominant form of the substance silica present in each zone. In saving time in the furnace we must
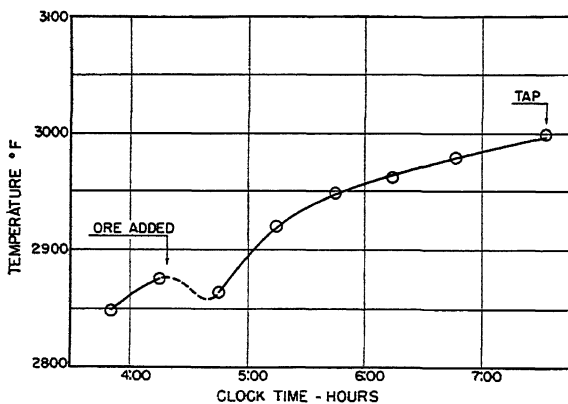
FIG. 2.—TEMPERATURE-TIME CURVE OF LIQUID STEEL IN THE OPEN-HEARTH FURNACE.

have a system which, because it is farther away from equilibrium, will, for the same

do it in the early stages of the heat and not during the last hour or so; for the end condi-

tion, both as to composition and temperature of the steel, must obviously be approached slowly if the degree of uniformity from one heat to another now required in so many steel products is to be attained. In other words, the temperature-time curve of the liquid steel should be as shown in Fig. 2, which represents actual measurements, by Sordahl, with the recording bath pyrometer.

THE INGOT

Passing over the operations of transfer of the liquid steel from furnace to ladle to molds—in both of which the time factor must not be left out of account—we come to the ingot. The ingot when poured must obviously be left in the mold until the solid skin has grown strong enough to permit the mold to be removed with safety. The stripped ingot in due course is moved to, and placed in, the soaking pit; but during this "time out" its outside should not cool too rapidly, for rapid local cooling is likely to initiate cracks which later will appear as surface defects. In any case the time out should be as short as practicable, in order to conserve heat. In certain steels, especially some of those containing added sulphur, it has been observed that the longer the interval between removal of the mold and the charging of the ingot into the soaking pit, the more numerous are the surface defects in the billet rolled from the ingot, which is an additional reason for operating so that this "time out" may be as short as possible. This increase in surface defects is due presumably to the combined effect of atmospheric oxygen and the sulphur in the steel, together producing a mixture of iron oxide and iron sulphide, which, being present in larger quantity the longer the exposure, and freezing at a lower temperature than iron sulphide alone, eats farther into the surface layers of the ingot. This suggested mechanism cannot, however, be regarded as established yet; the real mechanism may be more complex.

As to the desirable limits to the period of soaking an ingot, there seem to be few direct measurements of the temperature at the center of an ingot available, and
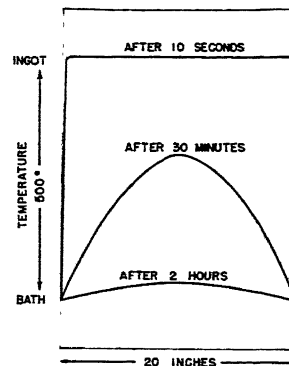
FIG. 3.—TEMPERATURE DIFFERENCE BETWEEN SURFACE AND AXIS OF 20 BY 20-INCH INGOT IN RELATION TO PERIOD OF IMMERSION IN BATH MAINTAINED AT A TEMPERATURE 500° LESS THAN INITIAL TEMPERATURE OF INGOT.

hence little information beyond that furnished by general experience. There is no doubt that, whether owing to some shortage of soaking-pit capacity relative to the capacity of the rolling mill, or to other reasons, the soaking period has at times been too short to ensure proper equalization of temperature through the ingot, or, at least, to yield the best product on rolling; further, that steel frequently has been damaged by overheating of the ingot surface in an attempt to get away with a short soaking period. In other words, steel has been supposed to be a better absorber and conductor of heat than it is in fact. Such data as are yet available do not enable us to state positively in how far the minimum time needed to soak an ingot of given size is determined by the rate of heat transfer to the steel, or by the conductivity through (heat diffusivity of) the steel, or by both jointly. If heat flow by conduction is the limiting factor, then Fig. 3 shows, for a 20 by 20-in. ingot, how the temperature difference between its axis and surface would decrease with time after it is plunged into a bath whose temperature differs from that

of the ingot surface by 500°, on the basis that there is zero resistance to transfer of heat between bath and steel and that the mean heat diffusivity of the steel within

HEATING OF STEEL PRODUCTS

Indeed, the proper heating of steel in its various forms from ingot to finished prod-
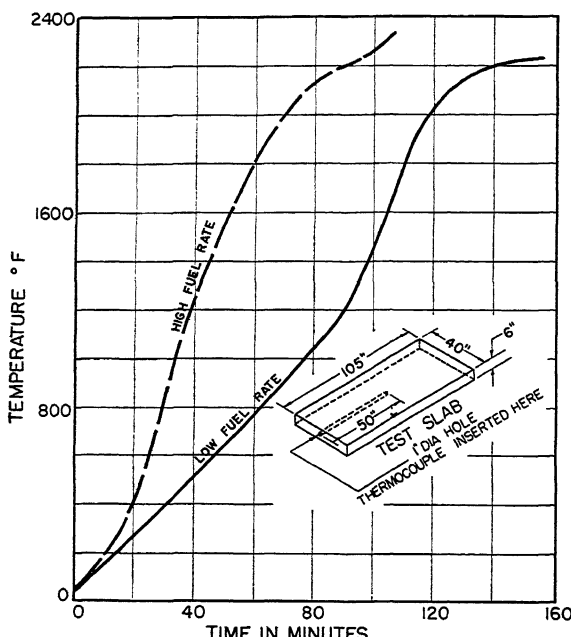
FIG. 4.—TEMPERATURE AT CENTER OF SIX-INCH SLAB WHILE IT IS BEING HEATED FOR ROLLING.

the temperature range considered is 1.0 sq. in. per minute. If the conductivity is in fact the limiting factor, the time required to bring about a given temperature distribution is proportional to the square of the diameter (or thickness) of the ingot; in other words, an ingot 20 in. thick will, other things being equal, require almost twice as much time as a 15-in. ingot to lessen the temperature difference between surface and center to the same amount. This suggests that it is unsafe to estimate the internal temperature of a piece of steel merely from a measurement of its surface temperature, particularly if the surface temperature has been changing rapidly; further, that there is a maximum *practicable* rate of heat input if substantially uniform temperature throughout the piece of steel is desired.

uct is a very important matter, which deserves further investigation now that heating furnaces under fine control and suitable pyrometric methods are both available. Fig. 4 shows some preliminary results of measurement of the temperature at the geometrical center of a slab 6 in. thick as it passed through a modern slab-heating furnace; one curve refers to a high, the other to a relatively low, rate of fuel input. For the less rapid heating, the rate of temperature rise, as the furnace was then operated, was much less through the lower part of the range than later (13° as compared to 25° per minute); these results indicate that furnace time could in principle be saved by increasing the initial rate of heat supply, but that the total time in the furnace cannot in this particular case safely be less than about 1½ hours.

A somewhat different example is presented in Fig. 5, which illustrates the rate of change of the temperature difference between the geometrical center of a pile
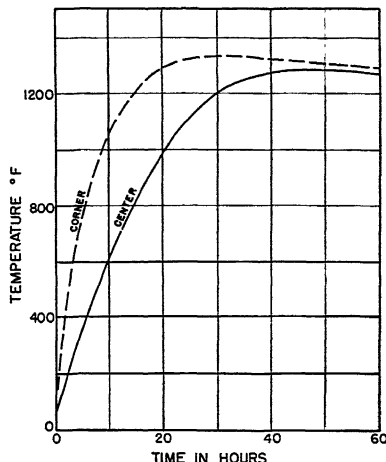
FIG. 5.—TEMPERATURE NEAR CORNER AND AT CENTER OF PILE OF SHEETS DURING ANNEALING.

40 by 90 by 40 in. of sheets and a location just inside a corner of the pile, the temperature of the annealing oven being substantially constant over the period; the heat was supplied mainly to the sides of the pile. After 20 hr.—by which time the outside sheet is substantially up to the final temperature—the difference is still about 300°F., and even after 40 hr. is as much as 50°F. In this case again it is obvious that little time can be saved by raising unduly the temperature of the outside sheets of the pile, and any such saving might well be more than offset by a loss of quality, particularly if the desired annealing temperature should be close to the transformation temperature of the steel. Incidentally, it may be remarked that the evidence favors the view that the heat is mainly transferred horizontally along each sheet rather than vertically from one sheet to the next; in other words, the resistance to heat transfer at the surface is far greater than the heat resistance (i.e., the reciprocal of the conductance) of the steel itself, a

point that is not always borne in mind by the designers and makers of heating equipment, from boilers to kettles and pans. In any case, the measurement and
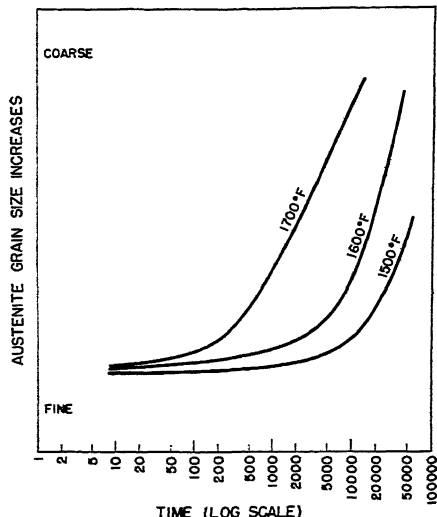
FIG. 6.—COARSENING OF AUSTENITE GRAINS WITH TIME IN SECONDS AT THREE TEMPERATURE LEVELS.

control of temperature of metal during annealing is very much improved over what it was in Howe's time, as a comparison of operating data in 1916 and 1941 shows conclusively.

ISOTHERMAL TRANSFORMATION

We have just outlined the practical limitation on rate of heating steel imposed by its mass and by the heat transfer across its surface; let us now take up some cases where time influences the result, no matter how small the piece of steel may be. The first is the growth of austenite grains. If small samples of a series of steels are held for a fixed period—say, half an hour— at a progressively higher temperature level, some will coarsen at a lower temperature than others, but if held long enough at a single temperature all will coarsen (Fig. 6), though at rates that may differ greatly. With increase of temperature, the rate for any given steel increases rapidly, and

the rates for the several steels become more nearly alike. This difference in response seems to be correlated with the presence of very fine solid particles of a

A second, and related, case is the time required for transformation of austenite, and how it depends upon the composition and grain size of the austenite and upon
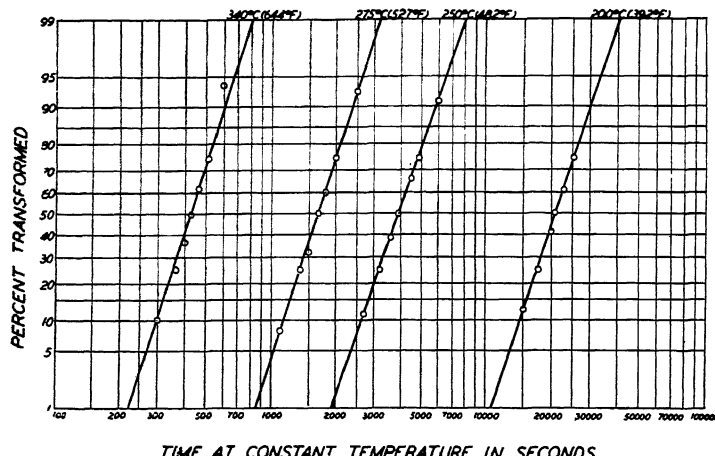
FIG. 7.—TIME OF TRANSFORMATION (t) OF AUSTENITE AT VARIOUS TEMPERATURE LEVELS, PLOTTED IN TERMS OF LOG $A/(1 - A)$ AGAINST LOG t.

high-melting compound, such as alumina, dispersed through the steel; but how far it depends upon the fineness, number or distribution of these particles, or upon some additional factor, remains to be established, present indications being that the very finest particles, beyond the range of the optical microscope, exert the dominant influence upon the rate of grain growth.

the temperature. In recent years this topic has been so much discussed that I need do no more than mention it and show Table 1, illustrating the influence of austenite grain size upon the time required for isothermal transformation of a single steel at various temperature levels. May I emphasize, however, that this type of information—which brings out clearly the effect of alloying elements, alone or in combination—combined with systematic investigations of the hardenability of steel, as made by a number of procedures, has set the whole subject of heat-treatment and hardenability on a sure, scientific basis, and has largely ended the kind of discussion which, to quote Howe again, "retained the hotness of the art itself, and a ferocity worthy of Mars, the patron of the metal."

TABLE 1.—*Influence of Austenite Grain Size upon Time Required for Isothermal Transformation*

| Temperature Level, Deg. F. | Time for 50 Per Cent Transformation of | | Ratio t_1/t_2 |
	Coarse Grain, t_1, Secs.	Fine Grain, t_2, Secs.	
1300	1,800	260	6.9
1200	500	150	3.3
1100	2,500	900	2.8
1000	1,200	750	1.6
900	30	30	1
800	35	35	1
700	40	40	1
600	25	25	1

Before leaving this topic of rate of isothermal transformation, there is one point to which I would advert; namely, that when we plot the proportion of austenite transformed (A) against time (t) at

a constant temperature, the curve closely resembles the logistic or autocatalytic curve which represents the progress of an autocatalytic reaction or the growth of a

mal transformation curve; their theoretical implication, unless they are merely a description of the probability of some happening, remains to be learned, though

NORMALIZED

CONTROLLED COOLED
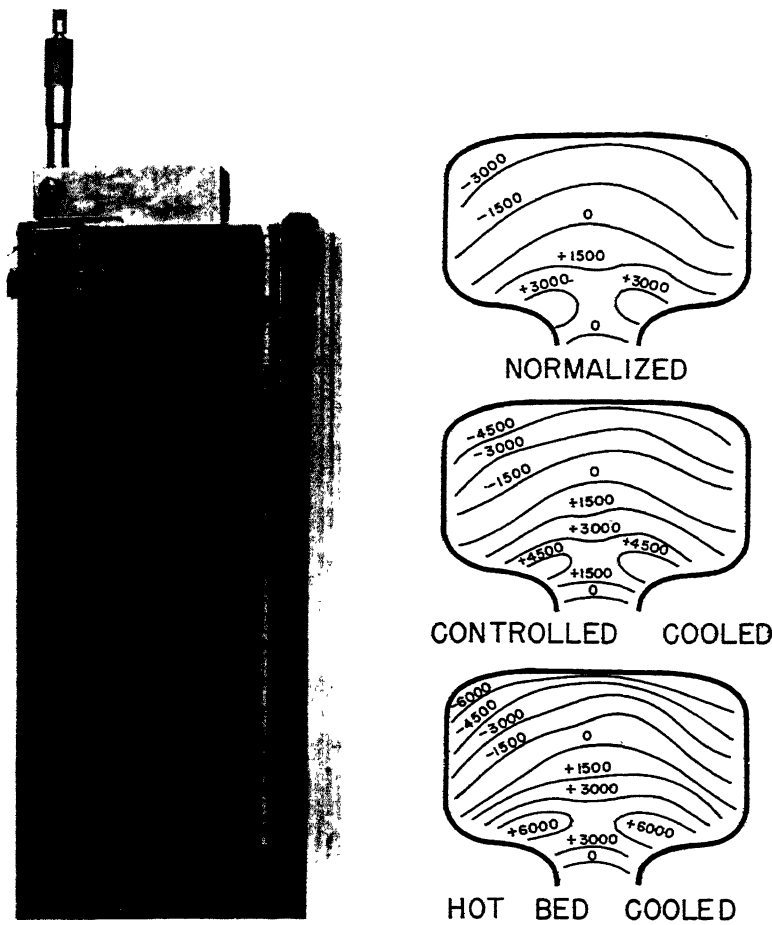
HOT BED COOLED

FIG. 8.—CONTOUR MAP OF MEASURED RESIDUAL STRESSES, IN POUNDS PER SQUARE INCH, IN HEAD OF RAIL WHICH HAD BEEN (a) NORMALIZED, (b) COOLED SLOWLY, (c) COOLED ON HOT BED. Tensile stress, +; compressive stress, −.

population. Following this indication, if we plot the data in terms of $\log A/(1 - A)$ against t or $\log t$, the graph so plotted is a straight line (Fig. 7); moreover, within a certain range of temperature, these lines for the several temperature levels are substantially parallel. These facts can be used to lessen greatly the number of observations required to set up a complete isother-

theories based on a mechanism of formation, and subsequent growth, of nuclei lead to a very similar description of the phenomenon in mathematical terms. Indeed, mathematics was developed largely as a means of enabling us to express, and reason about, the influence of time upon phenomena. As Willard Gibbs said, "mathematics is a language"; it is a succinct language

—*the* language for the description of complex phenomena that can be measured—and for this purpose is as far ahead of ordinary language as our numerals are to roman numerals for anything beyond simple addition and subtraction. Yet a mathematical formula is merely a convenient description, but in no wise an explanation, of the phenomenon measured.

TRANSFORMATION ON COOLING

It should now be clear that, in any heat-treatment, since the lag of structural change of steel falling in temperature is much greater than for a rising temperature, the most significant time period is that allotted to cooling through a certain range of temperature. Nevertheless, it is necessary to hold the steel at the austenitizing temperature long enough to ensure that all the carbides are dissolved (unless this is not required) and that the carbon so dissolved is distributed uniformly by diffusion through the austenite. With this achieved, the important rate of cooling is prior to the onset of the transformation; namely, that which, by determining the transformation level at which the change begins, determines the metallographic structure; for when once the transformation is complete the structure is not noticeably affected by the rate of further cooling unless the time at relatively high temperature should be so long that spheroidization of the carbides proceeds to an appreciable extent. When we are dealing with large pieces of steel, however, this later cooling rate exerts a significant influence upon the magnitude and distribution of the residual stresses as well as upon the prevalence of the so-called flakes or shatter cracks. For instance, Fig. 8 shows, for comparison, a contour map of the residual stresses in the head of a rail after it had been: (*a*) normalized and slowly cooled, (*b*) cooled very slowly, (*c*) cooled on the regular hot bed. The outcome of such observations is that rails are now being cooled from the rolling temperature under rigid control of time and temperature; and the indications are that such rails, which have been put into service within the last few years, are much safer than those made formerly. A similar control of cooling time of wheels and of other products, intermediate as well as finished, and of welds, is now common practice as a means of ensuring freedom from harmful residual stress.

DIFFUSION OF HYDROGEN

The available evidence indicates that shatter cracks are somehow related to the presence of hydrogen in the steel, though it seems as though hydrogen alone were not a sufficient cause. However this may be, they can be lessened, or eliminated, by a slow cooling, which gives the hydrogen time to diffuse out and away (and at the same time lessens the residual stresses). Indeed, it has been shown that the well-known increased resistance to impact of rails, as indicated by the drop test, during the first few days after they are made, goes hand in hand with a gradual loss of hydrogen, which is more rapid in summer than in winter. Thus we are led to a brief consideration of the process of diffusion, as of hydrogen or carbon, in solid steel, and how this is related to other phenomena, such as the effect of time upon the extent of carburization or decarburization of steel, under given conditions.

Hydrogen, whether reaching the steel surface as gaseous molecules or as ions formed in a liquid, diffuses fairly rapidly through steel, the actual rate depending both upon the effective pressure of the hydrogen at the surface of the steel and upon the temperature. For instance, at 1000°F. the diffusion constant is 1.9×10^{-4} sq. cm. per sec.; which means that at this temperature a steel plate 1 in. thick, exposed on both sides to hydrogen maintained at a given constant pressure, would be 50 per cent saturated (with respect to that pressure) in about ½ hr., 95 per cent

saturated in 2½ hr. and 99 per cent saturated in about 4 hr. The last period is obviously the minimum time of contact if we propose to measure the real solubility of hydrogen in steel of that thickness at that temperature; for any other thickness the corresponding time required is proportional to the square of the thickness. Incidentally, it may be remarked that at this temperature this solubility, expressed in terms of volumes of hydrogen, measured at normal temperature and pressure, per volume iron, is $0.064p^{1/2}$, where p is the hydrogen pressure expressed in atmospheres.

CARBURIZATION AND DECARBURIZATION

The diffusion constant of carbon in austenite, though much less than that of hydrogen, is greater than that of any other alloying element yet measured; its change with temperature is shown in Fig. 9. Clearly, the time required for carburization or decarburization is set by the rate of carbon diffusion. The relation between the elapsed time of contact with a carburizing atmosphere of constant carbon activity and the total amount of carbon that has then entered a ½-in. cylinder, initially

plied usually by scale)—the case is somewhat more complex, because oxygen is diffusing inward, though more slowly, as carbon is diffusing toward the surface.
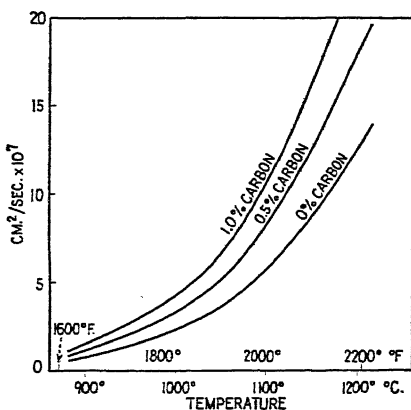
FIG. 9.—DIFFUSION CONSTANT OF CARBON IN STEELS IN RELATION TO TEMPERATURE.

In this case again it is probable that the discontinuity observed under the microscope, and used as a conventional measure of the depth of decarburization, does not imply a total absence of carbon at that level. I suspect, moreover, that some of the troubles ascribed to a loss in carbon
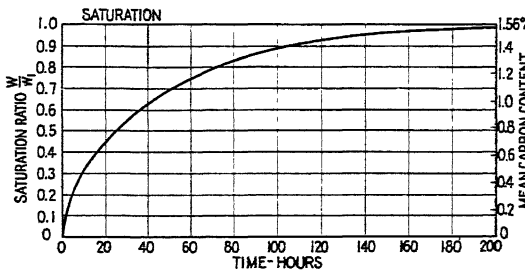
FIG. 10.—PROGRESSIVE MEAN SATURATION BY CARBON OF HALF-INCH IRON CYLINDER AT 1800°F.

pure iron, is illustrated in Fig. 10; this carbon is distributed so that there is a *continuously* diminishing percentage of carbon going inward from the surface, even though under the microscope there may appear to be a line of demarcation.

In the usual case of decarburization— that is, when the carbon is eliminated from the surface by reaction with oxygen (sup-

near the surface of the steel may at times be due in part to a gain in oxygen, possibly accompanied by the precipitation of some oxide particles.

By following the gradual loss of carbon from a piece of steel, maintained at constant temperature in an atmosphere which, without otherwise affecting the steel, removes the carbon as fast as it diffuses to

the steel surface, we can calculate the rate of its diffusion, and the result agrees with data obtained by the usual quite different method. Such an atmosphere is hydrogen

pearlite. Fig. 11 illustrates the change of hardness of a martensite with time at a series of temperature levels; and this general picture suggests—though of course
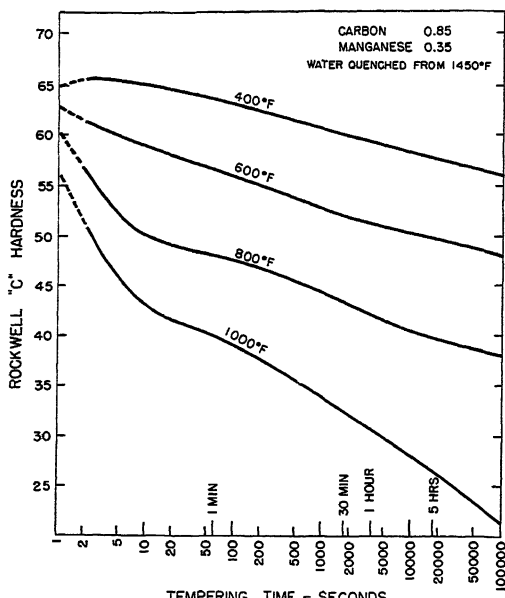
FIG. 11.—INFLUENCE OF TIME AND TEMPERATURE UPON TEMPERING OF MARTENSITE, ON BASIS OF MEASUREMENTS OF HARDNESS.

carrying a proportion of water vapor—e.g., 2 per cent at a temperature of 900°C. or above—which is large enough to oxidize carbon completely but does not oxidize iron. *Pure* hydrogen does not remove carbon rapidly at temperatures at which carbon diffusion is appreciable; the belief that hydrogen (or an ordinary reducing gas) is responsible for decarburization arose because the hydrogen used in the experimental work was not in fact free from oxygen compounds, particularly from water, a very small proportion of which quickens enormously the removal of carbon from the steel surface.

The rate of carbon diffusion is somehow related to a number of other phenomena of practical significance to the steel metallurgist; for instance, to the tempering of martensite and the spheroidization of

change of hardness is only an indirect measure of the progress of the structural change called tempering—that the rate of diffusion of carbon is the limiting factor in the over-all rate of this process. The same doubtless holds for spheroidization, for the progress of which there is again no direct quantitative measure. It would seem, moreover, that the rate of diffusion of carbon must play some role in setting the spacing of the lamellae in pearlite, the distance between lamellae being smaller the lower the temperature level at which the pearlite formed from austenite.

STABILIZATION OF STRUCTURE

Alloying elements other than carbon diffuse very much less rapidly, wherefore a long sojourn at high temperature is required to homogenize a steel thoroughly;

that is, to eliminate banded structure and similar inhomogeneities. Thus, a certain steel was not sensibly homogeneous until it had been held at 2250°F. for a period of

brought to a stable state by appropriate previous treatment. Direct experiment showed, for example, that the structure produced in 5 hr. at 1300°F. is indistin-
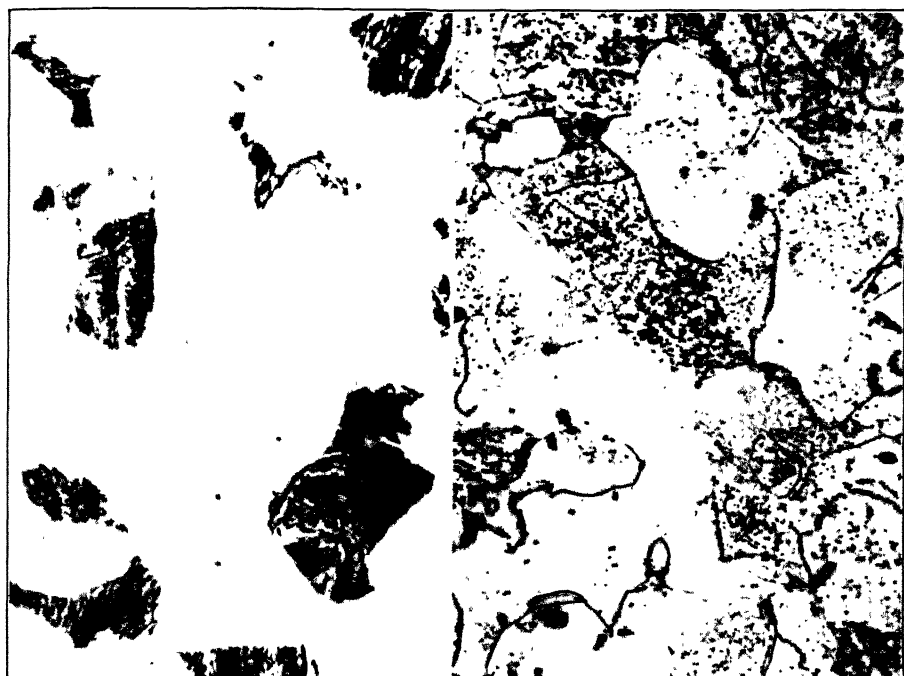
FIG. 12.—CHANGE OF STRUCTURE OF A CARBON-MOLYBDENUM STEEL AFTER 3000 HOURS AT 1100°F.
× 1000.

48 hr., this being done in an evacuated container to eliminate the disturbing effects of scaling; and it hardly needs remark that unless homogeneous samples are used one is hardly justified in considering the properties observed to be truly characteristic of steel of that composition. A specific case comes up in the measurement of creep, which is itself a very slow rate of yielding under stress at elevated temperature. To be significant, these measurements should extend over a period of 2000 hr. or more, for the structure changes over the first 500 hr. or so at temperature, as shown in Fig. 12, unless the steel is in a state that is substantially stable at the temperature in question, or if not (as frequently happens), has been

guishable from that produced in 5000 hr. at 1000°F. Again it may be pointed out that data on creep—or more generally on rate of strain at elevated temperature— are of little practical significance unless they refer to a structure that does not change appreciably with time at the temperatures at which it will be in service.

A somewhat different, though not unrelated, phenomenon is that of the so-called aging of steel. One example is illustrated in Fig. 13, which depicts change of hardness with time at the aging temperature. Aging is attributed to a precipitation in the steel of something—a carbide, oxide, nitride or whatever—though the major changes in mechanical properties appear before any visible precipitation has occurred; in any

case, the final appearance of a precipitate is proof that the steel had at some time during cooling become supersaturated with respect to something, and that this super-

carbon as a carbide suggests that the true solubility of carbon in ferrite at atmospheric temperatures is smaller than it is usually supposed to be. Howe stated it as
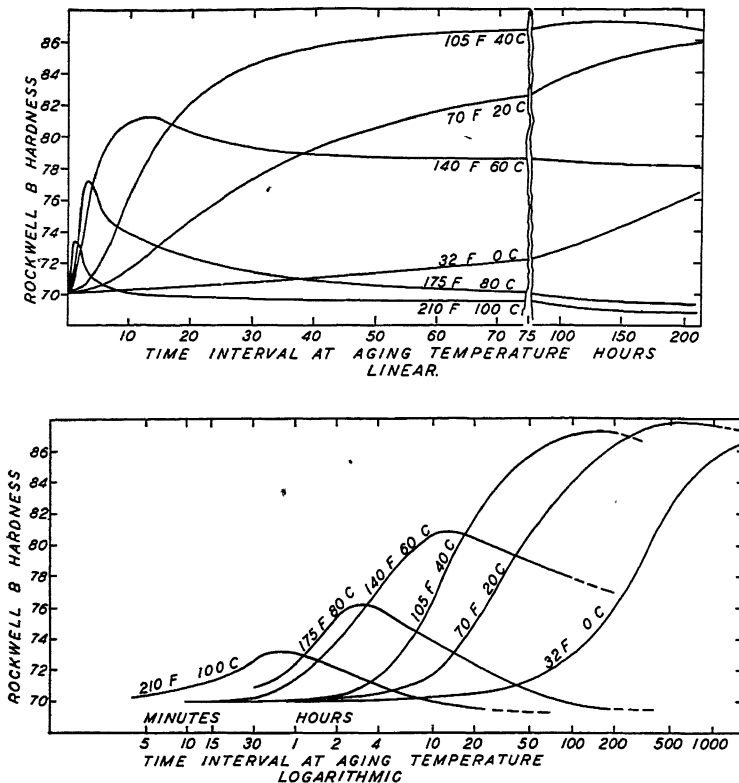
FIG. 13.—TYPICAL AGING CURVES; CHANGE OF HARDNESS OF A STEEL WITH TIME AT TEMPERATURE.

saturation was relieved by the sojourn at temperature or by the deformation brought about by cold-work in the so-called strain aging. This phenomenon proceeds faster, other things being equal, as the temperature is raised to the so-called blue-brittle range, when it is almost instantaneous; this complete precipitation is followed by a slow coagulation of the precipitated material, this process—the so-called over-aging—again being very much more rapid the higher the temperature, as illustrated in Fig. 13.

The fact that one kind of aging in a plain carbon steel is due to the precipitation of

0.06 per cent, whereas the present accepted value seems to be 0.01 per cent or less, and I would not be surprised if it is in fact less than this; for any determination of this quantity would tend to yield a high result because of the likelihood of some residual degree of supersaturation, which would lead to an overestimate of the carbon actually dissolved in the ferrite matrix. On the other hand, it has been shown recently that carbon entering austenite by diffusion may, at the eutectic temperature (1135°C., 2075°F.), build up to a concentration of 1.98 per cent, which is appreciably higher than the limiting value

heretofore accepted (1.7 per cent); but whether, under these conditions, the solid phase in contact with the steel and in equilibrium with the austenite is graphite or a somewhat less stable form of "carbon," remains to be established.

In view of this, and in general because many of the reactions in solid steel proceed only slowly, it is probable that our so-called equilibrium diagrams include many errors; for they have been based upon experiments lasting minutes or hours, whereas the attainment of real equilibrium may require days or even weeks, as, for instance, in the iron-manganese system. It is always a matter of difficulty to distinguish between real equilibrium and a condition that apparently has ceased to change merely because the rate of reaction is very small; when this is so the change is inappreciable until after a quite long interval, or after some special treatment, such as cold-working in the 18 per cent chromium, 8 per cent nickel stainless steel. It is to be expected that some of the anomalies in our present diagrams will disappear when, and only when, sufficient time is allowed to permit the attainment of true equilibrium between the several phases, establishing this as a fact by the only valid criterion; namely, that the same state is reached when approached from either side.

SURFACE PHENOMENA

Now a few words relating to the surface of steel, and what may happen to it. Careful experimental work has demonstrated that a plane steel surface, as of cold-rolled steel, will at a definite temperature absorb a perfectly definite quantity of a given gas, *provided* that all material previously attached to the metal surface has been eliminated by a series of alternate exposures to high vacuum and to the gas to be absorbed. The number of such cycles may be as many as 20, and occupy a period of a week or more; this repeated observation

illustrates the difficulty of removing the last trace of anything that previously had been in intimate contact with the steel surface. A steel surface treated in this way repeatedly with pure hydrogen is so clean that it is wetted by mercury, whereas an instant's exposure to air prevents this wetting. It would lead too far to go into this large question of absorption at a surface; I have mentioned it merely to emphasize the fact that two pieces of steel, which to all ordinary tests are identical, *may* differ at their surfaces because of some difference in prior treatment, and to that extent show a different initial rate of reaction with an external agent. To such difference in surface film may perhaps be attributed differences in rate of pickling, or generally in reactivity as indicated by the use of terms such as "incubation period" or "threshold value"; and they may be the basis for the belief that the nature of the first film formed seems sometimes to determine the subsequent course of the corrosive reaction.

Such a surface may (or may not) catalyze a reaction between gases in contact with it. If it does, the composition of the gas atmosphere as a whole will differ from that which is affecting the steel; and conclusions as to what would be a neutral atmosphere would not be completely valid. Perhaps this, which is in essence another case of failure to distinguish between a state of equilibrium and a condition of reaction, is responsible for some of the diverse statements and opinions with respect to the proper composition limits for a "controlled" atmosphere which shall be neutral to steel at temperature. I have already adverted to carburization and to decarburization, the progress of either of which depends upon the rate of carbon diffusion and upon the concentration of carbon maintained at the surface. Perhaps the most effective remover of carbon is an oxide scale, which reacts directly with the carbon as it reaches the surface; the depth

of decarburization of the rolled billet may therefore be dependent on whether the ingot, while it is being heated for rolling, loses thickness by scaling faster than is compensated by the diffusion outward of carbon to the moving scale-metal interface. All of these rates increase markedly with temperature, but the rate of increase may differ considerably from one to another; thus further knowledge may enable us to select a time-temperature schedule which will strike a better balance between the several competing rates encountered in bringing steel to temperature for rolling or other fabrication process.

No general lecture dealing with steel and time would be regarded as complete without some reference to corrosion, a large subject, which has caused much degradation of energy and vexation of spirit. I shall refer to it only by remarking that the term "corrosion" covers a multitude of different reactions, the course and progress of which depend not only upon the metal but also upon its environment; and that many are still hoping that some magician will produce out of his hat a test which will tell us *now* what some environment (seldom specifiable in precise detail) will do to the metal over a period of years— in other words, they are seeking by some so-called accelerated test to compress time, and I still doubt whether this can be done. Nevertheless, it can be said that this whole matter of corrosion is on a far better basis than it was, for recent years have brought advances in reliable knowledge of this large group of phenomena which have greatly clarified them, even though much remains to be done.

CONCLUSION

Enough examples have been adduced to emphasize the need for taking into account the time required for the proper operation of various processes in steel metallurgy. Since the publication of Howe's book, our knowledge of both equilibrium and the

rate of approach to the state of equilibrium has become wider and more precise, and correspondingly more useful in practice. In recent years many papers dealing, directly or indirectly, with questions involving time as a factor have been published—a larger number perhaps than on any other topic; many points that were obscure have been cleared up, but many others remain to be settled by experimental investigation, for the answer cannot be foretold. There is opportunity to set up more satisfactory correlations between some of these apparently different phenomena than have yet been reached; any such correlation would be empirical— since there is no satisfactory detailed theory of reaction rate, even in gaseous systems, and far less in liquids and solids— but none the less useful. These remarks may not, to use a phrase of Howe's, "convey a very clear idea to an unwilling mind"; yet the number of minds willing and equipped by training to think these things through has been increasing rapidly since his time.

In conclusion I cannot do better than again quote, this time from his preface.

As befits such an attempt as this, though I try to explain and illustrate clearly the visible phenomena, my chief aim is to stimulate others to think profoundly, in order that some among them may in due time push discovery further beyond its present very early stage. Those of us who are working and thinking on this subject today are only crying in the wilderness, in the hope of inciting our successors.

With this general aim I have acted on Tyndall's sage words: "Right or wrong, a thoughtfully uttered theory has a dynamic power which operates against intellectual stagnation; and even by provoking opposition is eventually of service to the cause of truth."

The true task of the teacher is to excite thought. Hence I do not hesitate to offer such hypotheses as I can devise, not with the belief —hope should not enter into consideration— that they will endure, but with the aim of stirring others to seek the truth by destroying them. This, I take it, is the true function of most hypotheses, and this purpose should be in the heart of every philosophic student. Laws

are useful, and where opportunity offers I try to deduce them. But because the causes beneath those laws are of a higher order of importance, it is to these that I have chiefly addressed myself.

For my part, I have aimed to distinguish inferences from observations, personal interpretations from what would generally be regarded as facts, and suggest that we need many more complete and reproducible observations before we can expect to describe these time phenomena in terms of any law, even perhaps of any satisfying hypothesis.

Correlations of Some Coke Properties with Blast-furnace Operation

BY HJALMAR W. JOHNSON,* ASSOCIATE MEMBER A.I.M.E.

(Chicago Meeting, April 1941)

It has long been accepted that blast-furnace practice varies to some degree with the coke used. While the qualities desirable in iron have been known for some time, the qualities in coke that produce such iron have not been established. There are no objective standards for blast-furnace coke, which is usually described in general terms, as good or bad.

Many experienced operators believe that coke cannot be measured objectively except by using it in the furnace, noting the result, and labeling the coke according to furnace operations. This is admittedly unscientific, and besides is useless for the two main purposes for which a measure of coke quality is needed: (1) to produce the best possible coke from the coals and equipment on hand; (2) to test new coals and determine their value for blast-furnace coke. In seeking such an objective measure, much work has been done on tumbler tests, shatter tests, sizes of coke, porosity, specific gravity, reactivity or combustibility and other tests, but as yet very little has been published in which conclusive correlations have been established between such objective measures and furnace operation.

In our study of the problem during the past 8 years we have developed no new measures of coke quality, but we have collected data that are presented here in the hope that they may assist in further work, so that at some future time there may be developed such positive measures. The purpose of this paper is to show that there are variations in coke and that such variations do influence the operation of blast furnaces. At the same time we must remember that there are variations in blast-furnace operation and it may be the blast furnace that is at fault. This correlation of coke properties with blast-furnace operation will be worked out in the following steps:

1. Discussion of a period when a change in the coke resulted in an increase in efficiency on one furnace and a decrease in efficiency on another.

2. Adaptation of the inefficient furnace to the available coke so that normal efficiency was restored.

3. The use of radial distribution: a discussion of the effect of size of ore layer in adapting blast-furnace operation to the coke.

4. An example of a change in size of coke and the detrimental influence on the production of one furnace.

5. An example of a change in size of coke, together with manufacturing data, to show why it changed, the conclusion being that coke is a product with an optimum value.

6. Illustration of the fact that coke has different optimum values on two furnaces, with discussion on adaptation of operation so the optimum values will be the same.

7. Limitations of the use of screen tests as an objective measure of coke quality.

8. Importance of uniformity in coke.

FUNCTIONS OF COKE AND QUALITIES REQUIRED TO PERFORM THESE FUNCTIONS

Coke has three important functions in a blast furnace: (1) to furnish most of the

---

Manuscript received at the office of the Institute June 13, 1941. Issued as T.P. 1402 in METALS TECHNOLOGY, December 1941 and printed in *Proceedings* of Blast Furnace and Raw Materials Committee, A.I.M.E., 1941.
* Superintendent, Blast Furnace Department, Inland Steel Co., East Chicago, Indiana.

heat required for the operation, (2) to provide voids in the furnace stack for proper gas flow, (3) to provide voids in the bottom of the furnace so that iron and slag can accumulate in the hearth.

The value of any particular coke will be in proportion to its ability to fulfill these functions. The amount of heat produced per pound of coke can be readily determined by analysis. Among the varied properties that result in the required voids in the furnace are:

1. Initial size.
2. Range in size.
3. Uniformity in size in furnace.
4. Ability to withstand breakage.
5. Ability to withstand abrasion.
6. Type of fines produced after degradation.
7. Shape of pieces.
8. Behavior of coke pieces on reheating in furnace.
9. Resistance to abrasion and crushing at high temperatures.
10. Weight per cubic foot.
11. Percentage of voids effective for gas flow per pound of coke.
12. Uniformity from load to load.

To these might be added the property of reactivity or combustibility. Perhaps also there is some rebonding of the individual pieces when subjected to pressure at high temperatures.

Excellent correlations have been established at individual plants between some of these properties and blast-furnace operation and, as shown by Campbell and Wagner,[1] by combination of these properties. In general, they have been too limited to afford a basis for predicting furnace operation. Either the properties measured are minor ones and others, known or unknown, are the significant ones, or it is the combination of all the properties that determines its value as a blast-furnace fuel. To measure all of these properties is obviously impossible, so other methods should be considered.

[1] References are at the end of the paper.

METHODS OF APPROACH

The methods of approach used in this paper have been: (1) screen tests of coke and (2) oven-operating data.

The manufacture of coke can be divided into four steps: (1) selection of coals, (2) preparation of the coal charge, (3) heating the coal charge, (4) pushing, quenching and preparation of coke. Detailed investigation of each of these four divisions reveals many variables in each one. If there is a change in any one variable it will result in a change in the coke produced. The fact that the difference cannot be seen or measured does not prove that the difference is not there. Our measure may not be accurate enough, or we may not have the right measure.

However, it is obvious that if all factors are kept constant the coke will be constant, and so will the screen tests of the coke. If variations are found in the screen tests, it is clear that the coke has changed; that is, one or more variables have been introduced in the manufacture. Study of the details of manufacture should then reveal which of the variables has changed. By this method we have found that two of the most significant variables are coking time and flue temperature.

Our procedure has been to study the size of coke as charged into the blast-furnace skip and note the results obtained with changes in size. The manufacture of the coke in turn has been considered, to observe what factor has changed to cause the alteration in size. And finally, correlations have been established directly between pertinent data on the manufacture of coke and the results on the furnaces. In all cases the blast furnaces have been used as the final testing medium.

METHOD OF MAKING SCREEN TESTS

No. 4 furnace was equipped with grizzlies to screen the coke going into the skips, while the other furnaces had no screening facilities; When No. 4 furnace was in opera-

tion all screen tests were made on that furnace and the samples were taken after the coke had gone over the grizzlies. The sample then represented the coke going into No. 4 furnace skip. The same coke was going into the other furnaces but it was

the 8-hr. turn, and samples were taken on one, two or three turns per day.

The furnace equipped with grizzlies was believed to afford the most accurate samples because at the time the grizzly was stopped and the sample box put in place
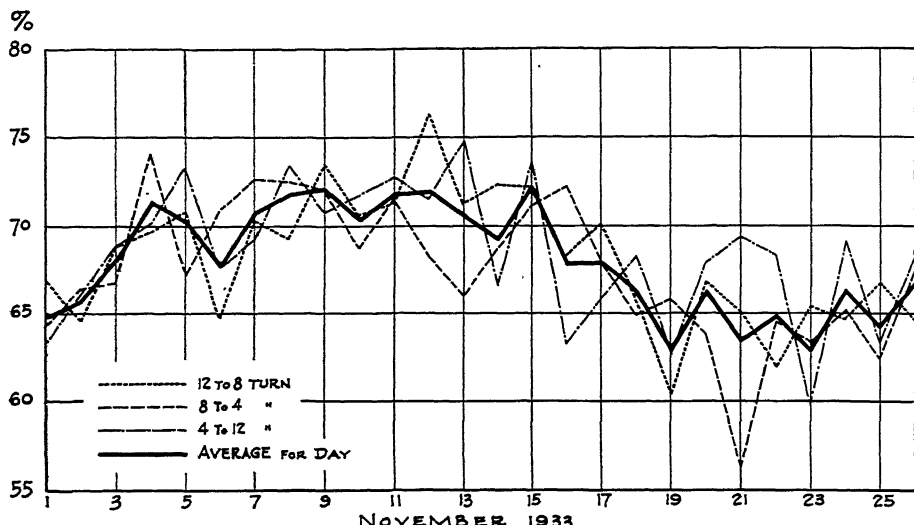
FIG. 1.—PERCENTAGE OF PLUS 2-INCH COKE FOR EACH 8-HOUR TURN AND AVERAGE FOR DAY AT NO. 4 FURNACE.

not screened and so contained from 4 to 8 per cent of fines. When looking at screen tests taken on No. 4 furnace, but considering data on No. 2 or No. 3 furnace, from 4 to 8 per cent of fines should be added to the minus 1¼-inch.

The following procedure was used in taking samples: When a skip of coke was to be charged, about one half a skipload of coke was pulled into the buggy. The grizzly was stopped, a steel box large enough to catch the whole stream of coke was placed on top of the skip, the grizzly was started and the entire stream was pulled into the box for a moment. The sample box, with from 50 to 75 lb. of coke, was then raised and the coke it contained was dropped on a 4-in. screen. This was done every half hour from 8 a.m. to 2 p.m. Fourteen samples of 50 to 75 lb. constituted the sample for

the coke that constituted the sample was resting directly on the grizzly. As any movement of structure, such as cars operating on the highline, would cause the fine coke to filter down to the doors and give a sample containing excessive fines, the sample was not pulled directly from the bin, but from the part of the grizzly that extended beyond the bin.

The results of the screen tests taken on each of three turns from Nov. 1 to Nov. 26 are shown graphically in Fig. 1, together with the average for the day. The data plotted are the percentages of coke that remained on a 2-in. screen. The curve of the individual turns is much more irregular than the average of the three, which is fairly smooth. It is doubtful whether the individual peaks in the average curve are correct, but a smooth average line drawn

through the curve representing the average of the three turns is believed to be correct.

METHOD OF MEASURING FLUE TEMPERATURES

Mr. E. J. Gardner, superintendent of the coke plant, reports that flue tempera-

that the coke is satisfactory but the operation of the blast furnace is inferior. It is essential to adjust the operation of the furnace as well as possible to the coke available before beginning to make correlations. And it is equally essential to know the limits of furnace adjustments. Certain
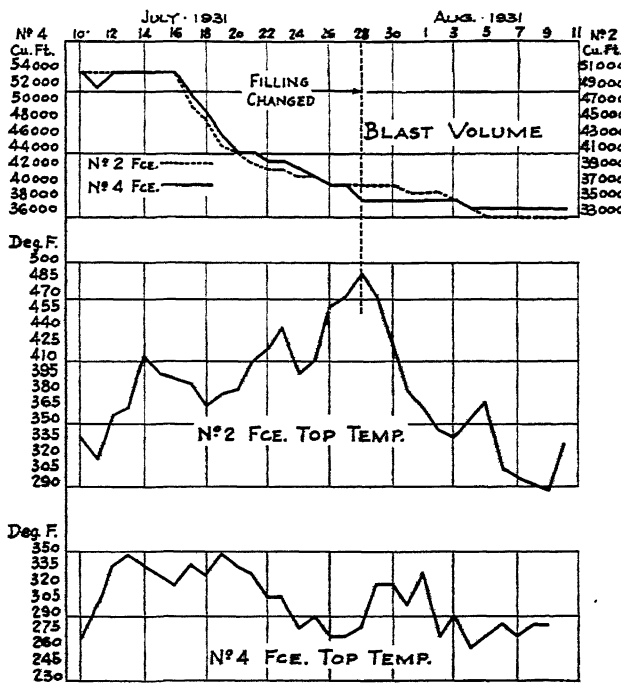
FIG. 2.—OPERATING DATA FOR NO. 2 AND NO. 4 FURNACES.

tures were taken as follows: "We start at one end of the battery 15 min. after reversal, on the coke side, taking the seventh flue on every eighth wall, returning on the pusher side from the opposite end, taking the seventh flue on the same walls as on the coke side. These temperatures are added and averaged and reported as the temperatures of the flues for that particular day."

DISADVANTAGE OF USING THE BLAST FURNACE AS A TESTING MEDIUM

When the blast-furnace practice is poor, we cannot leap to the conclusion that the coke is inferior, as it may just as easily be

changes, for example, in filling are known to improve furnace operation, so that without any change in the coke the operation of the furnace has been better adjusted to the coke available.

This point can be illustrated. Two furnaces were performing satisfactorily on full wind when it became necessary to curtail operation and the wind was reduced gradually, at the same rate on both. The decreased need for coke made it necessary to increase the coking time at the ovens. Under such conditions there is an increase in the size of coke, but for this particular period no data are available. As shown in Fig. 2, while the wind was decreased there

was a gradual increase in top temperature on No. 2 furnace until July 28, but on No. 4 furnace there was a gradual decrease. In Fig. 3, it is shown that while there was a gradual decrease in burden on No. 2 furnace there was a gradual increase in burden on No. 4 furnace. No changes had

neither conclusion could be drawn. It is such conflicting evidence that makes it difficult to relate coke quality and furnace performance; and it is probable that many confusions between producers and consumers of coke arise over situations such as these.
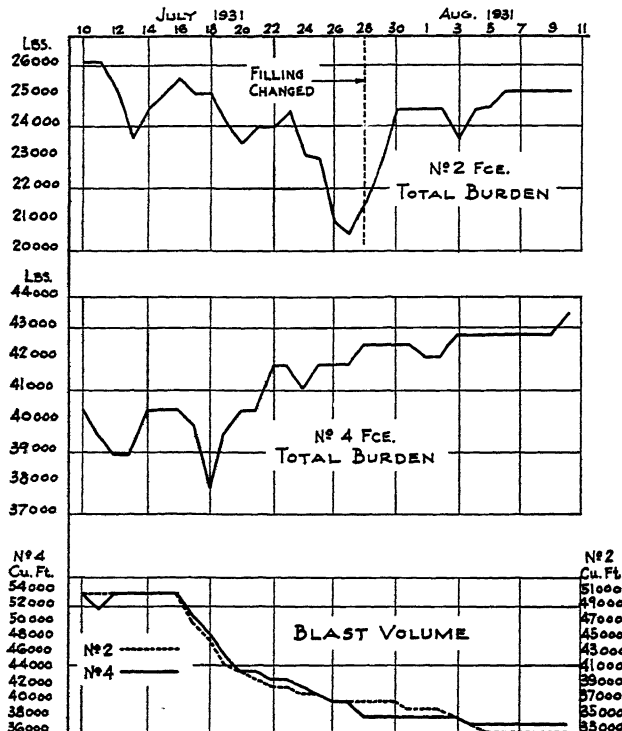
FIG. 3.—OPERATING DATA FOR NO. 2 AND NO. 4 FURNACES.

been made in the ore or stone used, method of filling, or other factors. The two variables were the decrease in wind blown and increase in coking time at the ovens.

If only No. 2 furnace had been in operation, the decrease in burden of 21 per cent would have been convincing evidence that the increase in coking time was causing the production of inferior coke. If only No. 4 had been in operation, probably the conclusion would have been that the increase in coking time was beneficial. Since the same coke was being used on both furnaces, with opposite results, it was apparent that

On July 28 a change was made in the filling of No. 2 furnace, of which the details will be discussed later. Immediately there was a decided improvement, an abrupt decrease in top temperature, and a decided increase in burden. This simply amounted to an adaptation of the operation of the furnace to the coke available. Closer examination of the charts reveals the fact that the burden on No. 4 furnace between Aug. 7 and Aug. 11 was higher than it was before the decrease in wind, while on No. 2 furnace it was about the same. This indicates that the coke was being used to

better advantage on No. 4 furnace than on No. 2, and we can conclude that the change in filling on No. 2 furnace was not the best adaptation that could have been made. Since No. 4 was able to carry more burden with the decreased wind, No. 2 should have been able to do it also, had the proper adaptation been made. This point will be discussed later.

Effect of Size of Ore Layers on Radial Distribution

The fundamental question then arises: With the same change in wind blown and the same coke, why did one furnace increase in efficiency and the other decrease? To understand this it will be necessary to review the influence of the size of ore layer on the radial distribution of the gases. Ordinarily a skipload of ore is charged, then a skip of stone and one of coke, making three layers on the large bell. The large bell is then lowered and the material slides off into the furnace. There are many variations, but this is a typical charging sequence.

When the big bell lowers, the material falls into the furnace in fairly distinct layers, with relatively little mixing, and so there is first a layer of ore in the furnace, then a layer of stone and on top a layer of coke. The characteristics of these layers are important, because they influence the flow of gas.

C. C. Furnas and T. L. Joseph[2] pointed out that when ore falls into the furnace it assumes its angle of repose about directly below the large bell. This angle varies for different types of ore and for different degrees of moisture, but approximates 35°, and the angle of repose for coke is about 28°. The peak of the ore may be almost directly under the edge of the bell or against the wall, or anywhere between, dependent upon the velocity with which it leaves the bell and the distance it drops.

While any system of filling results in layers of ore, stone and coke, it is the size

of these layers, particularly that of the ore layer, that determines whether the filling is good or bad.

This is illustrated in Fig. 4, which shows sections through the top of a 17-ft. furnace equipped with a 13-ft. bell. It is assumed in this case that the ore and coke leave the bell with zero velocity, so that the peaks of both are directly under the edge of the bell, and that the stock line is immediately below the lowered bell. The top section shows a layer of coke at an angle of 28° and on top of this a layer of ore with its angle of repose at 35°. Since ore has so steep an angle, it is obvious that an ore layer of considerable thickness can be built up without reaching into the center. In the case illustrated, when the ore just reaches the center of the furnace there are 12¾ in. of ore at the peak, and 9⅛ in. at the wall. An ore layer of 25,064 lb. is needed to fill these requirements.

This difference in thickness of ore and coke layers automatically indicates more or less what the gas travel will be. The coke is large in size and produces the voids, while the ore is small and tends to fill these voids. Consequently, the greater the ratio of coke to ore in any given section, the more effective voids there will be and the greater the gas velocity. Another factor in the resistance to gas flow is the segregation into coarses and fines. Directly below the edge of the bell are the small pieces of ore and coke, and the farther the pieces are from this vertical plane on either side, the larger they are. It is clear that the areas with the maximum amount of coke will also have the largest pieces of coke, and the areas with the minimum of ore will have the largest pieces of ore. From this it follows that the minimum flow is directly under the edge of the bell, because there is the maximum thickness of ore layer for thickness of coke layer and a concentration of fines of both these materials. From the zone directly under the bell toward the center of the furnace, gas flows are in-

creasing and the maximum flow is at the center of the furnace.

If it becomes desirable—for reasons to be discussed later—to increase the flow up the center, it can be done by increasing the voids; that is, placing less ore at the center. If the size of the ore layer is decreased from

a circle of coke alone that is 7 ft. in diameter, which is 16.9 per cent of the total area of the stock line. It is apparent that this is a large proportion of the total and such a furnace would have a flow up the center excessive enough to make that furnace extremely inefficient. To our knowledge no
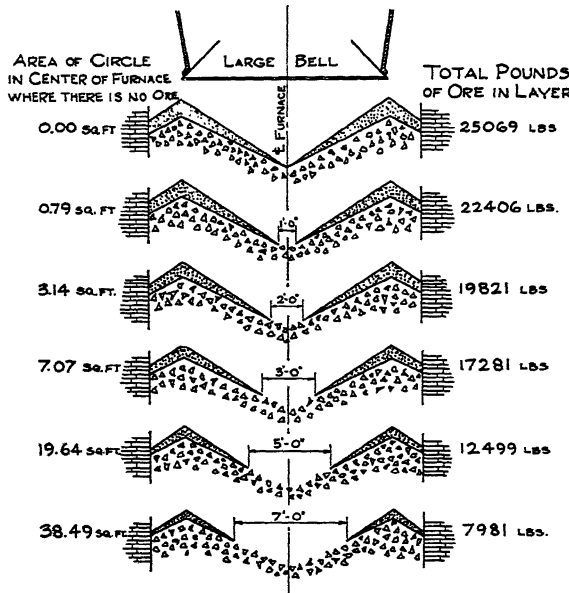
FIG. 4.—EXTENT OF ORE LAYERS IN FURNACE WITH PEAK UNDER EDGE OF BELL.

25,069 to 22,406 lb., the ore will not quite reach the center, and there will be a circle 1 ft. in diameter at the center consisting of only the maximum-sized pieces of coke. At first glance this circle looks large and an astonishing loss through this zone can be imagined, but a circle 1 ft. in diameter has an area of only 0.79 sq. ft., which is only 0.35 per cent of the total area of the stock line.

A further increase in flow up the center can be effected by decreasing the ore layer to 17,281 lb., so that the center circle, consisting only of large pieces of coke, will be 3 ft. in diameter and have an area of 7.07 sq. ft. This area will be only 3.1 per cent of the total stock-line area. Changing to an ore layer of only 7981 lb. produces

furnaces in the United States with bell and stock-line dimensions as shown or larger operate on such a small ore layer.

Discussions of gas flow are frequently meaningless because the sizes of ore layers and charges are not clearly defined. For instance, one furnace with a coke unit of 11,000 lb. may be charged: ore, stone, coke; dump; ore, coke, coke; dump. If the two skiploads of ore are of the same size, actually the size of the ore layer is better represented by a coke unit of 5500 lb. In another case, a coke unit of 11,000 lb. may mean a filling of ore, stone, coke, ore, coke, coke, followed by dumping of the bell. Such a charge approximates the first filling in that there are two independent layers of ore, but their different location results in

less gas flow up the walls. Actually this may be termed a large unit, as all the material is lowered at once, but it approximates a small unit because the individual layers of ore are small.

is, a decrease in the proportion going up through the center means a larger proportion going up through the rest of the stock line, or vice versa. This variation is the most important one in filling.
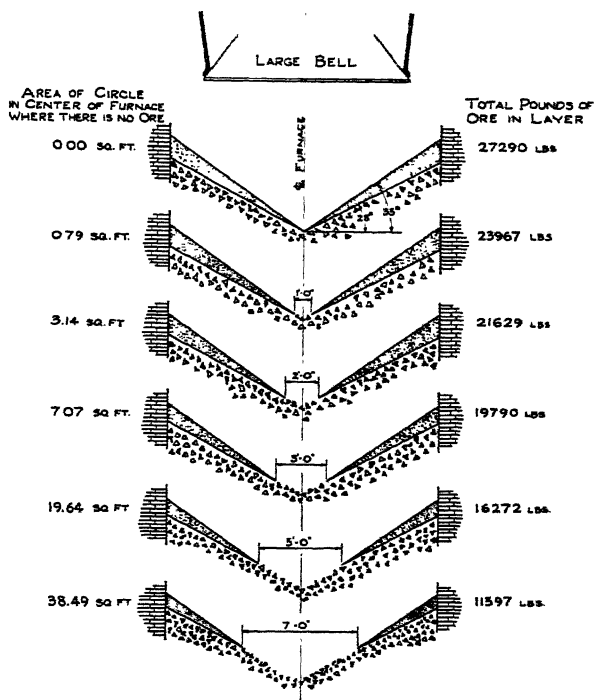
FIG. 5.—EXTENT OF ORE LAYERS IN FURNACE WITH PEAK AGAINST WALL.

It can be argued that since the material does not leave the bell at zero velocity the contour of the ore will not be as shown here, but as diagramed by Furnas and Joseph. In Fig. 5 are shown the same data with the peak of the ore adjacent to the wall. It is evident that the same general conclusions can be drawn from either assumption.

This presentation has attempted to establish one point; namely, that the amount of gas flow up through the center of a furnace can be regulated by varying the size of the ore charge. By controlling the proportion of gases going up through the center, the proportion going up through the rest of the stock line is also controlled; that

However, the limitations must be clearly understood. The chief limitation is that it does not correct gas flow to compensate for lack of uniformity in size of material charged, a correction that must be made by sizing. The important application is that with this system of charging, and under a given set of conditions, there is an optimum size of ore layer that will result in the right amount of gas flow through the center and a certain proportionate amount through every annular ring out to the wall.

Many other factors, of course, influence the radial distribution, such as inwall batter, height of stock line and wind blown. It is also affected by other variations, such

as the sequence of the ore in the charge, but the limits of this paper do not permit discussion of them.

ADAPTING FURNACE OPERATION TO COKE AVAILABLE BY CHANGE IN FILLING

In the previous section it was shown that a change in coke had opposite results on two furnaces and that a change in filling caused a decided improvement in the operation of one furnace. The importance of size of ore layer was next discussed. The following section is to discuss the filling that resulted in decrease in efficiency on one furnace and increase on the second, and the change in filling that corrected the operation of the inefficient furnace.

No. 2 furnace had a 19-ft. hearth, with a 17-ft. stock line and 13-ft. bell, while No. 4 furnace was 20 ft. in the hearth with a 17-ft. 6-in. stock line and 13-ft. bell. The routine of filling was the same on the two furnaces, but the coke units were of different sizes.

TABLE 1.—*Filling Order, Typical Charge*

NO. 2 FURNACE	NO. 4 FURNACE
Coke unit, 10,400 lb. and 17,000 lb., respectively	
One skip ore	One skip ore
One skip stone	One skip stone
One skip coke	One skip coke
Dump big bell	Dump big bell
One skip ore	One skip ore
One skip coke	One skip coke
One skip coke	One skip coke
Dump big bell	Dump big bell

Since there were two ore layers per charge, and the coke unit on No. 4 furnace was 63 per cent larger than on No. 2 furnace, the individual ore layers on No. 4 furnace were approximately 63 per cent larger; that is, each ore layer on No. 2 furnace was about 12,000 lb. and on No. 4 furnace it was 20,000 lb. Since the bell and stock-line diameters were very near the same size, there was a much larger open center on No. 2 furnace than on No. 4, and as the wind was reduced a larger proportion of the gas could escape up through the center on No. 2 furnace. This increased percentage of

gas flow up through the center caused poorer gas-solid contact, and eventually a cold furnace. Decreasing the burden to correct the cold furnace only aggravated the evil of the open center.

On July 28 operation on No. 2 furnace improved after the filling was changed by doubling the ore layer every sixth charge. This large ore layer every sixth charge was effected by changing the sequence of that charge to the following:

> One skip ore
> One skip ore
> One skip stone
> > Dump big bell
> One skip coke
> One skip coke
> One skip coke
> > Dump big bell

The larger layer of ore every sixth charge extended farther toward the center of the furnace, increased the resistance to flow of gas in that zone, and forced more gas up the intermediate and outside zones. The result was better gas-solid contact, and the furnace so improved in efficiency that soon it was back on a normal burden.

The change in filling improved the radial distribution of the gases by decreasing the amount of gas flow up through the center zones. But this improvement did not necessarily achieve the ideal radial distribution. Possibly the furnace would have made greater progress with still less gas flow through the center, as would have happened if every third charge instead of every sixth had been the large one.

Rate of Gas Flow and Radial Distribution

The rate of gas flow in every annular ring is determined by the voids in this ring and the character of material present. If there are no changes in materials or method of filling, the voids should be the same and the gas flow in each annular ring the same. In No. 2 furnace, the materials were not the

same, as the coke was changing because of the longer coking time. However, there were two other changes that are likely to cause more gas flow through the center on less wind.

The first change was the decrease in velocity of gases and its influence on the "lifting" of the fine particles. Furnas[3] has pointed out the decided decrease in pressure drop that occurs when particles are lifted from the bed and held in suspension by the gas stream. This occurs primarily in the annular rings under the edge of the bell, not in the center, where there is no fine material. When the wind is reduced, the gas velocity decreases, especially in the annular ring under the edge of the bell, and so some material that was being lifted is dropped back into the bed and offers resistance to flow. But no such change has occurred in the center. The greater resistance in the outer annular rings, where there is fine ore, results in a decrease in gas flow there, but in the center zone, where there has been no increase, there will be more flow.

A second change was in the degree of packing of material as it dropped off the bell. On full wind, the high upward velocity resists the falling material, but when the wind velocity is lessened the materials hit the stock line with more force and greater packing results. The material in the center of the furnace rolls rather than falls into place, so the gas velocity has little influence there. With more packing in the annular rings under the edge of the bell, there is an increase in resistance and less gas flow. Since there is no change up through the center of the furnace, there is an increase in flow in that zone.

INFLUENCE OF CHANGE OF SIZE OF COKE ON FURNACE OPERATION, CASE I

The preceding illustration shows that the size of ore layer can have a decided influence on the radial distribution of the gas. It must be recognized that a change in

size of coke can have a similar effect on the radial distribution of the gas, and so on furnace efficiency.

If a certain coke is being charged into a furnace, there is segregation of coarse and fines as it drops onto the stock column, and this, together with all other factors that affect radial gas distribution, causes a certain gas flow in every annular ring. If the size of this coke is changed—for instance, by change in coal mix—probably there will be some change in the voids in all the annular rings in the stock column, either for better or worse. Following is an illustration of such a change in the size of coke and the effect on furnace operation.

On two occasions it had been noted that when the size of coke increased above a certain amount a furnace operating at less than normal wind dropped off in efficiency. The larger coke was found to occur during a period of increasing coking time on both occasions. Still, it was impossible to say that the large coke was the cause of the difficulty because the wind on the furnace was also changing, so a test run was made during which the size of the coke was increased while the wind was held constant.

Constant Factors

The period of controlled operation ran from Nov. 18 to about Dec. 20, and all factors that influenced furnace operation and were within control were held constant. It was necessary to make a minor adjustment of manganese ore on the twentieth, to reduce the manganese in the iron, but that was the only ore change made during the entire period. Every charge of ore that went into the furnace for over one month had identical amounts of the individual ores. One ore was the change ore, and it was varied as the furnace needed more or less burden. The method of charging was the same during the entire period, even the order of pulling the various ores into the scale car. So also was the filling mark, amount of water on the ore, grade of iron,

size of tuyeres and wind blown. The furnace operated well during the entire period; no off iron, hanging or slipping occurred to introduce a variable.

The daily screen test of the coke is shown in Fig. 6, including a figure that

average diameter of each screen size by percentage of that size (Table 2).

The correct average diameter of the coke through 1¼ in. is not known and we arbitrarily assume the figure of 0.56 in. Another figure might be more correct, but
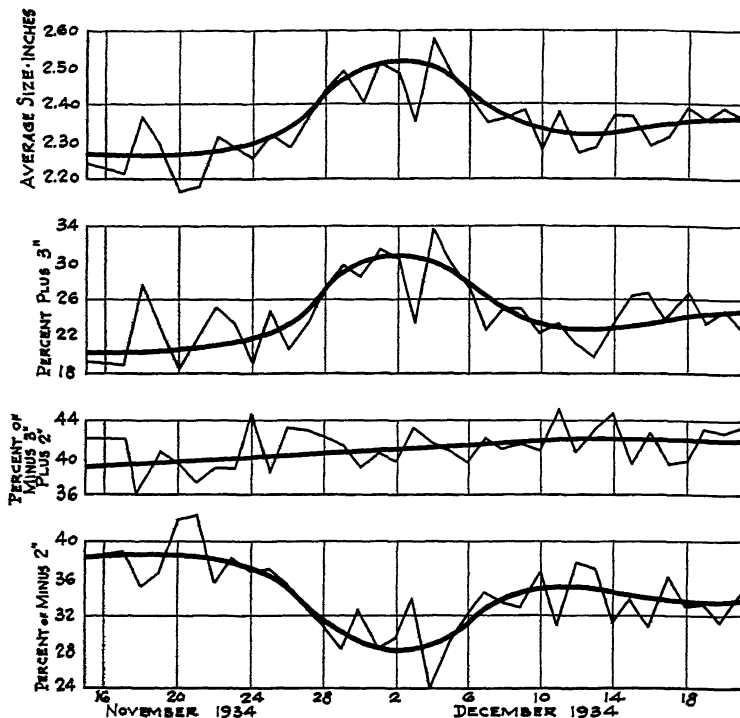
FIG. 6.—SCREEN TEST OF COKE.

represents the average size. This was determined by multiplying the assumed

TABLE 2.—*Average Size of Coke, No. 4 Furnace*

8:30 a.m. to 2:30 p.m., Dec. 4, 1934

Screen Size	Percentage	Average Diameter, In.	Size Factor
Inch			
On 4............	3.06	4.5	13.77
3............	30.94	3.5	108.29
2............	41.90	2.5	104.75
1¼............	16.60	1.63	27.06
Through 1¼.....	7.50	0.56	4.20
			258.07

Average diameter of pieces, or average size = 2.58 inches.

this makes no difference because we are interested in relative values only.

All of the ore used was from the stock pile and varied little in chemical and physical characteristics. During the test, more iron was required and 1000 cu. ft. of wind was added on Dec. 3. Fig. 7 shows the total pounds of burden charged and the average coke size. From Nov. 18 to Nov. 30, the total burden was constant and all charges of ore that went into the furnace during the 12-day period were identical. It was necessary to reduce the burden on the thirtieth because the furnace was getting cold. Some of this was restored later

and further reductions were made on the first and second. The burden cuts were not excessive, the silicon averages for the two days were 0.91 and 0.99, respectively; that is, about 10 points lower than the average. The burden was gradually restored after Dec. 3. By Dec. 7 it was normal and by

normal. The furnace was shut down for change of tuyere sizes on Dec. 17, after which the wind was increased.

Data on Furnaces

There was a drop in tonnage from 520 tons to 485 tons per day, or a decrease of
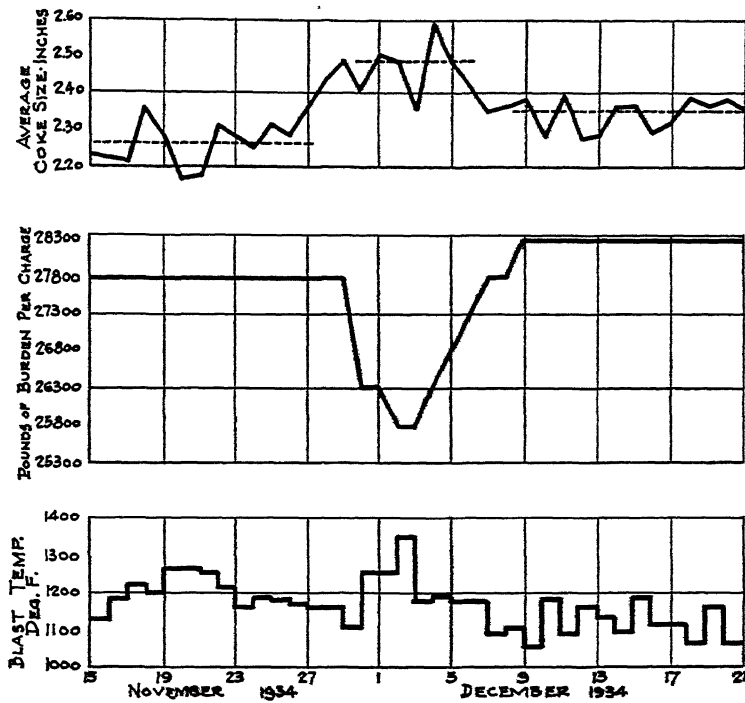
FIG. 7.—COKE SIZE AND FURNACE DATA.

Dec. 9 it was 500 lb. more than normal, and so it remained for the rest of the period.

The average size was about 2.25 in. during the first of the period and on Dec. 27 or 28 it started to increase. Apparently the first increase in size was beneficial, as the blast temperature for Dec. 28 was below normal. However, the larger size seemed detrimental, because immediately afterward the blast temperature was increased above normal and the burden decreased. After the coke had reached the maximum size and started to decrease, the burden was gradually restored, and when the size was again normal the burden was

6.7 per cent (Table 3). At the same time there was an increase in coke consumption

TABLE 3.—Results on No. 3 Furnace

Period of Time	Tonnage	Coke per Ton Iron, Lb.
Nov. 15–29, incl........	520	1,590
Nov. 30–Dec. 8........	503	1,661
Dec. 2–Dec. 7........	485	1,707
Dec. 9–Dec. 17........	520	1,572

from 1590 to 1707, or 6.1 per cent. The maximum reduction in burden was from 27,800 to 26,000 lb., or 6.2 per cent. Since the wind was constant and the decrease in

tonnage was proportional to the increase in coke consumption, the weight of coke per skip was certainly close to the same amount.

The test run can be divided into three small periods; from Nov. 15 to Nov. 27, inclusive; from Dec. 1 to Dec. 5, inclusive; from Dec. 9 to Dec. 21, inclusive. The middle period had the largest coke; the days during the transition have been

2.48 in. during the middle period was too large. It is surprising that such slight differences in screen tests could have such a noticeable effect on furnace efficiency. The narrowness of the range indicates the need for accurate control in the manufacture of coke.

Two points should be stressed concerning this test: (1) It is not claimed that any of the three sizes had an absolute value greater

TABLE 4.—*Average Data*

Period of Time	Average Wt. of Sample	Blast Temperature, Deg. F.	Top Temperature, Deg. F.	Average Burden, Lb.	Coke Ash, Per Cent	Iron Analysis, Per Cent		Screen Test of Coke, Per Cent			Coke Size, In.
								Plus 3-in.	Plus 2-in.	Minus 2-in.	
Nov. 15–27.........	1,139	1201	242	27,800 −5.8 %	5.04	1.08	0.026	22	41	27	2.27
Dec. 1–5..........	1,208	1227	278	26,200 +8 %	6.04	1.05	0.029	30	41	29	2.48
Dec. 9–21.........	1,184	1120	252	28,300	6.54	1.14	0.027	24	42	24	2.35

omitted. Table 4 shows average data for the three periods.

Discussion of Data

The average analysis of the iron during the three periods was approximately the same, so the temperature of the furnace during the periods must have been comparable. When the coke size was 2.27 in. during the first period, it took an average of 1201°F. blast to maintain 27,800 lb. of burden with a coke ash of 5.04 per cent. During the second period 1227° blast was required to maintain 26,200 lb. of burden; that is, 5.8 per cent less. However, the coke ash had increased 1 per cent, so it is fair to assume that 1 per cent of the 5.8 per cent loss was due to higher ash. During the last period only 1120° blast was required to maintain 28,300 lb. of burden, an increase of 8 per cent, when the coke size was 2.35 in., although the coke ash had increased to 6.54 per cent.

These data indicate that the last size (2.35 in.) was the best. The first size (2.27 in.) was too small and the size of

than the other, or that the coke in any one period was better than another; it is conceivable that the furnace could be adapted through proper change in filling so that the efficiency would be the same for each of the three sizes; (2) the increase in size of coke resulted from several changes, including the substitution of one high-volatile coal for another and an increase of 5 per cent in the low-volatile coal used. The increase in size was not the result of a change in the processing—that is, an increase or decrease in coking temperature —but of a change in the coals used. The processing may have been ideal in both cases. It is interesting that the greatest efficiency occurred with the highest percentage of ash.

INFLUENCE OF CHANGE IN TEMPERATURE OF OVENS ON SIZE OF COKE AND EFFECT ON NOS. 3 AND 4 BLAST FURNACES ON FULL WIND

The illustrations given have pointed out that a change in the size of coke can affect the radial distribution and so furnace effi-

ciency, and also that the proper radial distribution must be worked out for each coke; that is, the furnace must be adapted to the coke. The next experience serves to

Manufacture of Coke

In Fig. 8 are plotted the coking time, temperature of flues and sliding brick, amount of heat per pound of coal carbon-
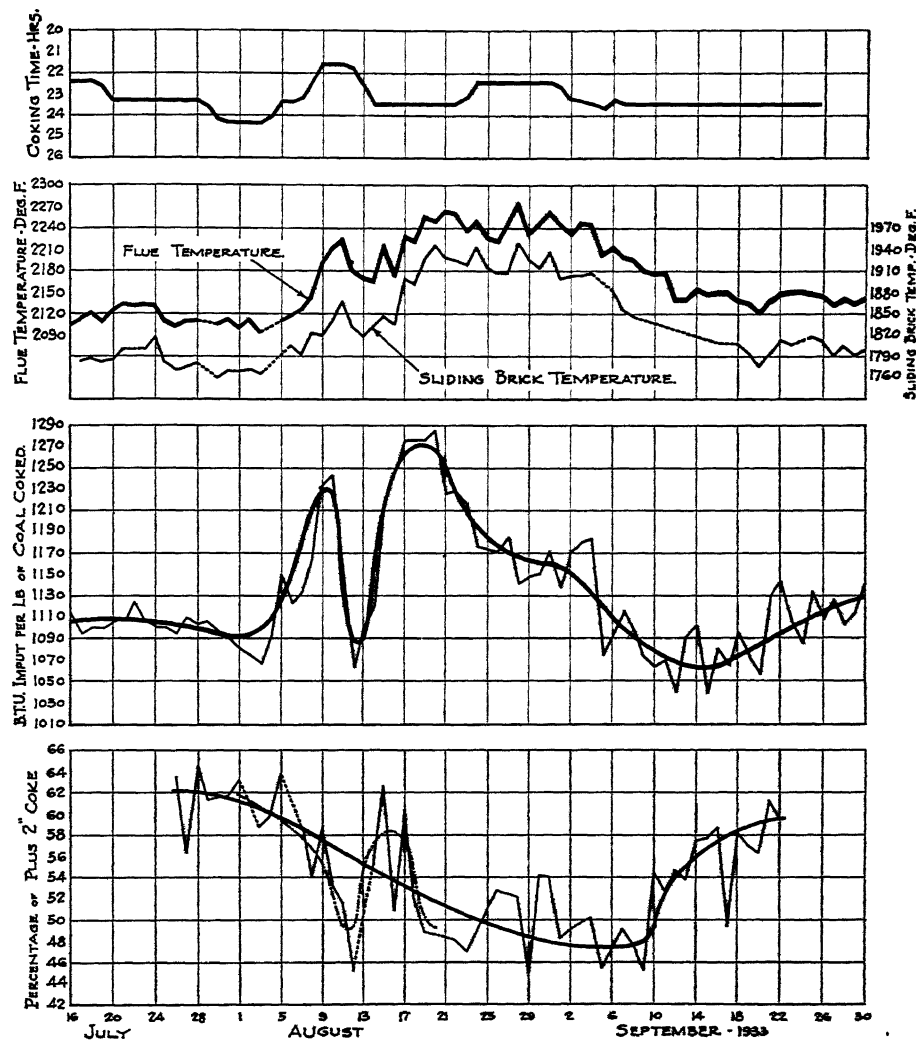
FIG. 8.—EFFECT OF OVEN OPERATION ON SIZE OF COKE.

confirm these two points and to bring in several new ones, which are: (1) Coke is a product with a maximum value; (2) oven operation influences the type of coke produced; (3) change in size of coke has different effect on different furnaces.

ized and the screen tests of coke going into the skips of the blast furnaces. On Aug. 3 a test run was started at the ovens and the temperature was gradually increased, while the coking time was increased to a maximum on Aug. 11. Then both were decreased

again to Aug. 15, which caused a decrease in the percentage of plus 2-in. coke from 62 to a minimum of 46. With the decrease in temperature, there was again an increase in size of coke on Aug. 15, then a gradual decrease, as oven temperatures were increased, until Sept. 9. The curve showing the British thermal units per pound of coal shows the decided increase in heat applied during the first part of August, a decided decrease about Aug. 12 to 14, and a subsequent increase.

The correlation between temperature of the ovens, the heat per pound of coal carbonized, and the screen test of coke is close. It might have been expected that there would be a decrease in flue temperature after Aug. 20 when the heat input had attained the maximum and was decreasing. It must be recalled that to bring a battery of ovens to a higher temperature than normal requires a large input of heat, but once that temperature has been attained only a small amount of heat input above normal is required to maintain the higher temperature. Actually, the heat input was much above normal until Sept. 4, when it was rapidly reduced to normal. This change in heat input is reflected both in the temperatures of the flues and in the size of coke. The lag between heat input in the oven and change in coke size is apparent from Sept. 9 to Sept. 30. There was a gradual increase in coke size with a constant heat input, showing the effect of the gradual loss of temperature of the block of ovens. None of the three measures is extremely accurate, so we cannot say definitely at what stage the coke attained the maximum temperature.

On Sept. 4 and 5 the test was discontinued at the ovens because of difficulty in pushing the coke; that is, because of "stickers." The temperatures were not the maximum but the coking time had been increased slightly, which makes hotter coke. There was no difficulty in pushing previous to Sept. 4, and this fact, coupled with the consistently smaller size of coke during the period from Sept. 4 to 9 indicates that at that time the coke had attained its highest temperature. It can be said that starting with the last of July there was a gradual increase up to Sept. 4 in temperature of the coke pushed, and with this gradual increase in temperature there must have been gradual change in the properties that are affected by increase in temperature.

Influence on Blast-furnace Operation

The tons of iron produced per day are plotted in Fig. 9, together with the screen test of the coke. With the first increase in flue temperatures there was a decided improvement in production on No. 4 furnace, although the wind was constant. Apparently the coke made at somewhat higher temperatures was more desirable for this particular furnace. However, further increase in temperature was accompanied by a gradual decrease in tonnage. With increasing temperature at the ovens there was a gradual improvement in tonnage on No. 3 furnace and maximum efficiency was reached 20 days later than on No. 4. But with further increases in oven temperature came a decided loss in efficiency on both furnaces. Here is an example showing that there is an optimum temperature of coking. Underheating the coke is detrimental, overheating the coke is detrimental, and somewhere in between there is an optimum for a particular furnace. The optimum temperature of coke for one furnace may not coincide with that for another furnace, as this case shows. The operation of either of the furnaces might have been adjusted somewhat so that the point of optimum size for two furnaces would coincide more nearly. A given oven or group of ovens can produce only one coke. If the coke produced is kept constant, there is an opportunity to adjust furnace operating conditions to obtain maximum efficiency. It should be noted that when the

coke was much overheated, both furnaces suffered badly. The coke was deficient in some qualities and no amount of furnace changes would adapt the furnaces to that coke.

may have been due entirely to poor judgment on the part of the furnace foreman, who let the blast temperature get too high, so that the furnace had a spell of hanging and slipping. At the time of writing, the
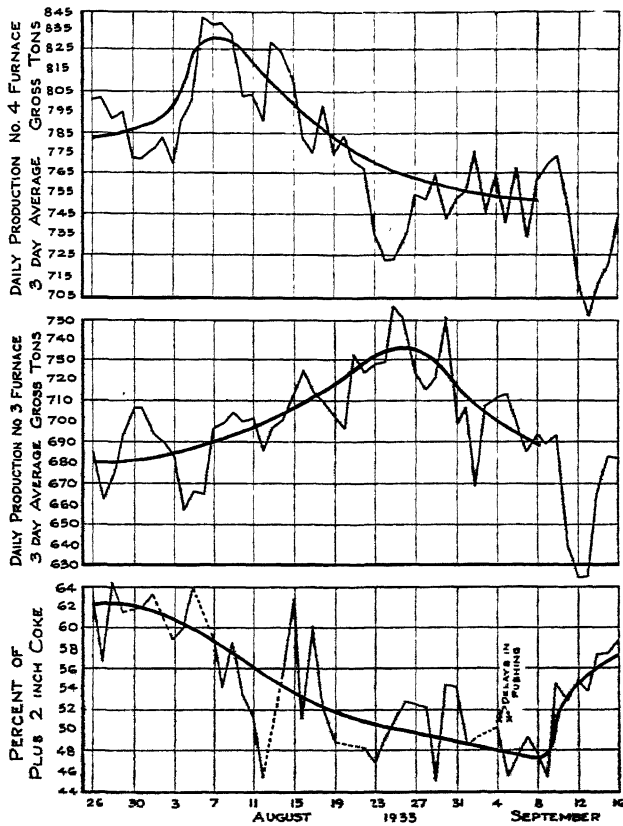
FIG. 9.—EFFECT OF CHANGE IN COKE SIZE ON FURNACE OPERATION

The decided drop in tonnage on Aug. 24 and 25 does not fit into the curve. The furnace worked irregularly for several days, then became too hot, and the average blast temperature for those days was 150° lower than the average from July 26 to Aug. 19. It is believed that the drop in tonnage was due to this irregularity, while it may have been influenced somewhat by the change in coke.

We have asserted repeatedly that coke is only one of many variables in furnace operation. This particular drop in tonnage

detailed data of this period are not available, so the cause cannot be definitely established. The decided drop in tonnage from Sept. 12 to 14, on both furnaces, probably was the result of the abnormal coke on Sept. 9, which followed from the difficulty in pushing on Sept. 4 and 5.

Other Changes in Furnace Operation

No changes whatsoever were made in the materials used on No. 4 furnace from July 26 until Aug. 26, and the changes made at that time merely consisted of

exchanging similar ores. The filling was the same, tuyeres the same and the wind was maintained at the standard of 54,000 cu. ft. Maintenance of this wind became difficult, so it was gradually reduced to 52,000

be presented to explain every case where a change in coke reacted in one way on one furnace and in another way on another furnace, but this cannot be done. If one merely wishes to measure the quantity of

Nº 3 FURNACE.

Nº 4 FURNACE.
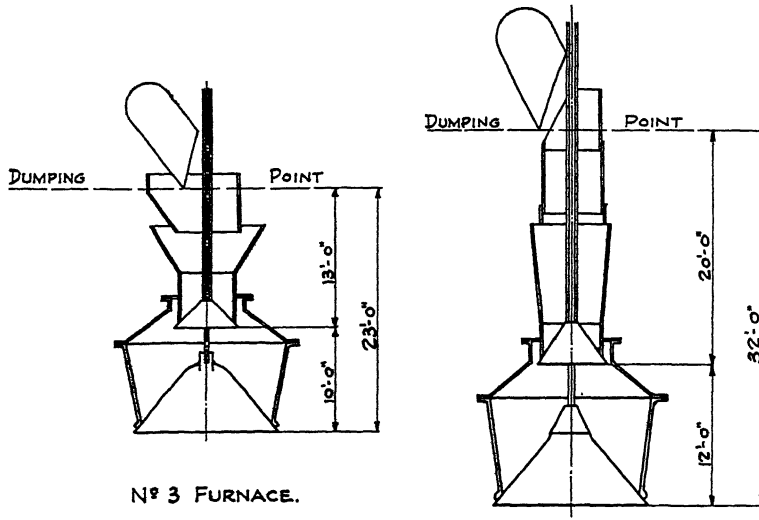
FIG. 10.—COMPARISON OF FURNACE TOPS.

and 53,000, but when the coke size again became normal the wind was returned to 54,000. There were some slight changes in the burden on No. 3 furnace but similar changes have been made many times without any effect. The wind was constant from Aug. 8 to the end of the period, as were also the tuyeres, filling, and other factors over which the operator has control.

Why the Same Coke Reacts Differently on Different Furnaces

It is easy to accept the statement that coke varies in quality, some good and some bad, and the tendency is to assume that it should be good or bad on all furnaces. The illustration just presented, however, is typical of what really happens; that is, changes in coke do not react in the same way on all furnaces. Many other experiences confirm this conclusion. It would be more comfortable if logical reasons could

gas flowing through a pipe with a Pitot tube, it is necessary to have at least 10 diameters of straight pipe to get a reasonably accurate reading, and one does not even attempt to do it near a bend. If it is so difficult to forecast the flow of gas under such simple conditions of constant flow, temperature, and pressure, and physical character of the pipe, it would be the height of optimism to expect to forecast the flow in the furnace that is filled with broken solids, under constantly changing temperatures, pressure, character of materials and physical condition of the furnace. Even identical furnaces do not react identically to the same coke, because their other conditions are not identical.

It is believed that in the case just described the furnaces reacted differently because of differences in design. Assume that two furnaces are using the same coke and the operation has been adjusted so

that each is operating efficiently. Now assume that the temperature of coking is increased, causing more cross fractures. Such coke will break up more readily when handled. If the coke is abused more when going into one furnace than when going into another, the coke will be broken up more and the operation will suffer accordingly. Fig. 10 gives the general arrangement of the top in the two cases, showing that the coke dropped a total of 23 ft. on No. 3 furnace and 32 ft. on No. 4 furnace. As would be expected, it was No. 4 furnace that first lost in production, owing to excessive oven temperatures. When the coke became so hot that there were too many cross fractures, both furnaces lost in efficiency.

Furnaces vary in height, and opinions differ as to the merits of increased height, but certainly the higher a furnace, the more abuse a coke will receive in going from the stock line to the tuyeres. The added height is an advantage provided the coke can stand it, but if the coke is weak the benefit derived from the added height will be lost in the detrimental effect on the coke.

If two furnaces of different heights, say 85 and 95 ft. respectively, are operating on the same coke, the higher furnace, other things being equal, will have lower coke consumption. But a detrimental change in coke will have less effect on the shorter furnace than on the taller one. On the other hand, an improvement in the quality of the coke will affect the shorter furnace less than the taller one.

Maximum Value

This example brings out clearly the fact that coke is a product that has an optimum, or maximum value, and this is one of the reasons that correlations between physical tests of coke and results in a blast furnace are difficult to establish. That a material may have an optimum or maximum value is not unusual. A familiar case is the

crushing strength of certain insulating bricks. As temperatures increase from room temperature, there is a gradual increase in strength up to a certain temperature, after which there is a decrease.
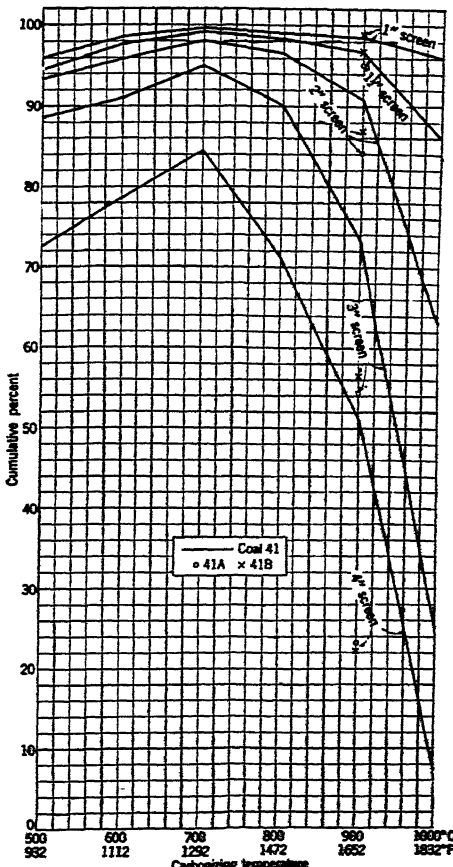
FIG. 11.—SCREEN ANALYSIS OF COKE FROM BECKLEY COAL AND BLENDS WITH PITTSBURGH BED (WARDEN MINE).
(From *Bull.* 411,[4] p. 51.)

If an oven of coal is heated just enough to cement the coal particles together, the resultant coke is very poor. However, with each increment of increase in temperature up to a certain point, there is improvement in quality. Going to the other extreme, coke that is overheated is small, contains many cross fractures and so is undesirable, but with each increment of decrease in tem-

perature there will be improvement. Somewhere these two lines will meet, and this will be the point of optimum value.

That coke is a product with an optimum
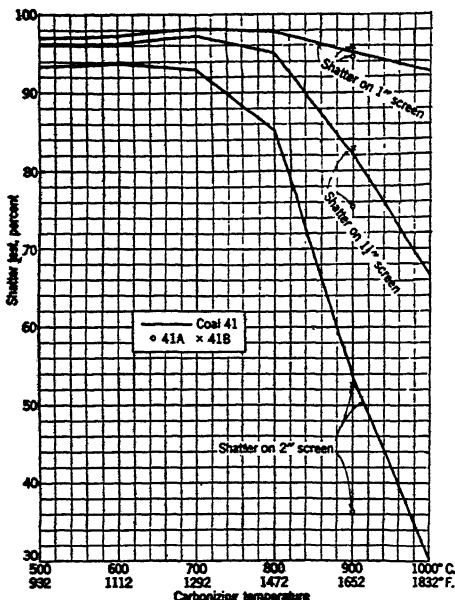
FIG. 12.—SHATTER TESTS OF COKE FROM BECKLEY COAL AND BLENDS WITH PITTSBURGH BED (WARDEN MINE).
(From *Bull.* 411,[4] p. 52.)

or maximum value is well illustrated by tests made by the Bureau of Mines on coals in an experimental oven.[4] Three figures from *Bulletin* 411 (the paper cited) are reproduced (Figs. 11, 12, 13). Fig. 11, giving the screen analysis of the coke, shows an increase in the size of coke produced up to 1292°F. and then a decrease to a minimum at 1832°F. Fig. 12 shows the shatter tests of the same coke on 2-in., 1½-in. and 1-in. screens. In all three cases there is an improvement in the ability of the coke to resist breakage starting at 932°F. The maximum value on the 2-in. shatter was at 1112°F., for the 1½-in. shatter at 1292°F. and the 1-in. somewhere between 1292° and 1472°F. Fig. 13 shows the results of the tumbler tests as measured by percentage of coke

on the 1½-in., 1-in. and ¼-in. screen. There is a definite increase in the percentage on the 1½-in. screen with increasing temperature up to 1292°, then a
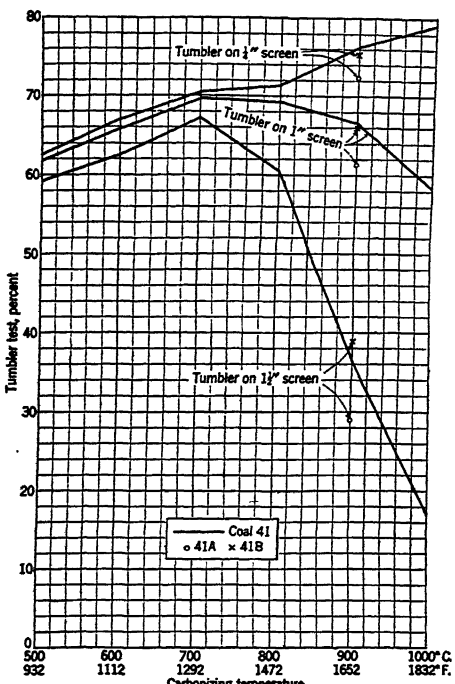
FIG. 13.—TUMBLER TESTS OF COKE FROM BECKLEY COAL AND BLENDS WITH PITTSBURGH BED (WARDEN MINE).
(From *Bull.* 411,[4] p. 53.)

decrease. The maximum value as measured on the 1-in. appears to lie between 1292° and 1472°F., but as measured by the ¼-in. the maximum value is at 1832°F.

It is apparent that the maximum value as measured by each of these three tests is different, but lies between 1112° and 1832°F. The maximum value of the coke for any particular test varies also with the sizes considered. We have no measure whereby we can combine all of these tests into one individual result to plot against furnace operation. An examination of the three curves would indicate that the zone from 1275° to 1450° would include most of the peaks and would represent the best

coke. These temperatures represent approximately average commercial practice.

A point that leads to confusion in field tests but is apparent in such laboratory tests is that results may lie on either side of a maximum value. Referring to the results of the tumbler test on a 1-in. screen, it will be noted that at 1220°F. the percentage on a 1-in. screen after the test was 68 per cent while at 1544°F. it was also 68 per cent. When the coking temperature is known, and we see that the points obviously lie on either side of a maximum value, this is easy to understand. However, in the field, a similar test may give 68 per cent one time and 68 per cent another and we may conclude that the coke was the same, while actually it might be very different because the coke was made at different temperatures.

It should be noted that each square represents 36°F. and examination of the chart reveals what a small increment of change in each of the properties will cause that change in temperature. However, data will be presented to show that a difference of about this amount in average flue temperatures will make a significant difference on furnace operation. Consequently, it is very difficult to measure such small increments of change accurately enough to reflect changes in the coke.

OPTIMUM VALUE OF COKE DETERMINED FROM FLUE TEMPERATURES AND FURNACE DATA

Effect of Change in Oven Temperature on Efficiency of No. 2 and No. 4 Furnaces during Summer of 1932

In the preceding section it was shown that coke had an optimum value and the point of optimum value was not the same for two different furnaces. Another illustration of this same point will be presented to substantiate this conclusion and to demonstrate several other facts:

1. Direct correlation of coke-oven and furnace data.

2. Effect of small variations in flue temperatures on the coke and blast-furnace operation.

3. The confusion presented by optimum value in a study of coke-consumption data for several furnaces.

The disadvantage of using the blast furnace as a testing medium was pointed out earlier in the paper and was illustrated by examples in which the practices on Nos. 2 and 4 furnaces were compared during a period when there was a change, both in the operation of the furnaces and in the manufacture of coke. It was shown that the change in coke reacted favorably on No. 4 furnace and unfavorably on No. 2 furnace. It was shown that by changing the filling of No. 2 furnace, putting in a double ore layer every sixth charge, and so decreasing the gas flow through the center, we adapted the furnace operation to the coke.

While there was decided improvement, it is probable that by still further decreasing gas flow through the center—that is, putting more ore to the center—the furnace might have been adapted still better to the coke available. Actually, this was done later when the big ore layer was used every third instead of every sixth charge, but even with this additional change we cannot say that the operation of No. 2 furnace had been adjusted to the same efficiency as No. 4 furnace.

Subsequent experience proved that it was not, and the following case not only substantiates this point but also brings out the opposite effect of change in coke manufacture on two blast furnaces. No. 2 and No. 4 furnaces were operated continually at reduced wind from July 1931 until March 1933. The period to be discussed extends from May 1, 1932 to Dec. 15, 1932. The wind was practically constant throughout the period. From July through November it was necessary to

fan No. 2 furnace for a short period every day, but this operation did not influence the factors to be discussed. All other factors that influence furnace operation, over

The curve for No. 4 furnace shows a low burden for coke made at less than 1950°F. and increasing amounts of burden with increasing oven temperatures up to about
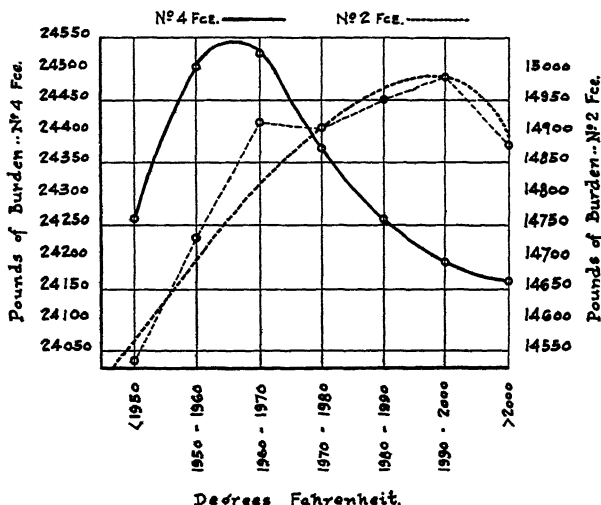
FIG. 14.—POINTS OF OPTIMUM FLUE TEMPERATURE FOR NO. 2 AND NO. 4 FURNACES DURING PERIOD OF MAY 1 THROUGH DEC. 15, 1932.

which the operator has control, such as method of filling or size of tuyeres, were constant throughout the period.

As little flue dust is produced on slow wind, a substitute method of measuring furnace performance used during this period was to compare the pounds of iron per charge. The average temperature of the flues at the coke ovens was divided into ranges of 10°, the first range being all temperatures less than 1950°F., the next range from 1950° to 1960°, and so forth at 10° intervals, up to the last column, which included all temperatures of over 2000°. After the seven columns of flue temperatures had been established, the burden on the furnace for a particular day was noted, together with the flue temperature, and this burden was inserted in its proper column. This was done for every day from May 1 to Dec. 15 on each furnace. Results of these data are presented graphically in Fig. 14.

1960° to 1970°, but further increases in temperature caused a decided drop of burden. This curve clearly illustrates that for this furnace, operating under these conditions, the coke had a maximum value when produced with flue temperatures about 1960° to 1970°. On the other hand, the burden on No. 2 furnace increased with increasing oven temperature up to a maximum, which occurred when the flue temperatures ran from 1990° to 2000°. Further increase in temperature caused a decrease in burden. Here again it can be said that for this particular furnace, operating under these conditions, the coke produced reached its maximum value at about 2000° flue temperature, and at ranges above or below this temperature the coke was of less value.

If the foregoing analysis is correct, a change in oven temperatures in certain ranges should have opposite effects on both furnaces. In Fig. 15 are plotted the average

flue temperatures of the ovens from Sept. 1 to Nov. 28, together with the burdens on No. 2 and No. 4 furnaces. The latter represent the pounds of burden on the furnace

lower flue temperature, and decreased with the increase in flue temperatures.

This substantiates the curves of optimum value previously established. During Sep-
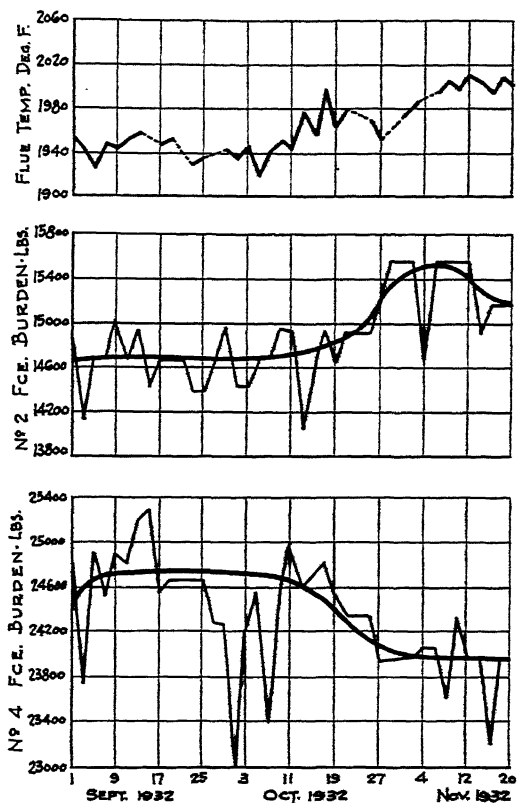
FIG. 15.—OPPOSITE EFFECT OF CHANGE IN FLUE TEMPERATURE ON No. 2 AND No. 4 FURNACES.

at midnight of each day. These were convenient to plot, but resulted in a very uneven line because burden reductions were sometimes made just before midnight and may already have been put back just after midnight.

The flue temperatures were fairly constant at about 1950° during September, increasing somewhat in October and decidedly during the middle of November. With the lower flue temperature the burden on No. 2 furnace was constant and with increasing flue temperature there was decided increase in burden. On No. 4 furnace the burden was constant with a

tember, the coke produced was close to the optimum value on No. 4 furnace. The coke was less suited to the furnace after the increase in flue temperature. The coke produced during September was far from the optimum value for No. 2 furnace, but the optimum value was approached as the temperature was increased. The average blast temperature for each day indicated that there was no change in this factor that could have influenced results.

Coke Consumption

These data can be presented in still another way to illustrate the confusing

fact that a coke has a different optimum value for each furnace operating under its given set of conditions. Coke consumption for the seven months on the two furnaces

"worse," the consumption would increase on both in the same ratio. This did not occur. As the coke consumption decreased on one furnace and increased on the other,
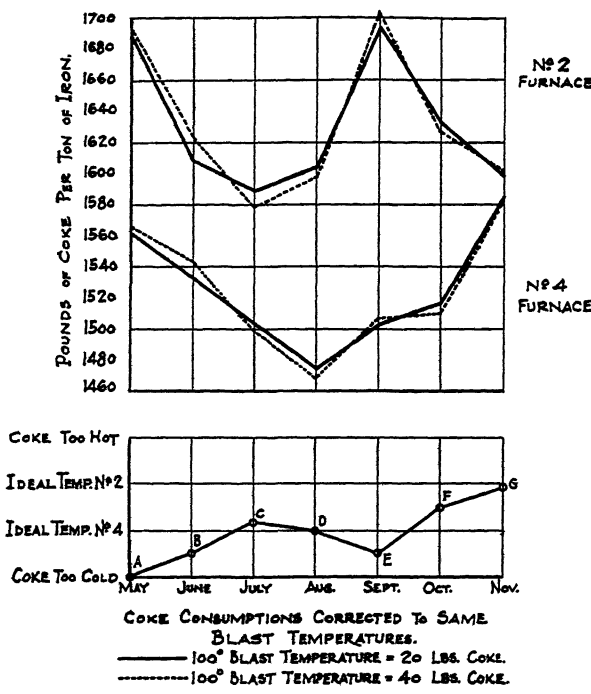
FIG. 16.—COKE CONSUMPTION.

is plotted in Fig. 16. There are two lines for each furnace, representing the coke consumed, and corrected to the same average blast temperature for the seven months for each furnace, one line representing a correction of 20 lb. of coke per 100° of blast temperature; the second representing 40 lb. of coke per 100° of blast temperature. The correct amount is not known but probably lies between the two, and in this case it is immaterial which is chosen as correct. One striking characteristic of this chart is that there seems to be no relationship between the coke consumption on the two furnaces. One would expect that if the coke had been a good deal "better" one month, the coke consumption would decrease on both furnaces the same amount, or if it had been

the coke must have been more desirable for the one furnace and less desirable for the other.

From the curves of optimum flue temperatures just studied, we know that the optimum temperature of coking for No. 2 is above that for No. 4 furnace. In the lower part of Fig. 16 are drawn four horizontal lines. The top line indicates coke made at too high a temperature, the next one coke made at the optimum temperature for No. 2 furnace; the next, coke made at the optimum temperature for No. 4 furnace, and the bottom line, coke made at too low a temperature for both furnaces.

Since the coke consumption was high on both furnaces during May, the coke was made either too hot or too cold. Since it is

relatively higher on No. 2 than on No. 4 furnace, we can assume that it was too cold, and this is represented by A on the chart. In June the coke consumption dropped on both furnaces, although considerably more on No. 2 than on No. 4. Evidently, the temperature of coking represented by B came closer to the ideal on both furnaces. The greater decrease in coke consumed on No. 2 than on No. 4 may be explained on the basis that small deviations from the ideal have relatively little effect up to a certain point, and beyond that point increase rapidly in effect. In July, the coke consumption dropped about the same amount on both furnaces, and so the temperature of coking must have increased, and in doing so approached the optimum temperature for No. 2 furnace, which in turn brought it relatively closer to the optimum for No. 4. This is represented by point C.

In August the coke consumption dropped on No. 4, so the temperature must have been closer to the óptimum for that furnace as represented by point D. In doing so, it moved farther away from the ideal temperature for No. 2 and should have caused an increase in coke consumption. This proved to be the case. In September the coke consumption increased on both furnaces, so the temperature of coking must have moved still farther away from the ideal of both, as represented by point E. In October the coke consumption dropped very decidedly on No. 2 and little or none on No. 4. Obviously the temperature of coking must have increased drastically, as represented by point F. In November the coke consumption decreased still further on No. 2 furnace, so the temperature of coking must have approached still closer the optimum for No. 2, as represented by G. In doing so, it moved still farther away from the optimum for No. 4, and should have caused an increase in coke consumption. The chart shows that this actually happened.

This reasoning was based on the hypothesis previously proved, and clearly demonstrates the confusion that is introduced into the study of the application of coke to blast furnaces by the fact that the coke has an optimum value, which may be different for different furnaces.

Establishing Relative Temperatures of Coke from Coke-plant Data

Conclusions based on logical analysis may seem purely theoretical, but in this case the processing data necessary to check them are available.

TABLE 5.—*Coke-plant Data, Summer of* 1932

1932	Average Flue Temperature, Deg. F.	Average Coking Time, Hr.	Average Coal Mixtures		
			Slack	Egg	Pocahontas
May....	1969	44:10	69	20	11
June....	1992	43:55	45	45	10
July....	1969	47:47	44.5	44.5	11
Aug....	1965	48:14	42.5	42.5	15
Sept....	1948	46:15	85	0	15
Oct....	1958	46:58	86.7	0	13.3
Nov....	1992	47:44	85[a] 42.5[b]	0[a] 42.5[b]	15[a] 15[b]

[a] Nov. 1 to 11.
[b] Nov. 11 to 30.

The temperature of an oven of coke is a function of the flue temperature and time of coking. Unfortunately, there is no yardstick whereby the two variables, coking time and flue temperature, can be combined into one coke temperature. However, they can be compared easily; that is, if there are two months on the same coking time, the conclusion can be reached that the month with the higher flue temperature will have the hotter coke; and if the average flue temperature is the same, the one with the longer coking time will have the hotter coke.

The significant data on the processing of coke during the period mentioned are listed in Table 5.

If the months of May and July are compared, it is evident that the temperatures were the same, 1969°F., but the coking times were 44:10 and 47:47 hr., respectively. Since other conditions were the same, it can be assumed that the coke was hotter during July than in May. Comparing other months in the same manner, the conclusions of Table 6 can be drawn.

TABLE 6.—*Conclusions from Table 5*

Comparison of	Temperature, Deg. F.	Time	Pocahontas, Per Cent	Conclusion
May........	1969	44:10	11	Coke in May was colder than in July
July........	1969	47:47	11	
May........	1969	44:10	11	Coke in May was colder than in June
June........	1992	43:55	10	
September..	1948	46:15	15	Coke in September was colder than in August
August.....	1965	48:14	15	
September..	1948	46:15	15	Coke in September was colder than in October
October.....	1958	46:58	13.3	
June........	1992	43:55	10	Coke in June was colder than in November
November..	1992	47:44	15	
November..	1992	47:44	15	Coke in November was hottest because the temperature was the highest and coking time about the longest
October....	1958	46:58	13.3	Coke in October was colder than in November
November..	1992	47:44	15.0	

Comparison of the relative coke temperatures in Fig. 16, obtained by comparing coke consumptions on the furnaces, with the relative temperatures obtained from the coke-plant data (Table 6), shows that they check exactly. It is probable, therefore, that the hypothesis is correct, and that under the conditions that obtained the changes in temperature and coking time are significant.

Operation of No. 4 Furnace when Flue Temperatures Were Abnormally High

The study described in the foregoing pages was based on a period when the coking temperatures and coking time varied within a narrow range and the effect of this variation was noted on two furnaces that were operating very efficiently. What happens when the temperatures of coking get out of this range; that is, abnormally high? Unfortunately, certain variables, particularly changes in coal, came into the picture during December, January and February, which made us hesitate to use the data for that period, and No. 2 furnace was blown out in March for relining. However, conditions on No. 4 furnace in March and succeeding months were comparable to conditions during the previous summer.

In Fig. 17 are plotted the pounds of iron per charge, top temperature, and coke consumption during the spring of 1933, showing wide variation in furnace efficiency. The lag between change in flue temperature and the effect on the furnace is considered in Fig. 18 by use of a plot of coke data a week ahead of that of the furnace data. The high flue temperature on March 1 correlates with the very low burden, high top heat, and high coke consumption. As the flue temperature decreased during March, there was a decrease in coke consumption and the minimum occurred when the oven temperature was also at the minimum. A gradual increase in flue temperatures again caused a decrease in burden and increase in coke consumption, and later a drop in flue temperatures resulted in a decrease in coke consumption. It should be noted that the minimum flue temperature of 2000° with about 48-hr. coke resulted in a maximum burden of 23,000 lb. of iron per charge. Previous analysis showed that the optimum temperature of 1965 occurred with a burden of about 24,550 lb. of iron

per charge and about the same coking time. It can be assumed, therefore, that further decreases in flue temperatures would have resulted in still higher efficiency.

SIZE OF COKE AS INDICATION OF QUALITY

The data just presented showing the effect of changes in flue temperature on furnace operation can be applied only to the
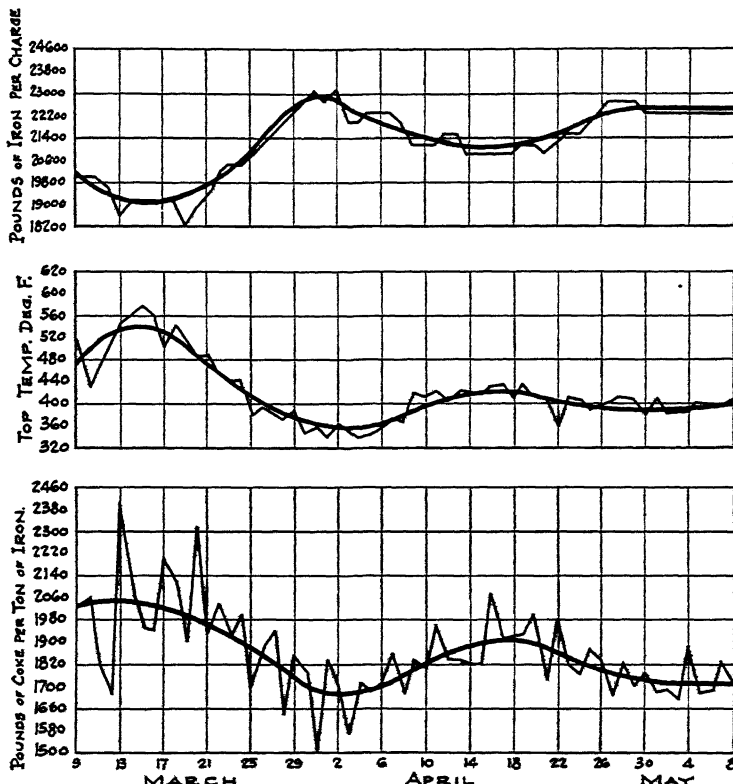
FIG. 17.—NO. 4 FURNACE PRACTICE DURING SPRING OF 1933.

The high flue temperature of 2100°, which obtained early in March, led to a burden of only 19,000 lb. of iron per charge, against a maximum of 23,000 lb. during the latter part of the month, an increase of 21 per cent. But it must not be concluded that this coke was 21 per cent better, as by changes the operation of the furnace may have been better adapted to the coke. What should be recognized is that variations in the manufacture of coke do alter the product, and consequently affect blast-furnace operation. There is only one answer—that is, control.

local situation. It shows merely relative value but does not measure or describe the product so that similar coke could be produced elsewhere.

The two previous examples, wherein screen tests were used to correlate coke with furnace operation, indicate that this might be a useful objective measure. After making daily screen tests of coke at the blast furnaces for the past 6 years, we have concluded that in our case the size of coke certainly indicates coke quality, but it does not measure it. Coke has many different properties that affect the results

in a blast furnace, and size is only one. It is obvious that two cokes may be of the same size but may have decidedly different properties in other respects, just as steel

in coking time. Above the screen test is plotted the average tonnage produced on the furnace for the two periods of large and small coke. There was no decided
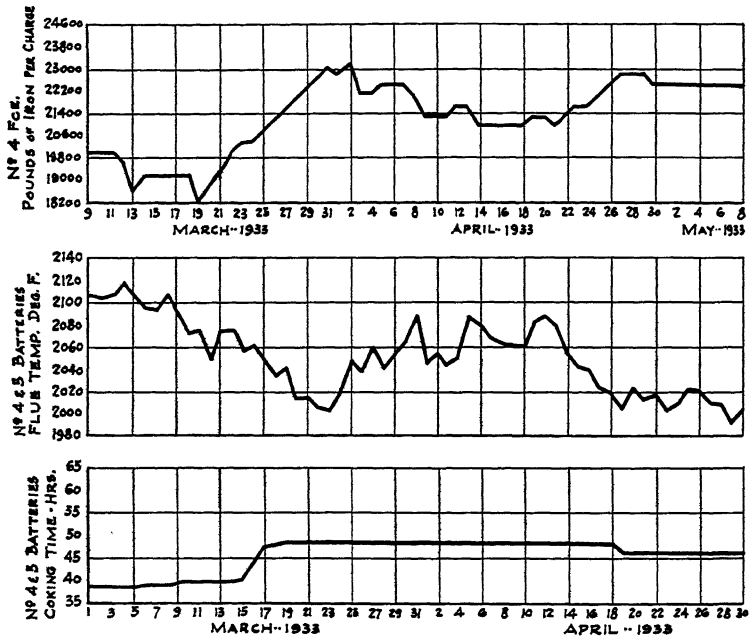
FIG. 18.—CORRELATION OF POUNDS OF IRON PER CHARGE WITH FLUE TEMPERATURES.

balls and eggs may have the same size but would react differently on a shatter test.

The following illustrations have been prepared to demonstrate both the usefulness and limitations of screen size as a measure of coke quality. We expect to show that two different cokes may have the same screen tests but entirely different effects on furnace operation, indicating the importance of some properties other than size.

Case 1

In Fig. 19 are plotted the tonnage on No. 4 furnace and the percentage of coke on a 2-in. screen. There was a decided decrease in size of coke from an average of 60.72 per cent on a 2-in. screen, on Aug. 3, to an average of 48.96 per cent on a 2-in. screen after that date, owing to a decrease

change in operation of No. 4 furnace, no decided change in burden, performance was very satisfactory and tonnage about the same, even a little better on the smaller coke. From this it can be inferred that coke can change from 60 to 49 per cent on a 2-in. screen without any change in furnace operation.

Case 2

In a previous paragraph it was pointed out that, according to Fig. 9, temperature change influenced size of coke and the operation on Nos. 3 and 4 furnaces. Furthermore, as the average size of coke decreased from 70 per cent on 2-in. screen during July and the first part of August 1933, to 49.65 per cent from Aug. 18 to Sept. 8, there was a decided dropping off in production on No. 4 furnace. But this size

is virtually the same as that in Fig. 19, 49 per cent, at a time when there was no ill effect. In one case this size of coke caused poor furnace operation; in the next case, good furnace operation.

peratures from Jan. 1 to 17 varied from 2250° to 2270°; the coking time was approximately 16½ hr.; and 41.06 per cent of the coke stayed on a 2-in. screen. On Jan. 17 a test was made in which the flue
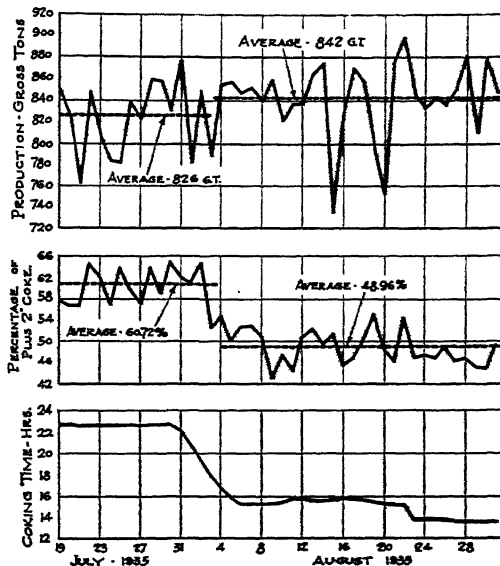
FIG. 19.—CHANGE IN COKE SIZE WITH SMALL VARIATION IN PRODUCTION ON NO. 4 FURNACE.

Case 3

The third example covers the operation of the same furnace, together with No. 3 furnace, during a period when a change in size of coke followed a decided drop in the oven temperatures. In Fig. 20 are plotted the

temperatures at the coke ovens were dropped to below 2200° for 5 days. The sharp increase on Jan. 25 to a maximum of 2285° was a result of delays in pushing. Exact data on the temperatures between Jan. 17 and 20 are missing, and a straight

TABLE 7.—*Operation on No. 4 Furnace*

Case	On 2-in. Screen, Per Cent	Period	Coke Size Produced by	Furnace Efficiency	Normal Size
1	48.96	Aug. 1935	Normal operation	Good	49 % + 2″
2	49.65	Aug. 1933	Excessive temperature	Poor	65 % + 2″
3	49.10	Jan. 1936	Low temperature	Poor	41 % + 2″

tonnages produced on Nos. 3 and 4 furnaces for January. These are 3-day averages; that is, the tonnage plotted for any given day is the average of the tonnage for that day, the previous day, and the following day. Below this are plotted the average oven temperature, the percentage of plus 2-in. coke and coking time. The flue tem-

line connecting these two points is assumed as approximately true. Beginning on Jan. 17, an upward trend in the plus 2-in. coke reached a maximum on Jan. 19 and remained there for four days. In other words, from Jan. 19 to 22, there was more coke over 2 in. No screen tests were made on Jan. 23 and 24, but tests on Jan. 25

showed again a decrease in size, together with the increased oven temperature, which was the result of a delay in pushing, followed by an increase in size and another decrease in temperature.

much better when the coke was smaller; that is, with 41.96 per cent on a 2-in. screen.

The relations indicating cause and effect are more striking if the three cases are tabulated (Table 7).
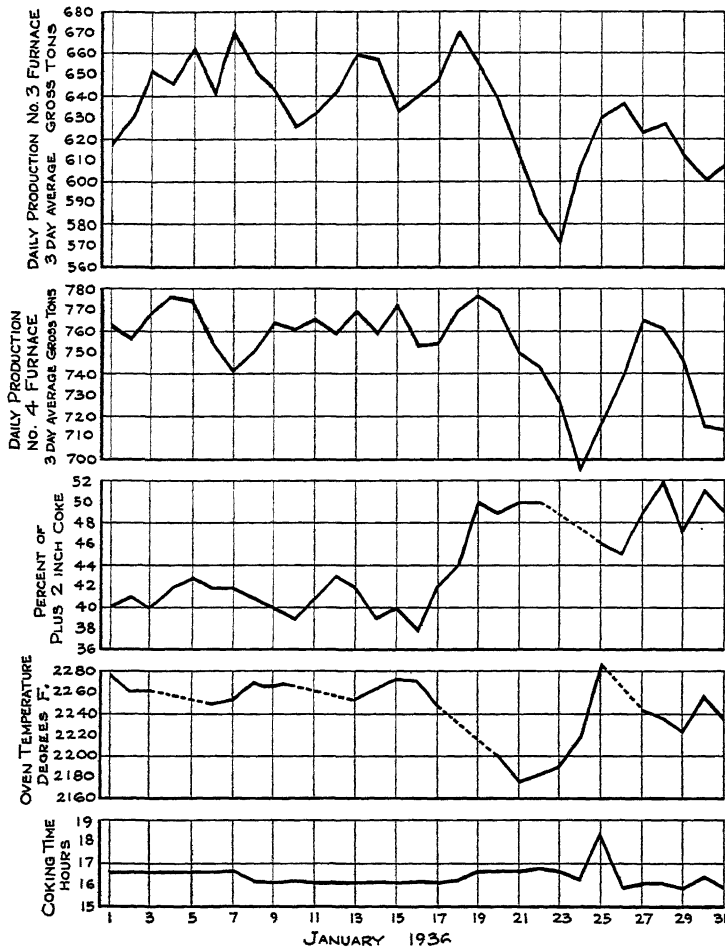
FIG. 20.—DECREASE IN SIZE OF COKE WITH DECREASE IN OVEN TEMPERATURE AND EFFECT ON NOS. 3 AND 4 FURNACES.

The drop in tonnage on both Nos. 3 and 4 furnaces was very marked, and correlates with the increase in size of coke, which was a result of the extreme decrease in the temperature of the ovens. The furnace operation was poor when there was an average of 49.10 per cent on a 2-in. screen, and was

In case 2, normal processing would have produced coke with 65 per cent on a 2-in. screen but the coke was overheated, so that when it was measured at the furnace it was 49.65 per cent on a 2-in. screen. In case 1, the processing was normal and the size of 48.96 per cent on a 2-in. screen is the size

that usually results from these ovens on short coking time at correct coking temperatures. Case 3 showed poor results with coke of 49.10 per cent on a 2-in. screen, but

coke. The second is that for a given coal mix and a given coking time, correct oven operation will produce a coke of a certain or normal size. The size may be altered by
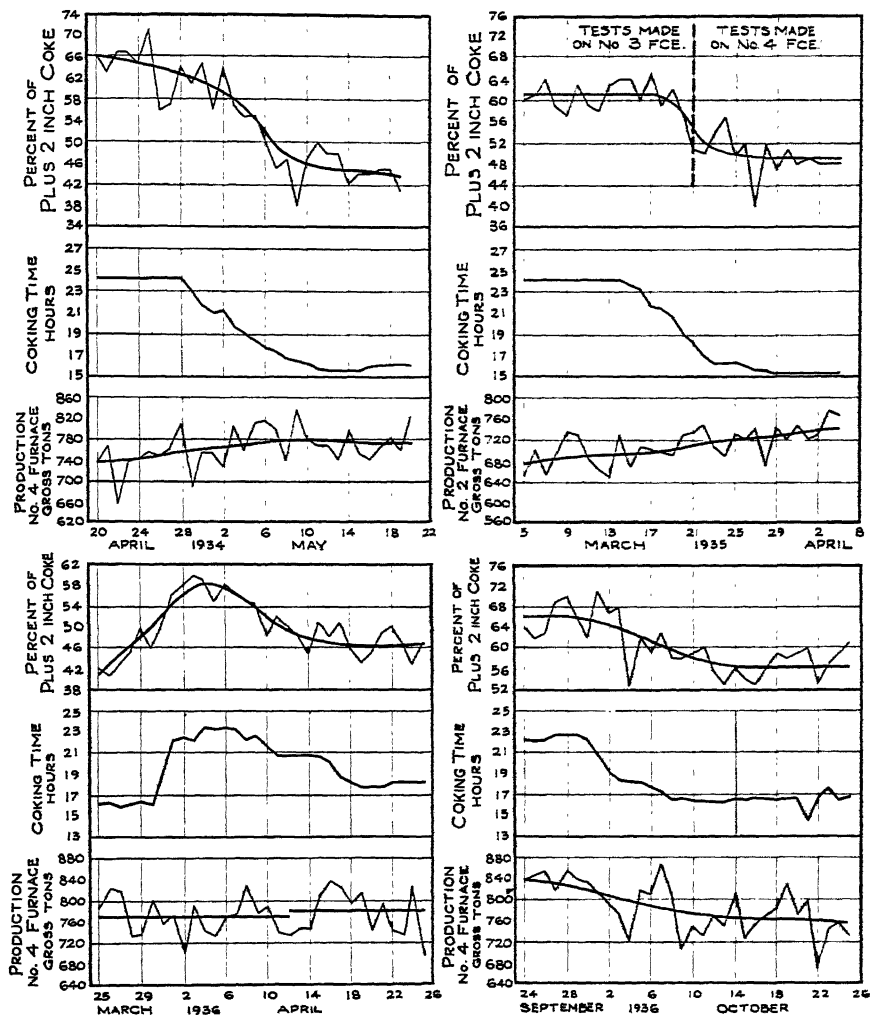
FIG. 21.—DECREASE IN SIZE OF COKE WITH DECREASE IN COKING TIME AND VARYING EFFECT ON FURNACE OUTPUT.

this size was caused by unusually low oven temperature. If this coke had been pushed at the normal temperature it would have been 40 per cent on a 2-in. screen.

From the data in Table 7 two conclusions can be drawn. The first is that size is much less important than other properties of

changes in the temperature of coking, but this will cause changes in other properties of the coke, which may have a detrimental effect on furnace operation.

The question now arises, "What is normal size?" This is very difficult to answer. In Fig. 21 are four cases in which

the coking time was increased from about 16 hr. to something more than 23 hr. When the coking time was short, 45 to 50 per cent of the coke was on a 2-in. screen at the blast furnace, but every time the coking time was long—that is, more than 23 hr.—65 to 70 per cent of the coke was retained on a 2-in. screen. So for a given set of coals under a given processing, there will result a coke of a certain size, containing definite properties. A drastic change in manufacture may cause the coke to be of a different size, but also of different properties. It would have been possible, in any of the cases of longer coking time illustrated in Fig. 21, to increase the temperature of the ovens and decrease the coke size to 50 per cent on 2-in., but definite overheating of the coke would have been necessary. It also would have been possible to increase somewhat the size of the coke produced at 16 hr. by decreasing the oven temperatures, but this likewise would have resulted in an abnormal coke of inferior quality.

Importance of Uniformity in Furnace Operation

The blast furnace is a continuous process in which gases are passing upward at high velocity through 50 or 100 individual layers of coke and ore. Obviously the coke as well as the ore in each layer must be of suitable quality. One or two abnormal layers can interfere with the continuous stream of gas.

The coke is made by a batch process, and individual ovens differ. One abnormal oven makes a batch of 10 tons, which constitutes as many as four or five individual layers in a blast furnace. This amount can seriously interfere with the flow of gases, and so with furnace operation. Unfortunately, the data to illustrate this point fully are not available, but there is recorded an example of one abnormal layer of coke that was sufficient to upset a furnace very badly.

The coke was abnormal in that it was unusually dirty and small. It had been recovered from the flue dust after a screening operation at the sintering plant. The Hum-mer screens were equipped with a ⅜ by 1¼-in. cloth. The oversize that accumulated was rescreened and appeared clean enough to use, so it was put into an ore bin for use in the furnaces. The furnace was being charged as follows:

ONE CHARGE
Coke unit 10,800 lb.
One skip ore
One skip stone
One skip coke
   Dump big bell
One skip ore
One skip coke
One skip coke
   Dump big bell

The furnace was taking about 40 charges per 8-hr. turn. On the first charge of each 8-hr. turn the one skip of coke for the first half of the charge was the rescreened coke, and the rest of the coke charged was the usual furnace coke. After this had been done for several weeks, there began to be an increasing amount of irregularity in the operation. One morning at 10:30 a.m., the blast pressure, which normally is 16 to 17 lb., went up to 28 or 29 lb. for several hours, then came back to normal. The small coke was then taken off the furnace, as it was suspected of having caused the high pressure. After performance of the furnace had been checked for the previous several weeks and additional evidence noted to substantiate that conclusion, it was decided to discontinue permanently the use of the reclaimed coke after what remained in the bin had been used up. One skipload was charged every 8 hr. Since there were three skips of coke per charge and 40 charges per 8-hr. turn, there were actually 119 skips of regular coke for the one skip of small coke in the furnace at one time. On the wind blown at the time, it took about 8 hr. for a charge to come through.
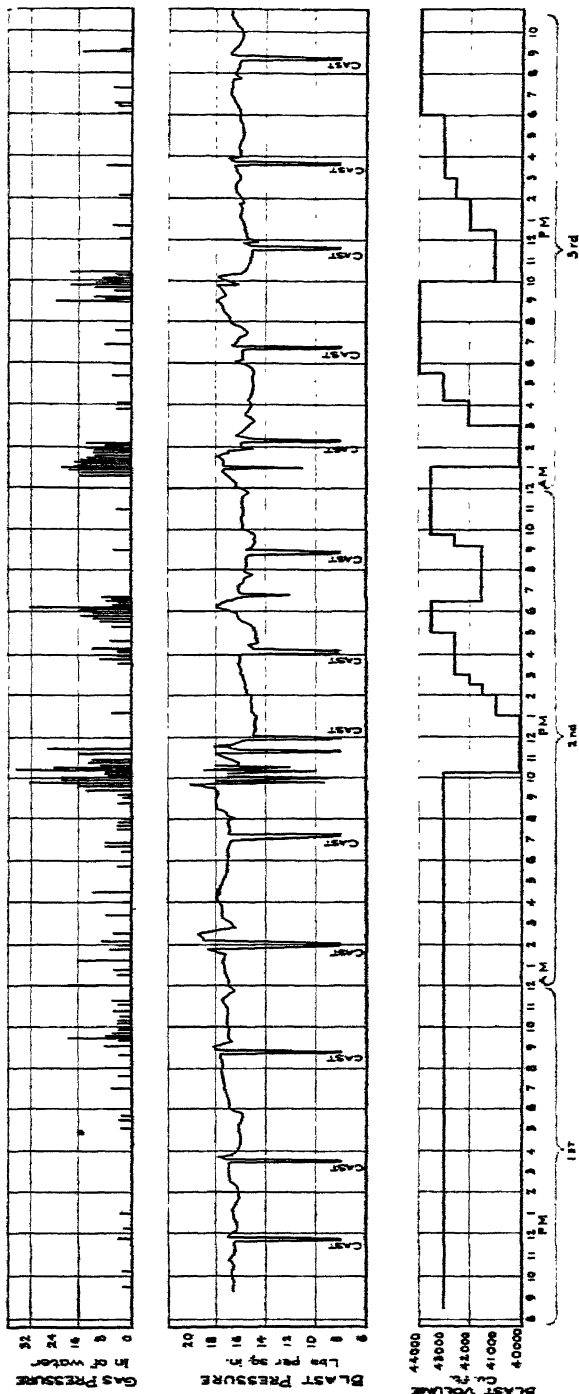
FIG. 22.—OPERATING DATA FOR NO. 3 FURNACE, DECEMBER 1935.

The first charge of reclaimed coke was at 8:00 a.m. on Dec. 1. The top gas pressure, the blast pressure and the wind blown are shown in Fig. 22. The use of the small coke had no effect until the skipload charged at 8:00 a.m. on Dec. 2. One hour later the blast pressure increased, the furnace slipped several times in spite of an extreme decrease in the wind blown, and the condition continued for 2½ hr. Another skipload was charged about 4:00 p.m. About 1½ hr. later there was an increase in blast pressure, a series of slips for several hours, then normal operation. The skipload put in at midnight had the same effect, and the one at 8:00 a.m. the next morning. This coke was then discontinued definitely and the irregularity stopped. There is not an exact record of the time the skiploads went in, as the order to the stockhouse was for the man coming to work to put in one skipload on his first charge and the time of relief varied with the individuals.

The regularity of the hanging and slipping shortly after the charge of small coke makes the cause and effect connection positive. The explanation is that the one layer was deficient in voids, and acted as a plug in the stock column after it had descended some 10 or 15 ft. into the furnace. It did not permit the gas to pass through at the same pressure as did the normal layers, and caused a building up of pressure, which would finally blow through. This would be repeated several times until the material worked down into the furnace to a point where the deficiency in voids was less critical, or until the slipping had blown out enough fine material to create the necessary voids.

Why did the first few loads go through the furnace without trouble? Evidently they contained more voids than later skips. As the bin was being emptied, the dust adhering to the coke was shaken down, and the segregation left the last skips with larger amounts of fine material.

One "spell" of hanging and slipping as produced by one skipload of the fine coke can upset the furnace for several days and cause the loss of several hundred tons of production. The incident just related is of little importance in itself because such conditions do not occur frequently, but the principle of uniformity is extremely important and nonuniformity resulting from another cause or material will have a similar effect. Each oven of coke pushed is a distinct product, loaded in a car with three or four others, dumped into some furnace coke bin, and later makes several layers in the furnace. Though all other ovens pushed may have been satisfactory, one abnormal oven may upset the furnace.

SUMMARY

An attempt has been made to add to the knowledge on the complicated problem of establishing some objective measure of blast-furnace coke. If this were not a difficult problem, such measures would have been established long ago.

Nor have we been able to establish any new objective measure. There are 10 or 15 properties of coke that are important, and there is no one yardstick available to measure all of them, except the blast furnace. Because this is true, it seems logical to consider a different method of approach, using the furnace as a testing medium.

The manufacture of coke is divided into four steps: (1) selection of coals, (2) preparation of the coal charge, (3) heating, (4) pushing and preparation. If all variables making up these four steps are kept constant, the product will be constant. Then screen tests of the coke will show the same results. In this study, detailed investigations were made of the manufacture when there were changes in the size, to see what variables had been affected. Of the many variables investigated, coking time and temperature were found most significant.

In this paper we have attempted to establish three facts:

1. Before considering the quality of coke used, it is first necessary to adapt the furnace to the coke available. No conclusion regarding the quality of coke is worth while until the best possible gas flow has been worked out for the particular furnace.

2. Coke is a product that has an optimum value. Certain objective measures also have a maximum value. Consequently, it is impossible to establish any straight-line relationship between such properties and the results in a blast furnace. It was shown that the point of optimum value on two blast furnaces as measured by flue temperatures and coke size did not coincide.

3. The use of screen tests of coke as an objective measure of coke quality was discussed. It was concluded that the size of coke may be an indication of coke quality but is not a measure of it.

Some excellent correlations have been worked out in individual plants between some one objective measure and furnace operation, and, as Campbell and Wagner[1] have indicated, combinations of some objective measures. The superior coke is a combination of many properties. The significant variable in one process may be measured by the shatter test and in others by some other variable, such as weight per cubic foot. Consequently, the one may serve as a useful guide at one plant, the other as a useful guide at a different plant.

For most plants, the source of coal and equipment available are fixed. The problem is to make the product most useful for most efficient blast-furnace operation. More is to be gained if less attention is paid to objective measures and more to the control of the many variables that in combination produce blast-furnace coke. Any improvement in control will result in more constant product, and this in turn will facilitate study of the results in the blast furnaces. Then by controlled experiments the optimum coke for a particular plant can be readily determined.

REFERENCES

1. F. W. Wagner and R. W. Campbell: Physical Testing of Coke and Correlation with Furnace Operation. Unpublished manuscript received from authors.
2. C. C Furnas and T. L. Joseph: Stock Distribution and Gas-solid Contact in the Blast Furnace. U. S. Bur. Mines *Tech. Paper* 476 (1927).
3. C. C. Furnas: Flow of Gases through Beds of Broken Solids. U. S. Bur. Mines *Bull.* 307 (1929).
4. A. C. Fieldner, J. D. Davis, W. A. Selvig, R. Thiessen, D. A. Reynolds, C. R. Holmes and G. C. Sprunk: Carbonizing Properties of West Virginia Coals and Blends of Coals from Alma, Cedar Grove, Dorothy, Powellton A, Eagle, Pocahontas and Beckley Beds. U. S. Bur. Mines *Bull.* 411 (1938).

Effects of Scrap in the Blast-furnace Burden

By C. L. T. Edwards*

(Chicago Meeting, April 1941)

In the preparation of this paper, the author has drawn upon experience with the operation of a blast furnace on 100 per cent scrap burden, which he believes was the first operation of its kind in the country. It is the writer's further belief that much of the controversy attending discussions of this subject may be obviated by the presentation of a group of facts that should be known by blast-furnace men and open-hearth men alike.

The following question has been raised: "Is iron made with scrap in the blast-furnace charge as good iron as that made without scrap—made with straight ore?" This question may be answered in part by the fact that the open-hearth men of the Bethlehem Steel Co. who used pig iron from a blast furnace that operated on 100 per cent steel scrap found no difficulty in the processing of such iron other than that to be expected from the known analysis.

OPERATION WITH 100 PER CENT STEEL SCRAP

During World War I, there was accumulated at the Bethlehem plant of the Bethlehem Steel Co. some 22,000 tons of alloy-steel turnings and borings. This scrap material was highly corroded and, like alloy-steel turnings of that period, were as a drug on the market. There was also a small tonnage of scale, rich in valuable metal. If this scrap could be worked up into pig iron, it would become readily available for use in the open hearth.

In order that the pig iron should contain the maximum percentage of nickel, permission was obtained from the Management to try a 100 per cent scrap operation. Accordingly, a blast furnace was swung over on July 25, 1919; the percentage of steel scrap increased more or less irregularly until July 29, when 100 per cent steel turnings were charged. Except for occasional charges of nickel scale as an "extra," the operation continued uninterruptedly until Aug. 27, when the furnace was swung back to the regular ore—ore and scrap—operation. During this period, the furnace production ranged from a low of 568.60 tons to a maximum of 766.07 tons.

At the swing-over from 100 per cent scrap to the regular burden, the charge hung up rather severely. While the latter condition has nothing to do with the object of the paper, a brief discussion of the experience will appear later because of the interest it may have for blast-furnace operators.

In Table 1, results of the first and last days of the ore charge are shown, July 25 and July 29. The last column shows a summary for the period of maximum scrap charge.

The furnace employed had a hearth 16 ft. 0 in., bosh 22 ft. 0 in., stock line 15 ft. 6 in., bell 11 ft. 6 in., batter ¾ in., bosh angle 73° 27' and a Baker-Neuman top, with gas-engine blowers.

Analyses Range of Material Charged

Gravel: SiO_2, 64.40 to 70.54 per cent; Al_2O_3, 3.52 to 4.58; CaO, 7.27 to 9.49; MgO, 5.09 to 6.14; FeO, 1.67 to 3.34, ignition loss, 9.50 to 13.83.

TABLE 1.—*Operation on Nickeliferous Pig Iron*
D FURNACE IN 1919

Charge and Products	July 25 Tons	July 25 Per Cent	July 29 Tons	July 29 Per Cent	Aug. 4 Tons	Aug. 4 Per Cent	Aug. 9 Tons	Aug. 9 Per Cent	Aug. 17 Tons	Aug. 17 Per Cent	Aug. 24 Tons	Aug. 24 Per Cent	July 30 to Aug. 25 Tons	July 30 to Aug. 25 Per Cent
Ore														
Daiquiri	375	50	—	—	—	—	—	—	—	—	—	—	—	—
Ontario	225	30	102.0	80	—	—	—	—	—	—	—	—	10.7	—
Charlotte	151	20	—	—	—	—	—	—	—	—	—	—	—	—
Scale	—	—	25.5	20	—	—	63.4	Extra	32.1	Extra 32.2T	—	—	968	—
		Pounds per Round		Pounds per Round		Pounds per Round		Pounds per Round		Pounds per Round		Pounds per Round		
Scrap, etc.														
Turnings	168	—	659.0	—	628.6	—	634	—	748.4	—	750	—	17,405	275
Gravel			74.4	—	84	—	136.5	—	150.0	—	134.5	—	3,474	
Stone														
Calcite	128.3	5,100	102.3	6,400	121.8	8,800	127.3	8,400	147.8	8,800	150.5	9,200	4,972	
Dolomite	128.3	5,500 / 5,700	102.3	7,800	121.8	8,800	127.3	8,000	147.8	9,200	150.5	9,400	2,974	
Coke	446.5	6,000	263.9		325.9		301.6		357.2		370.0		9,200	
		Approximately		Per Cent		Per Cent		Per Cent		Per Cent		Per Cent		Per Cent
Pig	737.4		745.7		757.7		706.8		715.7		712.4		18,101	
Si		1.22		0.71		1.09		1.24		1.45		1.11		1.08
S		0.043		0.042		0.027		0.028		0.040		0.040		0.042
P		0.108		0.061		0.061		0.050		0.061		0.074		0.061
Mn		1.63		1.07		0.550		0.538		0.480		0.483		0.535
Ni		0.827		1.91		2.21		2.00		1.85		2.10		2.166
C		4.61		4.74		4.38		4.58		4.79		4.60		4.58
Cr				0.90										
Slag														
SiO₂		34.50		34.3		35.4		35.0		36.5		44.7		46.2
Al₂O₃		11.75		7.8		8.1		8.02		8.47		10.3		8.3
S		2.03		0.96		0.98		1.30		1.12		1.23		1.22
Blast														
Pounds per Sq. In.	13.47		10.3		17.7		16.4		15.6		19.9			
Cu. Ft. per Min.	42,228		34,428		41,008		41,280		39,716		37,122		37,050	
Temp., Deg. F.	1,075		1,367		1,272		1,157		1,304		1,334		1,280	
Gas														

ᵃ Gross tons, 2240 pounds.

Coke: ash, 12.78 per cent; sulphur, 0.91; volatile matter, 0.74; fixed carbon, 86.58; phosphorus, 0.030; moisture, 5.76.

Limestone (calcite): SiO_2, 2.50 to 4.08 per cent; MgO, 2.05 to 4.83; CaO, 51.4.

Limestone (dolomitic): SiO_2, 4.18 to 7.55 per cent; MgO, 20.28; CaO, 29.54.

Scale: Fe, 59.00 per cent; SiO_2, 13.2; Ni, 1.61.

Steel Turnings: Fe, 92.8 per cent; Mn, 0.50; Si, 0.11; S, 0.034; P, 0.022; Ni, 2.12; Cr, 1.00.

Product

Pig-iron Average for Run: Si, 1.08 per cent; S, 0.032; P, 0.0619; Mn, 0.535; Ni, 2.106; C, 4.58; Cr, 0.90.

Slag Average: SiO_2, 36.24 per cent; Al_2O_3, 8.83; S, 1.22.

Unquestionably, if a run of this sort were to be repeated today, a substantial improvement all along the line would be anticipated. Better furnace distribution would be obtained because of the modern filling system. A siliceous material of more uniform analyses would be used and a far superior grade of basic flux is available. In retrospect, the venture proved a success from the start, although there had been considerable misgiving concerning the feasibility of such an operation. All of the pig iron produced was used in the production of forging steels of the highest quality, and no difficulty was reported from the metallurgical or open-hearth departments.

In the production of pig iron from 100 per cent steel scrap, the physical quality of the iron, whether as hot metal or cold, was so little different from that normally expected from a furnace operating on 100 per cent ore that no one paid any particular attention to it. When the furnace came "hot" and the sulphur below 0.04 per cent, the usual graphite made its appearance in the cast house.

Scrap Classification

There are two separate and distinct classes of scrap for blast-furnace use:

1. *Iron Scrap*, on the order of iron castings, cast-iron borings, pig iron, iron-ladle, mixer and runner scrap, ingot molds and the high-carbon irons.

2. *Steel Scrap*, on the order of machine-shop turnings and borings, crops, punchings, flashings, detinned billets, plate, pipe, structurals and any of the miscellaneous steel junk collected by the old-fashioned rag picker.

Because of their effects on blast-furnace practice and the general use for which the pig iron is intended, the principal elements for immediate consideration are shown in the two composite mixtures (Table 2). It is

TABLE 2.—*Elements in Two Classes of Scrap*

Element	Cast-iron Scrap, Per Cent	Steel Scrap, Per Cent
Silicon.........	0.30 to 3.25	0.002 to 0.50
Sulphur........	0.03 to 0.250	0.015 to 0.065
Phosphorus.....	0.060 to 0.800	0.010 to 0.105
Carbon.........	2.15 to 4.75	0.020 to 1.20
Manganese......	0.40 to 0.85	0.250 to 2.00

to be noted that while the two classes of scrap vary widely within themselves, there is just as great a difference between the two general classifications. As the percentage of either of the two classes of scrap is increased in the furnace burden, the effect on the metallurgy of the furnace becomes more marked. A tremendous change accompanies a switch from steel to cast-iron scrap in the burden; in fact, the effect may be more marked than the switch from a basic ore mixture to a foundry ore mixture. From analyses shown, it will be seen that the use of scrap in the blast furnace cannot be promiscuous.

Smelting versus Melting

The opinion has been rather general that the charging of scrap into the blast furnace constitutes a cupola operation. This is by no means true, as in the blast-furnace operation with a 100 per cent scrap charge, no ore in the burden, it is essential for

proper operation to carry a normal blast-furnace slag. Therefore this constitutes a smelting rather than a melting process.

Normally, about 85 per cent of the sulphur entering the blast furnace enters with the coke. Cast-iron scrap may carry as much as 0.16 per cent of its weight in sulphur, or more. The normal smelting operation will reduce this sulphur content to 0.025 per cent or less in the pig iron. As for the sulphur in the fuel (coke), from 90 to 98 per cent will be eliminated with the slag.

It is general practice to reduce up to 1.25 per cent by weight of silicon in basic pig iron. The reduction of this silicon, as well as the removal of sulphur in the slag, requires a certain minimum of temperature. This means that 98.75 units of pig iron must be raised to the minimum degree of superheat in order that 1.25 units of silicon may be reduced and the necessary minimum of sulphur removed.

A further indication of the intensity of the smelting operation is found in the carbon content of the pig iron from 100 per cent steel scrap. Although the scrap consisted of forging-quality steel, the carbons in the pig iron ranged up to 4.74 per cent and possibly higher. From our experience with chromium, we know that the excessive carbons shown are due largely, if not entirely, to the presence of that element.

The question as to the effect of 10 or 100 per cent scrap in the blast-furnace charge cannot be answered in a few words. When discussing the effect of scrap on quality of pig iron, unless we can qualify our statement with the proviso that other things shall be equal, our commitment has little meaning. So many variables enter into the operation and production of a blast furnace that it becomes necessary to make corrections for inequalities; otherwise, irregularities are inevitable.

If it became imperative that the author answer the question, What effect does 10 per cent or 100 per cent, scrap in the blast

furnace have on pig-iron quality? the answer would be, in two words, no effect. One can no more attribute a particular quality in pig iron to the use of scrap in the furnace burden than he can to the use of magnetite or hematite. Different qualities will be found in the pig irons produced from Adirondack and Swedish ores, if for no other reason than that the Adirondack ores are titaniferous. Both, however, are magnetic.

As the percentage of steel scrap in the blast-furnace charge increases, the slag volume per ton of pig iron decreases, thereby drying up the mix. The effect is analogous to that of gradually switching from a foundry mix to a basic mix. In such cases, where a furnace is set up on a siliceous mixture, the addition of steel scrap to the charge will be accompanied by a decrease in silicon content of the pig iron. In such cases, the basic open-hearth man will say that the addition of "scrap" to the blast-furnace charge leads to better steel-making iron. When a furnace is set up for a fairly lean mixture, the addition of cast-iron scrap will cause a tendency toward a higher silicon pig (given the same sulphur). In such cases, the open-hearth man will claim that his results are not so good, even though his cost of pig iron may be a little less.

When the open hearth is served with cast-iron scrap as a substitute for pig iron, and with highly corroded steel scrap, all of which is to be used in the production of high-quality steels, the problem becomes difficult in the open hearth. By processing these scraps in the blast furnace, the sulphur is removed from the cast iron; the oxides, as such, are removed from the steel scrap, and the product delivered to the open hearth as a "quality" raw material.

The effect that any pig iron has on a steelmaking mix is not especially due to the use of a particular raw material in the blast furnace but is, rather, a matter of balance. The percentage of silicon in the pig iron must vary with the percentage of pig iron

in the open-hearth charge. When lowering the silicon content as a result of additions of steel scrap to the blast-furnace charge, this naturally speeds up the open hearth, providing a proper temperature has been maintained in the hot metal.

ECONOMICS AND QUALITY

The economy of every blast-furnace operation is different from that of every other blast-furnace operation. Of primary importance in the use of scrap is the question of economy, and the strategic position of a furnace in relation to its sources of raw materials will probably be reflected in the quality of its product. The scope of this subject is so broad that it can only be touched upon briefly with examples:

1. In order to work a heat of steel in the open hearth, it is necessary that the bath contain a certain minimum percentage of carbon. Where a plant has the facilities to do so, it can purchase rusty steel turnings, impregnate them with carbon and silicon in the blast furnace and deliver the product to the open hearth as hot metal. The advantage to be gained by such practice will be determined by the relative costs of melting in the open hearth and smelting in the blast furnace.

2. Cast-iron scrap frequently is used as a substitute for pig iron in the open hearth. Such scrap can be desulphurized in the blast furnace and delivered to the open hearth as hot metal.

3. Steel scrap of known source may be impregnated with carbon and silicon in the blast furnace, bessemerized into high-quality steel, or duplexed through the open hearth into special steels.

4. When fuel prices become the dominant factor in the matter of costs, the use of iron or steel scrap in the blast furnace becomes a matter of immediate importance, as the fuel ratio may be reduced from 40 to possibly 50 per cent.

5. Desirability in the use of scrap changes daily, the principal determining factors being relative costs of iron in the form of iron ore, steel, cast-iron scrap; the effect of coke prices on pig-iron costs, the need for production, spread between costs and selling prices and the uses for which the pig iron is intended.

The author believes the following statements to be as axiomatic with scrap in the blast-furnace burden as when operating with ore only, and that furnacemen may feel safe in accepting them literally; also, that open-hearth operators should consider the merits of such points in so far as such knowledge may assist in diagnosing certain difficulties peculiar to their operations:

6. Other things being equal: (a) as the temperature of the blast-furnace hearth increases, the carbon content of the pig iron and the ratio of graphitic to combined carbon will increase; (b) increase in silicon content will be accompanied by a decrease in total carbon and an increase in the ratio of graphitic to combined carbon.

7. Silicon and sulphur are diametrically opposite in their effects upon carbon in pig iron, silicon favoring graphitization, while sulphur causes carbon to enter the combined form.

8. Slow cooling favors graphitization.

9. The silicon content of the pig iron does not vary uniformly with the hearth temperature when the ratio of silica to bases in the slag-forming material varies, and the silicon will not vary uniformly with temperature when the volume of slag-forming material varies.

CONCLUSION

There appears to be no reason fundamental in nature for any difference in the qualities of pig irons produced from ore and from scrap. When differences do occur, they are complementary with the nature of the materials involved, and such variables are inherent in ore mixtures, just as in mixtures that include scrap.

When residual elements such as copper, nickel or chromium appear in pig iron,

cognizance should be taken of such occurrence and provision made for their digestion in the open hearth.

Before scrap additions are made to the blast-furnace burden, the economics of the proposed practice and the use for which the pig iron is intended should be given fullest consideration.

NOTES FROM EXPERIENCE

First consideration had to be given to the necessity of producing an iron that could be used in the production of special steels—hence the liberal slag volume.

Fuel requirements were judged through a combination of calculation and deduction. The trend in fuel consumption accompanying increasing percentages of steel turnings was known.

We learned quickly that as the percentages of scrap increased beyond normal there was an accompanying decrease in top temperature. With 100 per cent steel scrap we dropped the stock line about 12 ft. below normal, otherwise the top temperature would have been below the dew point. Lowering of the stock line would, almost certainly, have been forced in any event, because of the blast pressure.

Furnace symptoms indicated an extensive cooling of the furnace, well down in the inwall.

Daily consumption of fuel was not a clear indication of daily production. Volume of casts varied widely. Regardless of fuel consumption, the temperature of succeeding casts showed little variation and

the reduction of silicon did not materialize as anticipated.

The daily log shows no undue blast pressure until the swing-over from scrap to ore. Because of the cooled condition of the furnace, a few blanks of coke were charged, followed by a conservative allowance of fuel for the normal ore charge and the furnace filled to regular stock line. Shortly thereafter, the pressure suddenly rose to the point where no gas appeared to be passing through the furnace. The tuyeres continued bright but showed no life.

The diagnosis for the high pressure condition was that the weight of the ore burden caused several of the large blankets of turnings to collapse when hot, thereby sealing the furnace. At this point, a steam blower was put on the furnace with instructions to turn as slowly as possible, giving about 5 to 8 lb. pressure. In about 3 hr. the pressure relaxed without a slip and the blast increased rapidly to normal. We may assume that the steel scrap absorbed carbon before melting, thereby lowering its melting point, after which the melt ran ahead of the coke, followed by drop in pressure.

In further operations with 100 per cent scrap, it is the author's suggestion that when switching from scrap to ore, the lowest stock line permitted by top temperature be maintained until it is reasonably certain that the last charge of steel turnings has been digested, after which a reasonable charge of fuel should be made for the purpose of preheating, and the furnace should be filled to the normal stock line.

Temperature Gradients through Composite Carbon Columns and Their Application to Blast-furnace Linings

By F. J. Vosburgh,* Member A.I.M.E., and M. R. Hatfield*

In a recent article,† it was shown that in the blast furnaces in Germany that are lined with carbon blocks no cooling plates are used, and that shower cooling is employed on the hearth and bosh sections. While one of the authors was in Germany he was told that one furnace was being operated without even the shower cooling on the bosh section, though the hearth section was shower-cooled. In discussion of this interesting situation with a number of blast-furnace operators in this country, it was made clearly and promptly evident that shower cooling was very unpopular, probably because of its messiness and its ineffectiveness.

Both of the causes for the dislike of shower coolings are reasonable ones. Shower cooling can be and frequently is messy, but the present cooling of blast furnaces leaves much to be desired on that score. Shower cooling is ineffective as compared with plate cooling, so far as its usefulness in keeping the bricks cool enough not to melt or fall to pieces is concerned.

However, the introduction of carbon linings changes the situation. No one is concerned with keeping a carbon lining cool, for no temperature in the blast furnace has any effect on carbon, which is just as stable at 3000°F. as it is at 70°F. The only concern is for the shell—to keep it cool enough for safety and comfort—and for that shower cooling is sufficient.

Of course, with only the shell to cool, instead of the shell plus all the refractory material, much less water would be required, and the necessity for constant attention to the flow would be lessened, as the hundreds of inlets and outlets would be eliminated. Probably half of the water used in cooling a blast furnace is used for cooling the shaft and tuyeres and the remainder for the bosh and hearth sections.

However, in view of the dislike of shower cooling in the United States, and particularly because at least one German blast furnace is operated with no cooling of the bosh section, thought was given to the possibility that a carbon-lined blast furnace might be operated without any cooling of the entire carbon-lined portion. For that reason a series of experiments was performed to determine what might be the temperature of the shell of a blast furnace protected by a carbon lining and operated under varying conditions up to a maximum inside temperature of 3000°F.

Experimental Procedure

A schematic diagram of the experimental setup is shown in Fig. 1 and a photograph of the entire assembly in Fig. 2.

The heating element was a carbon tube nominally 2⅝ in. o.d. by 2 in. i.d. by 30 in., used as a resistor. Power was furnished by a 15-kva. transformer operating

at 60 cycles on 220 volts. Temperatures up to 5000°F. were attainable. The current was controlled between 200 and 650 amp. The terminals were water-cooled graphite blocks. To prevent oxidation, the tube was packed in charcoal particles and nitrogen was circulated through it. The blocks tested were of different grades of carbon and graphite, all 3½ in. square and 12 in. long. One end of the first block above the tube was cut out to fit the curvature of the tube. The second block was cemented to the first and then followed 4 in. of coke particles held in an asbestos sleeve, this setup representing a typical carbon lining for a blast furnace as generally used abroad. Above the coke particles was a steel plate 1 in. thick, to represent the blast-furnace shell.

The test column was surrounded by 9 in. of charcoal particles plus 2½ in. of Sil-O-Cel brick, all contained in a Transite box. The upper face of the steel plate was uncovered and exposed to the air. Pre-

which could be separated even during a run to give the desired heat control.

Temperatures above 1800°F. were taken with a Leeds and Northrup optical

T - Thermocouple
P - Optical pyrometer
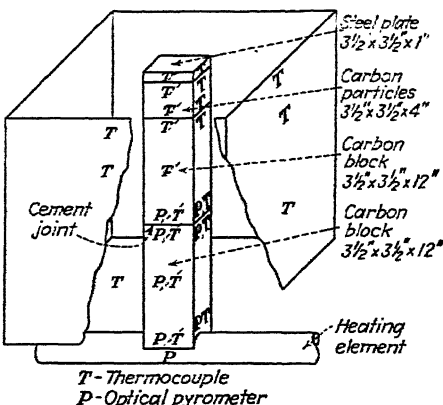
FIG. 1.—DIAGRAM OF TEST-COLUMN ASSEMBLY.

pyrometer; lower temperatures by iron-constantan thermocouples or copper-constantan couples, each one calibrated for the range in which it was used. The
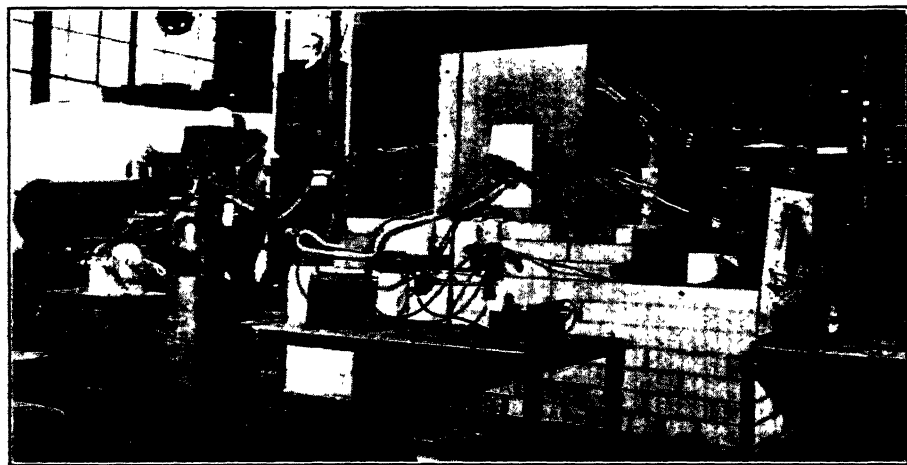
FIG. 2.—EXPERIMENTAL SETUP.

liminary tests indicated the necessity for additional insulation to prevent radial heat losses, and this was accomplished by surrounding the column with a series of graphite cylinders, one above another,

location of the points at which temperatures were taken are indicated in Fig. 1.

The most serious problem in experimenting with carbon materials at high temperatures is to prevent air oxidation,

since carbon begins to oxidize at 662°F. (350°C.). The charcoal particles served very well, since the charcoal consumed the entering oxygen before it could attack the carbon blocks. The protection of the carbon sight tubes for the optical pyrometer was difficult, but was accomplished after some preliminary trials.

The setting up and testing out of the apparatus was the more difficult part of the experiment. The taking of actual readings after a condition of equilibrium was reached took relatively little time.

TABLE 1.—*Cooling of Steel Shell*

Test Column	Type of Cooling	Interior Temperature of Steel Plate, Deg. F.[a]
12-in. grade S carbon backed by 12 in. Carbocell (porous carbon) (Fig. 4).*	None	324
	Air blast:	
	10 ft. per sec.	244
	25 ft. per sec.	230
	50 ft. per sec.	180
	Water-vaporized, 1.1 lb. per hr. per sq. ft.	162
24-in. grade CB-4 carbon in two 12-in. sections (Fig. 3).	None	353
	Air blast:	
	10 ft. per sec.	253
	25 ft. per sec.	225
	50 ft. per sec.	160
	Water-vaporized, 1.5 lb. per hr. per sq. ft.	176
12-in. grade AGX graphite backed by 12-in. Carbocell (porous carbon) (Fig. 5).	None	378
	Air blast:	
	10 ft. per sec.	226
	25 ft. per sec.	176
	50 ft. per sec.	147
	Water-vaporized, 2 lb. per hr. per sq. ft.	165

[a] Bottom sections of test columns kept at approximately 3000°F. throughout runs.
* Carbocell is a trade-mark of the National Carbon Company, Inc.

The resistor-tube current would be set at a predetermined amperage to produce a temperature at the bottom of the column of 1300° to 1400°F. Continual adjustment was necessary during the first few hours because the resistance of the tube varied with the temperature changes. As equilibrium was approached the current remained steady. Usually 3 days was required for attainment of equilibrium, and duplicate readings over

a period of 5 hr. were considered satisfactory evidence that thermal equilibrium had been reached. Readings were taken for the ranges 1300° to 1400°F., 2100° to 2300°F., and 3000° to 3100°F.

Measurements on methods of cooling the steel shell followed, while the bottom of the column was held at approximately 3000°F. First, air streams were directed across the steel plate at velocities of about 10, 25 and 50 ft. per second, allowing 24 hr. for reaching equilibrium at each rate. Finally water cooling was employed. This was accomplished by welding strips of metal around the plate to form a shallow box having the plate itself as the bottom. Water was run dropwise onto the plate and the amount needed to maintain a constant depth over the plate as the water vaporized was measured.

RESULTS

The data on temperature gradients summarized in Figs. 3 to 5 represent several types of carbon stock available for lining blast furnaces. Fig. 3 shows the data for carbon stock such as is now used for lining various types of ferroalloy furnaces, and probably the best grade for blast-furnace use. The thermal conductivity at room temperature is 2 B.t.u. per square foot per degree Fahrenheit per hour per foot. Data represented by Figs. 4 and 5 were taken more to make comparisons of materials having different thermal conductivities than with any idea that such materials would be used in lining blast furnaces, since both the porous carbon and the graphite would be much more expensive than the CB-4 (carbon block) material, while the S-grade carbon would be 50 per cent higher in cost. The thermal conductivity of the porous carbon material is 1 B.t.u. per sq. ft. per deg. F. per hr. per ft.; for the graphite material it is 45 transversely and not less than 75 longitudinally, while for the S-grade it is 3 (Table 2).

The general conclusions that can be drawn from the experimental work confirmed the knowledge that carbon is a suitable refractory material and indicated or softening at those temperatures, there is no necessity for cooling the furnace walls, insofar as protection of the carbon lining is concerned. The insulating quali-
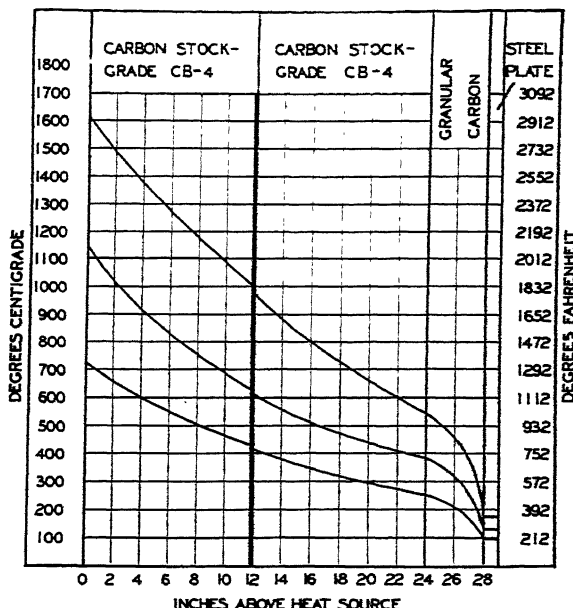

FIG. 3.—TEMPERATURE GRADIENT THROUGH TWO SECTIONS OF GRADE CB-4 CARBON.

that even at the temperatures encountered in a blast furnace it has an application as a lining material for certain parts of the furnace. Since there is no deterioration ties of carbon materials are shown by the temperature-gradient curves for the various grades of materials in Figs. 3 to 5. The equilibrium temperatures to be expected

TABLE 2.—*Thermal Conductivities of Furnace-lining Stock*

| Material	Temperature Range, Deg. F.	Data Source	Heat Flow through Length of Test Column, B.t.u. per Hr. per Sq. Ft.	Transverse, Thermal Conductivity K, B.t.u. per Sq. Ft. per Hr. per Deg. F. per Ft.
CB-4 grade carbon	Room 1000–1800 1800–3000	 Fig. 3 Fig. 3	 1,120 1,120	2 1.4 1.0
S-grade carbon........................	Room 2000–3100	 Fig. 4	 1,170	3 1.2
AGX (graphite)........................	Room 2400–2700	 Fig. 5	 1,255	45 2.7
Carbocell stock (porous carbon)	Room 1100–2000 1100–2200	 Fig. 4 Fig. 5	 1,170 1,255	1 1.1 1.1
Coke particles........................	400–1100	Figs. 3–5	1,120–1,255	0.55
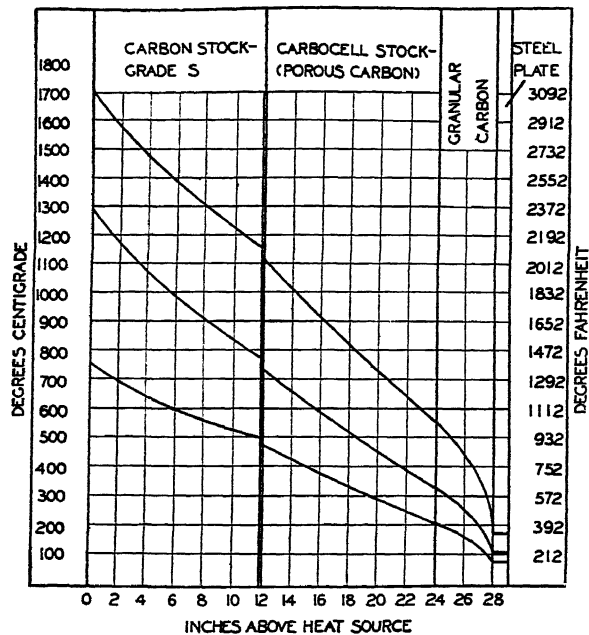
FIG. 4.—TEMPERATURE GRADIENT THROUGH GRADE S CARBON BACKED BY CARBOCELL STOCK (POROUS CARBON).
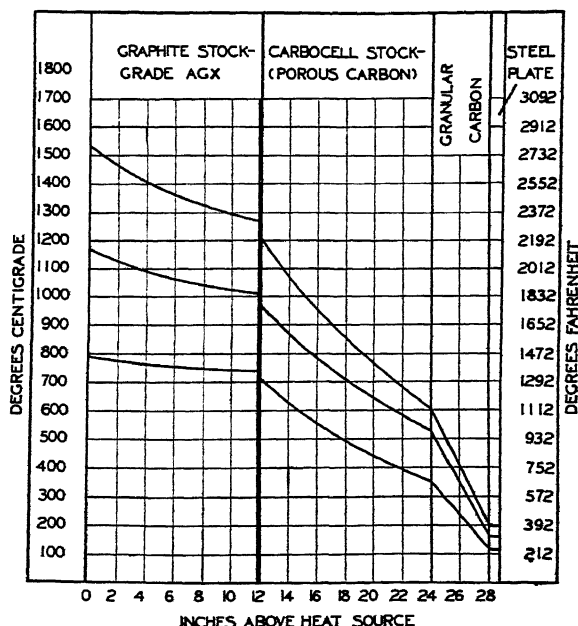
FIG. 5.—TEMPERATURE GRADIENT THROUGH GRADE AGX GRAPHITE BACKED BY CARBOCELL STOCK (POROUS CARBON).

at any point within the lining for any temperature within a furnace may be predicted by interpolation of the curves.

It is clearly evident from the curves that, even when the hot end of the carbon blocks was kept at 3000°F., the maximum temperature to be expected in a blast furnace, the temperature of the plate representing the shell of the furnace is at a relatively low temperature. It is believed that the conclusion may be drawn from the data that a blast furnace lined with carbon up to the mantel may be safely run with no cooling of that part of the furnace, except for the tuyeres. It is presumed that regardless of the data, emergency cooling of some sort would be provided; shower cooling, water troughs or air blast.

Elimination of the expensive plate cooling of the lower half of a blast furnace by the substitution of a simpler form of cooling should markedly reduce the cost of blast-furnace construction. As carbon blocks basically are more expensive than ceramic brick, the saving in construction of the cooling section is important in that the total cost for either type of lining is approximately equal.

The reduction in the amount of water used would be of little importance except when water is scarce or expensive on account of treatment. The reduction in heat losses would probably be of little consequence, not over 2 per cent at a maximum. The reduction in maintenance might be an item of some importance.

It is possible that the fact that the uncooled carbon lining could be operated safely at higher temperatures than the water-cooled bricks would have some value metallurgically, in view of the effect of higher temperatures on silica and sulphur.

An Evaluation of Factors Affecting Iron Oxide in Open-hearth Liquid Steel

By J. E. Gould,* Member A.I.M.E., and H. J. Hand†

(New York Meeting, February 1942)

Many independent studies are being made on slag-metal relationships in the open-hearth furnace, and these studies cannot help but result in an ultimate improvement in the quality of open-hearth steel of both the open and killed types. In maintaining quality control at the National Tube Company's plant, emphasis has been placed on an evaluation of the iron oxide content of the steel in as quantitative a manner as possible, in order that the most desirable level of oxidation might be obtained for a given type of steel, and to secure a more precise basis for final deoxidation. In the past, various methods were used for estimating FeO content of the metal at tap to ensure uniform and thorough deoxidation of killed steel, avoiding overdeoxidation to minimize the amount of inclusions present and to make as sound a steel as possible. For the open-type steels, such control involves obtaining the necessary level of oxidation for the most suitable action of the steel in the molds to provide good surface quality and cross section for the specific grade involved.

While rapid analytical methods are available for determination of FeO in the liquid metal, such methods are still not sufficiently rapid for routine control on the open-hearth floor, nor do such analyses provide information as to what causes high or low FeO values. The method of sampling can still be considered a problem in view of the variability encountered in taking simultaneous duplicate tests. With the accurate rapid methods now available for determining carbon in the metal, estimating slag basicity and obtaining temperatures of liquid metal, it was believed possible to determine the influence of the various furnace reactions in establishing the state of oxidation at a given time. Simultaneous slag and metal tests were used in this analysis, aided by statistical methods, to determine the factors that affect the metal FeO, and also to make a quantitative evaluation of these factors.

Data obtained are from actual furnace operations, the metal test being of the spoon, Herty type, and taken in duplicate. Metal temperatures were taken with the open-tube bath pyrometer developed by the Research Laboratory of the United States Steel Corporation. This method of taking open-hearth metal temperature was invented by Collins and Oseland,[1] and was developed into its present form by L. O. Sordahl,[2] of the Research Laboratory. The instrument and its mode of operation have been fully described by Sordahl and Sosman in three publications.[3,4,5] Slag components were obtained by chemical analysis. Data were taken from four 165-net-ton furnaces during the working period of the heat. Recognizing that additions of ore affect the metal FeO, no tests were included within 30 min. after ore additions. In all, 65 tests (48 heats) were used in this study.

[1] References are shown at the end of paper.

Constituents determined, each of which was considered of potential effect on metal FeO, are shown in Table 1. Also shown are the maximum, minimum, and average values.

TABLE 1.—*Slag and Bath Components Considered, and Range of Variation*

Component, Per Cent	Minimum	Average	Maximum
Steel:			
[C]	0.04	0.28	1.03
[Mn]	0.07	0.13	0.21
[FeO]	0.07	0.19	0.38
Slag:			
(SiO₂)	8.04	12.85	23.40
(CaO)	33.94	43.71	51.08
(P₂O₅)	0.99	1.89	2.79
(MnO)	3.81	6.08	13.29
(FeO)	12.40	18.71	30.85
(Fe₂O₃)	2.35	5.91	9.33
(Total Fe)	12.36	18.62	30.23
$R = \dfrac{\% \, CaO}{\% \, SiO_2 + 0.634 \, \% \, P_2O_5}$	1.70	3.12	5.15
Temperature, deg. F	2890	2967	3055

Fetters and Chipman[6] have developed a method for estimating FeO in the metal from carbon in the metal, total slag FeO, with correction for slag basicity, and they say that by use of this estimation FeO may be predicted within a standard deviation of 15 per cent. By this method of expressing prediction, the absolute accuracy of the prediction decreases as the carbon content decreases or as the FeO of the metal increases. B. M. Larsen[7] considers that the more fundamental factors controlling FeO in the metal are: slag basicity, carbon content, and temperature of the metal; whereas the effect of iron oxide content of the slag is not a primary factor usable directly for control.

The statistical methods employed in the current analysis are those involving multiple correlation, which is an entirely different method of attack from that used by Fetters and Chipman,[6] in that the methods employed herein enabled: (1) evaluation of the *independent quantitative* effect of each factor, even though intercorrelated with other factors affecting FeO in the metal;

(2) the simultaneous consideration of all factors in the determination of [FeO]* in a given case; (3) an estimate of the *importance* of the various factors considered individually or simultaneously on the regulation of [FeO]; (4) a measure of the improvement in the variation in [FeO] values after eliminating the quantitative effect of the influencing factors (this establishes the accuracy within which [FeO] can be predicted). These methods are described by Ezekiel,[8] Wallace and Snedecor,[9] and Smith,[10] discussion of which is beyond the scope of this paper. Suffice it to say that these methods require, because of the multiplicity of the calculations involved, the use of punched tabulating cards and fully automatic calculating machines for completion of calculations within a reasonable period of time. Solution of the equation involved, considering the seven factors used, gives the individual effect of each of the factors. We are also enabled to determine any interdependence existing between the factors.

The seven factors considered in their effect on [FeO] were: carbon, manganese, slag MnO, slag FeO and Fe₂O₃, temperature, and R value.

PRESENTATION OF RESULTS

Since, as aforementioned, the solution of the equation immediately integrates the results of all factors concerned, we have a solution in the empirical equation:

$$x_1 = a + b(f)x_2 + c(f)x_3 + d(f)x_4 + \cdots s(f)x_n \quad [1]$$

where x_1 is the dependent variable and x_2, x_3, etc., are the independent variables being investigated with a, b, c, etc., determining the slope of the relationship.

For carbon, the equilibrium expression at one atmosphere is $K_c = \dfrac{1}{[C][FeO]}$, and in

---

* Brackets refer to metal percentage, parentheses to slag percentage.

the solution of the equation herein the function of this variable has been taken to be the hyperbolic function expressed by the equation, $y = a + \frac{1}{bx}$. In the absence of any contrary evidence, the effectiveness of all other factors was taken to be linear. Subsequent checks were made for curvilinearity on the resultant equation, giving confirmation to these assumptions.

It is interesting to call attention to the approach of the statistical methods of solution. The equations were worked out, direct correlations between the factors obtained, and the interdependent correlations* determined before any attempt at graphical representation of the data was made. Solution of the empirical Eq. 1 gives the following equations for [FeO]:

$$[FeO] = -0.322 + \frac{0.0092}{[C]} + 0.0798[Mn]$$
$$+ 0.0011(MnO) + 0.0019(FeO)$$
$$+ 0.0034(Fe_2O_3) - 0.0067R$$
$$+ 0.00013T_F \qquad [2]$$

$$[FeO] = -0.299 + \frac{0.0092}{[C]} + 0.1188[Mn]$$
$$+ 0.0003(MnO) + 0.0035(Fe)$$
$$- 0.0082R + 0.00012T_F \qquad [3]$$

$$[FeO] = -0.296 + \frac{0.0092}{[C]} + 0.1280[Mn]$$
$$+ 0.0035(Fe) - 0.0085R$$
$$+ 0.00012T_F \qquad [4]$$

Elements are expressed in percentages, R in units, and temperature in degrees Fahrenheit.

All factors studied are included in Eqs. 2 and 3, with Eq. 3 expressing total iron in the slag instead of FeO and Fe$_2$O$_3$ separately as used in Eq. 2. Eq. 4 considers only

those factors found to be of most probable statistical significance with total iron being used instead of FeO and Fe$_2$O$_3$, since Eqs. 2 and 3 account for equal percentages of total variation (90 and 89.2 per cent).

In Eq. 4, the five remaining factors are carbon, manganese, total iron in the slag, basicity, and temperature. Carbon in the metal and total iron in the slag are of unquestionable statistical significance, and the remaining three factors, while in the expected direction, are of inconclusive statistical significance. A more positive statement concerning manganese, basicity, and temperature cannot be made because of the limited amount of data and, more likely, the slight effect that these factors may actually have.

In Table 2, the total percentage of the *separate determinations* is shown to be 89.4 per cent. The interpretation of this value is that this is the percentage of all variation in [FeO] that has been accounted for by the factors considered based upon the data under consideration. The percentage of *direct determination* (72.9 per cent) represents the magnitude of the direct effect of each of the factors (carbon, manganese, total iron in the slag, basicity, and temperature) on [FeO]. The difference between the 72.9 and 89.4 per cent represents the added effectiveness of the *intercorrelation* between these factors.* The figure shown for $\bar{S}(0.0247)$ represents the new standard deviation for the data after evaluating the effective factors. This compares with the original standard deviation of the distribution of 0.075 for all of the [FeO] determinations. Unconsidered variables account for

---

* Direct correlation, as used in this paper, refers to the measured effect of one variable on another with other factors varying at will. Interdependent correlation is interpreted as the effect of one variable on another with all other considered factors *constant*. See Table 4 for direct correlations.

* To illustrate the full implication of separate and direct determination, without mathematical involvement, *all* variation would be accounted for if the percentage of either were 100. If percentage of direct determination is 100, then there is no combined effect between the variables. The difference between separate and direct determination is a measure of the magnitude of joint effects between the variables that are incapable of direct evaluation.

the remaining variation, and it is most reasonable to assume that these unconsidered variables are related to sampling and analytical limitations rather than to mathematical limitations. The greatest evidence substantiating this assertion is that the duplicate tests for [FeO] showed a standard deviation only slightly lower than the $\bar{S}$ found (0.018 was the standard deviation for the duplicate tests).

ganese almost a 50:50 probability of being due to chance alone.

In order to illustrate the degree to which each of the five significant factors affects [FeO], an evaluation has been given in the center portion of Table 2. This is further brought out in Figs. 1 and 2.* As the factor increases from the minimum to the maximum value encountered (as given in Table 1), the FeO can change within the values

TABLE 2.—*Data Relative to Significance and Determination of Factors Studied*

Factor	Significance		Independent Quantitative Effect on FeO from Equation 4	Per Cent Determination from Equation 4	
	From Equation 2	From Equation 3			
	p^a	p^a	Most Probable Value	Separate	Direct
C]....	Less than 1 in 1 billion	Less than 1 in 1 billion	From 0.05–0.06 % C, FeO decreases 0.031 % From 0.10–0.11 % C, FeO decreases 0.008 % From 0.30–0.31 % C, FeO decreases 0.001 % From 0.60–0.61 % C, FeO decreases 0.0005 %	+77.0	67.4
[Mn].... (MnO)... (FeO).... (Fe₂O₃)... (Fe)..... R........ Temperature....	3 out of 5 4 out of 5 1 out of 3 1 out of 3 1 out of 3 1 out of 4	2 out of 5 9 out of 10 1 out of 50 1 out of 4 1 out of 4	+0.006 % FeO for 0.05 % Mn increase +0.0035 % FeO for 1 % Fe increase −0.004 % FeO for 0.05 R increase +0.012 % FeO for 100°F. increase	−4.6 +15.6 −1.4 +2.8	0.6 4.4 0.4 0.1
			Total per cent accounted for..........	89.4	72.9

a Probability that effect of factor is due to chance.
Standard deviation of error (S) considering all variables.......................... 0.0247.

The prime importance of carbon in determining the [FeO] is evident from Table 2, since it accounts for three fourths (77 per cent separate determination) of the total variation explained, and the effect of carbon from Eqs. 2 and 3 can be due to chance less than one time in one billion. The significance of the effect of total iron in the slag is brought out by the probability that this effect could be due to chance is one time out of fifty. The measured effect of iron in the slag as compared with carbon indicates the total iron in the slag to be about one fifth as important. The effects of manganese, basicity, and temperature, if real, are small. Statistically, basicity and temperature have a one out of four probability of being a chance effect, with man-

shown in Table 3. It is well to bear in mind that in considering each of the factors—for

TABLE 3.—*Change in FeO*

Variable	Per Cent [FeO]		
	For Minimum of Variable	For Maximum of Variable	For Range of Variable
[C]	0.12	0.34	0.22
(Fe)	0.16	0.23	0.07
T₁	0.18	0.20	0.02
R	0.17	0.20	0.03
[Mn]	0.18	0.20	0.02

example, total iron in the slag—when that factor is considered, the other four factors are at their average value.

* The numeral beside each point indicates number of results used in obtaining value.

Previous investigators, from theoretical considerations, have shown values for the FeO-carbon equilibrium product from 0.008 to 0.01. It is interesting to note that

FeO in the metal is shown, with all other factors maintained at their average value. The points shown are adjusted to the average value for each of the remaining vari-
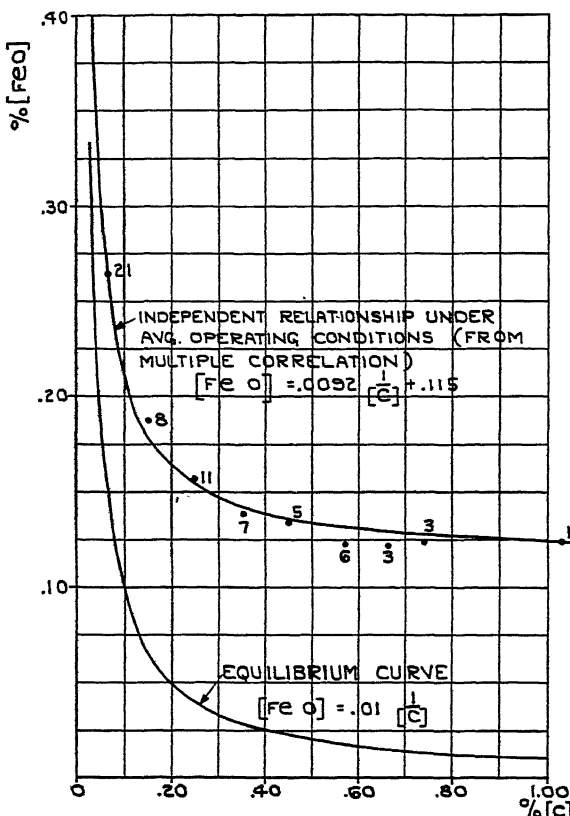

FIG. 1.—RELATIONSHIP BETWEEN CARBON AND FeO IN METAL (OTHER OBSERVED FACTORS CONSTANT).

the statistical considerations here have shown this constant to be 0.0092, with a constant supersaturation for all carbon contents. In Fig. 1, this supersaturation is shown to be 0.115 per cent, this being the difference between the two equations as follows:

Equilibrium curve $[FeO] = \dfrac{0.01}{[C]}$

Developed curve $[FeO] = \dfrac{0.0092}{[C]} + 0.115$

In Figs. 1 and 2, the direct relationship between the factor considered and per cent

ables; for example, a point plotted on the carbon curve (Fig. 1) is for the average (Fe), [Mn], R, and temperature for all of the data. The close agreement of these data with the curves is apparent, except with that for residual manganese, and indicates that the linear curves for all but carbon are probably the best fit. For carbon, the hyperbolic curve is virtually a perfect fit. A word of caution is necessary at this point; that is, that extrapolation beyond the range actually encountered for the variable considered may be precarious. To illustrate

this, additional data were obtained with total iron less than 12 per cent (not used in this analysis), which indicated that below this value the effect on [FeO] became

becomes more basic in character, the available iron in the slag for reduction becomes less, because of formation of stable lime ferrites.
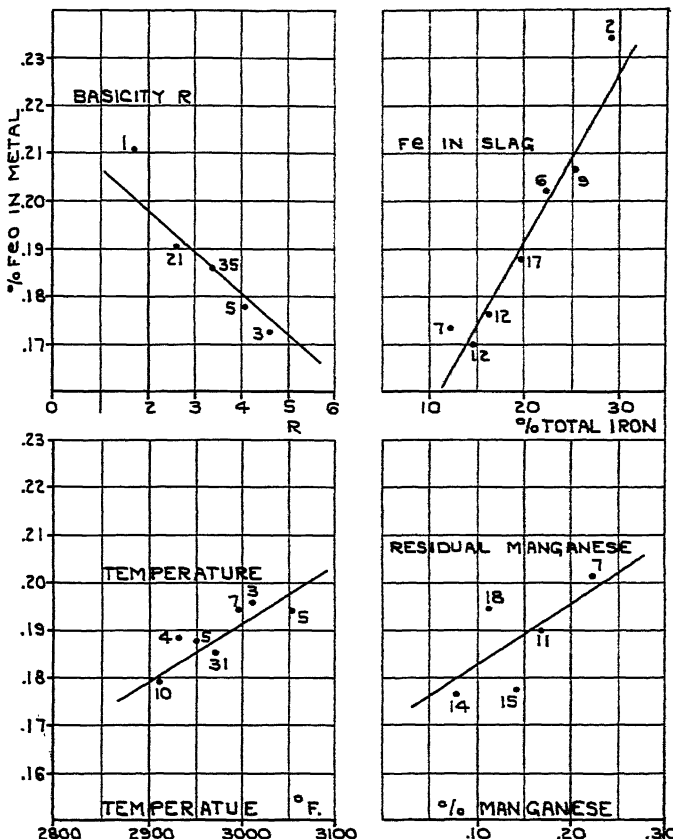

FIG. 2.—INDEPENDENT RELATIONSHIPS OF BASICITY, FE IN SLAG, TEMPERATURE AND RESIDUAL MANGANESE WITH FeO IN METAL.

negligible. It will further be noted that [FeO] increases with increasing temperature, but decreases with increasing basicity. The reason for the latter is not readily apparent, but Fetters and Chipman[6] found this to be true, and an additional check made by the present authors on data from another plant also confirmed it. The explanation may be related to the fact that the direct correlation between slag basicity and [FeO] is positive, but as the slag

In Fig. 3, a comparison between direct correlation of carbon and metal FeO obtained from our data and that obtained by Fetters and Chipman[6] is shown. Also included is the curve from Fig. 1, showing the independent relationship of carbon unaffected by (Fe), [Mn], temperature, and R. The intercorrelation of these factors affects the curve to the extent that [FeO] is shown as too low at high carbons and too high at low carbons, simply because the

direct correlation curve does not strictly follow the hyperbolic curve as does the independent curve.

Since the carbon relationship as already

from the carbon effect can be visualized. While carbon is the most important single factor on the whole in its effect on [FeO], it is clearly seen from this figure that above
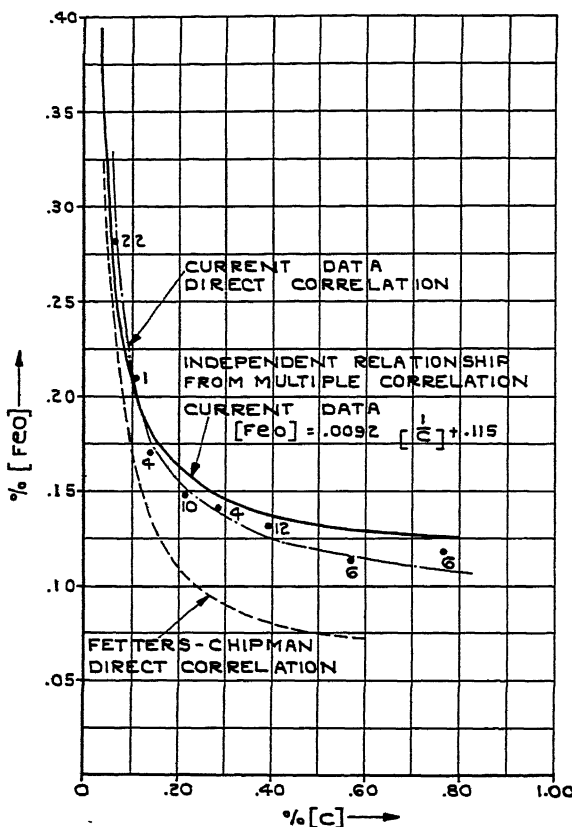


FIG. 3.—DIRECT CORRELATION OF CARBON WITH METAL FeO, COMPARED WITH INDEPENDENT RELATION AND FETTERS-CHIPMAN DIRECT CORRELATION.

shown is for the *average* value of the effective factors, it would be interesting to perceive the effect of carbon on [FeO] for extreme values of total Fe in slag and of temperature. This is shown in Fig. 4. In the upper part of the curve the carbon-FeO relationship is shown for 10 per cent and 30 per cent Fe in slag. The in-between curve is the relationship between carbon and [FeO] with the average (Fe) value at *each* of the *carbon* points rather than the average for all points. In this figure the magnitude of the effect of (Fe) on [FeO] as distinct

0.20 per cent carbon total Fe in slag is a very important consideration. The lower curve in a similar manner illustrates the minor effect of temperature.

In working through the statistical methods employed it is possible to obtain the direct correlation between all of the variables studied with but little additional effort. In Table 4, these correlation values are given (perfect correlation is 1). Attention is directed to the fact that carbon correlates very well with all of the factors studied except basicity. Accordingly, the

value of the other factors affects carbon, and in that manner considerable variation in relationship between carbon and [FeO] is possible, depending upon the types of slags carried on the bath. The authors believe that the only satisfactory manner in which

SUMMARY

The object of this study has been to determine and evaluate mathematically the factors affecting FeO in open-hearth liquid metal. It has been found that carbon is of paramount effect, total Fe in slag is second
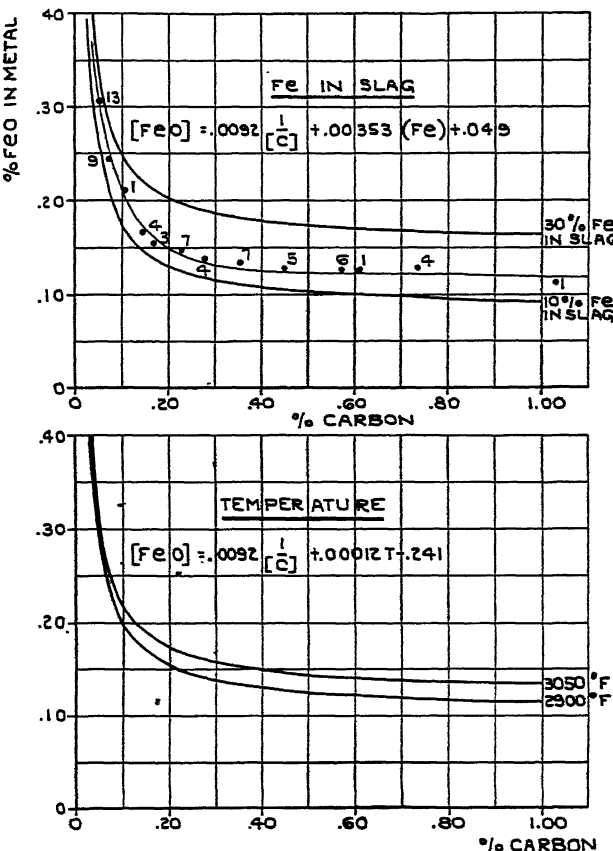

FIG. 4.—EFFECTS OF CARBON ON FeO IN METAL AS INFLUENCED BY EXTREME VALUES OF TOTAL FE IN SLAG AND TEMPERATURE.

this true relationship can be established is by a method that makes due allowance for all these other factors (statistical approach to steel-plant data) or by keeping them constant (virtually impossible even with laboratory methods). Note also that [FeO] has a high correlation constant with several of the factors, each of which is of probable significance, as shown from the multiple correlation study.

in importance, and temperature, basicity of slag, and residual manganese may be statistically significant in effect; but such effect, if real, is minor in magnitude. The influencing factors have been found to account for 90 per cent of variation in FeO in metal and enables it to be determined mathematically almost as accurately as duplicate tests will analyze. The carbon relationship as determined statistically

TABLE 4.—*Summary of Direct Correlations: Slag, Bath Composition and Temperature*

Factor	[Mn]	(FeO)	(Fe₂O₃)	(Fe)	(MnO)	R	Temperature	[FeO]
[C]	−0.625	+0.764	+0.579	+0.747	−0.390	+0.216	+0.508	+0.944
[Mn]		−0.741	−0.574	−0.719	+0.807	−0.286	−0.139	−0.575
(FeO)			+0.828	+0.988	−0.540	+0.464	+0.175	+0.750
(Fe₂O₃)				+0.886	−0.511	+0.542	+0.013	+0.584
(Fe)					−0.550	+0.515	+0.161	+0.742
(MnO)						−0.494	−0.066	−0.341
R							−0.009	+0.192
Temperature								+0.497

$n = 65$.
r (correlation coefficient) must exceed 0.363 in order to be significant.

from actual data has been found to fit the thermodynamic equilibrium curve with a constant supersaturation.

ACKNOWLEDGMENT

The authors wish to acknowledge the help furnished by R. W. Dilworth, D. B. Collyer, and A. Messig in performing the calculations required to set up the multiple correlation equations; to I. H. Schaible for collecting the open-hearth data; and to the National Tube Co. for permission to publish the findings of this investigation.

REFERENCES

1. U. S. Patent No. 2020019 (Nov. 5, 1935).
2. U. S. Patent No. 2184169 (Dec. 19, 1939).
3. Sordahl and Sosman: *Instruments* (May 1940) 13, 127–130.
4. Sordahl and Sosman: *Steel* (May 20, 1940) 106 (21), pp. 44–47.
5. Sordahl and Sosman: Temperature, Its Measurement and Control in Science and Industry," American Institute of Physics, 1941, pp. 927–936.
6. Fetters and Chipman: Slag-metal Relationships in the Basic Open-hearth Furnace. *Trans.* A.I.M.E. (1940) 140, 170.
7. B. M. Larsen: Controlling Reactions in the Open-hearth Process. *Trans.* A.I.M.E. (1941) 145, 67.
8. M. Ezekiel: Methods of Correlation Analysis. New York, 1941. John Wiley and Sons.
9. H. N. Wallace and G. W. Snedecor: Correlation and Machine Calculation. Iowa State College, Division of Industrial Science, Department of Mathematics (January) 1925.
10. B. B. Smith: The Use of Punched-Card Tabulating Equipment in Multiple Correlation Problems. U. S. Department of Agriculture, Bureau of Agricultural Economics (October) 1923.

DISCUSSION

(*T. S. Washburn presiding*)

R. C. Good,* Pittsburgh, Pa.—Have the authors found it possible to use the developed formula to calculate the loss of manganese from additions made to the steel in the furnace prior to tapping?

K. L. Fetters,* Pittsburgh, Pa.—The authors' utilization of the methods of multiple correlation directs attention to the wide and fruitful field that awaits investigation by such methods.

Fetters and Chipman[6] used partial correlation methods to express the FeO in the metal in terms of the carbon in the bath and the FeO in the slag. They determined values of the constants f, g, and h for a great many heats for the equation

$$[FeO]_M = \frac{f}{C} + g(FeO)_{Total} + h$$

Their data included heats from eight different producers of steel and the only subclassification that was made was the division of the data into several ranges of slag basicity. On looking back at that paper, it is now evident that the tests from one of the plants (or perhaps more) were not consistent with the indications of the balance of the data. Much improved accuracy of estimate, approaching that of the present authors, might have been obtained by elimination of these now questionable data. Similarly, had the data of Gould and Hand been available at the time of this previous study, they would have been inconsistent with the general indications of the balance of the data. This does not detract in any way, however, from the validity of the conclusions reached by Gould and Hand, and certainly the results show good consistency for their plant. There is also added accuracy to be gained in the allowance that has been made for temperature in the present case, which could not be done in the previous instance

* Metallurgical Engineer, Electro Metallurgical Co.

* Assistant Professor of Metallurgy, the Carnegie Institute of Technology.

because of the unavailability of temperature determinations. Fig. 5 shows the generally accepted average value of the carbon-oxygen relation for open-hearth data, and in the same
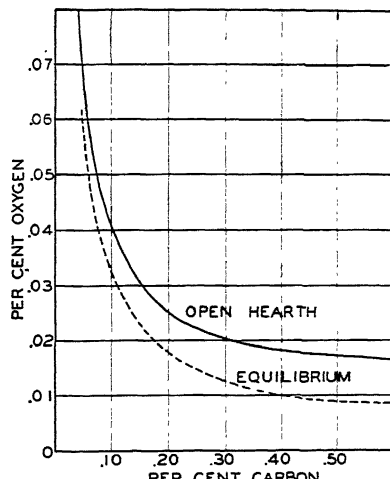

FIG. 5.—CARBON-OXYGEN RELATIONS IN THE OPEN HEARTH AND AT EQUILIBRIUM.

figure the equilibrium curve based on the recent Marshall-Chipman[7] work. The present results are well above the usual open-hearth values. and the present authors' plot of the equilibrium curve in their Fig. 1 is from earlier data and represent lower values than are accepted at present.

The high values that Gould and Hand show for the carbon-oxygen product based on their tests are undoubtedly to be explained by their sampling method, which involves the repouring of tests and which previously has been found to give higher and more erratic oxygen results than does the bomb test.

The authors' Fig. 2 calls for some comment. This figure shows the independent relationship between the FeO in the metal and other variables of interest. In each case, the trends have been determined by the methods of multiple correlation, and purport to show the relation between just two variables with all other variables at their average value. This statistical concept should not be confused with any physicochemical implication where such constancy of all but two of the components of a reaction is impossible. An instance will make

[7] S. Marshall and J. Chipman: Trans. Amer. Soc. Metals (1942) 30, 695–741.

this clear. The authors show that as the manganese in the bath increases (with all other variables at their average value), the FeO in the bath increases. Now consider the reaction

FIG. 6.—PETROGRAPHIC THIN SECTION OF OPEN-HEARTH FINISHING SLAG SHOWING UNDIS-SOLVED DICALCIUM SILICATE. × 100.

between FeO in the metal and manganese in the metal according to the equation:
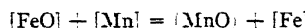
$$[FeO] + [Mn] = (MnO) + [Fe]$$

The equilibrium constant for this reaction may be written as:

$$K = \frac{a_{FeO} \times a_{Mn}}{a_{MnO} \times a_{Fe}} \quad \text{or}$$

$$K' = \frac{[FeO] \times [Mn]}{(MnO) \times [Fe]}.$$

The likelihood is small that the FeO and the manganese in the metal both increase at constant values of the other variables. Independent relations as determined statistically by the methods of multiple correlation are therefore not to be confused with the physicochemical relations that may exist between the same variables.

One should always temper conclusions that have been drawn on the basis of the chemical analyses of slag samples, since these analyses may include undissolved phases as well as those which were liquid and therefore effective in the slag-metal reactions. Fig. 6 shows the appearance of the petrographic thin section of a slag typical of many open-hearth finishing slags. The "blocks" are dicalcium silicate, Ca_2SiO_4, that was not in solution in the liquid slag but

that would have been determined by analysis. It would be of interest to study the slag-metal relations between a series of slag and metal samples where all the slag samples represented slags in which all phases were in solution and therefore effective.

The stated purpose of this paper is to set up better methods for estimation of the FeO in the metal than heretofore were available. It seems pertinent, therefore, to ask the authors how the method works in practice, and how many of the factors they find it necessary to determine to estimate the FeO in the metal with usable accuracy for deoxidation calculations.

G. SOLER,* Canton, Ohio.—The paper presented by Gould and Hand appears to have immediate practical value. Carbon is shown to be the major factor in the control of FeO in open-hearth liquid metal, with total Fe in the slag as a secondary factor. Temperature exerts only a minor effect.

In steelmaking practice a definite oxygen end point governed by oreing down to a constant carbon could be attained when the heat is tapped and carbon to meet the final analysis is added to the ladle. The final deoxidizing additions of aluminum and silicon could be made to the steel based on the total iron content of the slag. This type of control would be especially valuable in the making of semikilled steels. In the making of fully killed steels, usually a surplus of deoxidizing agents is added, consequently such close control methods would not be fully utilized.

J. E. GOULD and H. J. HAND (authors' reply). In reply to Mr. Good's question: No attempt has been made to calculate the loss of manganese from final additions, although possibly this could be done by estimating the FeO in the metal from the carbon and total iron in the slag and correlate this estimate with the actual manganese loss.

* Manager Research and Mill Metallurgy, The Timken Roller Bearing Co., Steel and Tube Division.

We agree with Dr. Fetters that statistical concepts must not be confused with established physicochemical concrete implications, and Dr. Fetters correctly questions the validity of increase in FeO in the metal with increased residual manganese. However, attention is called to Table 2, which indicates that the effect of residual manganese on FeO in the metal is due to chance, which is 3 in 5 from Eq. 2 and 2 in 5 from Eq. 3. It is very likely, then, that the indicated effect of [Mn] on [FeO], as shown in Fig. 2, is due entirely to chance, and certainly is due to its conflict with established physicochemical theory. It would probably be better to consider residual manganese along with MnO in slag as ineffective factors. As to how the method works in practice, we would state that carbon and total iron in the slag would be the only factors required in any practical program for utilizing the information in connection with deoxidation. Actually, for low-carbon steels under 0.10 per cent carbon, carbon in the bath would probably be sufficient, except for a wide variation of total iron in the slag. For intermediate carbon steels, up to, say, 0.25 per cent carbon, both carbon content and total iron in the slag would be necessary, and for high-carbon steels the total iron in the slag would be sufficient.

In reply to Mr. Soler's remarks, we would state that the greatest utilization of our data is made on fully killed steels, to avoid adding too great a surplus of deoxidizing agents, particularly additions of aluminum and silicon.

It might be added, also, that extensive developments are occurring in the field of applying methods of multiple correlation which serve to speed up the calculation technique and develop methods designed to answer other pertinent questions in connection with the problem involved. While in this investigation iron oxide in the metal was made the independent variable, in other studies it could serve as a dependent variable and determination could be made of its effect.

Distribution of Manganese and of Sulphur between Slag and Metal in the Open-hearth Furnace

By L. S. Darken* and B. M. Larsen,* Member A.I.M.E.

Some years ago we collated all laboratory data then available to us on the distribution at equilibrium of manganese and of sulphur between metal and simple slags, and used the results in setting up an equation, which proved to be in accord with determinations of the distribution ratio of manganese and of sulphur between liquid steel and open-hearth slag, over a wide range of operating conditions. We now present an outline of our calculations and inferences on these two closely related questions, which are of especial importance because of the advisability of conserving manganese wherever possible. In general, our results show that in the open-hearth furnace equilibrium between metal and slag, with respect to both manganese and sulphur, is substantially attained during the finishing period of the heat, or in about a half hour to an hour after any additions were made. This implies that the end result will be identical whether manganese is added as alloy or metal to the liquid steel or as oxide to the slag. The proportion of total manganese retained by the steel is favored: (1) by use of the minimum amount of lime, consistent with other operating limitations, required to give a lime-silica ratio of about 2.4, which usually corresponds to a minimum practical slag volume; (2) by a high concentration in the slag of MnO relative to FeO; (3) by high operating temperature. Absorption of sulphur by the slag from the liquid metal is

favored: (1) by large slag volume; (2) by a high concentration of active (or "free") lime and of manganese oxide dissolved in the slag; (3) by low concentration of silica, iron oxide, and phosphate dissolved in the slag.

Distribution of Manganese between Slag and Metal at Equilibrium

On the basis that the distribution of manganese between liquid steel and slag is controlled by the reaction

$$\text{FeO} + \text{Mn} \rightleftharpoons \text{MnO} + \text{Fe} \quad [A]$$
$$\text{slag} \quad \text{metal} \quad \text{slag} \quad \text{metal}$$
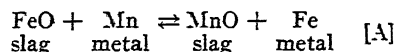
the distribution at equilibrium, at a given temperature, is expressed by the equilibrium constant for this reaction, which is defined as

$$K'' = \frac{a_{MnO} \cdot a_{Fe}}{a_{FeO} \cdot a_{Mn}} \quad [1]$$

where a is the activity of the molecular species denoted by the subscript. The activity of each of the several components, although it is not known precisely, is approximately equal to the concentration of each component expressed as its mol fraction; that is, as the ratio of the number of mols of the given component to the total number of mols of all the molecular species present in the metal or slag, as the case may be. Moreover, since the activity, or concentration, of iron in the liquid metal is in fact substantially constant, the term a_{Fe} may be combined with K'' to give a new constant K'. Making these changes,

and rearranging, Eq. 1 may be written:

$$[Mn] = \frac{(MnO)}{(FeO)} \times \frac{1}{K'} \qquad [2]$$

where $[Mn]$ represents* the mol fraction of manganese in the metal and (MnO) and (FeO) represent that of MnO and FeO respectively in the slag.

Inasmuch as the total number of mols in the metal (per unit weight) is sensibly constant, $[Mn]$ is directly proportional to the weight per cent of manganese, and it is convenient to express it in this manner. Moreover, since the total number of mols in the slag appears in both numerator and denominator of the ratio $(MnO)/(FeO)$ it cancels out; so that in this case we may simply use the number of mols of MnO and FeO present in any given amount of slag, which for convenience, we have taken as 100 grams. For practical use, therefore, it is convenient and sufficient to use Eq. 2 in the form

$$[Mn]_w = \frac{1}{K} \times \frac{(MnO)}{(FeO)} \qquad [3]$$

where K is a new constant.

This relation shows that the concentration of manganese in the metal is controlled by the *ratio* of the concentration (activity) of MnO in the slag to that of FeO, and that for the simple system represented by reaction A, the weight per cent of manganese in the metal at a given temperature can be predicted from observed values of this ratio, provided the value of the constant K for that temperature is known.

---

* In accordance with usage, brackets denote the concentration of a constituent in the metal phase; parentheses, that of a constituent of the slag. If the symbol for a given constituent appears in italics, the concentration is expressed as a mol fraction; that is, as the number of gram-molecular weights of the given constituent divided by the total number of gram-molecular weights of all the molecular species present. If the symbol for the constituent is in Roman type, the concentration is expressed as mols per 100 grams of slag or metal, as the case may be. The subscript w after the parenthesis or brackets indicates that the concentration is expressed in weight per cent as determined directly by chemical analysis.

A laboratory determination of this constant for a wide range of temperatures has been made by Körber[1] with results that can be represented, in terms of our units, by the equation

$$\log K = \frac{10710}{T} - 2.877$$

where T is expressed in degrees absolute on the Fahrenheit scale; thus the necessary data for the simple system are at hand. In the open-hearth furnace, the slag is, however, a much more complex system than that involved in the simple reaction A; hence, in endeavoring to apply Eq. 3 to open-hearth data, we are forced to make some simplifying assumptions with respect to the constitution of the slag. These are:

1. That all the manganese in the slag is present as free MnO.

2. That all the iron in the slag is present either as free FeO or Fe_2O_3.

3. That all the Fe_2O_3 is in effect reduced to FeO at the slag-metal interface according to the reaction

$$Fe_2O_3 + Fe \rightarrow 3FeO \qquad (B)$$
$$\text{slag} \qquad \text{metal} \qquad \text{slag}$$
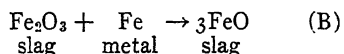
so that each mol of Fe_2O_3, as determined by analysis, is equivalent to 3 mols of FeO. On this basis the total equivalent FeO* is the sum of the FeO existing as such and the FeO equivalent to the Fe_2O_3 present; throughout this paper this total equivalent FeO is used whenever the concentration of FeO is involved.

4. That the influence of the other oxides present in significant quantity in the slag—specifically, CaO, P_2O_5, SiO_2—can be char-

---

[1] References are at the end of the paper.
* The calculation of the equivalent FeO is illustrated by the following example: Suppose a slag contains 14 per cent FeO and 2.5 per cent Fe_2O_3 per 100 grams of slag. There are, therefore, $14/72 = 0.195$ gram mol of FeO and $2.5/160 = 0.0156$ gram mol of Fe_2O_3. But each mol of Fe_2O_3 is, according to reaction B, equivalent to 3 mols of FeO; hence, the equivalent FeO is $0.195 + 3 \times 0.0156 = 0.242$ mol FeO per 100 grams slag.

acterized by an appropriate coefficient, commonly called the basicity ratio, which expresses the effective concentration of CaO in relation to that of SiO_2. The very small residual concentration of phosphorus in the metal indicates a very small degree of dissociation of the lime phosphate compounds in the slag, and we assume, as has been done by others, that it combines with lime to form $4CaO \cdot P_2O_5$, an assumption that yields satisfactory results not only in correlating observations on the actual distribution of manganese between slag and metal, but, as is shown later, yields satisfactory results for the analogous distribution of sulphur. As a matter of fact, as long as the concentration of P_2O_5 in the slag is 3 per cent or less, it makes little difference whether one assumes the compound present in the slag to be $4CaO \cdot P_2O_5$ or $3CaO \cdot P_2O_5$.

On this basis, the ratio L of the concentration of "effective" CaO to that of SiO_2 is

$$L = \frac{(CaO) - 4(P_2O_5)}{(SiO_2)}$$

which is a measure of the number of mols of CaO that are available for combination with each mol of silica, or of other oxide aside from P_2O_5. Thus, a ratio of 2 signifies that 2 mols of CaO are available for combination with each mol of SiO_2.

With the aid of the above set of assumptions, we can compare the concentration of manganese in the metal as calculated by means of Eq. 3 with that observed in open-hearth practice, and can estimate how the presence of an appreciable amount of other oxides influences the distribution of manganese between slag and metal. In order to make such a comparison, we collected a group* of more than 100 fairly complete analyses, both of slag and of metal, of samples taken from basic open-hearth heats, covering a wide range of composition

of both steel and slag, in which the following favorable conditions obtain: (1) the bath temperature appeared to be satisfactorily measured; (2) the composition of both slag and metal was obtainable by analysis of substantially simultaneous samples; (3) the final reactions were proceeding slowly enough to justify belief in a reasonably close approach to equilibrium between slag and metal. The manganese content in the metal, calculated from these data, by means of Eq. 3 and of Körber's values for the equilibrium constant K, was compared with the result of direct determinations of manganese in the metal, as is illustrated in the following typical example. The available data were:

Temperature 2910°F., for which $K = 2.0$
The metal contained 0.32 per cent Mn
The slag contained 10.95 per cent MnO,
    14.0 per cent FeO,
    2.5 per cent Fe_2O_3

In 100 grams of slag there were 10.95 grams or 0.154 gram mol of MnO; the equivalent FeO, as used in Eq. 3, is 0.242 mol; hence,

$$[Mn]_x = 1\tfrac{1}{2} \times \frac{0.154}{0.242} = 0.28$$

which compares very well with the observed value of 0.32 per cent. In this case, the ratio M of the observed to calculated value of $[Mn]$ is 0.32 0.28 or 1.14.

The results of the whole series of comparisons made as just outlined are given in Fig. 1, in which, for the sake of clarity, the ratio M has been plotted as a function of the basicity ratio L as defined earlier.

the literature, particularly in the papers listed below:

A. N. Diehl: Yearbook, Amer. Iron and Steel Inst. (1926) 404-440.
H. Schenck: *Archiv Eisenhüttenwesen* (1929-30) 3, 505-530.
E. Maurer and W. Bischof: *Ergebnisse der angew. Physik Chem* (1931) 1, 109-197.
P. Bardenheuer and Thanheiser: *Mitt. K. W. I. Eisenforsch.* (1935) 17, Abt. 280.
Our own data, available when these calculations were made, are presented in Table 1.

TABLE 1.—*Slag and Metal Analyses*

Heat No.	Test No.	Temp. °C	Metal %C	Metal %Mn	Metal %S	Slag %S	Slag %SiO₂	Slag %CaO	Slag %Fe₂O₃	Slag %FeO	Slag %MnO	Slag %P₂O₅	Slag %MgO
I	1	1540	0.80	0.28	0.075	0.157	26.3	40.5	3.1	7.5	11.6	2.9	4.3
	2	1550		.24	.059	.233	22.3	39.0	3.6	9.6	14.2	2.8	4.7
	3	1565	.18	.24	.064	.288	19.7	43.0	4.3	10.3	12.6	2.6	5.4
II	1	1540	.80	.24	.062	.178	24.3	43.0	4.3	5.2	11.1	3.0	6.9
	2	1550	.70	.24	.061	.253	23.5	40.0	4.8	7.2	11.6	3.4	5.7
	3	1560	.50	.22	.064	.247	22.0	40.5	6.3	8.5	11.6	3.1	5.4
	4	1570	.21	.20	.069	.288	20.0	40.5	6.7	10.7	10.1	2.8	6.7
	5	1575	.09	.20	.064	.302	16.8	44.5	9.4	9.5	8.8	2.4	6.9
III	1	1535	.52	.16	.067	.274	16.9	47.0	6.9	14.3	4.1	2.7	3.3
	2	1565	.13	.16	.056	.356	15.9	46.5	8.0	10.8	8.3	2.6	2.7
IV	1	1540		.10	.060	.178	19.6	48.0	8.6	10.3	3.9	4.1	2.5
	2	1570		.16	.044	.274	15.4	44.0	10.0	12.2	10.2	3.2	2.7
A	1	(1530)?	.46	.12	.066	.123	23.1	42.5	5.0	10.95	6.2	3.7	2.5
	2		.24	.26	.055	.343	20.7	41.5			14.5	2.6	3.3
	3	1560	.19	.29	.055	.210	20.0	42.5	.86	13.40	13.4	2.7	2.9
VI	1	1535	.50	.11	.069	.123	23.0	44.0	6.44	10.9	6.4	3.2	3.1
	2	1530	.28	.18	.058	.247	20.8	41.5	3.58	12.2	13.4	2.7	2.5
	3	1560	.16	.19	.051	.192	19.0	45.0	6.58	10.2	10.5	2.8	2.5
VII	1	1535	.27	.12	.064	.164	20.4	49.5	7.86	7.7	4.5	3.2	3.6
	2	1560	.22	.12	.057	.302	16.5	44.5	5.72	12.9	10.9	2.7	3.3
	3	1570	.13	.20	.043	.343	16.5	45.0	7.86	11.0	10.8	2.8	3.6
VIII	1	1540	.09	.06	.057	.274	12.4	37.0	10.4	24.8	4.1	2.0	5.4
	2	1560	.08	.08	.048	.288	11.4	39.75	12.3	21.8	3.6	1.7	4.9
	3	1575	.08	.08	.046	.302	11.0	39.5	11.6	23.1	3.5	1.7	5.4
	4	1580	.08	.08	.045	.343	10.3	42.0	12.15	23.2	3.1	1.5	7.8

Heat	Test												
IX	1	1545	.47	.08	.084	.137	23.6	43.0	4.72	9.9	5.2	3.8	5.8
	2	1560	.25	.08	.076	.137	23.1	43.0	5.29	9.4	4.9	3.8	6.3
	3	1590	.07	.08	.070	.206	19.8	44.5	6.58	13.4	4.4	3.2	5.1
	4	1595	.09	.18	.062	.274	16.5	47.0	7.00	13.0	5.2	2.7	5.8
X	1	1540	.10	.08	.058	.315	14.8	43.0	9.44	17.3	4.1	2.8	6.2
	2		.05	.08	.039	.302	13.2	46.0	8.08	16.9	3.6	2.7	5.1
	3	1570	.11	.12	.040	.383	11.8	45.75	8.51	19.1	4.1	2.3	4.9
XI	1	1530	.08	.08	.062	.274	15.4	43.0	8.3	19.6	5.0	2.7	3.8
	2	1560	.09	.08	.056	.274	14.85	45.0	12.4	15.8	4.5	2.4	4.2
	3	1565	.08	.08	.048	.274	13.65	45.5	11.6	16.6	4.2	2.6	3.6
	4	1575	.07	.12	.045	.288	12.35	43.5	10.4	18.9	5.3	2.1	5.3
XII	1	1535	.14	.12	.084	.226	24.4	45.5	5.3	8.1	5.8	2.7	6.5
	2	1550	.14	.27	.076	.274	21.4	48.0	6.7	6.8	6.5	2.1	6.0
	3	1570	.10	.22	.061	.398	18.8	49.0	7.0	7.9	6.5	2.3	5.3
XIII	1	1540	.19	.12	.106	.178	20.4	49.5	6.9	13.1	5.5	3.0	3.6
	2	1540	.13	.24	.077	.480	16.4	50.5	7.4	10.7	5.2	2.7	2.2
	3	1565	.10	.16	.054	.549	14.0	51.5	7.4	12.6	5.7	2.2	3.4
XIV	1*	1575	.24	.10	.039	.261	12.6	40.0	14.3	17.4	4.6	2.5	8.2
	2	1595	.08	.18	.038	.274	12.1	44.0	11.5	16.3	10.3	1.9	4.2
XV	1*	1560	.10	.08	.044	.377	14.6	49.0	8.58	12.9	4.65	3.2	4.5
	2	1580	.13	.12	.038	.377	12.6	49.0	7.29	14.7	6.72	2.8	3.8
XVI	1*	1565	.06	.06	.061	.329	15.4	41.5	10.01	16.7	4.65	3.1	4.9
	2	1585	.09	.20	.046	.425	15.4	41.5	8.72	12.2	11.88	3.1	4.2

Note: The first test in each heat was taken shortly after complete melt-down (except those marked *), the final test shortly before tap. Bath temperature was measured by optical pyrometer, sighted on dark bubbles in the slag, with a correction determined by comparison with two other methods; it was also compared to the tapping temperature on the stream leaving the furnace.

If there were perfect agreement between calculated and observed values for $[Mn]_{ur}$, the points would lie on a horizontal straight line corresponding to the ratio $M = 1.0$.

FeO are substantially free rather than combined with SiO_2 or other oxides; or more generally, that both MnO and FeO are combined to the same extent; moreover,
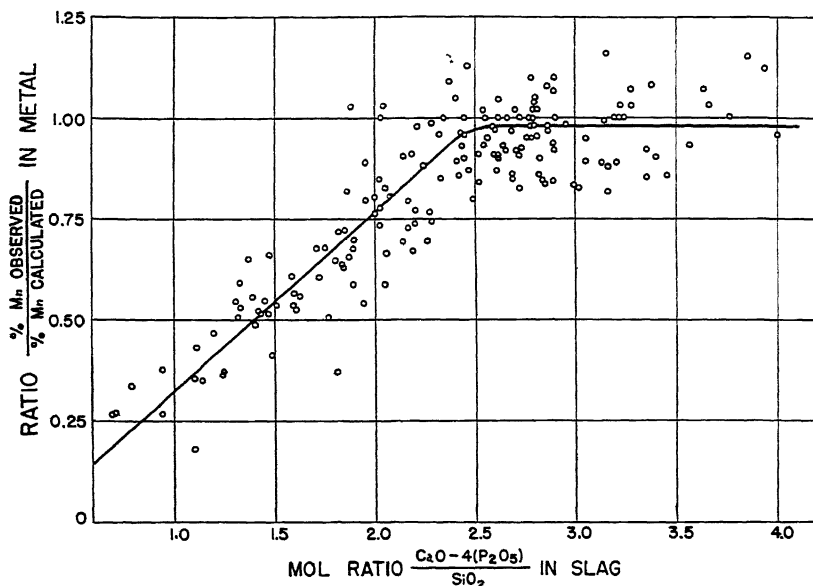

FIG. 1.—COMPARISON OF RATIO M OF OBSERVED TO CALCULATED RESIDUAL MANGANESE IN OPEN-HEARTH HEATS AS RELATED TO LIME-SILICA RATIO L.

In view of the probable inaccuracies in the data, arising from errors in sampling and analysis from errors in temperature measurement and from possible lack of attainment of equilibrium (since it is difficult to be sure in practice that equilibrium is in fact established) perfect correlation is not to be expected; the scatter, as shown in Fig. 1, proves to be surprisingly small and the general trend is clearly evident.

When L is greater than about 2.4, M is reasonably constant and is close to unity, indicating that over this range of basicity the manganese concentration in the open-hearth bath can be calculated with satisfactory accuracy from the equilibrium constant for the simple reaction represented by reaction A, on the basis of the specific assumptions made. From this it is inferred that, whenever L exceeds the value of about 2.4, the molecules of both MnO and

that the Fe_2O_3 indicated by analysis behaves as though it were FeO of equivalent oxygen content; and, further, that near the slag-metal interface it is not present to an appreciable extent as an "inactive" compound, such as a lime ferrite, even though some such compound may be present near the upper surface of the slag.

The marked decrease in M when L is less than about 2.4 suggests that the silica in the liquid slag is present predominantly as a stable dibasic silicate. When L is greater than 2.4, it is probable that the predominant silicate is $2CaO.SiO_2$, but as the ratio of *available* CaO to SiO_2 decreases toward 2 the activity of CaO, or the effective concentration of "free" CaO, becomes small, and other molecules, such as MnO, FeO, MgO, begin to take the place of lime in dibasic silicates such as $CaO.MnO.SiO_2$, $CaO.FeO.SiO_2$ or $CaO.$-

MgO.SiO$_2$, with a resultant removal of "free," or active. MnO or FeO from the slag. Were MnO and FeO equally active in entering such combinations, the effective activity ratio a_{MnO}/a_{FeO} (and hence M) would remain almost unchanged; but the fact that as L decreases from 2.4 the actual concentration of manganese in the metal is progressively lower than that calculated on the basis that FeO and MnO are equally available for reaction indicates that MnO has a greater tendency than FeO to be "neutralized" as a dibasic silicate. This interpretation suggests further that these dibasic compounds are fairly stable. being but little dissociated into their components at ordinary steelmaking temperatures; and that tricalcium silicate ($3CaO.SiO_2$), though it may be formed in the more basic slags. is not present as such unless there is more than enough CaO to combine with all the SiO$_2$ as dicalcium silicate (that is, $L > 2$).

This general picture of the slag is helpful in the discussion of the distribution of sulphur between metal and slag.

DISTRIBUTION OF SULPHUR BETWEEN METAL AND SLAG

The sulphur in the liquid metal is, when present within the usual range of concentration, all dissolved; for convenience in expression, it will be regarded as present as FeS, and the assumption, as before, will be that its activity is proportional to its mol fraction; hence, because this is always small, to its concentration as determined by analysis. It could be present also as MnS, but certain calculations, mentioned later, indicate that less than 5 per cent of the sulphur can justifiably be thought to be present in the liquid metal as MnS.

In the liquid slag phase the only molecular species containing sulphur significant to our present purpose are FeS, MnS, CaS. This statement requires some discussion in view of the fact that analysis of solid open-hearth slag usually indicates that

some 20 to 40 per cent of the total sulphur is present as sulphate. probably mostly as calcium sulphate. Nevertheless, there can be little. if any, sulphate at the slag-metal interface when the equilibrium between slag and metal is established.

The reaction in the slag is

$$CaSO_4 \rightleftharpoons CaS + 2O_2 \qquad [C]$$
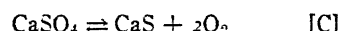
and its equilibrium constant $= \dfrac{a_{CaS}}{a_{CaSO_4}} p_{O_2}^2$ whence it follows that the activity ratio a_{CaS}/a_{CaSO_4} at equilibrium varies inversely as the square of the partial pressure (p_{O_2}) of oxygen existing at any point within the slag. From data in the literature on related reactions. it is possible to calculate the equilibrium attained in this reaction over the range 2750° to 3050°F. with ample accuracy for our present purpose; because of this. and of the fact that the mode of derivation is rather complex, it will not be discussed further except for the statement that the concentration of sulphate becomes insignificant when p_{O_2} is 10^{-5} or less. At the slag-metal interface, p_{O_2} is actually not larger than 10^{-8}, whence a_{CaS}/a_{CaSO_4} [and presumably (CaS)/(CaSO$_4$)] would be at least 10^7.* Accordingly we proceed on the basis, as stated above, that the total sulphur in the slag, as determined by analysis, is—as far as the present purpose is concerned—present as sulphide. This basis is supported by the fact that the proportion of sulphate to sulphide, as determined on a large number of slags. bears no relation to slag composition, and by the circumstance that the above assumption yielded the most consistent and reasonable interpretation of the observed distribution of sulphur as related to slag composition.

---

* At the upper slag surface, p_{O_2} undoubtedly is considerably higher and, though not accurately known, may well be high enough to cause absorption of oxygen and formation of CaSO$_4$; this, together with the oxidation occurring during removal, freezing and grinding of the slag sample, accounts for the sulphate found by analysis.

On this basis, then, for the liquid slag, $(S) = (FeS) + (MnS) + (CaS)$ where (S) is the total number of gram atoms sulphur for 100 grams slag, as determined by analysis; accordingly, the sulphur distribution ratio

$$\frac{(S)}{[S]} = \frac{1}{[S]} ((FeS) + (MnS) + (CaS)) \quad [4]$$

[S] being the corresponding concentration, expressed in appropriate units, of sulphur in the metal. The problem, therefore, is to evaluate, with sufficient accuracy, the activity of each of these three sulphides in a complex silicate solution.

As a first step in this direction, consider the following pair of similar reactions proceeding to substantial equilibrium in the liquid slag:

$$FeS + CaO \rightleftarrows CaS + FeO \quad [D]$$
$$FeS + MnO \rightleftarrows MnS + FeO \quad [E]$$
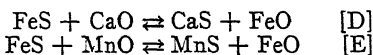
We may write

$$(CaS) = B'' \frac{(CaO)_f}{(FeO)} \times (FeS) \quad [5]$$

and

$$(MnS) = C'' \frac{(MnO)}{(FeO)} \times (FeS) \quad [6]$$

where $(CaO)_f$ represents the "free" or "active" CaO, as defined later. Assuming, as before, that mol fraction is proportional to activity for each of the molecular species here concerned,* and changing the units

_____

* It may be noted that such expressions in terms of molal concentration are useful if the ratio of activity to mol fraction (or activity coefficient γ) remains reasonably constant over the range considered, even though the solutions are far from ideal. For example, the data of Chipman and TaLi[2] on the reaction

$$H_2 + FeS \rightleftarrows H_2S + Fe$$
$$\text{gas} \quad \text{liquid} \quad \text{gas} \quad \text{liquid}$$
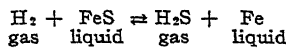
indicate a linear relation between the ratio p_{H_2S}/p_{H_2} (which is proportional to the activity of sulphur) and the sulphur content of iron up to 1.2 per cent sulphur by weight. Thus γ_{FeS} is apparently nearly constant over this range, even although, as noted later, this solution must deviate considerably from ideal behavior.

correspondingly, by dividing $[S]$ by N_m, the total number of mols per 100 grams metal, and each of the several slag terms by N_s, the total number of mols per 100 grams of slag, Eq. 4 is transformed to

$$\frac{(S)}{[S]} \times \frac{N_m}{N_s} = \frac{(FeS)}{[S]} \times \frac{N_m}{N_s}$$
$$\left(1 + B'' \frac{(CaO)_f}{(FeO)} + C'' \frac{(MnO)}{(FeO)} \right) \quad [7]$$

On the basis of the assumption made earlier that all sulphur in the metal is present as FeS, the number of mols of sulphur in the metal is equal to the number of mols of FeS; hence, the term $\frac{(FeS)}{[S]} \times \frac{N_m}{N_s}$ is equivalent to $\frac{(FeS)}{[FeS]} \times \frac{N_m}{N_s}$, which is the equilibrium constant for the interchange reaction

$$FeS \rightleftarrows FeS$$
$$\text{metal} \quad \text{slag} \quad [F]$$
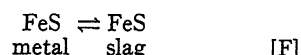
Denoting the value of this equilibrium constant by A', we may write:

$$\frac{(S)}{[S]} \times \frac{N_m}{N_s} = A'$$
$$\left(1 + B'' \frac{(CaO)_f}{(FeO)} + C'' \frac{(MnO)}{(FeO)} \right) \quad [8]$$

During the refining period of the open hearth, the liquid metal is always a quite dilute solution for which N_m is substantially constant; furthermore, the value of $[S]$ and of (S)—expressed as mols per 100 grams of metal and slag, respectively—is directly proportional to the weight per cent of sulphur in the metal or slag. Incorporating these changes in Eq. 8 and adjusting the constants, gives

$$\frac{(S)_w}{[S]_w} = N_s$$
$$\left(A + B' \frac{(CaO)_f}{(FeO)} + C' \frac{(MnO)}{(FeO)} \right) \quad [9]$$

But if the slag and metal are substantially at equilibrium, the ratio

(MnO)/(FeO) can be expressed in terms of the manganese content of the metal and the equilibrium constant for the distribution of manganese according to reaction A. Thus, from Eq. 3,

$$\frac{(MnO)}{(FeO)} = K[Mn]_w$$

whence, as an alternative to Eq. 9,

$$\frac{(S)_w}{[S]_w} = N_s$$

$$\left(A + B'\frac{(CaO)_f}{(FeO)} + C[Mn]_w \right) \quad [9a]$$

The value to be used for (FeO) in Eq. 9a is the total equivalent FeO as calculated in the study of the distribution of manganese.

The ratio $(S)_w/[S]_w$, that is, the ratio of the sulphur content of the slag to that of the metal, *as determined experimentally*, is now expressed explicitly in terms of the following factors: (1) the total number of mols in the slag, N_s; (2) the effective concentration of "free" lime relative to that of FeO in the slag; (3) concentration of manganese in the metal; (4) three constants, A, B' and C. And from the relationships expressed by these equations certain useful qualitative conclusions can be drawn at once regarding the influence of these factors upon the distribution of sulphur between slag and metal at equilibrium; specifically, other things being equal, the concentration of sulphur in the metal is lessened and that in the slag is increased:

1. By an increase in the ratio $(CaO)_f/$(FeO), which is simply a statement of the fact that a high effective concentration of free lime relative to that of FeO in the slag aids in desulphurizing the metal.

2. By an increase in the ratio $(MnO)/$(FeO), or by what is equivalent, raising the concentration of manganese in the metal. This is, in effect, a statement of the influence of the distribution of manganese on that of sulphur.

3. By an increase in N_s, the total number of mols per 100 grams of slag. This con-

clusion is significant in that it shows that a change in the molecular species existing in the slag may influence the distribution of sulphur, even though the reacting molecules do not themselves contain sulphur. For example, a reaction between CaO and P_2O_5 or SiO_2 to form a phosphate or silicate decreases the total number of mols and in consequence lessens the value of the ratio $(S)_w/[S]_w$. For most effective desulphurization of the metal, therefore, it is desirable to have as large a value of N_s as is consistent with other requirements.

If it is desired to go beyond these qualitative deductions to a quantitative use of Eq. 9, it is necessary to evaluate the several concentrations and constants appearing therein. The values of $(S)_w$, $[S]_w$, $[Mn]_w$. (MnO) and (FeO), the last being the total equivalent FeO as defined earlier, are directly determinable in any given case by chemical analysis, but the values of the constants A, B', and C, and of N_s and $(CaO)_f$, are not so determinable. They can, however, be determined with satisfactory accuracy by other methods, as is shown in the sections that follow; the constants, which need be evaluated but once, from laboratory data and from statistical studies, and the terms N_s and $(CaO)_f$, by making certain simplifying assumptions.

Determination of Constant A

The simplest and most direct method of evaluating the constant A is from data on slag-metal melts in which: (1) no manganese is present; (2) the concentration of free or active CaO is substantially zero; (3) the constitution of the slag is simple enough to permit a reasonably accurate calculation of N_s, the total number of mols. Under these conditions, the second and third terms within the parenthesis of Eqs. 9 vanish, leaving the relation

$$A = \frac{(S)_w}{[S]_w} \times \frac{1}{N_s} \quad [10]$$

in which all the terms on the right-hand side are experimentally determinable. The conditions listed above appear to be met satisfactorily by the measurements of Bardenheuer and Geller[3] for the distribution of sulphur between liquid iron and an FeO slag. Their numerical data inserted in Eq. 10 give a value of $A = 2.6$ for a temperature of 1600°C. This value, which we consider the best for this constant, is entirely in accord with the indications of other methods. It is, for example, in excellent agreement with the data published by Fetters and Chipman.[4]

It is also interesting to note that it is within the range obtained from a study of the melting diagram of the system Fe-FeS, which indicates a positive deviation from Raoult's law so great that the system appears to be on the verge of exhibiting liquid immiscibility.

If the liquid in this system were an ideal solution, and if the solutions of FeS in slags with which the liquid metal is in equilibrium were also ideal, the mol fraction (activity) of FeS in each would be equal; that is,

$$\frac{(S)_w}{N_s} = \frac{[S]_w}{N_m}$$

where N_s is the total number of mols per 100 grams of slag and N_m is the corresponding value for the metal. From this it follows that

$$\frac{(S)_w}{[S]_m} = \frac{N_s}{N_m}$$

and substituting in Eq. 10

$$A = \frac{1}{N_m}$$

Since the metal is a quite dilute solution, N_m is substantially equal to the number of mols of iron present per 100 grams of metal, and on this basis

$$A = \frac{1}{100\frac{1}{56}} = 0.56$$

If, however, solutions of FeS in Fe are not ideal, the value of A should be 0.56 multiplied by the activity coefficient of FeS in molten iron, and if this activity coefficient can be evaluated the correction can be made.

In many binary nonideal solutions, for a given component, the value of its activity coefficient, γ, is approximated by the expression

$$\log \gamma = \alpha(1 - \text{mol fraction})^2 \quad [11]$$

where α is a constant. It can further be shown that if this relation holds, the condition that the system just border on immiscibility is that $\gamma = 0.87$; hence, at low sulphur content, $\log \gamma_{FeS}$ approaches 0.87, or $\gamma_{FeS} = 7.4$, whence

$$A = 0.56 \times 7.4 = 4.1.$$

The inflection, which indicates an approach to a miscibility gap in the melting curve of the system Fe-FeS, occurs at about 1350°C., so that the calculated value 4.1 would be expected to be slightly greater than the true value and considerably greater than that obtaining at higher temperatures as the system approaches ideal behavior more closely. Extrapolation of the data of Bardenheuer and Geller indicates that at 1350°C. A has a value of about 4, in remarkably good agreement with the estimate made as above. As the miscibility gap does not, in fact, appear in the system at 1600°C., these considerations indicate that at 1600°C. the value of A is less than 4.1 but greater than 0.56.

The measurements of Körber[5] on the high-sulphur portion of the system iron-manganese-sulphur permit a more accurate estimate of the activity coefficient γ_{FeS}. For instance, his data show that at 1600°C. a slag composed of FeS and MnS, in which the mol fraction of FeS is 0.5, is in equilibrium with liquid metal containing 6 per cent sulphur and 1 per cent manganese; that is, it is in equilibrium with metal in which the mol fraction of FeS is 0.11.

On the basis that the solution of FeS in MnS is ideal, $\gamma_{FeS} = \frac{0.5}{0.11} = 4.5$, whence $A = 0.56 \times 4.5 = 2.5$, again in good agreement with the value obtained from the measurements of Bardenheuer and Geller.

Finally, Chipman and Ta Li,[2] in comparing their equilibrium data for the reaction

$$H_2 + FeS \rightleftharpoons H_2S + Fe \qquad [G]$$
$$\text{gas} \quad \text{metal} \quad \text{gas} \quad \text{metal}$$
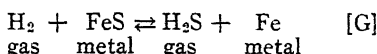
at 1600°C. with an extrapolation of corresponding data of Britzke and Kapustinsky for lower temperatures, find a discrepancy of 0.65 log units when mol fractions are used in place of activities. If this discrepancy is considered as occasioned by the departure from ideality of solutions of FeS in iron at the higher mol fractions, $\log \gamma_{FeS} = 0.65$, whence $\gamma_{FeS} = 4.5$ and $A = 0.56 \times 4.5 = 2.5$. The agreement between this value and that obtained from the measurements of Bardenheuer and Geller, must, however, be regarded as fortuitous, in view of the uncertainties involved in the extrapolations made by Chipman and Ta Li.

The selected value, $A = 2.6$, sets about the minimum value of the sulphur distribution ratio. In certain systems in which the slag is relatively acid and the manganese content of the metal is also low, a value of the ratio $(S)_w/[S]_w$ as low as 1.5 has been observed, which happens when the value of N_s is as low as about 0.6.

Determination of Constant C

Having thus evaluated the constant A, the value of C can be determined from measurements of the sulphur distribution ratio in a slag-metal system containing manganese but with a slag such that the effective concentration of lime approaches zero; provided, of course, that the total number of mols in the slag N_s can be approximated with satisfactory accuracy. Data that meet these conditions have been reported by Bardenheuer and Geller[3] for the system Fe-Mn-O-S (containing small amounts of S) and by Meyer and Shulte[6] for the system Fe-Mn-S. CaS being absent in each case. A replot of these several sets of data yields a value for C of 9.1 and 11.0, respectively.

These values are in reasonable agreement with the results of a statistical analysis by Fetters and Chipman[7] of data for 650 open-hearth heats, though these results are not strictly comparable. For example, on the assumption that the average value of N_s is 0.80, Fig. 16 of their paper indicates that C is 14 for a basicity ratio above 2.5 and 10 below 2.5. Moreover, Körber's measurements on the system Fe-Mn-S at 1600° are in good agreement with the results reported by Meyer and Schulte and correspond to a value of 11 for C.

An approximate value for C may also be obtained from the solubility product of MnS in iron saturated with graphite as determined by Joseph and Holbrook.[8] Taking into account the increase in the distribution ratio of FeS between slag and metal occasioned by the presence of carbon, as is discussed later in this section, it is found that for steel, $C = 8$.

Reviewing these several estimates of C, we have selected the rounded value of 11.0 as best.

Determination of Constant B'

If the value of the constant A is known, that of constant B' can be determined from data on the distribution of sulphur between metal and a slag containing CaO but no manganese. Suitable data for synthetic slags of CaO and FeO have been reported by Bardenheuer and Geller.[3] They plotted their data directly in terms of percentage of the several constituents, but a better method is that indicated by Eq. 9; that is, to plot the ratio $(S)_w/[S]_w \times \frac{1}{N_s}$ against the ratio $(CaO)_f/(FeO)$, the term

(FeO) being as before the total equivalent FeO, and the term (CaO)$_f$, the concentration of free lime, being calculated on the basis that the small amount of SiO$_2$

Evaluation of N_s and of $(CaO)_f$

An accurate calculation of the number of mols of the several constituents coexisting in a liquid slag is hardly feasible at present
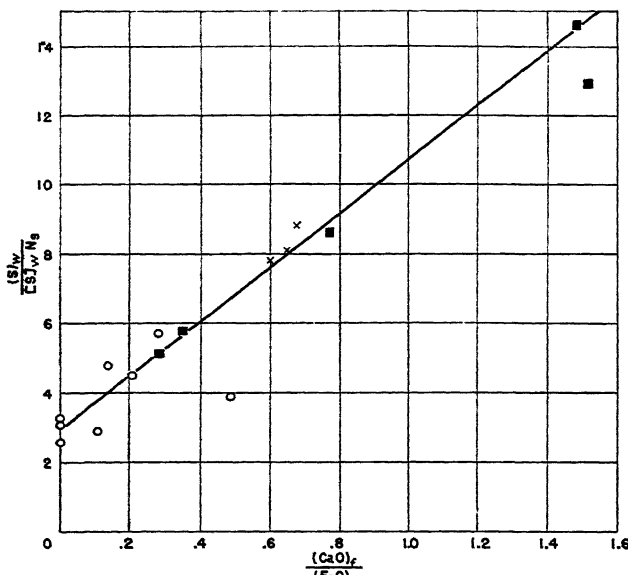

FIG. 2.—EFFECT OF (CaO)$_f$/(FeO) RATIO ON DISTRIBUTION OF SULPHUR BETWEEN METAL AND SYNTHETIC SLAGS.
(Data from Bardenheuer and Geller's laboratory melts).

present is combined as 3CaO.SiO$_2$, an assumption whose justification is discussed later. When data are plotted in this manner (Fig. 2), the intercept gives the value of A and the slope the value of B', which for the curve shown is 7.7.

The data of Fetters and Chipman[4] on the distribution of sulphur in the system CaO-MgO-FeO-SiO$_2$ lead to the somewhat lower value of 6 for the constant B'. Their data do not extend, however, to the high concentrations of CaO near the binary system CaO-FeO; moreover, it is impossible to approximate the binary system satisfactorily because of the high amount of Fe$_2$O$_3$ present, presumably as a ferrite, at equilibrium; consequently, more weight was given to melts containing the presumably inert diluent CaF$_2$. Therefore the value $B' = 7.7$ has been selected as the best.

but a satisfactory estimate can be made on the basis of the following reasonable assumptions:

1. The significant compounds present are FeO, MnO, CaO, 4CaO.P$_2$O$_5$, and various calcium silicates.

2. In a slag whose basicity is above about 2.0, all the FeO and MnO are uncombined, a view that is justified on the basis of the data presented for the distribution of manganese (Fig. 1).

3. The concentration of free SiO$_2$ is vanishingly small and the silicates present, which are chiefly disilicates or trisilicates, contain but one mol of SiO$_2$ so that the number of mols of the several silicates present is the number of mols of SiO$_2$ as given directly by chemical analysis.

4. No ferrite is present, an assumption that is based upon the low oxygen pressure existing at the slag-metal interface.

5. No compound of the type $R_2O_3.RO$ is present.

6. In the more basic slags, the solubility of MgO is so small as to be negligible.

close to the full line, intercepting the abscissa at a ratio $L = 2.0$, which indicates that there is essentially no free lime in a slag for which L is less than 2.0; in other
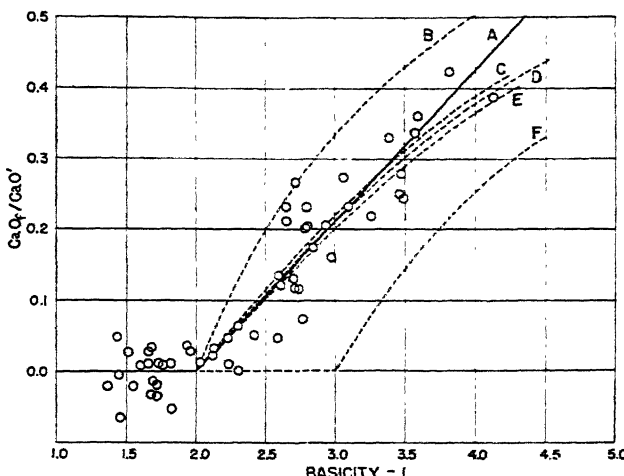

FIG. 3.—OPEN-HEARTH DATA SHOWING RELATIONSHIP BETWEEN RATIO $(CaO)_f/(CaO)$ AND THE LIME-SILICA RATIO.

A, best straight line through points.
B, theoretical curve for $K' = \infty$
C, theoretical curve for $K' = 0.40$
D, theoretical curve for $K' = 0.35$
E, theoretical curve for $K' = 0.30$
F, theoretical curve for $K' = 0$

On the basis of these assumptions:

$$N_s = (FeO) + (MnO) + (SiO_2) + (P_2O_5) + (CaO)_f \quad [12]$$

where all quantities are in mols per 100 grams and $(CaO)_f$ is the number of mols of "free" or uncombined CaO. Comparing this expression with Eq. 9 shows that the only factor not directly determinable by chemical analysis of slag or metal is $(CaO)_f$, hence these equations may be used to calculate the concentration of "free" lime in an open-hearth slag. This has been done for about 50 analyses of slag-metal pairs taken from open-hearth furnaces, with the results shown in Fig. 3, in which the ratio $(CaO)_f/(CaO')$, where $(CaO)_f$ is the number of mols of "free" lime per 100 grams of slag and (CaO') is the difference $(CaO) - 4(P_2O_5)$, is plotted as a function of the basicity ratio L. The points fall reasonably

words, the compound $2CaO.SiO_2$ is stable and does not dissociate appreciably, a conclusion that is supported by the fact that there is a sharp peak in the phase diagram for the system $CaO-SiO_2$ at the composition corresponding to the compound $2CaO.SiO_2$. This approximate linearity of the ratio $(CaO)_f/(CaO')$ over an appreciable range of the ratio L is to be expected on the basis that there is an equilibrium between $2CaO.SiO_2$ and $3CaO.SiO_2$, as is shown later in the section on the constitution of liquid slags.

In view of the approximate character of the data, the solid line in Fig. 3 suffices as a basis for calculating the value of $(CaO)_f$, since this line may be represented by the equation

$$\frac{(CaO)_f}{(CaO')} = 0.21(L - 2) \quad [12a]$$

whence $(CaO)_f = 0.21 \, (L - 2).(CaO')$. This relation may be substituted in Eqs. 9 and 9a to give:

$$\frac{(S)_w}{[S]_w} = N_s \left[2.6 + 1.6 \frac{(CaO')}{(FeO)} (L - 2) + 11.0[Mn]_w \right] \quad [13]$$

where the only quantity that cannot be evaluated directly from chemical analysis is N_s, the total number of mols per 100 grams of slag. But N_s may be evaluated for a slag with a basicity ratio greater than 2.0 by combining Eqs. 12 and 12a, thus,

$$N_s = (FeO) + (MnO) + (SiO_2) + (P_2O_5) + 0.21(L - 2).(CaO')$$

When the ratio L is less than 2.0, N_s can be evaluated satisfactorily by assuming that disilicates other than $2CaO.SiO_2$ are present in the slag; that is, that, if possible, one mol of SiO_2 is always combined with 2 mols of metallic oxide; thus, when L is less than 2.0

$$N_s = (SiO_2) + (MnO) + FeO + (P_2O_5) - 2[(SiO_2) - 1/2(CaO')] \quad [14]$$

This approximation admittedly is a rough one, but it is sufficiently accurate for the present purpose, since when L is less than 2.0 the ratio $(S)_w/[S]_w$ is small and not sensitive to a change in the value of N_s.

Equations 13 and 14, which are based primarily on laboratory studies of simple slag systems, now provide a comprehensive relation governing the influence of the several factors involved upon the desulphurizing power of an open-hearth slag, in which each of the factors is expressed in terms of a quantity readily calculable from chemical analysis of the slag or metal.

Before proceeding to test the extent to which this relation represents the behavior of the slag-metal system in a commercial furnace, two of the assumptions implicit in Eq. 13 should be discussed a little further; i.e., the effect of temperature, which has been, thus far neglected, and the con-

sequences of the assumption that all the sulphur in the metal exists as FeS.

Effect of Temperature

Since none of the terms of Eqs. 13 or 14 involves temperature explicitly, it is of interest to see to what extent this neglect influences their accuracy. For example, the constants A, B' and C are known to vary somewhat with temperature and the use of $[Mn]_w$ instead of $(MnO)/(FeO)$ ignores the fact that for a given slag the concentration of manganese in the metal increases with temperature. The magnitude of the influence of temperature may be estimated in either of two ways: (1) by direct measurement, or (2) from the heat of the several reactions involved.

Bardenheuer and Geller measured the constant A at different temperatures, with results that indicate that in the neighborhood of 1600°C. A decreases about 1.4 per cent for an increase of 10°C. Similarly, they found that C decreases about 7 per cent for a corresponding increase in temperature.

From the heats of formation given by Schwarz,[9] the heat of the reaction

$$FeS + CaO \rightleftharpoons CaS + FeO \quad [H]$$
$$\text{slag} \quad \text{slag} \quad \text{slag} \quad \text{slag}$$
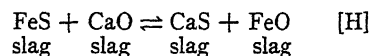
is $\Delta H = 16,520$ cal. per mol.

Assuming as a first approximation that ΔH is constant with temperature:

$$\frac{d \ln B''}{dT} = \frac{d \ln \frac{(CaS)(FeO)}{(CaO)(FeS)}}{dT} = \frac{\Delta H}{RT^2} \quad [15]$$

or at 1600°C.,

$$\frac{\Delta H}{RT^2} = \frac{16520}{1.98 \times (1873)^2} = 0.00235$$

and as B' is proportional to $B''A$

$$\frac{d \ln B'}{dT} = 0.00235 - 0.0014 = 0.001$$

or, near 1600°C., the constant B' increases about 1 per cent for an increase in temperature of 10°C. Insofar as the constant $B(= 1.6)$ of Eq. 13 was evaluated empiri-

cally from B', its temperature coefficient cannot be determined quantitatively, but it seems likely that it is positive and somewhat greater than that of B'.

Raising the temperature, therefore, tends to increase the concentration of CaS and to decrease the FeS and MnS in the slag, but whether the net effect is to help or hinder desulphurization of the metal depends on the relative concentration of the three present. As a matter of fact, however, the difference between the desulphurization ratios calculated on the basis of the temperature coefficients estimated above and those calculated directly from Eq. 13 is less than the normal scatter of the observed ratios, hence the net effect of change in the temperature of the open hearth on the distribution of sulphur is apparently small and appears to be negligible for our present purpose, a conclusion that was reached by Chipman and Fetters[4] also.

Form in Which Sulphur Exists in the Metal

In deriving Eq. 13 it was assumed that the activity of sulphur in the metal is directly proportional to its weight per cent; that is, that $\gamma_{[S]}$ is constant. Although the data of TaLi and Chipman show that this is true in the binary system Fe-S up to 1.2 per cent S, it does not necessarily follow that this simple proportionality holds in the presence of other elements. In particular, the effect of the presence of manganese and carbon needs to be considered before the equation may be applied to steelmaking.

The influence of manganese probably is to lessen the activity coefficient of sulphur in steel because of the presence of MnS in the metallic phase. It may readily be shown that if a homogeneous equilibrium is set up so that both FeS (or Fe_xS) and MnS are present, Eq. 9 becomes

$$\frac{(S)_w}{[S]_w} = \frac{N_s}{1 + K_m[Mn]_w} \left(A + B' \frac{(CaO)_f}{(FeO)} + C[Mn]_w \right) \quad [16]$$

where

$$K_m = \frac{[MnS]}{[FeS][Mn]_w}$$

Suppose that 10 per cent of the sulphur in a bath containing 0.4 per cent Mn exists as MnS and the other 90 per cent as FeS—i.e., $K_m = 0.28$—then, in a bath containing 4.0 per cent Mn the ratio of MnS to FeS would be $0.28 \times 4.0 = 1.12$. In this case the constants A, B', C would appear to be smaller by the factor $\frac{1}{1 + K_m[Mn]_w} = 0.47$. The value of the constant C obtained from the data of Meyer and Schulte is confirmed by that of Körber at high manganese concentration, and, as mentioned previously, the value thus obtained is essentially the same as that obtained from other data at low manganese content. Although the data show considerable random departure from a linear variation, nevertheless they indicate quite definitely that at about 4 per cent Mn the factor $\frac{1}{1 + K_m[Mn]_w}$ is close to unity and certainly is not lower than 0.7, which indicates that at 1600°C. the sulphur existing in the liquid metal as MnS is less than 5 per cent of the total and probably is very much less under normal open-hearth conditions.

The influence of carbon upon the activity of sulphur may be estimated from some hitherto unpublished data obtained here in association with R. W. Gurry, which indicate that at 1500°C. in an atmosphere of nitrogen the solubility of FeS in iron saturated with graphite (about 4 per cent carbon) corresponds to a sulphur content of about 1.5 per cent. (These data also suggest that low-sulphur steel might be produced more easily by desulphurizing the hot iron from which the steel is made than from the steel itself.) The effect of the much smaller amount of carbon present in the open hearth at the finishing stage may be roughly estimated by assuming that the logarithm of the distribution coefficient A

varies linearly with the percentage of carbon, thus at 1500°C.

$$\log A = 0.48 + 0.18\ [C\%]$$

and at 1600°C.

$$\log A = 0.42 + 0.18\ [C\%]$$

At 0.20 per cent carbon A would have the value 2.9 instead of 2.6. The "constants" B, B', and C also would have values about 10 per cent higher.

Thus, the equation developed is most accurate when applied to low-carbon molten steels. This limitation is not too serious, since in application to open-hearth data interest in the sulphur distribution is usually limited to the end of the heat where the carbon is usually low. The normal scatter of operating furnace data tends to mask this effect of various carbon content.

Correlation with Open-hearth Data

In view of the possible inaccuracies in open-hearth data, arising from errors in sampling and analysis and from possible lack of attainment of equilibrium, such data are best treated in large numbers. For this purpose, the authors collected a group* of 231 fairly complete analyses, both of slag and of metal, covering a wide range of composition, and including a number of unpublished data as well as those available in the literature. Comparison of these data with Eq. 13 was made by two general methods: first, analytical and graphical checks on the values of the constants; second, a direct comparison of the observed and calculated distribution of sulphur.

The values of the three constants A, B and C (obtained analytically to fit Eq. 13) that fit best the 231 actual open-hearth heats are compared in the following table with the values selected on the basis of laboratory data.

*See footnote to page 89.

Constants	Mean Values from 231 Open-hearth Analyses	Evaluated from Laboratory Data
A	2.8	2.6
B	1.4	1.6
C	10.0	11.0

The agreement is most gratifying and indicates that Eq. 13 is substantially correct and that the selected values of the constants are good to about 10 per cent. Graphical methods applied to the 231 heats likewise yield values of these constants that agree with the selected values within the inherent subjective error.

The final check is the comparison of the observed and calculated distribution of sulphur between metal and slag. The use of this method is best illustrated by an example. For instance, in one case, a metal containing 0.031 per cent S and 0.31 per cent Mn was presumably in equilibrium with a slag of the following composition:

SiO_2, 12.8 per cent; CaO, 41.0; FeO, 18.4; Fe_2O_3, 4.5; MnO, 14.0; P_2O_5, 1.8; S, 0.27. The observed sulphur distribution ratio therefore is:

$$(S)_w/[S]_w = \frac{0.27}{0.031} = 8.7$$

The distribution ratio calculated by means of Eq. 13 is obtained as follows:

The slag contains $\frac{41.0}{56} = 0.732$ gram mols of CaO per 100 grams of slag, hence,

$$(CaO) = 0.732$$

There are $1.8/142 = 0.013$ mols P_2O_5 whence

$$(CaO') = (CaO) - 4(P_2O_5) = 0.680$$

The total equivalent FeO is

$$(FeO) = \frac{18.4}{72} + 3\frac{4.5}{160} = 0.342$$

The term $(SiO_2) = \frac{12.8}{60} = 0.213$
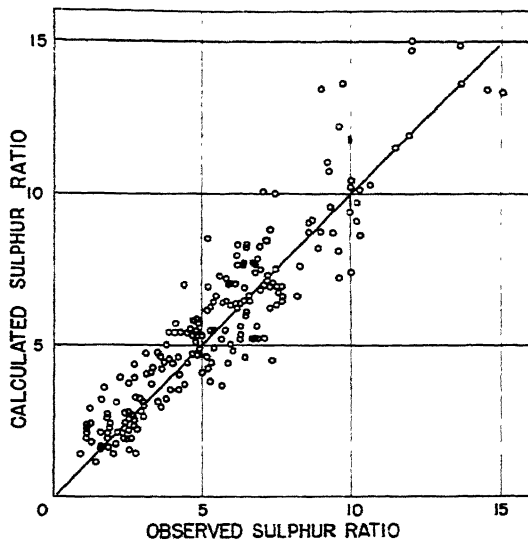
FIG. 4.—COMPARISON BETWEEN OBSERVED AND CALCULATED VALUES OF SULPHUR DISTRIBUTION RATIO IN ACTUAL OPEN-HEARTH HEATS.
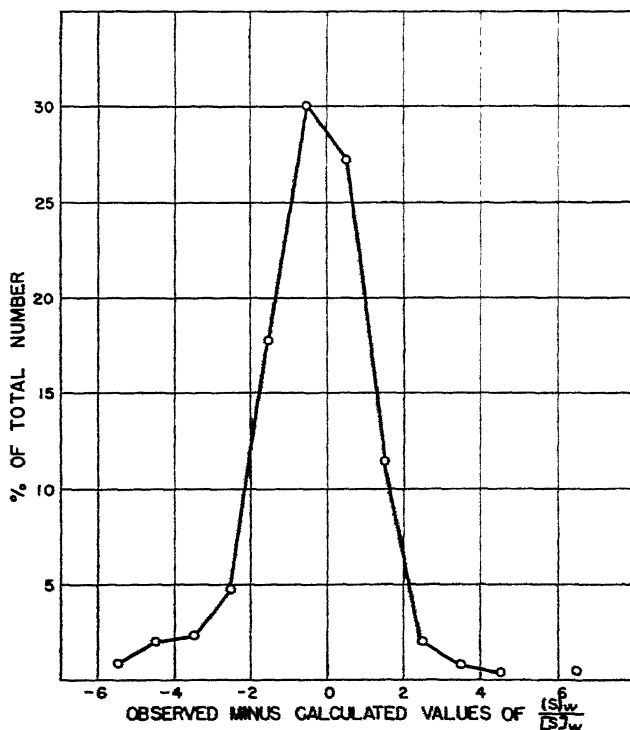

FIG. 5.—FREQUENCY CHART OF DIFFERENCE BETWEEN OBSERVED AND CALCULATED VALUES OF SULPHUR DISTRIBUTION RATIO.

The basicity ratio then is

$$L = \frac{0.732 - 4(0.013)}{0.213} = 3.19$$

The influence of CaS on the desulphurization is characterized by the expression

$$1.6 \frac{(CaO')}{(FeO)} (L - 2) = 3.8$$

The effect of manganese is given by

$$11[Mn]_w = 11[0.31] = 3.4$$

There yet remains the evaluation of N_s, which depends upon the calculation of $(CaO)_f$ and (MnO). From Fig. 3 at $L = 3.19$, the ratio $(CaO)_f/(CaO') = 0.25$, whence $(CaO)_f = 0.680 \times 0.25 = 0.170$. Since L is greater than 2.0, it is assumed that all the MnO is free, whence $(MnO) = \frac{14.0}{71} = 0.198$. With these we may now compile N_s:

$$N_s = (FeO) + (MnO) + (SiO_2) + (P_2O_5) + (CaO)_f$$
$$= 0.342 + 0.198 + 0.213 + 0.013 + 0.170$$
$$= 0.936$$

The calculated distribution ratio from Eq. 13 is

$$\frac{(S)_w}{[S]_w} = 0.936[2.6 + 3.8 + 3.4]$$
$$= 9.1$$

The calculated ratio is 9.1 as compared with an observed ratio of 8.7.

The correlation thus obtained for the 231 sets of data is illustrated in Fig. 4, in which the observed ratio is plotted against the calculated ratio. If the correlation were perfect the points should all fall upon the straight line shown, whereas if the calculated ratio is greater or less than the observed ratio the points fall above or below the line, respectively. It is evident that the points are distributed at random on either side of the line, indicating that

Eq. 13 is a fair representation of the average of the open-hearth data collected. The extent of this fit is illustrated also by the frequency curve in Fig. 5, which shows the relative frequency of the difference between the observed and calculated ratio. Since 54 per cent of calculated values come within 1 unit of the observed values, and 84 per cent come within 2 units, and since the curve is nearly symmetrical with respect to the ordinate of zero deviation, the fit can be considered very satisfactory.

The fact that Eq. 13, which is based largely on laboratory studies, applies, within the probable limits of error, to open-hearth data covering a wide range of slag compositions justifies the conclusions that: (1) The equation expresses quantitatively at least the main factors involved in desulphurization in steelmaking; and (2) the assumptions involved regarding the compounds existing in the slag give a useful picture of the constitution of the slag.

CONCLUSIONS REGARDING INFLUENCE OF DIFFERENT FACTORS INVOLVED IN DESULPHURIZATION

Some of the qualitative conclusions drawn from Eq. 13 have been pointed out in an earlier section. It now becomes of interest to extend these conclusions to a quantitative basis, and to aid in this discussion a set of seven illustrations, in the form of typical analyses of slag and metal taken from actual open-hearth data and covering a fairly wide range of composition, is given in Table 2. For convenience, the table also includes for each pair of analyses the derived value of the significant factors appearing in Eq. 13.

It is evident from Eq. 13 that, other things being equal, the effectiveness of desulphurization is increased:

1. By increasing N_s, the total number of mols per 100 grams of slag. Thus, comparison of columns 2, 6 and 7 in Table 2 with columns 1, 3, 4 and 5 shows how the ratio $(S)_w/[S]_w$ is increased when the value

of N_s is increased from about 0.70 to slightly over 1.0. The range of variation of N_s indicated in Table 2 is significant; for even though these values are in general only approximate, and may be a little lower than the true total number of mols, they show how, at a given weight per cent, the activity of a given constituent can vary because of a change in its mol fraction resulting from a change in N_s caused by the formation or dissociation of other molecules. The effect of the concentration of silica should be especially emphasized in this connection; even though it does not appear explicitly in Eq. 13, it is none the less significant in that it has a considerable influence on the value of N_s. Thus, an increased concentration of SiO_2 leads to the formation of complex silicate molecules with a consequent reduction in N_s, which in turn results in decreased power to desulphurize.

It is also clear that, quite apart from its lower cost, lime has an advantage over other alkaline earth oxides, such as barium or strontium oxide, in that it has the smallest molecular weight and therefore contains the largest number of mols per unit weight, which results in a higher value of N_s.

This effect of the total number of mols in the slag emphasizes that the desulphurizing power of a slag may be influenced by the concentration of molecules that do not contain sulphur, nor even react with sulphur, a fact that has not been widely recognized.

2. By increasing the basicity ratio L; comparison of columns 1 and 2 in Table 2 shows that as L is increased from 2.15 to 5.60, the ratio $(S)_w/[S]_w$ increases from 3 to 14.9. Here again the concentration of silica is significant even though it does not appear explicitly in Eq. 13, because the term (SiO_2) is involved in the value of L. Thus, an increase in silica tends to lessen the power to remove sulphur by combining with CaO to form calcium silicates, thereby decreasing the concentration of free lime, and hence of CaS. It should be pointed out

TABLE 2.—*Typical Slags and Desulphurizing Power*

Slag No.	1	2	3	4	5	6	7
CaO, per cent.	38.6	45.0	43.1	52.9	48.0	33.0	42.2
FeO, per cent.	17.0	21.2	7.7	7.2	10.3	19.0	15.7
Fe_2O_3, per cent.	5.5	9.5	3.2	1.9	8.6	7.0	3.1
MnO, per cent.	5.1	5.7	12.8	5.9	3.9	25.0	10.0
SiO_2, per cent.	17.7	8.4	22.3	22.7	19.6	7.0	8.9
P_2O_5, per cent.	1.87	0.71	0.92	1.62	4.1	1.0	1.8
MgO, per cent.	11.0	6.3	6.0	5.9	2.5	6.0	8.2
Mn, per cent.	0.08	0.12	0.43	0.31	0.10	0.44	0.23
C, per cent.	0.032	0.02	0.41	0.40	0.25	0.04	0.14
(CaO)	0.688	0.803	0.768	0.944	0.856	0.588	0.753
$4(P_2O_5)$	0.053	0.020	0.026	0.046	0.115	0.028	0.051
(CaO')	0.635	0.783	0.742	0.898	0.741	0.560	0.702
(FeO)	0.340	0.474	0.167	0.136	0.305	0.396	0.276
(MnO)	0.072	0.080	0.180	0.083	0.055	0.350	0.141
(SiO_2)	0.295	0.140	0.372	0.378	0.326	0.117	0.148
(P_2O_5)	0.013	0.005	0.006	0.012	0.029	0.007	0.013
(CaO)$_f$	0.020	0.406		0.071	0.042	0.272	0.323
N_s	0.740	1.105	0.725	0.680	0.757	1.142	0.901
L	2.15	5.60	1.99	2.37	2.27	4.74	4.74
$1.60 \dfrac{(CaO')}{(FeO)} (L - 2)$	0.5	9.5		3.9	1.0	6.2	11.2
$11[Mn]_w$	0.9	1.3	4.7	3.4	1.1	4.8	2.5
$2.6 + 11[Mn]_w + 1.60 \dfrac{(CaO')}{(FeO)}, (L - 2)$	4.0	13.4	7.3	9.9	4.7	13.6	16.3
$(S)_w/[S]_w$	3.0	14.9	5.3	6.7	3.6	15.5	14.7

that the significant factor is, in effect, the ratio of $(CaO)/(SiO_2)$, and that a slag low in lime may be an effective desulphurizer if the silica is low and the residual manganese is high, as is illustrated by the data in column 6 of Table 2. The use of bauxite in moderate amounts—that is, with Al_2O_3 in the slag not exceeding about 6 per cent—appears to have no significant influence on the removal of sulphur. The alumina probably tends to combine to some extent with lime but this is offset by the fact that it aids by thinning the slag and dissolving lime.

3. By conditions that promote a high concentration of residual manganese in the metal, as is illustrated by comparison of columns 1 and 3, which demonstrate that an increase in $[Mn]_\omega$ from 0.08 to 0.43 per cent is accompanied by an increase of the desulphurizing ratio from 3.0 to 5.3. It should also be noted that in a slag high in SiO_2 or low in lime, so that the basicity ratio L is less than about 2.4 (Fig. 1), the free MnO in the slag, and in consequence the residual manganese in the metal, is lowered through entrance of manganese into the silicates so that the concentration of MnS in the slag is lessened.

4. By a low concentration of FeO in the slag, as is illustrated by comparison of columns 4 and 5 of Table 2, which show that the low concentration of FeO in slag 4 is a major factor in contributing to its superior desulphurizing power. On this basis, and other things being equal, a given slag becomes less effective in removing sulphur toward the end of a heat when the carbon is low and the FeO is high. In low-carbon heats, however, it is easier to obtain a fluid slag with high lime and low silica, and if such conditions are obtained (slag 2, Table 2) sulphur may be effectively removed even though the slag is of necessity high in iron oxide.

Considered in the light of these considerations, the effect of fluorspar on the removal of sulphur appears to be due chiefly to its tendency to hasten the solution of lime, although it may react in part to contribute some free lime.

In passing, it should be pointed out that the best recovery of residual manganese in the steel occurs with a slag whose basicity ratio is between 2.3 and 2.5 (Fig. 1). In more acid slags, the lowered activity of MnO due to silicate formation more than offsets any advantage gained from a smaller slag volume, whereas in more basic slags increasing iron oxide content and slag volume both tend to diminish the recovery of manganese.

In this discussion, slag volume and the related amount of any constituent contained in the slag must not be confused with the concentration of that constituent in the slag. The whole of the treatment of slag-metal equilibrium and the calculation of the sulphur distribution ratio are based on relative concentrations, and have nothing to do with the amount of the several phases present, such as slag and metal. But obviously the total amount of sulphur absorbed by a slag of given composition increases with the weight of slag; that is, for a given slag composition, which determines the sulphur distribution, the total number of pounds of sulphur contained in the slag increases with the weight of slag per ton of steel, and therefore enters the general economy of the operation. Greater slag volume tends to increase fuel and lime consumption, slow up rate of production, and increase loss of iron and manganese, so that the use of large slag volume for the purpose of removal of sulphur involves a definite loss in general efficiency. It is much better therefore, when possible, to effect the necessary removal of sulphur by decreasing the silicon and increasing the manganese content in the charge and using a minimum amount of limestone.

At best, the slag in the basic open hearth can be expected to contain only 0.2 to 0.5 per cent S. It is therefore important to

maintain a low sulphur content in all miscellaneous material charged, as well as in the pig iron and scrap. In adding extra burnt lime for sulphur elimination at 0.030 to 0.040 per cent S in the metal, for example, a lime with a sulphur content of even 0.1 per cent would not be very efficient for the purpose, and with 0.25 to 0.30 per cent S it would be almost useless, since the extra sulphur introduced into the bath would roughly be the same as the resulting increase in the "sulphur-absorbing power" of the slag. Similarly the sulphur content of ore, fluorspar and other materials should be kept as low as possible.

In a given practical problem of minimizing sulphur in the steel, the following means are available: (1) decrease the silicon and sulphur content of charge, (2) increase the manganese content of charge, (3) increase lime addition and, if necessary, accompany with more manganese, MnO, or fluorspar to secure a more favorable slag composition. All other methods being insufficient, it would be necessary to develop a means of removing the first slag from the furnace, and build up one or more successive slags on the metal, using low-sulphur slag-forming materials.

Constitution of the Liquid Slag

The fact that the basic assumptions made regarding the composition of the liquid slag led to an equation that fits operating data so well indicates that these assumptions are substantially correct, a fact that significantly extends the available evidence on the constitution of the liquid slag, and in particular confirms the inferences made earlier in the discussion of the distribution of manganese. For example, since in Eq. 13 the term (FeO) appears in both the B and C terms, the apparent applicability of the equation to slags of such widely different composition supports our belief that in the more basic slags ($L > 2.4$), FeO and MnO are not combined but are present almost entirely as such;

moreover, that very little Fe_2O_3 enters into the formation of ferrites or other inactive compounds. Apparently Fe_2O_3, lime ferrites, $CaSO_4$ and similar oxygen-rich compounds exist chiefly at the top surface of the slag where the oxygen pressure is relatively high, their essential function being to carry oxygen from this zone to the slag-metal interface.

Fig. 3 provides not only a definite indication of the stability of $2CaO.SiO_2$, as well as of other dibasic silicates, but also evidence for the presence of molecules of $3CaO.SiO_2$ which, however, would seem to have a much greater tendency to dissociate than do molecules of the disilicate. Moreover, it is even possible to obtain a rough idea of the amount of this dissociation, which is represented by the reaction

$$3CaO.SiO_2 \rightleftharpoons 2CaO.SiO_2 + CaO \quad [I]$$

for which the equilibrium constant is

$$K = \frac{(CaO)(2CaO.SiO_2)}{N_s(3CaO.SiO_2)} \quad [15]$$

From stoichiometric relations, we may write

$$(CaO') = (CaO) + 2(2CaO.SiO_2) + 3(3CaO.SiO_2) \quad [16]$$
$$(SiO_2) = (2CaO.SiO_2) + (3CaO.SiO_2) \quad [17]$$

and if these equations are combined with Eq. 15, with the definition of the basicity ratio L, namely

$$L = \frac{(CaO')}{(SiO_2)}$$

it is possible to obtain a single relation in which three of the variables are eliminated. The three most convenient ones to eliminate are (SiO_2), $(2CaO.SiO_2)$ and $(3CaO.SiO_3)$. The last two of these three can be evaluated by simultaneous solution of Eqs. 16 and 17, thus:

$$(2CaO.SiO_2) = 3(SiO_2) - (CaO') + CaO$$
$$(3CaO.SiO_2) = (CaO') - 2(SiO_2) - CaO$$

These relations may now be substituted in Eq. 15, which can be solved for (SiO_2) to give

$$(SiO_2) = [(CaO') - (CaO)]$$
$$[(CaO) + KN_s]/[3(CaO) + 2KN_s] \quad [18]$$

Substituting this expression in the definition of L,

$$L = \frac{3\gamma_{CaO} + 2K'}{(1 - \gamma_{CaO})(K' + \gamma_{CaO})} \quad [19]$$

where $\gamma_{CaO} = (CaO)/(CaO')$ and K' is $KN_s/(CaO')$. The term γ_{CaO} is essentially the activity coefficient of CaO and is the factor plotted against the basicity ratio L in Fig. 3. In Eq. 19, the value of γ_{CaO} corresponding to a given value of L depends upon the value assumed for K', which in turn is directly related to the equilibrium constant K for dissociation of $3CaO.SiO_2$. For example, if $K' = \infty$, the trisilicate is completely dissociated and the variation of γ_{CaO} with L is that represented by curve B in Fig. 3. On the other hand, if $K' = 0$—that is, none of the $3CaO.SiO_2$ present is dissociated—the variation of γ_{CaO} with L is represented by curve F in Fig. 3. For intermediate values of K', there are a whole family of curves lying between the limiting curves B and F. The straight line A, which has been drawn as the best line representing the open-hearth data shown by the circles, corresponds to a value of K' of about 0.35, which is equivalent to a value of K of about 0.25. This implies that under average conditions obtaining in the slag something of the order of half of the $3CaO.SiO_2$ is dissociated.

Since the relation between γ_{CaO} and L is not very sensitive to a change in the value of K', a change of 30 per cent causing a shift from the line C to line E in Fig. 3, K' may be considered as constant within the range of other errors, and the value 0.35 may be used in calculating the constitution of the slag. This picture of the liquid slag still remains very sketchy and incomplete.

We need more evidence on such details as the solubility of MgO and $2CaO.SiO_2$ at various temperatures, more precise data on the dissociation of calcium phosphates, $3CaO.SiO_2$, $CaO.Fe_2O_3$, etc., and more information as to the mode of occurrence of Al_2O_3, MgO, CaF_2, etc. in the liquid slag.

SUMMARY

It has been possible to express quantitatively and with satisfactory accuracy the distribution of manganese and of sulphur between liquid metal and slag in the basic open-hearth furnace over a wide range of slag composition. The distribution ratio at equilibrium depends upon concentration factors that are directly determinable from the chemical analysis of slag and metal, in the case of sulphur involving also three constants that have been evaluated from laboratory determinations of equilibrium between liquid iron and simple slags. This leads to the following practical conclusions with respect to the conservation of manganese and the elimination of sulphur in making basic open-hearth steel.

Retention of manganese in the steel is favored by a high concentration in the slag of MnO relative to FeO, which implies that maximum retention is obtained where the slag is basic enough, or rich enough in lime, to liberate essentially all the MnO from complex silicates, yet not so basic as to have an increased concentration of FeO and the associated increase in slag volume. The optimum slag composition for maximum retention of manganese is one corresponding to an effective lime-silica (basicity) ratio between 2.3 and 2.5.

A high distribution (concentration) ratio of sulphur in slag to sulphur in metal is favored by: (1) high concentration of effective or "free" CaO and MnO in solution in the slag; (2) low concentration of FeO in the slag; and (3) low concentration of SiO_2 and P_2O_5 in the slag, such as to favor a large total number of molecules (N_s) per unit weight of slag; or, in other

words, to bring to a minimum the number of large silicate and phosphate compound molecules present in the liquid slag.

The foregoing statements apply to concentration relationships, but the amount of slag present per unit weight of steel is in practice also a factor. With respect to maximum recovery of manganese in the metal, the requirement is simply minimum slag volume, and this presumably is dependent upon the practical minimum of silicon in the charge, with lime adjusted thereto so that the 2.3–2.5 lime-silica ratio is obtained. Good sulphur retention in the slag is also consistent with such a low slag volume up to a certain point, insofar as it can be promoted by a low-silicon, high-manganese charge; but if still better elimination of sulphur is required, or if the charge is high in silicon, more lime must be added, with a consequent increase in slag volume and a resultant decrease in manganese recovery.

The satisfactory agreement between data from a large number of open-hearth heats, covering a wide range of slag composition, and the equation, which is based on certain simplifying assumptions, corroborates the validity of these assumptions and leads to the following conclusions regarding the constitution of the slag and metal.

In the metal substantially all the sulphur can be regarded as being present as FeS; less than 5 per cent as MnS.

In a slag for which the lime-silica (basicity) ratio has a value greater than about 2.0, substantially all the MnO and FeO are "free" instead of being combined with other oxides to form less simple compounds. In these same slags, lime and silica are combined to form the very stable dicalcium silicate ($2CaO.SiO_2$), which at steelmaking temperatures is not dissociated in appreciable extent.

Lime present in excess of that required to form the dicalcium silicate is available for the compound $3CaO.SiO_2$, which, however, dissociates much more than the disilicate.

In less basic slags both MnO and FeO replace lime in $2CaO.SiO_2$ to some extent, MnO apparently being somewhat more active in this respect.

The compounds calcium sulphate and calcium ferrite, which are continuously formed to some extent at the upper slag surface, appear to be dissociated to a much greater extent at the slag-metal interface. Thus, these act as oxygen carriers downward through the slag: the most important can be regarded as ferric oxide, the concentration of which relative to ferrous oxide is decidedly less at the bottom than at the top of the slag layer. The activity of oxygen at the interface seems to be closely approximated by assuming that it is equivalent to the total oxygen in both ferrous and ferric oxide, as determined by analysis, even though the ferric oxide may not be completely reduced at the interface.

REFERENCES

1. P. Körber: *Stahl und Eisen* (1932) 52, 133–144.
2. J. Chipman and Ta Li: *Trans. Amer. Soc. Metals* (1937) 25, 435–465.
3. Bardenheuer and Geller: *Mitt. K. W. I. Eisenforschung* (1934) 16, 77–91.
4. K. L. Fetters and J. Chipman: *Trans. A.I.M.E.* (1941) 145, 95.
5. F. Körber: *Stahl und Eisen* (1936) 56, 433.
6. Meyer and Shulte: *Archiv Eisenhüttenwesen* (1934) 8, 187.
7. K. L. Fetters and J. Chipman: *Trans. A.I.M.E.* (1940) 140, 170.
8. T. L. Joseph and W. P. Holbrook: *U. S. Bur. Mines R.I.* 3240 (June 1934).
9. C. Schwarz: *Archiv Eisenhüttenwesen* (1932) 6, 227.

DISCUSSION

(Frank G. Norris presiding)

C. B. Post,* Reading, Pa.—This paper represents a step in determining the intermolecular compounds present in liquid slags at steelmaking temperatures. Although caution should be exercised in being too definite regarding the intermolecular compounds present in liquid slags by this method of analysis, nevertheless the conclusion is justified that the orthosilicate ($2CaO·SiO_2$) is the principal silicate of calcium in basic slags. This view is sup-

* Metallurgical Department, Carpenter Steel Co.

ported indirectly by the recent experimental work of Fetters and Chipman.[4] The presence of tricalcium silicate at high lime contents is necessary to explain the phenomena of "falling" slags in basic electric-arc furnace slags.

that progress can be hastened by extrapolation of existing data. This paper by Darken and Larsen is of the latter type, and measured in the light of the general problem referred to earlier, these authors have many equations to consider

TABLE 3.—*Calculations Based on Table 2*

Slag Number	(CaO)[a]	(FeO)[a]	K_{1e}[b]	K_{2e}[b]	$\Sigma S \cdot [S]$		[Mn]	
					Calc.	Anal.	Calc.	Anal.
1	20	7	1.7	0.13	2.3	3.0	0.09	0.08
2	25	6.2	0.5	0.13	9.1	14.9	0.12	0.12
3	28	3.7	2.8	0.13	5.3	5.3	0.38	0.43
4	36	3.0	3.0	0.13	6.7	6.7	0.28	0.31
5	23	5.5	2.0	0.13	2.9	3.6	0.11	0.10
6	18	7.0	0.47	0.13	10.0	15.5	0.50	0.44
7	26	5.5	0.55	0.13	10.3	14.7	0.28	0.23

[a] Free lime and FeO; percentage by weight as determined from tables of Schenck.
[b] After values of constants in reaction

$$\frac{\Sigma S}{[S]} = \frac{(CaO)}{(FeO)_{k \cdot K_{1e}}} + \frac{[Mn]}{K_{2e}}$$ on page 168—Schenck.

In focusing attention only on the behavior of manganese and sulphur at lime-silica ratios in the neighborhood of 2.5, we must not lose sight of the fact that dissociation constants for all of the silicates, $FeO \cdot SiO_2$, $MnO \cdot SiO_2$, $2CaO \cdot SiO_2$, etc., should be known in relation to one another in order to have faith in conclusions drawn from limited data, such as that obtained from the basic open hearth only. The general problem is to be able to state at what stages certain slag-metal reactions are at equilibrium in the various processes of steel refining. Thus, all such methods of calculating equilibrium reduce essentially to a set of self-consistent equations, which are in fact, a system of bookkeeping for experimental data relating to these slag-metal reactions in steel refining.

Viewed in this light, we can differentiate between the researches of Körber and Olsen, of Chipman and his associates, of Maurer and Bischoff, H. Schenck and his co-workers at the Krupp Works, P. Herasymenko, Count Bo Kalling of Jernkontorets, and C. H. Herty, Jr. The first two groups of workers have preferred to attack steelmaking problems concerning slag-metal reactions in a purely experimental manner, never committing themselves to any conclusions except those supported by *direct* experimental data. The other workers have directed their efforts toward obtaining correlations between operating and laboratory data on steel-refining problems, so

before it can be said that they are presenting an acceptable means of studying slag-metal reactions.

H. Schenck[10] considered equilibrium in steel-making reactions, and the assumptions used by Dr. Schenck are quite at variance with the assumptions used by Darken and Larsen, yet Schenck's methods lead to a prediction of the bath composition with as good agreement as found by Darken and Larsen for the manganese and sulphur reactions. Furthermore, Schenck extended his equilibrium studies to all of the reactions commonly met in steel refining, and was able to build up a set of self-consistent equations that reproduced equilibrium conditions in both acid and basic processes of steel refining.

To illustrate further, we have taken the analyses of slags shown by Messrs. Darken and Larsen in Table 2 and calculated these slags on the basis of Schenck's methods to predict the manganese content of the bath and the sulphur ratio existing between the slag and metal for these cases. These calculations are summarized in Table 3.

Comparison of the values shown in Table 3 with those obtained by Darken and Larsen show that Schenck's methods will certainly calculate the manganese content from slag analysis as well as the methods proposed by

10 H. Schenck: Physikalische Chemie der Eisen-hüttenprozesse, 2. Berlin 1934. Julius Springer.

Darken and Larsen, and furthermore, in these few isolated cases will almost calculate the sulphur distribution ratio as well as these authors, except for the high-lime, low-silica slags.

Now consider the totally different picture of intermolecular compounds to be inferred from Schenck's methods and those of Darken and Larsen. Schenck assumed the silicates of iron, manganese and calcium to be of the form $2FeO \cdot SiO_2$, $2MnO \cdot SiO_2$ and $(CaO \cdot SiO_2)$. Dissociation constants for these silicates were evaluated from acid and basic open-hearth data. On this basis, the "free" lime at any lime-silica ratio would be greater by Schenck's methods than that found by Darken and Larsen. In considering the sulphur reaction, Schenck ignored the concentration of FeS in the slag ($A = 0$) and threw the burden of carrying the sulphur on the lime content. In evaluating the "equilibrium constant" for the sulphur reaction, Schenck found that the constant defined by $\frac{(CaO)[S]}{(FeO)(S)}$ was not constant, but a function of the silica content of the slag (because the lime was too dissociated at high silica contents). The point is that even though Schenck's picture is far out of line with the suspected intermolecular compounds, nevertheless a group of self-consistent equations was presented that reproduced equilibrium between slag and metal reactions in the acid and basic open hearth and in Bessemer and Thomas converters.

This comparison between Schenck's method and those of Darken and Larsen is made merely to point out that the final conclusion regarding the intermolecular composition of slags is to a large measure a function of the initial assumptions that must be made to start unraveling the problem. Thus Darken and Larsen choose to assert that the MnO and the FeO contents are substantially uncombined when the lime-silica ratio is equal to and greater than 2.5. The validity of this assumption is an open question because it can be shown that, within the limits of error commonly met with in slag analyses and computational errors, some small part of the MnO and FeO contents are combined with silica even at fairly high lime-silica ratios, as indeed is necessary when finite dissociation constants are given for the silicates of iron and manganese in order to reproduce acid-slag

processes. Similarly, the "free" lime contents shown by Darken and Larsen in Fig. 2 is entirely a function of their assumed equation for the sulphur ratio, for correlating data on this reaction.

The main contribution made by Messrs. Darken and Larsen to this problem of equilibrium in steel-refining practices is one that has been inferred in the work of Körber and Olsen, and Darken,[11] i.e., slags and metal systems with few exceptions obey closely Raoult's law for regular solutions over a wide range of concentration of the constituents. The apparent deviations in some steelmaking reactions from the laws of regular solutions have been shown by this and other works to be due mainly to an incorrect formulation of the intermolecular slag composition.

L. S. DARKEN AND B. M. LARSEN (authors' reply).—In our paper we attempted to derive open-hearth slag-metal equilibrium relationships from available laboratory data on relatively simple equilibria; and pointed out in detail that there is relatively good agreement between the values of the constant derived from the several sources by direct and by indirect methods. The application of data derived from investigation of simple systems to the complex slag of the open hearth involves of necessity some postulates as to the activity of the several constituents, since none of these activities (except that of the oxides of iron) has been directly measured or is likely to be in the near future; and we chose to attack this problem from the viewpoint of molecular constitution. The picture now presented, which admittedly was selected to fit the data as well as possible, is quite sketchy and incomplete. Nevertheless, it does seem to tie together a variety of miscellaneous experimental results with steelmaking experience. In this sense the proposed equations are more than "a system of book-keeping" for slag-metal equilibrium. It is shown that the constant for the distribution of iron sulphide is essentially identical whether determined experimentally on a simple system or derived statistically from slag-metal data; the same is true of the constant in the manganese term of the desulphurization equation. The coefficient of the lime term was determined

[11] L. S. Darken: Trans. A.I.M.E. (1940) 140, 204.

with the aid of open-hearth data, since no experimental data on the activity of lime in silicate melts were known to the authors. Since two terms of the equation were now known and there was good agreement between experiment and practice, thus verifying the method, it was thought that a third term could be obtained by difference without too great error.

The procedure of the present paper is quite different from that of Schenck, who by rather complex methods derived equilibrium constants mainly from slags of the type to which they were to be applied rather than from laboratory data on simple systems. Frequently his equilibrium "constants" were not constant even after correction of the concentration for compound formation. Thus the coefficient for the lime terms in Schenck's desulphurization equation is not constant but varies twentyfold as a function of silica content. Such a correction term is purely empirical and has little, if any, justification from a physicochemical standpoint. Admittedly we endeavored to avoid such empirical terms by making several stated hypotheses, but these hypotheses, which are clearly stated in the paper, by no means affect the order of magnitude of the results on desulphurization. For example, in most cases it makes but little difference whether the slag phosphorus is considered combined as $4CaO \cdot P_2O_5$ or as $3CaO \cdot P_2O_5$, or whether the equivalent FeO is calculated by the method given or by some other method, although statistically the two examples employed seem to fit best.

The criticism appearing in the discussion is somewhat inconsistent; at one place there is the statement that "the 'free' lime (Fig. 3) is entirely a function of the assumed equation for the sulphur ratio," and at another that the main contribution of the present paper has already been inferred from other work—that Raoult's law is obeyed over a wide range of concentration in slag-metal systems. If it is granted that Raoult's law (with proper choice of constituents) holds, then the free lime as shown in Fig. 3 follows by rigorous physico-chemical reasoning from the data and not from an "assumed equation."

The main object of the present paper has been to demonstrate that the slag-metal equilibria considered may be deduced from laboratory data by physicochemical methods without the aid of empirical adjustment terms. As present knowledge is limited, this end may not have been completely attained, but we hope that a step has been made in that direction.

Significance of the Bessemer End Point

By H. T. Bowman*

(New York Meeting, February 1942)

For more than 80 years the Bessemer process has depended upon the ability, skill, and judgment of the blower, although as early as the 1860's it was recognized that the process would benefit by some type of instrumental control.[1] However, instruments with sufficient recording speeds did not exist, so the end-point determination was always dependent upon the blower's eye. This placed an obstacle in the way of precise experimental work, because of the absence of the necessary records and reference points as reported by Work.[2] The use of the photocell provided the instantaneous record of the blow that made this experimental work possible and provided more scientific control for the process as discussed by Graham.[3] A brief description of the progress of the blow will illustrate the recording function of the instrument.

The silicon in the iron is being oxidized during the first minutes of the blow, as pointed out by Henning[4] in a table showing the order of metalloid elimination. The product of this oxidation is a solid that remains in the converter, so there is virtually no flame during this part of the blow. This low flame luminosity is illustrated by the flame recording shown in Fig. 1, where the silicon blow is plainly marked. The dull flame of the silicon blow gradually gives way to the brilliant carbon flame as the increasing quantities of carbon monoxide formed inside the converter burn to dioxide upon contact with

the atmosphere above the vessel. When the carbon reaches some low value under 0.20 per cent, there is insufficient monoxide formed to maintain the dioxide flame, so its intensity drops. Throughout the flame drop carbon continues to burn, until at some value around 0.05 per cent an arrest occurs in the recorded drop. This point has been designated as the end point.

The period of time from this end point until the vessel is turned upon its side and blowing has stopped has been called the afterblow. This afterblow is used as a measure of the degree of metal oxidation, and uniformity demands that it be controlled within narrow limits. Iron and blowing conditions are likely to change several times during a turn, necessitating corresponding changes in end-point control. It is the purpose of this paper to discuss these changes, the factors that make them necessary, and their bearing upon the quality of steel.

Carbon-FeO Relationship

In the Bessemer process oxidation relationships are precise. Fig. 2 shows a graph of the carbon-FeO relationship. The familiar "bomb-test" method, described by McCutcheon and Rautio,[5] was used for obtaining these and all other dissolved FeO values herein reported, all tests being taken from the converter before deoxidation unless otherwise noted. All tests of 0.10 per cent carbon and above were obtained from metal blown for duplexing. McGinley and Woodworth[6] reported iron oxide values for blown metal, but their tests were obtained by a different method than were those

reported here. With this exception there is little information in the literature relative to dissolved oxides in Bessemer steel. The results herein reported are for one set of

the carbon and FeO analyses shown. The blow recorded at the extreme right was blown with 15 blanked tuyeres in the bottom. With approximately the same
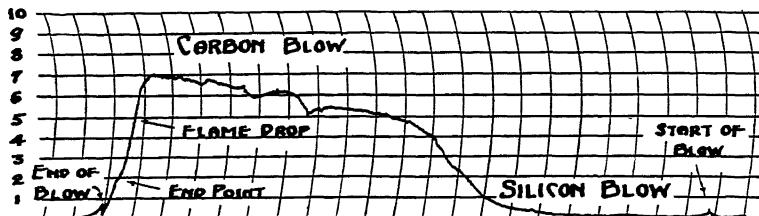

FIG. 1.—TYPICAL PHOTOCELL RECORDING OF BESSEMER BLOW.

operating conditions only. Similar information gathered under other conditions, particularly in the low-carbon range, would be of interest and value.

The curve in Fig. 2 demonstrates how the metal is protected from overoxidation until the low carbon values are reached, and shows that the rate of metal oxidation increases rapidly when the carbon reaches

length of afterblow as the preceding blow the retarded rate of oxidation is evidenced by the lower FeO analysis.

INFLUENCE OF OPERATING VARIABLES

Effect of Bottom Conditions.—The bottoms of the vessels used in gathering these data contain 35 tuyeres, each tuyere having seven holes of $\frac{5}{8}$-in. diameter. As is com-
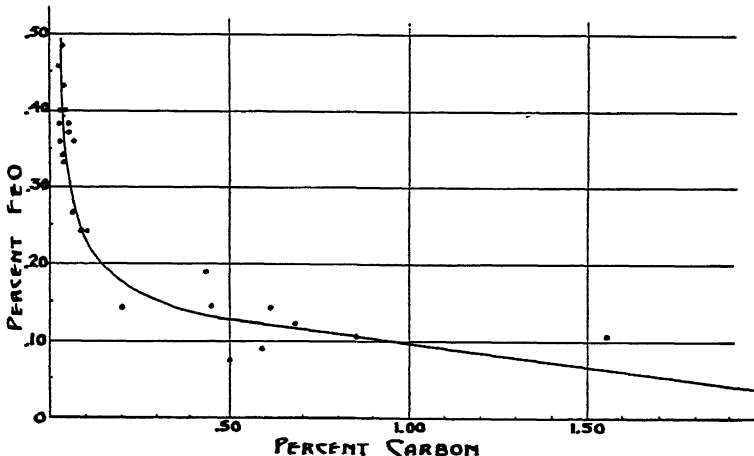
FIG. 2.—RELATIONSHIP OF CARBON AND IRON OXIDE IN BLOWN METAL.

these lower values. These points, of course, all lie in the region shown as the flame drop in Fig. 1.

To give a clearer picture of the relationship of the flame recording to this carbon-oxidation ratio, several examples are shown in Fig. 3. Each of these blows was turned down at the point marked χ, resulting in

mon practice in the industry, some of these tuyeres are blanked off as they become too short for continued safe use. This restricts the amount of air supplied to the converter and thus affects end-point control to a considerable degree. McCaffery[7] and Fulton[8] have advanced considerable information concerning blast restrictions and variations.

To minimize such variables, a constant blowing pressure is maintained at 25 lb. per sq. inch.

The effect of a change in bottom condi-

Iron Composition.—Changes in iron composition, principally in regard to silicon content, affect the rate of oxidation at the end of the blow. Experience has shown that


| %Carbon | .10 | .06 | .04 | .04 | .04 |
| %FeO | .24 | .27 | .37 | .48 | .40 |
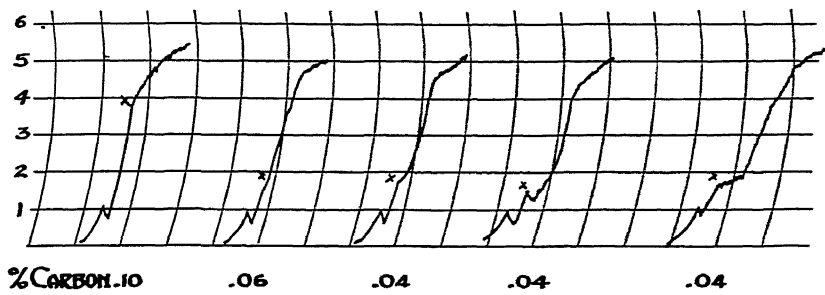
FIG. 3.—CARBON AND DISSOLVED FeO IN RELATION TO TURNDOWN POINT.
x marks the point where vessel was turned down.

tions is further illustrated in Fig. 4. These two heats were blown to the same end point and afterblow, but on different bottoms. The restricted blast volume of the blanked-up bottom resulted in less oxidation, as evidenced by the higher metalloid

it is very easy to overblow, or overoxidize, low-silicon iron, whereas high-silicon iron must be given a longer afterblow than normal to avoid a young, or underoxidized heat. The significance of this phase of control is discussed in Yocum's paper on
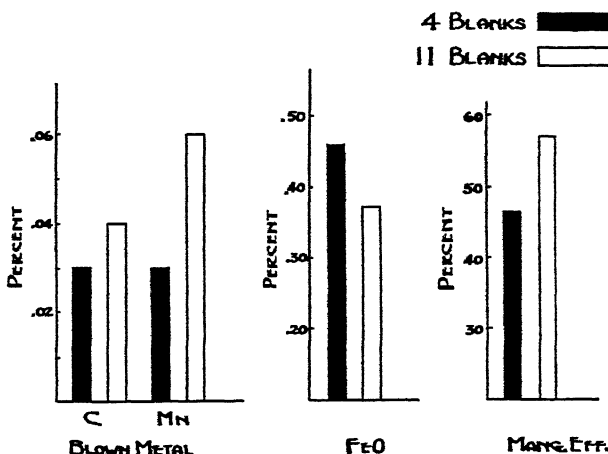
FIG. 4.—SPECIFIC EXAMPLE ILLUSTRATING EFFECT OF BLANKED TUYERES ON DEGREE OF METAL OXIDATION.

content, lower FeO analysis, and greater manganese efficiency. The small number of blows used in this graph and others that follow represent typical results and are not intended to establish definite points of reference.

dephosphorization.[9] Effective control requires an accurate knowledge of the silicon analysis of the iron being blown. Reported cast analyses and mixer averages are sometimes misleading—for example, a test from a mixer average of 1.35 per cent Si

may actually analyze either 1.10 per cent or 1.55 per cent Si. These discrepancies are by no means the rule, but unless detected they may result in a substandard blow.

analysis of the iron for each blow. Each of these blows was made with four blanked tuyeres in the vessel bottom. The length of silicon blow, corrected for the number of
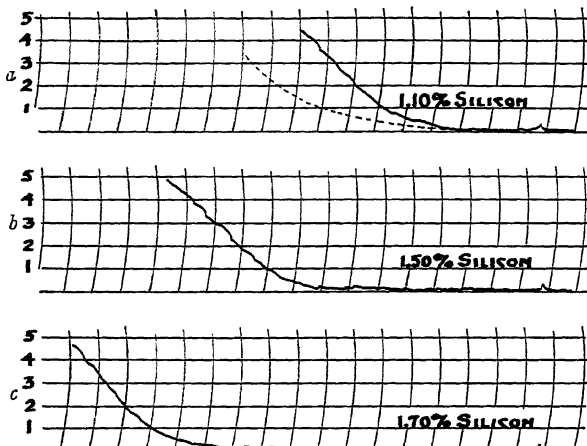
FIG. 5.—LENGTH OF SILICON BLOW RELATED TO SILICON CONTENT OF IRON.
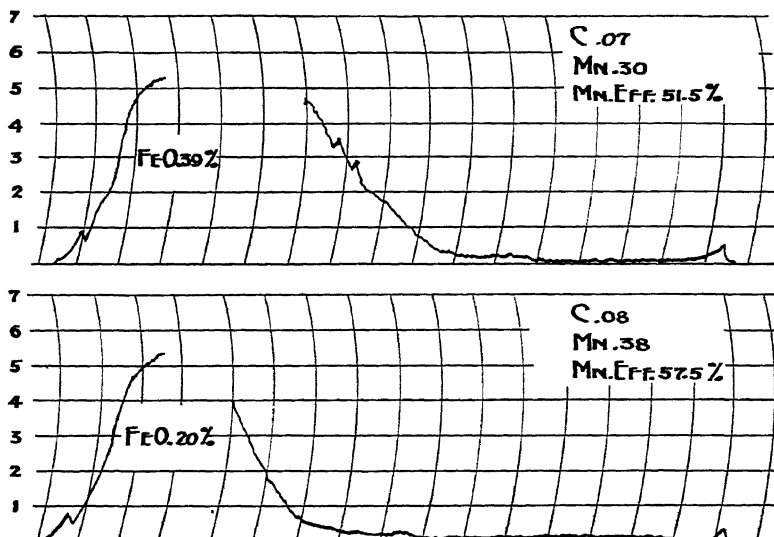
FIG. 6.—SPECIFIC EXAMPLE ILLUSTRATING GREATER DEGREE OF METAL OXIDATION THAT OCCURS WHEN LOW-SILICON IRON IS BLOWN.

The part of the flame recording known as the "silicon blow" furnishes a sufficiently accurate means of measuring this silicon content. In Fig. 5 are shown the early parts of three blows with the actual silicon

blanked tuyeres and the weight of iron, correlates closely with the silicon analysis of the iron. This relationship is quite apparent. The dotted line in Fig. 5a is a silicon blow made from 1.10 per cent Si

iron, but blown with eight tuyeres blanked instead of four, further illustrating the blast restriction due to blanked tuyeres.

To attain the same degree of metal

Temperature.—Degree of oxidation and temperature are generally listed as the two major factors to be controlled in the Bessemer process, and much has been
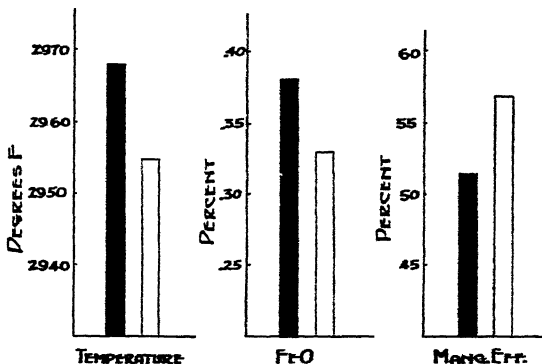
FIG. 7.—SPECIFIC EXAMPLE ILLUSTRATING EFFECT OF TEMPERATURE ON DEGREE OF METAL OXIDATION.

oxidation, a longer afterblow should be allowed for high-silicon iron than for iron with a lower silicon content. This is demonstrated in Fig. 6, where the silicon blow and the flame-drop portions of two blows are shown, one from 1.20 per cent and the other

written on the ill effects of poor temperature control on steel quality. Another angle, worthy of development, is that of the effect of temperature variation on degree of oxidation. With the wide temperature variations possible in blowing metal for
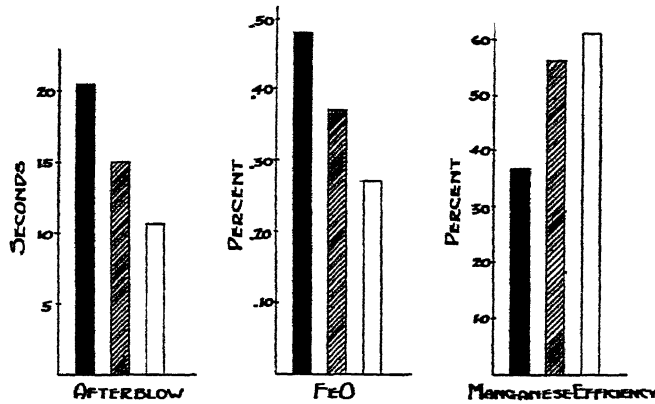
FIG. 8.—SPECIFIC EXAMPLE ILLUSTRATING EFFECT OF AFTERBLOW LENGTH ON DEGREE OF METAL OXIDATION.

from 1.45 per cent Si iron. These blows were made with the same number of tuyeres blanked and were given the same length of afterblow, as shown. The greater oxidation of the lower-silicon iron is reflected in the ladle analyses and the manganese efficiencies of the two blows.

duplexing, it was fairly simple to develop the higher degree of oxidation that accompanies hot blowing. However, it was decided to illustrate the less spectacular phase, that of the difference in the degree of oxidation between two consecutive blows given the same length of afterblow, but

blown at different temperatures. Fig. 7 shows the results from two such blows. The temperature variation is only that normally encountered in Bessemer practice, yet this

AFTERBLOW AND OXIDATION

Many examples could be given to show the significance of the length of afterblow
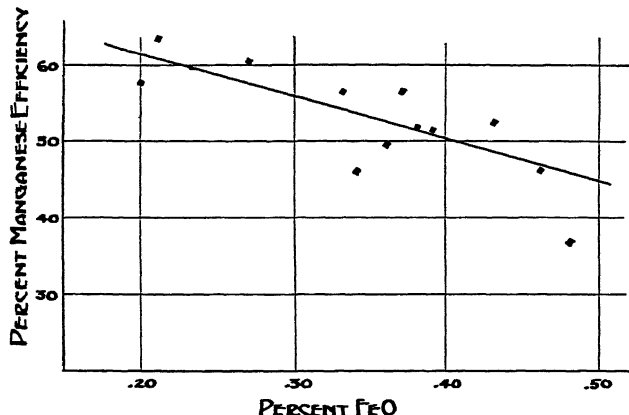
FIG. 9.—DISSOLVED FeO RELATED TO MANGANESE EFFICIENCY.

was sufficient to affect the degree of oxidation and manganese efficiency as shown.

When the blower encounters a hot heat, he must choose between pulling the heat young to avoid overoxidation and blowing

on the degree of metal oxidation. The information given in Fig. 8 was obtained on three consecutive blows made on the same bottom, but given different lengths of afterblow. The degree of oxidation follows
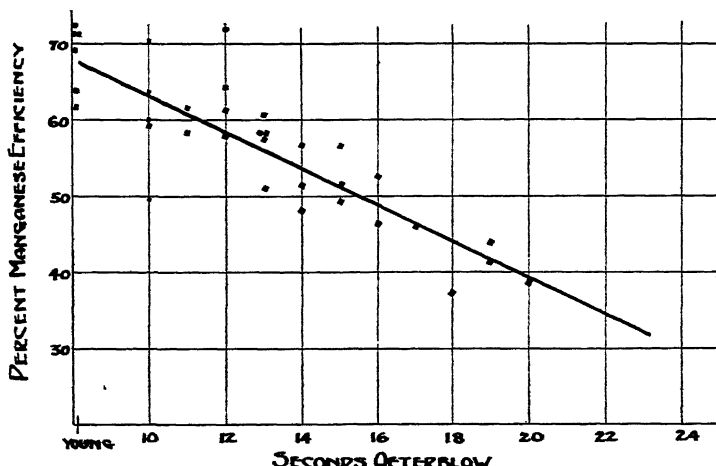
FIG. 10.—LENGTH OF AFTERBLOW RELATED TO MANGANESE EFFICIENCY.

it to the end point, with certain overoxidation. The risk in the former practice is that a high-carbon heat may result while in the latter extra deoxidizers are required, with attendant uncertainty of control.

the same trend as the afterblow length, and, as would be expected, the manganese efficiency was poorer on the overoxidized blow. The blow that was given the 21-sec. afterblow was considerably below standard

in surface quality, while the others were normal for capped steel practice. This phase of the significance of control will be more thoroughly developed later in this paper.

MANGANESE EFFICIENCY

In view of the need for conservation of manganese, it seems pertinent to show Fig. 9, illustrating the relationship between manganese efficiency and the FeO content of the blown metal. Since the length of afterblow is the primary factor in the control of the FeO in the metal, a relationship should exist between the length of afterblow and manganese efficiency. Fig. 10 shows this relationship very clearly. As a matter of interest, and to illustrate the validity of these data, Fig. 10 was made up from the information obtained on the blows reported in Fig. 9, then an equal quantity of information obtained about a year previous was superimposed on the chart without changing the trend in any way.

MECHANICALLY CAPPED BESSEMER

Much Bessemer steel is teemed into "bottle-top" molds as effervescing, open steel, and then mechanically capped to stop the rising action. The primary purpose of this practice is to obtain a uniform cross section of ingot with maximum yield possibilities. One 22 by 24 by 76-in. ingot was chosen from a representative blow of six ingots and split through the vertical axis (Fig. 11). The freedom from pipe and low degree of segregation are worthy of note.

Pouring Practice.—Correct practice for capped steel requires a rising, or growing steel, controlled within narrow limits. This, of course, requires that the metal temperature and degree of oxidation be controlled closely. It is readily understood that variation of oxidation may cause a difference in the quality of two blows, but such variations often cause nonuniformity within the individual blow. The steel pourer judges the condition of the blow during the pouring of the first ingot and tries to control the

FIG. 11.—SPLIT BESSEMER CAPPED INGOT. ANALYSIS, PER CENT

Spot	C	Mn	P	S
1	0.11	0.43	0.095	0.031
2	0.10	0.43	0.093	0.027
3	0.09	0.41	0.097	0.027
4	0.21	0.42	0.212	0.079
5	0.14	0.41	0.129	0.044
6	0.10	0.39	0.097	0.032
7	0.10	0.40	0.095	0.028
8	0.10	0.41	0.103	0.031
9	0.09	0.40	0.098	0.028
10	0.09	0.41	0.099	0.029
11	0.09	0.41	0.090	0.027
12	0.09	0.42	0.091	0.028
13	0.09	0.41	0.090	0.028
14	0.09	0.40	0.097	0.032
15	0.09	0.42	0.095	0.030
16	0.10	0.41	0.096	0.031

rate of gas evolution accordingly. Over-oxidation or underoxidation changes the rate of gas effervescence in the mold, so that the first or second ingot of an over-

two of the overblown heats on this chart were blown on blanked-up bottoms. While the young heats were not as bad as those overblown, they were for the most part
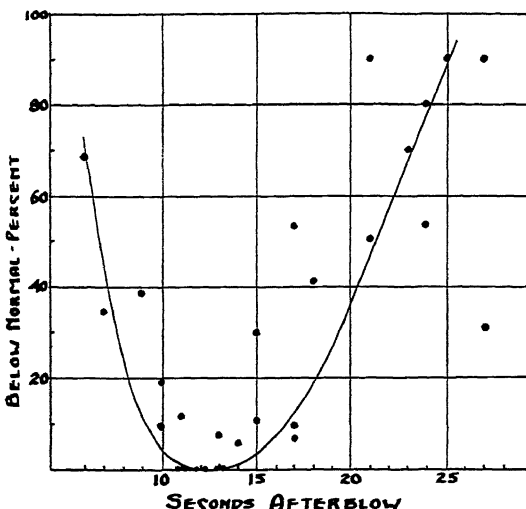

FIG. 12.—AFTERBLOW RELATED TO SURFACE DEFECTS (MATERIAL REQUIRING RECONDITIONING).

blown heat may not be properly controlled and bleeders and unsound interiors are formed. Bleeders are ingots on which metal spurts between the top of the mold and the cap because of excessive internal gas pressure or poor capping practice.

Surface and Interior Quality.—In the early days of the photocell investigation, many blows were followed to evaluate the different blowing practices, and it was discovered that overoxidation or underoxidation usually caused poor surface or unsound internal structure, or both. One such investigation, involving 29 heats, is reproduced in Fig. 12. The evidence is overwhelmingly against anything over a 17-sec. afterblow, and it is rather definite that the young blow can be expected to give surface trouble. The afterblows as reported in this chart have been corrected for blanked tuyeres, so that there can be no question on that score. However, to the advocates of the extended afterblow for a blanked-up bottom, it might be pointed out that all but

definitely inferior to those in the 10 to 15-sec. afterblow range.

As a combined illustration of external and internal quality as related to the afterblow, an investigation was made of bar-mill skelp and the steel performance was followed closely in the tube mill. The results of this investigation are shown in Fig. 13. The afterblow portions of the flame recordings show one young, one normal, and two overblown heats. Blow D could be classed as severely overblown. The graph depicting the skelp-mill surface and edge quality has the same trend as that of the preceding graph. The follow through of the tube-mill performance gave a very similar curve, the principal tube-mill defects being laminations.

Since these data were obtained before the photocell instrument was used as a control, it has seemed advisable since the inauguration of the control to promote similar investigations at intervals. Results of the most recent study are shown in Fig. 14.

Again there are the three degrees of blow-ing—young, normal and overblown. This time manganese efficiencies, which attest to

note. A limited number of data indicates that the best steel performance is attained when the ladle FeO is between 0.20 and
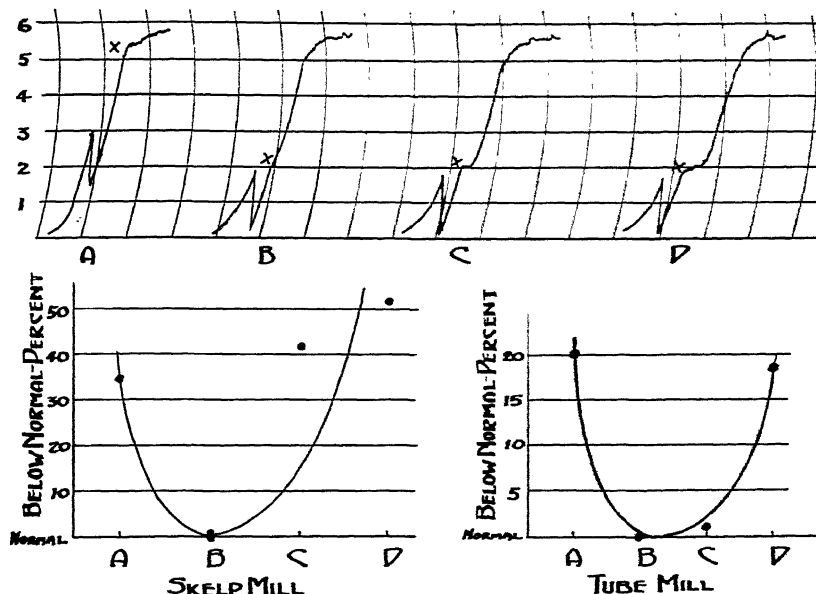

FIG. 13.—BLOWING PRACTICE RELATED TO SURFACE QUALITY AND TUBE-MILL PERFORMANCE.
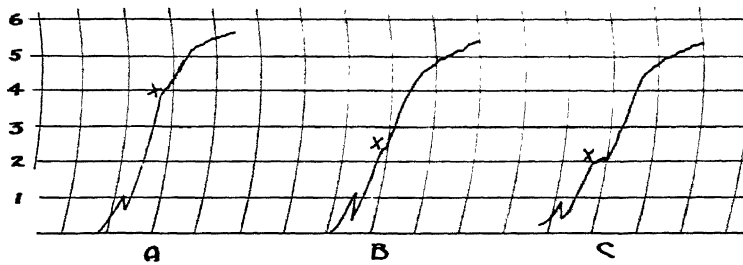
Surface	Normal	Normal	40% Below Normal
% Ladle FeO	.22	.28	.30
% Mang. Eff.	71.5	58.2	44.0

FIG. 14.—BLOWING PRACTICE RELATED TO SURFACE, MANGANESE EFFICIENCY, AND DISSOLVED FeO IN LADLE.

the degree of metal oxidation, are reported. Again the overblown heat was substandard in quality, though the young heat was fully up to standard in this case.

Range of Oxidation.—The ladle FeO values reported in Fig. 14 are worthy of

0.28 per cent when making capped Bessemer steel.

Type of Defects.—Experience in the manufacture of capped Bessemer steel has shown that the overblown heat usually causes a heavier type of surface defect than

the young blow. The latter usually shows a light slivered condition referred to as "dirty" surface.

*Etch Tests.*—Fig. 15 pictures etch tests

FIG. 15.—ETCH TESTS OF TWO TOP BILLETS FROM FOUR INGOTS OF OVERBLOWN BESSEMER HEAT (CAPPED STEEL).
Top row, top billets; second row, second billets.

taken from the two top billets from four ingots of an overblown heat. The segregation is rather characteristic for this blowing practice. The rimmed pattern shown in the billets at the left indicates that this ingot fell away and rimmed in after it hit the cap. This illustrates the lack of pouring control that may be encountered with irregular blowing practice.

RIMMED BESSEMER

Blowing Practice.—While not as important from the tonnage angle as capped steel, rimmed Bessemer is important as a source of material when ductility and surface are required rather than cross-sectional uniformity. In blowing steel for rimming ingots the end-point control is somewhat the reverse of that for capped practice; in the latter, overblowing is critical whereas for good rimming practice underoxidation must be avoided. Severe overblowing, however, is still to be avoided, because it causes excessive segregation, greater metal loss, lower manganese efficiency, and sometimes impaired surface.

The young, underoxidized heat contains insufficient dissolved FeO to promote good

rimming action, giving rising ingots. In the lower portion of the ingot the pressure of the evolved gas is too low to force itself up through the metal. These trapped gases form blowholes immediately beneath the ingot surface and cause the ingot to grow. Subsequent heating in the soaking pits is very likely to scale off the primary ingot surface, exposing the blowholes to oxidation, which in turn causes substandard surface quality.

Surface Quality.—In Fig. 16 surface defects are plotted against length of afterblow on five consecutive rimmed heats that were followed closely from iron to billet hot bed. The young blow represents very poor practice. The FeO in solution in the ladle on this blow was only 0.24 per cent, the ingots all growing in the molds to the extent of 6 to 10 in. Surface defects were prevalent on the billets from the bottom half of every ingot on this blow, while very few defects appeared on the upper billets. On the other hand, the defects that appeared on the severely overblown heat (26-sec. afterblow) were confined mostly to the first and last ingots, indicating that a controlled rate of gas evolution was attained throughout most of the pour.

Range of Oxidation.—From the preliminary data now at hand it seems that a minimum of 0.28 to 0.30 per cent dissolved

FeO in the ladle is necessary to promote good rimming action. Very limited data indicate that ladle FeO values above 0.35 to 0.37 per cent, while they give a very nice

is that oxysulphides are the sources of machinability. Overblowing, with increased contact between iron oxide and sulphur, should promote the formation of these
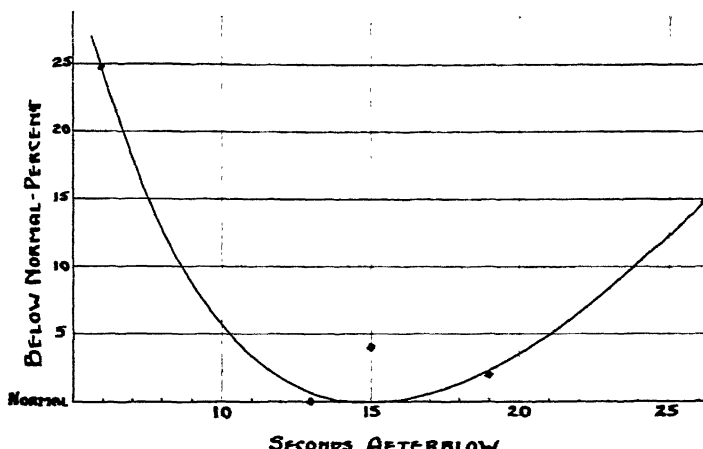

FIG. 16.—AFTERBLOW RELATED TO SURFACE DEFECTS OF RIMMED BESSEMER.

rimming action, cause excessive segregation in the top portion of the ingot.

Temperature.—Although well known, the effect of temperature on rimming action should be mentioned. A cold heat often rims poorly, even though it contains enough FeO to promote the rimming action. Cold heats where the ladle FeO content was as high as 0.29 per cent have given poor rimming action and substandard billet surface. On hot heats the excessive temperature delays the formation of the chill crystals that start the inward freezing of the metal. Gas evolution proceeds without metal solidification, and should this condition last long enough before the metal begins to rim in there will be insufficient gas left to maintain the proper action and the ingot will grow, much the same as the ingots of a young heat grow.

SCREW STEEL

Blowing Practice and Machinability.—End-point control is subject to considerable variation in the manufacture of Bessemer screw steel. One contention, held for years,

sulphides. The degree to which this path may be followed is limited only by the amount of billet reconditioning that will be countenanced by plant management, for, generally speaking, the more the overblowing, the greater the reconditioning costs. Machining of the center piercing or drilling type is often retarded by such overblowing because of the excessive segregation that accompanies this blowing practice. An elaborate etch testing program developed this information in a striking manner, which led to the adoption of the afterblow length that gave the soundest internal structure. This is in the neighborhood of 15 to 16 sec. under normal blowing conditions. Surface quality is enhanced also by this length of afterblow.

Sulphur and the End Point.—Sulphur additions to the vessel change the appearance of the flame during the flame drop and also lower the recorded end point on the electric-eye chart. The flame appears more red and gives off large quantities of red-brown fumes. This causes the heat to look overblown before the end point is

actually reached, and in many plants where all of the sulphur is added to the vessel the blow is turned down during the flame drop.

KILLED AND RECARBURIZED BESSEMER

The tonnage of killed and recarburized Bessemer is relatively small, but enough

of the slag to run into the ladle with the metal is difficult to overcome.

The slag analysis is a good indication of the degree to which the blow itself has been oxidized. In Fig. 17 is shown the slag analysis in FeO and SiO_2 for blows ranging from 0.70 per cent carbon duplex metal
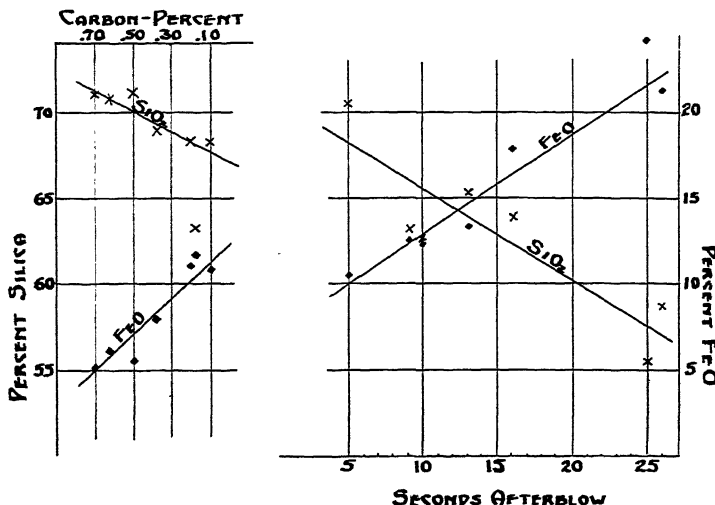
FIG. 17.—FeO-SILICA RELATIONSHIP OF SLAG TO CARBON CONTENT OF DUPLEX BLOWN METAL AND AFTERBLOW OF BESSEMER HEATS.

has been produced to prove that the overblow is to be avoided. For low-carbon killed steel the flow should be turned down at the end point, assuring the carbon desired, but avoiding excessive oxidation. For recarburized steel, the general practice is to pull the heat as soon as the flame drop is definitely reached.

Bessemer Slags

The Bessemer slag is purely the result of the oxidation processes taking place in the converter, performing none of the functions of the open-hearth slag. The slag will be dry and coarse in appearance at any point of turndown before the flame drop. At the end point there is sufficient FeO contained in the slag to hold it together as a dry, pasty mass. With any extension of the afterblow, the slag takes on a wet, mushy appearance, and with severe overblowing the tendency

down to severely overblown Bessemer heats. Comparatively little iron is lost in the slag in any blowing practice that terminates the blow before the end point is reached, whereas an appreciable amount of iron is contained in the slag of an overblown heat.

SUMMARY

This paper has dealt specifically with degree of metal oxidation and its effect on steel quality. It has shown graphically that the degree of metal oxidation is dependent upon carbon content until the low-carbon values are reached.

The effect of blanked tuyeres in slowing the rate of metal oxidation has been described.

The length of silicon oxidation period has been shown to reflect accurately the silicon content of the iron being blown; also the influence of variable iron-silicon content on

rate of metal oxidation at the end of the blow is shown.

Increase in temperature of blown metal has been shown to increase the solubility of iron oxide with a corresponding decrease in recovery of manganese.

It has been brought out that when all operating variables were constant, the length of afterblow determined the degree of metal oxidation.

The importance of temperature and oxidation control in the production of various types of Bessemer steel has been indicated.

Brief reference has been made to the effect of blowing practice on slag characteristics and composition.

ACKNOWLEDGMENT

The author expresses sincere appreciation for the assistance and cooperation of associates, which has made this work possible.

REFERENCES

1. F. Kohn: Iron and Steel Manufacture, 112. 1868.
2. H. K. Work: Trans. A.I.M.E. (1941) 145, 132–150.
3. H. W. Graham: Trans. A.I.M.E. (1941) 145. 113–131.
4. C. C. Henning: Trans. A.I.M.E. (1935) 116, 137–158.
5. K. C. McCutcheon and L. Rautio: Trans. A.I.M.E. (1940) 140, 133–139.
6. E. E. McGinley and L. D. Woodworth: Trans A.I.M.E. (1941) 145, 151–159.
7. R. F. McCaffery: Yearbook Amer. Iron and Steel Inst. (1931) 351–381.
8. J. S. Fulton: Trans. A.I.M.E. (1941) 145, 175–193.
9. G. M. Yocum: Trans. A.I.M.E. (1941) 145, 160–174.

DISCUSSION

(T. S. Washburn presiding)

K. L. FETTERS,* Pittsburgh, Pa.—The author has added an interesting contribution to the series of papers on the Bessemer that have appeared in recent years. Coming soon after the Gould-Hand paper (see p. 76), this paper calls to mind that the methods of multiple correlation might profitably be applied to studies of the Bessemer process in order to tell more about the interrelations of the variables.

Several questions seem in order: What do scale or ore additions do to the length of the silicon blow and to the carbon-oxygen relation? Does steam have any effect on the final oxygen content of the metal? When sulphur is under 0.025 per cent. is there any difference in the shape of the afterblow curve? It has been stated by many blowers that the flame does not look the same when the sulphur is unusually low.

Has the expression of "normal" surface quality been based on the average of some quality rating or rejection, the average of which has been considered as "normal"?

H. T. BOWMAN author's reply.—Ore additions shorten the silicon blow. We have been unable to detect any effect of steam on the final oxygen content of metal. The end point is sometimes less distinct with low-sulphur metal.

Yes, our expression "normal" refers to an average quality rating based on predetermined standards.

R. B. SOSMAN,* Kearny, N. J.—There has never been a satisfactory explanation of the sudden appearance of the so-called end point as seen in the Bessemer flame. Its sharpness indicates some discontinuous phenomenon. This discontinuity cannot be in the composition of the metal because carbon is still present and is still oxidizing. I suggest that a possible explanation may be found in the phenomenon of liquid immiscibility. Liquid iron at a given temperature will dissolve a certain amount of oxygen. If it takes up additional oxygen a second liquid phase is formed, which may be considered a molten oxide but actually contains considerably more iron than the composition represented by the formula FeO. I picture the atmosphere in the Bessemer vessel as being filled with flying droplets of liquid metal. When the saturation or immiscibility point is reached, each of these drops suddenly becomes coated with the second liquid phase. It is not a stable equilibrium because oxygen may still be reacting with carbon in the interior of the drop, but that reaction is relatively slow and a temporary supersaturation may therefore occur. This sudden change in the character of the liquid surface of the droplets would be accompanied by a similarly sudden change in the appearance

* Assistant Professor of Metallurgy, the Carnegie Institute of Technology.

* Research Laboratory. U. S. Steel Corporation.

and spectrum of the flame. The occasional uncertainty in the end point is also consistent with this explanation. The characteristic spectrum lines will disappear sharply sometimes, then reappear for a few seconds and disappear again for a final end point. Such an effect would result from incomplete mixing of the body of metal, such that a fresh lot of liquid droplets would be a little short of saturation although the droplets in suspension a few seconds earlier had reached the immiscibility stage.

Observations in the Making and Use of Sulphite-treated Steels

By E. L. Ramsey* and L. G. Graper,† Members A.I.M.E.

THE present program of increased production of armament and lend-lease material for mechanized war has created a problem for the shops that must do the machining. They have naturally turned to the steel producers to provide them with a steel that can be accurately machined with the greatest possible speed. The adding of sulphur to steel as an aid to machinability has long been practiced; however, it may cause red shortness in rolling and may result in billets with seams and cracks, which must be removed before rolling can be continued. This conditioning of billets slows down production and adds to the cost of making steel.

Experience with various grades of sulphur steel made to different specifications has shown that Bessemer sulphur steels roll better than similar grades made in the open hearth, and also that low-carbon steels that are open or semikilled as tapped roll better than completely deoxidized or killed steels. This has led to the belief that oxygen plays an important part in the rolling qualities of sulphur-bearing steels.

It is generally held that the red shortness of sulphur steels is due to the low melting point of the sulphide compounds that separate out at the grain boundaries when the steel solidifies. At the rolling temperature of steel these sulphide compounds melt and cause cracking.

Adding Sulphur as a Sulphite

These difficulties can be avoided if sulphur is introduced into the steel by means of an anhydrous sulphite, such as sodium sulphite or sodium bisulphite, which—upon decomposition—forms sulphur dioxide. It is assumed that, in this case, the oxygen of the sulphur dioxide forms part of the sulphide inclusions in the steel, and raises their solidification temperature enough so that the formation in the steel of a low-melting eutectic is prevented. The result is the prevention of hot shortness and a more uniform distribution of inclusions.

Fig. 1 shows photomicrographs of steels made with sulphur, while Fig. 2 illustrates the structure of steels made with sodium bisulphite. These samples were cut from the steels as cast—that is, before rolling—and were polished and lightly etched to bring out the grain boundaries. Fig. 1 shows that sulphide inclusions segregate more or less at the grain boundaries, and it can be seen how the continuity of these low-melting inclusions would cause red shortness. Fig. 2 shows that the sulphide inclusions are more or less uniformly distributed throughout the matrix. This arrangement of inclusions has no apparent effect on the rolling qualities of a steel. This statement has been substantiated by the observation of the rolling of over 6000 tons of steel made with a sulphite addition.

Results

As stated before, the sulphur dioxide is added to steel by means of the decomposi-
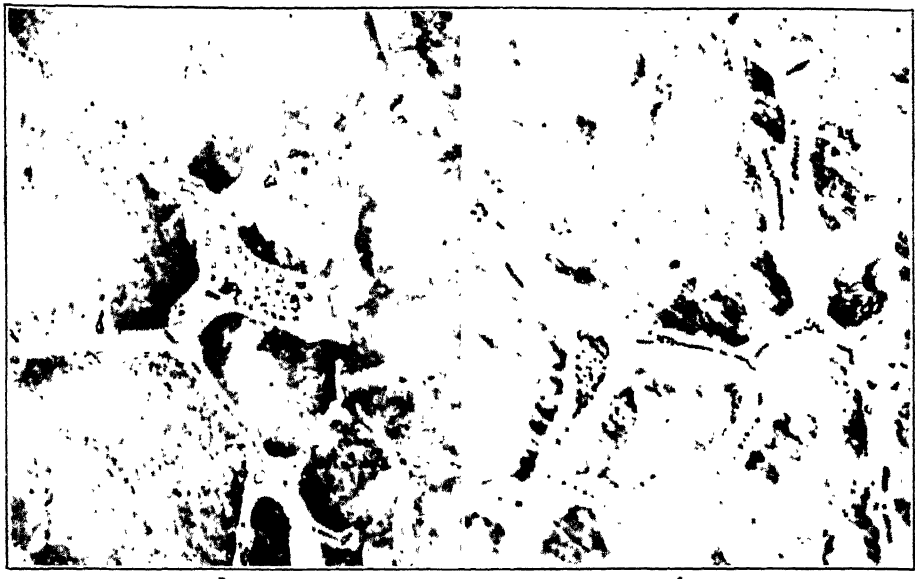
FIG. 1.—STRUCTURE OF STEELS MADE WITH SULPHUR. × 300.
a. Composition: C, 0.48 per cent; Mn, 0.94; P, 0.029; S, 0.184; Si, 0.21.
b. Composition: C, 0.36 per cent; Mn, 0.67; P, 0.022; S, 0.165; Si, 0.22.
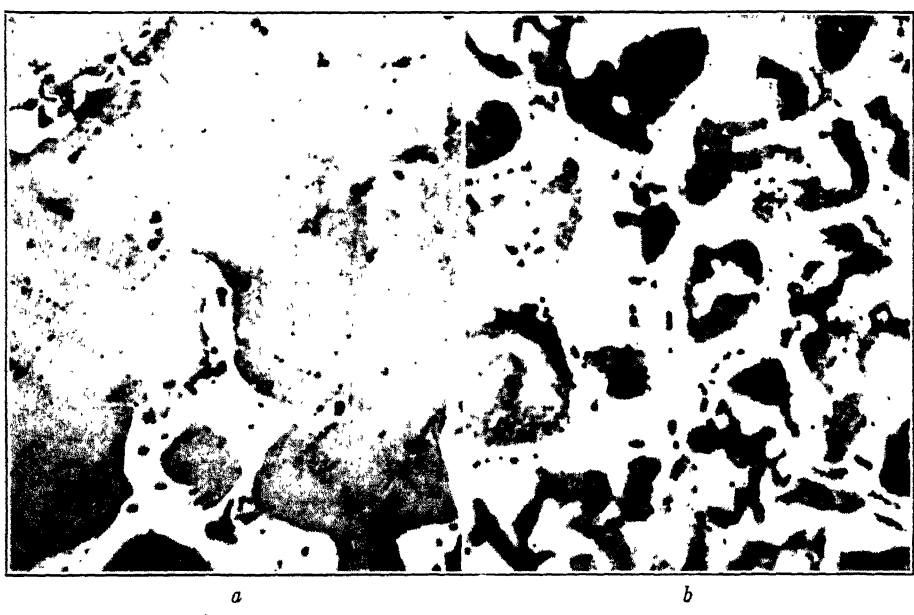
FIG. 2.—STRUCTURE OF STEELS MADE WITH SODIUM BISULPHITE. × 300.
a. Composition: C, 0.50 per cent; Mn, 0.80; P, 0.022; S, 0.160; Si, 0.21.
b. Composition: C, 0.36 per cent; Mn, 0.67; P, 0.022; S, 0.101; Si, 0.22.

tion of an anhydrous sulphite, principally sodium sulphite or bisulphite. In general, sulphites, upon being heated, decompose easily into sulphur dioxide and the oxide of the metal. For example:

$$Na_2SO_3 + heat \rightarrow Na_2O + SO_2$$
$$Na_2S_2O_5 + heat \rightarrow Na_2O + 2SO_2$$
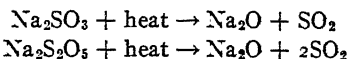
. The addition of sodium sulphite to molten metal causes a vigorous reaction, liberating sulphur dioxide, which is taken up by the metal, and sodium oxide, which is a strong base and reacts readily with the oxides of the deoxidation reactions, forming a fluid slag that rises to the top of the steel. Some of the reactions may be as follows:

$$Na_2O + SiO_2 \rightarrow Na_2SiO_3$$
$$Na_2O + Al_2O_3 \rightarrow 2NaAlO_2$$
$$Na_2O + 6SiO_2 + Al_2O_3$$
$$\rightarrow Na_2O.Al_2O_3.6SiO_2$$
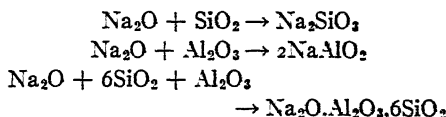
The actual analysis of the resulting slag is as follows: SiO_2, 36.14 per cent; Al_2O_3, 28.77; MnO, 5.55; FeO, 3.24; Na_2O, 21.15; S, 1.27.

The percentages of 36.14 for SiO_2 and 28.77 for Al_2O_3 indicate that large amounts of refractory inclusions have been washed from the steel. These inclusions are abrasive, and their removal is shown by the increased tool life that is reported by the machine shops.

The addition of a sulphite to steel can be made either to the ladle while the steel is being tapped, or to the molds. It is preferable to make the addition to the ladle and to add it after all other ladle additions have been made. The efficiency or recovery of the sulphur from the sulphite is fairly constant, being between 65 to 70 per cent, which makes it possible to meet an 0.020 per cent sulphur range without difficulty. The practice has been to use sodium sulphite when sulphur up to 0.050 per cent is wanted, and sodium bisulphite for a sulphur content up to 0.090 per cent. When higher sulphur is specified, additional stick sulphur is used,

because of the large volume of bisulphite necessary to meet the high specifications.

Experience with a large number of heats of steel made with sulphite addition to various specifications has shown no effect on grain-size control or on the recovery of manganese, silicon, and other alloying elements. Most of the heats made have been fully killed steels with sulphur in the lower ranges. Some typical results obtained in the machine shop are as follows:

Several heats of S.A.E. 1060 steel were made, rolled into $1\frac{1}{16}$-in. bars, and machined to 1-in. diameter. The sulphur range was specified as 0.040 to 0.070 per cent. Sulphite-treated steel machined 23 per cent faster and with an increase of over 300 per cent in tool life when compared with the same kind of steel made with stick sulphur. The mechanical properties also were more uniform in the sulphite-treated steel, and the impact values were approximately twice the impact values of the sulphur-treated heats.

Gears of S.A.E. 5140 steel, in which the sulphur content had been raised to 0.038 per cent by addition of sodium sulphite, were compared with ordinary S.A.E. 5140 gears. These gears are first rough-machined, rough-ground, finish-machined on cone automatics, and then cut. The sulphite-treated steel, after the first rough-machining operation, had a better finish and were close enough to size so that the next operation, the rough grinding, was omitted and the gears were put directly through the cone automatic machines. In both machining operations, the number of pieces produced was 50 per cent more before retooling was necessary. In the final cutting of the gears, no difference in speed of operation was noticed, except that the finish was much better; so much so that complete transmissions are being made and will be given thorough tests on the dynamometer.

Steels for many other parts have been sulphite-treated. S.A.E. 4140 has been

made into axle shafts and connecting rods, X1335 has been used for shells; 4120 for gears; 1340 for shells; X1015 for camshafts; et cetera.

SUMMARY

As the result of this preliminary investigation it is believed that adding sulphur to steel by means of a sodium sulphite will produce:

1. A steel that can be rolled as well as if no sulphur were added.

2. A steel with fewer refractory inclusions because of the cleansing effect of sodium oxide.

3. A steel with more uniform distribution of sulphide inclusions.

4. A steel that can be machined with greater speed, more accuracy, better finish, and much longer tool life.

It is also believed that these objectives can be accomplished with no effect on grain-size control, recovery of other alloying elements, or mechanical properties in the lower sulphur ranges.

These initial studies of the production of steels of improved rolling and machining properties are especially important at this time, when it is necessary to produce a first-class product, in the greatest quantities possible, that can be machined in a minimum of time, especially in the conservation of machine tools and in increasing the output of shells and other war materials that must be machined in large tonnages.

It should be pointed out that any large-scale treatment of steel with sulphite and bisulphite will require additional provision on the part of the chemical industry to supply the material needed. This may have to be considered in the light of other requirements in order to correlate properly this production with other war requirements of the industry.

This paper is a brief preliminary summary of experiments, observations in practice, and results obtained to date. Much research remains to be carried on, plans for which are under way. It is likely that many other adaptations of this process are possible, and any contribution the steel industry can make toward the speeding up of the war effort will no doubt be of great value to the country at large.

A Magnetic Determination of the A_3 Transformation Point in Iron

By B. A. Rogers,* Member A.I.M.E. and K. O. Stamm*

Because it is the basis of the economically important operation of hardening steel by quenching, the A_3 transformation in iron has been the subject of numerous investigations. Although the contributions to this subject are interesting, no general review will be given here. Readers who care to follow the matter further are referred to the comprehensive summary by Cleaves and Thompson,[1] which covers the literature to about 1935. Their references to 53 papers on the subject suggest that further investigation is hardly justifiable. However, considerable interest has developed recently concerning the reversibility of the transformation. From thermodynamic considerations, the transition ought to occur at the same point on heating or cooling, if the change of temperature is sufficiently slow. Yet all of the earlier investigators found a difference of several degrees. Burgess and Crowe,[2] who used thermal methods, obtained average temperatures of 912° for Ac_3 and 900°C. for Ar_3 on electrolytic iron. Their data indicate a considerable range of temperature over which the change occurs, both on heating and on cooling. Terry[3] measured the susceptibility in the critical range and estimated from the steepest parts of his curves that Ac_3 came at 918° and Ar_3 at 903°C.

Ishiwara[4] was one of the first investigators to report a shorter interval between the temperature of the change in the two directions. He measured the change of susceptibility of kaolin-coated samples of steel, in a hydrogen atmosphere, at rates of heating and cooling so low that about 3 or 4 hr. were required for the transformation to complete itself. His results show some variability between samples, but indicate that the difference between Ac_3 and Ar_3 is in the vicinity of 6°C. Roberts and Davey[5] measured the space lattice in pure iron in the vicinity of 900°C. and concluded that a change occurs reversibly between 907° ± 3° and 910° ± 3°C., probably between 907° and 910°C. Wells, Ackley, and Mehl[6] made dilatometric determinations of the Ac_3 and Ar_3 points in samples of hydrogen-treated carbonyl iron maintained under a vacuum. They used three rates of heating and cooling: 2°, ½°, and ⅛°C. per min. and found the spread between the two points decreased with low rates. At the slowest rate, the Ac_3 transition occurred at 909° to 909.5°C. and the Ar_3 change at 907°C. in three of the samples believed to contain the lowest percentages of alien elements. They concluded that if the rate of temperature change and the content of alien elements were low enough, the A_3 transformation would be completely reversible at 909.5° ± 1°C.

The question of reversibility is an interesting one and when some iron with especially small percentages of alien elements became available the opportunity to conduct an investigation was welcomed. This iron was prepared by the Division of

Metallurgy of the National Bureau of Standards and was made available by Dr. J. G. Thompson, of that organization. A magnetic method was selected because electromagnet, a furnace for heating the sample, and a balance for measuring the force on it. A Frantz[3] magnet was employed. The furnace and magnetic balance
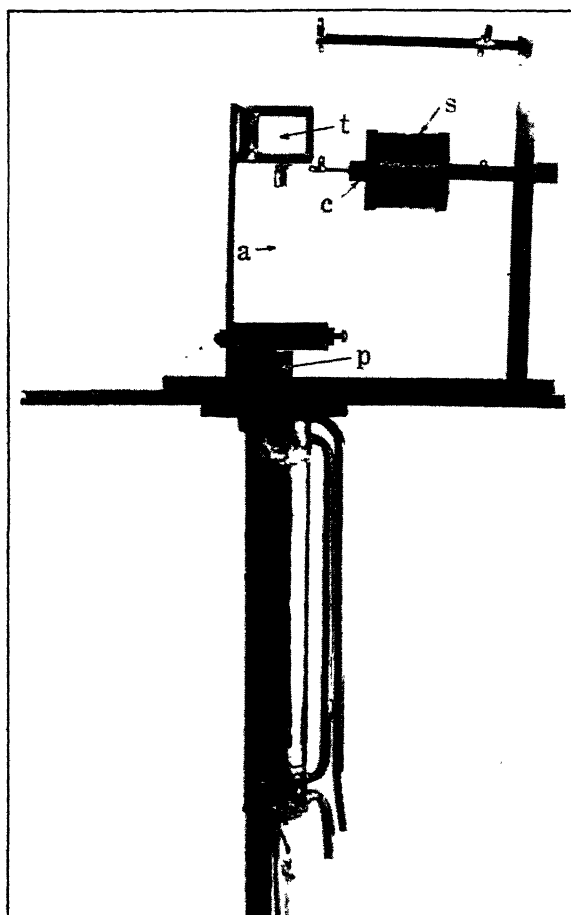

FIG. 1.—COMBINATION OF MAGNETIC BALANCE AND SAMPLE FURNACE.

suitable equipment had already been set up for other purposes.

THE APPARATUS AND ITS MANIPULATION

The apparatus will be described briefly, although the details of its construction have been published already.[7] It is based upon Curie's method of measuring the force on a specimen placed in a nonuniform magnetic field. The elements are: an are combined in one structure, as illustrated in Fig. 1, reproduced from the paper cited. The working parts of the balance are: the silica balance beam a pivoted at p and the combination of solenoid s and core c, which takes the place of the weights on a mechanical balance. In using the balance, the pull on the specimen is determined by noting the current through s necessary to hold the indicator t at its

zero position. The force corresponding
to any current is read from a table obtained
by methods to be described. The sample
end of the balance beam is not visible in
Fig. 1 because of its location within the
cylindrical furnace shell. This shell, which
has water-cooled ends, fits snugly in the
air gap of the magnet.

The interior of the furnace is illustrated
in Fig. 2, which shows the region near the
specimen x. The silica sample container g
is fused to the lower end of beam a; b is
the refractory tube on which platinum
wire w is wound.* A conception of dimen-
sions is obtained from the distance of ½ in.
between the horizontal lines on the graph
that shows the variation in temperature
along the vertical axis.

Since the previous paper was written,
the apparatus has been improved by the
addition of a controller of the kind de-
scribed by Reid.[9] This instrument, which
was operated in conjunction with a Leeds
and Northrup type K potentiometer, was
connected to thermocouple h in Fig. 2.
The temperatures recorded during the
experiment were read from a Tinsley
Vernier potentiometer connected to ther-
mocouple k. Both couples were made of
matched 22-gauge chromel-alumel wires.
As judged from the movement of the
galvanometer connected to the Tinsley
unit, the total variation of temperature at
junction k was about 0.2°C. for any
setting of the controller. In general, read-
ings of temperature and also of force on the
sample were taken at 15-min. intervals.
Any changes of the temperature con-
troller were made immediately after
these readings.

Because of its importance, the method of
preparing the sample will be given in some
detail. The dimensions of the sample were

about ⅛-in. diameter by ³⁄₁₆-in. length
and its weight about 0.3 gram. It was
placed in a closed-end, clear, fused-silica
tube of 4-mm. internal diameter, which
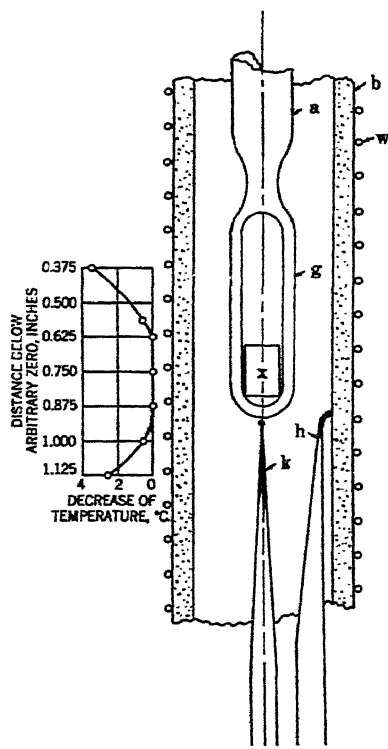
FIG. 2.—PART OF FURNACE NEAR SAMPLE.

was then evacuated to a pressure of about
0.0005 mm. Hg. Next, the end of the silica
tube containing the sample was heated to
about 800°C. and held at this temperature
for about ½ hr. before being sealed off.
The evacuated capsule, having a cavity
length of about ¾ in., was then attached
by use of a torch to the silica balance
beam, care being taken to have the sample
at the proper distance from the pivots.
Finally, the balance beam was replaced
in the position illustrated in Fig. 1.

CALIBRATION OF EQUIPMENT

Three calibrating operations were re-
quired. The first concerned thermocouple

---

* The heating element was wound nonin-
ductively; that is, the currents in adjacent
wires were in opposite directions. As a result,
the magnetic field produced by the heating
current was very slight.

k, located under the specimen container; the second involved the relation between the current through the magnetic balance and the actual force; the third was a redetermination of the field of the electromagnet. In addition, the variation of furnace temperature near the sample was examined.

The thermocouple k was checked against a similar couple that had been calibrated at the National Bureau of Standards. It was used throughout the tests but was cut off and rewelded twice. As a further

room temperature. The position of the sample in the magnetic field was the same in both balances and also coincided with that of the samples studied in the transformation experiments. Current plotted against the square root of mechanical force yielded a straight line having the equation $I = 114.4 \sqrt{w}$. This equation was used to set up a table for converting current to grams weight.

Redetermination of the constant of the magnetic field was undertaken as a result of having more exact data on some of the

TABLE I.—*Composition of Samples Obtained from National Bureau of Standards*

Ingot No.[a]	Content of Alien Elements, Per Cent									
	Cu	Si	Be	Al	C	S	P	O₂	N₂	H₂
2	<0.002	0.001	<0.001	nil	0.001	0.002_3	<0.0005	0.000_3	0.000_2	0.000_2
3	<0.002	0.003	<0.001	nil	0.001	0.002_6		0.000_5	0.000_4	0.000_1
18	<0.002	nil	nil	nil	0.001	0.001_1		0.003_0	0.000_1	0.000_2

[a] The arc spectrum of each ingot was examined for the presence of sensitive lines of 49 elements. Determinations of Cu, Si, Be, and Al are recorded above, the expression "nil" meaning that the amount of the impurity, if present at all, was less than the sensitivity of the analytical method. None of the following 45 elements could be identified in any of the ingots: Ag, As, Au, B, Ba, Bi, Ca, Cb, Cd, Ce, Co, Cr, Ga, Ge, Hf, Hg, In, Ir, K, Li, Mg, Mn, Mo, Na, Ni, Os, Pb, Pd, Pt, Rh, Ru, Sb, Sc, Sn, Sr, Ta, Th, Ti, Tl, U, V, W, Y, Zn, and Zr.

check on the accuracy of the apparatus, a measurement was made of the melting point of silver containing less than 0.01 per cent of alien elements when sealed in a capsule in the same way as the iron specimens. Three determinations at different times gave 960.5°, 961.5°, and 961.0°C. The first was obtained while the couple was in its original condition and corresponds to the period when most of the work on the Bureau of Standards iron was done.

The relationship between current through the magnetic balance and the force in grams was found by measuring samples of slightly magnetic alloys of approximately the same size as the specimens of iron, both in the magnetic balance and in a mechanical balance that had been built for determining the mass susceptibility of substances at

calibrating equipment. The procedure has already been described.[7] The new value for $H \dfrac{dH}{dy}$ is 26.02×10^6 oersteds.oersteds per centimeter.

Exploration of the temperature in the furnace was conducted by placing a 22-gauge chromel-alumel thermocouple junction at a sequence of $\frac{1}{8}$-in. intervals along the axis of the furnace while the temperature of the heating element was held constant by an auxiliary couple connected to the controller. The deviation of temperature in the vicinity of the sample is shown on the graph which forms a part of Fig. 2.

SAMPLES USED

Samples from five different pieces of iron were tested. Three pieces were rods

furnished by the National Bureau of Standards. The analyses of these rods, which were from ingots 2, 3, and 18,[10] are given in Table 1. The other two were a

the Ac₃ and Ar₃ transformations. The sample of Fig. 3 was not carried above the Ac₃ temperature, whereas that of Fig. 4 was.
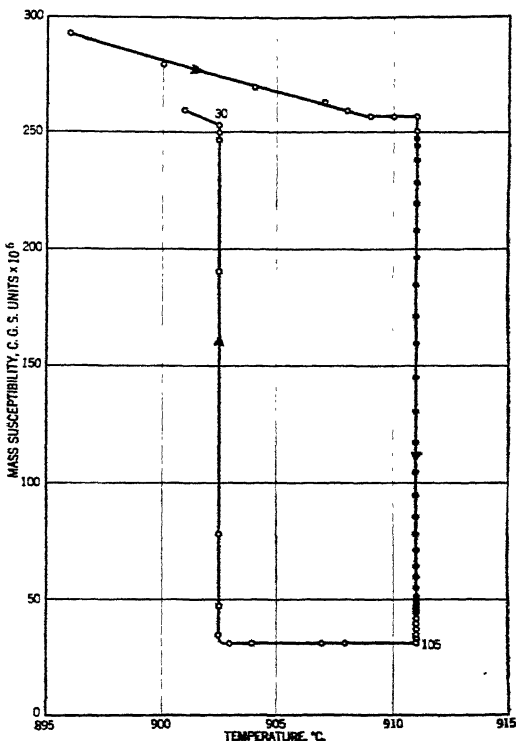

FIG. 3.—SUSCEPTIBILITY-TEMPERATURE LOOP FOR A₃ TRANSFORMATION OF IRON. TEMPERATURE OF SAMPLE NOT CARRIED ABOVE A₃ POINT. INGOT NO. 2.

Sample weight, 0.2914 gram. Numbers along curve show time in minutes between plotted points when other than 15. Closed circles indicate a period of 5 minutes between points.

specimen of Armco ingot iron and a length of wire drawn down from an ingot made by adding 0.051 per cent copper to electrolytic iron.

EXPERIMENTAL RESULTS

The data from runs on ingot 2 will be used to illustrate the results of the investigation. Tests on ingot 3 were as detailed as those on No. 2 and yielded essentially identical data. Ingot 18 was studied less fully, but its behavior was in general agreement with that of the other two ingots.

Figs. 3 and 4 show how the susceptibility changes as the sample passes through

The performances of the two samples were similar. As the temperature was increased in small steps from 896°C., the susceptibility first decreased and then, for a few degrees below the Ac₃ point, remained constant. The length of this horizontal portion amounts to 2° in Fig. 3 and 3.5°C. in Fig. 4. All samples of iron from the National Bureau of Standards showed a flat region extending over an average interval of about 3°C.; but the length of this portion could not be determined exactly because the apparatus is not more precise than corresponds to $\pm 2 \times 10^{-6}$ c.g.s. units at this susceptibil-

ity. Upon reaching the Ac_3 temperature, the sample did not begin to transform at

formation temperatures. Of the 13 measurements of the Ac_3 change, two were
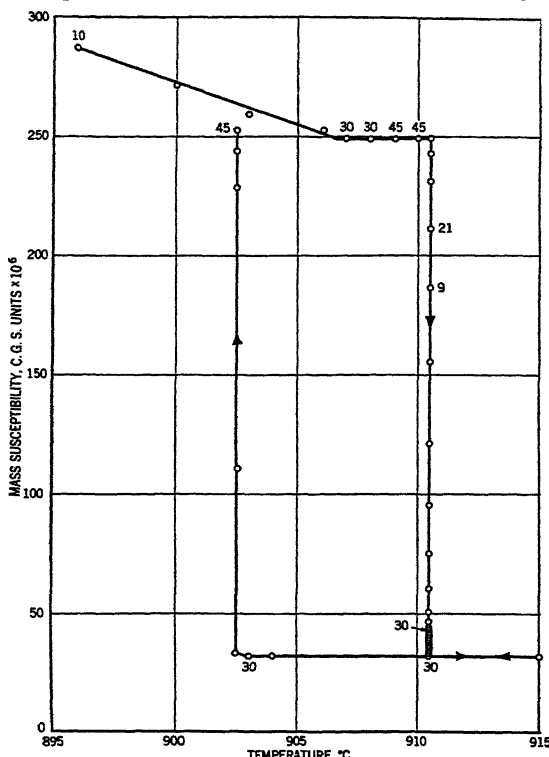
FIG. 4.—SUSCEPTIBILITY-TEMPERATURE LOOP FOR A_3 TRANSFORMATION OF IRON. TEMPERATURE OF SAMPLE CARRIED ABOVE A_3 POINT. INGOT NO. 2.

Sample weight, 0.3033 gram. Numbers along curve show time in minutes between plotted points when other than 15.

once but remained in the alpha condition for 15 min. or more—as much as 45 min. in one case. Once the transformation began, its rate increased gradually to a maximum value and then decreased as the sample approached the gamma condition. According to Fig. 3, the temperature of the Ac_3 transformation is 911° and according to Fig. 4 it is 910.5°C. The latter figure is probably nearer the correct one, as it was the one determined on all three ingots during the first runs on the original calibration of the thermocouple. Table 2 shows the summary of the data for the five different samples of Bureau of Standards iron employed in determining the trans-

outside the 910.5° to 911.0°C. range. One of these was at 910° and the other at 911.5°C. Probably both were the result of some incorrect experimental condition. but the cause for the discrepancies was not determined.

The periods of about 4 hr. for the Ac_3 transition depicted in Fig. 3 and about 5½ hr. for that shown in Fig. 4 represent the time required at a temperature very slightly above the point where the iron will transform at all. A sample held not more than 1°C. below its transformation temperature did not change during a 6-hr. period. On the other hand, an increase of one or two degrees in temperature caused

the transformation to complete itself in a few minutes.

ured in these experiments is about 30 $\times$ 10^{-6} c.g.s. units—approximately one-
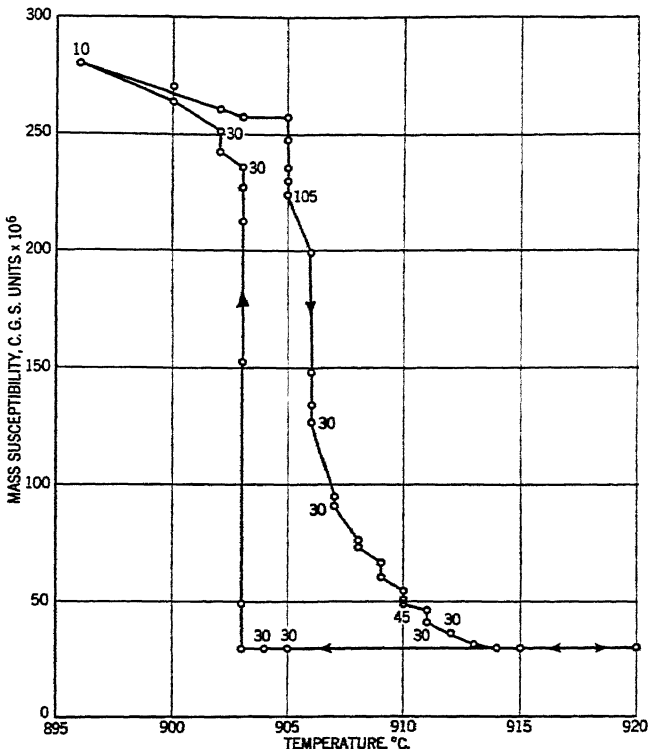

FIG. 5.—SUSCEPTIBILITY-TEMPERATURE LOOP FOR A$_3$ TRANSFORMATION OF IRON SUPERFICIALLY OXIDIZED AT LOW TEMPERATURE. INGOT NO. 2.

Sample weight, 0.3048 gram. Numbers along curve show time in minutes between plotted points when other than 15.

A decrease in the temperature of the sample produced no evidence of the Ar$_3$ transformation until 902.5°C. was reached. At this point the change began slowly, attained a maximum rate greater than that of the Ac$_3$ transition, and then decreased in speed again. Comparison of Figs. 3 and 4 reveals that the temperature of the Ar$_3$ change does not depend on whether the sample has previously been taken above the Ac$_3$ point. As shown in Table 2, the gap between Ac$_3$ and Ar$_3$ was found to be either 8° or 8.5°C. when 0.5° settings were made. The former figure may be considered the minimum interval.

The susceptibility of gamma iron meas-

TABLE 2.—*Temperature of Transformation of Samples of Bureau of Standards Iron*

Ingot No.	Tria No.	Temperature of Ac$_3$ Transformation, Deg. C.	Temperature of Ar$_3$ Transformation, Deg. C.	Temperature Difference between Ac$_3$ and Ar$_3$, Deg. C.
18	1	911.0[b]	902.0[b]	9
	2	911.0[b]	902.5	8.5
	3	910.5		
	4	910.5		
3	1	910.5	902.5	8.0
	2	910.5	902.5	8.0
	3	910.0		
2	1	910.5	902.5	8.0
	2	910.5		
	3	910.5		
	4	910.5		
3[a]	1	911.0	903.0	8.5
2[a]	1	911.0	902.5	8.5

[a] Data on this sample were taken two months later than on others. The apparatus had been partly dismantled and reassembled.
[b] No settings made at half degrees.

eighth of the minimum of about 250×10^{-6} c.g.s. units measured on alpha iron—and is constant within the limits of accuracy of the equipment. The results for gamma

behavior, samples of ingots 2 and 3 were oxidized lightly—at about 0.5 mm. Hg pressure—over their entire surfaces before their containers were sealed. This coating
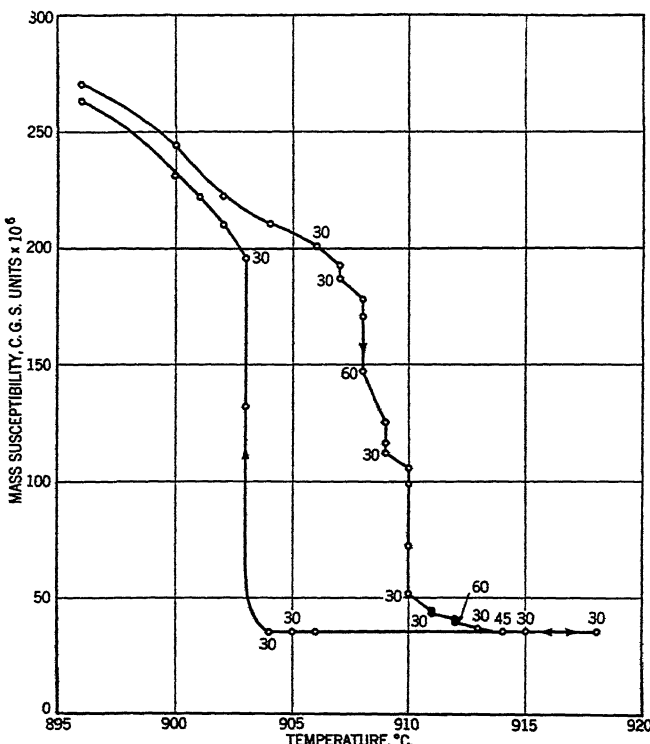

FIG. 6.—SUSCEPTIBILITY-TEMPERATURE LOOP FOR A₃ TRANSFORMATION OF ARMCO INGOT IRON. Sample weight, 0.2729 gram. Numbers along curve show time in minutes between plotted points when other than 15.

iron agree reasonably well with the data selected by Cleaves and Thompson[1] but the value for alpha is larger than their mean figure of 190×10^{-6} c.g.s. units. The average field intensity in the locality of the sample was about 8600 oersteds in all cases.

During a run on a sample, one spot of which had been accidentally oxidized slightly during the sealing-off operation, the susceptibility was observed to drop slightly at 909° and then hold steady and to repeat this behavior at 910° before decreasing continuously during transformation at 911°C. To determine whether the coating was responsible for this unusual

disappeared during the test on the samples, a fact that indicates that the substance of the coating was absorbed by the metal. An attempt was made to estimate the amount of gas taken up, by weighing a sample on an Ainsworth microbalance before and after it was oxidized. The increase in weight, 0.009 mg., was so small that a definite statement will not be ventured. If the amount is correct, the percentage of oxygen introduced scarcely exceeds the 0.003 per cent in ingot 18, which behaved normally.

The form of the transformation loop obtained with an oxidized specimen of

ingot 2 is illustrated in Fig. 5. Three differences from the loop obtained with unoxidized material may be noted: (1) the sample began to transform at 905°C.;

the rapid decrease in susceptibility of the untransformed iron, the temperature of 914°C. necessary to complete the transition, the slightly higher susceptibility of
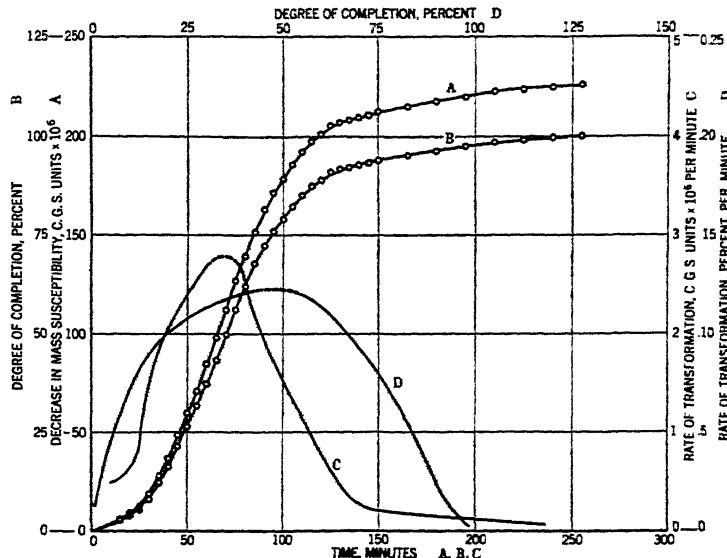

FIG. 7.—CURVES DERIVED FROM DATA PLOTTED AS FIG. 3. INGOT NO. 2.
A, decrease in susceptibility-time curve for Ac_3 transformation.
B, degree of completion-time curve for Ac_3 transformation.
C, rate of transformation-time curve for Ac_3 transformation.
D, rate of transformation-degree of completion curve for Ac_3 transformation.
Sample weight, 0.2914 gram.

(2) it transformed partly, then stopped at successively higher temperatures, and (3) it was not completely in the gamma condition until the temperature reached 914°C.

Ingot 3 behaved in a similar manner, except for a rounded top on the loop and an Ar_3 point of 901.5°C. No explanation of the behavior of the oxidized samples will be offered. Inhomogeneous distribution of oxygen does not appear responsible. After the samples have undergone the diffusion effect corresponding to one transformation loop, they will still transform at a low temperature if reheated.

A run was made on a sample of Armco iron to compare its transformation loop with that of material from the National Bureau of Standards. The principal features of the resulting graph (Fig. 6) are

the gamma form, and the similarity of the Ar_3 change to that of previous samples. Possibly, the susceptibility of gamma iron is related to composition. The figure of 50×10^{-6} c.g.s. units observed for the previously mentioned piece of electrolytic iron containing 0.051 per cent copper supports this suggestion.

Fig. 7 presents four curves derived from the data already plotted as Fig. 3. Curve A shows the progress of the transformation with time. Its ordinate points give the decrease in susceptibility below the value for the alpha condition at 911°C. Curve B gives the same information expressed as percentage of the total change of about 225×10^{-6} c.g.s. units. Curve C shows the change in the rate of transformation as

time progresses. It was derived graphically by drawing tangents to curve A and calculating their slopes. The shape of curve C near its maximum is in doubt.

cent of the material has changed over, but the exact course of the curve in this region is again uncertain.

Fig. 8 illustrates the effect of raising the
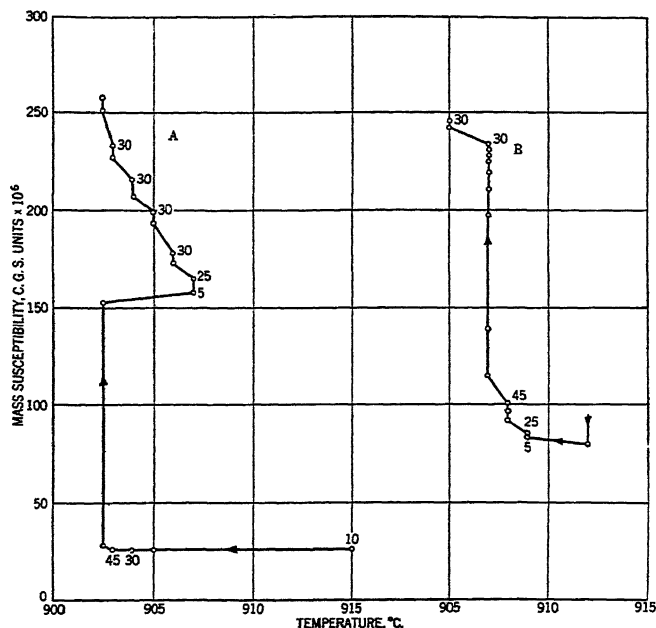
FIG. 8.—SUSCEPTIBILITY-TEMPERATURE CURVES.

A, susceptibility-temperature curve for Ar$_3$ transformation interrupted by increase in temperature.

B, susceptibility-temperature curve for Ac$_3$ transformation interrupted by decrease in temperature.

Sample weight, 0.3051 gram. Numbers along curves show time in minutes between plotted points when other than 15.

Probably, a rounded maximum exists at about 60 min. in agreement with the assumption of a continuous change in slope of curve A at the same abscissa distance, but curve A can be drawn as a straight line through the interval from about 100 to 140 $\times$ 10^{-6} c.g.s. units of susceptibility without doing violence to graphic procedure. Under the circumstances, the ascending and descending branches of curve C have been connected by a dotted line. Curve D gives the rate of transformation as the percentage of the total change occurring per minute plotted against the percentage already transformed. The maximum rate of transformation obviously occurs when about 50 per

temperature while the Ar$_3$ transformation is in progress and of lowering it during the Ac$_3$ change. In the first instance, as shown by curve A, there is a slight tendency for the transition to continue at temperatures as high as 907°C., but the action stops after a short time. A decrease of the temperature from 907°C. causes the transformation to begin anew, but the action soon ceases. Completion of the change into the alpha state does not take place until the usual Ar$_3$ temperature of 902.5°C. is reached. Curve B shows that if the Ac$_3$ change is interrupted by a reduction in temperature, the sample demonstrates a not very persistent tendency to revert to the alpha condition at 909°C. Further

decrease of temperature to 907°C. allows the reversed transformation to proceed nearly to its full extent. Some slight variation of the samples whose transformations were interrupted in this way was observed. In every instance, the sample refused to continue the Ar_3 change to completion when the temperature was raised above 902.5°C. In most instances, a sample in process of going from the alpha to the gamma state would return to the former if the temperature were dropped to about 907°C., but often the return appeared to be not quite complete.

The data just discussed suggest that the transformation tends to be reversible at about the temperature of the Ac_3 change but that the Ar_3 change is suppressed by some unknown factor. The situation may be somewhat akin to the phenomenon commonly called "undercooling" in the solidification of some metallic elements, but the action of the undercooling influence appears to be remarkably constant.

SUMMARY

The investigation of the A_3 transformation by measurement of susceptibility has yielded a number of facts, which are listed in the following summary:

1. The Ac_3 transformation of iron with very small content of alien elements will complete itself at a fixed temperature, which is in the vicinity of 910.5°C. At this temperature, the rate of transformation is so slow that several hours are required for the change from the alpha to the gamma condition. An increase of about a degree in the temperature of the specimen will cause the reaction to take place much more rapidly.

2. The Ar_3 transformation in iron occurs at about 902.5°C. and runs at perhaps three or four times the speed of the corresponding Ac_3 change.

3. The minimum difference in temperature found in this investigation between Ac_3 and Ar_3 was 8°C. All samples showed an interval of either 8° or 8.5°C.

4. The presence of a small amount of oxide—at least, material occurring in an oxide coating—distorts the transformation loop by causing the Ac_3 transition to begin several degrees below its normal temperature and end several degrees above it. The Ar_3 transformation is less affected.

5. The maximum rate occurs when about 50 per cent of the material has been transformed. The rate of change near the end of the transition is much less than the rate near the beginning.

6. If the temperature is reduced to 907°C. before the Ac_3 transformation is completed, the iron reverts (for some samples, at least) to the alpha condition. If the temperature is raised to some point between 903° and 907°C. before the Ar_3 transition is finished, the susceptibility continues to rise slowly for a short time, but action eventually ceases.

REFERENCES

1. H. E. Cleaves and J. G. Thompson: The Metal—Iron, 105–108. Engineering Foundation, New York, 1935. McGraw-Hill Book Co.
2. G. K. Burgess and J. J. Crowe: Critical Ranges A_3 and A_4 of Pure Iron. Nat. Bur. Stds. *Bull.* 10 (1914) 315–368.
3. E. M. Terry: The Magnetic Properties of Iron, Nickel and Cobalt above the Curie Point and Keesom's Quantum Theory of Magnetism. *Phys. Rev.* (1917) 9, 394–413.
4. T. Ishiwara: On the Magnetic Investigation of A_3 and A_4 Transformations in Pure Iron and Steels. *Sci. Repts.* Tohoku Imp. Univ. Sendai (1917) 6, 133–138.
5. O. L. Roberts and W. P. Davey: An X-ray Study of the A_3 Point of Iron and Some Iron-Nickel Alloys. *Metals and Alloys* (1929–1930) 1, 648–654.
6. C. Wells, R. A. Ackley, and R. F. Mehl: A Dilatometric Study of the Alpha-Gamma Transformation in High Purity Iron. *Trans.* Amer. Soc. Metals (1936) 24, 46–66.
7. B. A. Rogers and K. O. Stamm: An Apparatus for Determining Thermomagnetic Behavior of Slags, and Some Preliminary Results Obtained with It. A.I.M.E. *Tech Pub.* 1133 (*Metals Tech.*, Dec. 1939).
8. S. G. Frantz: Magnetic Separation Method and Means. U. S. Patent 2056426 (1936).
9. W. T. Reid: An Electronic-Contacting Galvanometer for Temperature Control. Temperature—Its Measurement and Control in Science and Industry. (Symposium under Amer. Inst. Phys.), 611–616. New York, 1941. Reinhold Pub. Corporation.
10. J. G. Thompson and H. E. Cleaves: Preparation of High-Purity Iron. *J. Res. Nat. Bur. Stds.* (1939) 23, 163–177.

DISCUSSION

(Cyril Wells presiding)

S. EPSTEIN,[*] Bethlehem, Pa.—At and near the transformation temperatures, the authors show that very lengthy time intervals were required for the specimens of iron used to go through the A_3 transformation. It would be of interest to know how such slow rates of transformation affected the grain size.

J. K. STANLEY,[†] Pittsburgh, Pa.—In Fig. 7, curve *B*, Rogers and Stamm show that the isothermal transformation of alpha to gamma iron follows a reaction-rate curve that has been so successfully treated by Johnson and Mehl.[11]

If the isothermal reaction-rate curves for the alpha-gamma change for ingot No. 2 are plotted from the data in Figs. 3 and 4, two quite similar but not coincidental curves result. Similar reaction-rate curves for the gamma-alpha change can be plotted; they too are similar but not coincidental. This is interesting because it indicates that two samples from the same ingot do not give identical isothermal reaction-rate curves, probably as a consequence of some inhomogeneity, either chemical or physical.

The isothermal reaction-rate curve is quite common in metallurgy—the decomposition of austenite, recrystallization, etc. This reaction-rate curve is a combination of two kinetic processes—the formation of a new phase in the matrix or old phase (nucleation) and the growth of these new phases or nuclei until the entire matrix is transformed.

The differences exhibited in the curves can probably be attributed to variations in nucleation or growth. But then we ask: "What would cause such variations?" Possibly chemical composition, variable grain size, or physical condition such as strains or deformation. That the physical state would have an effect is possible but not probable; the heating to such a temperature would have relieved the strains recrystallized the material. The variable grain size could be eliminated by starting with single crystals of iron. In this way, the

reaction-rate curves as affected by impurities, particularly carbon, might be determined.

Rogers and Stamm say (page 138) that the inhomogeneous distribution of oxygen does not appear to be responsible for the irregular curves obtained, as in Figs. 5 and 6. These curves are quite similar in character to dilatation-temperature curves obtained by Wells, Ackley, and Mehl[6] for nonuniform distribution of carbon in iron. I wonder if the authors would elaborate a little more on why they think this irregularity is not due to inhomogeneous distribution of oxygen.

T. D. YENSEN,[*] East Pittsburgh, Pa.—The present determination of the A_3 point in iron establishes a new high as far as experimental accuracy and purity of samples are concerned. The results show definitely and strikingly that these samples transform from alpha to gamma at 910.5° and from delta to alpha at 902.5°, and most of us undoubtedly will conclude that there can be no further argument in regard to the question as to whether iron has or has not allotropic transformation points. The evidence is too convincing. And yet the question apparently will not remain submerged.

In the first place, what about the spread between the A_{c3} and the A_{r3} points? The present authors obtain a spread of 8°C., whereas Wells, Ackley and Mehl[6] obtained only 2° to 2.5° (909° to 907°). Does this mean that the samples used by Wells, Ackley and Mehl were of a higher purity than those of Rogers and Stamm? While evidence presented in the way of chemical analysis is to the contrary, spread is undoubtedly a measure of the amount of foreign elements. The more carbon is added to iron, the greater is the spread between A_{c3} and A_{r3}.

In the second place, what about the time required for the transformation to go to completion? Several hours for a 0.3-gram sample. Where does the transformation start? And why does it start there? Presumably because of a concentration of foreign atoms. But, you will say, the samples in the present case contain an insignificant amount of impurities, 0.001 per cent C, etc. It is not always realized how many atoms this represents. In a cubic millimeter of

iron containing 0.001 per cent C there are roughly 10^{18} iron atoms and 5×10^{13} carbon atoms. Of course, if uniformly distributed there is only one carbon atom for every 20,000 iron atoms (a cube with 27 atoms on the side). But even so, just think how much trouble one fifth columnist can do in a town of 20,000. And the carbon atoms may be concentrated and start trouble in one place, then diffuse to another place and so continue until the entire crystal has been transformed. But let someone else do the arguing.

Some time ago I received from a Russian scientist, Prof. T. A. Lebedev, a booklet entitled "Basic Principles of a New Theory of Iron-carbon Alloys," published in Leningrad in 1939, with the request that it be published in this country. This booklet contains a short chapter entitled "The Cause of Allotropy of Iron." I have had it translated, and I think it is of sufficient interest to include some quotations from this chapter as a part of this discussion.

QUOTATIONS FROM T. A. LEBEDEV'S BOOK*

The Cause of the Allotropy of Iron

Since the times of Osmond, most investigators have accepted allotropy as a peculiarity of the internal state of the iron, something inseparable from the concept of iron itself.

The first investigator to advance a bold suggestion that was in complete disagreement with the prevailing traditions was the Russian engineer, P. N. Ivanoff. In the year 1925 he wrote, "There are absolutely no proofs of the presence of such allotropic forms. . . . "

Starting from the analysis of the iron-carbon diagram, Ivanoff came to the logical conclusion that the first cause of an allotropic transformation in iron is carbon. Shortly afterward, the American investigator, Yensen, came to the same conclusions absolutely independently of Ivanoff. Yensen observed that with the decrease of the carbon content in a silicon alloy, a smaller amount of silicon is needed in order completely to prevent the gamma modification of iron. The conclusion suggests itself that iron within a minimum amount of admixtures should not have any gamma modification.

While metallurgists as a whole are not re-

sponding to this idea, individual investigators are beginning to come to the thought that the concepts of the allotropy of iron really need a suitable revision. Thus, for instance. Professor Rosenhain made the following statement at the 1930 convention of German metallurgists, "We have discovered that the transformation points of very pure iron undergo a quite unexpected shift which perhaps has a connection with the ideas with respect to the entirely possible absence of allotropic transformations in absolutely pure iron."

On the basis of a mathematical analysis of different data on the effect of admixtures upon the transformation $\alpha \to \gamma$ Prof. V. N. Swetchnikoff also admitted in 1932 the possibility of the absence of allotropic transformations in pure iron. Finally, Scheil admits that Yensen's hypothesis may be right for pure iron at normal (atmospheric) pressure. Recently Esser was compelled to pronounce himself in favor of the monotropy of pure iron and to assume that "allotropy is not encountered in ideally pure iron and that it is caused by those inclusions which are inevitably contained in practice in the material."

One fact that compels us in one way or another to doubt Osmond's hypothesis is undoubtedly the existence of the so-called delta iron, and that the range of this wedging-in depends to an extent upon the quality of the admixtures in iron. Consequently, the problem of the allotropy of pure iron should be solved at present on the basis of the following considerations: Is it permissible, in the so-called technically pure iron (thousandth parts of one per cent of admixtures), to reduce the effect of these admixtures to insignificant dimensions, or is it exactly these admixtures that are to be considered as responsible for the reaction of the transformation $\alpha \to \gamma$. It may seem incredible that such small quantities of admixtures are able to cause a total recrystallization of the iron, but one should not forget that our ideas of "small" and "large" are very relative, and it is just these "small" admixtures that sometimes cause a change in the alloy (changes in crystallization, in magnetic properties, in mechanical qualities, and so on).

Entirely good reasons compel us to reckon very seriously with the insignificant amounts of carbon that usually are present in technically pure iron. And, however small may be these

* Basic Principles of a New Theory of Iron-carbon Alloys, chap. 3, pp. 28-36.

amounts, we should not forget that the possibility of the transformation of iron from alpha to gamma will depend not so much on the carbon content as on the forces of affinity between the iron and carbon atoms and on how strongly the alpha iron will resist the indicated transformation.

If the force of affinity between the atoms of iron and carbon is sufficiently great, even a small amount of carbon will be able to transform great masses of iron from the alpha modification into gamma. Here it is possible to foresee the fact that in the specially pure iron grades, the point Ac₃ should move up with increasing rate as the percentage of carbon decreases. A great number of investigators who tried to determine the point Ac₃ in pure iron have found that the temperature of the transformation α → γ increases in some cases to more than 930°. From the point of view of the anti-allotropic hypothesis, this circumstance fully conforms to law, since it is expected that with increasing purity of iron the points A₃ and A₄ will gradually draw together and finally disappear entirely in absolutely pure iron.

With respect to the influence of carbon, interesting data can be obtained from the work of Wells and his associates. In technically pure iron (C = 0.012 per cent), the whole course of transformation α → γ depends most clearly upon the distribution of carbon. A nonuniform distribution of carbon (unannealed alloy) results in that the transformation α → γ extends over a considerable temperature interval starting evidently in places with high carbon concentration. For a more uniform distribution of carbon, the whole transformation α → γ takes place between 904° and 907° and has the appearance of a process that has started simultaneously throughout the sample. If the question were raised, what is the active element that starts the transformation of the iron in the direction of α → γ (the iron itself or the carbon) one would be justified in answering: "The active element undoubtedly is the carbon." How can one contend that the allotropy of iron manifests itself as an inherent property in the face of the fact that an amount of 0.012 per cent carbon affects the 99.988 per cent of iron so clearly and undeniably? Not one fact has been observed that would confirm the "inherent" iron allotropy. On the contrary, every newly discovered fact shows more clearly the function of the admixtures, which produce very often a false allotropy of metals.

There is a sufficiently well founded assumption that for small contents of carbon the allotropic transformation does not affect the whole volume of the iron. Experiments have shown that, depending on the uniformity of distribution of carbon, the same samples yield dilatometric effects, entirely different as to magnitude. Finally, the thermal effects of the transformation α → γ found by different authors are far from always coinciding with one another. The table given shows that the investigators have failed to prove the constancy of the thermal effect of the transformation α → γ which would be absolutely indispensable for a constant and complete allotropic transformation.

Therefore, the facts observed in modern metallurgy are bringing the anti-allotropic hypothesis to the fore.

B. A. ROGERS AND K. O. STAMM (authors' reply*).—Mr. Epstein's question brings up an interesting point. Unfortunately, we did not set aside any samples for microscopic examination at the time of the experiment and, after the work was finished and the apparatus dismantled, we realized that the specimens had been put through such a variety of experiments that their thermal history was quite complicated. Under the circumstances, an examination seemed unprofitable.

Mr. Stanley comments on the difference in the isothermal reaction-rate curves for ingot No. 2, as derivable from Figs. 3 and 4, and suggests some possible causes for this variation. However, difference in temperature is probably the most prominent cause. It is true that for any given run the variation of temperature in the furnace did not exceed ±0.1°C. and that the temperature of the sample presumably changed by only a small fraction of this amount, but the setting for different runs might easily have differed by 0.1°C. Since a rise in temperature of 1°C. was observed to increase the rate of transformation by several hundred per cent, a much smaller difference in temperature might exert an influence greater than the factors named by Mr. Stanley.

---

* Published by permission of the Director, Bureau of Mines.

Our statement that the inhomogeneous distribution of oxygen does not appear to be responsible for the type of curve obtained in Fig. 5 was based only on the opinion that several hours at about 900°C. should permit fairly thorough diffusion of the oxygen in this small sample of metal, but it may not be correct. It was noted that when such a sample was again brought up to the transformation temperature, its behavior was generally similar to that in the first run.

Dr. Yensen mentioned the difference in spread between the Ac₃ and Ar₃ points obtained by Wells, Ackley, and Mehl[6] and in the present experiments. The investigation by Wells, Ackley, and Mehl evidently was carried out with unusual care. On the other hand, we believe that our own results are correct for the samples that were used. Lacking a satisfactory explanation of the discrepancy, we did not discuss the point. The assumption that the spread will increase as the percentage of impurities becomes greater is a natural one to make. Yet, as Dr. Yensen says, the opposite results have been obtained in our experiments. Although the Ac₃ transformation shown in Fig. 5 covers a range of temperatures, it is possible that a dilatometric test would show changes in length mostly at temperatures corresponding to the upper part of the loop in our Fig. 5, and in this case an observer using this method would conclude that a smaller interval exists for very slightly oxidized material than for the uncontaminated metal. This question of spread is one that needs further investigation. Some effect similar to undercooling in liquid metals may be involved in the transformation.

Dr. Yensen has also questioned the existence of the gamma phase in iron uncontaminated by any trace of foreign atoms and has presented arguments for this theory in the form of quotations from chapter 3 of the book on Basic Principles of Iron-carbon Alloys by Prof. T. A. Lebedev. References cited by Professor Lebedev[12-15] show that the experi-

mental basis for such arguments rests mainly on two observations, of which the first is the decrease in the amount of alloying element necessary to close the gamma loop in certain ternary alloys as the percentage of carbon is decreased and the second, the occasional high values reported for the A₃ transformation point in iron specified as being especially free from carbon and other alien elements.

Three component alloys, such as iron-carbon-silicon or iron-carbon-chromium, should always be studied from the viewpoint of a ternary system. A study of diagrams of this type as illustrated, for example, by Fig. 11 in the paper by Köster and Tonn,[16] brings out the fact that the surfaces that bound the alpha and alpha plus gamma spaces extend farther from the iron corner as the percentage of carbon is increased through the lower values. As a result, the traces of these surfaces that appear as the gamma loop on vertical sections parallel to the iron-silicon side will bulge more and more as the sections are taken at greater carbon contents. Conversely, as the carbon content decreases, the gamma loop as depicted by these sections tends to shrink. Its limiting position is reached as the carbon content for the successive sections diminishes to zero and the section coincides with the iron-silicon side. The decrease in extent of the gamma loop is thus seen to be a perfectly normal behavior, and any supposition that it will disappear when no carbon is present is quite unjustifiable.

Arguments based on reported high values for the A₃ transformation involve two assumptions: (1) that the reported values are correct, and (2) that the increase in temperature of the A₃ transformation does not reach a maximum value for iron with absolutely no alien atoms. The question of the temperature of the A₃ transformation point in iron of a very high degree of purity has been carefully examined by Cleaves and Thompson[1] and also by Cleaves and Hiegel.[17] Cleaves and Thompson[1] rejected the high

[12] T. D. Yensen: Iron-Silicon-Carbon Alloys. Constitutional Diagrams and Magnetic Properties. *Jnl.* Iron and Steel Inst. (1929) 120, 187–202.

[13] M. A. W. Svetchnikoff: Sur les transformations polymorphes du fer aux points A₃ et A₄. *Rev. de Mét., Mem.* (1932) 29, 583–587.

[14] M. V-N. Svetchnikoff: De l'effet des éléments additionnés sur le polymorphisme du

fer. *Rev. de Mét., Mem.* (1933) 30, 200–210.

[15] H. Esser: The Allotropy of Iron. Iron and Steel Inst., *Carnegie Schol. Mem.* (1936) 25, 213–234.

[16] W. Köster and W. Tonn: Die α-γ-Umwandlung in den Dreisoffsystemen des Eisens. *Archiv Eisenhüttenwesen* (1933–1934) 7, 193–200.

[17] H. E. Cleaves and J. M. Hiegel: Properties of High-purity Iron. *Jnl.* Res., Nat. Bur. Stds. (May 1942) 28, 643–667.

values in summarizing the data on the subject and indicated that the best evidence pointed to about 910°C. Cleaves and Hiegel dealt more particularly with the iron prepared at the National Bureau of Standards—probably the purest yet produced—and show that the value of approximately 910°C. was obtained by three different methods, of which our investigation is one. Under the circumstances, the reports of values appreciably above 910°C. should be considered to require confirmation.

As to the second assumption, the proponents of the no-gamma-range-in-pure-iron theory have advanced no reason for believing that the gamma phase will disappear rather than that the temperature of the A₃ transformation will attain some maximum value. Without evidence, the idea remains pure speculation.

We should also like to point out that the transformation from the body-centered to the face-centered-cubic atomic arrangement, as it occurs at 1400°C. in a cooling mass of iron, involves a change from a condition in which each atom has 8 neighbors to one in which it has 12. In other words, the metal no longer has a kind of homopolar binding that is capable of holding neighboring atoms in certain positions but becomes close-packed. The rearrangement of valence electrons necessary to produce such an alteration is of a fundamental nature and one not likely to be influenced by the presence of one carbon atom in 20,000 iron atoms. To suppose that one carbon atom has such power would imply a sphere of influence of much greater radius than that calculated in other ways.

In conclusion, we agree that the question of the existence of the gamma phase in iron containing no alien atoms can be settled finally only by experiments on such material. We do believe, however, that the advocates of the no gamma theory have yet to produce evidence that justifies uncertainty concerning current views.

The Solubility of Carbon as Graphite in Gamma Iron

By R. W. Gurry*

(New York Meeting, February 1942)

In the course of a series of measurements of the rate of diffusion of carbon in austenite at about 960°C. (1760°F.) and 1110°C. (2030°F.), it became necessary to determine carbon concentration when austenite is saturated with graphite, because of indications that the hitherto accepted value of the solubility of graphite in this temperature range is too low. Specimens of carbonyl iron were saturated at temperature in a hydrogen-toluene atmosphere which was in equilibrium with graphite. The carbon content of the steel was measured either by combustion or by the loss of weight after substantially complete decarburization in an atmosphere of hydrogen saturated at room temperature with water vapor. The absence of carbide or graphite as a phase at temperature was demonstrated by microscopic examination of saturated specimens that had been drastically quenched.

The mean result of concordant measurements is that gamma iron saturated with respect to graphite contains 1.39 per cent carbon at 957°C. (1755°F.) and 1.89 per cent at 1110°C. (2030°F.). These two values, plotted along with what appears from the literature to be the best value (0.69 per cent) at the iron-graphite eutectoid temperature (738°C. or 1360°F.), yield a curve that is almost linear, and which, continued upward through a short interval, leads to a limiting solubility of 1.98 per cent at the iron-graphite eutectic temperature

1135°C. (2075°F.) instead of the commonly accepted value of about 1.7 per cent.

Experimental Procedure

The samples of carbonyl iron, with the exception of those for microscopic examination, were cylinders 3.8 cm. long, 0.475 cm. in diameter. They were placed in a graphite holder and suspended in a vertical furnace, the temperature of which was controlled precisely by means of the resistance of the platinum winding.[1] In the empty furnace the range of temperature over a distance of 4 cm. at the heat center was 9°C. (16°F.) but at a given location the temperature remained within ±0.5°C. (0.9°F.); it was measured by inserting a platinum-rhodium couple calibrated at the melting point of palladium, 1555°C. Since the presence of the sample probably improved the uniformity of temperature, it was decided to consider the average temperature of the sample to be 3°C. lower than the maximum measured in the empty furnace with the same setting of the controller. Data were obtained in the vicinity of two temperatures, 960°C. (1760°F.) and 1110°C. (2030°F.). The samples for microscopic examination, 2.2 cm. long, 0.475 cm. in diameter, were suspended individually on pure iron wire; for these no temperature correction was applied.

The carburizing gas passed into the furnace was dry, oxygen-free hydrogen saturated at room temperature with toluene; this quickly produced on the

[1] References are at the end of the paper.

surface of the specimen a layer of graphite. Preliminary tests showed that the final carbon content of the steel is independent of the rate of flow of the carburizing gas up to a rate of 40 c.c. per min.; at higher rates the final carbon content was variable and somewhat greater, presumably because of the higher carbon activity of the intermediate decomposition products of toluene as compared with that of the final stable product graphite. Consequently, the rate of flow was kept below 40 c.c. per min. except at the start of the carburizing period, when it was increased somewhat in order to produce a more rapid approach to saturation. The final carbon content observed under the experimental conditions is believed to be that of austenite that is in equilibrium with graphite at the temperature; the main reason for this belief is that there was no trend of final carbon content with increasing time in the furnace up to 240 hr., the maximum period over which observations were continued.

The samples at 960°C. (1760°F.) were carburized for at least 140 hr., those at 1110°C. (2030°F.) at least 44 hr. Calculations based on an integrated solution of Fick's law[2] show that this minimum time should in each case be sufficient for the sample to reach about 99.9 per cent of saturation, provided that the surface is always kept saturated. Some samples were carburized for a very long period to verify by comparison the state of saturation, also to allow time for precipitation of any carbide or graphite that may have had that tendency.

After the prescribed length of time in the furnace the samples for microscopic examination were quenched in brine at room temperature, the others simply cooled at the top of the furnace tube. Before the determination of carbon all graphite was removed from the surface of the sample by sandpapering in a lathe. Carbon content was determined by the usual combustion method, which was checked frequently with a standard 1.01 per cent carbon steel from the Bureau of Standards; or by the weight loss on decarburization, which was accomplished by passing hydrogen, saturated with water at room temperature (a mixture which at these high temperatures oxidizes carbon in steel but not iron) at a rapid rate over the specimen, which later was cooled for weighing in the furnace atmosphere at the top of the furnace. The furnace and the temperature distribution during decarburization were the same as for the carburizing process described above; the temperature was in each case within 9°C. (16°F.) of that at which the sample was saturated. The sample was suspended in a molybdenum wire holder together with a completely decarburized iron specimen, so that its weight might be corrected for the very small loss due to vaporization of iron. Decarburization was allowed to proceed until the sample lost weight at approximately the same rate as did the originally decarburized specimen. Both procedures yielded identical results.

RESULTS

The measurements of the solubility of graphite in austenite at temperatures about 960°C. (1760°F.) and 1110°C. (2030°F.) are recorded in Table 1.

TABLE 1.—*Solubility of Graphite in Austenite*

Sample No.[a]	Temperature, Deg. C.	Carburization Time, Hr.	Carbon Content, Per Cent	Method of Carbon Determination
1	957	140	1.38	Weight loss on decarburization
3	957	140	1.39	Combustion
6	956	240	1.39	Combustion
2	1104	44	1.86	Weight loss on decarburization
4	1110	50	1.91	Combustion
5	1115	69	1.91	Combustion
9	1105	120	1.87	Combustion
7	1106	120	1.865	Combustion
8	1106	240	1.88	Combustion

[a] Samples 1 to 5 were cylinders 3.8 cm. long, the others 2.2 cm.; all were 0.47-cm. diameter.

Figs. 1 and 2 are typical photomicrographs, at an original magnification of 1000 diameters, of specimens that had been saturated with graphite, at 956°C. (1753°F.) and 1106°C. (2023°F.), respectively, and then quenched in brine, polished, and etched in 4 per cent picric acid in alcohol. Fig. 1, representing sample 6, shows an interlocking group of martensite needles with only a small amount of retained austenite (white); Fig. 2, representing a field close to the surface of specimen 7,

as being the concentration of saturation with graphite, or at least not in excess of this solubility.

The results of the determination of graphite solubility are shown in Fig. 3 along with data reported by Söhnchen and Piwowarsky[3] and by Wells,[4] which appear to be the best of the several sets of measurements recorded in the literature. The solubility given by Söhnchen and Piwowarsky for the lower temperature range is, in the light of present knowledge

FIG. 1.—MICROSTRUCTURE OF SAMPLE 6, 1.39 PER CENT C.; SATURATED WITH GRAPHITE AT 956°C. (1753°F.) AND QUENCHED IN BRINE. X 1000.

shows a great deal of retained austenite with much less martensite. At the center of the latter sample, where the quench was less drastic, the grain boundaries contain a small amount of pearlite resulting from the high-temperature transformation of some austenite. The short transverse black lines visible in both figures are microcracks commonly associated with high-carbon martensite. No area examined showed evidence of the presence of any graphite or carbide whatever at temperature; the carbon content therefore can be considered

of phase relations in the iron-graphite system, certainly too high, but their values for the higher temperatures appear to be better and are roughly in accord with the present measurements. Wells' data consist of two values, one for 738°C. (1360°F.) the other for 840°C. (1544°F.), which, when extrapolated linearly to 957°C. (1755°F.) and 1110°C. (2030°F.), indicate that the solubility at these temperatures is 1.27 and 1.68 per cent carbon, respectively, whereas our direct determinations at these same temperatures give 1.39 and 1.89

per cent carbon, respectively. On the other hand, a smooth curve, which is very nearly a straight line, can readily be drawn through the two points representing the present measurements and Wells' point representing the eutectoid composition

Fig. 3, which passes through the two points representing our measurements and through the point representing Wells' data for the eutectoid composition and temperature.

It should be noted that the determinations recorded in Table 1, as interpreted,

FIG. 2.—MICROSTRUCTURE OF SAMPLE 7, 1.865 PER CENT C.; SATURATED WITH GRAPHITE AT 1106°C. (2023°F.) AND QUENCHED IN BRINE. × 1000.

(0.69 per cent carbon) and temperature (738°C., 1360°F.). It is difficult, however, to draw a smooth curve through both of Wells' points and the present measurements. It seems likely, therefore, that Wells' value for the solubility at higher temperature is too low and that the solubility curve can be represented with satisfactory accuracy by the solid curve in

indicate that the true solubility of graphite in austenite is at higher temperature appreciably greater than would be inferred from the selected phase diagram published by Epstein.[5] For example, from extrapolation of the present measurements over only 25°C., the maximum solubility of graphite in austenite—that is, at the temperature of the iron-graphite eutectic, at present

accepted as 1135°C. (2075°F.)—is 1.98 per cent, whereas the diagram indicates a value of 1.7 per cent, though on an earlier page of the same book (p. 112) there is a

tions of the stability of iron carbide as compared with graphite and iron saturated with graphite; so it is of interest to compare the solubility curve for graphite,
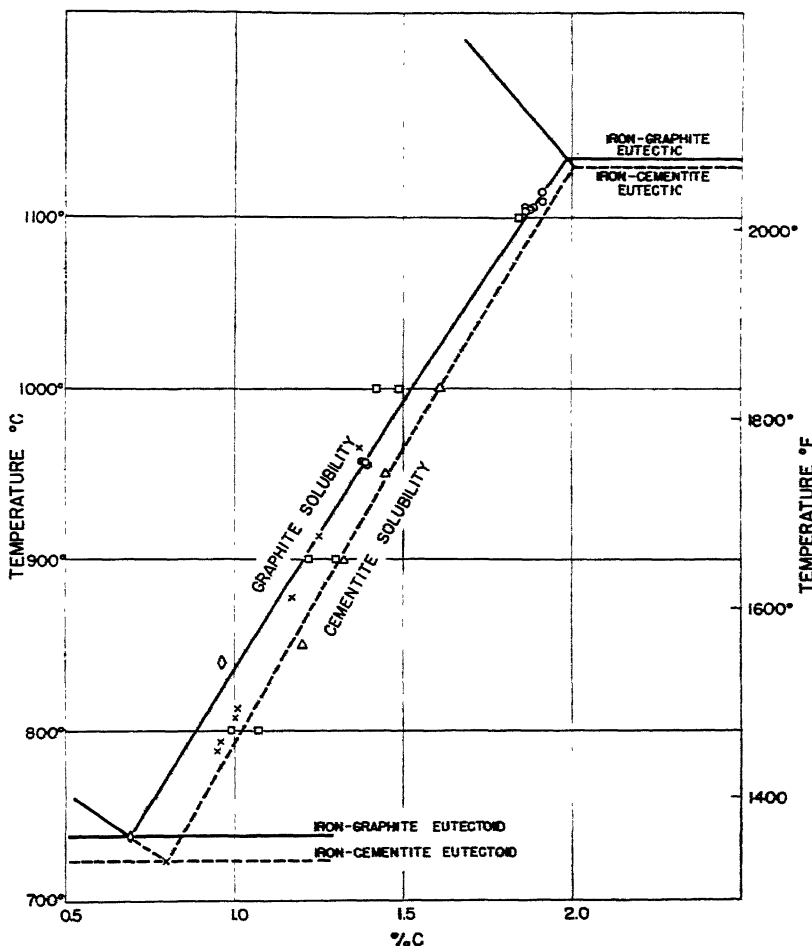

FIG. 3.—PROPOSED GRAPHITE (SOLID LINE) AND CEMENTITE (BROKEN LINE) SOLUBILITY LINES OF IRON-CARBON DIAGRAM, AND DATA OF SOME INVESTIGATORS.
Investigators: for graphite solubility Söhnchen and Piwowarsky (squares), Wells (diamonds), Gurry (circles); for cementite solubility Bramley and Lord per Kelley (triangles), and Mehl and Wells (crosses).

statement that the probable carbon content at this point is 1.7 ± 0.3 per cent.

Although the present measurements yield no direct information on the solubility of cementite in austenite, they have an indirect bearing through established rela-

as given in Fig. 3, with corresponding data for iron carbide. The best of the data for cementite solubility appear to be those of Bramley and Lord[6] and of Mehl and Wells.[7] Bramley and Lord's measurements were made by allowing mixtures of carbon

monoxide and carbon dioxide to come to equilibrium with steels of known carbon content. The equilibrium ratio $CO:CO_2$ increased with carbon content up to a given content and then remained constant for all steels with higher carbon. That percentage of carbon at which the maximum ratio of CO to CO_2 was first attained was considered to be the concentration beyond which Fe_3C was present as a separate phase, and this carbon content was taken to represent the solubility of carbide. The results so obtained, as interpreted by Kelley,[8] yield a cementite solubility curve which fits in well with our present knowledge of this system and is consistent with the data of Mehl and Wells for the eutectoid composition and temperature. This curve, shown by the dotted line in Fig. 3, lies to the right of the graphite-solubility curve, a condition that must hold if, as Wells and others have shown, cementite is unstable with respect to graphite and austenite saturated with graphite in this range of temperature.

Mehl and Wells worked with a series of alloys of known carbon content whose transformation temperature was determined either dilatometrically or by examination of quenched specimens under the microscope. The curve drawn through the points representing their data is much steeper than the dotted line in Fig. 3, and, indeed, appears to have too steep a slope; for comparison of their data at the higher temperatures with the selected line for the solubility of graphite (solid line in Fig. 3) would indicate that cementite is stable relative to graphite and iron saturated with graphite at all temperatures above 915°C. (1679°F.). This is not in agreement with Wells'[4] observation at 1125°C. (2057°F.) showing that cementite is unstable at least up to this temperature.

The dotted line in Fig. 3, which represents the data of Bramley and Lord, and passes through the point corresponding to the eutectoid composition and temperature

determined by Mehl and Wells, appears, therefore, to be more consistent with the selected curve for the solubility of graphite than is the curve drawn through all the data of Mehl and Wells. On linear extrapolation these two solubility curves would intersect at a point corresponding to 1280°C. (2336°F.), which is proposed as the temperature at which iron carbide becomes stable relative to graphite in austenite saturated with graphite.

For both graphite and cementite solubility, there appears to be a consistent discrepancy between the results of the solubility measurement according as it is made directly by analysis of a sample of iron or steel that was held at constant temperature long enough to allow it to become saturated with carbon by diffusion from an atmosphere containing carbon, as was done in the present measurements and by Bramley and Lord; or as it is derived from observations of the lowest temperature at which carbon, or carbide, in a specimen of given carbon content, appears to be all in solution after a given number of hours, which is basically the method of Wells, and of Mehl and Wells. It is difficult to understand how the former method, which gives the higher solubility, should yield a result in excess of the true solubility when there is no evidence of the existence of a second phase at temperature; it is inferred, therefore, that in the latter method, as carried out, the time at temperature was not sufficient to establish equilibrium, and, in particular, presumably, to assure a thoroughly uniform distribution of carbon in the austenite phase.

SUMMARY

The solubility of graphite in austenite, determined by carburizing samples to saturation at constant temperature, is 1.39 per cent carbon at 957°C. (1755°F.) and 1.89 per cent carbon at 1110°C. (2030°F.). Microscopic examination after quenching showed the carburized samples to be free from graphite or cementite at temperature. The maximum solubility of graphite in austenite, determined by a short linear extrapolation to 1135°C. (2075°F.), the temperature of the iron-graphite eutectic, is 1.98 per cent carbon.

A cementite-solubility curve, based on data reported in the literature, and consistent with the measured solubility of graphite, has been selected. The intersection of this curve with that for the solubility of graphite indicates that cementite is unstable relative to graphite and austenite saturated with graphite below about 1280°C. (2336°F.).

REFERENCES

1. H. S. Roberts: *Jnl.* Opt. Soc. Amer. and *Rev. Sci. Instr.* (1925) 11, 171.
2. D. H. Andrews and J. Johnston: The Rate of Absorption of Water by Rubber. *Jnl.* Amer. Chem. Soc. (1924) 46, 640.
3. Söhnchen and Piwowarsky: Über den Einfluss der Legierungselemente Nickel, Silizium, Aluminium und Phosphor auf die Löslichkeit des Kohlenstoffs im flüssigen und festen Eisen. *Archiv Eisenhüttenwesen* (1931) 5, 111.
4. C. Wells: Graphitization in High-purity Iron Carbon Alloys. *Trans.* Amer. Soc. Metals (1938) 26, 289.
5. S. Epstein: Alloys of Iron and Carbon, 1, 157. New York, 1936. McGraw-Hill Book Co.
6. Bramley and Lord: Equilibria between Mixtures of Carbon Monoxide and Carbon Dioxide at Various Pressures in Contact with Steel of Different Carbon Concentrations at 750° to 1150°. *Jnl.* Chem. Soc. (1932) 1641.
7. Mehl and Wells: Constitution of High-purity Iron-carbon Alloys. *Trans.* A.I.M.E. (1937) 125, 429.
8. K. K. Kelley: Thermodynamic Properties of Metal Carbides and Nitrides. U. S. Bur. Mines *Bull.* 407 (1937).

DISCUSSION

(John Marsh presiding)

C. WELLS* AND R. F. MEHL,* Pittsburgh, Pa.—
The subject studied by the author is an important one, upon which new and better

* Carnegie Institute of Technology.

information must be welcomed. Other workers have engaged themselves on this same problem; if new work on an old subject is to be considered as an addition to our knowledge, it must be based on better reasoning, or based on better experimental technique, or be more complete. We do not think that the present work meets such requirements.

Wells used a dilatometric method to determine the eutectoid temperature and a single graphite solubility value in the iron-graphite system. By suitably plotting and extrapolating the dilatometric results procured at a number of heating and cooling rates the equilibrium temperatures A_{1cr} and A_{zr} were obtained. The advantage of such a procedure is that equilibrium is approached from both sides. Wells also used the familiar microscopic method for the determination of both the eutectoid temperature in the iron-graphite system, and the A_{cm} line in the iron-cementite system, but this was done only after it had been first shown by the dilatometric method that the soaking times chosen were sufficiently long to give a close approach to equilibrium at the temperatures chosen; one point on the A_{cm} line as determined microscopically was checked—and accurately checked—by the dilatometric method; if times of annealing employed in using the microscopic method at this low temperature may be taken as adequate in view of the check, surely no objection can be raised to results at higher temperatures using the same time of annealing, for the rate of diffusion increases markedly with temperature. The dilatometric method was used to establish the A_1 temperature in the iron-cementite system. The microscopic method is entirely reliable if it is shown that the times of annealing are adequate, and is entirely free from any assumptions concerning the phase relationships involved; the approach to equilibrium from both sides as employed in the dilatometric method is the orthodox proof that the values obtained are in reality equilibrium values.

The author's suggestion that the cementite-solubility line of Mehl and Wells is inaccurate because of inadequate annealing times leads to an interesting comparison with the author's times. In the author's experiment in approaching saturation, carbon must diffuse over a radius in excess of 2 mm., whereas in the specimens employed by Mehl and Wells it had

to diffuse only over very short distances, since carbide particles were on the average only about 0.005 mm. apart. At temperatures 5°C. below the A_{cm} line thousands of small carbide particles were observed, distributed uniformly through the sample. Calculations show that for the author to obtain as close an approach to equilibrium as obtained by Mehl and Wells his specimens would have had to be heated for several years at temperature.

The experiments performed by Mehl and Wells in determining the cementite-solubility line were so surrounded by experimental precautions, and gave such consistent results, employing the simplest of the principles for the establishment of phase diagrams, that they should hardly be lightly dismissed.

It is difficult to understand why Gurry uses the eutectoid compositions and temperature values given by Wells (iron-graphite system) and by Mehl and Wells (iron-cementite system) when these are based on an extrapolation involving the A_{cm} data which he does not accept. Also, one wonders why the author considers only that part of Bramley and Lord's investigation involving the determination of the A_{cm} line between 850° and 1000°C. when work was done covering the range 800° to 1050°C. Gurry accepts Kelley's interpretation of Bramley and Lord's results, which gives different A_{cm} values from those published by Bramley and Lord. Since Gurry accepts the A_{cm} line based on Bramley and Lord's work as being more accurate than that of Mehl and Wells, any extrapolation to the A_1 line should be made on that basis. If this were done both iron-graphite and iron-cementite eutectoid points would be moved to the right of those now shown in Gurry's present suggested diagram. Incidentally, it appears that the A_{cm} data of Bramley and Lord may be questionable on the basis of nonattainment of equilibrium; work on this point is underway.

Mr. Gurry, who uses Bramley and Lord's results as a basis for his proposed A_{cm} line (Fig. 3), would no doubt not accept the $A_{g r}$ line proposed by the same authors in the same paper, for this line, as shown in Fig. 4, is considerably to the left of that proposed by the author and of that proposed by Wells, although it is consistent with the A_{cm} line of Mehl and Wells in so far as it falls to the left.

According to the author's diagrams, it should be possible to heat his 1.98 per cent C homogeneous specimens at temperatures close to but above the eutectic temperature without melting and completely dissolving the carbide (or graphite). It is suggested that such experiments be made by the author to test the validity or nonvalidity of the unusually high solubilities proposed for temperatures near the eutectic; in previous work on the constitution of iron-carbon alloys there has been no basis for such high solubilities.

Fundamentally, the question involved in interpreting the author's results is what equilibrium, if any, do they represent. It is by no means clear that they represent the equilibrium solubility of graphite in austenite. It will be observed that the amount of carbon his samples absorbed increased as the velocity of flow increased above 40 c.c. per minute. If the solution of carbon above this rate of flow did not provide the equilibrium solubility of graphite in austenite, how can it be certain that the solution at 40 c.c. per minute did provide this equilibrium solubility? Hydrocarbons are all unstable; between graphite at one extreme and toluene at the other, the equilibrium solubility of carbon will vary from a minimum to some unknown maximum; the occurrence of soot on the samples is no proof that an equilibrium of the austenite with graphite was established, and it seems more likely, judging from the mass of information on the reaction of austenite with carbonaceous gases and with carbon in the absence of gases, that the reaction was one between austenite and some undetermined decomposition product or products of toluene, providing a solution of carbon in austenite in excess of the equilibrium graphite solubility. This problem is a complicated one, requiring much study for full elucidation.

The reaction studied by the author is an interesting one. If graphite and cementite solubility values determined by orthodox methods were accepted and the carbon absorption with various mixtures of hydrocarbon gas and hydrogen determined at various rates of flow and over a range of temperatures, much progress might be made in such studies. It has seemed to us for some years that reactions of this sort are much in need of detailed study; their importance in commercial gas carburizing should justify them practically.

R. W. GURRY (author's reply).—The first part of the discussion by Wells and Mehl, in so far as it is concerned with my conclusions, deals with the suggested solubility curve for ce-

saturated with carbon at 1023°C. (1873°F.) in a mixture of hydrogen and toluol flowing at the rate of 4 c.c. per min. The specimens were then cleaned, broken in two, and one half of each was
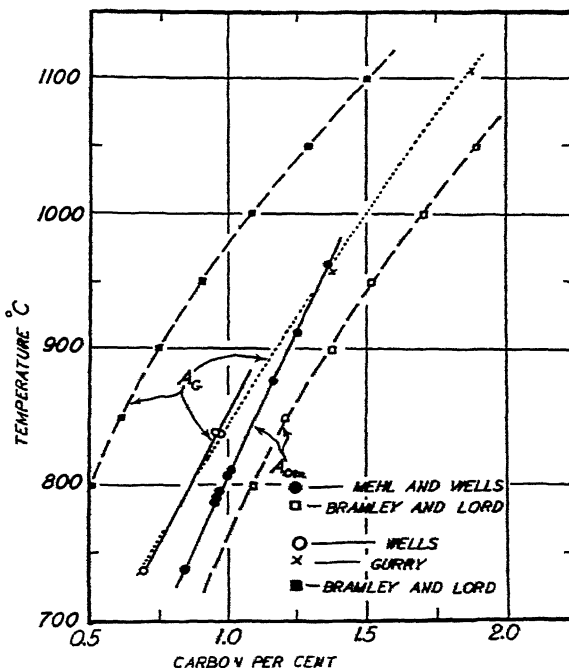

FIG. 4.—CURVES SHOWING SOLUBILITY OF CARBON IN AUSTENITE WHEN IN EQUILIBRIUM WITH GRAPHITE (Ag LINES) AND CEMENTITE (A_{cm} LINES) AS DETERMINED BY GURRY, BRAMLEY AND LORD, AND MEHL AND WELLS.

mentite. Since the position of this curve is admittedly based solely on inference, and since no useful purpose would be served by a further exchange of opinions at this time, this reply is confined to a consideration of the second part of their remarks, in which they point out, with some justification, that the evidence presented in the paper does not establish beyond question that the carburized samples were in equilibrium with graphite. Since this question was raised when the paper was presented, some additional measurements have been made to demonstrate that the results for a sample that is in equilibrium with graphite are the same as those reported in the paper, and at the same time, by providing data at a third temperature, to corroborate the position and shape of the solubility curve for graphite in Fig. 3.

These additional measurements were made on three cylinders of carbonyl iron, which were

used for analysis. Although the time of treatment ranged from 216 to 420 hr., the final carbon content of all the samples was 1.57 per cent, a result that agrees satisfactorily with the solubility curve shown in Fig. 3.

The remaining piece of each cylinder was then further carburized in contact with graphite at a higher temperature. In carrying out these measurements it was necessary to be sure that the carbon used was true graphite and not one of the pseudographitic forms described by Biscoe and Warren.[9] We have been informed (communication from Prof. John Chipman) that Professor Warren finds that Acheson graphite is entirely graphitic, and accordingly Acheson graphite powder No. 38 was used in these tests. The three pieces of carburized iron were sealed

[9] Biscoe and Warren: *Jnl. Applied Physics* (1942) 13, 364.

in a single evacuated silica tube along with some graphite and about 3 mg. of Fe_2O_3, the latter being added to provide a trace of oxygen as a carrier for the carbon. After 331 hr. at 1095°C. (2003°F.) the tube was broken, and one specimen, removed for analysis, contained 1.81 per cent carbon. The remaining two specimens were sealed as before in another silica tube and were held an additional 172 hr. at 1106°C. (2023°F.) in contact with graphite, after which one specimen, removed for analysis, contained 1.86 per cent carbon. After being again sealed in a silica tube along with graphite and Fe_2O_3, and held at a temperature of 1112°C. (2034°F.) for an additional 192 hr., the third specimen likewise contained 1.86 per cent carbon. Each of the last two specimens was quenched by smashing the silica tube so as to allow the specimen to fall into iced brine. Examination of the quenched specimens under the microscope revealed a complete absence of graphite or carbide at temperature, just as in the specimen illustrated in Fig. 2.

The results of these tests, in which the specimen must have been in equilibrium with graphite because if its carbon content had been greater than the solubility of graphite some carbon should have diffused out of the sample, are in excellent agreement with the data reported in Table 1, and confirm the conclusion that the solid curve in Fig. 3 represents the solubility of carbon as graphite in gamma iron.

In passing, it may be pointed out that in the light of Warren's researches one may justifiably raise the question whether the free carbon observed in certain irons or steels under the microscope, and commonly called graphite, is in fact graphite.

Diffusion in Metal Accompanied by Phase Change

By L. S. Darken*

(New York Meeting, February 1942)

THE manufacture and treatment of metals comprises operations whose effectiveness depends in large measure upon diffusion phenomena. The significance of such phenomena has, for a few simple cases, long been understood, but in more complex cases it has not been adequately recognized. This paper presents a mathematical analysis of some of the cases in which diffusion leads to the formation of a new phase within the metal, and this analysis provides a basis for interpreting quantitatively many apparently diverse experimental observations recorded in the literature, some of which are outlined in the following pages.

OBSERVATIONS RECORDED IN LITERATURE

An outstanding instance is the general type of phenomenon in which diffusion of an element into an alloy is followed by a phase change, which most frequently is a reaction (precipitation) of the diffusing element with one or more components of the alloy to form a compound. Thus in certain alloys heated in contact with oxygen not only the usual oxide scale appears but, in addition, beneath the surface, a well-defined zone in which free oxide particles are dispersed with notable uniformity. This zone, commonly referred to as the subscale or zone of internal oxidation, is remarkable in that the visible boundary between it and the unaltered metal is usually sharp. Such a subscale, which appears to have been recognized

first in oxidized copper alloys, has been described and studied by C. S. Smith,[1] by Rhines,[2] and by Rhines, Johnson and Anderson;[3] but it appears also in other alloys when they are exposed to conditions that bring about the precipitation of some compound, not necessarily an oxide.

Another clear case of this same kind is the diffusion of carbon into a steel containing an element such as molybdenum, chromium, vanadium or tungsten, whose carbide is less soluble in iron than iron carbide, the result being that some part of that element is precipitated as a dispersed carbide. A similar phenomenon may occur on the welding of two alloys each of which contains one of a pair of elements that react to form a compound or a new phase of any sort. But in addition to the precipitation of a compound formed from the diffusing element, other effects may result merely from the presence of the diffusing element. For instance, if homogeneous austenite, nearly saturated with respect to carbon, is heated in contact with silicon in the absence of oxygen, one would expect to find, behind the several iron-silicon phases analogous to a scale, a zone of austenite containing dispersed carbide, because of the fact that silicon decreases the solubility of carbon in iron. As still another example, oxidation of an alloy may result in diffusion toward the surface of one or more of the constituents; for instance, during oxidation of a steel containing an element such as copper, which is less prone to oxidation than iron, there is a notable enrichment of copper just beneath the scale-metal interface. As an example of a yet more

complex case, it is well known that a steel containing somewhat more than the usual proportions of copper and sulphur is particularly likely to develop troublesome surface defects when heated in an oxidizing atmosphere. Consideration of both phase equilibria and diffusion phenomena leads to the conclusion that, under the conditions stated, oxygen diffuses inward, thereby depleting manganese near the surface, while the content of both copper and sulphur increases near the scale-metal interface. This shift in concentrations may give rise to a further change, in that the sulphur, initially present mainly as relatively harmless solid particles of manganese sulphide, may react to form a low-melting liquid containing iron, copper and sulphur; this liquid has a much larger volume than the initial manganese sulphide and constitutes an observable surface defect. The over-all reaction at the treating temperature may be written:

$$
\begin{array}{llll}
\text{MnS} & + & \text{Cu} & + \text{Fe} + \text{O}_2 \\
\text{solid} & & \text{dissolved} & \text{gas} \\
\text{particles} & & & \\
& \rightarrow & \text{MnO} & + \text{Fe-Cu-S} + \text{FeO}_x \\
& & \text{solid} & \text{liquid} \quad\quad \text{solid} \\
& & \text{particles} & \text{scale}
\end{array}
$$
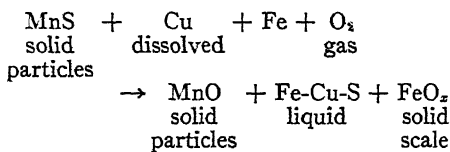
though other reactions may also take place.

Thus the role of diffusion in the complex phenomena involved in the heat-treatment of many types of steel is often unsuspected; for most papers on diffusion deal only with relatively simple cases, and so it is not surprising that the metallurgist does not perceive that some of his practical difficulties involve rather complex cases of diffusion. In general, when, any condition that induces diffusion of an element is imposed at the surface of a homogeneous alloy, a multiphase zone results, provided that the diffusion shifts the gross composition so that more than one phase is stable over a finite range of composition. It is on this basis that Rhines,[2] also Scheil and Kiwit,[4] have shown how the number

and nature of oxidic subscale zones can be predicted from an isothermal section of the phase diagram of the system.

It is to be remarked, however, that since diffusion takes place only by virtue of a composition, or more precisely, an activity, gradient, any system in which diffusion occurs is not at equilibrium; consequently, reasoning based on an equilibrium diagram alone cannot be strictly valid. It is here assumed, as has been done tacitly by others, that equilibrium prevails locally even though the system as a whole is far from equilibrium—in other words, that diffusion is slow compared with the rate of reaction to form a new phase. This assumption is reasonable in many cases, though not in all—for instance, the austenite-pearlite transformation under many conditions, and the Liesegang band formation, noted by Rhines in the beryllia and alumina subscales in copper, which implies that the solubility product of these oxides was exceeded for an appreciable time before precipitation occurred. The present paper deals only with cases in which the time for diffusion is so great compared with that for reaction that the latter may be ignored.

The mathematical treatment on the basis of Fick's law of the fundamental diffusion of one element into another to form a homogeneous solid solution is well established and has been widely utilized. The formation during oxidation of subscale on dilute alloys of copper has been treated mathematically by Rhines, Johnson and Anderson,[3] whose results are rigorous and complete, under the specific boundary conditions considered, if only subscale forms, and are reasonably satisfactory if both subscale and scale form simultaneously. These authors assume, however, rather than demonstrate, the existence of a sharp boundary between subscale and homogeneous alloy; also, that all reaction with the diffusing element (oxygen) takes place at this sharp boundary.

The purposes of the present paper are: (1) to demonstrate the conditions necessary for the existence of a sharp boundary; (2) to furnish a simple method of calculating the composition and thickness of the subscale; and (3) to show how the method may be extended to cover, at least approximately, related but more complex cases. Throughout this discussion it is assumed, as noted above, that local equilibrium is established; that is, that the rate of phase change is very rapid compared with the rate of diffusion. Also, the authors have adopted the convention of referring to the surface of contact between metal and scale as the *interface*, whereas the relatively sharp limit to the subscale is referred to as the *boundary* between subscale and unaltered metal. Finally, since the treatment of diffusion involves the number of atoms diffusing rather than the total weight of the migrating substance, concentrations are expressed in terms of mols or atomic per cent rather than as weight per cent. Any exception to this rule is specifically noted.

SIMULTANEOUS FORMATION OF SUBSCALE AND NONADHERENT SCALE

First, the case that can be treated most simply and most rigorously is considered; namely, the unidirectional and isothermal diffusion of an agent U, for instance, oxygen, corrosive to an alloy, originally homogeneous, composed of a base metal M and a small proportion of an alloying element V, which forms with U a compound UV, which precipitates whenever its solubility product is exceeded. The depletion of V in the metal matrix resulting from this precipitation gives rise to a concentration gradient of V such that V tends to diffuse in a direction opposite to U. It is postulated that sufficient time is allowed for the attainment of a steady state; that is, it is assumed that the concentration, or more strictly, the activity, of U remains constant at the interface

between the metal and its corrosive environment; moreover, that relative to the metal as a whole, this interface moves inward at a constant rate and so remains parallel to the original surface of the metal, which is assumed to be plane. The mathematical statement of these postulates in terms of D_u and D_v, the diffusivity of U and V, respectively, and of K, the solubility product of UV, and the general expressions for the distribution of U, V and UV as derived by combining these assumptions with Fick's law are given in section I of the Appendix (see p. 169). Assuming different relative values of D_u, D_v, and K, the variation in molar concentration of U, V, and UV with distance from the moving interface may readily be calculated for a variety of conditions (illustrated by the four typical examples in Fig. 1).

Since what is commonly observed under the microscope is the distribution of the precipitated compound UV, the curve referring to UV is of most immediate interest. Comparison of this curve in Figs. 1a to 1d leads to the following significant conclusions.

When K is zero (Figs. 1a and 1b) there is a discontinuity in the concentration of UV corresponding to a sharp boundary between subscale and unaltered metal; moreover, the concentration of UV is equivalent to the initial concentration of V. When K is greater than zero (Figs. 1c and 1d) the discontinuity becomes an inflection, which is less steep the greater the value of K or of the ratio D_v/D_u; that is, the boundary between subscale and unaltered metal becomes more diffuse as K or the ratio D_v/D_u increases. Thus, it is demonstrated that on the basis of the postulates listed above, the subscale should have a well-defined boundary whose sharpness decreases as the solubility product of the precipitated component increases, or as the diffusivity of V increases relative to that of U. Since the value of the solubility product and of the ratio D_v/D_u changes

fairly rapidly with temperature, this means that the sharpness of the boundary of the subscale may vary considerably with the temperature at which the diffusion

as the distance between the moving boundary and the point of inflection on the concentration curve for UV, is substantially independent of the value of K and
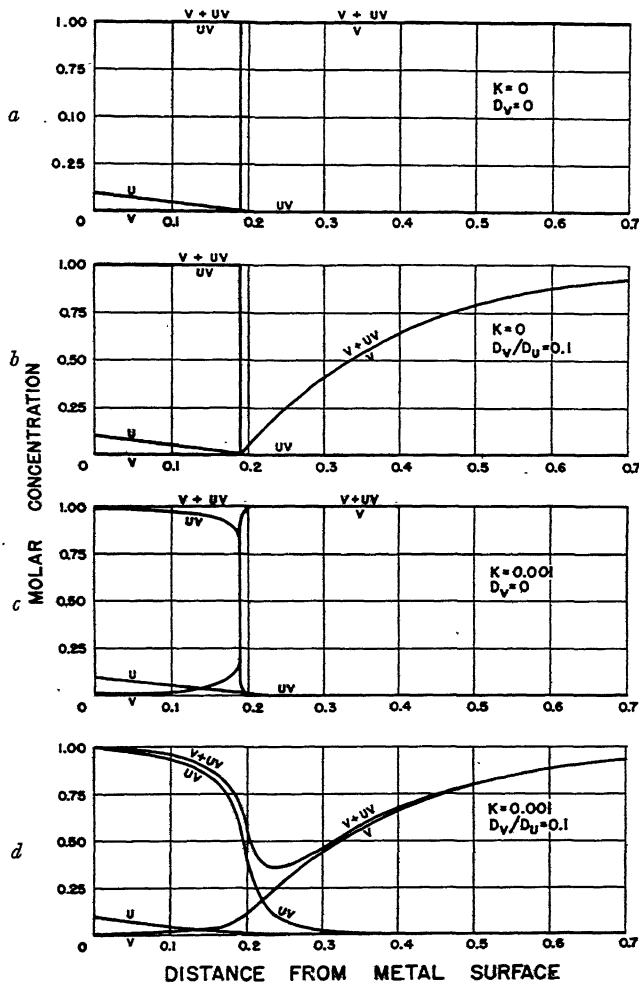

FIG. 1.—SUBSCALE AND NONADHERENT SCALE.

Distribution of element U and V of compound UV, as influenced by value of solubility product of UV and of ratio $D_V : D_U$.

occurs. Obviously, if K is greater than the product of the initial concentration of V and the solubility of U, no precipitation occurs and no subscale is formed.

The relations given in section I of the Appendix also indicate that the thickness X of the subscale, defined in terms of Fig. 1

of D_v, at least over a fairly wide range of these factors, and that it may be calculated with an error less than that of measurement of the position of the boundary as observed under the microscope by the relation

$$X = \frac{D_u}{r} \ln \left(1 + \frac{u_0}{v_0} \right) \qquad [1]$$

in which r is the rate of scaling—that is, the rate of motion of the interface between metal and the corroding agent—u_o is the solubility of U in the pure base metal, and v_o is the initial concentration of V, both in units that are chemically equivalent. This relation shows that the depth of subscale increases as the diffusivity and solubility of U increases and decreases with increasing rate of scaling or with increasing solubility of V. It is not appreciably influenced by the value of the solubility product K.

SUBSCALE FORMATION UNACCOMPANIED BY SCALE FORMATION

For dilute alloys this case has been treated rather completely by Rhines, Johnson and Anderson,[3] whose assumptions, however, as evidenced by the schematic diagram in Fig. 3 of their paper, are not quite consistent with the hypothesis that local equilibrium is attained in the vicinity of particles of the precipitated phase UV. In fact, it is difficult to picture any physicochemical conditions corresponding to the precise assumptions made by them. This reflection, however, has no bearing on the simplified equation actually used, which involves in essence the assumption that the solubility product is zero. They also omitted to point out explicitly, though they implied, that the proportion of UV in the subscale may be very large in comparison with v_o. This "build-up" of V, resulting from the migration of V in a direction opposite to that of U, is illustrated schematically in Fig. 2 for the case of zero solubility product; it is obvious that the two shaded areas must be equal if none of V is lost, as by evaporation.

The equation describing the rate of growth of the subscale in the absence of a scale can be expressed most readily in terms of the "build-up" of V in the subscale. Thus it is shown in section II of the Appendix that the rate of growth of subscale may be expressed by the equation

$$\frac{X^2}{t} = 2D_u \frac{u_o}{u_m} \left[1 + \frac{u_o}{12u_m} - \frac{1}{240} \left(\frac{u_o}{u_m} \right)^2 + \cdots \right]^2 \quad [2]$$

where X is the depth to which precipitation extends at time t, D_u and u_o are, as before, the diffusivity and solubility of U, respectively, and u_m is the mean concentration of U in the subscale. Since V tends to "build up" in the subscale, u_m is not the amount of U required to react with the initial concentration of V but rather with the amount actually present, plus $\frac{1}{3}u_o$.* In section III of the Appendix it is shown further that:

$$\frac{v_s}{v_o} = 1 + \frac{2G \sqrt{D_v}}{\sqrt{X^2/t}} \quad [3]$$

where v_s is the concentration of V, as UV, in the subscale, v_o its initial concentration and D_v its diffusivity, and G is a function that is given graphically in Fig. 3 as a function of $\frac{1}{2} \frac{X^2}{t} \sqrt{D_v}$. The quantity u_m is readily found from v_s by multiplying by the weight ratio in which U and V react and adding $\frac{1}{3}u_o$.

Equations 2 and 3 together permit the calculation of both the depth of penetration X and the "build-up" of V in the subscale. Usually the term shown in brackets in Eq. 2 differs negligibly from unity and may be omitted. In many cases the "build-up" is negligibly small, hence Eq. 3 may be neglected; when this is not so, an approximate value of X^2/t may be found from Eq. 2 and substituted in Eq. 3 to find a more accurate value of u_m; the approximation seldom needs to be repeated more than once or twice. These equations are of somewhat wider application than the simplified equation of Rhines, Johnson and Anderson, and are considerably easier to handle than the

* The average amount of U actually present in true solution in the subscale zone is approximately $\frac{1}{2}u_o$. However, the quantity u_m is not strictly an arithmetic mean value. The contribution to this term of the dissolved amount of U is $\frac{1}{3}u_o$, as has been shown by Rhines, Johnson and Anderson.[3]

complete solution given by these authors. Application of these relations to the experimental data given in their paper shows that the two methods give identical numerical results for the dilute range covered.
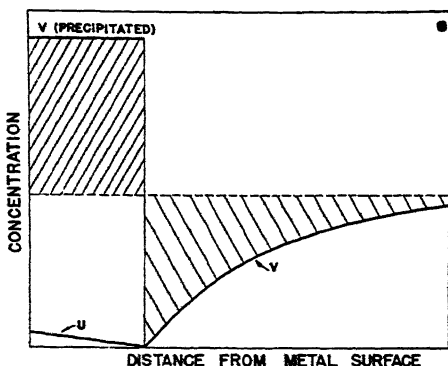

FIG. 2.—SUBSCALE WITHOUT SCALE.
Influence of diffusion of V when solubility product is zero.

The equations may be used also to determine the diffusivity of the migrating elements from data on subscale formation; for instance, the measurements of C. S. Smith[1] on the oxidation of copper-silicon alloys yield the diffusion coefficient of oxygen in copper. The values so derived are compared (Fig. 4) with the data reported by Ransley,[5] the same values of the solubility of oxygen in copper[6] being used in each case, and with the diffusivity of silicon in copper taken from Rhines and Mehl.[7] The agreement is seen to be good.

It is of interest to note that the equations on which the parts of Fig. 1 are based reduce to approximate forms of Eqs. 2 and 3 if r is set equal to dx/dt; i.e., if steady-state conditions are approximated at corresponding rates of increasing subscale thickness in the case when no scale forms on the surface. This implies that these diagrams represent also the conditions in the present case provided that the "build-up" of V in the subscale is not too large, and that the diagrams are altered so that the deficiency of V in the single-phase region

appears as a uniform excess concentration in the subscale zone.

SUBSCALE FORMATION AT HIGHER ALLOY CONTENT

The preceding discussion deals with the formation of a subscale in which the volume of the precipitated phase UV is small compared with that of the metal in which UV is dispersed. In practice this condition is sometimes not fulfilled, for V may be present in sufficient quantity so that its diffusion plays a major role. In this case the rate of subscale growth is relatively very slow and Eq. 3 may be used, as shown in section III of the Appendix, in the approximate form

$$\frac{v_s}{v_0} = 1.1 \frac{D_v}{\alpha} + 1 \qquad [4]$$

where $\alpha (= X/\sqrt{t})$ is the parameter describing the rate of motion of the subscale-metal boundary relative to the mass of metal. If, further, the rough approximation is made that the rate of diffusion of U is proportional to the volume percentage (β) of the base metal M in the subscale, the approximate form of Eq. 2 may be transformed to the following relation, which holds for the case in which only subscale is formed:

$$\alpha' = \sqrt{2D_u\beta \frac{u_0}{u_m}} \qquad [5]$$

where α' again characterizes the rate of subscale growth but must be distinguished from α on account of the volume difference. Eqs. 4 and 5 together describe approximately the subscale formed. In any given case u_m, v_s, and the ratio α'/x are functions of β, and may be so expressed providing the composition and density of the precipitated phase are known.

In the case of the oxidation of iron-silicon alloys (U is oxygen, V silicon) the ratio of α' to α is approximately $\dfrac{2}{x+\beta}$ on the basis that the precipitated oxide is SiO_2.

Combining Eqs. 4 and 5 with this relation, expressing u_m and v_s approximately in terms of β, and estimating the solubility of oxygen in iron as 0.07 per cent and the ratio of the diffusivity of silicon to that of oxygen in

that is, the alloy content appears to be on the borderline between that at which subscale does and does not form. Similarly, Scheil and Kiwit[4] point out that at 1000°C. the rate of scaling of silicon steel drops off
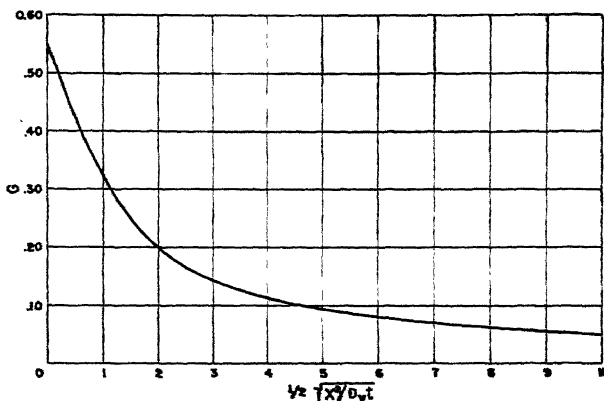

FIG. 3.—VALUES OF FUNCTION G.

iron as $\frac{1}{2}0$, we obtain

$$(1 + \beta)^3 \sqrt{1 - \beta} \doteqdot v_s' \qquad [6]$$

where v_s' is now the initial concentration of silicon *in weight per cent*. This is only a crude approximation based on the stated assumptions, but it serves to illustrate the form of the relationship between initial alloy composition and the amount of precipitated oxide in the subscale. The striking feature of this relation, which is shown graphically in Fig. 5,* is that it predicts an upper limit to the alloy concentration at which a subscale may form; in iron-silicon alloys this limit appears, as shown, to be in the vicinity of 2 to 3 per cent silicon. If scale and subscale were formed simultaneously, the corresponding limit would be somewhat higher.

This prediction is confirmed by experiment. For example, it has been observed in this Laboratory that a steel containing 3.25 per cent silicon, when scaled in CO_2 at 1000°C. develops subscale only in patches;

markedly as the silicon content increases in the range 3 to 4 per cent, the scaling rate being very low when the steel contains more than 4 per cent silicon. This would be anticipated from the foregoing reasoning, on the basis that at a silicon content higher than that corresponding to the nose of the curve in Fig. 5 the rate of diffusion of silicon outward is great enough to prevent the diffusion of any oxygen into the metal; under these conditions the silicon is oxidized only at the scale-metal interface, forming a skin of SiO_2 that is relatively impervious to oxygen and therefore greatly lessens the scaling rate thereafter.

INWARD DIFFUSION OF MORE NOBLE ALLOYING ELEMENTS DURING SCALING

When steel containing an element less easily oxidized than iron is exposed to a corrosive atmosphere, the alloying element frequently accumulates to a marked degree at or near the scale-metal interface. In copper-bearing steels this phenomenon is particularly pronounced, and undoubtedly is largely responsible for the difficulty often

---

* No definite experimental evidence bearing on the physical significance of the upper portion of the curve seems to be available.

encountered in obtaining a good surface on such steels. Often the build-up of the more noble metal at the scale-metal interface, provided that the scale is adherent, can be

As an example of the use of Eq. 7 and Fig. 3, if in a specific case $\alpha/2\sqrt{D_r}$ has the value 2, G from Fig. 3 has the value 0.20, whence $v_b/v_o = 11$, or the percentage of V
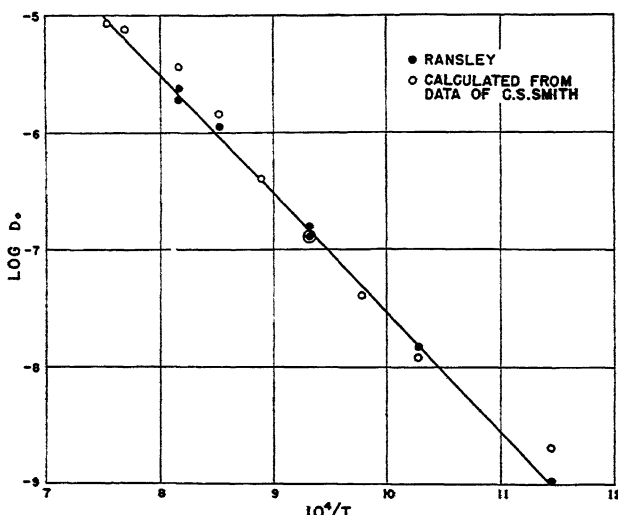

FIG. 4.—COMPARISON, DIFFUSIVITY OF OXYGEN IN COPPER AS CALCULATED FROM DATA ON SUBSCALE AND AS REPORTED BY RANSLEY.

described with sufficient degree of approximation by the relations developed in section III of the Appendix. There it is shown that if, by some process such as scaling, base metal is removed from a plane surface at a rate inversely proportional to the amount already removed, whereas the alloying element V is not, the relation between its concentration at the interface (v_b) to its original concentration (v_o) is

$$\frac{v_b}{v_.} = 1 + \alpha/2G\sqrt{D_v} \qquad [7]$$

where α is the parameter describing the rate of scale formation, $X(= \alpha\sqrt{t})$ is the distance of the scale-metal interface from the original surface at time t, and D_v is again the diffusivity of V. Values of the ratio v_b/v_o are shown graphically as a function of $\alpha/2\sqrt{D_v}$ in Fig. 6. For large values of $\alpha/2\sqrt{D_v}$, Eq. 7 may be simplified to

$$\frac{v_b}{v_o} = 1 + \frac{\alpha^2}{2D_v} \qquad [8]$$

would be approximately 11 times as great at the scale-metal interface as in the initial homogeneous alloy, provided that none of V passed into the scale. Clearly, if 11 times the initial percentage of V exceeds its solubility, and if the time required for its formation is not too great, there will form a new phase, which may admix with the scale. If the value of v_b read from Fig. 6 does not exceed its solubility, it seems reasonable to suppose that very little of the more noble alloying constituent V will be found in the scale; for in that case, on the basis that V is sufficiently noble so that none of it oxidizes, yet all of the base metal oxidizes in the scale, its activity in the scale would be unity, and in the metal less than unity. Since all the scale was, at the time of its formation, in intimate contact with the metal, this condition is not possible unless an infinitely steep activity gradient occurs at the scale-metal interface; under the condition, as stated previously, that there is

local equilibrium at all times, such an infinitely steep gradient is impossible.

The rate of scaling of iron in air and carbon dioxide has been measured by

FIG. 5.—TYPICAL ILLUSTRATION (IRON-SILICON ALLOYS) OF LIMITING CONCENTRATION FOR SUBSCALE FORMATION AT HIGHER ALLOY CONTENT.

Heindlhofer and Larsen,[8] with results that indicate that α has the value 2.8×10^{-4} cm. per sec.$^{1/2}$ at 1000°C. Reliable data on the diffusity of copper in iron are not available, but its diffusivity in nickel as reported by Grube and Jedele[9] is 1.2×10^{-5} sq. cm. per day at 1000°C. If the diffusivity of copper in iron be considered as the same, and independent of concentration in the range o to 10 per cent, D_v is 1.4×10^{-10} sq. cm. per sec., hence $\alpha/2 \sqrt{D_v} = 12$, and v_b/v_o is approximately 300. As the limiting solubility of copper in austenite is about 10 per cent at 1000°, it follows that if a homogeneous copper-iron alloy containing more than $\dfrac{10 \text{ per cent}}{300} = 0.03$ per cent copper is scaled in air or carbon dioxide at 1000°C. it is to be expected that the copper at the surface will build up to 10 per cent and that there will be formed a copper-rich alloy phase, corresponding in amount to all the copper over 0.03 per cent in the scaled metal, some of which may pass into the scale. If the initial iron alloy contained less than 0.03 per cent copper such a phase would not form and the copper would remain almost totally in the austenite. The value 0.03 per cent copper is, of course,

only approximate, since it depends upon an assumed value of the diffusivity of copper in iron. The total amount of copper, in excess of the initial content in the austenite,
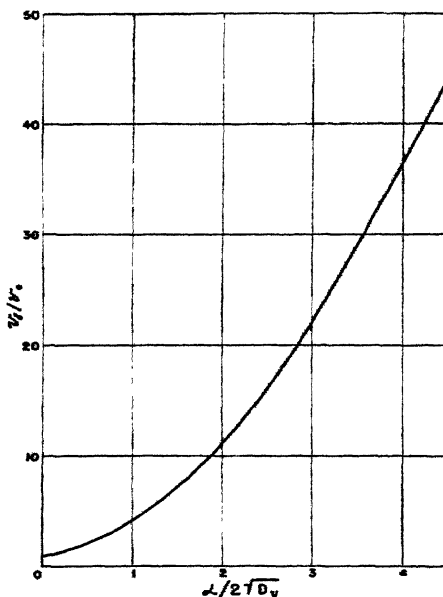
FIG. 6.—"BUILD-UP" OF MORE NOBLE ALLOYING ELEMENTS AT SCALE-METAL INTERFACE.
Variation of ratio of concentration at interface to initial concentration (v_b/v_o) with diffusivity D_v, and scaling rate parameter α.

is clearly 0.03 per cent of the total amount of iron scaled; at the end of an hour at 1000°C. this is about 4.2×10^{-5} grams per sq. cm. of surface.

Similar reasoning may be applied to a variety of examples not involving an oxidic scale. Hicks[10] has shown that if iron is heated in chromium chips at 1200°C. there results a rim of high chromium content which is separated from the low-chrome core by a sharp boundary. The formation of such a rim of ferritic iron-chromium solid solution on a core of austenite is analogous, from the diffusion viewpoint, to the formation of an oxidic scale, though of course in the common oxides the range of solid solutions is not as great as in the iron-chromium alloys.

Since iron-silicon alloys also have a closed gamma loop, the diffusion of silicon into austenite undoubtedly would produce a like occurrence, except that there would be several distinct rims, corresponding to the several silicon-iron solid solutions analogous to the several oxide zones (wustite, magnetite, hematite) formed on iron scaled in air or oxygen. If carbon is present in the austenite into which the silicon diffuses it should behave as copper does during the scaling of copper-bearing steel, the solubility of carbon being very low in ferrite. If the rate of formation of the rim, the diffusivity, and the solubility of carbon were known, the behavior of the carbon could be predicted by the method outlined for copper—again on the basis that the heterogeneous reaction rate is rapid compared with the diffusion rate.

ROLE OF THERMODYNAMICS IN INTERPRETING DIFFUSION PHENOMENA

Most of the preceding discussion was limited to the simultaneous diffusion of several elements in a single phase; moreover, it was assumed that the diffusion processes taking place at the same time did not occur in the same volume elements except in the vicinity of the subscale metal boundary. The problem of the simultaneous diffusion of more than one element into a metal is much more complex. Mehl and Rhines[11] have measured the rates of the simultaneous diffusion of nickel and silicon into copper and compare these rates with those of each of these elements diffusing individually into copper. At a concentration less than 1 per cent, the diffusivity is not greatly affected by the simultaneous diffusion of the other element. At higher concentrations the rate of diffusion of the more rapidly diffusing silicon is markedly decreased by the presence of nickel, whereas that of the more slowly diffusing nickel is influenced but little, if at all, by the pres-

ence of silicon. Although this is not the place for an extended discussion of this complex phenomenon, it is perhaps worth while to point out the bearing of equilibrium considerations on diffusion.

It is commonly stated that diffusion of an element occurs by virtue of its concentration gradient. Clearly, this is not strictly so, for two phases in equilibrium may be placed adjacent to each other without the occurrence of diffusion, although there may be an infinitely great gradient (discontinuity) of concentration at the interface. From the viewpoint of phase equilibrium this is so obvious that it need hardly be mentioned, for the definition of equilibrium precludes the possibility of interdiffusion between phases that already are in equilibrium. Thus, cementite (Fe_3C) in intimate contact with austenite saturated therewith exhibits no tendency to lose carbon to the austenite; in fact, austenite supersaturated with respect to cementite tends to lose carbon to produce this higher-carbon phase—that is, carbon diffuses from a region (austenite) where it is present at a lower concentration to a region (cementite) where it is present at a higher concentration. The rule that diffusion takes place in the direction of lower concentration applies at best only to a single-phase region; thus, it is true that carbon diffuses *in the austenite* in the direction of lower carbon concentration, which is toward the austenite-cementite interface. For any one phase of a binary system this rule is valid and is expressed quantitatively by Fick's law, modified if necessary to allow for variation of the diffusion coefficient with concentration. For a system of more than two components it is no longer necessarily true that a given element tends to diffuse toward a region of lower concentration even within a single phase. This may be shown by equilibrium considerations which enable us to predict the direction of diffusion. Let us consider two alloys, one composed of the base metal A and an alloying element B, the other composed of

A, B, and a third constituent C; and suppose, for the sake of simplicity, that on the isothermal-phase diagram the composition of both of these alloys is represented by points that lie within the same single-phase region. Further, let it be assumed that the amount of B per unit volume is the same in both, and that the rate of diffusion of A and of C is so slow that B may be considered the only diffusing element. Under these conditions it might be expected that if the two alloys were welded together no diffusion of B would occur, since no concentration gradient of B would exist. But only in special cases, such as an ideal solution, would the activity of B be the same in the two alloys. Since it is rather rare for a metallic solid solution to be ideal, it is to be expected that in general the activity of B in the two alloys would be different, and often very different; that is, the two would not be in equilibrium with respect to B; neither, of course, would they be in equilibrium with respect to A or C; but it has been postulated that these diffuse so slowly that any change in composition is brought about only by the motion of B. Under these circumstances B would move from the alloy in which its activity is higher into that in which its activity is lower, so that diffusion would result in an inequality in the concentration of B. Similarly, when the activity gradient of B does not have the same sign as the concentration gradient, B apparently will diffuse "uphill." Such cases may not be numerous in practice, nevertheless the activity change brought about by the presence of other components cannot be ignored in treating diffusion phenomena.

In general, the isothermal diffusion coefficient (D in the ordinary form of Fick's law), which has been shown to be a function of composition even in binary systems, becomes in systems of more than two components a function not only of the concentration of each constituent but also of the concentration gradient of each; that is, the value of the diffusion coefficient is

significant only in conditions identical with those under which it was measured. Obviously, the utility of a coefficient that is a function of so many variables is limited. This suggests that the "driving force" in diffusion phenomena might better be represented as an activity gradient than as a concentration gradient. On this basis, Fick's law for unidimensional diffusion would be modified to the following:

$$\left(\frac{\partial x}{\partial t}\right) x = D_a \left(\frac{\partial^2 a}{\partial x^2}\right) t \qquad [9]$$

where x represents concentration and a, activity. Eq. 9 reduces to the ordinary form of Fick's law in the case of an ideal solid solution, or in any short concentration range—e.g., dilute solid solution—in which the activity is proportional to the concentration. The coefficient D_a would be expected to be essentially constant at constant temperature in a limited portion of a single-phase region of the system under consideration, provided that the differences in concentration under consideration do not materially alter the other factors affecting the rate of diffusion. Since diffusion is always a mutual phenomenon, it is clear that when the alloy content is so high that the movement of the base metal is large, Eq. 9 cannot apply, because only one activity appears in the equation. Sufficient data on activities and diffusion rates are not available to check the applicability of the foregoing equation to ternary systems. It may, however, be applied to a binary system in which the diffusion coefficient, as usually expressed, is found to vary with concentration. To do so necessitates the assumption of some specific relation between activity a and atomic concentration x; in many instances the following expression is probably adequate:

$$a = x e^{\beta x} \qquad [10]$$

where β is a parameter. Where the diffusion

coefficient D varies with concentration, Fick's law is usually written

$$\frac{\partial u}{\partial t} = \frac{\partial}{\partial x}\left[D\left(\frac{\partial u}{\partial x}\right)\right] \qquad [11]$$

By aid of expression 10, and ignoring any volume change, the relation between D, a variable, and D_a, assumed to be constant, is

$$D = D_a e^{\beta u}(1 + \beta u) \qquad [12]$$

which permits the evaluation of β from measured values of D, or the prediction of the manner of variation of D with concentration from a value of β determined by measurement of activity. It is to be noted that for an ideal solution $\beta = 0$, hence $D = D_a$; that is, there is no variation of D with concentration.

The easiest method of comparison is to determine whether the value of β derived from activity measurements is in agreement with that obtained from diffusion measurements. For iron-carbon alloys, both types of measurement have been made. The activity of carbon in austenite has been measured by Bramley and Lord[12] and also by Dünwald and Wagner,[13] the latter reporting a value of $\beta = 0.10$ at 940°C., u being expressed as atomic per cent carbon. The isothermal activity-concentration data of Bramley and Lord at 900° or 1000°C. correspond approximately to $\beta = 0.04$. Kelley,[14] in computing the heat of solution of cementite in austenite, finds that Bramley and Lord's data over the temperature range and composition range covered are not in disagreement with the assumption that solutions of carbon in austenite behave thermodynamically as an ideal solution of iron carbide in iron. This assumption, which is made by many investigators, corresponds approximately to the value 0.065 for β (up to the vicinity of 1 per cent carbon by weight). Recent measurements made by M. J. Day in this Laboratory (not yet published) on the equilibrium of iron-carbon alloys with H_2-CH_4 mixtures lead to

$\beta = 0.09 \pm 0.01$ at 1000°C. It is believed that this value is more accurate than the earlier ones.

From the measurements of Wells and Mehl[16] on the rate of diffusion of carbon in pure austenite, $\beta = 0.07$ at 1000°C. Their measurements on the rate of diffusion of carbon in an iron containing 16 per cent manganese, which appear to be more precise, correspond to $\beta = 0.09$. The average agrees well within the experimental error with the value 0.09 from activity data. Thus it has been shown that in austenite the increase of the diffusivity of carbon with increasing carbon percentage is in agreement with that calculated on the hypothesis that the rate of diffusion across any plane is proportional to the activity gradient, instead of the concentration gradient, at that plane.

This single example, of course, is not evidence that all cases of variation of diffusivity with composition may be similarly interpreted; nevertheless, it demonstrates the value of making use of thermodynamic functions in interpreting diffusion phenomena. Further qualitative confirmation of this interpretation is offered by the fact that the diffusion coefficient of manganese in iron does not vary as much with percentage of manganese as does that of carbon with carbon content; in fact, the manganese content must be raised by 50 per cent to double its diffusivity, whereas the diffusivity of carbon in iron almost doubles between zero and one per cent. This would be anticipated, since the solid solution of manganese in austenite approaches ideality much more closely than does the solid solution of carbon in γ iron.

SUMMARY

1. It has been shown that the rate of growth and composition of an oxidic subscale formed on an alloy may be predicted from the knowledge of diffusion constants, phase relations, and boundary conditions.

2. The analogy between oxidic subscale formation and other diffusion phenomena frequently encountered in alloys is pointed out, and the physical limitations to these phenomena are discussed.

3. An interpretation of the behavior of an alloying constituent during scaling has been presented.

4. Large apparent deviations from Fick's law may be expected in systems of more than two components, defined in terms of concentration. It is suggested that the activity gradient rather than the concentration gradient be regarded as the "driving force" in diffusion; for since activity is successfully used instead of concentration in interpreting equilibrium, it should have like merit in interpreting the approach to equilibrium by diffusion.

APPENDIX

The author will be glad to furnish a mimeographed copy of the Appendix on request, or it may be obtained in the form of microfilm or photostat. For the two latter, write to the American Documentation Institute, Science Service Building, 1719 N Street Northwest, Washington, D. C., asking for Document No. 1639 and enclosing 28¢ for microfilm or $1.00 for photostat (6 × 8 inches).

REFERENCES

1. C. S. Smith: *Min. and Met.* (1930) 11, 213; (1932) 13, 481; *Jnl.* Inst. Metals (1931) 46, 49.
2. F. N. Rhines: *Trans.* A.I.M.E. (1940) 137, 246.
3. P. N. Rhines, W. A. Johnson and W. A. Anderson: *Trans.* A.I.M.E. (1942) 147, 205.
4. Scheil and Kiwit: *Archiv Eisenhüttenwesen* (1936) 9, 405.
5. C. E. Ransley: *Jnl.* Inst. Metals (1939) 65, 147.
6. F. N. Rhines and C. H. Mathewson: *Trans.* A.I.M.E. (1934) 111, 337.
7. P. N. Rhines and R. F. Mehl: *Trans.* A.I.M.E. (1938) 128, 185.
8. Heindlhofer and Larsen: *Trans.* Amer. Soc. Steel Treat. (1933) 21, 865.
9. Grube and Jedele: *Ztsch. Elektrochem.* (1932) 38, 799.
10. L. C. Hicks: *Trans.* A.I.M.E. (1934) 113, 163.
11. R. F. Mehl and F. N. Rhines: *Trans.* A.I.M.E. (1940) 137, 301.
12. Bramley and Lord: *Jnl.* Chem. Soc. (1932) 1641.
13. Dünwald and Wagner: *Ztsch. anorg. allg. Chem.* (1931) 199, 321.
14. K. K. Kelley: U. S. Bur. Mines *Bull.* 407 (1937).
15. M. J. Day: Work as yet unpublished.
16. C. Wells and R. F. Mehl: *Trans.* A.I.M.E. (1940) 140, 279.

DISCUSSION

(John Marsh presiding)

R. F. MEHL* AND H. SELTZ,† Pittsburgh, Pa.—This discussion will relate chiefly to the latter part of the paper, in particular to the treatment of Fick's law and the comments concerning the gradients active in diffusion. This is a matter of considerable basic importance and it will be well to inspect any suggestion of change in fundamental concepts with considerable care.

The idea of employing some other expression than concentration in Fick's law is not new.[17] When it was observed that the diffusion coefficient varies with concentration, it became desirable to explain this variation; if this could be done by the use of some term other than concentration, but related to concentration, so that in plotting this term no variation with concentration would longer ensue, progress could have been made. This matter was considered with care when work in diffusion at this institution began some 8 years ago. The thermodynamic quantity activity was considered, but shortly rejected, not only on theoretical but also on factual grounds.

There is no necessary relation between thermodynamic quantities and kinetic or rate phenomena. It can certainly not be assumed that "activity gradients" have any significance in diffusion phenomena. The attempt to merge thermodynamics and kinetics has led to much confusion. The only successful application of thermodynamic activities to kinetic problems has been to reactions in solutions. Here, however, the modern theory assumes that the rate-determining reaction is the decomposition of an intermediate "complex" and that the concentration of this complex is determined by an equilibrium state. The activities thus appear from the usual thermodynamic expression of this equilibrium.

It is difficult to see how activities can be introduced logically into Fick's diffusion equation, since this equation is based on a statistical concept of the process of diffusion. The author

* Professor of Metallurgy, Carnegie Institute of Technology.
† Professor of Physical Chemistry, Carnegie Institute of Technology.

[17] Cf. W. Jost: Diffusion und Chemische Reaktion in Festen Stoffen. Dresden and Leipzig, 1937. Steinkopf.

assumes a hypothetical case of two metals $A + B$, in solid solution, in contact with another solid solution of $A + B + C$, with the concentration of B the same in both alloys but with the activity of B smaller in the latter than the former. Hence, he says, if A and C diffuse with negligible rates, B will diffuse uphill into the $A + B + C$ alloy. Thermodynamically, however, the only requirement is that a homogeneous alloy of uniform composition throughout must ultimately obtain. This, obviously, can be achieved by the diffusion of C, which, even though it has a negligible diffusion coefficient, is exposed to an infinite concentration gradient.

Existing data appear to deny any applicability of activities to diffusion data. The copper-nickel system has been shown to form almost perfect solid solutions over the entire concentration range.[18] The value of D, however, varies about tenfold, a direct contradiction to the activity theory of diffusion. The copper-zinc system, in a concentration range of from $0 \rightarrow 22$ atomic per cent of zinc, shows a fifteen-fold increase in D. While no activity data are available, it is highly improbable that a variation in activity coefficient sufficient to account for this would ever appear. The data on activities in the iron-carbon system are too uncertain in view of the small variation of D with concentration to be of much probative value.

The problem of the factors that control the variation of D with concentration still remains. It would appear that much more information concerning the nature of the solid solution state will be required before real advances can be made.

The application of activities to interface reactions seems to be more confusing than helpful. It is artificial to say that an infinite concentration gradient exists at an interface between two phases of equilibria. In such a case there is no true concentration gradient, for this can occur only in a simple phase. Nor does the rejection of a phase from a solid solution, as in simple precipitation, imply "uphill" diffusion. This matter has been discussed frequently in the last decade. The nucleus of a new phase appears at a region momentarily enriched by concentration fluctuations on an atomic scale.

When the nucleus has appeared, the usual concentration discontinuity as a phase interface is established. Growth of the nucleus proceeds by normal downhill diffusion in the matrix.[19]

L. S. DARKEN (author's reply).—It is indeed true, as stated by Mehl and Seltz, that the attempt to merge thermodynamics and kinetics had led to much confusion. Yet in the simplest terms all cases of nonequilibrium involve a force, a motion, and a resistance to motion. Often the force may be expressed as the gradient of a potential; under appropriate conditions this potential is the chemical potential, in terms of which activity is defined. That chemical potentials are fundamental to the diffusion problem is shown clearly by Jost;[17] the fact that no satisfactory solution of the problem has as yet been obtained is no evidence to the contrary. Stearn and Eyring,[20] who have also pointed out the bearing of the activity coefficient on the diffusivity, derive a relation (Eq. 20 of their paper) giving the diffusivity D as a function of various quantities including the activity coefficient. They write that this correction term involving the activity coefficient "can be added when vapor pressure or electromotive force data are available. For example, in cases where the activity plotted against the concentration shows a maximum or minimum the diffusion rate will drop to zero under the maximum or minimum conditions." Stearn, Irish and Eyring[21] have developed a similar relation (Eq. 29 of their paper) between diffusivity and activity coefficients in liquids. Fig. 2 of their paper shows the observed relation between diffusivity and concentration as compared with that calculated from activity. They comment: "In spite, however, of the incompleteness of the data and the necessary crudeness of handling, the obvious correlations in Fig. 2 between trends of the experimental points and calculated averages of D_1/D_{rel} indicate the general soundness of Eq. 29."

The statement of Mehl and Seltz in regard to the A-B-C alloys that "thermodynamically, however, the only requirement is that a

[18] H. Seltz: Perfect Solid Solutions. Jnl. Amer. Chem. Soc. (1934) 56, 307.

[19] R. F. Mehl and L. K. Jetter: The Mechanism of Precipitation from Solid Solutions. Symposium on Precipitation Hardening. Amer. Soc. Metals (Oct. 1939) 342.
[20] A. E. Stearn and H. Eyring: Jnl. Phys. Chem. (1940) 44, 955.
[21] A. E. Stearn, E. M. Irish and H. Eyring: Jnl. Phys. Chem. (1940) 44, 981.

homogeneous alloy of uniform composition throughout must ultimately obtain" is true only in a limited sense. It is general practice in experimental work to follow rapid reactions, or equilibria that are rapidly attained, while ignoring simultaneous reactions which are so slow as to exert no appreciable effect on the reaction or equilibrium under investigation. For example, the properties of hydrogen-oxygen mixtures at room temperature may be investigated in spite of the fact that the mixture is unstable. A majority of organic compounds are thermodynamically unstable, yet their properties, reactions and equilibria with other substances are quite properly investigated in spite of the fact that in sufficiently long time such compounds might decompose by reactions quite different from those of immediate interest. Likewise, if, in a given alloy, one diffusion process is reasonably rapid and another very slow, it is quite proper to conduct an experiment on a time scale such that the rapid diffusion process may be investigated and the slow one ignored. For example, in measuring the diffusion of water from one solution to another through a semipermeable membrane, the diffusion of the solute (or solutes) through the membrane is commonly ignored; this is entirely justifiable provided the diffusion of the solute is slow enough to be inappreciable in the time of measurement. The thermodynamic requirement that both sides of the membrane must eventually come to the identical composition, though correct, is not a fruitful principle in such cases.

The modified form of Fick's law (Eq. 9) given in the present paper was developed by reasoning similar to that of Jost with the additional hypothesis (similar to that of Eyring) that the mobility (as well as the driving force) is a function of the activity. The author is under no illusions that it is exact; moreover, this equation is applicable only over a limited range of concentration, as is stated clearly in the paper.

The data on copper-nickel alloys, cited by Mehl and Seltz as evidence that diffusivity is not constant in an ideal system, do not by any means prove their point. The claim that these alloys are ideal solutions is based upon Seltz's[18] study of the relation between the liquidus and solidus curves in the phase diagram, which, however, does not demonstrate that both liquid and solid behave as ideal solutions but merely

indicates that any departure from ideal behavior is, very roughly, the same in each. The activity cannot be evaluated from such data alone, unless one phase be a pure component. The statement by Mehl and Seltz that in this system the value of D varies tenfold is also somewhat misleading, in that it implies that D varies with composition over the whole range whereas it is in fact constant within the experimental error over the range 0 to 60 per cent copper.[12] The copper-zinc alloys, for which D is stated to vary fifteenfold, is cited as another example of a system in which the variation of diffusivity cannot be accounted for by a variation of activity. As a matter of fact, the exact opposite is true, since these alloys provide an excellent illustration of a system in which the change in diffusivity is accounted for by the change in activity. Thus, the data on the vapor pressure of zinc in brass have been reviewed and discussed by Johnston,[13] who showed that between 15 and 45 atomic per cent of zinc the activity coefficient changes by a factor of 3.5. A plot of these data indicates that up to 35 atomic per cent zinc the activity may satisfactorily be represented by the form of Eq. 10, with β about 0.06. Inserting this value of β in Eq. 12 it is found that between zero and 20 atomic per cent zinc the diffusivity would be expected to vary by a factor of slightly over 7. This is in good accord with the measured diffusivities of Rhines and Mehl.[7] From Fig. 9 of their paper the diffusivity of copper at 840°C. is about 6×10^{-10} sq. cm. per sec. when the amount of zinc is small, but rises to about 45×10^{-10} sq. cm. per sec. at 20 atomic per cent zinc; the ratio of these two is almost identical with the predicted value of 7. The scatter of the experimental data on the diffusivity prevents comparison at the other two temperatures investigated.

The author does not pretend to have given anything approaching a final answer to the problem of diffusion in metals; in the last section of the paper he merely attempted to point out the bearing of the thermodynamic potential, hence, the activity, on diffusion phenomena, a relation that he feels is well substantiated by the work cited.

[12] R. P. Mehl: Trans. A.I.M.E. (1936) 122, 11.

[13] J. Johnston: Trans. A.I.M.E. (1919) 64, 416.

Weight Change as a Criterion of Extent of Decarburization or Carburization

By R. W. Gurry*

WHEN a steel in the austenitic state, with all its carbon in solution, is maintained, at constant temperature, in contact with a gas that removes the carbon from the surface, yet without otherwise altering the composition of the steel, the change in weight of the specimen, after any period of exposure, is a direct measure of the amount of carbon it has then lost. The purpose of the present paper is to show how, by application of established mathematical reasoning based on the fundamental diffusion law and on certain postulates, this loss of weight yields a complete picture of the distribution of carbon throughout a specimen of regular shape after any period of exposure, with all the accuracy required in any practical occurrence of decarburization. Precisely the same is true for the gain in weight during the reverse process of carburization, or for the gradual gain or loss of any element, so long as the steel comprises only a single phase at temperature, provided always that the experimental conditions conform to the postulates. The change in carbon content from surface to center of the specimen is always continuous, when everything is in solution, even though under the microscope the decarburized zone (or carburized rim) may appear to be sharply defined.

The experimental procedure is described and some typical results are presented, which are then interpreted by application of the diffusion law.

EXPERIMENTAL PROCEDURE

Initially an endeavor was made to follow the gain of weight during the process of carburization in a hydrogen-toluene atmosphere, but it was soon found that the specimen became coated with graphite, which could not be removed without some loss of metal; therefore it was decided to continue carburization until the steel was saturated throughout, to remove all graphite from the surface of the specimen, and then to follow the loss of weight during decarburization in a moist hydrogen atmosphere at the same temperature as that used for carburizing.

The carburizing procedure has been described in an earlier paper;[1] it suffices to state here that the carburization lasted about 140 hr. at 760°C. (1760°F.) and 44 hr. at 1110°C. (2030°F.), these periods being long enough—on the basis of the calculations presented later—to ensure that the specimen was about 99.9 per cent saturated at each temperature. The specimen was a cylinder about 3.8 cm. long and 0.475 cm. in diameter; the materials were carbonyl iron, a commercial low-metalloid iron, and a steel with 3.6 per cent nickel and the usual proportion of other elements.

The fully carburized specimen, after cooling at the top of the furnace tube, was placed in a lathe and sandpapered to remove all graphite; then the diameter was measured with a micrometer caliper, and the initial weighing (corresponding to complete saturation) was made. By means of a

[1] References are at the end of the paper.

molybdenum holder, it was suspended in the furnace, through which was now passed purified hydrogen saturated with water at room temperature. After appropriate intervals it was raised in the furnace and cooled in this atmosphere, then weighed. The temperature was never lower than that used for carburizing, but occasionally was slightly higher. With the specimen there was a similar cylinder, previously completely

rate of carbon loss, but was substantially realized early in the run. All of the 10 runs made on any of the three original materials yielded concordant results at each temperature; two typical series of experimental results. both on the carbonyl iron, are presented in Table 1. They are expressed, for reasons that will appear later, in terms of $w w_1$ against $t a^2$, where w is the loss of weight up to the time t, w_1 the loss of

TABLE 1.—*Observed Values of w/w_1 at Various Values of t (in Seconds), Compared with Values Calculated from a Mean Value of D_m*

(1) $t \times 10^{-3}$, Seconds Observed	(2) $t/10^6 a^2$ Observed	(3) $D_m t/a^2$ Calculated	(4) $w w_1$ from Col. 3, Calculated	(5) $w w_1$ Observed	(6) Difference, Col. 4 − Col. 5	(7) Col. 6 as Per Cent of Col. 5
		Radius of cylinder $a = 0.242$ cm.; $w_1 = 0.0737$ gram; Temperature, 958°C. (1756°F.); $D_m = 2.3 \times 10^{-7}$ sq. cm. per sec.				
3.6	0.0611	0.0141	0.260	0.257	0.003	1.2
9.0	0.153	0.0352	0.388	0.388	0.000	0.0
20.1	0.341	0.0784	0.550	0.541	0.009	1.7
26.4	0.449	0.103	0.613	0.628	−0.015	−2.4
51.0	0.866	0.199	0.779	0.769	0.010	1.3
75.9	1.29	0.297	0.877	0.849	0.028	3.3
133.8	2.27	0.522	0.966	0.933	0.033	3 5
215.5	3.66	0.842	0.995	0.976	0.019	1.9
284.	4.81	1.11	0.999	0.991	0.008	0.8
		Radius $a = 0.240$ cm.; $w_1 = 0.0983$ gram; Temperature, 1113°C. (2035°F.); $D_m = 11.0 \times 10^{-7}$ sq. cm. per sec.				
1.80	0.0312	0.0343	0.385	0.378	0.007	1.9
5.40	0.0935	0.103	0.613	0.607	0.006	1.0
12.6	0.218	0.240	0.827	0.801	0.026	3.2
27.0	0.467	0.514	0.965	0.933	0.032	3.4
50.4	0.872	0.960	0.997	0.986	0.011	1.1
72.0	1.248	1.37	0.999	0.996	0.003	0.3

decarburized, the purpose of which was to make possible correction for loss of weight by vaporization of iron; this correction was small, the rate of loss being about 0.0023 and 0.004 mg. per hour, at 960°C. (1760°F.) and 1110°C. (2030°F.), respectively, for the size of specimen and rate of gas flow used. At 960°C. the rate of flow of moist hydrogen, initially about 450 c.c. per minute, was lessened to about 110 c.c. per minute, toward the end of the run; at 1110°C. the corresponding rates were 810 and 240. The aim of this adjustment of flow was to keep the surface of the steel completely decarburized throughout the run; this may not have been quite achieved at the very start, for this would require a very large

weight after infinite time, and a is the radius of the cylindrical specimen. Thus w_1 corresponds to saturation with carbon at the temperature, and the ratio w/w_1, derived directly from experiment, represents the fractional saturation of the specimen as a whole at the time t, a being of course constant for any given specimen.

Our task now is to derive from this fractional saturation at any instant the corresponding distribution of carbon content from axis to surface of the specimen. This is accomplished by appropriate integration of the fundamental equation that defines D, the diffusion coefficient; though the mathematical analysis is rather complex, the final results are simple and, when brought

together into a table or diagram, are readily applied toward the solution of a variety of practical problems. For the present, we anticipate the results derived later, by pointing out that, since in the case of carbon diffusing in iron D varies with the carbon content,[2] we must use a mean value D_m because at any instant there is a wide range of carbon content within the specimen from axis to surface; and that, with the value of D_m given in Table 1, we are able to reproduce the observed values of w/w_1 with a difference nowhere greater than 3.5 per cent, these differences being tabulated in columns 6 and 7. This degree of accuracy of prediction by use of a single value of D_m—which, moreover, is close to what would be chosen from the data of Wells and Mehl—is ample for practical purposes; and permits us to extend the results to other regular shapes and sizes of specimen, to any time interval, and to any temperature within the stable austenite range.

INTERPRETATION OF EXPERIMENTAL
RESULTS BY APPLICATION OF
DIFFUSION LAW

The fundamental law defining the diffusion coefficient D at any constant temperature is

$$\frac{\partial c}{\partial t} = D \frac{\partial^2 c}{\partial x^2}$$

where $\partial c/\partial x$ is the concentration gradient (in this case, change of carbon content with distance x from the center of the specimen) of the diffusing substance at any point in the sample, and $\partial c/\partial t$ is the rate of change of concentration with time at the same point.

This differential equation can be integrated, and so brought into usable form for direct comparison with experiment, if the following postulates are made:

I. That the initial carbon content (c_o) is uniform throughout the specimen; it need

not correspond to saturation with carbon, though it does in our experimental work.

II. That the carbon concentration at the surface $(x = a)$, is a constant (c_1) from beginning to end of the process of decarburization; this implies that as fast as the carbon reaches the surface by diffusion outward, it is there immediately brought to the concentration c_1 by the atmosphere in contact with the specimen.

III. That D, at any one temperature level, is independent of carbon content c.

The first integration gives the carbon distribution through the sample at any time after the start of the treatment; the second integration of this distribution over all values of x from zero to a, the radius of the cylinder, or half thickness of the plate or slab (large enough in other dimensions so that end effects may be neglected) gives an expression for the total amount of diffusing substance that has passed the surface of the sample at any time. Specifically, the result is a convergent series expressing the ratio w/w_1 (again the fractional saturation* at time t) in terms of the quotient Dt/a^2; evaluation of the expression for the cylinder and for the plate, respectively, yields results, for even values of Dt/a^2, brought together in Table 2.† It will generally be found easier to use a graph of these functions; either a plot of w/w_1 directly against Dt/a^2 (shown in Fig. 1) or, for increased accuracy at low values of w/w_1, against $\sqrt{Dt}/a$. In practice, if a specimen does not conform exactly to either of the shapes

---

* In general, if the specimen was not initially saturated with carbon, w_1 is the weight loss at infinite time when the carbon concentration would have been everywhere brought to the value in equilibrium with the reagent; conversely, in the case of carburizing, w_1 is the gain in weight at infinite time.

† The reader interested in details of the integrations and calculations will find them in a paper by D. H. Andrews and J. Johnston;[3] in one by A. B. Newman,[4] who gives numerous tables and includes the results for the case of a sphere; and in one by B. Serin and R. T. Ellickson.[5]

presented here, approximate calculations can usually be made by appropriate interpretation of the results given for the cylinder and the plate.

TABLE 2.—*Calculated Values of w/w_1 Corresponding to a Series of Values of the Quotient Dt/a^2 for a Long Cylinder of Diameter $2a$, or Infinite Plate or Slab of Thickness $2a$*
w = Change in Weight after Time t; w_1 That after Infinite Time

Dt/a^2	w/w_1	
	Cylinder	Plate
0.005	0.157	0.078
0.01	0.216	0.110
0.02	0.300	0.161
0.03	0.360	0.195
0.05	0.453	0.251
0.1	0.606	0.357
0.15	0.709	0.438
0.2	0.781	0.503
0.3	0.878	0.612
0.4	0.932	0.698
0.6	0.978	0.816
0.8	0.993	0.887
1.2	0.9993	0.958
2.0	1.0000	0.994

In the derivation and calculation of the corresponding pairs of values in Table 2, no assumption was made as to the individual values of t, a, or D (except that D is a constant); consequently the table is valid for any values whatever of these factors, provided always that the measurements are made under conditions such that our three postulates are valid. For a given value of w/w_1 in Table 2, t is inversely proportional to D for a specimen of given size and shape; and for given D, t is proportional to the square of the diameter, or thickness, of the specimen. Consequently the table enables us immediately to draw the curve relating any of the variables by introducing values for the quantities that remain constant; since for any one specimen under consideration at present, D, a, and w_1 are fixed, a curve can be plotted to give directly the relation between w,

as measured, and t. The specimens were cylinders about 10 times as long as their diameter; calculation from the theory shows that these may, for the present purpose, be considered as differing inappreciably from an infinite cylinder. Accordingly, the values for the cylinder, Table 2, would be applicable to these decarburization experiments, provided that the three postulates were valid; we have reason to believe that the first two were, but know, from the work of Wells and Mehl, that D is in fact not constant, but is about twice as great when the iron is saturated as when it is only one tenth saturated with carbon at the temperature.

In line with this it was found, for the cylinder tested at 958°C. (Table 1), by inserting the value of a, assuming several reasonable values of D, and selecting for the resulting Dt/a^2, a corresponding value of w/w_1 from Fig. 1, that no single value of D would yield a curve coinciding throughout the range with the experimental points (Fig. 2) representing these data. For instance, if D is taken as 2.3×10^{-7} sq. cm. per sec., w/w_1 as calculated agrees satisfactorily with that observed for values of w/w_1 from 0 to 0.8; whereas if D is taken as 1.6×10^{-7}, the agreement is good for values of w/w_1 between 1 and 0.9. Accordingly, since we are primarily interested in the early stages of the process, where w/w_1 is less than 0.8, the value 2.3×10^{-7} was chosen for D_m at this temperature 958°C.; the results so calculated are compared with the experimental data in Table 1, also in Fig. 2, where the points representing the observations are seen to be close to the calculated curve. That the divergence between the curve for this value of D_m and the experimental points should become appreciable as w/w_1 exceeds 0.7 is entirely reasonable in view of the curves in Fig. 3 that represent the distribution of carbon throughout the specimen at any time.
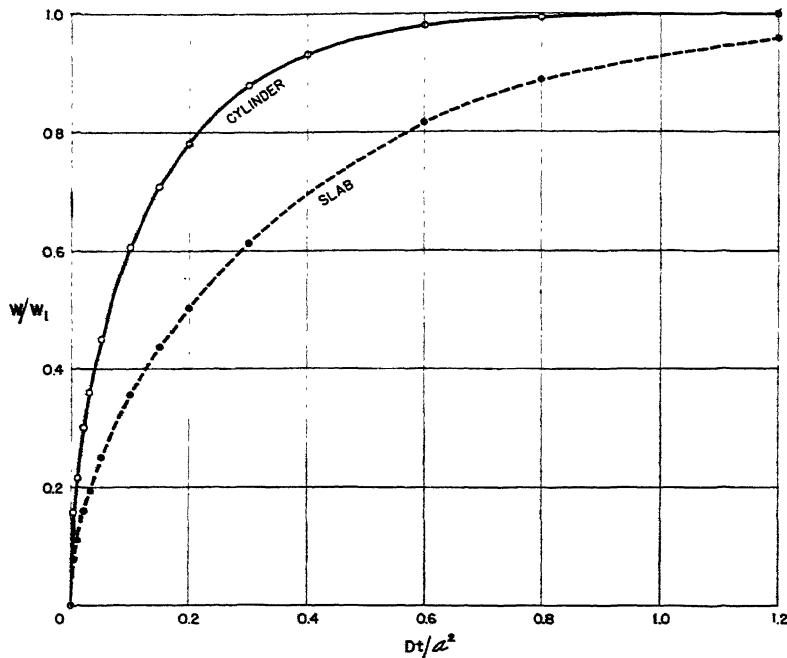
FIG. 1.—RATIO w/w_1 IN TERMS OF QUOTIENT Dt/a^2.
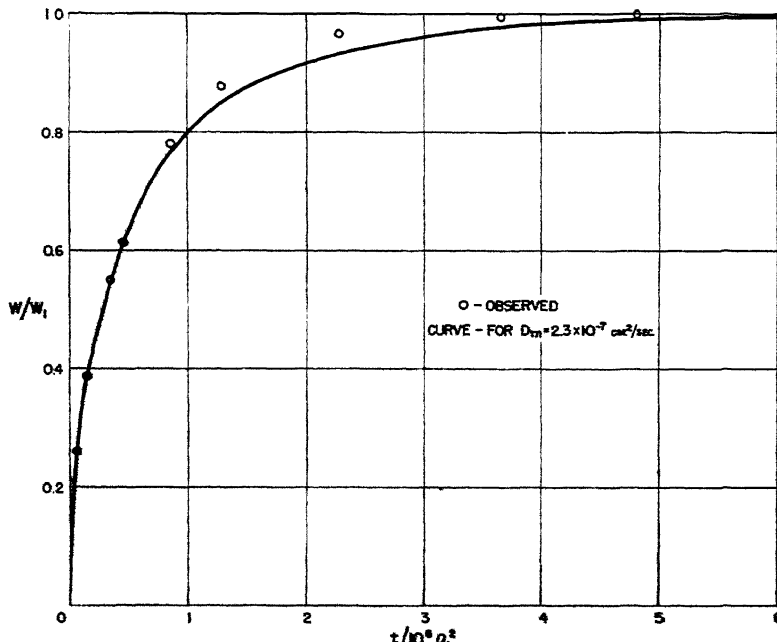
FIG. 2.—COMPARISON OF EXPERIMENTAL POINTS AND CALCULATED CURVE FOR CYLINDER TESTED AT 958°C.

GENERAL CONCLUSIONS

This comparison (Table 1) shows that the whole series of observations, covering a hundredfold range of time, is reproduced within about 3.5 per cent by assuming a single mean value of D. Now it is to be pointed out that, although any portion of the range of data for any one sample could be closely reproduced by choice of a single value of D, in practice usually the interest would be in only a limited portion of the range; namely, the portion referring to a relatively short time interval, no matter whether the interest is in decarburization or in carburization. This circumstance, in conjunction with the fact that in practice the condition of postulate II (and occasionally of postulate I) would be fulfilled only approximately, leads us to believe that a single value of D_m, such as that used in Table 1, describes, accurately enough for all practical purposes, the course of the · curve representing the change of weight of a specimen with the period of exposure, at constant temperature, to a decarburizing agent.

The samples (Table 1), originally of carbonyl iron, give values of D_m of 2.3×10^{-7} and 11.0×10^{-7} at temperatures 958°C. (1756°F.) and 1113°C. (2035°F.), respectively. All samples investigated, including the low-metalloid iron and the nickel steel, gave almost identical results; consequently, these values of D_m are considered to be applicable to any steel containing small amounts of any alloying element, except the steels that readily form an insoluble carbide phase.

It is interesting to see how the value of D_m that best fits the experimental data compares with values of D interpolated from the data of Wells and Mehl. At 958°C., where the carbon concentration (c) ranges from 1.39 per cent (namely, that in equilibrium with graphite)[1] to zero, the best value of D_m corresponds to a carbon content of 0.65 per cent, which is about 47 per cent of the maximum; at 1113°C.,

at which the maximum carbon in solution is 1.90 per cent.[1] D_m corresponds to 0.87 per cent C, again about 47 per cent of the range. This close approach to 50 per cent of the range, which would be the first estimate of the effective mean carbon content throughout the specimen and over the time interval, although perhaps fortuitous, suggests that at any temperature a similar mean value may be used. Since the measurements of Wells and Mehl have shown that (1) the ratio of the values of D pertaining to two specified values of c is substantially independent of the temperature, and (2) for any given concentration a plot of log D against the reciprocal of the absolute temperature T is a straight line, we felt justified in believing that values of D_m, derived on the basis that the plot of log D_m against $1/T$ is linear, would be sufficiently accurate for all practical purposes. Such values are listed in Table 3.

TABLE 3.—*Values of D_m for Use at Various Temperatures*

Deg. F.	Deg. C.	$D_m \times 10^7$
1400	760	0.15
1500	816	0.35
1600	871	0.77
1700	927	1.6
1800	982	3.0
1900	1038	5.4
2000	1093	9.1
2100	1149	15.0

On this basis can be computed, from the data of Tables 2 and 3, what will happen during the process of loss (or gain) of carbon by diffusion through austenite, provided always that all the carbon present is in solution.* By this means, for instance, what will happen to a thick piece may be predicted from observations on a thin piece; or observations over a short time

---

* If in the diffusion process anything is precipitated—or, indeed, if any phase change occurs—the situation is more complex, and the theoretical treatment here does not apply directly; on this type of phenomenon, see a paper by L. S. Darken.[a]

may be utilized to tell how long an interval will be required to achieve any specified level of carbon content (e.g., substantially complete saturation or elimination of carbon—the required interval being far longer than it is commonly assumed to be). It should be mentioned that when w_1 corresponds to saturation, the value of w_1 to be used need not be determined experimentally but can be computed from the solubility with respect to graphite or

and the plate at round values of w/w_1; when expressed in these terms, they are independent of the value of D or of t. In this figure the abscissa is expressed in terms of the ratio x/a, where x is the distance from the center and a the radius of the cylinder or the half thickness of the slab; the ordinate is the quotient $(c - c_o)/(c_1 - c_o)$, where c_o is the initial (uniform) concentration of carbon, c_1 is the constant carbon concentration maintained at this

TABLE 4.—*Carbon Distribution*

w/w_1	Value of x/a							
	0.95	0.9	0.8	0.7	0.6	0.5	0.3	0.0
	VALUES OF $\frac{c - c_o}{c_1 - c_o}$ FOR CYLINDER (ROD) OF RADIUS a							
0.1	0.435	0.097	0.006	0.001	0.000	0.000	0.000	0.000
0.2	0.726	0.475	0.112	0.025	0.010	0.002	0.000	0.000
0.3	0.823	0.653	0.363	0.160	0.059	0.016	0.001	0.000
0.4	0.875	0.755	0.525	0.330	0.185	0.095	0.023	0.003
0.5	0.908	0.821	0.647	0.483	0.342	0.230	0.095	0.035
0.6	0.931	0.864	0.732	0.605	0.483	0.378	0.228	0.140
0.7	0.950	0.901	0.805	0.712	0.619	0.535	0.405	0.320
0.8	0.968	0.937	0.873	0.811	0.750	0.695	0.605	0.541
0.9	0.984	0.968	0.937	0.904	0.874	0.847	0.800	0.767
	FOR SLAB OF HALF THICKNESS a							
0.1	0.703	0.435	0.100	0.020	0.004	0.000	0.000	0.000
0.2	0.842	0.688	0.420	0.223	0.105	0.045	0.007	0.000
0.3	0.890	0.787	0.590	0.420	0.282	0.180	0.063	0.015
0.4	0.918	0.842	0.690	0.550	0.422	0.320	0.177	0.090
0.5	0.935	0.874	0.754	0.640	0.536	0.443	0.305	0.223
0.6	0.950	0.902	0.807	0.718	0.633	0.558	0.447	0.376
0.7	0.963	0.928	0.856	0.788	0.724	0.667	0.582	0.530
0.8	0.976	0.951	0.905	0.860	0.817	0.780	0.720	0.687
0.9	0.987	0.975	0.951	0.929	0.908	0.890	0.861	0.843

carbide, as the case may be, at the temperature.[1]

Moreover, the fortunate circumstance that the assumption of a mean value of D makes it possible to reproduce the experimental data likewise makes possible the computation of the distribution of carbon within the specimen at any value of t or of w/w_1 (which are, of course, not independent variables if D and a are fixed). This is readily done, on the assumption that D is constant, by appropriate substitution in the first integrated form of the fundamental differential equation. The results are presented in Fig. 3 for the rod

surface, and c is the local concentration at the distance x; and the curves are drawn for a series of equidistant values of w/w_1. Although evaluated under the assumption that D is constant, the curves in Fig. 3 have been shown, by the laborious process of numerical integration, to agree closely with the corresponding distribution that prevails in an actual specimen where D varies with carbon concentration. Thus, with the aid of these curves, measured values of the ratio w/w_1 are transformed directly into a measure of the thickness of the "decarburized zone," for any specified limiting carbon content at the
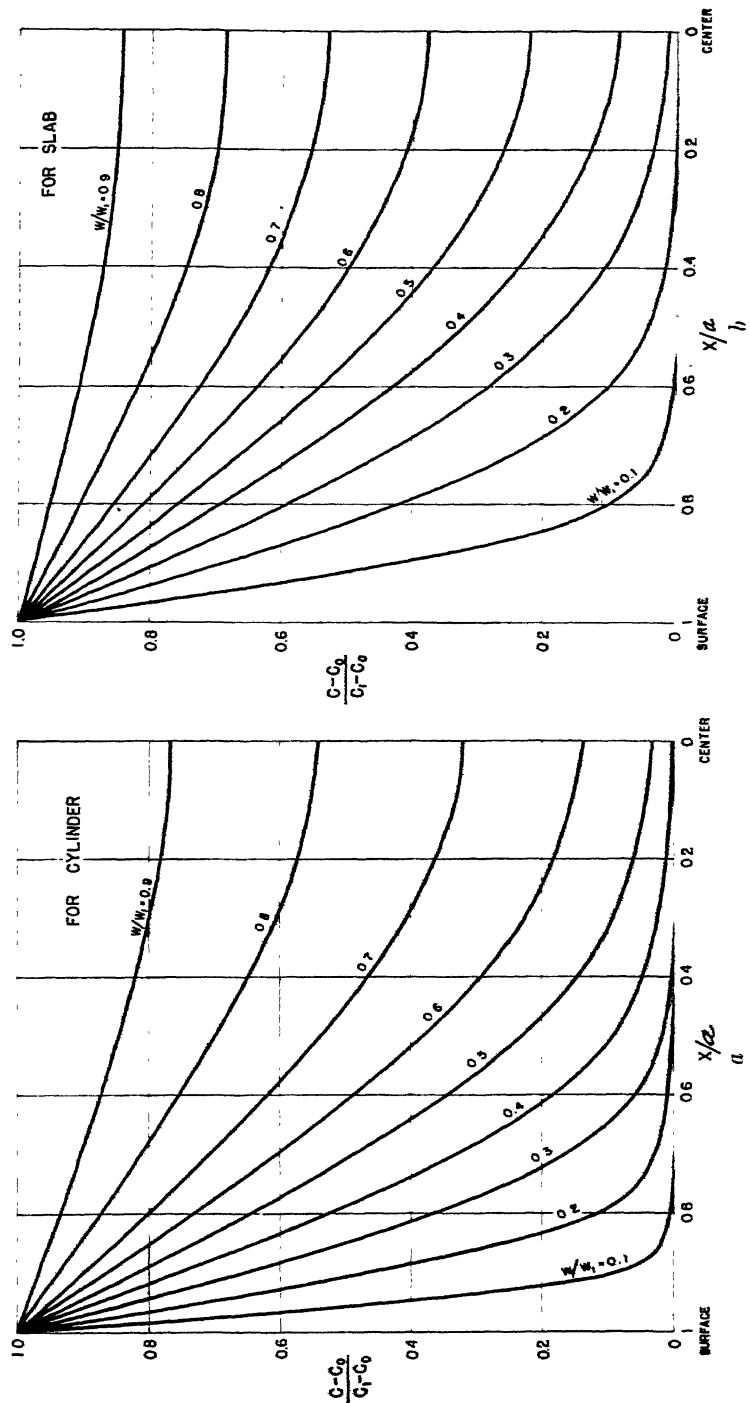
FIG. 3. — CALCULATED DISTRIBUTION OF CARBON THROUGHOUT SPECIMEN.

inner boundary of this zone. Because the scale of Fig. 3 may be too small for certain applications, the numerical data on which the curves are based are given in Table 4.

The general conclusion, therefore, is that the data in the several tables or figures make it possible to describe, with ample accuracy for practical purposes, the progress of any decarburization reaction provided the initial concentration of carbon (c_o) was uniform throughout the piece and the surface concentration (c_1) was constant throughout the period (postulates I and II); and they apply equally to any cylinder or slab at any temperature in the austenitic range.

APPLICATION TO PROCESS OF CARBURIZATION

Although up to this point consideration has been given primarily to the process of decarburization, it has been intimated that the theory presented pertains as well to the reverse process of carburization. Thus, Table 2 and Fig. 1 can be applied directly to calculations of the carburizing process by now considering w to be the weight gain after time t, and w_1 the ultimate weight gain after infinite time. The carbon distribution is calculated from Table 4 under the same definition of terms as before: c_o is the uniform initial concentration, c_1 the constant surface concentration, and c the local concentration at distance x from the center; but ($c - c_o$) and ($c_1 - c_o$) now have positive values, although their ratio, given in the table, is positive in either case.

It is to be borne in mind that, as before, Tables 2 and 4 and Fig. 1 are strictly applicable only when: (1) the initial concentration is uniform, (2) the surface is maintained at constant carbon concentration, and (3) D is independent of carbon concentration. The conditions required by these three postulates are met, or approximated, as in the process of decarburization. Since the data from a few preliminary carburization runs seem to be fitted reason-

ably well by the value of D_m already given, and since this value corresponds, as shown earlier, to about half-saturation with carbon, it is believed that the values of D_m in Table 3 can be applied to carburization as well as to decarburization.

The usefulness of this general method of interpretation of phenomena depending upon diffusion is illustrated by a pair of examples that show how to apply it readily as a means of solving a specific problem.

The first problem is to determine the carbon distribution in a $\frac{1}{2}$-in. plate ($a = 0.635$ cm.), originally of very low carbon content, say zero, after it has been carburized for 3 hr. at 1800°F. First of all, let us calculate the value of Dt/a^2. Converting to the proper units, $t = 10,800$ sec., $a = 0.635$ cm. and, from Table 3, D_m at this temperature is 3.0×10^{-7} sq. cm. per sec.; Dt/a^2, therefore, is 0.0080. Since at such a low value of Dt/a^2 Fig. 1 does not yield a sufficiently precise value of w/w_1, a similar plot of w/w_1 is used against $\sqrt{Dt}/a$, which shows that for the sample in question the fractional saturation w/w_1 is 0.10. Assuming that the carburizing atmosphere maintained the surface at substantial saturation with cementite, at this temperature about 1.56 per cent C,[1] the carbon distribution throughout the sample after 3 hr. at 1800°F. is as shown by the curve for $w/w_1 = 0.1$ in Fig. 3b, where c_o is now zero and $c_1 = 1.56$ per cent. The actual carbon content c at any point from the center ($x = 0$) to the surface ($x = a$) is now apparent; obviously, it is very small when x/a is less than 0.6; that is, at a depth greater than 0.1 in. from the surface.

The second problem is to find the time required at 1700°F. to decarburize a 0.375-in. rod, originally 1.0 per cent carbon, to such an extent that at a distance of 0.015 in. below the surface the carbon concentration will be 0.5 per cent, with a certain commercial gas whose decarburizing power is not known. First, a preliminary test is made to ascertain the decarburizing

power of the gas, under conditions as nearly as possible the same as will be used later for the commercial treatment. Accordingly a weighed piece of the 0.375-in. rod about 2 in. long, that is, long enough so that the end effect will be relatively small, is placed in the gas at 1700°F. After a period of one hour the weight has dropped from 28.4000 grams to 28.3724 grams, or $w = 0.0276$ gram. For this test piece, the value of Dt/a^2 is computed to be 0.00254, since $a = 0.476$ cm., $t = 3600$ sec. and D (from Table 3) is 1.6×10^{-7} sq. cm. per sec.; and a graph of the theoretical w/w_1 against $\sqrt{Dt}/a$ for a cylinder shows that this corresponds to $w/w_1 = 0.110$. Inserting the measured weight loss w, we find that $w_1 = 0.0276/0.110 = 0.251$ gram, corresponding to a loss of $0.251(100)/28.40 = 0.885$ per cent of carbon from the original 1 per cent carbon sample; thus the surface of the test sample was, in effect, maintained by the decarburizing gas at a carbon concentration of $1.00 - 0.885 = 0.115$ per cent. This is an average surface concentration, and it is not implied that this value remained absolutely constant throughout the period; in general, it would be well, whenever possible, to expose the test sample for, roughly, the same length of time as will be used later for the real treatment.

With a knowledge of the carbon concentration that our atmosphere is capable of maintaining on the surface of the specified sample, it is a simple problem to calculate the time required to produce the desired carbon distribution. In this example, $c_o = 1.0$ per cent, $c_1 = 0.115$ per cent, and at the distance 0.015 in. below the surface $c = 0.5$ per cent, corresponding to $(c - c_o)/(c_1 - c_o) = 0.565$; and x/a is $(0.1875 - 0.015)/0.1875 = 0.92$; according to Fig. 3a these conditions correspond to $w/w_1 = 0.2$. Fig. 1 (or, more conveniently, a graph of w/w_1 against $\sqrt{Dt}/a$) indicates that this state will be reached when Dt/a^2 is 0.0085; again inserting values of D and a as before, we find the time of treatment

t to be 12,100 sec., or about 3 hr. 20 minutes.

SUMMARY

Experimental observations of the loss in weight of a steel specimen after various time intervals during a decarburization process at constant temperature, show, when interpreted on the basis of an integrated form of the fundamental diffusion law, that, at any one temperature, in spite of the fact that the diffusion coefficient of carbon in iron varies appreciably with carbon concentration, the absolute weight loss can be predicted within 3.5 per cent by the use of a properly selected mean value of this coefficient. The mean coefficient so derived, values for which are given for a series of temperatures from 1400° to 2100°F., agrees very closely with that interpolated from the measurements of Wells and Mehl for a carbon content corresponding to half-saturation at the temperature.

By the use of this mean coefficient, in conjunction with other data presented in tables and figures, the amount and distribution of carbon that would be present after any time interval can be calculated for a steel cylinder or plate maintained at constant temperature in a constant carburizing or decarburizing atmosphere, provided that certain easily realizable experimental conditions obtain, and that all the carbon in the steel is and remains in solution.

REFERENCES

1. R. W. Gurry: The Solubility of Carbon as Graphite in Gamma Iron. This volume, page 147.
2. C. Wells and R. F. Mehl: Rate of Diffusion of Carbon in Austenite in Plain Carbon, in Nickel and in Manganese Steels. *Trans.* A.I.M.E. (1940) 140, 279.
3. D. H. Andrews and J. Johnston: The Rate of Absorption of Water by Rubber. *Jnl.* Amer. Chem. Soc. (1924) 46, 640.
4. A. B. Newman: The Drying of Porous Solids: Diffusion Calculations. *Trans.* Amer. Inst. Chem. Engrs. (1931) 27, 310.
5. B. Serin and R. T. Ellickson: Determination of Diffusion Coefficients. *Jnl.* Chem. Physics (1941) 9, 742.
6. L. S. Darken: Diffusion in Metal Accompanied by Phase Change. This volume, page 157.

DISCUSSION

(A. B. Greninger presiding)

C. WELLS* AND R. F. MEHL,* Pittsburgh, Pa.—The object of the present discussion is primarily to evaluate the usefulness of the

during carburization to reach a constant value of carbon concentration than for surfaces covered with graphite.

Some time ago Mehl and Wells calculated concentration-penetration curves, taking into account the variation of D with carbon con-
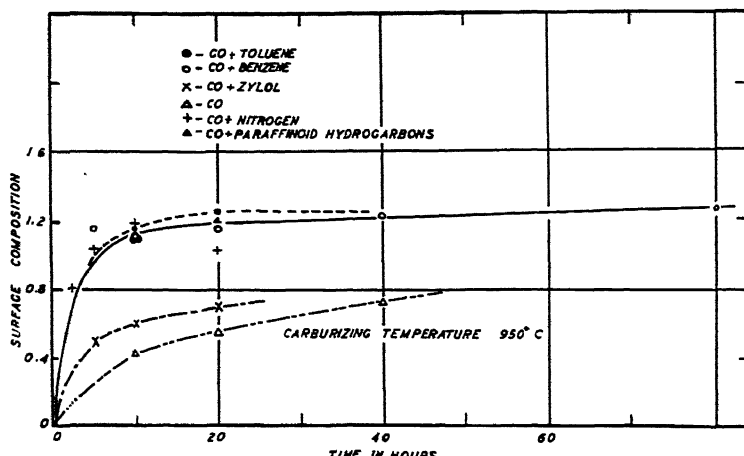
FIG. 4.—RELATION BETWEEN SURFACE COMPOSITION AND TIME WHEN CARBURIZING IS DONE IN VARIOUS HYDROCARBONS.

A graphite layer was observed on specimen surfaces carburized in CO + toluene, CO + benzene, and CO + nitrogen. Data were taken from papers by Bramley and by co-authors. Normal commercial carburizing times usually are between three and eight hours.

results obtained by the author as applied to commercial carburizing practices.

It has long been recognized that if the three postulates given by the author were correct it would be possible to calculate accurately from the method he used not only variations of compositions in carburized cases and variations of thicknesses of cases with temperature and time, but also average D values as was practiced by Dunn.[7] Unfortunately, however, at least two of the postulates are incorrect, for actually the carbon concentration at the surface is *not* a constant from the beginning to the end of either the decarburization or carburization process, and D is *not* independent of carbon concentration. A plot of surface composition against time of carburizing as observed by Bramley and co-authors† is shown in Fig. 4. The figure shows that it took longer for specimen surfaces not covered with graphite

* Carnegie Institute of Technology.
[7] Dunn: *Jnl.* Chem. Soc. (1926) **129,** 2973.
† References to series of papers by Bramley and co-authors are given in paper by Wells and Mehl: *Trans.* A.I.M.E. (1940) **140,** 305.

centration (not done by the author), and assuming that the surface concentration remains constant during carburization. Comparisons between the calculated curves of Mehl and Wells and the experimentally determined curves of Bramley and co-authors showed the agreement to be poor when short times of carburization were considered and good when long times were considered, which simply means that if the total time of carburization is sufficiently long the surface concentration can be assumed constant without causing an appreciable error in the results obtained, but if the time of carburization is short the assumption is unwarranted. Commercially carburizing times are usually relatively short (3 to 8 hr. at about 1700°F.), except in the carburizing of armor plate, when the times may extend to two or three weeks, and it is believed that curves calculated on Gurry's assumptions will in general not agree with those determined experimentally when relating to carburizing times covering the range used in general commercial carburizing practices. It was the failure to get

good agreement between calculated concentration-depth curves and experimentally determined curves obtained under conditions normally used in industry that convinced Mehl and Wells that predictions of the distribution of carbon in carburized steels at given times and temperatures cannot be made accurately until the solution of Fick's law of diffusion includes conditions that allow for: (1) the change of surface composition with time and (2) the change of D with concentration. The relation between D and concentration is already known, but the relation between surface composition and time of carburization has not yet been worked out in terms of the factors controlling it.

Commercially there are other factors that make it difficult to calculate accurately concentration-penetration curves directly applicable to general carburizing practice, for not only does the surface composition tend to increase with carburizing time but it may be varied from time to time during carburizing, by the practice of changing the atmosphere periodically to eliminate soot deposited on articles being carburized. Again, in pack carburizing the time of bringing the charge to temperature may be long compared with the time at the carburizing temperature, in which case temperature variation must be considered as a factor in determining carbon variation and case thickness. Furthermore, the effect of alloying elements present in many carburizing steels no doubt have an appreciable effect on the surface composition, and therefore on effective carburizing.

For the present, it is doubtful whether one can do better than accept the curves available showing composition variations and case depths in carburizing steels when packed-carburized [A.S.M. Handbook (1939) 1038–1039, Figs. 1 and 2] or gas-carburized [A.S.M. Handbook (1939) 1041, Fig. 5] at various carburizing temperatures and times. Such data give sufficient information to estimate closely enough for all practical purposes about what depths of case and what composition variations to expect under the carburizing conditions usually present in commercial practice.

R. W. GURRY (author's reply).—The stated object of the discussion by Wells and Mehl is "to evaluate the usefulness of the results ob-

tained by the author as applied to commercial carburizing practice." This is a question in which the author is likewise greatly interested, since the practical limits to the use of his method have not as yet been established, but it must be pointed out that the only acceptable ground for evaluation is direct test and that the matter can hardly be regarded as settled on the basis of the arguments advanced by Wells and Mehl, which in essence reduce to mere opinion.

It is true, as Wells and Mehl have stated, that when the change in average carbon content is large, which commonly means that the period of carburization or decarburization is long, the results obtained by this method are relatively insensitive to a departure from the fundamental postulates, but that they become more sensitive as the period of exposure decreases. A difference of opinion, therefore, arises as to the effective validity of postulate II for a relatively short period of treatment.

In this connection, the data of Bramley and his colleagues cited by Wells and Mehl deserve some comment. It is evident from the work of Bramley and Lawton[3] that in the series of investigations cited the rate of gas flow was in general so slow that for a considerable period after the start of a test the surface concentration of carbon was not uniform but decreased along the length of the specimen with increasing distance from the gas inlet. It is not surprising, therefore, that the surface layer did not reach its maximum concentration of carbon until the sample had been exposed to the gas for many hours, and in such circumstances the author's method admittedly might not be satisfactory.

On the other hand, there are many applications in which conditions are much more favorable. For example, in the preliminary work of the present investigation a comparison of the amount of carbon absorbed in half an hour with the result of a numerical integration indicated that under the conditions of test the surface must have become substantially saturated with carbon within a few minutes. Moreover, the commonly observed formation of iron carbide on the surface of a specimen that has been carburized for a relatively short time

[3] Bramley and Lawton: Iron and Steel Inst., *Carnegie Schol. Mem.* (1927) 16, 35.

indicates that carbon is being supplied to the surface faster than it can diffuse into the metal.

A suitable atmosphere during decarburization likewise results in the removal of carbon at such a rate that the surface concentration is in effect rapidly reduced to zero, a typical example of such an atmosphere being moist hydrogen.[9] In the present work, calculations based on data obtained after an exposure of $\frac{1}{2}$ hr. indicated that the surface was almost completely decarburized within a few minutes.

In view of these observations, it is evident that it is difficult, if not impossible, to decide *a priori* whether the method is or is not appli-

[9] Bramley and Allen: *Engineering* (Jan. 22, 1929); (Feb. 19, March 11, 1932).

cable. The only trustworthy basis for judgment is direct test. The author does not claim that his method will work in every case but the evidence available indicates that it is applicable in enough cases to warrant its consideration.

In the matter of the variation of D with carbon content, it is only necessary to repeat that direct test has shown that the use of a mean coefficient enables the representation of the observations over the whole range from saturation to complete decarburization with an accuracy of 3.5 per cent, which is deemed ample for many purposes. Should much greater accuracy be required, resort must be had to some more complex method.

Rate of Nucleation and Rate of Growth of Pearlite

By Frederick C. Hull,* Robert A. Colton,† and Robert F. Mehl,‡ Member A.I.M.E.

It is known that pearlite forms from austenite by a process of nucleation and growth, and that the rate of formation of pearlite may be described by a rate of nucleation and a rate of growth.[1,2] The manner in which these two quantities operate to produce the observed isothermal reaction curve has been analyzed in a paper published in 1939.[3] Two types of process were described: (1) that in which nucleation occurs at the grain boundaries of the parent phase, with the nodules growing toward the centers of the grains, initially as hemispheres and then after impingement as roughly radial-columnar structures; and (2) that in which nucleation occurs generally, with the nodules growing to full spheres until impingement with other growing nodules restricts growth. Both cases are met in the formation of pearlite from austenite (Fig. 1);[2,4] the former, occurring near the knee of the S-curve, has been named "grain-boundary transformation," and the latter, occurring at temperatures near Ae₁, has been named "group-nodule transformation."

In developing our knowledge of the factors that determine the rate of formation

of pearlite from austenite, it is important[1,2] to obtain data on the rate of nucleation and the rate of growth of pearlite. Such data, when obtained near the knee of the S-curve, will furnish information of use in understanding the factors that affect hardenability; when obtained at higher temperatures, such data will be useful in understanding the behavior of steels that during heat-treatment react to pearlite.[2]

It is the purpose of this paper to present data on the rate of nucleation and the rate of growth of pearlite in dependence upon composition, grain size, temperature, and the degree of homogeneity of the parent austenite. The studies are restricted chiefly to plain carbon commercial steels.*

PREVIOUS DATA ON RATE OF NUCLEATION AND RATE OF GROWTH

Data on the rate of nucleation and the rate of growth of pearlite have been published by Scheil and Lange-Weise,[5] by Mirkin and Blanter,[6,7] by Mehl,[1] and by Dorn, De Garmo and Flanigan.[2] It is difficult to interpret the data, for in most cases too little information is given on austenitizing temperatures and times, the state of homogeneity of the austenite (presence or absence of carbide, etc.), austenite grain size, and mode of formation of pearlite at the temperatures given. Except for the approximations of Mehl and the work of Dorn, austenite grain size was disregarded, though it is well known

Fig. 1.—Modes of transformation of austenite to pearlite. × 100.

a and c illustrate grain-boundary transformation; b and d show group-nodule transformation. a and b are photomicrographs of steel A. Pretreated by holding ½ hr. at 875°C. and oil-quenching. Austenitized ½ hr. at 875°C., grain size No. 5. Gradient quenched and partially transformed 480 sec. at 690°C., respectively. c and d are photomicrographs of steel B. Annealed 1 hr. at 950°C.; austenitized ½ hr. at 875°C., grain size No. 4¼; reacted 5 sec. at 600°C. and 540 sec. at 680°C., respectively.

that grain size affects the rate of reaction and therefore presumably the rate of nucleation.

RATE OF REACTION AS DETERMINED BY RATE OF NUCLEATION AND RATE OF GROWTH

The reaction equations employed herein are those published earlier.[3] We shall consider, first, general nucleation as it may be applied to reaction near Ae_1 and, second, grain-boundary nucleation as it may be applied to reaction near the knee. Although nucleation near Ae_1 occurs at the grain boundary, the nodule grows so much larger than the austenite grain (Fig. 1) that the process operates with respect to impingement as though nucleation were wholly general and it may therefore properly be treated as one of general nucleation.[4,5]

General Nucleation (Group-nodule Transformation)

The rate of nucleation is taken as the number of nuclei forming per unit time per unit volume of unreacted matrix. This is designated as N_v, expressed in number of nuclei per cu. mm. per sec. The rate of growth is taken as the rate at which the nodule radius increases with time. It is designated as G, expressed in millimeters per second. N_v and G may remain constant as the reaction proceeds, or may vary; analytical methods are available for calculating the rate of reaction in either case.[3]

Assuming that N_v and G remain constant during the reaction, assuming also that nucleation is random without regard for matrix structure (vide supra) and that the reaction product forms true spheres up to the moment of impingement upon other growing nodules, we may write

$$f(t) = 1 - e^{-\frac{\pi}{3} N_v G^4 t^4} \quad [1]$$

where $f(t)$ is the fraction transformed as a

function of time t. The shape of this curve when plotted on a logarithmic time scale is given in Fig. 2.
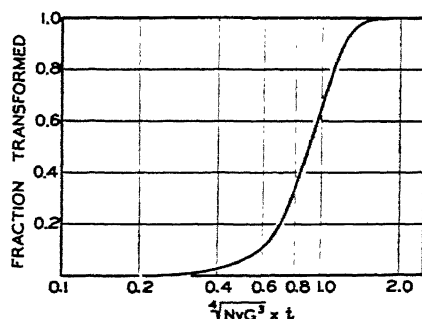
FIG. 2.—MASTER REACTION CURVE FOR GENERAL NUCLEATION.

If N_v varies with time (it will be seen that it does), we may write

$$N_v(t) = N_0(1 + \alpha t + \beta t^2 + \gamma t^3) \quad [2]$$

and the corresponding reaction equation may be written

$$f(t) = 1 - exp.$$
$$\left\{ -\pi N_0 G^3 \left(\frac{t^4}{3} + \frac{\alpha t^5}{15} + \frac{\beta t^6}{45} + \frac{\gamma t^7}{105} \right) \right\} \quad [3]$$

It has proved convenient to consider the rate of nucleation as constant with time even though it is known to vary, and we have relied therefore mainly on Eq. 1. Departures from an ideal state of homogeneity in austenite provide centers of easy nucleation within the grain, distributed at random; this leads to true general nucleation. Such a condition is afforded by the presence of deoxidation products, and by undissolved carbide and undissipated carbon concentration gradients.[2,4]

The application of Eq. 1 to group-nodule transformation involves the use of the quantity N_v. It is known, however,[2,4] that group nodules are nucleated at grain boundaries. The equation may properly be applied, but it will be found that N_v varies with austenite grain size. The rate of nucleation per unit grain-boundary area may

be derived, however, simply by dividing N_r by the grain-boundary area per unit volume, and this will be designated as N_s, expressed in number of nuclei per square millimeter per second.

Grain-boundary Nucleation (Grain-boundary Transformation)

For transformation near the knee of the S-curve, assuming that nuclei form at grain boundaries, that nodules grow only into the grain in which the nucleus appeared, forming hemispheres of which the shape is modified by impingement upon other nodules originating in the same way in the same grain,[3] and that N_s and G remain constant with time, we may derive a series of master curves, for the isothermal reaction in which the fraction transformed (ordinate) is plotted against a function of time (abscissa) and in which the several curves represent different values of the "shape factor,"

$$\lambda = \frac{a^3 N_s^*}{G}$$

The variables are thus N_s, G and the grain size a, defined as the grain radius in millimeters. Variations in these quantities affect both the rate of reaction and the shape of the isothermal reaction curve.[3]

CALCULATION OF RATE OF NUCLEATION AND RATE OF GROWTH FROM EXPERIMENTAL DATA

Rate of Growth

The rate of growth is determined simply by measuring the radius of the largest nodule found in each of a series of samples reacted for increasing time periods. Plotting this radius as a function of time provides a curve of which the slope is the rate of growth G[5] (Fig. 3). The accuracy of the method depends upon inspecting samples

of sufficient size, with a sufficiently large number of nodules, so that the nodule upon which the measurement is made—the largest nodule visible—may be taken as that which had formed at the first instant of reaction and had thus grown farthest; it depends also upon inspecting a sufficient number of nodules so that one among the nodules that had formed in the first instant of reaction will have been cut by the surface at its maximum diameter. Apart from exercising care in the extent of the inspection of the sample, the closeness with which the plotted points will fall to a single curve will offer assurance of the adequacy of the measurement. The fact that the curve is always a straight line simplifies the latter test.

The curve does not always intersect the origin, as it should if the reaction began at the moment of attainment of the reaction temperatures and if the first stages of growth were equally as rapid as the latter. The curves presented here intersect the time axis close to the origin; the significance of the time intercept is not certain. It will be observed later that the rate of nucleation at the beginning of the reaction is very low; this circumstance will decrease the chance of finding a nodule that had formed at the first instant and had been cut along its major axis. It appears best to draw a curve through the plotted radii regardless of whether the curve passes through the origin or has a time-axis intercept.

In steel H, containing 1.1 per cent C, the grain-boundary mode of transformation was observed at all temperatures; the rate of growth of pearlite was calculated from the radial rate of growth of the hemispherical nodules. Steels E, F and G, which are slightly hypereutectoid, exhibited incompletely formed networks of cementite around the austenite grains upon reaction at high temperatures; group nodules were formed and G was determined in the usual manner. In hypoeutectoid steel I the ferrite network was continuous and quasi-group

---

* See full discussion in ref. 3 of the necessity for and usefulness of this type of plot.

nodules were formed;[4] G was taken as the radial rate of growth of such nodules. The actual rate of growth of pearlite must be somewhat greater owing to a time lag in the nucleation of pearlite in adjacent

Rate of Nucleation—Group-nodule Transformation

Method 1.—The method by which Scheil and Lange-Weise[5] determine the rate of
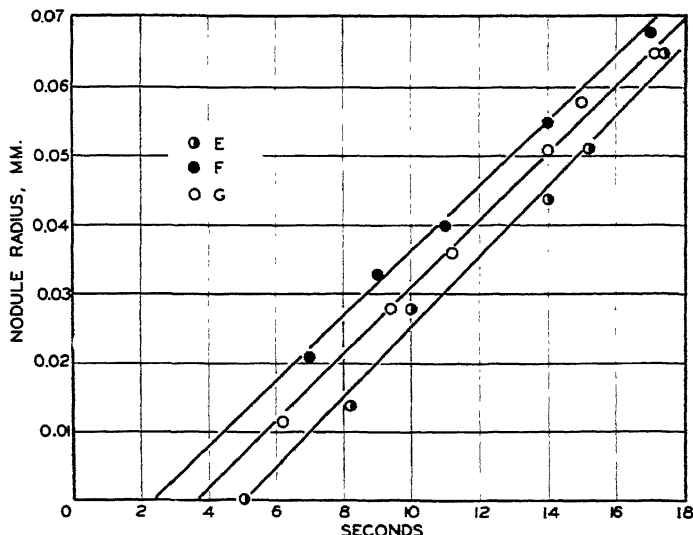
FIG. 3.—MAXIMUM NODULE RADIUS VERSUS TIME IN FORMATION OF PEARLITE IN STEELS E, F, AND G AT 680°C.
Austenitized 1½ hr. at 1100°C. and transformed at 680°C.
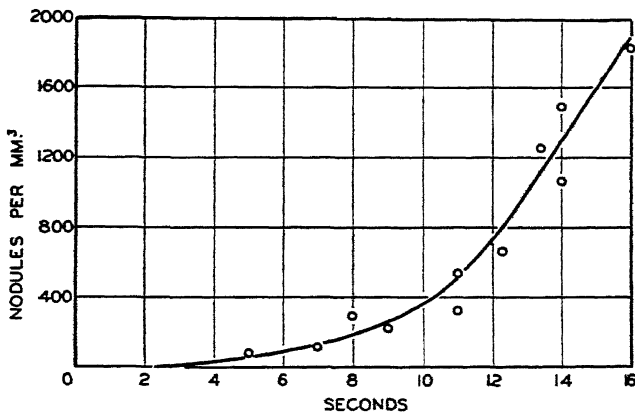
FIG. 4.—NUMBER OF NODULES PER CUBIC MILLIMETER OF VOLUME VERSUS TIME AT 680°C.
Steel F pretreated 1 hr. at 875°C., oil-quenched; austenitized 1½ hr. at 1100°C.; A.S.T.M. grain size No. 4¼.

"pockets" of austenite. Reaction at low temperatures suppressed the proeutectoid constituents.

nucleation is, in brief, as follows: For each of a series of partially reacted samples there is determined (a) an experimental

plane distribution curve of nodule radii, (b) a calculated spatial distribution curve, (c) the total number of nodules per unit volume, and (d) the percentage of trans-

as to the constancy of G versus time or its uniformity from nodule to nodule.

Method 2.—All the available experimental evidence indicates that the rate of
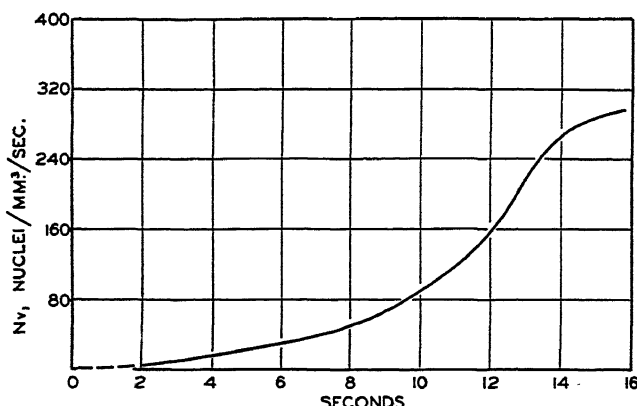
FIG. 5.—RATE OF NUCLEATION OF PEARLITE IN STEEL F VERSUS TIME AT 680°C.

$N_r(t)$ expressed as number of nuclei per cubic millimeter of untransformed austenite per second; calculated from Fig. 4, as described in text; approximately 20 per cent transformation in 16 seconds.

formation. A plot of the number of nodules per unit volume versus reaction time (Fig. 4) is then made and $N_r(t)$* is calculated by dividing the slope of this curve at any time by $u(t)$, the corresponding fraction of the austenite not transformed† (Fig. 5).

$N_r(t)$ can be determined in this way only for the beginning of the reaction. Beyond about 20 per cent transformation, the method loses precision owing to the difficulty of counting the number of nodules after impingement becomes serious, and owing also to errors in applying the theoretical plane distribution curve to the odd shapes that result when nodules grow together.

This method is very time-consuming and was used in only one instance for the determination of $N_r(t)$. It possesses the advantage that no assumption is necessary

growth of pearlite is a constant for a given reaction temperature. This fact fortunately simplifies the derivation of $N_r(t)$, for the necessary data may be obtained from a single partially reacted sample and the reaction curve. Except for Fig. 5, all variations in the rate of nucleation with time were derived by this method.

The plane distribution curve is found experimentally as before, and the spatial distribution curve of nodule radii is calculated by the methods outlined by Scheil.[9] The spatial distribution function, $\phi(R)$, is defined in such a way that $\phi(R)\Delta R$ is the number of nodules per cu. mm. of the sample of radius R to $R + \Delta R$. It has been assumed that the theoretical plane distribution curve for Scheil's statistical grain shape furnishes a closer approximation to the curve for a pearlite nodule than would the curve for a sphere.

The number of nuclei formed per cu. mm. of the *sample* (not of the untransformed austenite) from the time t to $t + \Delta t$ equals $N_r(t)u(t)\Delta t$. At the time the reaction is

---

* The rate of nucleation as a function of time at constant temperature, expressed as number of nuclei per cu. mm. of untransformed austenite per second.

† Scheil and Lange-Weise based their rate of nucleation on a unit volume of the sample and did not need to correct for transformation.

interrupted, t_E, these nodules will have attained a radius

$$R = (t_E - t)G \qquad [4]$$

lack of homogeneity of the steel from one specimen to another than to errors in the method of calculation.
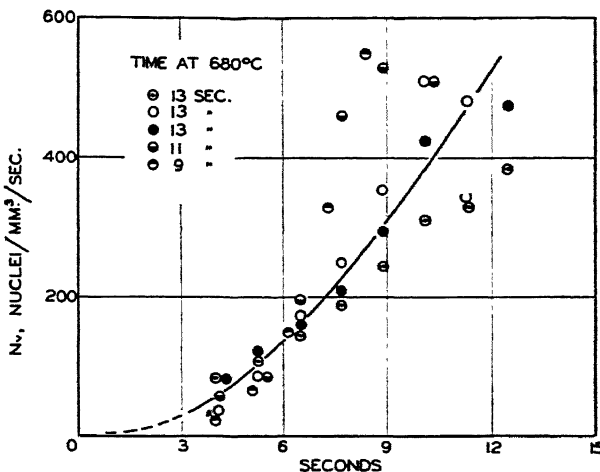
FIG. 6.—DUPLICATE DETERMINATIONS OF N_v AS A FUNCTION OF REACTION TIME AT 680°C. BY METHOD 2.
Steel G held 1 hr. at 875°C. and oil-quenched; austenitized $\frac{1}{2}$ hr. at 1100°C.; A.S.T.M. grain size No. $3\frac{1}{2}$.

By definition,

$$N_v(t)u(t)\Delta t = \phi(R)\Delta R$$

and since

$$\Delta R = G\Delta t$$

$$N_v(t) = \frac{\phi(R) \cdot G}{u(t)} \qquad [5]$$

where the corresponding values of t and R are given by Eq. 4. As soon as impingement becomes serious, this method, like method 1, becomes ineffective, for the reasons cited above.

The results of several duplicate determinations of $N_v(t)$ by method 2 are plotted in Fig. 6.* The data from which the plane and spatial distribution curves were calculated are listed in Table 1. The scatter of the points may be attributed more to a

* The time axis intercept of the nodule radius versus time curve introduces a degree of uncertainty into the $N_v(t)$ calculations. We have chosen to assume that all nuclei formed after this time (3.5 sec. for Fig. 6), and, therefore, N_v is shown as a dotted line during the incubation period.

Method 3.—It is very laborious and for purposes of comparison not necessary to determine the variation of N_v with time. If N_v is assumed constant, and reaction proceeds by the group-nodule mode of transformation so that Eq. 1 applies, N_v can be calculated from a knowledge of G and the time for 50 per cent transformation, employing the relation

$$\sqrt[4]{N_v G^3} \cdot t_{0.5} = 0.9 \qquad [6]$$

The values of N_v appearing in the tables were calculated by this method.

Grain-boundary Transformation

Method 4.—Measurement of N_v from a count of nodules on the surface of polish is not now possible, for this would require a knowledge of the theoretical plane distribution curve for hemispherical nodules, which is not available. It is possible that approximations of this distribution might be made, yielding values reasonably close to the real values, but since this type of

FIG. 7.—FOR DESCRIPTIVE LEGEND SEE OPPOSITE PAGE.

(d)

(e)
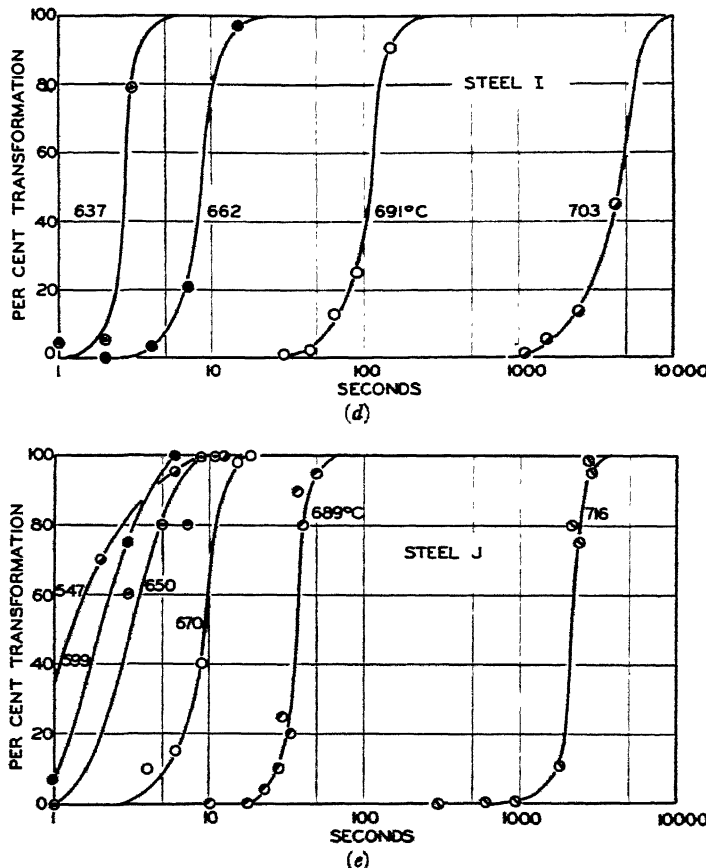
FIG. 7.—ISOTHERMAL REACTION CURVES FOR STEELS A, B, H, I AND J.
Table 3 contains all data relative to pretreatment, austenitizing times and temperatures, and grain sizes.

transformation obtains near the knee of the S-curve where the rate of reaction is very rapid, it would be difficult to obtain a series of samples with precisely measured times of reaction. No attempt has been made to develop or apply such a method.*

Method 5.—The isothermal reaction curve is procured, the rate of growth determined directly, and the grain size is determined. The isothermal reaction curve is

fitted to one of the family of master curves for this type of reaction, and the value of N, computed.[3] Since this method relies upon an accurate reaction curve, difficult to obtain near the knee of the S-curve in plain carbon steels, it is not generally useful, though probably it could be used on alloy steels.

Method 6.—Since experimental difficulties were too great to permit a satisfactory determination of N, near the knee of the S-curve, a more approximate method was used. The nodules are assumed to be spherical and the nucleation to be general in type; i.e., the case is assumed identical

* Dorn, De Garmo and Flanigan[22] have derived a method by which N, can be calculated for grain-boundary transformation. It has been successfully applied to a steel containing 0.92 per cent C, 1.53 per cent Mn, 0.20 per cent Si, and 0.26 per cent Mo.

with group-nodule transformation, and method 3 applied. Obviously, the method cannot yield true N_s values, but those

TABLE 1.—*Duplicate Determinations of $N_r(t)$ at 680°C. for Steel G.*
PLANE DISTRIBUTION CURVES OF NODULE RADII[a]

Radius in Divisions (1 division = 0.00667 mm.)	Number of Nodules in Marked Area				
	13 Sec. at 680	13	13	11	9
0–1	30	52	34	47	38
1–2	41	62	44	64	33
2–3	42	63	47	52	17
3–4	31	42	38	25	8
4–5	26	33	28	12	3
5–6	21	21	21	6	
6–7	12	10	14		
7–8	7	4	7		
Marked area, sq. mm...	2.14	2.29	2.02	2.71	3.23

[a] Data from which Fig. 6 was calculated.

calculated should serve for purposes of comparison.

The temperature at which the transition from group-nodule to grain-boundary transformation occurs is the same as that at which the application of method 3 begins

mercial wirebar steels, deoxidized with silicon. These are the steels used by M. Gensamer for the study of the mechanical properties of controlled microstructures.[10,11] They have been used also for a study of pearlite spacing by G. E. Pellissier, M. F. Hawkes, W. A. Johnson, and R. F. Mehl.[12] Photomicrographs illustrating the modes of pearlite formation in steel B at different temperatures have been published.[4] Steels C and D are steels made from a single heat, one part deoxidized with aluminum (D), furnishing a "fine-grained steel" and one part not treated with aluminum (C), furnishing a "coarse-grained" steel.[13] Steels E, F, G and H are carbon tool steels, made with differences in deoxidation treatment. These steels were partially deoxidized in the furnace, and all had aluminum additions in the ladle. Steel I is a silicon-killed forging-grade steel;* J is a high-purity steel, prepared by the method described earlier.[14]

Isothermal Transformation Technique

The technique employed is that described by Davenport and Bain.[15,16] For high reac-

TABLE 2.—*Steel Compositions*

Steel	Composition, Per Cent						
	C	Si	Mn	P	S	Cr	Ni
A	0.78	0.18	0.63	0.014	0.030		
B	0.80	0.24	0.74	0.019	0.029	0.01	0.11
C	0.79	0.21	0.62				
D	0.78	0.23	0.63				
E	1.02	0.13	0.19	0.013	0.010	0.03	0.03
F	1.01	0.16	0.15	0.011	0.011	0.05	0.03
G	1.02	0.31	0.26	0.014	0.012	0.06	0.02
H	1.10	0.24	0.26	0.014	0.011	0.04	0.02
I	0.57	0.10	0.46	0.025	0.03		
J	0.93	0.002	<0.004	<0.005	0.0001	<0.0005	0.006

to yield N_s data of no physical significance. This transition zone corresponds to a value of the shape factor $\lambda = \dfrac{a^3 N_s}{G}$, equal to 0.1.[4]

EXPERIMENTAL METHODS

Materials

The composition of the steels used are listed in Table 2. Steels A and B are com-

tion temperatures, in the neighborhood of 690° or 700°C., where there is no danger from recalescence, pieces up to $\frac{5}{16}$ in. square were used. At lower temperatures, especially near the knee of the S-curve, where the possibility of appreciable recalescence must be carefully considered, all

* Ferromanganese added in furnace, ferrosilicon added in ladle, no mold addition.

TABLE 3.—*Rate Data on Steels* A, B, F, H, I, J

STEEL A

As-received material (hot-rolled). Austenitized ½ hr. at 875°C.; A.S.T.M. grain size No. 5¼. Grain-boundary area = 42 sq. mm. per cu. mm.

Temperature of Reaction, Deg. C.	Time of 50 Per Cent Reaction, $t_{0.5}$ Sec.	Rate of Growth, Mm. per Sec., G	Rate of Nucleation per Cu. Mm. of Volume, N_v	Rate of Nucleation per Sq. Mm. of Grain-boundary Area, N_s
700	2,500	0.3×10^{-3}	6.2×10^{-4}	1.5×10^{-5}
690	400	0.85×10^{-3}	5.9×10^{-2}	1.4×10^{-3}
680	105	1.7×10^{-3}	1.1	2.6×10^{-2}
660	32	3.8×10^{-3}	11.9	0.28
640	16	6.2×10^{-3}	46.5	1.1
620	11	8.0×10^{-3}	106.0	2.5
600	7.0	9.0×10^{-3}	294	7.0
560	5.4	8.5×10^{-3}	$1,130$	27
520	5.0	7.0×10^{-3}	$1,700$	40
500	5.0	5.4×10^{-3}	$6,630$	160

STEEL B

Pretreatment: Annealed one hour at 950°C. and cooled at 4° per min. Austenitized ½ hr. at 875°C. A.S.T.M. grain size No. 4¼. Grain-boundary area, 29 sq. mm. per cu. mm.

710		0.003×10^{-3}		
700	6,000	0.10×10^{-3}	0.51×10^{-3}	0.017×10^{-3}
689	1,000	0.40×10^{-3}	10.2×10^{-3}	0.35×10^{-3}
680	320	1.0×10^{-3}	6.2×10^{-2}	2.2×10^{-3}
670	110	1.7×10^{-3}	0.91	0.031
660	47	2.8×10^{-3}	4.8	0.136
650	25	3.6×10^{-3}	36	1.24
629	10	6.1×10^{-3}	274	9.4
600	5	7.9×10^{-3}	$2,130$	73.5

STEEL F

Pretreatment: Held 1 hr. at 870°C. and oil-quenched. Austenitized ½ hr. at 1100°C.; A.S.T.M. grain size No. 4¼. Grain-boundary area = 29 sq. mm. per cu. mm.

715		0.26×10^{-3}		
700		1.9×10^{-3}		
690	36	3.0×10^{-3}	1.5	0.05
680	22	4.7×10^{-3}	27	0.93
660	10	8.0×10^{-3}	130	4.5
640	4.6	12.0×10^{-3}	850	29
625	3.1	13.8×10^{-3}	$2,700$	92
600		15.0×10^{-3}		

STEEL H

As-received material (annealed). Austenitized ½ hr. at 900°C. A.S.T.M. grain size No. 5. Grain-boundary area = 38 sq. mm. per cu. mm.

720	4,500	1.68×10^{-5}	0.337	0.0089
714	345	1.17×10^{-4}	29.1	0.77
703	80	5.17×10^{-4}	117	3.1
691	28	1.7×10^{-3}	212	5.6
662	6	1.10×10^{-3}	383	10.1

STEEL I

As-received material (annealed). Austenitized ½ hr. at 900°C. A.S.T.M. Grain size No. 5. Grain-boundary area = 38 sq. mm. per cu. mm.

703	4,500	0.5×10^{-4}	1.3×10^{-2}	3.4×10^{-4}
691	110	2.75×10^{-3}	0.22	5.7×10^{-3}
662	8.6	5.0×10^{-3}	9.7×10^{2}	25
637	2.6	2.30×10^{-3}	13.8×10^{6}	3.6×10^{4}

STEEL J

Furnace-cooled from the carburizing temperature. Austenitized ½ hr. at 875°C. A.S.T.M. grain size No. 1. Grain-boundary area, 9.5 sq. mm. per cu. mm.

720.7		0.015×10^{-3}		
716	2,100	0.072×10^{-3}	9.0×10^{-6}	9.5×10^{-6}
689	37	1.95×10^{-3}	4.7×10^{-3}	4.9×10^{-3}
670	9.6	4.50×10^{-3}	0.85	9.0×10^{-2}
650	3.0	5.95×10^{-3}	39	4.1
599	2.0	6.5×10^{-3}	300	31
547	1.3	6.6×10^{-3}	800	84
500*	13	1.42×10^{-3}		
466*	17	0.54×10^{-3}		

* Reaction product was bainite.

specimens were $\frac{1}{8}$ in. thick or less. With a clean and well stirred lead bath, there is no observable rise in temperature during reaction, and the reaction takes place within 5°C. of the bath temperature.[2] During austenitizing, prior to quenching, the steels were held in a purified nitrogen atmosphere in order to prevent scaling; slight decarburization of the surface was

accuracy of measurement of ±0.5°C. Long reaction times were measured with a stop watch and short reaction times with a chronograph.

The percentage reaction after interrupted isothermal reaction was determined either by comparing the microstructure with standard charts or by planimetric evaluation of the extent of reacted areas.

TABLE 4.—*Rate Data on Steels* C *and* D *at* 680°C.

Pretreatment: Annealed one hour at 970°C., furnace-cooled.

Steel	Austenitized ½ hr. at Deg. C.	A.S.T.M. Grain Size	Grain-boundary Area, Sq. Mm. per Cu. Mm.	Time of 50 Per Cent Reaction, $t_{0.5}$ Sec.	Rate of Growth, Mm. per Sec., G	Rate of Nucleation per Mm. of Volume, N_v	Rate of Nucleation per Sq. Mm. of Grain-boundary Area, N_s
C	875	4	27	93	2.1×10^{-3}	0.95	0.035
C	730	6¾	70	18	2.0×10^{-3}	675	9.6
D	875	7¼	84	40	2.2×10^{-3}	27.6	0.33
D	1,025	3	19	120	2.3×10^{-3}	0.30	0.016
C	925	3	19	165	2.2×10^{-3}	0.083	0.0044

observed; in measurements of percentage of transformation, N_v and G, the decarburized surface was avoided.

Temperature measurements in both furnace and lead bath were made with

TABLE 5.—*Effect of Austenite Heterogeneity on Variation of Rate of Nucleation with Time*[a]

Radius in Divisions (1 division = 0.00667 mm.)	Minutes at 1000°C.				
	15	30	45	60	90
	Number of Nodules in Marked Area				
0–1	64	65	45	51	40
1–2	84	82	58	60	50
2–3	64	77	49	46	35
3–4	43	47	34	36	25
4–5	27	36	18	21	13
5–6	18	16	11	13	7
6–7	11	7	5	4	4
Marked area, sq. mm.....	1.48	1.72	1.70	1.87	2.49

[a] Data from which Fig. 13 was calculated.

chromel-alumel thermocouples calibrated against a platinum:platinum-rhodium secondary standard thermocouple certified by the Bureau of Standards, providing an

The austenite grain size was established either by comparison of the grain size revealed by a gradient quench with the standard A.S.T.M. charts, or by comparison of the fracture with standard fracture samples; these methods give essentially equivalent results (within ¼ grain-size number) in the range of grain sizes considered.[17]

EXPERIMENTAL RESULTS AND DISCUSSION

Isothermal Reaction Curves

For the purposes of determining the rate of nucleation and the rate of growth, and of assessing the effect of variations in austenitizing treatment upon these rates, it was necessary to obtain isothermal reaction curves over a range of temperature. A series of such curves for steels A, B, H, I and J are reproduced in Fig. 7. These curves can be assembled into a conventional S-curve, by reading off constant percentages of reaction; e.g., 2.0 and 98 per cent. Fig. 8 gives the S-curve derived for the high-purity steel J.

Rate of Growth

Rates of growth were determined by plotting the largest observed nodule radius

as a function of time, as stated above. Figs. 3 and 9 give a number of such plots, showing that the points fall upon straight lines and that in the ordinary case a small time intercept is observed. All of the values of G quoted here have been obtained from curves of this sort. Fig. 10 gives G plotted as a function of reaction temperature for steels A, B, C, F, H and J. A, B, C and J are eutectoid steels and steels F and H are hypereutectoid. The data from which these curves have been plotted are given in Tables 3 and 4. In the neighborhood of 570°C. (that is, near the knee of the S-curve), the values of G are somewhat lower than they should be, for recalescence causes the reaction to proceed at a temperature very slightly higher than the bath temperature; as stated above, the maximum difference between the temperature of the sample and the temperature of the bath is not greater than 5°C. affecting G but little.[2]*

The rate of growth is quite insensitive to structural variation in the austenite. Steels C and D, from the same heat, differing only in the fact that D had been deoxidized with aluminum and thus contained alumina and a small amount of residual alloyed aluminum whereas steel C had not been given this deoxidization practice and therefore contained but little alumina and no alloyed aluminum, gave, nevertheless, identical values of G. Fig. 9 and Table 4 give the data on G at 680°C. obtained on these steels with various austenitizing treatments. These variations in austenitizing produced different grain sizes and different degrees of austenite heterogeneity. The range in the A.S.T.M. grain size is from No. 3 to No. 7¼; the steel austenitized at 730°C. contained a considerable number of undissolved carbide particles. Despite these

* Owing to uncertainty as to the nature of the decomposition product, it was impossible to determine whether or not G for *pearlite* passed through a maximum with continued undercooling.

structural variations in the austenite, it may be seen that G remains invariant within the experimental error. It is clear from these data that G is a *structure-insensitive*
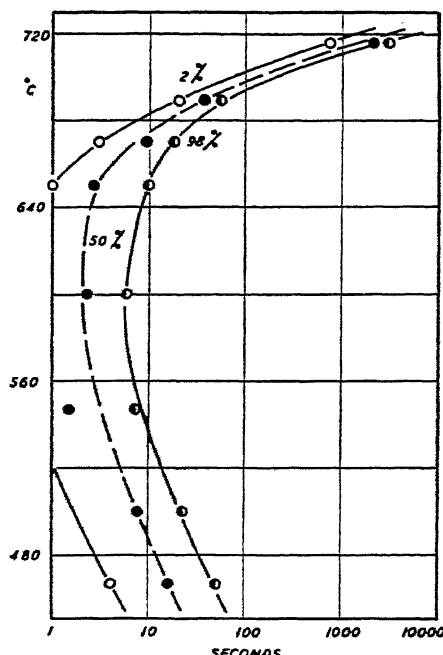
FIG. 8.—S-CURVE FOR HIGH-PURITY STEEL J.
Austenitized ½ hr. at 875°C.; grain size No. 1. At temperatures above 700°C. nucleation was almost exclusively at the surface of the specimens.

property. This is a fortunate circumstance, for with G remaining constant at a given reaction temperature for a given simple-carbon eutectoid steel, whatever its austenitizing treatment, variations in reaction rate must originate in variations in the rate of nucleation and the grain size, thus simplifying the study of the factors controlling hardenability.

It is known that alloy content has an effect upon G.[1] The effect of the manganese content on G at 680°C. may be seen in the data listed in Tables 3 and 4. It will be observed that G decreases with increase in manganese, from 3.4×10^{-2} mm./sec. in the steel with no manganese to 1.0×10^{-3}

FIG. 9.—MAXIMUM NODULE RADIUS VERSUS REACTION TIME AT 680°C.
Steels C and D annealed at 950°C. and austenitized ½ hr. at temperatures indicated. Austen-
ite grain sizes and calculated rates of growth are listed in Table 4. It is to be noted that grain size,
austenite heterogeneity, and deoxidation practice do not affect G.
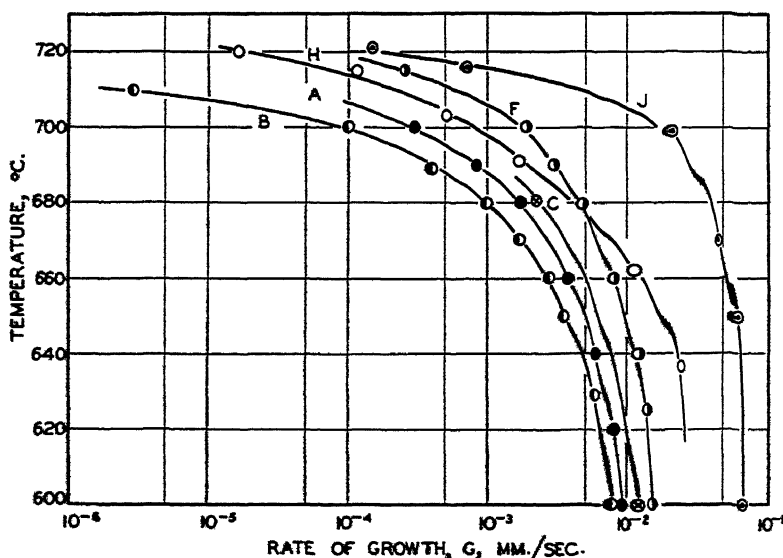
FIG. 10.—RATE OF GROWTH OF PEARLITE AS A FUNCTION OF REACTION TEMPERATURE FOR STEELS
A, B, C, F, H AND J.
Data are listed in Tables 3 and 4 along with pretreatment, austenitizing time and temperature,
and grain size for each steel.

in the steel with 0.74 per cent Mn. The variation of G with percentage of manganese is plotted in Fig. 11; the value for the high-purity alloy is not included in this

Rate of Nucleation

Variation of N with Time.—The rate of nucleation, expressed either as N_v or N_s,
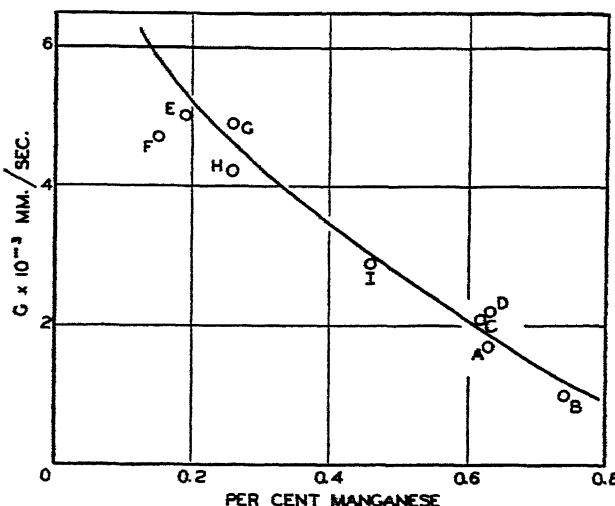
FIG. 11.—EFFECT OF MANGANESE CONTENT ON RATE OF GROWTH OF PEARLITE AT 680°C.
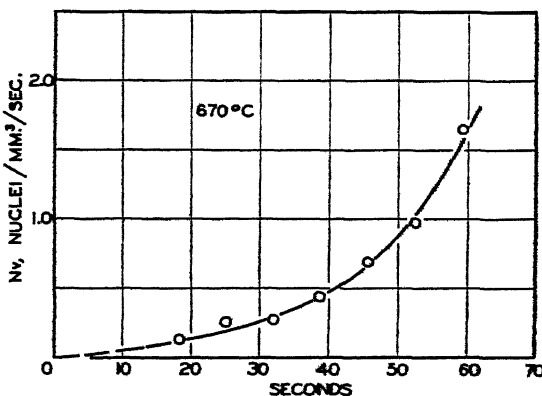
FIG. 12.—RATE OF NUCLEATION, N_v, AS A FUNCTION OF TIME FOR STEEL B AT 670°. Annealed 1 hr. at 950°C.; austenitized ½ hr. at 875°C. A.S.T.M. grain size No. 4¼. $N_v(t)$ determined by method 2.

diagram, for it lies far above the curve drawn. The values of G plotted are lower than they would be if the steels contained only the amount of manganese listed, for the residual alloying elements invariably present in commercial steels must act, as manganese does, to decrease G.

has been found to increase with time during isothermal reaction; this behavior seems to be general, for it has been found in all of the steels for which the variation of N with time has been measured. Figs. 5 and 6 show $N_v(t)$ for steels F and G at 680°C. The variation of N_v with time for steel B

is plotted in Fig. 12 for a reaction temperature of 670°C. This curve was obtained by method 2, in a sample that had been about 15 per cent transformed. It is an inherent difficulty of the successive subtraction method that errors originating in the original divisions accumulate in the later ones. The values of N in the later stages of the curves plotted therefore lose precision; it is impossible at the moment to say whether N continues to increase with time or assumes a constant value, or decreases.*

It will be seen later that the rate of nucleation is markedly affected by the state of heterogeneity in the austenite. At the moment we may inquire concerning the effect of austenite heterogeneity upon the variation of N with time at constant reaction temperature. Steel G was austenitized at 1000°C. for 15, 30, 45, 60, and 90 min., respectively. The A.S.T.M. grain size was found to be No. 5 throughout. The results of this study are given in Fig. 13; the data from which N_v was calculated, in Table 5. The N-curves have the same shape and appear to differ only in vertical displacement. This displacement is not a simple upward shift, but appears to be given by a constant multiplying factor at any value of the time. Apparently austenite heterogeneities, carbide, etc., do not furnish nuclei that are all

active immediately at the start of reaction, but, like grain boundaries, merely furnish loci with a high degree of probability of nucleation; even carbides do not act as "germ nuclei" (*vide supra*).

Variation of N with Temperature.—Since N varies with time during isothermal reaction, a full representation of N versus temperature of reaction would require a three-dimensional plot. It is hardly expedient to attempt to obtain the data for such a plot, for the determination of the variation of N with time at high temperatures is very laborious, and, moreover, it is impossible to obtain trustworthy information on this variation at low temperatures (*vide supra*). Since much can be learned from comparative values of N, as derived for different temperatures of reaction, different austenitizing treatments, different deoxidation treatments, and for different compositions, we shall employ the simplified calculation outlined in method 3. This method, when applied to group-nodule transformation, yields true *average* values for N_v; when applied to grain-boundary transformation it can yield only approximate average values of N_v.

The values of N_v calculated in this way are listed in the summary table (Table 3); since pearlite is known to nucleate at the austenite grain boundary at all temperatures,[2] the rate of nucleation per unit grain-boundary area N_s may be calculated; values of N_s are also listed in the tables.* The data listed in the tables are also plotted in Fig. 14.†

---

* It is interesting that N_v has been shown to increase in a similar way with time for the recrystallization of the solid solution of iron with 1 per cent Si; in this case there is good evidence that N_v passes through a maximum (J. K. Stanley and R. F. Mehl, p. 260, this volume). The temptation is strong to ascribe the increase in N_v during the formation of pearlite to the nucleating effect of strain engendered by the volume increase accompanying the formation of pearlite, but this reason can hardly be invoked to explain the analogous effect observed in recrystallization, for in the latter the volume change accompanying the relief of cold-work (4 per cent reduction in thickness by tensile elongation) is very minor.[2] The increase of N_v with time is directly opposed to the behavior that would be predicted by Avrami's "germ nuclei" theory.[1b,20]

* N_v divided by the grain-boundary area in sq. mm. per cu. mm. for a given A.S.T.M. grain size yields N_s. (These values are tabulated in the Metals Handbook, 1939 Edition, page 760, Amer. Soc. Metals.)

† These data have been used to check Avrami's[18] assumption of an isokinetic temperature range for the formation of pearlite. The product $G \times t_{0.5}$ and the ratio $\dfrac{G}{N_s}$ have been found to vary markedly over the temperature range studied, contrary to the constancy of these quantities expected on the basis of Avrami's theory.
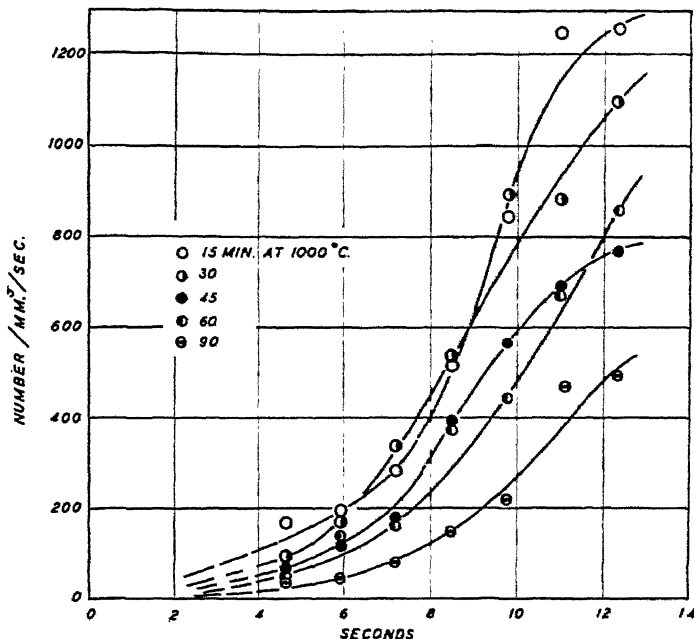
FIG. 13.—RATE OF NUCLEATION FOR STEEL G AT 680°C. AS A FUNCTION OF AUSTENITIZING TIME AT 1000°C.

Pretreatment consisted of holding at 875°C. for 1 hr. and oil-quenching. The austenite grain size was A.S.T.M. No. 5 for all samples indicating that the change in N with austenitizing time was due to increased austenite homogeneity. $N_v(t)$ determined by method 2.
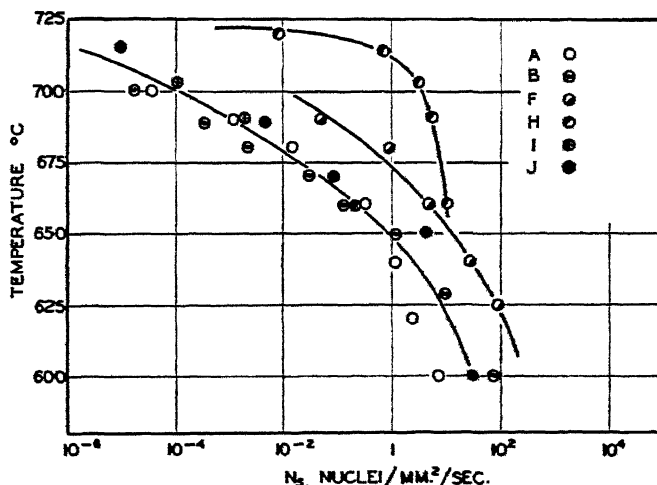
FIG. 14.—RATE OF NUCLEATION, N_s, AS A FUNCTION OF REACTION TEMPERATURE FOR STEELS A, B, F, H, I AND J.

Pretreatment, austenitizing time and temperature, and grain size appear in Table 3. N_s determined by method 3.

Effect of Austenite Heterogeneity upon N. The conversion of the cementite-ferrite aggregate into austenite is a process dependent upon time. It occurs in three

less homogeneous the austenite, with a free carbide particle acting as a point for easy nucleation, and with loci of high carbon concentration in austenite acting in a
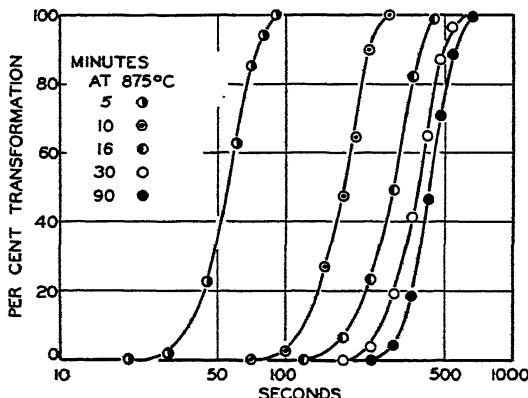

Fig. 15.—Effect of austenitizing time at 875°C. upon rate of reaction of steel B at 680°C. Rates of nucleation calculated by method 3 from these curves are listed in Table 6.

stages: (1) the formation of heterogeneous austenite by a nucleation and growth process, leaving residual undissolved carbide, (2) the final solution of carbide, and, finally, (3) the dissipation of carbon concentration gradients. The longer the austenitizing

similar capacity either directly or by a rapid rejection of carbide particles.

The effect of austenite heterogeneity was studied by austenitizing steel B at 875°C. for a series of time periods ranging from 5 to 90 min. and then reacting to pearlite at

Table 6.—*Effect of Time at Austenitizing Temperature on Transformation Rate of Steel B at 680°C. and 593°C.*

Pretreatment: Annealed one hour at 950°C. and cooled at 4°C. per min. $G = 1.0 \times 10^{-5}$ mm. per sec. at 680°C.; 8.0×10^{-5} at 593°C.

Time at 875°C., Min.	A.S.T.M. Grain Size	Grain-boundary Area, Sq. Mm. per Cu. Mm.	Reaction Temperature					
			680°C.			593°C.		
			$t_{0.5}$	N_v	N_s	$t_{0.5}$	N_v	N_s
5	6½	57	57	62.5	1.1	2.7	2.4×10^4	4.2×10^2
10	5½	42	198	0.43	0.01	3.0	1.6×10^4	3.8×10^2
16	4½	35	300	0.081	0.0023	3.25	1.2×10^4	3.3×10^2
30	4½	29	378	0.057	0.0020	3.50	0.85×10^4	2.9×10^2
90	3½	25	420	0.021	0.00084	4.0	0.50×10^4	2.0×10^2

treatment at constant temperature or the higher the temperature of austenitizing, the more nearly will the austenite approach a state of true homogeneity.[2]

There is evidence that suggests that the rate of nucleation may be the greater the

680°C. The austenitizing treatment provided a series of samples exhibiting undissolved carbide at the shorter times and far more homogeneous austenite at the longer. Reaction curves and N_s were determined (the latter by method 3); the

reaction curves are given in Fig. 15, and the values of N_v and N_s are listed in Table 6.

The grain size increases from A.S.T.M.

is probably the result of this undissolved carbide; the steady decrease of N_s with time of austenitizing from 10 to 90 min. is probably to be associated with the gradual
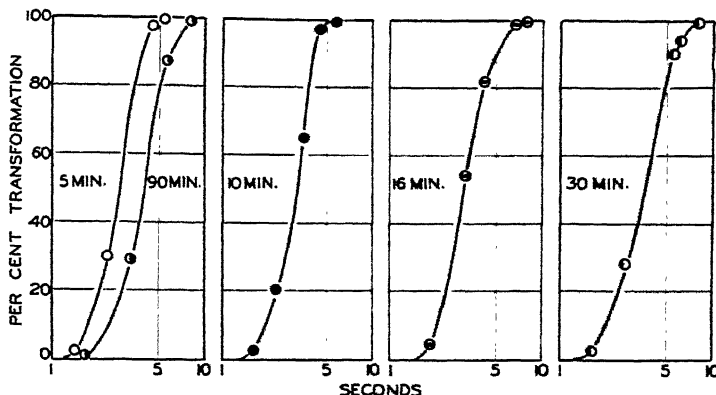

FIG. 16.—EFFECT OF AUSTENITIZING TIME AT 875°C. UPON RATE OF TRANSFORMATION OF STEEL B AT 593°C.

Rates of nucleation calculated by method 3 are listed in Table 6.

No. 6¼ at 5 min. of austenitizing to No. 3¾ at 90 min. Curves such as those given in Fig. 15 have been taken ordinarily as an illustration of the effect of austenite grain size upon reaction rate.[2] The true effect of grain size for the group-nodule mode of transformation is purely one of the extent of grain-boundary area, with decreasing grain size affording increasing surface area and a proportionally increasing number of nuclei. If the curves given actually represent the effect of grain size *alone*, the rate of nucleation per unit grain-boundary area N_s calculated from the measured values of N_v should be a constant irrespective of grain size. It is thoroughly clear that the values of N_s given in Table 6 are not constant but decrease very greatly as the time of austenitizing is increased. The higher values of N_s at the shorter austenitizing times must originate in austenite heterogeneity. After 5 min. of austenitizing many undissolved carbide particles were observed; after 10 min. carbide could still be detected, but appeared absent after longer times. The very high value of N_s after 5 min., and even after 10 min.,

elimination of carbon concentration gradients. It is to be emphasized, therefore, that the reaction curves given in Fig. 15, and others like them, cannot be taken as an illustration of the effect of grain size alone on the rate of reaction: They represent, in fact, the combined effect of increasing grain size and decreasing austenite heterogeneity.

Fig. 16 shows a group of reaction curves for the same steel austenitized at the same temperature and for the same time periods but reacted at 593°; Table 6 shows the N_v and N_s data calculated. This temperature of reaction was chosen because it is near the knee of the S-curve (though not quite at it) and the reaction curves should therefore be suggestive of the behavior of the steel with respect to depth of hardening. It will be observed that there is now far less variation in rate of reaction with time of austenitizing. The variation in N_s is correspondingly small. Apparently the rate of reaction and the rate of nucleation at the knee of the S-curve are far less sensitive to differences in austenite heterogeneity than at higher temperatures. It appears

that little change in these quantities and little change in depth of hardening will be observed unless there are numerous small carbide particles left undissolved,[2] and it is

A.S.T.M. grain-size variation of No. 7 to No. 1½. Here again the reaction curves may not be taken as an illustration of the effect of grain size on the rate of reaction.
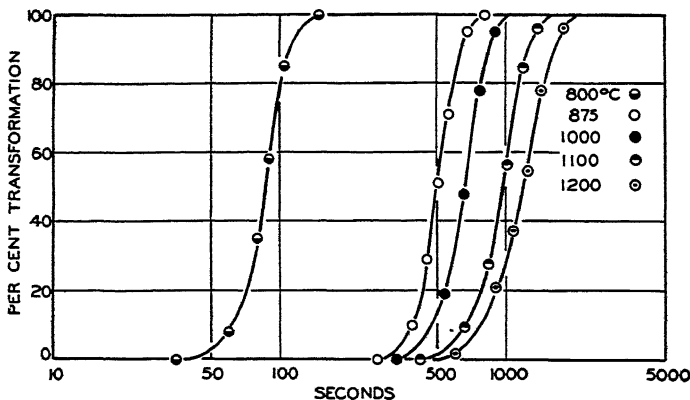
Fig. 17.—Effect of Austenitizing Temperature upon Rate of Reaction of Steel A at 690°C.
Grain sizes and rates of nucleation calculated by method 3 appear in Table 7. Austenitizing treatments were ½ hr. at temperatures given.

clear that the rate of reaction at temperatures near Ae₁ cannot be used to predict the rate of reaction at the knee and the correlated hardenability.

for the values of N_s listed vary by a factor even larger than that obtaining in the study of the effect of austenitizing time at constant temperatures.* The high value of N_s

Table 7.—*Effect of Austenitizing Temperature on Rate of Transformation of Steel* A *at* 690°C. *and* 593°C.

Pretreatment: Heated ½ hr. at 875°C. and quenched in oil. $G = 0.87 \times 10^{-2}$ mm. per sec. at 690°C.; 9.6×10^{-2} at 593°C.

Austenitized ½ Hr at Deg. C.	A.S.T.M. Grain Size	Grain-boundary Area, Sq. Mm. per Cu. Mm.	Reaction Temperature					
			690°C.			593°C.		
			$t_{0.5}$	N_v	N_s	$t_{0.5}$	N_v	N_s
800	7	76	87	17.2	0.23	2.1	3.8×10^4	0.50×10^2
875	5	38	504	16×10^{-2}	4.2×10^{-4}	2.4	2.2×10^4	0.59×10^2
1000	4	27	714	3.8×10^{-2}	1.4×10^{-4}	2.7	1.4×10^4	0.51×10^2
1100	3	19	985	1.1×10^{-2}	0.56×10^{-4}	3.8	0.36×10^4	0.19×10^2
1200	1½	12	1,170	0.53×10^{-2}	0.44×10^{-4}	6.5	0.041×10^4	0.035×10^2

The effect of austenite heterogeneity upon the rate of nucleation may be studied also by varying the temperature of austenitizing at constant time. Such a study was performed on steel A; the reaction curves are shown in Fig. 17, and the data are given in Table 7. The temperature of austenitizing varied from 800° to 1200°C., producing an

after austenitizing ½ hr. at 800°C. doubtless originates in the effect of the undis-

---

* Davenport and Bain[21] studied the effect of austenitizing temperature upon the rate of transformation of a eutectoid steel at 675°C. Mehl[3] has shown that the increase in grain size was insufficient to account for the observed decrease in reaction rate, in accord with the findings above.

solved carbide that was evident in a sample quenched to martensite; no carbide could be detected in samples austenitized at the higher temperatures, and the decrease in curves are given in Fig. 18, and the data are listed in Table 7. It may be seen again that the different degrees of austenite heterogeneity produce but a slight variation in
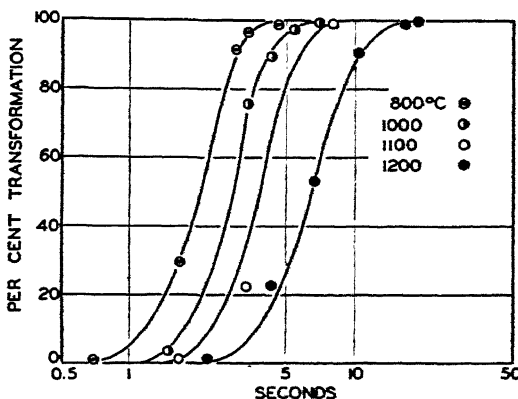
FIG. 18.—EFFECT OF AUSTENITIZING TEMPERATURE UPON RATE OF TRANSFORMATION OF STEEL A AT 593°C.

Grain sizes and rates of nucleation calculated by method 3 are in Table 7. Austenitizing treatments were ½ hr. at temperatures given.
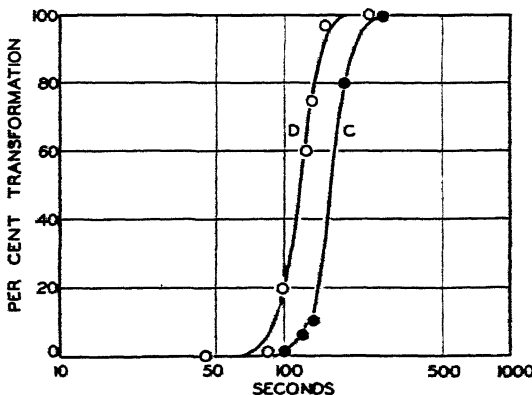
FIG. 19.—EFFECT OF DEOXIDATION PRACTICE UPON RATES OF TRANSFORMATION AT 680°C. OF STEELS C(C.G.) AND D(F.G.) AT CONSTANT GRAIN SIZE, No. 3.

Rates of nucleation calculated by method 3 appear in Table 4.

N_s with temperature of austenitizing increasing beyond 875° is doubtless the result of the progressive elimination of carbon concentration gradients. In contrast to G, it is clear, therefore, that N_s is markedly *structure-sensitive*.

Similar studies were made employing identical austenitizing treatments but with reaction to pearlite at 593°C. The reaction the reaction rate and in N_s at this lower temperature.

Effect of Deoxidation Practice upon N.— It has frequently been assumed that the products of furnace, ladle, or ingot deoxidation of steel may act as nuclei and thus appreciably alter the rate of reaction at the knee of the S-curve and the correlated depth of hardening.[2] There can be no ques-

tion that some deoxidation products do operate as active nuclei, for nodules of fine pearlite have been observed to form at such particles, producing a variety of

FIG. 20.—EFFECT OF DEOXIDATION PRACTICE UPON RATES OF TRANSFORMATION OF STEELS C AND D AT 593°C.

A.S.T.M. grain size No. 4 in both steels. Rates of nucleation calculated by method 3 are listed in Table 8.

general nucleation.[2] The question remains, however, as to whether these particles alter the rate of reaction enough to give a measurable difference in depth of hardening.

It is not an easy matter to produce an answer to this question by the examination of a series of commercial steels even though the full heat and deoxidation history of the

in the state of austenite heterogeneity can produce variations in rate of reaction and in depth of hardening masking the effect sought. In view of this, steels C and D were selected as most suited for the analysis.

As stated, steels C and D were made from the same heat, one part deoxidized with aluminum, steel D, yielding a nominally fine-grained steel, and one part not, steel C, providing a nominally coarse-grained steel. These two steels were austenitized to the same grain size, producing in both cases austenite of a high degree of homogeneity, and reacted at 680°C. The reaction curves are given in Fig. 19, and the data are listed in Table 4. The isothermal reaction rate curves are but little affected, and, correspondingly, the values of N_s differ but slightly: The value of N_s is 3.6 times greater in the aluminum-deoxidized steel that had been the more thoroughly austenitized and, consequently, the effect of deoxidation products in increasing N_s seems real, though it is small. In similar studies at a reaction temperature of 593°C., steel D was still faster in reacting than C, but the rates of nucleation differed only by a factor of two. The reaction curves are

TABLE 8.—*Rate Data on Steels* C *and* D *at* 593°C.

Pretreatment: Annealed one hour at 970°C. Furnace-cooled. Rate of growth, $G = 12.5 \times 10^{-3}$ mm. per second.

Steel	Austenized ½ Hr. at Deg. C.	A.S.T.M. Grain Size	Grain-boundary Area, Sq. Mm. per Cu. Mm.	Time of 50 Per Cent Reaction, $t_{s.s}$ Sec.	Rate of Nucleation per Cu. Mm. of Volume, N_v	Rate of Nucleation per Sq. Mm. of Grain boundary Area N_s
C	900	4	27	2.3	1.2×10^4	440
D	1,005	4	27	1.9	2.6×10^4	950

samples be known, for commercial steels contain very appreciable quantities of residual alloying elements, nickel, chromium etc., about which information is nearly always lacking, yet which can have a measurable effect upon the rate of reaction and upon the depth of hardening; furthermore, commercial steels vary markedly in response to austenitizing and a difference

plotted in Fig. 20, and the data are given in Table 8.

SUMMARY

1. Methods are given by the use of which: (a) the rate of growth of pearlite nodules from austenite may be measured and (b) the rate of nucleation of pearlite nodules from austenite may be measured either precisely or approximately.

2. Rates of growth and rates of nucleation were determined for a series of 10 steels, over a range of temperatures and for different degrees of austenite heterogeneity.

3. It is shown that the rate of growth remains constant with time during isothermal transformation; the rate of nucleation increases.

4. It is demonstrated that the rate of growth is insensitive to variations in austenite grain size and the degree of austenite heterogeneity; it is shown that the rate of nucleation is very sensitive to like variations.

5. It is observed that the products of deoxidation with aluminum exercise a very minor effect upon the rate of nucleation per unit grain-boundary area.

6. The effect of austenite heterogeneity upon the rate of transformation and upon the rate of nucleation is found to be far more marked at high reaction temperatures than at temperatures near the knee of the S-curve.

7. The interest these results bear to commercial heat-treatment is discussed.

ACKNOWLEDGMENT

One of the authors wishes to acknowledge the granting of a fellowship by the Westinghouse Electric and Manufacturing Co.; all are indebted to Mr. J. P. Gill, of the Vanadium Alloys Steel Co., and to Mr. R. L. Stephenson, of the Carnegie-Illinois Steel Corporation, for furnishing certain of the steels used in this research.

REFERENCES

1. R. F. Mehl: Physics of Hardenability. Hardenability of Alloy Steels, Amer. Soc. for Metals Symposium, 1939.
2. R. F. Mehl: Structure and the Rate of Formation of Pearlite. 16th Campbell Memorial Lecture, Amer. Soc. for Metals (Oct. 1941).
3. W. A. Johnson and R. F. Mehl: Reaction Kinetics in Processes of Nucleation and Growth. Trans. A.I.M.E. (1939) 135, 416.
4. F. C. Hull and R. F. Mehl: The Structure of Pearlite. Preprint, Amer. Soc. Metals (Oct. 1941).
5. E. Scheil and A. Lange-Weise: Statistical Structure Investigations, III—Velocity of Crystallization and Formation of Nuclei in the Transformation of Austenite into Pearlite. Archiv Eisenhüttenwesen (1937-1938) 2, 93.
6. I. L. Mirkin and M. E. Blanter: Linear Velocity of Crystallization and Rate of Nucleus For-

mation during Secondary Crystallization of Alloy Steel. Metallurgie (1936) 11, 43.
7. I. L. Mirkin: Rate of Nucleus Formation and that of the Growth of Eutectoid Grains in the Secondary Crystallization of Special Steels. Trudy Moscov. Inst. Stali im. I. V. Stalina (1938) 10, 77-90.
8. F. C. Hull: Discussion. Ref. 3.
9. E. Scheil and H. Wurst: Statistical Structure Investigations, II—Measurement of Spatial Grain Size. Ztsch. Metallkunde (1936) 28, 340.
10. M. Gensamer, E. B. Pearsall and G. V. Smith: Mechanical Properties of the Decomposition Products of Austenite. Trans. Amer. Soc. Metals (1940) 28, 380.
11. M. Gensamer, E. B. Pearsall, W. S. Pellini and J. R. Low: Tensile Properties of Pearlite, Bainite, and Spheroidite. Preprint No. 19, Amer. Soc. Metals (Oct. 1941).
12. G. Pellissier, M. F. Hawkes, W. A. Johnson and R. F. Mehl: Interlamellar Spacing of Pearlite. Preprint No. 41, Amer. Soc. Metals (Oct. 1941).
13. G. V. Cash, T. W. Merrill and R. L. Stephenson: Effect of Deoxidation Practice on Hardenability. Trans. Amer. Soc. Metals (1941) 29, 755.
14. R. F. Mehl and C. Wells: Constitution of High-purity Iron-carbon Alloys. Trans. A.I.M.E. (1937) 125, 429.
15. E. S. Davenport and E. C. Bain: Transformation of Austenite at Constant Subcritical Temperatures. Trans. A.I.M.E. (1930) 90, 128.
16. E. S. Davenport: Isothermal Transformations in Steels. Trans. Amer. Soc. Metals (1939) 27, 837.
17. Metals Handbook, 1939 Ed., 754. Amer. Soc. Metals.
18. M. Avrami: Kinetics of Phase Change, I—General Theory. Jnl. Chem. Physics (1939) 7, 1103.
19. M. Avrami: Kinetics of Phase Change, II—Transformation-Time Relations for Random Distribution of Nuclei. Ibid. (1940) 8, 212.
20. M. Avrami: Kinetics of Phase Change, III—Granulation, Phase Change and Microstructure. Ibid. (1941) 9, 177.
21. E. S. Davenport and E. C. Bain: General Relations between Grain Size, Hardenability, and Normality of Steels. Trans. Amer. Soc. Metals (1934) 22, 879.
22. J. E. Dorn, E. P. De Garmo and A. E. Flanigan: Nucleation and Growth Rates of Pearlite. Trans. Amer. Soc. Metals (1941) 29, 1022.

DISCUSSION

(A. B. Greninger presiding)

G. A. ROBERTS,* Pittsburgh, Pa.—During the course of the investigation reported in this paper, the question arose as to the nature of the slight shift of the rate of nucleation per unit grain-boundary area (N_s) with increasing times of austenitizing at any one temperature. The authors eliminated the effect of grain-size changes in their consideration of the part played by austenite heterogeneities in changing the rate of nucleation at subcritical temperatures by dividing the rate of nucleation per unit volume (N_v) by the grain-boundary area to obtain the rate of nucleation per unit grain-boundary area (N_s). The data presented show that this quantity (N_s) drifts considerably with

* Vanadium-Alloys Steel Company Graduate Fellow, Carnegie Institute of Technology.

time of austenitizing when carbides are visible and continues to shift even when carbon concentration gradients are active. It is postulated that perfect homogeneity would require N_s to remain constant, but this would be true only if there is no tendency for the grain corners (points of intersection of more than two grains) to be more active than the grain boundaries in producing pearlite nuclei. If this were true, a slight shift in the rate of nucleation per unit grain-boundary area (N_s) would be expected, for the number of corners per total grain-boundary area would decrease as the grain size is increased (corresponding to an increase in austenitizing time).

In order not to overlook this possibility, I have recently completed a study on numerous gradient quenched samples of commercial plain carbon steels of the type used in this paper and on several samples of high-purity iron-carbon alloys kindly supplied by Mr. T. G. Digges, of the National Bureau of Standards. The results of this investigation show that the shift in the rate of nucleation per unit grain-boundary area (N_s) reported by Messrs. Hull, Colton and Mehl cannot be explained away on a basis of grain-corner nucleation. A statistical study reveals that the corners act very similarly to the boundaries in nucleating pearlite, and that *on the average* the largest nodules (ones that were nucleated first) will be found without preference around the grain. It is clear, therefore, that the methods used to eliminate grain-size changes throughout the papers on this subject can be applied without fear of introducing complicating variables.

W. A. JOHNSON,* E. Pittsburgh, Pa.—The authors have mentioned several possible methods for measuring the rate of nucleation; they have also suggested that an average constant value of the rate of nucleation is much more easily measured and probably will suffice in most applications. I should like to suggest still another way in which information concerning the nucleation rate may be obtained.

Several years ago Austin and Rickett[21] described the use of "autocatalytic" and "probability" graph paper for plotting reaction curves portraying the rate of transformation of austen-

ite. The fact that reaction curves plot approximately as straight lines on either of these types of graph makes them useful for interpolating and for estimating the accuracy of the data. Unfortunately, the fact that there is no basis in theory for either of these types of plot severely limits their usefulness.

An examination of the various nucleation curves shown in the paper indicates that they are represented with fair accuracy by an equation of the form $N = N_0 t^x$. Employing such an expression for N and taking advantage of the observed fact that G is constant, a reaction equation for transformation by general nucleation may be derived easily;[3] it is

$$f(t) = 1 - \exp.$$
$$\left[-\frac{8\pi G^3 N_0 t^{(4+x)}}{(x+1)(x+2)(x+3)(x+4)} \right] \quad [1]$$

Transposing and taking logarithms twice, we obtain

$$\log \ln \left[\frac{1}{1-f(t)} \right]$$
$$= \log \frac{8\pi G^3 N_0}{(x+1)(x+2)(x+3)(x+4)}$$
$$+ (4+x) \log t \quad [2]$$

Thus a straight line will result if the logarithm of the natural logarithm of the reciprocal of the fraction untransformed is plotted against the logarithm of time.

It is possible, for convenience, to construct graph paper on the basis of Eq. 2 in such a way that we may plot directly percentage reaction versus time. Such paper will possess all the advantages of "probability" and "autocatalytic" paper, and will in addition furnish a rapid means of determining the rate of nucleation as a function of time.

A dilatometer reaction curve for steel B at 680°C., furnished by Dr. Hull, is shown plotted on this type of graph paper in Fig. 21. It is clear that the data fall rather accurately along a straight line. The deviation of the data at the beginning of the reaction is in reality small—the plot is greatly extended at the ends—and is well within experimental error. Comparing the measured slope of this line, 4.27, with its theoretical value of $(4 + x)$, x is found to be 0.27. From the lateral position of the line, N_0 is found to be 0.011. Thus the rate of nucleation is $N = 0.011 t^{0.27}$ per cu. mm. per sec. This equation yields a rate of nucleation of 0.054

* Westinghouse Research Laboratories.
[21] J. B. Austin and R. L. Rickett: *Trans.* A.I.M.E. (1939) 135, 398.

nuclei per cu. mm. per sec. at the time corresponding to 50 per cent reaction, which may be compared with an *average* rate of nucleation,

cant. It is hoped that future workers in this field will test this type of plot and determine its usefulness.
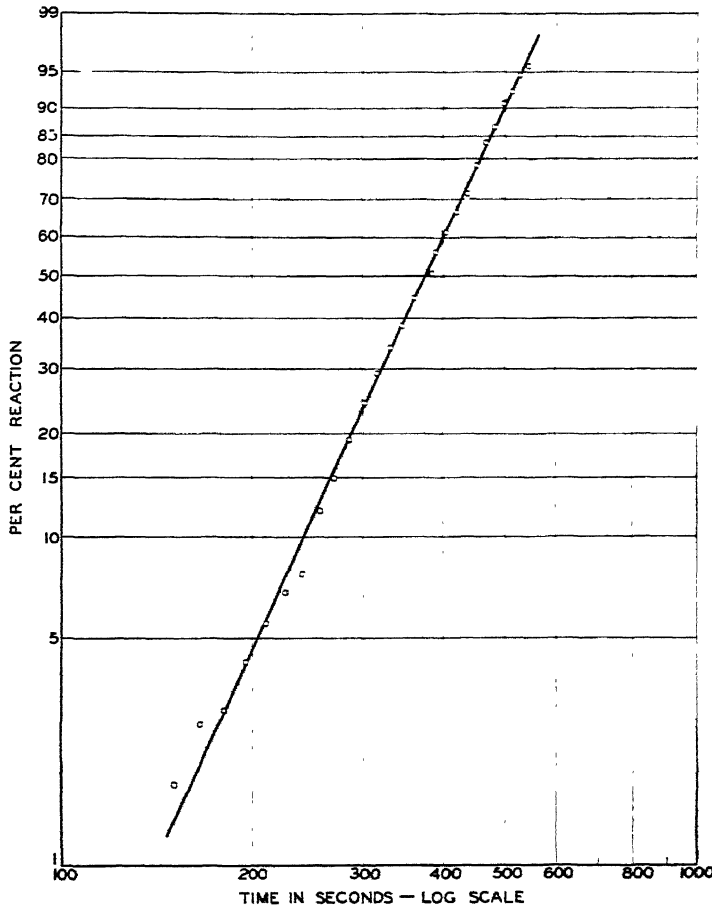
FIG. 21.—ISOTHERMAL DILATOMETRIC TRANSFORMATION CURVE FOR STEEL B PLOTTED ON "REACTION" GRAPH PAPER.

Sample was austenitized 30 minutes at $875°C$. and reacted at $680°C$.

based on the time for half reaction, of 0.034 nuclei per cu. mm. per sec.

No nucleation curve is given in the paper for this steel at the same temperature. However, all the nucleation curves given have about the same shape, and it is rather disturbing to note that all the published curves are concave upward, while the curve determined by the equation $N = 0.011t^{0.27}$ is concave downward. Unfortunately, only this one reaction curve has been plotted in this new way, so that it is not certain whether the anomalous result is signifi-

F. C. HULL (author's reply).—The authors are grateful to Mr. Roberts for providing the answer to a troublesome question. Because of the lack of definite information on the subject, they had been forced to assume that nucleation at grain-boundary edges and corners could be neglected in comparison with nucleation on the grain-boundary surfaces. Fortunately, this assumption has been justified by the investigation reported by Mr. Roberts.

Experimental difficulties limit direct measurements of the rate of nucleation to small

amounts of transformation. Dr. Johnson has now given an indirect method for estimating the variation of rate of nucleation with time for a considerable portion of the reaction. It appears that though N continues to increase with time, the rate of increase becomes much less than the initial rate. Many of the experimental curves for N versus time show a tendency to become concave downward after a short period of time, indicating that if measurements could be made at longer times, the curves might have the shape found by Dr. Johnson.

Lattice Relationships in Decomposition of Austenite to Pearlite, Bainite, and Martensite

By G. V. Smith,* Junior Member, and R. F. Mehl,† Member A.I.M.E.

The decomposition of austenite in steels, because of its immense practical importance, has been subjected to extensive study in recent years from the point of view of the mechanism of the process.[1-3] Although much information has been acquired, a number of questions, principally of theoretical interest, remain. One is that of the atomic-crystallographic mechanism by which each of the various reaction products forms.

The isothermal reaction products of the eutectoid decomposition in plain carbon steels (to which this study is restricted) have conveniently been classified in three general groupings—pearlite, bainite, and martensite. Of these several products, pearlite and martensite have been studied extensively, but bainite has received only scant attention. As a result, the mechanism of the formation of pearlite and that of martensite are now fairly well understood while a great deal of uncertainty exists regarding bainite.

PEARLITE

Pearlite forms from austenite by the precipitation of alternate platelets of cementite and ferrite, which grow into the austenite matrix.[2-5] The rate of reaction may be described in terms of a rate of nucleation and a rate of growth.[2,3]

Mehl and Smith[6] have attempted to determine the lattice relationships existing between the ferrite in pearlite and the parent austenite. Using a pole-figure method of analysis, it was found that a limited number of ferrite orientations resulted from the decomposition of a single grain of austenite; it was not possible, however, to decide between two assumed ideal relationships, both of which appeared to account for the experimentally determined pole figure. It was definitely shown, however, that the relationship obtaining was quite different from that determined for the proeutectoid separation of ferrite.[7] No attempt was made to determine the habit plane (matrix plane to which the precipitate lies parallel) of the pearlite lamellae.

Belaiew[5] earlier had stated that the number of directions assumed by the pearlite lamellae in a single grain of austenite was 12 (no details were given) and concluded wrongly, as Mehl and Smith[6] have pointed out, that the lamellae delineate the {210} planes of ferrite.*

MARTENSITE

It is known that martensite is a transitional constituent of body-centered tetragonal lattice,[9] and that it forms suddenly

* Belaiew assumed, too, the pearlite lamellae to be parallel to the lattice planes of ferrite rather than austenite.

by shearing movements[10] (requiring no concentration changes) when austenite is cooled through a certain temperature region.[11]

Kurdjumow and Sachs,[10] using a pole-figure method of analysis, determined the lattice relationship existing between austenite and the tetragonal martensite formed on quenching a 1.4 per cent carbon steel. An assumed ideal relationship

$$\{111\}_\gamma /\!/ \{110\}_\alpha$$
$$[110]_\gamma /\!/ [111]_\alpha$$

was found to fit the experimentally determined pole figure remarkably well.*

Kurdjumow and Sachs made no attempt to determine the habit plane but assumed it to be the conjugate plane, $\{111\}_\gamma$, of the lattice relationship cited above, and attempted to depict the atomic movements that must occur in the martensite transformation; this assumption appears now to have been in error, and the derived atom movements therefore not real.

Mehl, Barrett and Smith[7] made frequency counts of the martensite plate directions in several steels (including one of eutectoid composition) in a brief attempt to determine the habit plane of martensite. Although there was a great deal of scatter, the traces tended to group themselves in a maximum number of four, and this was taken as an indication that the martensite habit plane was the octahedral austenite plane. Greninger and Troiano,[13] in a recent and more thorough study, have shown that martensite does not delineate the octahedral planes of austenite, but, rather, an irrational one.

Nishiyami[14] has reported that the orientation relationship existing between the martensite-like constituent that forms in

an iron-nickel alloy of 30 per cent nickel and the original austenite is in accordance

with: $\{111\}_\gamma /\!/ \{110\}_\alpha$
$\quad\quad [211]_\gamma /\!/ [011]_\alpha$

More recently, Wassermann[15] has confirmed the Kurdjumow-Sachs relationship for martensite in steel and the Nishiyami relationship for the transformation product in iron-nickel alloys. It should be pointed out that the difference in orientations resulting from the two mechanisms is only about 5°. The Kurdjumow-Sachs relationship, however, leads to 24 final orientations from a single austenite grain, whereas the Nishiyami relationship gives but 12 orientations.

In further studies of iron-nickel alloys, Mehl and Derge[16] found the actual relationship to be dependent upon the temperature at which transformation takes place—at high temperatures (240°C.) the Kurdjumow-Sachs relationship obtained and at subzero temperatures, the Nishiyami; at intermediate temperatures both relationships were observed.

Greninger and Troiano[17] recently have determined the orientation relationship existing between austenite and the martensite-like product that forms in an iron-nickel-carbon alloy with 22 per cent nickel and 0.8 per cent carbon. The relationship was found to be about midway between the Kurdjumow-Sachs and the Nishiyami relationships.

To evaluate the atomic movements that occur in the formation of martensite, Greninger and Troiano analyzed the relief produced on a polished surface during the formation of martensite. It was concluded that a martensite plate is formed through the operation of two homogeneous shears, the first along an irrational plane of the matrix lattice (which is the habit plane of the martensite plate) and the second along a low-index plane of the martensite lattice, accompanied by a small dimensional readjustment.

---

* Mehl, Barrett and Smith[7] determined that the lattice relationship with respect to austenite of proeutectoid ferrite was in accordance with the same ideal relationship. Belaiew[12] earlier had shown the habit plane of proeutectoid ferrite to be $\{111\}_\gamma$.

The lattice relationship of martensite with respect to austenite in a eutectoid steel has not been reported.

BAINITE

Bainite is the name given to the structure or structures that form on isothermal transformation at temperatures intermediate between the pearlite and the martensite temperature ranges.

Davenport and Bain,[1] who first fully described these structures, suggested that in the formation of these intermediate structures there is a tendency for "the allotropic change to sweep across a grain ahead of carbide separation." the carbide separating as particles—not lamellae.

Reasoning from the extrapolation of the curve of interlamellar spacing of pearlite versus temperature it has been proposed that bainite is nucleated by ferrite.*

Greninger and Troiano[13] have determined the habit plane of bainite when formed at various temperatures, finding a continuous variation in this plane with temperature. Except for bainite formed at 450°C., which was found to be octahedral in habit, the habit plane was irrational.

EXPERIMENTAL PROCEDURE

In order to furnish further information upon the atomic-crystallographic relationships existing between austenite and its reaction products, experimental studies were undertaken to determine: (1) the orientation relationships between ferrite in bainite and the parent austenite, and between martensite and the parent austenite; (2) the composition or habit plane in bainite and martensite (in confirmation of ref. 13); (3) the orientation relationships between ferrite in pearlite and the parent austenite (in confirmation and extension of

ref. 6); and, (4) the composition or habit plane in pearlite.

Materials and Treatment

The steel used was a commercial steel of approximately eutectoid composition: 0.78 per cent carbon, 0.63 per cent manganese, 0.014 per cent phosphorus, 0.03 per cent sulphur. and 0.18 per cent silicon.

Large austenite grains, which are necessary for the study of orientation relationships, were obtained by heating to an elevated temperature for a sufficiently long time. It was found that 2-hr. heating at a temperature of 1350°C. sufficed to produce the desired large grains (1/4-in. diameter). To avoid decarburization, heating was carried out in an atmosphere of purified nitrogen at a pressure of about 10 in. of mercury. The specimens, 1/4 by 1/4 by 1/2 in., were cooled to 950°C. and quenched in lead or salt baths, held at constant temperature, and allowed to remain until completion of the reaction. The times necessary for completion were determined by metallographic examination and were found to be comparable with those given by the published S-curve. One specimen was allowed to transform to coarse pearlite by cooling in the furnace.

Analysis of Orientation

The determination of the lattice relationship in the eutectoid decomposition of austenite is beset with certain difficulties: first, with respect to the determination of the orientation of the parent crystal; and, second, with the respect to the determination of the orientations of the resultant products. The parent solid solution cannot be retained unchanged at room temperature to permit determination of its orientation, for, if transformation at constant temperature is only partial, martensite is formed in the final cooling (which would introduce added complexity). The determination of the orientation of an austenite grain at a temperature within the austenite range is

---

* See reference 2 for complete argument. The distinction made there between "upper" and "lower" bainite is probably not valid, nor does the argument appear now to be a strong one.

extremely difficult. For these reasons, an X-ray determination of the orientation of the parent austenite is not feasible, and indirect methods must be used. The products of austenite decomposition, the orientations of which are desired, are distributed in such a finely dispersed state as to preclude, or to render very difficult, the determination of the orientation of individual particles.

Two slightly different methods, depending upon the reaction product formed, were used for the determination of the orientation of the original austenite grain. When the product of transformation was bainite or martensite, the orientation of the original austenite was determined by a measurement of the trace directions of twin bands which were present in the austenite grain, and which were visible in the reaction product owing to the Widmanstätten structure assumed by the precipitate. One or more of these bands, which delineate the octahedral, {111}, planes of the austenite lattice,[18] were traced on two polished and etched surfaces, and plotted stereographically to obtain one or more {111} poles of the austenite lattice. This information when used in conjunction with trace normal measurement of other "twin bands" on only one surface gave the orientation of the original austenite grain with an accuracy estimated to be approximately 1°.

In specimens completely transformed to pearlite, no indication of austenite twin bands could be seen upon metallographic examination, and for this reason it was necessary to develop a variant of the former method. It was found that heating in the purified nitrogen atmosphere caused an etching of the surfaces, which outlined both the austenite grain boundaries and the twin bands; this etch was preserved by cooling to room temperature in the furnace, as with the coarse pearlite specimen, or (less effectively) by rapid cooling in salt after transformation. Measurement of the twin directions as described above

gave the orientation of the original austenite grain.

The only method available for the determination of the lattice relationship existing between austenite and its reaction products, pearlite, bainite and martensite, is that of the X-ray pole figure, and accordingly this method of analysis was used.* For a pole-figure analysis, the specimen is oriented with respect to the primary X-ray beam in a number of positions sufficient to allow reflections to occur from crystals of any possible orientation within the specimen. A stereographic plot is made of the reflections from a particular family of planes to show the distribution of the orientations present within the specimen.†

White radiation from a tungsten-target X-ray tube (of the Coolidge type) operated at 37 kv. and 10 ma. was used. Transmission Laue exposures were taken at intervals of 10° through a total angle of ±60°. Exposure times varied 8 to 12 hr. Pole figures were prepared for the {110} ferrite planes; no attempt was made to determine the cementite orientations. (Comments on this latter point will appear later.)

The habit plane of the various reaction products was determined stereographically by measurement of the trace directions on a single surface of polish of completely reacted specimens, the orientations of

---

* Greninger and Troiano[17] have successfully determined by X-ray diffraction methods the orientation of a single martensite plate formed in an Fe-Ni-C alloy. The martensite in this alloy forms in sufficiently large plates to permit such a determination; this is not true of the reaction products of plain carbon steel.

† The pole-figure method of evaluating lattice relationships is subject to certain limitations, depending upon the exactness and precision of the orientation relationship. Single spots or regions on the X-ray photogram are caused by diffraction from a number of separated crystal units, and may be interpreted erroneously if the scatter is sufficiently great; the reflections from groups of crystals that differ in orientation by only a few degrees may appear on the X-ray film to have risen from one group of crystals of which the orientation is a mean of the actual orientations.

which had been determined for the pole-figure studies.

EXPERIMENTAL RESULTS

Lattice Relationships

BAINITE

Bainite Formed by Isothermal Transformation at 450°C.—The time necessary for completion of reaction in a single crystal of austenite quenched to 450°C. was found to be less than $1\frac{1}{2}$ min. Because of the size of the specimens and of the short time necessary for transformation. it is probable that the specimen did not react isothermally at the bath temperature; this, however, in view of the results as a whole. is relatively unimportant. Metallographic examination failed to reveal any nodular pearlite; the results of the pole-figure analysis likewise indicate that no pearlite was present (pearlite will be shown to have an entirely different relationship) for all the diffraction spots were accounted for by one orientation relationship.

The results of the pole-figure analysis. after rotation into one quadrant of the stereographic projection to concentrate the data, are shown in Fig. 1. The three corners of the quadrant represent the cube. [100], directions in the original austenite. The triangles give the positions of the ferrite {110} poles required by the ideal lattice-orientation relationship proposed by Nishiyami, cited. The lines represent the observed reflections. It is felt that the experimental observations agree more closely with this relationship than with the Kurdjumow-Sachs relationship (which is the only other simple ideal relationship that approximates the observed orientations).

In order to provide stronger evidence, several X-ray exposures were taken with the specimen oriented with respect to the incident beam in such a manner that the reflection circles passed through the region shown in Fig. 2 (the reflection circles limiting the region investigated are shown

as dashed arcs). In the diagram. the ferrite {110} reflections resulting from the Nishiyami relationship are shown as triangles and those from the Kurdjumow-Sachs
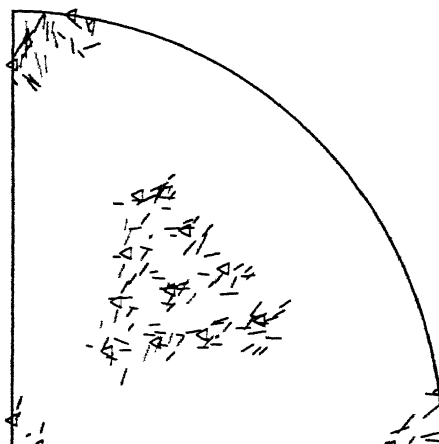
FIG. 1.—ONE QUADRANT OF FERRITE {110} POLE FIGURE FOR BAINITE FORMED BY TRANSFORMATION AT 450°C.
Triangles represent positions of {110} poles for Nishiyami relationship. Lines represent observed reflections.

relationship by circles. With the specimen oriented in this manner, four diffraction spots should be observed if the Nishiyami relationship is fulfilled and five should be observed if the Kurdjumow-Sachs relationship is fulfilled. Fig. 3 is a reproduction of an X-ray photogram, which shows only four spots (bracketed) for the 450°C. specimen when oriented in the manner described, thus confirming the Nishiyami relationship. The reflections from several such photograms taken at intervals of 2° are plotted as full lines in Fig. 2.

Bainite Formed by Isothermal Transformation at 350°C.—Single-crystal specimens held for 5 min. at 350°C. were not completely transformed, but 10 min. was sufficient for completion of the reaction.

One quadrant of the pole figure determined for the {110} ferrite planes is shown in Fig. 4. Here again the triangles, representing the required positions for the Nishiyami relationship, appear best to fit

the experimental data. The amount of scatter appears to be somewhat less than for the product formed at 450°C.

FIG. 2.—{110} FERRITE REFLECTIONS FOR 450°C. BAINITE IN REGION LIMITED BY DASHED ARCS OF CIRCLES.

Triangles give positions of {110} poles for Nishiyami relationship and circles for Kurd-jumow-Sachs relationship. Lines represent observed reflections.

FIG. 4.—ONE QUADRANT OF FERRITE {110} POLE FIGURE FOR BAINITE FORMED BY TRANS-FORMATION AT 350°C.

Triangles represent positions of {110} poles for Nishiyami relationship. Lines represent observed reflections.
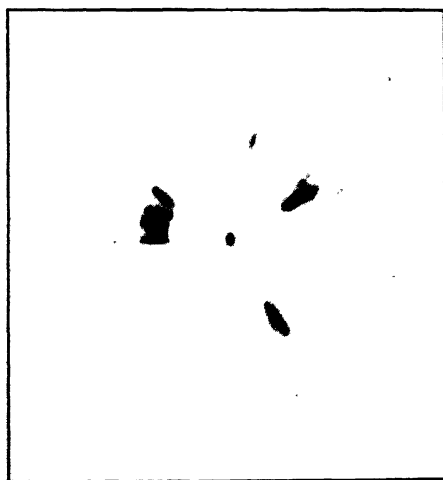
X-ray exposures taken at particular settings, as described, showed four spots, Fig. 5, to confirm the Nishiyami relation-

ship. The configuration of the X-ray photogram is identical with that for the 450°C. specimen, which is an indication that the

FIG. 3.—X-RAY PHOTOGRAM FOR 450°C. BAINITE.

Innermost streaks are {110} ferrite.

FIG. 5.—X-RAY PHOTOGRAM FOR 350°C. BAINITE.

orientation relationship with respect to austenite is the same in the two instances.

Bainite Formed by Isothermal Trans-formation at 250°C.—The time necessary

for completion of reaction at 250°C. was approximately 1½ hours.

One quadrant of the experimentally

FIG. 6.—ONE QUADRANT OF FERRITE {110} POLE FIGURE FOR BAINITE FORMED BY TRANSFORMATION AT 250°C.
Circles represent positions of {110} poles for Kurdjumow-Sachs relationship. Lines represent observed reflections.

FIG. 8.—ONE QUADRANT OF {110} MARTENSITE POLE FIGURE.
Circles represent positions of {110} poles for Kurdjumow-Sachs relationship. Lines represent observed reflections.

determined pole figure is shown in Fig. 6; the circles give the positions of the {110} ferrite reflections demanded by the Kurdjumow-Sachs relationship. This relationship

appears to fit the observations best, as shown more convincingly by the X-ray photogram of Fig. 7, with the specimen

FIG. 7.—X-RAY PHOTOGRAM FOR 250°C. BAINITE.

oriented as in the earlier instances. Five distinct streaks are evident.
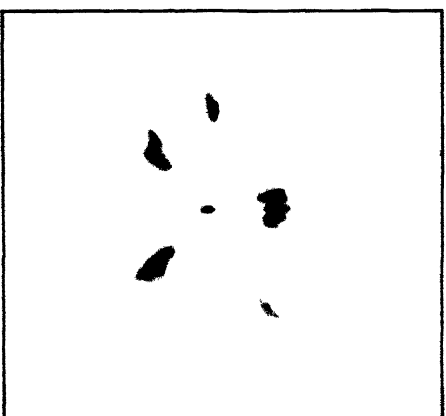
FIG. 9.—X-RAY PHOTOGRAM FOR MARTENSITE

MARTENSITE

The specimen used for the analysis of orientations in martensite was quenched in oil. Some concern was felt as to whether the tetragonal lattice of martensite would still be present after the grinding and polishing performed to reduce the thick-

ness of the specimen so that transmission Laue photograms might be prepared. An oscillation photogram with cobalt $K\alpha$ radiation, however, revealed the presence

FIG. 10.—REPRESENTATIVE PHOTOMICROGRAPH of COARSE PEARLITE. PICRAL ETCH. × 1500.

of a tetragonal lattice of axial ratio $\frac{c}{a} = 1.032$. (According to the investigations of Hägg,[19] the axial ratio of martensite in a steel of 0.80 per cent carbon should be 1.035.)

One quadrant of the experimentally determined pole figure is shown in Fig. 8. The circles, representing the Kurdjumow-Sachs relationship, appear to fit the observations satisfactorily. X-ray exposures taken at definite positions showed five streaks (Fig. 9).

PEARLITE

Pearlite Formed by Cooling in Furnace— Coarse Pearlite.—A photomicrograph representative of the pearlite structure obtained by cooling in the furnace is shown in Fig. 10. Apart from orientation differences, the X-ray photograms differed from those of bainite and of martensite by a greater vari-

ation in intensity of individual streaks. A typical photogram is reproduced in Fig. 11. It seems certain that many of these streaks were caused by diffraction from
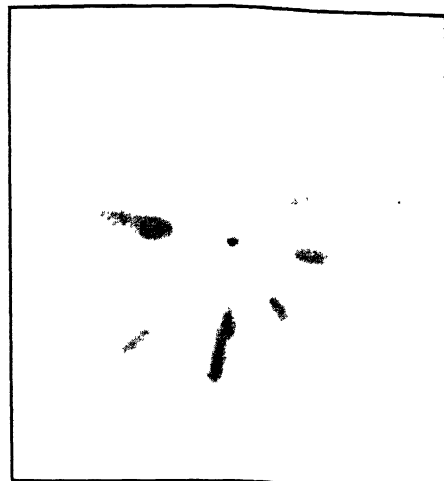
FIG. 11.—X-RAY PHOTOGRAM FOR COARSE PEARLITE.

cementite (see below). It was found, moreover, that in contrast with bainite and martensite, movement of the specimen in its own plane caused changes in the relative intensities of the streaks—occasionally new streaks appeared or old ones disappeared. This seems to indicate that a region of ferrite of a single orientation is greater in size than for the lower-temperature products. The reflections were sharper than those obtained by Mehl and Smith.[6]

All of these streaks, whether weak or intense, were plotted in a pole figure, one quadrant of which is shown in Fig. 12. (It will be shown that it is almost impossible to distinguish between reflections from a number of families of cementite planes and reflections from the ferrite {110} planes.) The circles and triangles of the plot give the positions of the {110} ferrite poles resulting from the two ideal relationships previously proposed.[6] The circles are for the relationship: $\{110\}_\gamma /\!/ \{112\}_\alpha$ and the $[112]_\gamma /\!/ [110]_\alpha$ triangles for the relationship:

$\{321\}_\gamma \mathbin{/\!/} \{331\}_\alpha$

$[331]_\gamma \mathbin{/\!/} [321]_\alpha$

Owing to the scatter in the data, it is difficult to decide between the two rela-
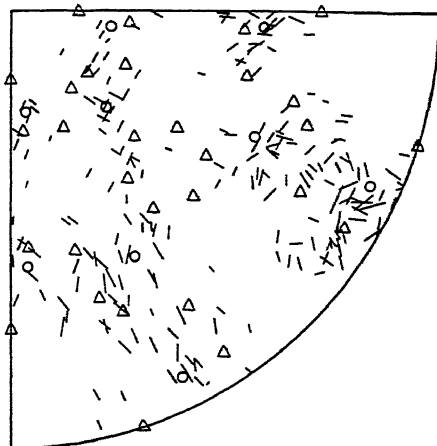
FIG. 12.—ONE QUADRANT OF $\{110\}$ FERRITE POLE FIGURE FOR PEARLITE FORMED IN FUR-NACE COOLING.

Circles and triangles show $\{110\}$ positions resulting from two ideal relationships given in text.

tionships, though the results appear slightly to favor the relationship represented by the circles. It was observed that in general the most intense diffraction streaks, when plotted on the projection, fell at positions near the circles of the diagram, and that the streaks weak in intensity plotted to other positions.

Pearlite Formed by Transformation at 580°C.—Fine Pearlite.—It was felt desirable to study both coarse and fine pearlite (whereas Mehl and Smith[6] had studied only the former) in order that the crystallographic data for pearlite might be made more complete.

The pearlite employed was relatively fine, formed by reaction at 580°C. for 45 sec., a time sufficient to permit complete transformation. Metallographic examination at 2500 diameters revealed that 5 to 10 per cent of the surface area was composed of resolvable pearlite. Undoubtedly, owing to the size of the specimen and the

rapid reaction rate, the specimen did not transform isothermally at the bath temperature.

The X-ray photograms of this specimen
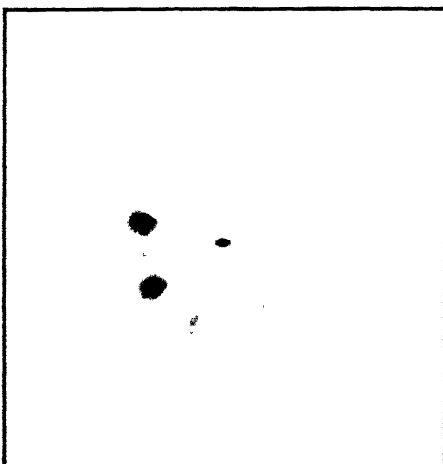
FIG. 13.—X-RAY PHOTOGRAM FOR FINE PEARLITE.

showed the streaks to be much more diffuse in appearance than for any of the earlier specimens. A typical photogram is shown in Fig. 13. One quadrant of a $\{110\}_\alpha$ pole figure plotted to one degree of intensity (the stronger of two estimated degrees) is shown in Fig. 14; the circles and triangles represent the same relationships as plotted in Fig. 12. The results again appear to be in better agreement with the relationship represented by the circles than with that represented by triangles.

DISPOSITION OF THE CEMENTITE

A determination of the orientations of the cementite in the various reaction products with respect to the parent phase would be welcome, for it would complete the crystallographic information for these transformations. Cementite exists in pearlite as alternate lamellae separated by ferrite, and in tempered martensite as discrete particles or globules, but some confusion exists as to its mode of distribu-

tion in the bainites; it would likewise be pleasant to have further light upon this latter point.

The experimental determination of the
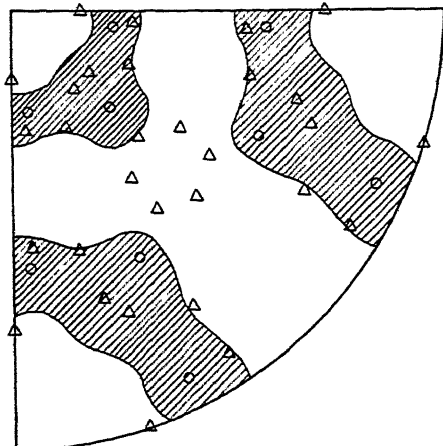
FIG. 14.—ONE QUADRANT OF {110} FERRITE POLE FIGURE FOR FINE PEARLITE.
Circles and triangles show {110} positions resulting from two ideal relationships given in in text.

cementite orientation relationships by X-ray diffraction methods is difficult, and the authors' efforts in this direction were not successful. It is to be expected that the reflections from the cementite of a eutectoid steel should be somewhat less intense than those of ferrite because of the small structure amplitude of the carbon atom (compared to iron), the complexity of the orthorhombic cementite lattice, and because cementite occupies less volume in the reacted steel than does ferrite. Moreover, consideration of the possible cementite reflections that may occur reveals a multiplicity, with many of the reflections coincident with reflections of ferrite. Hendricks[20] has observed, for example, that strong reflections from a cementite crystal occurred at d values (interplanar spacings) of 1.97, 2.01, 2.03, 2.06, and 2.10Å.; the d value for {110} ferrite is 2.02. In pole-figure work, it is almost impossible to distinguish (except possibly in intensity)

between diffraction streaks from ferrite {110} planes and those from a number of cementite planes.

In the work described in the preceding section, it was found that all of the diffraction streaks on the X-ray photograms of bainite could be accounted for by reflection from ferrite; the coarse pearlite, however, provided some streaks that might have originated from cementite. Such evidence may be found in the X-ray photogram of Fig. 11; the inner reflection circle, {110}, shows a slight difference in the position of the absorption edge (the sharp intensity change) on the various streaks. This behavior was observed in a number of photograms for this sample (and to a somewhat less pronounced degree in the fine pearlite specimen), but it was not observed in any of the photograms of bainite or martensite. A difference in absorption edge of this sort can be caused by diffraction from more than one lattice or by a large "grain size" in the specimen (two crystals of like orientation separated by a slight distance may reflect to different positions). The latter possibility seems unlikely in view of the fineness of the structure. More convincing proof that this possibility can be excluded was obtained by moving the specimen in its own plane to find that the displaced absorption edges still occurred. This observation, it is felt, offers rather strong proof that cementite reflections of sufficient intensity to be visible on the X-ray photogram—and thus render difficult the determination of the orientation relationship for the ferrite —did occur in the pearlite specimen.

If it is accepted that cementite reflections are observed in X-ray diffraction from pearlite, it is then reasonable to inquire why they were not observed for bainite. Long exposures (48 hr. as compared to the usual 8 to 12 hr.) were made of all the samples (including pearlite and martensite) to determine whether the cementite reflections might be observed in the photograms

of bainite and whether any new streaks might arise in the pearlite photograms. No new streaks were observed for the pearlite but (Fig. 15) new streaks, much less intense

FIG. 15.—X-RAY PHOTOGRAM FOR 450°C. BAINITE. EXPOSURE 48 HOURS.
Note streaks of low intensity in region of ferrite {110} reflection circle.

than the original ones, appeared for bainite: no new streaks appeared in the photograms of martensite. These new streaks from bainite exhibited about the same relative intensity for all the bainite specimens.

The martensite specimen was tempered for 12-hr. periods at increasing temperatures in intervals of 50°C. Some slight indication of the presence of low-intensity streaks was observed for tempering at 200°C. Streaks were clearly evident for tempering at 250°C., and were of the same relative intensity as those for the bainite specimens. It seems evident that these low-intensity streaks must represent diffraction from the cementite in the various reaction products.

The low intensity of cementite reflections in bainite and in tempered martensite is probably to be attributed to the difference in the mode of distribution of carbide in these structures compared with that in pearlite. A small particle size should cause a reduction in the intensity and sharpness of the diffraction streaks. The carbide present

in the tempered martensite structure (for low tempering temperatures—up to 250°C.) must be in a very finely dispersed state. A high degree of dispersion of the cementite.
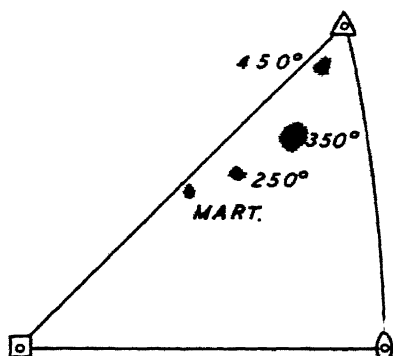
FIG. 16.—HABIT PLANES FOR BAINITE AND MARTENSITE STRUCTURES.

then, might be said to be the reason for the low intensity of the cementite streaks in the tempered martensite, and since the intensities of the streaks for the bainites are comparable with those for the tempered martensite, and much less than those for pearlite, it is not unreasonable to conclude that the cementite in the bainite structures is in a fairly fine state of dispersion, much finer than that in pearlite and similar to that in tempered martensite.

A finite and limited number of orientations of cementite was found in each of the samples—coarse pearlite, bainite, and tempered martensite—as shown by exposures taken with the specimen moved in its own plane. By comparison of the positions of the streaks, it was determined that these orientations were identical for the 450°C. and 350°C. bainite specimens and for the 250°C. bainite and the tempered martensite specimens.

ORIENTATION HABITS

Bainite and Martensite.—An average of some 10 to 15 measurements of each trace direction (the deviation from the average was ± 2° at the most and generally was less) was used for the evaluation of the habit

plane for each of the structures. The results are shown in the unit stereographic triangle of Fig. 16. They are in good agreement with those of Greninger and Troiano.[13]
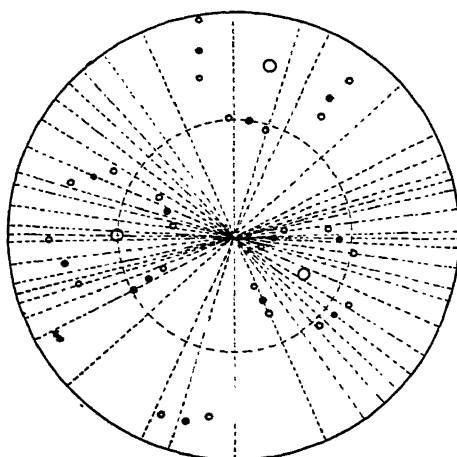
FIG. 17.—STUDY OF HABIT PLANE IN PEARLITE.
Large circles give positions of austenite {100} poles; small open circles give positions of austenite {521} poles; small filled circles give positions of austenite {722} poles. Trace normals are shown as dotted lines. Dotted circle represents angle subtended by range of pearlite spacing measured.

Pearlite.*—An attempt was made to determine the habit plane for pearlite by trace-normal studies. The pearlite used was formed on slow cooling. Only the fine straight lamellae were measured. In the plot of Fig. 17, the measured trace normals are shown as dotted lines on the stereographic projection of the austenite matrix (whose cube poles are given by the large circles). Earlier investigations[7,13] have suggested that the habit plane of proeutectoid cementite may be $\{521\}_\gamma$ or $\{722\}_\gamma$, and in view of the determined lattice relationships for ferrite in pearlite (which indicate cementite to nucleate pearlite—see discussion below) the poles of these families of planes were plotted on the projection;

$\{52\overline{1}\}_\gamma$ poles are shown as small open circles, $\{722\}_\gamma$ poles by small filled circles.

An attempt was made to limit the number of poles involved in the solution by considering the angle subtended by the range of pearlite spacing used for measurements.* This angle was found to be $55°$; it is plotted in Fig. 17 as a dotted circle concentric with the basic circle.

Because 22 traces are involved, it appears that some 24-plane family is a solution. By combining adjacent traces it is possible to reduce the number of traces, but reduction below 12 traces appears improbable. Many of the trace normals are satisfied by some pole of the $\{521\}_\gamma$ family and some by a pole of the $\{722\}_\gamma$ family. It is not possible, though, because of the scatter, to say that the 24-plane family $\{521\}_\gamma$ is the habit plane of pearlite, because a great many other families of planes may have given similar solutions.

METALLOGRAPHIC OBSERVATIONS CONCERNING FORMATION OF BAINITE

A brief metallographic study was made in an attempt to decide whether the bainite structures form by a process of nucleation and growth or whether the plates spring full-formed from the matrix lattice as they do in the transformation to martensite. It is felt that the metallographic studies to be described provide proof that the bainite structures form by a nucleation and growth process at all temperatures between that at which pearlite forms and that at which martensite forms.

The steel used is the same as that for the earlier work. The austenitizing treatment consisted in holding for ½ hr. at 900°C. Reaction was performed in a lead or salt bath and the specimens were quenched in water after holding for various times at the reaction temperature.

---

* The authors are indebted to Mr. R. A. Colton, of the Metals Research Laboratory, for assistance in this analysis.

* Since the pearlite was formed over a range of temperatures, this angle can be only an approximation.

The photomicrograph of Fig. 18 illustrates the characteristic feathery-like bainite that forms at temperatures immediately under the knee of the S-curve. This structure was found in a specimen reacted at limited regions* a definite proof would require a statistical consideration of sizes on the plane of polish.

This difficulty is not encountered with

FIG. 18.—STRUCTURE ILLUSTRATING PROGRESS OF TRANSFORMATION AT 495°C. NITALETCH. × 1500.

ture was found in a specimen reacted at 495°C. for 3 sec. Transformation is very rapid at this temperature—a specimen held for 8 sec. was completely transformed—and it is unlikely that the specimen reacted at this temperature; numerous nodules of pearlite were observed. The characteristics of the structure shown in Fig. 18 suggest strongly that bainite produced at high temperatures forms by a process of nucleation and growth: (1) it protrudes toward the center of the grain from the grain boundary—nucleation in processes of nucleation and growth is predominantly at the grain boundary; (2) the plates narrow to a wedge point, resembling proeutectoid ferrite, which is known to form by nucleation and growth. More conclusive proof would be furnished by a demonstration that the sizes of the reacted regions increase with increased reaction time; metallographic study seemed to show this to be true, but because the structure for such high reaction temperatures is confined to

bainite formed at lower temperatures, for reaction proceeds more generally throughout the austenite grain. Figs. 19 and 20 illustrate the progress of transformation at 250°C. for holding times of 6 and 10 min., respectively. The length and thickness of the plates are clearly seen to increase with increased holding time, a definite indication of progressive growth.

Figs. 21 and 22 show the progress of transformation at 200°C. A striking difference is to be seen between the structures of Figs. 20 and 21; the "needles" have become thicker for the lower temperature. However, with increased holding time at 200°C., narrow "needles," similar to those of the 250°C. bainite, are seen to form (Fig. 22), while the number of thick "needles" remains approximately the

* Feathery bainite forms largely if not exclusively at the austenite grain boundaries in the form of bundles of plates, and only at such high reaction temperatures that recalescence permits the formation of pearlite after only a small amount of bainite has formed.

same. The temperature of 200°C. is within the martensite temperature range,[11] therefore it seems likely that the thick plates are actually martensite, which formed on cooling or very rapidly at the bath temperature, between habit and orientation relationship, first discussed in the study of the Widmanstätten figure formed on the precipitation of alpha brass from beta,[21] is pronounced in the case of bainite.*
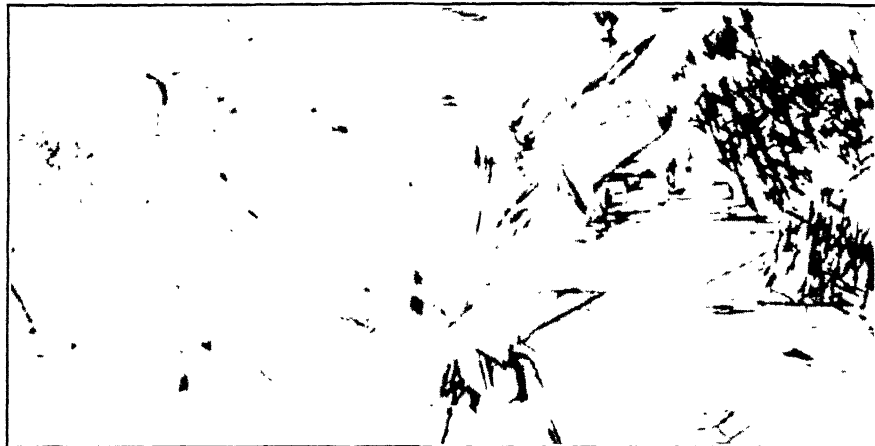
FIG. 19.   FIG. 20.
FIGS. 19 AND 20.—BAINITE FORMED ON HOLDING AT 250°C. NITAL ETCH. × 750.
Fig. 19. Held for 6 minutes. Fig. 20. Held for 10 minutes.

and which has had time to temper and become visible. The thinner plates, which form with increased holding time, then, represent a structure of the bainite type forming by a process of nucleation and growth. This is in conformity with the dilatometric curves of Davenport and Bain,[1] which show two stages of transformation for temperatures in the neighborhood of 200°C.

DISCUSSION OF RESULTS

Although this is essentially an experimental paper, several of the findings deserve comment. Most striking, perhaps, is the clear showing that even though the habit (composition) plane of bainite changes markedly with the temperature of formation, the orientation relationships between the ferrite in bainite and the parent austenite are nearly fixed (the orientation difference between the Nishiyami and the Kurdjumow-Sachs relationships is but 5°) This apparent lack of correlation

It is now certain that the orientation relationships may be relatively simple but that the habit plane may be relatively complex. And it is clear, moreover, that the atom movement or shearing mechanism that converts the lattice of the parent phase into the lattice of the resultant phase cannot be chosen with certainty on the basis of the orientation relationship alone. Greninger and Troiano[13] pointed out that the habit plane of bainite formed at low temperatures approaches that of proeutectoid cementite whereas that of bainite formed at high temperatures approaches that of proeutectoid ferrite, suggesting that the cementite lattice exercises a preponderant effect in the former case and the ferrite in the latter. Yet it will be observed that the orientation relationships change but slightly throughout. The matter evidently is complex; apparently different sets and

* See discussion of habit and orientation relationship by Sachs and by Mehl in the discussion of ref. 13.

different sequences of shearing operations are required to give a variation in habit plane while maintaining a similar orientation relationship (cf. ref. 17), but the prin-

by the relative intensities of X-ray diffraction. It is not possible, accordingly, to extrapolate the dimensions of the ferrite in pearlite to lower temperatures, as sug-
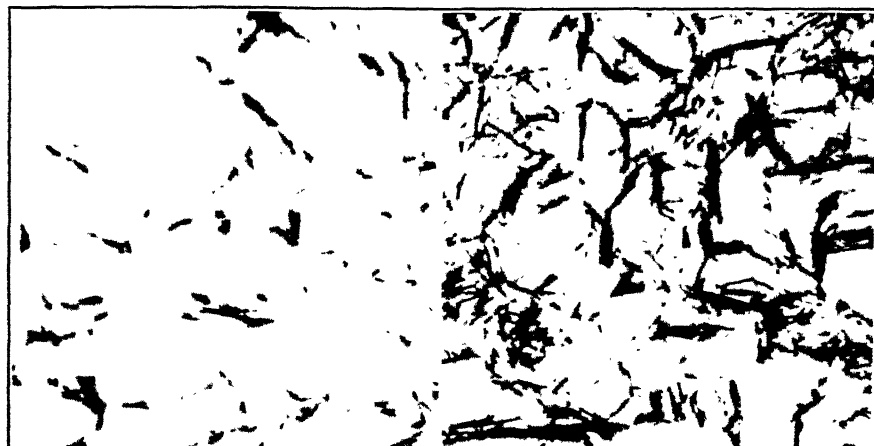
FIG. 21.   FIG. 22.
FIGS. 21 AND 22.—STRUCTURE RESULTING FROM HOLDING AT 200°C. NITAL ETCH. X 750
Fig. 21. Held for 15 minutes. Fig. 22. Held for 50 minutes.

ciples that determine the selection of these shearing mechanisms are not well understood.

The orientation relationship of ferrite in pearlite (both fine and coarse) with respect to the parent austenite is quite different from that exhibited by bainite and by martensite, and it will be well to explore this difference.

The orientation of ferrite in bainite with respect to austenite for bainite formed at high temperature, and the habit plane of this bainite, are identical crystallographically with those for proeutectoid ferrite. Proeutectoid ferrite, and bainite also, form by a process of nucleation and growth; since proeutectoid ferrite is necessarily nucleated by ferrite, it may be concluded that ferrite nucleates bainite formed at high temperatures. It is interesting that the size of the ferrite particles in bainite appears to be much greater than for ferrite in pearlite formed at temperatures just above the S-curve knee, as shown by microscopic evidence,[3] and as shown herein

gested earlier.[2] Cementite, however, shows the opposite behavior: the X-ray reflections from cementite in pearlite are much stronger than those from cementite in bainite; the particle size of cementite in bainite must be very small indeed.[*] There is ample reason to believe[1] that ferrite precipitates first in bainite as a supersaturated solid solution and that cementite precipitates later from this supersaturated solid solution. The platelike structure of bainite argues for this point of view, for platelike structures are normal in reactions when a single constituent forms.

The circumstances attending the formation of pearlite are quite different. The orientation relationship between ferrite in pearlite and the parent austenite precludes the operation of ferrite as the nucleating agent, and thus points to cementite as the nucleus.[6] After nucleation, growth is bipartite. With cementite and ferrite grow-

* See comments on this point based on electron-microscope photomicrographs of bainite, ref. 3.

ing concomitantly, platelike structures do not form; this seems to be generally true. The lamellae of pearlite frequently are wavy, and this must be attributed, it would seem, to factors inherent in bipartite growth. This robs the direction of the lamellae of precision in crystallographic position, though the study of the orientation of the plane of the lamellae included here at least suggests that the plane is of high index, as would be expected if the habit were determined by the precipitation of cementite.

SUMMARY

1. The orientation relationships between the ferrite in bainite and austenite were determined in a plain carbon eutectoid steel by the pole-figure method. Bainite formed at 450°C. and 350°C. displayed the Nishiyami relationship; bainite formed at 250°C. displayed the Kurdjumow-Sachs relationship.

2. Martensite was shown to exhibit the Kurdjumow-Sachs relationship.

3. The orientation relationships between the ferrite in both coarse pearlite (formed at high temperatures) and fine pearlite (formed near the knee of the S-curve) with respect to austenite were determined by the pole-figure method. Both showed the same relationship, identical with that determined earlier for coarse pearlite.[6]

4. X-ray diffraction effects from the cementite in pearlite, bainite, and tempered martensite were obtained, but the orientations of cementite were not determined. The diffraction from cementite in bainite is weaker in intensity than that in pearlite and similar in intensity to that in tempered martensite; this is taken as showing that cementite in bainite must be in a very fine state of subdivision.

5. The habit (composition) planes of bainite formed at several temperatures and of martensite were determined, confirming the previous work of Greninger and Tro-

iano. The habit plane varies markedly with the temperature of reaction though the orientation relationships remain nearly fixed.

6. The habit plane in pearlite was studied stereographically. The plane could not be determined but the evidence points to a plane of high index.

7. Metallographic studies suggest that bainite forms by a process of nucleation and growth.

REFERENCES

1. E. S. Davenport and E. C. Bain: *Trans.* A.I.M.E. (1930) 90, 117. See also subsequent papers from U.S. Steel Research Laboratory.
2. R. F. Mehl: Hardenability of Alloy Steels. Amer. Soc. for Metals (1938) 1.
3. R. F. Mehl: Sixteenth Campbell Memorial Lecture. Amer. Soc. for Metals, Oct. 1941.
4. H. C. H. Carpenter and J. M. Robertson: *Jnl.* Iron and Steel Inst. (1932) 125, 309.
5. F. C. Hull and R. F. Mehl: Preprint, Amer. Soc. for Metals (Oct. 1941).
6. R. F. Mehl and D. W. Smith: *Trans.* A.I.M.E. (1935) 116, 330.
7. R. F. Mehl, C. S. Barrett and D. W. Smith: *Trans.* A.I.M.E. (1933) 105, 215.
8. N. T. Belaiew: Discussion. *Jnl.* Iron and Steel Inst. (1932) 125, 330.
9. W. L. Fink and E. D. Campbell: *Trans.* Amer. Soc. Steel Treat. (1926) 9, 717.
10. G. Kurdjumow and G. Sachs: *Ztsch. Phys.* (1930) 64, 325.
11. J. M. Robertson: Discussion. *Trans.* A.I.M.E. (1930) 90, 117.
12. N. T. Belaiew: *Jnl.* Inst. Metals (1923) 29, 379.
13. A. B. Greninger and A. R. Troiano: *Trans.* A.I.M.E. (1940) 140, 307.
14. Z. Nishiyami: *Sci. Repts.* Tohoku Imp. Univ. (1934) 23, 637.
15. G. Wassermann: *Mitt.* K. W. Inst. Eisenforschung (1935) 17, 149.
16. R. F. Mehl and G. Derge: *Trans.* A.I.M.E. (1937) 125, 482.
17. A. B. Greninger and A. R. Troiano: *Trans.* A.I.M.E. (1941) 145, 289.
18. C. S. Barrett: *Trans.* A.I.M.E. (1937) 124, 48.
19. G. Hägg: *Jnl.* Iron and Steel Inst. (1934).
20. S. B. Hendricks: *Ztsch. Kristallog.* (1930) 74, 534.
21. R. F. Mehl and O. T. Marzke: *Trans.* A.I.M.E. (1931) 93, 123.

Hardenability Calculated from Chemical Composition

By M. A. Grossmann,* Member A.I.M.E.

(New York Meeting, February 1942)

Abstract

The hardenability of most steels can be predicted within 10 to 15 per cent provided the complete chemical composition is known, including "incidental" elements; and provided the as-quenched grain size is known; and provided, finally, that the composition and heating temperatures for hardening are such as to result in austenite free from carbide particles. In the method proposed herein, the steel is considered as having a base hardenability due to its carbon content alone (the hardenability of a "pure steel" of the given carbon content, without any other elements), and this base hardenability is multiplied by a multiplying factor for each chemical element present. After multiplying all these together, the final product is the hardenability. Grain size may be taken into account either in the base hardenability or after the multiplication. Hardenability is stated in terms of "ideal critical diameter", namely, the diameter of bar, in inches, that will just harden all the way through (absence of unhardened core) in an "ideal" quench, and the calculation may also be related to the Jominy test.

The data bring out certain features rather clearly. For example:

1. It is quite useless to attempt to predict hardenability unless all elements, including "incidentals," are known; thus an "incidental" chromium content of 0.20 per cent increases the hardenability by about 50 per cent.

2. The relative effectiveness of different alloys is sometimes unexpected; thus molybdenum when calculated in this way appears to be of the same order of effectiveness as manganese, rather than much more powerful, as would appear to be common experience; observe that

an increase from *no* manganese to 0.20 per cent Mn provides a multiplying factor of 1.67, and an increase from no molybdenum to 0.20 per cent Mo provides a factor of 1.63, an increase of over 60 per cent in each case. However, if to a steel containing 0.50 per cent Mn there is added "20 points of manganese," the factor is raised from 2.65 (for 0.50 per cent Mn) to 3.35 (for 0.70 per cent Mn), or an increase of only 26 per cent. Thus the first small addition of an element has a much more powerful percentage effect than an equal further addition when some is already present, and in most cases the effect of molybdenum is considered in relation to a steel in which molybdenum is absent.

3. If two elements are equally effective, a greater hardenability will be obtained by using, for example, 0.5 per cent of each than by using 1.0 per cent of either of them alone.

4. A knowledge of the as-quenched grain size is essential for precise work, since a difference of only one grain size number (say No. 7 instead of No. 6) makes a difference of almost 10 per cent in hardenability (in these units); this, however, does not apply to certain steels of high hardenability.

It should be emphasized that in chromium steels (over 0.30 per cent Cr) and chrome-molybdenum and chrome-vanadium steels, undissolved carbides are likely to be present in the steel as quenched, and that in such cases the charts can indicate only a maximum possible hardenability, whereas the extent of hardening actually obtained may be much less. Thus tests on a number of chrome-molybdenum steels have indicated a degree of hardening amounting to only 50 to 65 per cent of the maximum possible, and in chromium steels from full hardening (100 per cent) down to as low as 70 per cent. On the other hand, when the amount of such elements is small (Cr under 0.30 per cent, Mo up to 0.25 per cent in the

absence of Cr, and V up to 0.04 per cent), the charts provide reasonable approximations.

The precise figures on the charts are suggested as tentative, subject to some modification as more data accumulate, but the fundamental concept appears to be supported by tests made on a wide variety of steels, a few of the correlations being shown in Fig. 1.

INTRODUCTION—THE USE OF THE CHARTS

For those who may wish to calculate the hardenability of steels, without going through the intricacies of the derivations of the charts, it may be said at the outset that the actual calculation of hardenability by this method is extremely simple. It involves merely reading a factor from a chart for each chemical element present in the steel, and multiplying these factors together, the product being the hardenability. The latter is expressed as "ideal critical diameter," D_I, which has been defined[5] as the diameter of bar that just hardens all the way through in an ideal quench.

By way of explanation and review, it may be said that "hardening all the way through" means that the bar appears fully hardened throughout *when judged by a fracture or etch test;* the critical diameter is *just* hardened through, so that any larger size would show an "unhardened core" in a fracture or etch test. This means that the critical diameter is just half-hardened at the center (50 per cent martensite). The "ideal" quench is a perfect quench, in which the outside of the bar is instantly cooled to the temperature of the quenching medium, a condition that is never quite attained in practice, it is true, but which is a very useful reference point, as will presently be illustrated. To sum up, then, the calculations in this paper will estimate the hardenability of a steel in terms of "ideal critical diameter, D_I", which is the diameter of a bar of that steel that will just harden all the way through (as judged by fracture or

etch test) in the severest possible or ideal quench. This may be stated also in terms of the Jominy test by using Fig. 27 for conversion.

Suppose a steel has the chemical composition shown in Table 1, its as-quenched grain size being No. 7 (A.S.T.M.). The

TABLE 1.—*Example of Readings from Charts*

Element	Percentage in Steel	Factor
Carbon grain size 7.............	0.50	0.24
Manganese.....................	0.90	4.00
Phosphorus....................	0.020	1 05
Sulphur.......................	0.029	0 98
Silicon.......................	0.10	1.10
Nickel........................	0.28	1 10
Chromium.....................	0.30	1.70
Molybdenum...................	0.05	1.16
Copper.......................	0.05	1.02
Product.......................		2.40

factors shown in the last column of this table were read from the charts. Thus on the carbon chart, Fig. 18, at 0.50 per cent carbon read up to the line for grain size No. 7 and the value shown at the left is found to be 0.24 in. On the manganese chart, Fig. 14, the factor for 0.90 per cent Mn is found to be 4.00. Similarly, for 0.020 per cent P, the factor on the phosphorus chart, Fig. 4, is found to be 1.05, and in similar manner the factor is found for each element present.

These factors in the last column of the table are simply multiplied together, and the product is found to be 2.40. This means that the "ideal critical diameter" is 2.40 in.; or, in other words, it is estimated that a bar of that diameter of the stated composition at the stated grain size will just harden all the way through (absence of unhardened core) in an ideal (severest possible) quench.

For the behavior in any actual quench, it is necessary, of course, to know at least approximately the severity of quench employed. Thus still water is known to have a quenching severity approximately $H = 0.9$
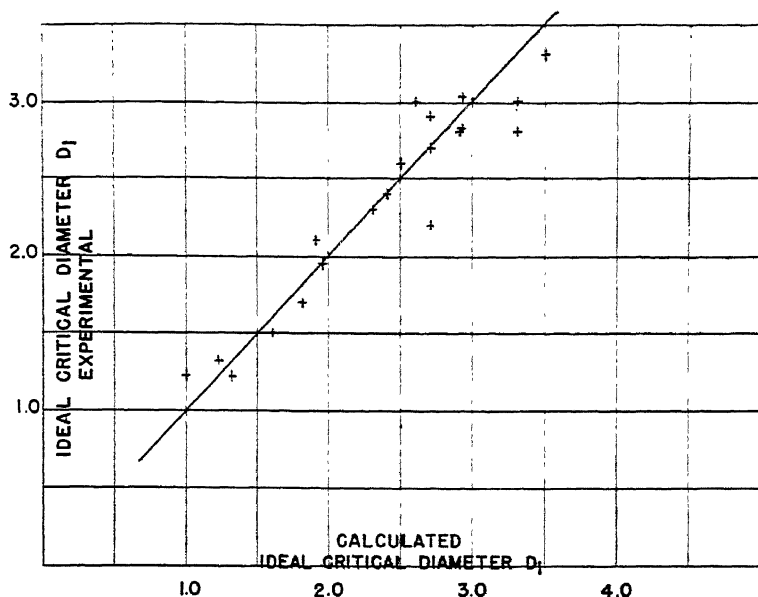
FIG. 1.—DATA ON A VARIETY OF STEELS, SHOWING RELATIONSHIP BETWEEN CALCULATED
HARDENABILITY AND THAT FOUND BY EXPERIMENT.
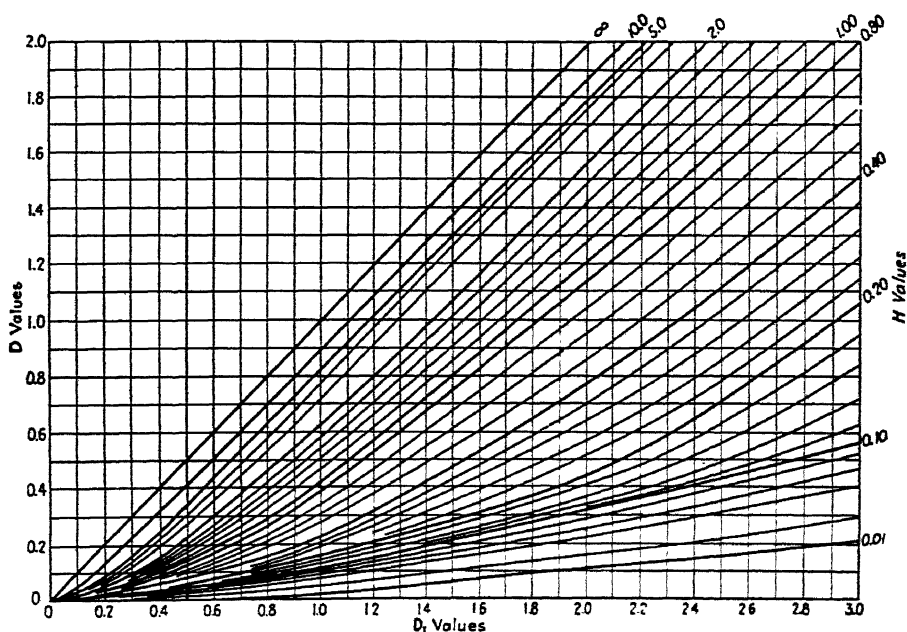
FIG. 2.—CHART FOR ESTIMATING CRITICAL DIAMETER IN ANY ACTUAL QUENCH OF KNOWN SEVERITY
WHEN HARDENABILITY OF A STEEL IS KNOWN IN TERMS OF IDEAL CRITICAL DIAMETER D_I.

to $H = 1.0$, and Fig. 2 shows that the steel of Table 1 in such a water quench would just harden through in a bar of about $1\frac{1}{2}$-in. diameter. This is found in Fig. 2 by reading the value 2.40 in. on the base line of abscissas marked D_I, reading straight up until it intersects the diagonal line for severity of quench, which (at the upper right) is marked 1.0, and from the intersection reading at the left the value 1.55 in. Or a moderately agitated oil quench is known to have a severity about $H = 0.4$. In Fig. 2, again upon reading from the abscissa D_I at the value 2.40, directly upward till it intersects the diagonal $H = 0.40$, and reading from the intersection over to the ordinate at the left, indicates a value about 1.05 in., meaning that in such an oil quench the steel of Table 1 would just harden all the way through (absence of unhardened core) in a bar a little over an inch in diameter.   .

A section at the end shows the relation of these data to the Jominy test, Fig. 28. In the present instance, the ideal critical diameter having been estimated as 2.40 in., consult Fig. 28 and find that this corresponds to a "Jominy distance" of about 0.36 in. Therefore, when such a steel is tested in a Jominy test, it would be half-hardened at about 0.36 in.; or, in other words, the hardness will have dropped off to about 48 to 50 Rockwell C at about 0.36 in. from the end of the Jominy bar.

DEVELOPMENT OF FORMULA AND CHARTS

A number of formulas have been suggested in the past for expressing the effects of elements on the strength, hardness or hardenability of steel. Among the more recent ones are that by Herty[1] for a hardness factor, and those by Burns, Moore and Archer[2] and Burns and Riegel[3] for hardenability.

In all prior proposals (as far as we are aware), the effects of the different elements were considered to be additive—that is, a

quantity was assigned for each element and the sum total represented the value sought. The scheme of multiplying, however, has been used in the computation of strength as a function of carbon and manganese content. The present system is based on the concept that a pure iron-carbon alloy (a "pure steel," other elements entirely absent) has a certain hardenability, and that each additional element (Mn, Si, etc.) is represented by a multiplying factor by which the base hardenability is multiplied. The total hardenability of the steel would then be the product of all the factors, one for each chemical element present in the steel, with a proper correction for grain size.

It may be mentioned that the clue to this behavior was obtained in two circumstances: (1) In studying the effect of very small additions of elements, it was striking that the hardenability was increased more than would be expected from a mere additive effect, and (2) in studying the effect of grain size, it had already been found[6] that a change in grain size introduced a multiplying factor for the hardenability. The following discussion indicates how the factors for alloys were developed.

Carbon

The proposed system begins with the hardenability of pure iron-carbon alloys, then applies a multiplying factor for each other element present. In the development of the data, however, pure iron-carbon alloys were not available, so it was necessary to develop first the factors for the elements commonly present in steel. The development of the carbon data will be found following the section on manganese.

Phosphorus

Coming, therefore, to the multiplying factors to be used for the different alloying elements, it will be recalled that the present scheme involves the hypothesis that the presence of a certain amount of chemical

(alloying) element multiplies the harden-ability by a certain factor; as, for example,

hardenability would be 5 per cent greater than if no phosphorus were present. In the
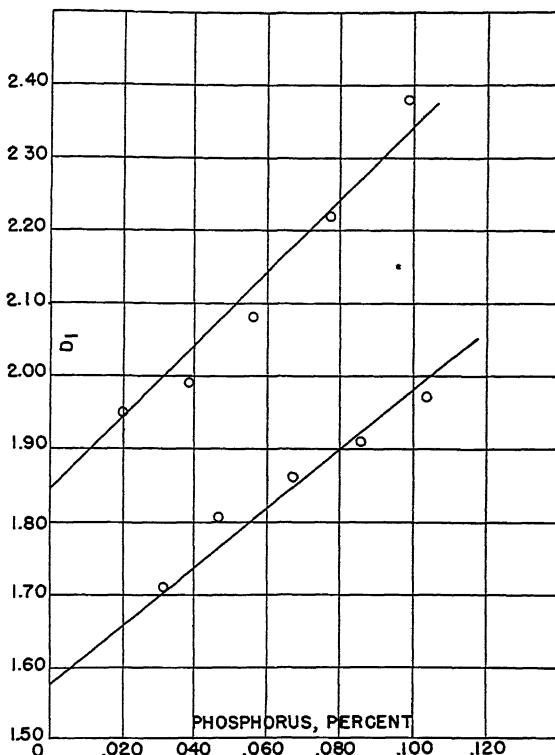
FIG. 3.—EFFECT OF PHOSPHORUS CONTENT ON HARDENABILITY, DETERMINED EXPERIMENTALLY.
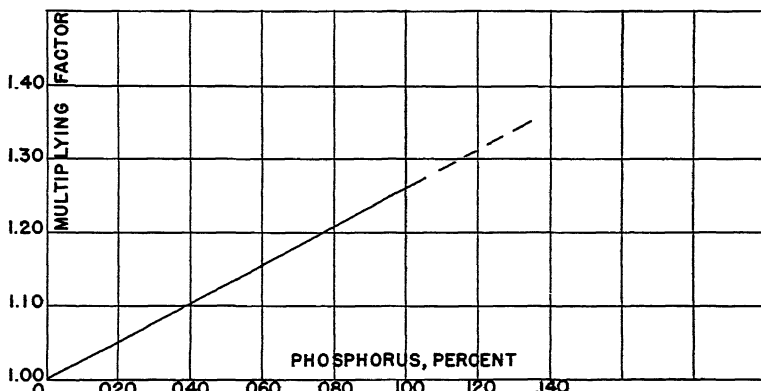
FIG. 4. MULTIPLYING FACTOR FOR CALCULATION OF EFFECT OF PHOSPHORUS ON HARDENABILITY.

that the presence of 0.020 per cent P in any steel would introduce a multiplying factor of, say, 1.05, meaning that the

experimental work on phosphorus, the effect of phosphorus was studied[5] in each of two steels, adding phosphorus to successive

ingots so that in each series the steels were identical except as to phosphorus content. The two steels had different hardenabilities, thus affording an opportunity to test the hypothesis of a "multiplying factor"; that is, in the steel of greater hardenability, the numerical increase in D_I due to phosphorus should be greater. The compositions of the two steels were as shown in Table 2.

This increase from 1.574 to 1.980 is an increase of 26 per cent in the value of D_I, for a phosphorus addition of 0.100 per cent. An increase of 26 per cent means, of course, a multiplying factor of 1.26, which is the factor shown in Fig. 4 for a phosphorus content of 0.100 per cent.

A question might well be raised as to how good the evidence is that the relationship is

TABLE 2.—*Steels for Study of Effect of Phosphorus*

Composition, Per Cent								Average Grain Size No.	Ideal Diameter, D_I
C	Mn	P	S	Si	Ni	Cr	Cu		
0.62	0.98	0.020	0.018	0.22	0.05	0.05	0.02	4.5	1.95
0.62	0.98	0.038	0.018	0.22	0.05	0.05	0.02	4.5	1.99
0.62	0.98	0.056	0.018	0.22	0.05	0.05	0.02	4.5	2.08
0.62	0.98	0.077	0.018	0.22	0.05	0.05	0.02	4.5	2.22
0.62	0.98	0.097	0.018	0.22	0.05	0.05	0.02	4.5	2.38
0.63	0.94	0.031	0.027	0.20	0.03	0.05	0.02	7	1.71
0.63	0.94	0.047	0.027	0.20	0.03	0.05	0.02	7	1.81
0.63	0.94	0.067	0.027	0.20	0.03	0.05	0.02	7	1.86
0.63	0.94	0.086	0.027	0.20	0.03	0.05	0.02	7	1.91
0.63	0.94	0.104	0.027	0.20	0.03	0.05	0.02	7	1.97

From the quenching experiments, the hardenabilities were deduced in terms of ideal diameter, and the results are plotted in Fig. 3 as ideal diameter D_I against phosphorus content. Two straight lines, one for each steel, are drawn to represent the increase in hardenability due to phosphorus. The slopes of these lines are such that the increase due to phosphorus is the same percentage in the high-hardenability steel as in the low-hardenability steel, and the points are not too far from these straight lines. Indeed, of the 10 points plotted, the one farthest away from either of the lines is less than 2.5 per cent away from the line in terms of D_I, which certainly is within the limits of expected experimental error. Fig. 3 thus provided the basis for Fig. 4, which shows the effect of phosphorus on hardenability in terms of a factor. For example, in Fig. 3 the extrapolated line at 0.0 per cent P shows a value $D_I = 1.574$ and the same steel at 0.100 per cent P shows a value $D_I = 1.980$.

a straight line as shown in Fig. 4. To this it can only be replied that with the data at hand a straight-line relationship expresses the factors as well as any other form of curve that might be drawn, and the accuracy of hardenability testing is not sufficiently good to warrant drawing small deviations that might be indicated. Furthermore, for manganese, to be described later, the straight line drawn in that case has been tested and found valid for a large number of heats at the extreme high end of the range, indicating that even with such large amounts of that element the straight-line relationship is still valid. It is true that for silicon and some other elements a curved line is indicated, in which the element becomes less effective as larger amounts are added, so that at large amounts the curve lies below the straight-line relationship, but the data indicate a straight-line relationship to be valid in many cases.

Sulphur

Sulphur lessens the hardenability of steel, and it is presumed to act in this

The tests were carried out on steels of the compositions shown in Table 3. The data are shown in Fig. 5 as D_I vs. sulphur
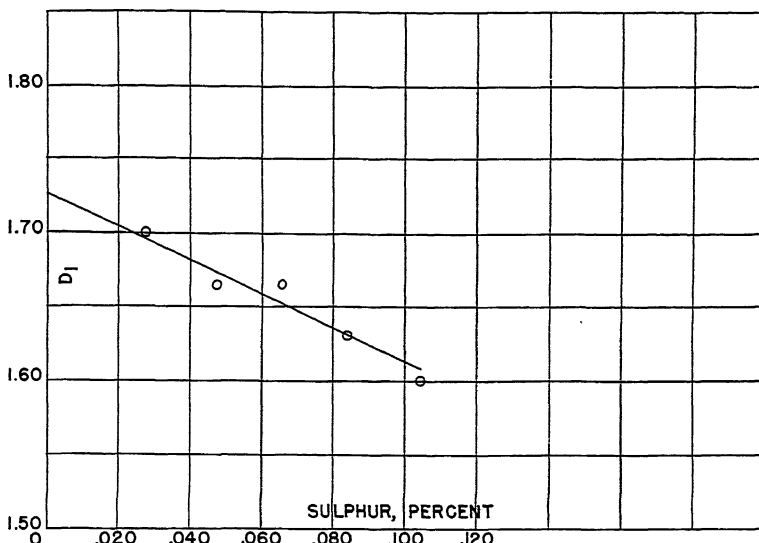

FIG. 5.—EFFECT OF SULPHUR CONTENT ON HARDENABILITY, DETERMINED EXPERIMENTALLY.
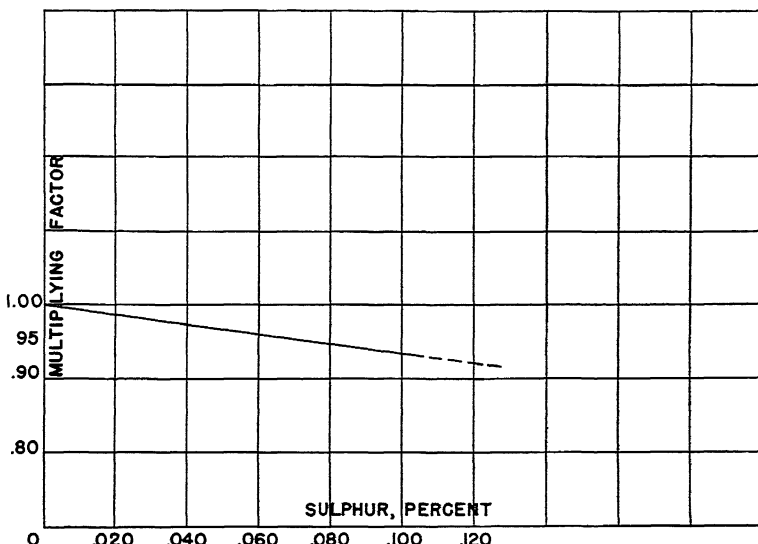
FIG. 6.—MULTIPLYING FACTOR FOR CALCULATION OF EFFECT OF SULPHUR ON HARDENABILITY.

manner because it forms a manganese sulphide (MnS), thus removing some of the manganese from the hardenability effect which otherwise the manganese might have.

content, the most probable straight line is again drawn through the points, and the resulting factors are shown in Fig. 6. Since sulphur lessens the hardenability,

the factor will always be some fraction less than 1.00.

It may be pointed out that the amount by which sulphur reduces the hardenability

order of 2 per cent are used. The curve shown in Fig. 8 is suggested as a probable close approximation, since it combines the effects of the small amounts in Fig. 7 with

TABLE 3.—*Steels for Study of Effect of Sulphur*

Composition, Per Cent								Average Grain Size No.	Ideal Diameter D_I Corrected to No. 5 Grain Size
C	Mn	P	S	Si	Ni	Cr	Cu		
0.65	0.86	0.019	0.027	0.22	0.04	0.06	0.02	6.2	1.70
0.65	0.86	0.019	0.047	0.22	0.04	0.06	0.02	6.2	1.665
0.65	0.86	0.019	0.065	0.22	0.04	0.06	0.02	6.2	1.665
0.65	0.86	0.019	0.084	0.22	0.04	0.06	0.02	6.2	1.63
0.65	0.86	0.019	0.104	0.22	0.04	0.06	0.02	6.2	1.60

TABLE 4.—*Steels for Study of Effect of Silicon*

Composition, Per Cent								Average Grain Size No.	Ideal Diameter D_I at No. 5 Grain Size
C	Mn	P	S	Si	Ni	Cr	Cu		
0.61	0.85	0.017	0.025	0.16	0.06	0.05	0.02	5	1.64
0.61	0.85	0.017	0.025	0.19	0.06	0.05	0.02	5	1.72
0.61	0.85	0.017	0.025	0.24	0.06	0.05	0.02	5	1.76
0.61	0.85	0.017	0.025	0.28	0.06	0.05	0.02	5	1.80
0.61	0.85	0.017	0.025	0.33	0.06	0.05	0.02	5	1.87

is less than would be the case if all of the sulphur were combined with manganese. In other words, this indicates that the entire amount of sulphur is not present as precipitated particles of MnS inclusions, meaning by inference that some of it probably is present as FeS and some of it possibly even dissolved.

Silicon

Again following the same procedure, results for silicon were obtained[5] from experimental ingots of the compositions listed in Table 4. These data result in Fig. 7 and thus indicate the effect of silicon in amounts up to about 0.35 per cent. However, this element is sometimes present in much larger amounts, notably in the silicomanganese steels, and a number of calculations were made on such steels. The results are shown in Table 5, and indicate that silicon is proportionately much less effective when amounts of the

the apparent lesser potency of the large amounts shown in the table.

TABLE 5.—*Effect of Silicon on Silicomanganese Steels*

Steel	Silicon Content, Per Cent	Apparent Hardenability Factor
Silicomanganese		
A...................	1.88	1.72
B...................	1.90	1.72
C...................	1.76	1.43
D...................	2.09	1.70
E...................	1.93	1.77

Nickel

The steels with nickel additions in the mold were tested as before, the compositions of the ingots being as shown in Table 6. These data resulted in Fig. 9 and the factors deduced from Fig. 9 are shown in Fig. 10. The accurate data extend to only 0.24 per cent Ni, and an extrapolation is suggested in Fig. 10 up to almost 2 per cent Ni. This

would, of course, be utterly unwarranted
if it were merely an extrapolation, but data
on steels with moderate nickel contents

Copper

No quantita ive data being available on
copper, it has been necessary to use an
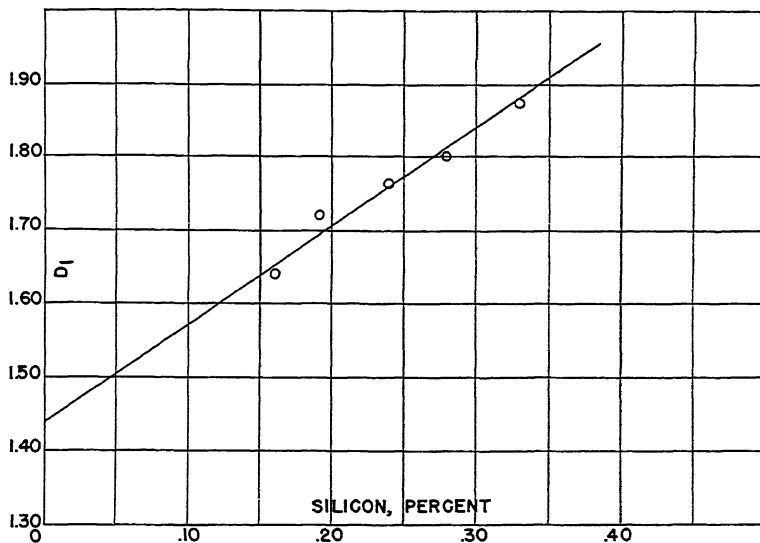
FIG. 7.—EFFECT OF SILICON CONTENT ON HARDENABILITY, DETERMINED EXPERIMENTALLY.
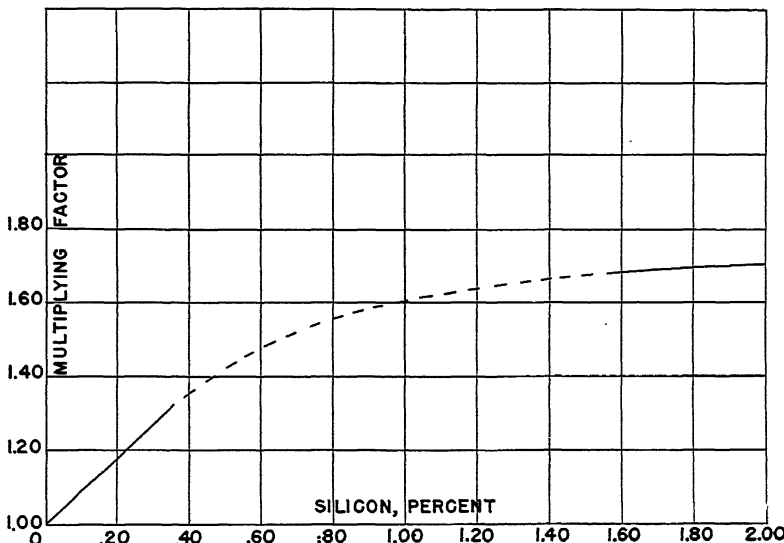
FIG. 8.—MULTIPLYING FACTOR FOR CALCULATION OF EFFECT OF SILICON ON HARDENABILITY.

below 2 per cent suggest the possible
validity of the line indicated. Data at 3 per
cent or more nickel are lacking.

approximation. It appears, from what little
is known of this element, that copper is a
weak alloying element for hardenability,

having an effect possibly rather similar to that of nickel. Since the copper content of heat-treating steels is usually small, pre-sumably it would introduce very little error

not be added together; the proper procedure is to use factors for the copper and the nickel separately.)
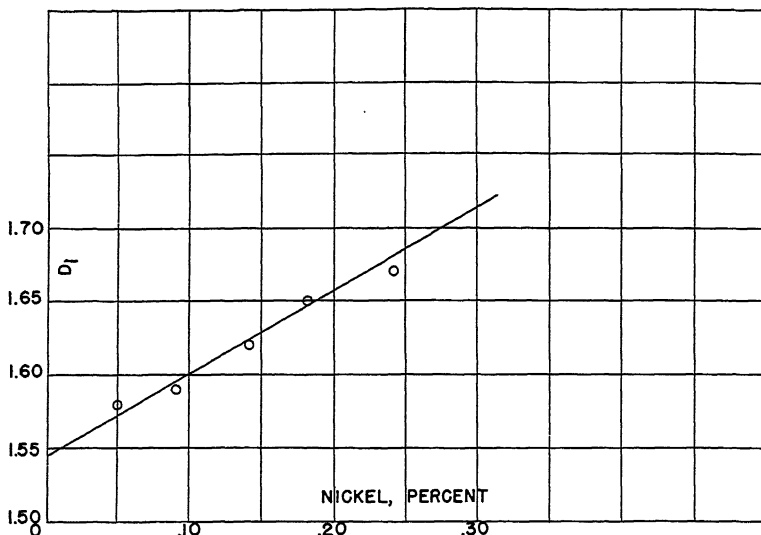
FIG. 9.—EFFECT OF NICKEL CONTENT ON HARDENABILITY, DETERMINED EXPERIMENTALLY.
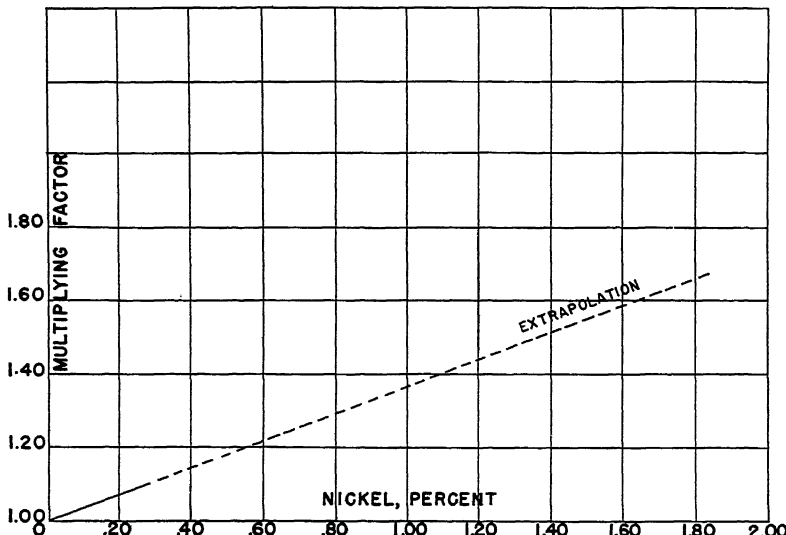
FIG. 10.—MULTIPLYING FACTOR FOR CALCULATION OF EFFECT OF NICKEL ON HARDENABILITY.

sumably it would introduce very little error to consider copper as being the same as nickel and to use the nickel relationship, Fig. 10, for the copper as well. (Needless to say, the nickel and copper contents should

Chromium

Data for chromium were developed as for the other elements, tests having been made on ingots of the compositions shown in

Table 7. These data lead to Fig. 11 and the resulting factors lead to the lower left-hand portion of the relationship shown in Fig. 12.

solved carbides ought to be calculated for their true lower carbon content (since less carbon is dissolved in the austenite), as well

TABLE 6.—*Steels with Additions of Nickel*

Composition, Per Cent								Average Grain Size	Ideal Diameter D_I Corrected to No. 5 Grain Size
C	Mn	P	S	Si	Ni	Cr	Cu		
0.58	0.89	0.019	0.027	0.18	0.05	0.05	0.02	6	1.58
0.58	0.89	0.019	0.027	0.18	0.09	0.05	0.02	6	1.59
0.58	0.89	0.019	0.027	0.18	0.14	0.05	0.02	6	1.62
0.58	0.89	0.019	0.027	0.18	0.18	0.05	0.02	6	1.65
0.58	0.89	0.019	0.027	0.18	0.24	0.05	0.02	6	1.67

TABLE 7.—*Steels for Study of Effect of Chromium*

Composition, Per Cent								Average Grain Size	Ideal Diameter D_I Corrected to No. 5 Grain Size
C	Mn	P	S	Si	Ni	Cr	Cu		
0.65	1.04	0.015	0.025	0.19	0.03	0.08	0.02	6.2	1.95
0.65	1.04	0.015	0.025	0.19	0.03	0.12	0.02	6.2	2.14
0.65	1.04	0.015	0.025	0.19	0.03	0.18	0.02	6.2	2.29
0.65	1.04	0.015	0.025	0.19	0.03	0.22	0.02	6.2	2.47
0.65	1.04	0.015	0.025	0.19	0.03	0.27	0.02	6.2	2.66

For larger amounts of chromium however, the situation becomes complicated because of a behavior not considered for the other elements described so far; namely, the effect of undissolved carbides. When carbides are not dissolved (and this is particularly likely to be true in steel of substantial chromium content), the undissolved carbides remove chromium from the austenite and therefore from its hardenability effect, and of course remove carbon from its effect as well. The crosshatched area shown in Fig. 12 has been drawn as a result of calculations on many chromium-bearing steels, heat-treated in some cases at a variety of quenching temperatures. Clearly, those heat-treated at the lower quenching temperatures will have a larger proportion of undissolved carbides, and the apparent hardenability factor for chromium will therefore be less, whereas of course those heat-treated at higher temperatures will show a larger apparent effect for chromium. Strictly speaking, such steels having undissolved carbides, after hardening, are particularly

as for their lessened chromium content, but this differentiation was not applied in Fig. 12. It is to be noted in Fig. 11 that the values up to 0.27 per cent Cr fall very close to a straight line, meaning that amounts of chromium up to possibly 0.30 per cent are completely dissolved and have their full effect. With larger amounts one can make a first approximation by assuming that at lower heat-treating temperatures the factor is likely to be in the lower portion of the crosshatched area, while the use of higher and higher heat-treating temperatures will cause the factor to approach the top of the crosshatched region.

Undissolved carbides in substantial amounts, after hardening, are particularly likely to be present in chrome-molybdenum and chrome-vanadium steels having as much chromium, molybdenum and vanadium as the S.A.E. 4100 and 6100 series. In the 4100 series, calculations of a number of S.A.E. 4140 steels, after hardening from normal quenching temperatures, indicated

about 50 to 65 per cent of full possible hardening: in other words, a fair approximation for the probable hardening of 4140 steels at normal quenching temperatures

FIG. 11.—EFFECT OF CHROMIUM CONTENT ON HARDENABILITY, DETERMINED EXPERIMENTALLY.

was found by calculating for maximum hardening, using Figs. 12 and 20, and then taking 50 to 65 per cent of this figure.

When the amounts of chromium, molybdenum and vanadium are small, however, the full effects are obtained as indicated in Figs. 12, 20 and 22.

Manganese

The evaluation of the manganese effect presented some difficulties because of the substantial amount present in all commercial heat-treating steels. Thus the grade of steel that had been selected for all

of these tests contained about 0.75 per cent Mn, and the amount of manganese that could be introduced by mold addition was of course rather limited. In this case the total range before and after the mold additions was only from 0.75 to 0.88 per cent Mn. Table 8[5] gives the compositions. It is clear that it would be wholly unwarranted to employ the change in hardenability from 0.75 to 0.88 per cent Mn for an extrapolation on the one hand down to 0 per cent Mn, and on the other hand up to 2 per cent Mn. It was, therefore, necessary to use a slightly different approach.

Up to this point the effects of all of the different elements present in plain carbon steels had been determined, including "residuals," with the exception of carbon

TABLE 8.—*Steels for Study of Effect of Manganese*

Composition, Per Cent								Average Grain Size	Ideal Diameter D_I Corrected to No. 5 Grain Size
C	Mn	P	S	Si	Ni	Cr	Cu		
0.61	0.75	0.021	0.021	0.18	0.04	0.06	0.03	4.9	1.46
0.61	0.79	0.021	0.021	0.18	0.04	0.06	0.03	4.9	1.56
0.61	0.83	0.021	0.021	0.18	0.04	0.06	0.03	4.9	1.63
0.61	0.88	0.021	0.021	0.18	0.04	0.06	0.03	4.9	1.69

and manganese. (It was necessary to know the effect of manganese before the carbon effect could be determined.) It happened that the hardenabilities of a variety of

obtained for the other elements, and it was thus possible to plot the estimated multiplying factors due to manganese for the above-mentioned steels ranging from 0.2 to
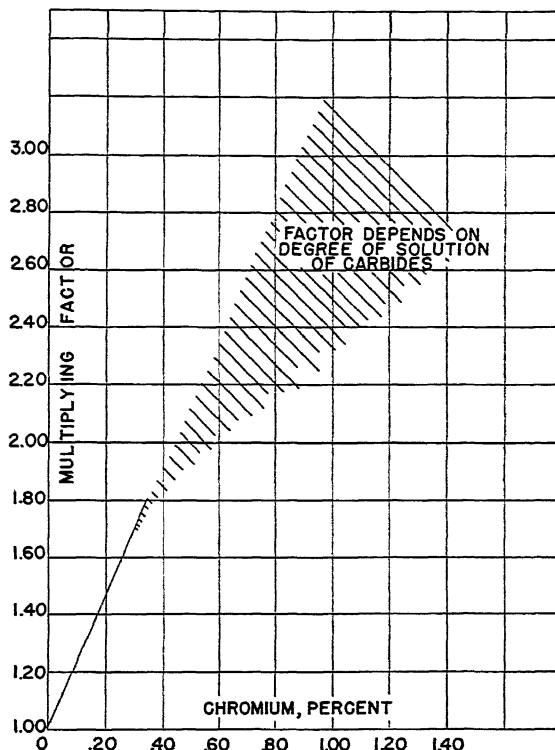
FIG. 12.—MULTIPLYING FACTOR FOR CALCULATION OF EFFECT OF CHROMIUM ON HARDENABILITY.

steels, ranging from 0.2 to 1.8 per cent Mn were available, and these were used to estimate the manganese effect by the following scheme. These data on manganese in the range 0.75 to 0.88 per cent were employed to obtain an approximate figure for the effect of manganese. This approximate figure, when employed in conjunction with the more precise determinations cited above for the other elements, made it possible to estimate approximately the effect of carbon, by the scheme indicated further on, in the discussion of carbon. These approximate figures for the carbon were used in conjunction with the figures

1.8 per cent Mn. This was done as shown in Fig. 13. The points shown there exhibit a rather consistent trend, even though the individual points show undue variation. This variation is accounted for in part by the fact that in some of the steels the analysis was not entirely complete, data not being always completely available on the "incidentals," and in part by the fact that the carbon effect was only a rough approximation, as just explained. Nevertheless, it seemed warranted to try the points in Fig. 13, by drawing a line *through the origin and parallel to the trend shown*. The resulting line, shown in Fig. 13, was

then tested as to its reliability. It turned out to be reliable and is in fact the adopted one shown in Fig. 14. It has since been

values were found to fall within a range plus or minus 10 per cent of the experimental values; and, furthermore, even in these
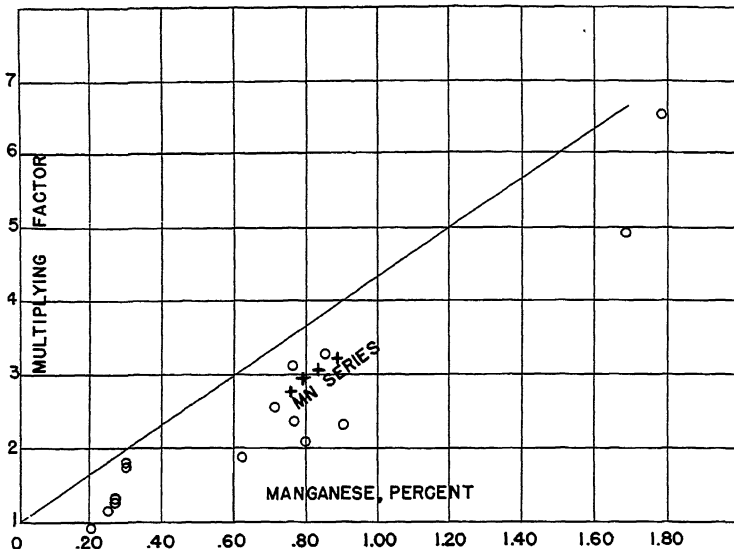
FIG. 13.—MULTIPLYING FACTOR FOR MANGANESE, ESTIMATED FROM A VARIETY OF STEELS.
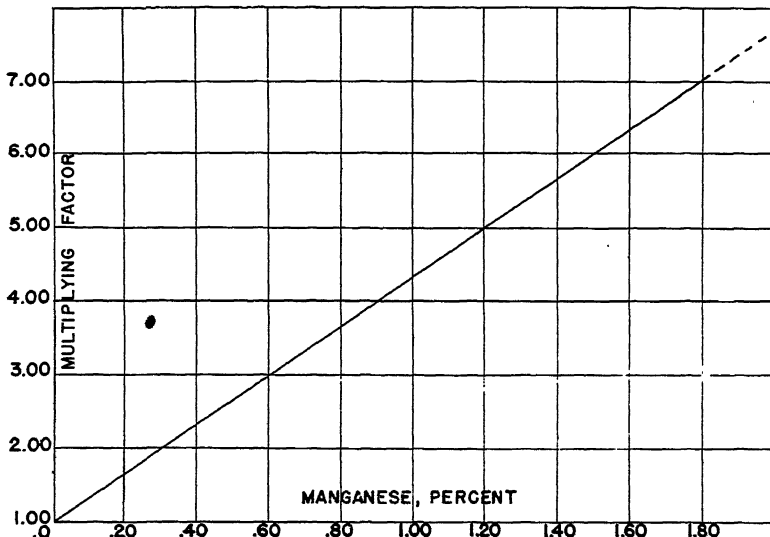
FIG. 14.—MULTIPLYING FACTOR FOR CALCULATION OF EFFECT OF MANGANESE ON HARDENABILITY.

tested on many different steels. Thus on a series of 73 heats of T-1340 steel containing from 1.5 to 2.0 per cent Mn, the calculated

high-manganese steels there were just as many calculated values above the experimental as there were below the experi-

mental, indicating that the departure was not due to the calculated manganese factor.

Thus the assumption of a straight-line relationship, as indicated in Figs. 13 and 14, appears to be fully supported by experimental data. Incidentally, this completed the list of elements needed for the determination of the carbon effect.

Carbon

As explained previously, we seek here to learn the hardenability of pure iron-carbon alloys (other elements entirely absent). Data on "pure steels" were not available in terms of "ideal critical diameter" as needed here (and indeed the experimental difficulties for such a measurement would be very great). Fortunately, however, two separate sets of data could be combined to indicate the probable values, and the resulting chart for pure iron-carbon alloys has worked out very satisfactorily in practice. The two prior investigations were:

Investigation 1.—Hardenability tests were made at the U. S. Bureau of Standards by Digges,[4] on iron-carbon alloys of high purity. Unfortunately for the present purpose, however, the ideal critical diameter could not be deduced directly from his data. Digges' experiments involved very small specimens ($\frac{1}{4}$ in. square by 0.040 in. thick) cooled at several rates, and he determined the cooling rate at which each steel was just fully hardened (97 to 99 per cent martensite). What we seek is the diameter of bar that, when given an ideal quench, will of course be fully hardened at the surface but will be just half-hardened (50 per cent martensite) at the center. It may be well to point out: (*a*) why Digges' data do not lead directly to the units in which we need to define hardenability here, and (*b*) how Digges' data nevertheless show *rate of change* of hardenability with carbon content, usable with our own units.

a. Digges' data do not lead directly to the data needed here. For a given carbon content, Digges gave the cooling rate (or cool-

ing time), in the range 1110° to 930°F., that would just cause the steel to harden fully. There is no convenient way of deducing from these figures the size of bar that, in an ideal (severest possible) quench, would be just half-hardened at the center. For the latter, it would have been necessary to know the "half-temperature time" (from the quenching temperature halfway down to that of the quenching medium), rather than the time from 1110° to 930°F., and to know that time for half-hardening (50 per cent martensite) rather than full hardening (97 to 99 per cent martensite). Had those data been given, it would have been possible to calculate the diameters by the use[5] of the formula.

$$D_I = k \sqrt{t}$$

where D_I is the desired "ideal critical diameter," k is a known constant and t is the half-temperature time.

b. Nevertheless Digges' data may be used to show *rate of change* of hardenability with carbon content, even when applied to our own units. Digges' data indicate a straight-line relationship between carbon content and "hardenability" (if we use his index for hardenability—namely, the cooling time from 1110° to 930°F., which will just provide full hardening). This relationship is shown in one of Digges' charts, reproduced as Fig. 15 herewith. Now we may make two assumptions which seem reasonable, which will enable us to check Fig. 15 against our own observations. We may assume first that the time from 1110° to 930°F. is a constant fraction of the "half-temperature time" (this is not by any means always the case, but is probably true for Digges' very small specimens), and we may assume second that the time for full hardening is a constant fraction of the time for half-hardening. If Digges' Fig. 15 is correct (and there are at present no theoretical indications to the contrary) and if the two assumptions are valid, there should be a "straight-line relationship"

between carbon content and half-tempera-
ture time (for half-hardening). The bearing
of this on our own data may be described as

But we have already concluded that a
straight-line relationship exists between
carbon content and (half-temperature)
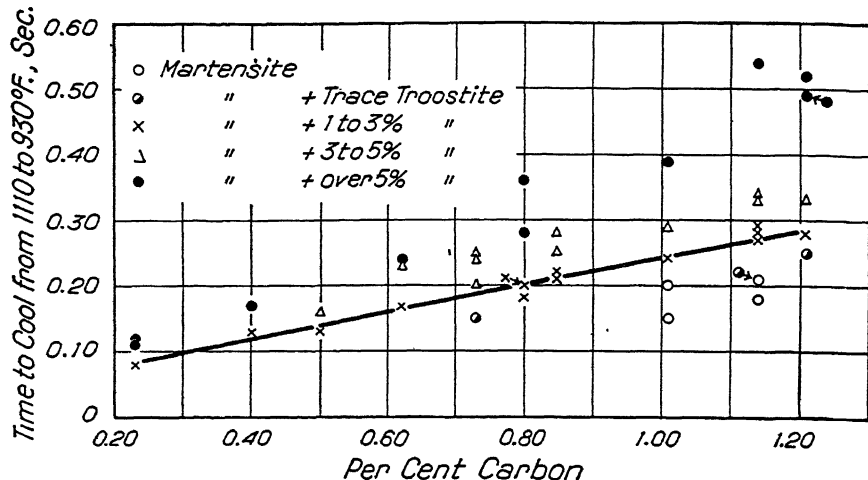
FIG. 15.—TIME REQUIRED FOR IRON-CARBON ALLOYS TO COOL FROM 1110° TO 930°F. WHEN
QUENCHED FROM 1700°F. SPECIMENS WERE ¼ INCH BY 0.040 INCH THICK. (*Digges.*)
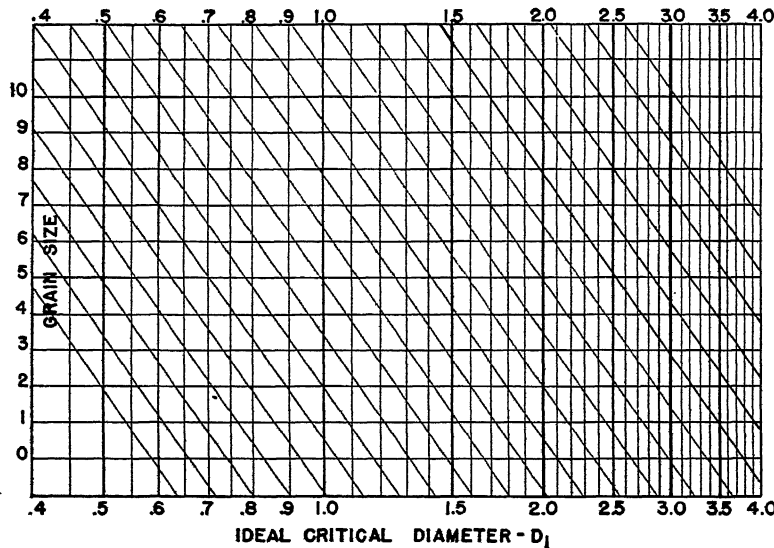
FIG. 16.—EFFECT OF GRAIN SIZE ON HARDENABILITY, IN TERMS OF IDEAL CRITICAL DIAMETER D_I.

follows: If we square the two terms in the
above formula, we have

$$D_I{}^2 = Kt$$

meaning that time t is proportional to $D_I{}^2$.

time, so that we now conclude that there is
a straight-line relationship between carbon
content and $D_I{}^2$ (the square of the ideal
critical diameter). This is the supposed
relationship that we can test on our own

data, which comprise the other source of information, item 2.

Investigation 2.—In our tests,[5] different amounts of carbon were added to successive ingots in an open-hearth heat, these successive ingots therefore being identical except as to carbon content. The analyses were as shown in Table 9.

refer again to the formula

$$D_I{}^2 = Kt$$

If, as Digges indicated, there is a straight-line relationship between carbon content and cooling time, then, as previously mentioned, the formula indicates that there should likewise be a straight-line relation-

TABLE 9.—*Ingots with Carbon Additions*

Composition, Per Cent								Average Grain Size	Ideal Diameter D_I Corrected to No. 5 Grain Size
C	Mn	P	S	Si	Ni	Cr	Cu		
0.41	0.79	0.015	0.026	0.20	0.07	0.07	0.03	4.6	1.34
0.54	0.79	0.015	0.026	0.20	0.07	0.07	0.03	4.6	1.52
0.68	0.79	0.015	0.026	0.20	0.07	0.07	0.03	5.0	1.75

TABLE 10.—*Effect of Elements Other than Carbon*

	Composition, Per Cent							Product of Factors without Carbon
	Mn	P	S	Si	Ni	Cr	Cu	
Percentage of element......	0.79	0.015	0.026	0.20	0.07	0.07	0.03	
Corresponding factor.......	3.63	1.039	0.982	1.186	1.025	1.16	1.01	5.274

In order to ascertain the hardenability effect of the carbon alone, it was necessary first to find the effects of all the other elements; namely, Mn, P, S, Si, Ni, Cr and Cu (other elements were absent). The derivation of these factors has been described. The total hardenability of the steels (in terms of D_I) is then divided by the factors for all of these elements, leaving as a quotient the derived values for carbon. The data are shown in Table 10.

The grain-size correction, Fig. 16, was prepared from other data,[6] as described below. From the previously obtained ideal diameters D_I at grain size No. 5, it was then possible to deduce the hardenability due to carbon alone, as in Table 11 (4th column).

These values could now be tested to see whether they accord with the behavior shown by Digges, as cited above; namely, "a straight-line relationship between carbon content and cooling time." We may

ship between carbon content and $D_I{}^2$ (since $D_I{}^2$ is proportional to cooling time t). In Fig. 17, carbon content is plotted against $D_I{}^2$ as taken from Table 11. The three

TABLE 11.—*Effect of Carbon Alone*

Carbon, Per Cent	Ideal Diameter D_I at No. 5 Grain Size	Divide by Factor for Other Elements	Ideal Diameter of Pure Iron-carbon Alloy at No. 5 Grain Size D_I, In.	$D_I{}^2$
0.41	1.34	5.274	0.2540	0.0647
0.54	1.52	5.274	0.2882	0.0831
0.68	1.75	5.274	0.3316	0.1098

points are quite close to the straight line drawn in Fig. 17, but this in itself would of course not be sufficient evidence of agreement. A much more important feature is the fact that the straight line is drawn through the origin, indicating zero hardenability at zero carbon content. It is this
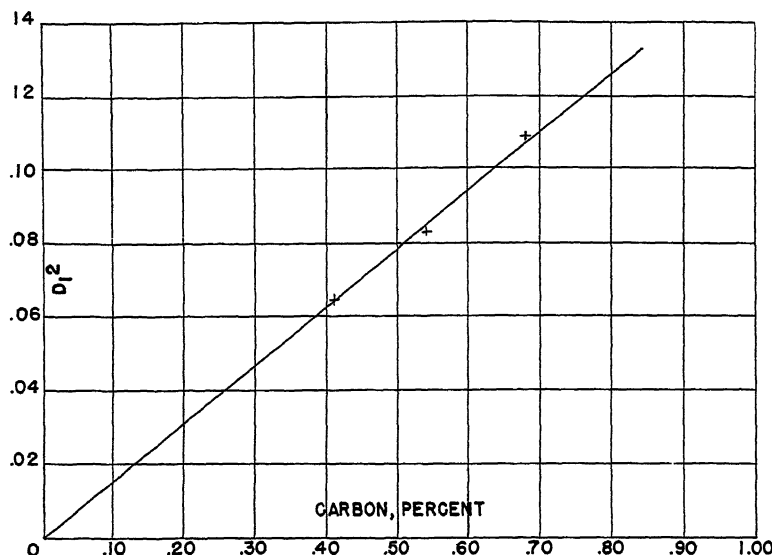
FIG. 17.—RELATION OF SQUARE OF IDEAL CRITICAL DIAMETER $(D_I{}^2)$ TO CARBON CONTENT, IN PURE IRON-CARBON ALLOYS.
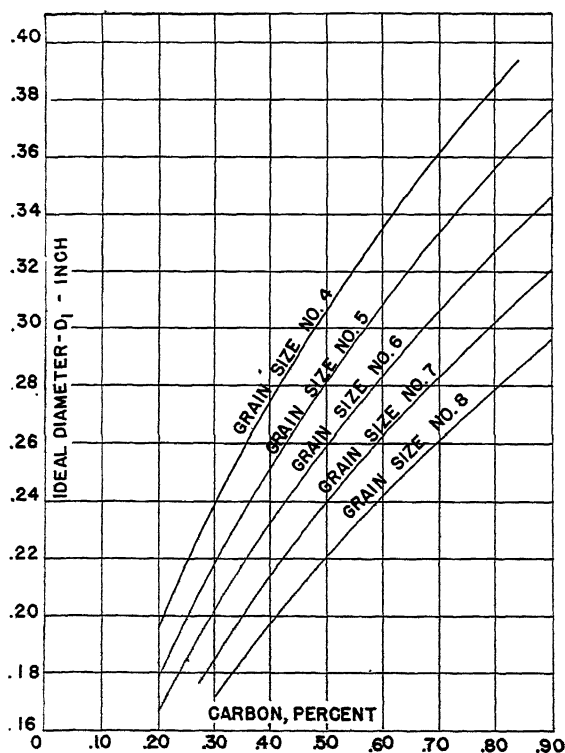
FIG. 18.—HARDENABILITY OF PURE IRON-CARBON ALLOYS, EXPRESSED AS IDEAL CRITICAL DIAMETER D_I.

feature that seems to show that our data accord with those of Digges: it is known that pure iron has practically negligible hardenability, and we find that a straight line can be drawn which begins at zero, and which is very close to our experimental points over the reasonably large range 0.41 to 0.68 per cent carbon covered by our tests. Also, measurements made on some published curves taken with Digges' instrument,[7] and allowing for the difference between full hardening and half-hardening as judged from isothermal transformation curves, give results of the same order of magnitude as those shown in Fig. 17. Digges' work was also done on materials having an austenite grain size approximately No. 5. These several reasons thus indicate that the line drawn in Fig. 17 is probably quite close to the correct value, and the line has been taken, therefore, as the working basis for the present data, to show the hardenability of pure iron-carbon alloys at grain size No. 5. Reading a series of values of D_I^2 from Fig. 17, and taking the square roots for the values of D_I, provides relationships between carbon and D_I which are plotted as the line in Fig. 18 marked "Grain Size No. 5."

Grain Size

The other lines in Fig. 18 are judged from Fig. 16 as follows. Fig. 16, as mentioned, shows the relationship between grain size and ideal diameter D_I, and was prepared from another chart developed previously.[6] In the earlier work it had been shown that an increase of one grain-size number caused a certain *percentage* increase in D_I^2, which means that the relationship between D_I^2 and grain size could be drawn as a series of parallel straight lines on semilogarithmic coordinate paper. If this was true, then it was clearly also true that the relation between grain size and D_I (not D_I^2) could likewise be drawn as a series of parallel straight lines on semilogarithmic coordinate paper. The result is shown in Fig. 16, the

position of the lines having been calculated from the earlier chart. Obviously then, the meaning of Fig. 16 is merely that if the hardenability (in terms of D_I) is known for a steel at one grain size, its hardenability at some other grain size can be read directly from Fig. 16. As an example, a steel having a hardenability of 0.75 in. at No. 10 grain size will be found to have a hardenability of 1.03 in. at No. 6 grain size. The lines in Fig. 18 for grain sizes other than No. 5 were calculated in this manner from the original line, which was for grain size No. 5.

It is true that Fig. 16 could be used for the complete steels after taking all the elements into account, but this would involve making the complete calculation for a steel at No. 5 grain size, and then correcting the completed steel for grain size according to Fig. 16. It thus provides a small short cut to read the carbon hardenability directly corrected for grain size as shown in Fig. 18. Incidentally, it may be pointed out that the austenitic grain size should be judged as closely as possible for accurate work. Thus, a designation 5 to 8 is not sufficiently close; the hardenability at grain size No. 5 is about 28 per cent greater than at grain size No. 8, whereas it has been shown in our tests that if grain size is taken into account properly the results predicted will usually accord with experiment within about 10 per cent. It is true that two different operators examining grain size may not agree within closer than one grain-size number; and, indeed, this variation could account for some of the discrepancies found in the application of the present formula.

Molybdenum

The test for molybdenum was again carried out on a series of ingots from a single heat, the compositions being as shown in Table 12. The data are plotted as before in Fig. 19, leading to the chart shown in Fig. 20. The highest amount tested in this series was 0.10 per cent, and it is seen that Fig. 20 extrapolates this line to 0.25 per cent. The

data for larger amounts of molybdenum are uncertain, and it is not yet possible to make any statements with assurance as to

It is to be remembered that undissolved carbides are generally present in steels of the S.A.E. 4140 type as quenched, as well as
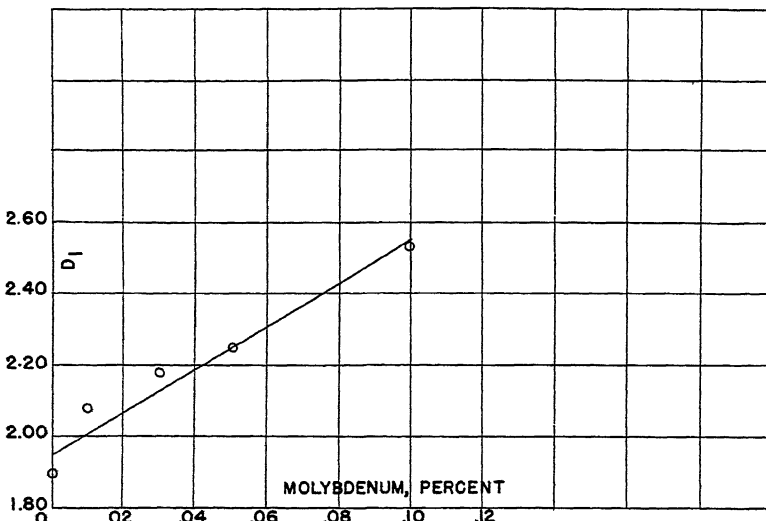

FIG. 19.—EFFECT OF MOLYBDENUM CONTENT ON HARDENABILITY, DETERMINED EXPERIMENTALLY.
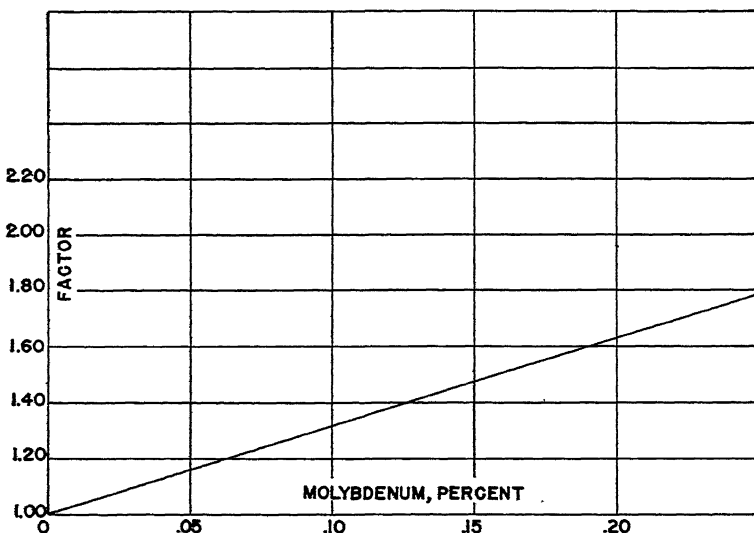
FIG. 20.—MULTIPLYING FACTOR FOR CALCULATION OF EFFECT OF MOLYBDENUM ON HARDENABILITY.

the upper portion of this line. The line, however, may be taken as an approximation, as it has also shown good correlation in a few tests on higher-molybdenum steels.

in others having equal or greater amounts of chromium and molybdenum. For discussion of these steels, refer to the section on chromium.

Vanadium

The test results for vanadium are shown in Table 13. Plotting this in terms of D_I vs.

It is evident that vanadium in very small amounts is an extremely powerful element for hardenability, since 0.04 per cent V
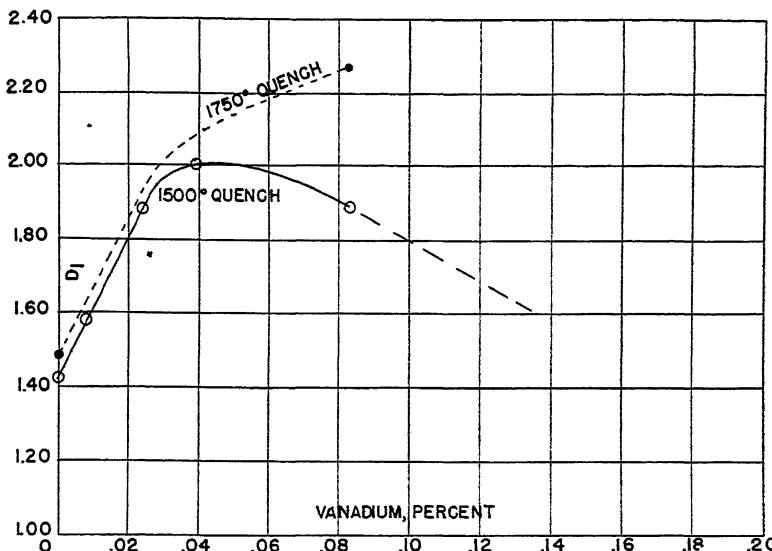
FIG. 21.—EFFECT OF VANADIUM CONTENT ON HARDENABILITY, DETERMINED EXPERIMENTALLY.
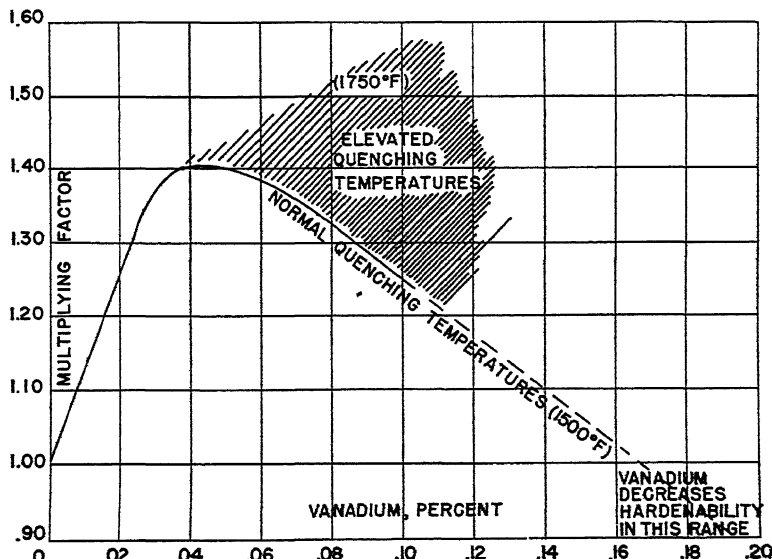
FIG. 22.—MULTIPLYING FACTOR FOR CALCULATION OF EFFECT OF VANADIUM ON HARDENABILITY.

vanadium content results in Fig. 21, leading to the factors for vanadium content shown in Fig. 22.

increased the hardenability by about 40 per cent. This compares, for example, with about 0.18 per cent Cr or about 0.13 per

cent Mo for an equal increase in harden-
ability of 40 per cent. The larger amount of
vanadium, for example 0.08 per cent, is seen
to have a lesser effect than 0.04 per cent,

It is quite clear under these circumstances
that the hardenability of a steel containing
a substantial amount of vanadium is
affected profoundly by the temperature of

TABLE 12.—*Steel for Test with Molybdenum*

Composition, Per Cent									Average Grain Size	Ideal Diameter D_I Corrected to No. 5 Grain Size
C	Mn	P	S	Si	Ni	Cr	Cu	Mo		
0.66	0.97	0.019	0.020	0.25	0.03	0.07	0.02	Nil	6.2	1.90
0.66	0.97	0.019	0.020	0.25	0.03	0.07	0.02	0.01	6.2	2.08
0.66	0.97	0.019	0.020	0.25	0.03	0.07	0.02	0.03	6.2	2.18
0.66	0.97	0.019	0.020	0.25	0.03	0.07	0.02	0.05	6.2	2.25
0.66	0.97	0.019	0.020	0.25	0.03	0.07	0.02	0.10	6.2	2.53

TABLE 13.—*Steels for Test with Vanadium*

Composition, Per Cent									Average Grain Size	Ideal Diameter D_I Corrected to No. 6 Grain Size	Quenching Temperature, Deg. F.
C	Mn	P	S	Si	Ni	Cr	Cu	V			
0.58	0.95	0.028	0.021	0.17	0.03	0.06	0.02	Tr.	6.	1.42	1550
0.58	0.95	0.028	0.021	0.17	0.03	0.06	0.02	0.008	6.0	1.58	1550
0.58	0.95	0.028	0.021	0.17	0.03	0.06	0.02	0.024	6.5	1.89	1550
0.58	0.95	0.028	0.021	0.17	0.03	0.06	0.02	0.039	6.5	2.00	1550
0.58	0.95	0.028	0.021	0.17	0.03	0.06	0.02	0.083	6.5	1.89	1550
0.58	0.95	0.028	0.021	0.17	0.03	0.06	0.02	Tr.	6.	1.48	1750
0.58	0.95	0.028	0.021	0.17	0.03	0.06	0.02	0.083	4.5	2.26	1750

TABLE 14.—*Steels with Aluminum Additions*

Composition, Per Cent									Average Grain Size	Ideal Diameter D_I Corrected to No. 5 Grain Size	Aluminum Addition in Molds, Lb. per Ton
C	Mn	P	S	Si	Ni	Cr	Cu	"Total Aluminum"			
0.65	0.87	0.014	0.024	0.14	0.03	0.04	0.02	0.003	3.5	1.62	0
0.62	0.87	0.014	0.024	0.14	0.03	0.04	0.02	0.006	4.7	1.59	¼
0.61	0.87	0.014	0.024	0.14	0.03	0.04	0.02	0.02	5.8	1.31	½
0.61	0.87	0.014	0.024	0.14	0.03	0.04	0.02	0.04	6.0	1.39	1
0.61	0.87	0.014	0.024	0.14	0.03	0.04	0.02	0.08	6.1	1.56	2

owing undoubtedly to the formation of
sluggish carbides, as these steels were
hardened from 1500°F. If the carbides are
taken into solution, however, by heating to
a higher temperature for the quench, the
effectiveness of the vanadium is increased.
For example, when the specimens were
quenched from 1750°F. the factor for
0.083 per cent V was 1.52, as compared
with a factor of 1.32 when the quenching
temperature was 1500°F.

heating for the quench. At ordinary quench-
ing temperatures, steels having substantial
amounts of chromium and vanadium, such
as the S.A.E. 6100 series, are quite certain
to contain appreciable amounts of undis-
solved carbides as quenched, so that they
harden to a much less extent than the
maximum indicated by the charts. On the
other hand, as with chromium, when only
small amounts of vanadium are present the
full hardenability effect of the vana-

dium is obtained at ordinary quenching temperatures.

FIG. 23.—EFFECT OF ALUMINUM CONTENT ON HARDENABILITY, DETERMINED EXPERIMENTALLY.
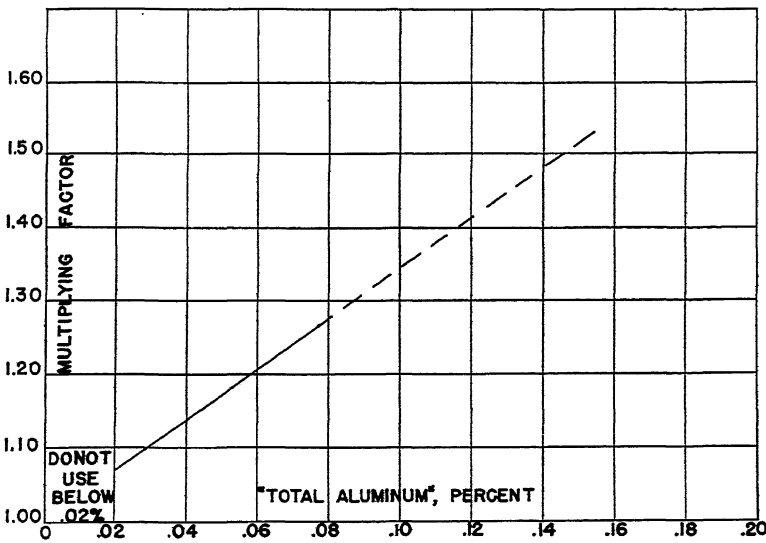
FIG. 24.—MULTIPLYING FACTOR FOR CALCULATION OF EFFECT OF ALUMINUM ON HARDENABILITY.

Aluminum

The effect of aluminum addition must be considered rather differently from that of the other elements, because of its effect on grain size and its rather complete elimina-

tion from steel when added in small amounts. The test ingots with different aluminum additions[5] gave the data of Table 14. In the first three ingots—namely, with 0, ¼ and ½ lb. per ton—the final steel contained very little aluminum. In the last two—namely, with 1 lb. per ton and 2 lb. per ton added—the residual alu-

minums were as shown. It was therefore concluded that the increase in hardenability in those two steels was due to the effect

slender basis the line shown in Fig. 24 was drawn. It is thus judged that aluminum is a powerful alloying element for hardenability,
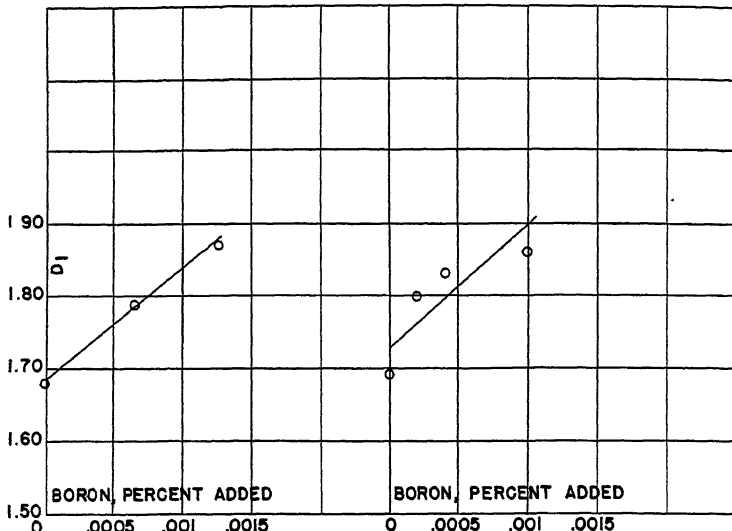
FIG. 25.—EFFECT OF BORON CONTENT ON HARDENABILITY, DETERMINED EXPERIMENTALLY.
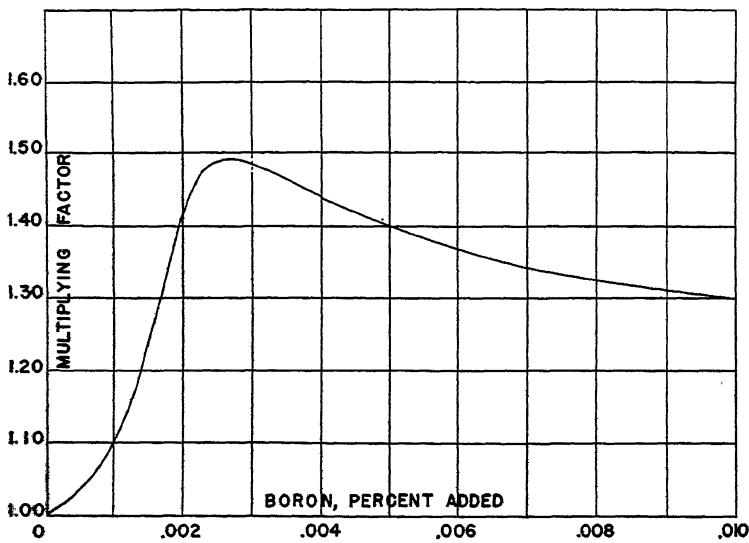
FIG. 26.—MULTIPLYING FACTOR FOR CALCULATION OF EFFECT OF BORON ON HARDENABILITY.

aluminum present in solution as alloy, and its hardenability effect could therefore be calculated. The points are plotted as shown in Fig. 23, and on this admittedly

having an effectiveness possibly of the order of chromium or manganese. The line in Fig. 24 must not be used below about 0.02 per cent Al.

It may be pointed out that the fine-grained steels, made fine-grained by the addition of aluminum, generally contain in the neighborhood of 0.025 per cent Al.

column, the first two steels are practically identical in hardenability *when corrected for grain size;* and, furthermore, they accord almost precisely with the calculated
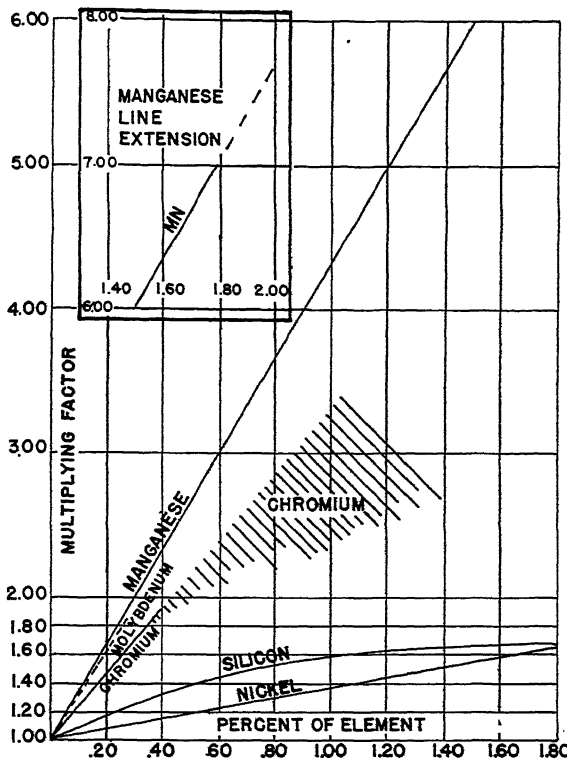
FIG. 27.—ASSEMBLY OF MULTIPLYING FACTORS FOR A VARIETY OF ELEMENTS.

This small amount would increase the hardenability by possibly only 5 per cent or so. Such a residual aluminum content is brought about by the addition of possibly ¾ lb. per ton, but if it were deemed advisable the hardenability could apparently be increased, say 20 per cent, by adding possibly 2 lb. of aluminum per ton (in the case of a medium-carbon steel) instead of the smaller amount required merely for grain-growth restriction.

The application of the present hardenability formula to these aluminum-treated steels brings to light an interesting circumstance. The first three steels give the results listed in Table 15. As shown by the third

figure. The third steel, however, even when corrected for its finer grain size, has much

TABLE 15.—*Three Steels with Aluminum Additions*

"Total Aluminum," Per Cent	Average Grain Size	Actual D_I Corrected to No. 5 Grain Size	Calculated D_I Corrected to No. 5 Grain Size
0.003	3.5	1.62	1.61
0.006	4.7	1.59	1.58
0.02	5.8	1.31	1.67

less hardenability than the other two, and likewise much less than the calculated value. It will be remembered that this steel

received its aluminum treatment in the mold, and it seems possible that particles (where the aluminum is added in the ladle) do not behave in this manner, as witness,
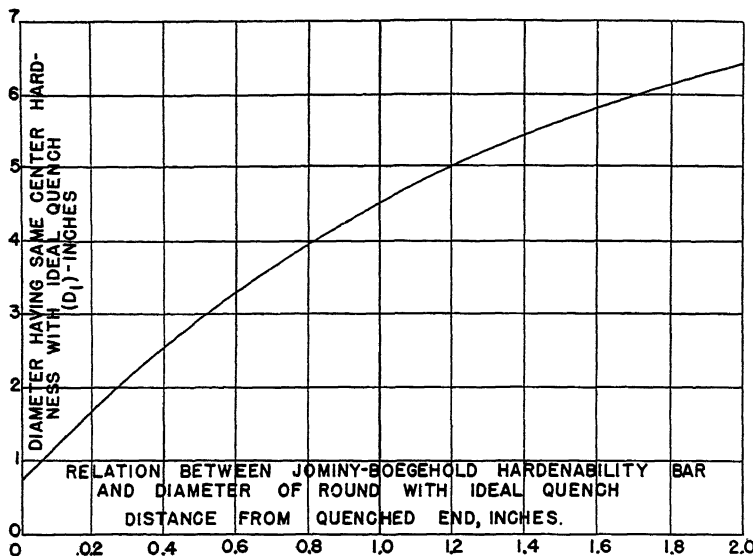
FIG. 28.—CHART FOR ESTIMATING IDEAL CRITICAL DIAMETER FROM JOMINY DISTANCE, OR VICE VERSA.
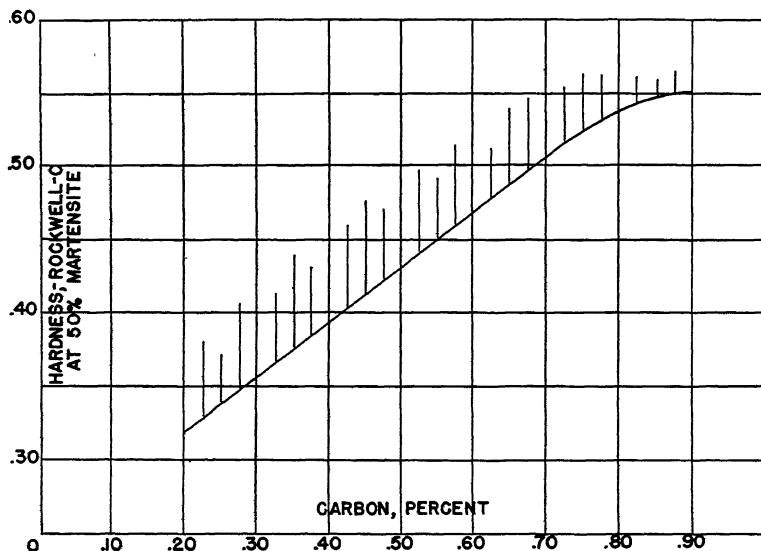
FIG. 29.—CARBON CONTENT IN RELATION TO HARDNESS OF 50 PER CENT MARTENSITE STRUCTURE. Solid line is for plain carbon steels. Shaded portion shows range encountered in low-alloy and medium-alloy steels.

of alumina, not eliminated from the steel, acted to nucleate pearlite and so lessen the hardenability. Ordinary commercial steels for example, the fact that commercial steels generally conform to the present proposed formula.

Boron

Boron is an outstandingly powerful element for increasing hardenability, having its maximum effect when adding the extremely minute amount of 0.0025 per cent. It is not possible to state the precise amounts actually remaining alloyed with the steel, since the analytical methods for such excessively small quantities are unsatis-

RELATION TO JOMINY END-QUENCH TEST

Data on hardenability will frequently be available or desired in terms of the Jominy end-quench test (distance from the quenched end), rather than in terms of ideal critical diameter. The relation between Jominy distance and ideal diameter has already been reported,[8] and Fig. 28 is a chart showing the relationship.

TABLE 16.—*Steels for Study of Effect of Boron*

Composition, Per Cent									Average Grain Size	Ideal Diameter D_I Corrected to No. 5 Grain Size	Factor
C	Mn	P	S	Si	Ni	Cr	Cu	B Added			
0.63	0.94	0.018	0.025	0.19	0.04	0.03	0.02	none	6.2	1.69	
0.63	0.94	0.018	0.025	0.19	0.04	0.03	0.02	0.0002	6.2	1.80	
0.63	0.94	0.018	0.025	0.19	0.04	0.03	0.02	0.0004	6.2	1.83	
0.63	0.94	0.018	0.025	0.19	0.04	0.03	0.02	0.0010	6.2	1.86	
0.66	0.86	0.014	0.028	0.24	0.03	0.04	0.02	none	6	1.68	
0.66	0.86	0.014	0.028	0.24	0.03	0.04	0.02	0.00065	6	1.79	
0.66	0.86	0.014	0.028	0.24	0.03	0.04	0.02	0.00125	6	1.87	
0.63	0.87	0.011	0.026	0.22	0.02	0.04	0.02	none	4.5	1.71	
0.63	0.87	0.011	0.026	0.22	0.02	0.04	0.02	0.0025	6	2.56	1.496
0.62	0.87	0.017	0.028	0.17	0.05	0.06	0.04	none	4.5	1.70	
0.62	0.87	0.017	0.028	0.17	0.05	0.06	0.04	0.005	5.5	2.38	1.40
0.61	0.90	0.012	0.023	0.17	0.05	0.08	0.03	none	4.5	1.75	
0.61	0.90	0.012	0.023	0.17	0.05	0.08	0.03	0.0125	5.5	2.25	1.286

factory. The data in Table 16 refer to percentages of boron added to the steel, the percentage recovery being unknown. The data for the first two heats, containing extremely minute amounts of boron, are plotted in Fig. 25. This provided a probable factor for the small amounts, and, together with the factors for somewhat larger amounts, as noted in Table 16, provided the figures for the general chart of Fig. 26. The reason for the drop in the curve with the larger percentages is not yet known, although there is some evidence that higher heat-treating temperatures produce an increased effect, suggesting that the boron is at least in part possibly present as stable carbides. The data in Figs. 25 and 26 refer to a quenching temperature of 1500°F.

Comparison

For purposes of comparison, the graphs for most of the principal alloying elements are assembled in Fig. 27.

Fig. 28 makes it possible to check results obtained in a Jominy test against the predictions of hardenability using the present proposed charts.

HARDNESS OF THE 50 PER CENT MARTENSITE STRUCTURE

In estimating critical diameter, the point of interest is the size of bar in which the structure is 50 per cent martensite at the center, or the depth in a quenched bar at which the structure is 50 per cent martensite. Clearly the hardness at this point is due in part to the martensite and in part to the nonmartensitic structure. When the nonmartensitic portion is fine pearlite (nodular troostite), as in the plain carbon steels, there is a quite regular relationship between the carbon content of the steel and the hardness of the 50 per cent martensite point, and this relationship is shown by the line at the lower boundary of the cross-hatched region in Fig. 29. But as the

hardenability of the steel increases, the character of the nonmartensitic portion changes (often to upper bainite or other complex structures) and the hardness of

hardens in any actual quench may be predicted by the use of Fig. 2. In order to be able to use Fig. 2, it is of course necessary to know the actual severity of quench. If it

TABLE 17.—*Severity of Quench*

	Oil	Water	Brine
No circulation of liquid or agitation of piece.................	0.25 to 0.30	0.9 to 1.0	2
Mild circulation (or agitation).............................	0.30 to 0.35	1.0 to 1.1	2 to 2.2
Moderate circulation..	0.35 to 0.40	1.2 to 1.3	
Good circulation...	0.4 to 0.5	1.4 to 1.5	
Strong circulation........................	0.5 to 0.8	1.6 to 2.	
Violent circulation..	0.8 to 1.1	4	5

TABLE 18.—*Typical Tests*

Average Grain Size	Composition of Steels, Per Cent									Calculated D_I	Actual D_I
	C	Mn	P	S	Si	Ni	Cr	Cu	Mo		
4.6	0.41	0.79	0.015	0.026	0.20	0.07	0.07	0.03		1.35[a]	1.34[a]
7	0.63	0.94	0.031	0.027	0.20	0.03	0.05	0.02		1.58[a]	1.71[a]
5	0.61	0.85	0.017	0.025	0.33	0.06	0.05	0.02		1.82[a]	1.87[a]
6.2	0.65	1.04	0.015	0.025	0.19	0.03	0.27	0.02		2.84[a]	2.66[a]
6.2	0.66	0.97	0.019	0.020	0.25	0.03	0.07	0.02	0.10	2.70[a]	2.53[a]
7	0.51	1.05	0.014	0.029	0.29		0.21	0.06		2.10	2.22
5	0.39	1.74	0.023	0.021	0.26	0.01	0.13	0.07		2.89	2.77
6	0.57	0.68	0.019	0.028	2.00		0.17	0.05		2.25	2.28
7	0.69	0.81	0.014	0.024	0.24	0.01	?	0.08	0.22	2.18	2.4
6	0.40	1.70	0.022	0.030	0.21	0.21	0.13	0.06	0.05	3.15	2.70
7	0.41	1.82	0.015	0.024	0.21	0.18	0.09	0.10	0.03	2.93	2.77
7	0.41	1.85	0.019	0.029	0.25	0.13	0.10	0.09	0.02	3.02	3.07
6	0.41	1.77	0.019	0.014	0.20	0.28	0.16	0.07	0.05	3.41	3.17
7	0.46	1.88	0.019	0.024	0.25	0.15	0.12	0.05	0.03	3.42	3.63
6	0.45	2.01	0.028	0.019	0.22	0.18	0.20	0.06	0.04	4.20	4.22

[a] Referred to No. 5 grain size.

the 50 per cent martensite point is higher. The crosshatched region in Fig. 29 indicates the range that may be encountered. In attempts to apply the proposed hardenability formula, it is desirable to know the hardness of the 50 per cent martensite point for the particular steel being investigated, though in most cases this can be judged readily from the point of inflection in a hardness distribution curve.

SEVERITY OF QUENCH

The ideal diameter D_I denotes (as mentioned previously) the size of bar that just hardens fully, without an unhardened core, in an ideal (severest possible) quench. Actual quenches in practice are less drastic than the ideal quench, so that the size that will just harden fully is smaller than the ideal diameter D_I. The size that just

is not feasible to ascertain the severity of quench experimentally, the figures in Table 17 may be used as a guide.

In the original article in which some of the present quantitative data were reported,[5] the severity of quench then estimated appears now to have been too high. In calculating ideal diameter D_I from the data there given, the figure adopted here as representing severity of quench was in most cases $H = 1.4$, and was in no case higher than $H = 2.0$.

RELIABILITY OF PREDICTIONS OF HARDENABILITY

The method proposed here for calculating hardenability has been checked against a very considerable number of tests, employing the graphs shown, and in

the great majority of cases the experimental values are found to be well within 10 per cent of the predicted values. A few typical instances are given in Table 18.

In the presence of substantial amounts of carbide-forming elements (Cr, V, etc.), the extent of hardening cannot be predicted (see discussion of those elements) although calculation can show the maximum possible hardenability and suggest the probable behavior.

To repeat the precautions: Be sure that all alloying elements are taken into account, including "incidentals"; ascertain the actual grain size at the hardening temperature; know the severity of quench as accurately as possible; do not overlook insoluble carbides when they may be present.

ACKNOWLEDGMENTS

The experimental work was for the most part carried out by the research staff of the South Chicago Works of the Carnegie-Illinois Steel Corporation, and it is a pleasure to pay tribute to their scrupulously careful work.

REFERENCES

1. C. H. Herty, D. L. McBride and E. H. Hollenback: Which Grain Size. *Trans.* Amer. Soc. Metals (1937) 25, 297.
2. J. L. Burns, T. L. Moore and R. S. Archer: Quantitative Hardenability. *Trans.* Amer. Soc. Metals (1938) 26, 1.
3. J. L. Burns and G. C. Riegel: Hardenability of Plain Carbon Steels. In volume entitled Hardenability of Alloy Steels, 262. Amer. Soc. Metals.
4. T. G. Digges: Effect of Carbon on the Hardenability of High-Purity Iron-Carbon Alloys. *Trans.* Amer. Soc. Metals (1938) 408.
5. Grossmann, Asimow and Urban: Hardenability, Its Relation to Quenching and Some Quantitative Data. In volume on Hardenability of Alloy Steels. Amer. Soc. Metals. 1939.
6. Grossmann and Stephenson: The Effect of Grain Size on Hardenability. *Trans.* Amer. Soc. Metals (1941) 1.
7. H. J. French: A Study of the Quenching of Steels. *Trans.* Amer. Soc. Steel Treat. (1930) 646, 798.
8. Asimow, Craig and Grossmann: Correlation between Jominy Test and Quenched Round Bars. *Jnl.* Soc. Automotive Engrs. (1941) 283.

DISCUSSION

(E. C. Bain presiding)

A. P. EDSON,* Bayonne, N. J.—For some time we have been concerned with the calcu-

* International Nickel Co., Research Laboratory.

lation of hardenability from the chemical composition of steel, and therefore find this paper most interesting. However, it raises one question: that is, the extent to which the relations shown can safely be regarded as linear. The composition ranges covered by the actual data used in this paper for determination of the factors for the various elements seem too limited in most cases to justify extensive linear extrapolation. A sufficiently short segment of any curve may be successfully represented by a straight line, which quickly comes to grief when extrapolated. The question then arises whether the linearity observed in the data presented is inherent in the relation or represents straight-line approximation over a very short range in a fundamentally nonlinear system. We have been accustomed to regard the influence of alloying elements on the hardenability of steel as generally better represented by an S-shaped curve, for we have encountered marked curvature and even reversals of the effects of some elements within the concentration limits discussed by Dr. Grossmann.

The data for the fine-grained steel of Fig. 3 might be somewhat better fitted by a straight line of lower slope, which we associate with steels of low hardenability, while the steels with 4.5 grain size show the rising characteristic associated with low-intermediate hardenability. If the two sets of data shown are joined in this figure, by shifting the upper curve 0.07 per cent phosphorus to the right in order to compensate for the hardenability effect of the difference in grain size, a combined curve represents the lower portion of the S-shaped hardenability curve.

It is believed that the interpolated range for the effect of silicon in Fig. 8 is incorrect. The curve for this element has been found concave upward in its lower reaches, with a maximum in the interpolated range at a point determined by the base composition of the steel. The curve is somewhat similar in shape to that shown for boron in Fig. 26.

In Fig. 9 and Table 6 the effect of nickel has been determined for "residual" amounts only. It is our experience that the effect of this element is not always a simple function of its concentration, and we therefore question the sixfold extrapolation of the data shown. To supplement the author's data on this element, in Table 19 data are submitted on three closely similar steels, which contain 1 per cent, 2 per

cent and 3.5 per cent of nickel. Because of minor differences of composition and grain size, the hardenabilities of these steels cannot immediately be directly compared. However, because the base compositions of these steels (exclusive of nickel) fall within the ranges studied experimentally by Dr. Grossmann, we may safely calculate from his formula the

TABLE 19.—*Effect of Nickel*

	1.00 Per Cent Nickel		2.02 Per Cent Nickel		3.50 Per Cent Nickel	
	Per Cent	Factor	Per Cent	Factor	Per Cent	Factor
Grain Size......................	7		6		6	
Carbon.........................	0.45	0.23	0.46	0.25	0.45	0.23
Manganese......................	0.73	3.40	0.77	3.45	0.66	3.15
Silicon........................	0.17	1.14	0.18	1.15	0.13	1.12
Calculated base D_I.............	0.89		0.99		0.88	
Observed D_I....................	1.60		2.50		3.10	
Nickel factor[a].................	1.80		2.53		3.52	

$$\text{[a]}\quad \frac{\text{Observed }D_I}{\text{Calculated base }D_I}.$$
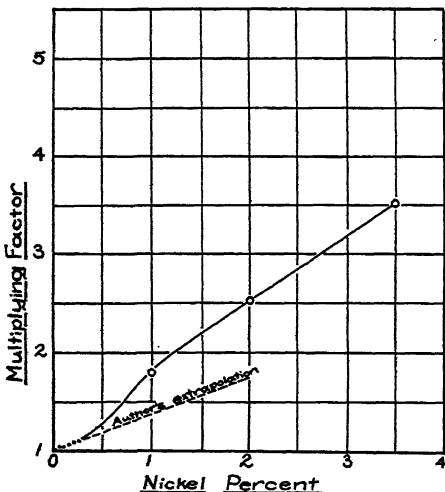
inherent hardenability of the base composition of each of these steels. If we now divide the observed ideal critical diameter of each steel by the D_I value calculated from its base composition, we eliminate the effects of all other known variables and secure factors for the effect of the three nickel concentrations involved. In Fig. 30 these data are plotted with those shown by Dr. Grossmann for the range 0.05 to 0.24 per cent nickel. Fig. 30 immediately reveals that these data can be reconciled only by an S-shaped curve in the region o to 1 per cent nickel. The author's linear extrapolation of his data is completely irreconcilable with the experimental points at 1 and 2 per cent nickel. All of the data shown in Fig. 30 could be fitted reasonably well by a straight line of approximately twice the slope chosen by Dr. Grossmann, but it is our belief that such a line does not represent the true relation, although it may provide an acceptable engineering approximation. The hazard inherent in extending a narrow range of data by means of extrapolation based on the concept of linearity is clearly shown in Fig. 30. The assumption that the effect of copper is equivalent to that of nickel in the complete absence of confirmatory data seems equally hazardous. Even for manganese, for which the author presents numerous data, the straight-line relation is not well established. The supplementary points shown in Fig. 13 indicate a general increase of hardenability with increasing manganese content, but contribute no support to the thesis of linearity, for they may be equally well or better fitted by a curve that is concave upward.

Another indication of a possible S shape for the curve that relates composition to hardenability may be secured by inspection of the data of Fig. 1. The calculated and experimental values in the range shown fall fairly well along a straight line, but for the steels of lowest hardenability the calculated ideal critical di-

FIG. 30.—EFFECT OF NICKEL VERSUS AUTHOR'S EXTRAPOLATION.

ameters tend to be lower than those observed, while for steels of high hardenability the reverse is true. These data could be fitted better by the suggested S-curve than by the straight line shown.

Indirect support for our belief in the S shape of the alloy content vs. hardenability curve is derived from a current paper by the writer.[9] In this paper on the maximum hardness developed in steel adjacent to metallic arc welds, we found, as does Dr. Grossmann, that hardening is related to composition by factors rather than by additive increments. However, weld-zone hardness is shown to be an exponential, rather than linear, function of alloy concentration in the composition range of common engineering steels. At higher alloy levels, the hardening effect of changes in composition becomes less until further alloy additions have little effect, and may even decrease hardening. Silicon has such an effect. We recognize, of course, that weld-zone hardness is not directly comparable to ideal critical diameter, but under the constant mild quenching conditions involved in welding it would seem that major changes in hardness should reflect changes in hardenability. If this is true, it becomes most difficult to reconcile the straight-line hardenability relation proposed in this paper with the thoroughly curvilinear relation found for weld-zone hardening.

Whatever the proper relation between composition and hardenability, we should like to see the range of data presented by Dr. Grossmann to determine the effects of the alloying elements considerably extended, if the use of the calculation described is not to be limited to "incidental" or "residual" alloy contents.

B. F. SHEPHERD,* Phillipsburg, N. J.—Too many of our scientific papers merely further our scientific knowledge. This, of course, is highly desirable, but the maximum good from any scientific research is obtained only when the scientific facts are practically applied to the better control of quality or improvement in quality of machinery parts. I wish many of our younger Doctors of Science would keep this angle in mind.

The present paper adds another stepping stone to our knowledge on the very important subject of hardenability. The calculations of hardenability from the chemical composition require, of course, the actual existence of samples and a complete chemical analysis. In addition, the as-quenched grain size must be determined, which involves hardening of specimens. Mr. Grossmann has shown previously that the "ideal critical diameter" can be determined by quenching several bars of varying size. It would seem that this previous procedure is a simpler method to determine hardenability than the complicated chemical, heat-treatment and mathematical formula described in the paper. The latter method would serve best to determine the manner in which the chemical composition should be altered in order to produce a desired hardenability.

Our attempts many years ago to control hardenability were based on extremely close chemical specifications for manganese and silicon. The influence of chromium was recognized by calling for 0.03 maximum. The steel was a simple carbon tool steel of hypereutectoid composition and most of my remarks will deal with this material.

In 1912 and 1913 we segregated heats of 1.05 carbon steel by analyzing every bar for chromium and utilizing them in groups of 0.015 plus or minus chromium. We could notice the difference between these groups on a carefully controlled, precise hardening operation.

Of course, chemical composition alone was not adequate and eventually we recognized the influence of grain size. Many specifications have since been prepared that use grain size and hardenability as a primary method of expressing the qualities desired, chemical analysis being relatively secondary.

I look forward to an extension of this idea and a recognition of what I must still call "personality," for lack of a better term. It is now quite generally recognized that steels of similar chemical composition may have the same hardenability and fracture characteristics at normal hardening temperatures. A profitable line of research would be to determine whether the difference in behavior between heats at the higher temperatures is reflected in a difference in service life of parts quenched from normal hardening temperatures where this difference is not evidenced.

[9] A. P. Edson: Weld Hardening and Steel Composition. *Metals and Alloys* (June 1942) 15, 966.
* Chief Metallurgist, Ingersoll-Rand Co.

I divided steels, by the P-F test, into four groups regarding their sensitivity to temperature:

1. The ones that were relatively insensitive to increase in case depth and increase in grain size.

2. The ones that were extremely sensitive and increased rapidly in both depth of hardness and coarseness of grain with slight increases in quenching temperature.

3. The steels that increased rapidly in penetration but did this with relatively small increases in coarseness of fracture.

4. The very rare type that was relatively insensitive to penetration but coarsened in grain rapidly.

We regularly buy large quantities of a tool steel that shows very little increase in *penetration or coarseness of grain* over a quenching range of 150°F.

Dr. Grossmann mentioned that the hardenability of hypereutectoid could be predicted only if the carbides were taken into complete solution. This work would require quenching temperatures that would be impractical. I do not know how extensively he has investigated this phase, but the undissolved carbides in hypereutectoid steels have considerable influence upon the hardenability.

Certain heats of the simple carbon steels of the same chemical composition have what I call a "stubborn" characteristic; that is, they require in a prehardening, normalizing treatment a considerably longer soak at temperature to produce similar structures.

If these steels are not given this longer soak at temperature, the hardenability will be different. Our soaking time for the prehardening normalizing quench must be considerably longer than necessary for normal heats in order to take care of a relatively small percentage of the so-called "stubborn" heats. It is much easier to add this extra time than to determine which heats are "stubborn" and handle them individually.

From the discussion of the severity of quench, it might seem that less severe quenches could be used to neutralize or compensate for higher hardenability. This is not the most desirable way of controlling the finished product. Any reduction in the severity of quench carries with it the definite possibility of soft spots on parts of intricate section. The best way to con-

trol depth of hardness is to use a very severe quench and the minimum hardenability material that will give the depth desired with this quench. Hardening strains can be taken care of in other ways.

J. B. AUSTIN,* Kearny, N. J.—I should like to ask Dr. Grossmann whether he has compared the multiplying factors for the different elements on the basis of atomic per cent rather than weight per cent; that is, on the basis of the presence of an equal number of atoms of alloying element.

H. J. FRENCH,† New York, N. Y.—I would like to ask a question concerning a detail that does not seem to have been mentioned in the paper. It relates to the control necessary when a given degree of hardenability is secured, not by additions of one or two alloying elements but from a combination of smaller additions of many elements, the majority of which may be oxidizable in molten iron. Have we under operating conditions in open-hearth steel manufacture the controls necessary to expect consistent adherence to a minimum hardenability without wasting alloys?

G. F. COMSTOCK,‡ Niagara Falls, N. Y.— The method of calculating hardenability described in this interesting paper should be useful in many instances when steels of fairly similar composition have to be compared rapidly. For comparing steels of very different analysis, however, the various precautions noted by the author should be carefully followed, and probably other instances of interrelated effects, such as that of sulphur on manganese, will be found as experience with the method develops. The factor for titanium, for instance, if that is eventually worked out, will probably be found to depend on the carbon content of the steel, as well as on the heat-treatment and possibly on other alloys.

The writer's experience agrees with the author's in regard to the remarkable effectiveness of small quantities of boron on hardenability, but not in the influence on grain size as reported in Table 16. As shown in another

---

* Research Laboratory, U. S. Steel Corporation.
† International Nickel Co.
‡ Titanium Alloy Manufacturing Co.

paper,[10] boron has been found to promote a tendency toward coarser grain size, at least in aluminum-deoxidized 0.40 per cent carbon steels. The tendency was marked when ferroboron was used, and could also be distinguished to a very slight degree in steels treated with complex deoxidizers containing boron together with the grain-refining elements titanium and aluminum.

M. A. GROSSMANN (author's reply).—With regard to the so-called linear relationship questioned by Mr. Edson, our position is as follows: There is at present no accepted exposition of the mechanism whereby alloys increase the hardenability; hence there is no theoretical reason to expect a particular form of line or curve; much less is there any occasion to believe that all elements would behave similarly. It seemed best therefore to draw the relationships in the manner suggested to us by the data; namely, a straight-line relationship for six of the elements and some form of curve for five.

With reference to the specific case of phosphorus, further data seem to indicate more than ever that a straight-line relationship is valid up to 0.100 per cent P. We are much interested in the comments on silicon and hope the precise data may be published. With regard to the hazards of extrapolation, we agree, of course, with Mr. Edson, and therefore have nothing to add to the reservations already made in the body of the paper. With regard to nickel, we feel constrained to point out that the data of his Table 19 disregard the "incidental" elements chromium, copper and molybdenum, which are therefore necessarily included in the so-called nickel factor. Perhaps this is why we have not been able to check his high nickel values. Some recent data seem to indicate a moderate upward trend in the nickel curve, up to a multiplying factor of about 3.0 for 3.5 per cent nickel.

We appreciate Mr. Shepherd's stimulating discussion. We agree, indeed, that the best way to arrive at a hardenability value for a piece of

steel is to "dunk" it in water and obtain an actual measurement and that the chief value of any "formula" is to estimate what chemical modification is needed for a desired change in hardenability.

With regard to Mr. Shepherd's well-known P-F test, the researches he suggests would indeed be informative. As to calculating the hardenability of hypereutectoid steels, we agree and even emphasize that undissolved carbides have an effect on the hardenability, and we therefore have no reason to believe that the proposed formulas would apply with any precision in such cases. As to "stubborn" heats with their carbides of probable slow rate of solution, and with regard to severity of quench, we agree with the tenor of Mr. Shepherd's remarks.

Following Dr. Austin's suggestion, we have plotted some of the factors against atomic per cent instead of weight per cent, and have not been able to discover any regular pattern of relationship, which means only what it says: We have not been able to discover it.

Mr. French raises a question about the necessary control in open-hearth steel manufacture in order to avoid wasting alloys, when using small amounts of a number of alloys. This is complicated in peacetime by the relation of the hardenability effect of the various alloys to their cost. To anyone mathematically inclined, we recommend this as an exercise, which we have found to be fascinating but far from simple. In wartime, when utmost use must be made of all alloys, possibly current experience with National Emergency (N. E.) steels (many of which contain small amounts of several alloys) may provide data as to adequacy of control in manufacture.

We note with interest Mr. Comstock's recommended precautions with regard to the interplay of elements. With regard to boron, we too have noted that there is sometimes a coarsening of the grain, though there is sometimes refinement. We would also agree that the titanium effect will probably be found to depend on the carbon content as well as the heat-treatment.

[10] G. F. Comstock: this volume, page 408.

Recrystallization of Silicon Ferrite in Terms of Rate of Nucleation and Rate of Growth

By J. K. Stanley* and R. F. Mehl,† Member A.I.M.E.

THE recrystallization of cold-worked metals is studied ordinarily by determining the temperatures required for complete recrystallization to occur within a given arbitrary time period, usually within 15 min. to 2 hr. The results obtained are conventionally assembled in a three-dimensional diagram relating this temperature to the amount of cold-work (percentage deformation) and the resultant grain size, though sometimes other modes of representation are employed.[1] Such three-dimensional diagrams are not complete, for the number of variables exceeds the number represented.

The process of recrystallization is characterized by a time-rate, a fact that is not portrayed upon ordinary recrystallization diagrams. It is known that recrystallization consists in the formation of new nuclei and the growth of these nuclei, a process that continues until the matrix is completely consumed and the original set of grains entirely replaced by the new. This knowledge is old.[2] Truly heterogeneous reactions invariably proceed by nucleation and growth; the decomposition of eutectoid solid solutions provides an example about which much is known,[3] and freezing, originally studied by Tammann, provides the classic example. Although recrystallization is not a heterogeneous reaction within the orthodox meaning of the term, the mechanism of the process is the same.

As in eutectoid inversion and freezing, it should be possible to study the rate of isothermal recrystallization as a function of time, and it should also be possible to analyze the isothermal reaction curve into the component rates of nucleation and growth that determine them.* Other methods, not employing the rates of nucleation and growth, have been used to represent the rates of such reactions, but these in general have been artificial and have not led to progress.[4,5]† The theory of recrystallization is not in advanced state; if recrystallization data were obtained in terms of the rate of isothermal recrystallization, and in terms of the rate of nucleation and the rate of growth of recrystallized grains, and in particular if the temperature coefficients of these rates were measured accurately, an adequate theory should be more readily developed.[27]

Such an effort requires proper experimental technique, but especially requires suitable methods of mathematical analysis to convert measurements made upon a surface of polish into values for the rate of nucleation and the rate of growth and to combine these into a rate of isothermal recrystallization. These methods are now available for the case of three-dimensional recrystallization (recrystallization of

* See discussion of this by R. F. Mehl[4] and also by W. A. Johnson and R. F. Mehl.[5]
† This objection can be raised to the method by Rothe[6] and that by E. Piwowarsky.[7]

massive pieces);[5] methods for the case of two-dimensional recrystallization (recrystallization of thin sheets where the diameter of the recrystallized grain is much greater than the sheet thickness) will be presented in the present paper.

The rate of recrystallization at constant temperature is the greater, the greater the degree of cold-work; it is the greater, the higher the temperature; and it is also the greater, the smaller the original grain size.[1,2] In some cases, crystal recovery, intruded between the cold-work and the recrystallization, has been observed to decrease the rate of recrystallization (*vide infra*). Finally, the rate frequently is changed by variations in composition, whether large or small.[2] These are the chief variables affecting the rate of recrystallization; they are, accordingly, also the variables that must be considered in analyzing the rate of recrystallization into the component rate of nucleation and rate of growth. The present paper will provide an account of the determination of the rate of nucleation, N, and the rate of growth, G, in the recrystallization of alpha iron with 1 per cent Si in solid solution, recrystallized at a single temperature after a single degree of cold-working; it will furnish methods by which the effect of the enumerated variables may be ascertained. The phenomenon of grain coalescence, occurring essentially subsequent to actual recrystallization,[2] will not be considered.

PRIOR WORK

A number of measurements of the rate of growth of recrystallized grains have been made; there have been few attempts to measure the rate of nucleation, and in general they have not been satisfactory. Concomitant measurements of the rate of nucleation and the rate of growth, and a determination of the corresponding isothermal recrystallization curve, obviously are required if the measurements are to throw much light on the recrystallization

process. There are no cases where this desideratum has been attained.

Rate of Growth

Polanyi and Schmid[8] measured G for the recrystallization of strained single crystals
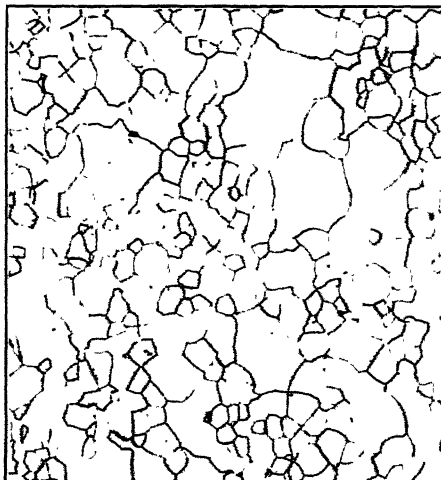
FIG. 1.—SILICON FERRITE BEFORE RECRYSTALLIZATION. ETCHED WITH NITAL. × 100.

of tin and found G to decrease with time. Hanemann[9] reported G to be constant with time in alpha iron. Van Arkel and van Bruggen,[10] working with polycrystalline aluminum, and van Arkel and van Amstel,[11] working with polycrystalline tin, stated that the rate of growth increases with deformation and temperature but did not actually measure G. Karnop and Sachs[12] determined G for polycrystalline aluminum, finding it to remain constant with time, and approximated the effect of temperature and percentage deformation upon G for the recrystallization of copper. Kornfeld and Pawlow[13] measured G for polycrystalline aluminum (wire), finding G constant with time and unaffected by prior recovery. They found that the curve of the radius of the recrystallized grain plotted against time intercepted the time axis at a positive
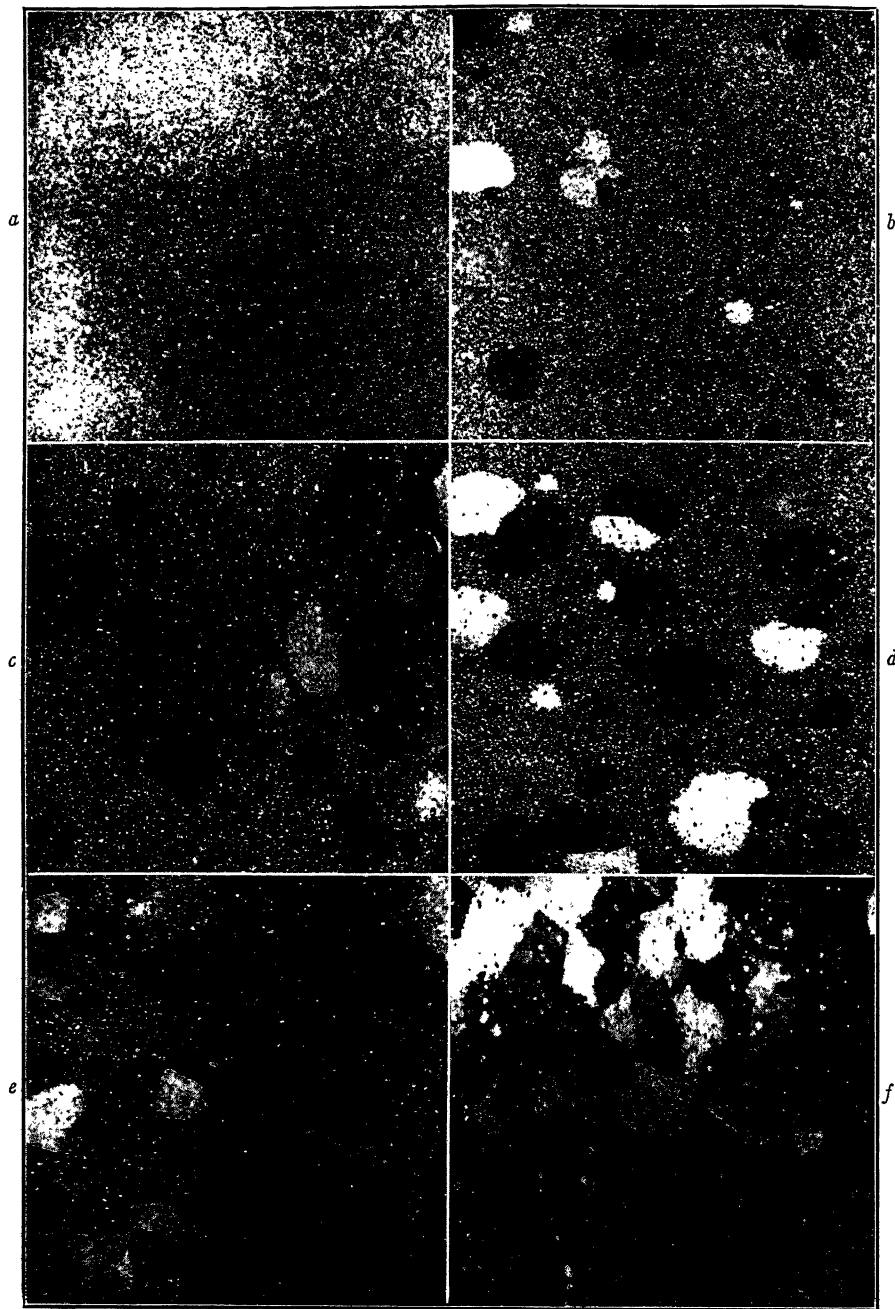
FIG. 2.—PROGRESS OF RECRYSTALLIZATION AT 770°C. IN SILICON FERRITE AFTER 4 PER CENT ELONGATION IN TENSION. ETCHED WITH 10 PER CENT NITAL. × 6.6.

Fig. 2a. 25 minutes. Fig. 2b. 70 minutes. Fig. 2c. 100 minutes. Fig. 2d. 120 minutes. Fig. 2e 150 minutes. Fig. 2f. 190 minutes.

value, providing an "induction period." Kornfeld[14] later reported that G varies with direction in a sample of aluminum wire bearing a preferred orientation. Kornfeld

anistropy in G for polycrystalline aluminum and reported that G varies exponentially with temperature. Kornfeld and Schamarin[19] reported on studies of G in single
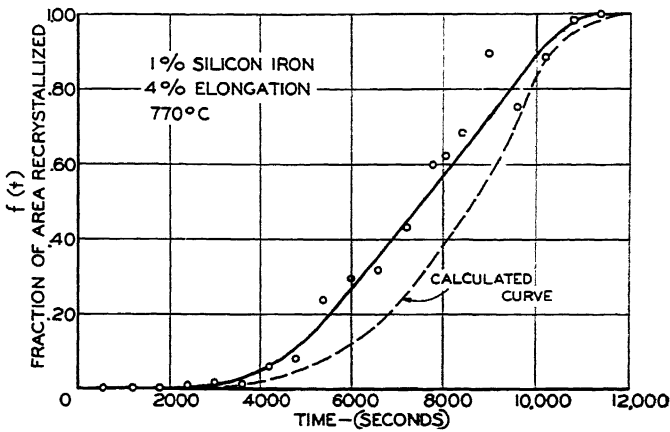
FIG. 3.—ISOTHERMAL RECRYSTALLIZATION CURVE.
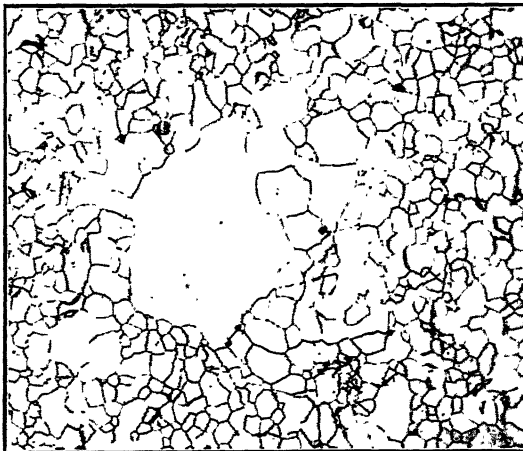
FIG. 4.—SMALL RECRYSTALLIZED GRAIN. ETCHED WITH 5 PER CENT NITAL. × 100.

and Sawizki[15,16] pointed out that the final grain size upon recrystallization is dependent upon the cooperation of N and G, and measured G for alpha ferrosilicon (0.6 per cent Si), tin, and cadmium, finding G constant with time. Kornfeld and Schamarin[17] found G in polycrystalline aluminum to remain constant with time and to increase as the prior strain is increased. Kornfeld and Pawlow[18] again studied the

crystals of aluminum, finding G not affected by recovery, as did Collins and Mathewson.[20] Ivernova[21] reported G in the recrystallization of steel to be unaffected by aluminum and vanadium additions. Masing and Staunau[22] measured G for the recrystallization of zinc sheet, finding G constant with time. Schmid and Boas[23] compared the rates of growth for polycrystalline tin[24] and the growth for a single crystal of alumi-

num[12] and find the growth to be greater in the polycrystalline material.

Rate of Nucleation

Karnop and Sachs[12] made an approximation of N in polycrystalline copper and of

MATERIALS FOR PRESENT TESTS

The analysis of the isothermal reaction curve in terms of N and G is much facilitated if the recrystallized grains grow to approximate spheres, for the geometrical
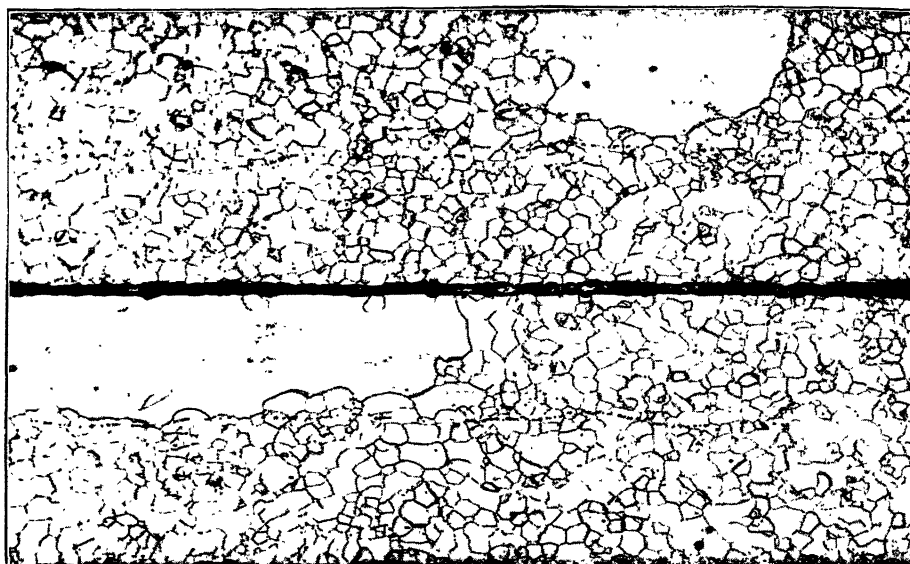
FIG. 5.—PHOTOMICROGRAPH TAKEN NORMAL TO SHEET. SHOWING NEW GRAINS APPEARING AT SHEET SURFACE. CROSS SECTIONS OF TWO SHEETS SHOWN. ETCHED WITH 5 PER CENT NITAL. × 100.

its variation with temperature and percentage deformation. Kornfeld and Schamarin[17] and Kornfeld[25] determined N for the recrystallization of polycrystalline aluminum, using a somewhat questionable method of analysis derived to apply to small samples, finding N to increase with time, to be decreased by prior recovery, and to increase with increasing deformation. Kornfeld and Pawlow[13] report N in polycrystalline aluminum to be decreased by prior recovery, and Kornfeld and Schamarin[19] report N in a single crystal of aluminum to be increased by prior recovery. Ivernova[21] approximated N in steels with aluminum and vanadium additions, finding that these alloys increase N. Collins and Mathewson[20] report recovery to lower N in the recrystallization of single crystals of aluminum.

considerations involved in developing the generalized reaction curve are simpler. Silicon ferrite was chosen for this first study because it has been shown that under suitable conditions the recrystallized grains grow into unusually perfect spheres (p. 147 of ref. 7). It has frequently been observed that metals generally develop recrystallized grains of a multitude of irregular shapes. The experimental determination of N and G is facilitated by simple surface studies on thin sheet, and the data are valid when the diameter of the recrystallized grain is much greater than the thickness of the sheet.

The silicon ferrite used had the following composition: silicon, 1.04 per cent; sulphur, 0.009; phosphorus, 0.010; manganese, 0.035; carbon, 0.006.

This material was prepared from electrolytic iron and high-purity silicon; the iron

was melted in an induction furnace under hydrogen and the silicon was added. The melt was cast, cleaned, forged, and hot-rolled to strip 0.100 in. thick by 1.25 in. wide. This strip was cleaned and cold-rolled to 0.012 in. thick (88 per cent reduction) in several steps without intermediate annealing. This was cut to 12-in. lengths and stacked and the sides of the stack were milled accurately to give the strip a width of 1 in. with accurately parallel sides. Throughout the cold-rolling and milling care was taken to avoid heating. A hole was drilled through one end of the stack to permit arrangement upon a horizontal rod; the strips were then annealed, in hydrogen that had been passed over hot copper and then through an activated-alumina drier, with ⅛-in. separation between adjacent strips, at 825°C. for 25 hr. This provided a grain size of A.S.T.M. number 7, 60 grains per square millimeter of surface. The structure produced is shown in Fig. 1.

METHODS OF TEST

Cold-work was performed by elongation in tension. This type of cold-work is the simplest, uncomplicated by gross complexities in flow and attendant macrostress patterns. The deformation was applied to a 7-in. gauge length; the sample was held in Templin grips, affording a high degree of axiality in loading, and the load was applied slowly by hand; elongation was measured by dividers. The uniformity of elongation was measured at a series of 1-in. lengths and found constant to 5 per cent.

The elongated pieces were cut with a jeweler's saw into 1-in. squares, the strip held between two pieces of soft wood. Care in this operation is important, for excessive distortion during cutting obviously will introduce a variation in recrystallization behavior.

These final samples were annealed for recrystallization as soon after the cold-rolling as possible, for it was observed that aging for 30 days at room temperature

produced a rapid decrease in the rate of nucleation. Evidently, in this material the rate of recrystallization is sensitive to recovery.
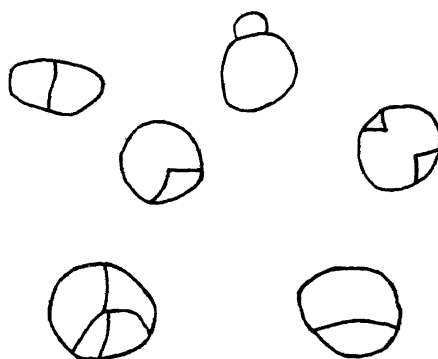
FIG. 6.—SKETCH OF TYPICAL COMPOSITE RECRYSTALLIZED GRAINS.

An attempt was made initially to procure the desired data by repeated anneals of a single sample; this is attractive for a number of reasons—for example, the rate of growth could be measured simply by observing the increase in diameter of a single grain after each of a series of periods of growth. This proved impossible, for the growth was observed to be irregular, and in some grains to have been entirely arrested; apparently the etching required to reveal the grain structure after each period of growth penetrated along the surface of the grain and impeded its subsequent growth.

This difficulty necessitated a statistical approach. Several samples of identical treatment were included in each anneal. Each sample was coated with a magnesia-acetone paste and packed with others, the pack held together with fine iron wire. Several such packs were prepared. Individual packs were tied to wire holders and were dipped into a lead pot for recrystallization. The temperature of the lead pot assumed a constant value in one minute after immersion and remained constant to ±3°C. A pack containing several samples was withdrawn from time to time, and cooled in Sil-O-Cel to avoid distortion.

Each sample removed was cleaned and etched in 10 to 15 per cent Nital to reveal the grain structure.

After etching, each sample was photographed at a magnification of 6.6 diameters
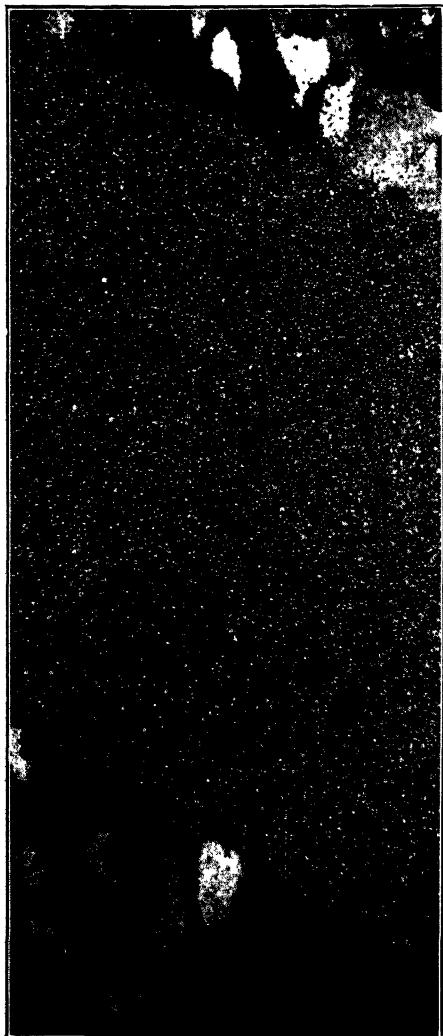
FIG. 7.—RECRYSTALLIZATION IN PARTLY DEFORMED SAMPLE. TIME OF RECRYSTALLIZATION 120 MINUTES. ETCHED WITH 10 PER CENT NITAL. × 6.6.

(Fig. 2) and the outlines of the recrystallized grains were traced on transparent paper. The area of the recrystallized grains

was determined by a planimeter (½ in. around the edges of the photograph was disregarded, for irregularities in recrystallization appeared there originating from the distortion of cutting). This area plotted against time provided the isothermal recrystallization curve, Fig. 3. The number of recrystallized grains to be used in calculating N was counted at each time interval. Seven to nine samples were used for each time period of recrystallization.

ANALYTICAL METHODS AND RESULTS

Structures

The structures produced on isothermal recrystallization at 770°C. after 4 per cent elongation in tension, at six time periods, are shown in Fig. 2. It is not an easy matter to recognize a recrystallized grain shortly after its birth, for it must be appreciably larger than the matrix grains in order to be identified with certainty (Fig. 4). The new grains first appeared nearly always at the surface of the sheet, Fig. 5. When such a grain had grown through the sheet it naturally exhibited a larger area on the side of the sheet where it had first appeared but the use of a large number of samples (seven to nine for each time period) suppressed errors from this source. The recrystallized grains frequently were not single crystals but showed a composite structure (Fig. 6).[7] A study of the orientation relationships subsisting among the separate parts enclosed by the outer boundary would be interesting and instructive; each separate part within each composite was counted as a single grain. Samples that had not been given the full 4 per cent deformation exhibited an interesting phenomenon (Fig. 7); this material has been observed to display an elongation at constant load at the yield point of 3 per cent, forming Lüders lines. In samples where this elongation had not been completed throughout, recrystallization occurred in the deformed regions and displayed a sharp boundary

between this and the adjacent undeformed region.

Data

The rate of nucleation N, representing the number of nuclei formed per unit of time per unit of untransformed area, was obtained by the following procedure. The gives the rate of nucleation for the whole area, uncorrected for the fraction of the area recrystallized; this rate, divided by the fraction of the material recrystallized at that instant in time, gives the true rate of nucleation N as a function of time (Fig. 9). The original data and these derived values are listed in Table 1.

TABLE 1.—*Recrystallization Data*

| Sample No. | Time, Sec. | Fraction Recrystallized | Number of Recrystallized Grains per Sq. Cm. | N | | Radius of Largest Grain, Cm. |
				Uncorrected for Percentage Recrystallization	Number of Nuclei Formed per Sec. per Sq. Cm.	
1	600	0.0002	0.2	3.1×10^{-4}	3.1×10^{-4}	0.006
2	1,200	0.001	1.0	4.6	4.6	0.031
3	1,800	0.002	0.8	6.7	6.7	0.049
4	2,400	0.007	5.3	8.6	8.6	0.043
5	3,000	0.013	2.6	13.0	13.1	0.068
6	3,600	0.013	2.9	18.2	18.8	0.058
7	4,200	0.053	5.3	26.8	28.2	0.095
8	4,800	0.070	5.3	33.2	37.4	0.118
9	5,400	0.236	11.4	40.0	49.5	0.134
10	6,000	0.295	10.0	40.0	54.8	0.171
11	6,600	0.321	11.5	40.0	65.6	0.162
12	7,200	0.434	13.8	36.8	70.8	0.172
13	7,800	0.596	18.8	33.9	80.6	0.173
14	8,100	0.621	16.9	32.0	82.0	0.217
15	8,400	0.677	20.5	26.1	84.3	0.214
16	9,000	0.898	22.3	19.4	88.3	
17	9,600	0.750	19.4	13.2	101.0	0.226
18	10,200	0.883	21.7	8.6	107.5	
19	10,800	0.984				
20	11,400	1.000				

TABLE 2.—*Typical Variation in Data Used in Obtaining Values for Table 1*

Sample No.	Time, Sec.	Fraction Recrystallized	Number of Recrystallized Grains per Sq. Cm.	Radius of Largest Grain, Cm.
Average for set No. 12.......	7,200	0.434	13.8	0.172
Individual values:				
4-115......	7,200	0.775	14.5	
5-133......		0.497	13.5	0.166
7-200......		0.435	16.2	
7-201......		0.503	16.0	0.197
7-202......		0.394	13.6	0.200
7-214......		0.198	12.2	0.148
7-215......		0.238	10.5	0.150

number of recrystallized grains per square centimeter of surface was counted for each recrystallization time interval. These values were plotted against time (Fig. 8). The slope of this plot, determined graphically, It is interesting to note in Fig. 9 that the values of N are low initially and then increase, the end of the curve beginning to turn downward, suggesting that N may in fact pass through a maximum. It is not possible to demonstrate this by direct measurements of N, for the nucleation curve loses precision at greater degrees of recrystallization, but indirect means may be employed. If a distribution curve of the frequency of occurrence of recrystallized grains in different size groups should show a maximum in a partly recrystallized specimen, it may be concluded that N passes through a maximum. Such a curve was prepared from one sample and a pronounced maximum was observed (Fig. 10), supporting the view that N does pass through a maximum. From a grain-size distribution of this sort, the rate of nuclea-

tion can be determined as a function of time from a single specimen.[26]

The rate of growth is obtained simply from the diameters of the largest recrystallized grains at each period of recrystalliza-

second. This curve may be represented by an equation of the type

$$r = G(t - c) \qquad [1]$$

where r is the radius, G the rate of growth,
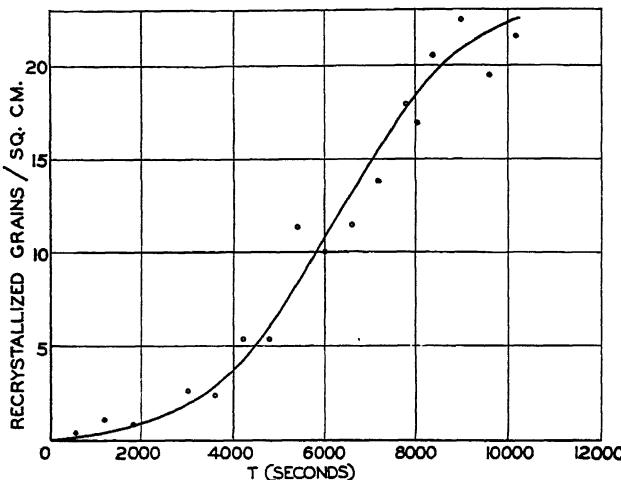
FIG. 8.—NUMBER OF RECRYSTALLIZED GRAINS IN DEPENDENCE UPON TIME OF RECRYSTALLIZATION (UNCORRECTED FOR PERCENTAGE RECRYSTALLIZATION). MANY SAMPLES.
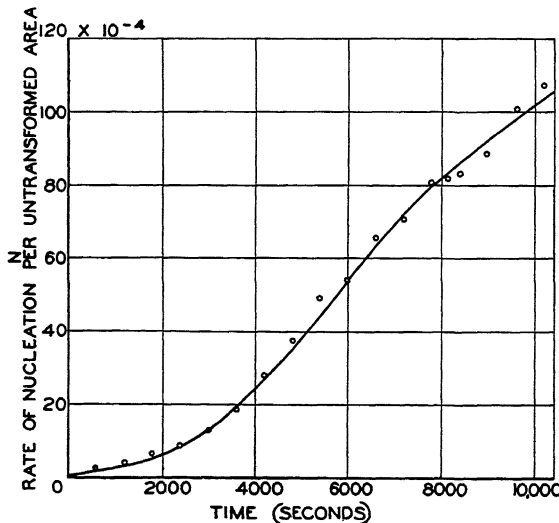
FIG. 9.—RATE OF NUCLEATION AS FUNCTION OF TIME. MANY SAMPLES.

tion, on the assumption that the largest grain in any sample had formed at the first instant of reaction; the slope of this curve is the rate of growth G expressed as the number of centimeters of radial growth per

t the time, and c a constant—the intercept on the time axis. The curve given in Fig. 11 supplies constants for this equation

$$r = 27 \times 10^{-6}(t - 555) \qquad [2]$$

The intercept on the time axis, c, 555 sec. in this case, sometimes designated as an incubation or induction period, may represent a time period of inactivity or may merely represent failure to observe grains nucleated at the first instant of time.

It has been shown that an analytical expression for the rate of reaction in terms of the rate of nucleation and the rate of growth is of considerable usefulness;[4,5] with it, if the rate of reaction and either N or G are measured, the other may be calculated. Since G is usually more readily measured than N, and less subject to variation with structural changes,[3] ordinarily it would be measured and N calculated. It becomes important, then, to derive the expression for the rate of recrystallization in terms of N and G.

It appears safe to assume[5] that the nuclei formed during the first 6000 sec. in Fig. 9, that section of the N-curve during which N increases with time, will play a dominant role in determining the rate of recrystallization, and those formed later a minor role. This section of the curve may be represented by a simple exponential of the type

$$N = a \ exp \ \{bt\} \qquad [3]$$

where t is the time, and a and b are constants. The values of a and b have been evaluated for Fig. 9 by the method of averages, as follows:

$$a = 2.2 \times 10^{-4}$$
$$b = 6 \times 10^{-4}$$

The general analytical expression, derived in the appendix, is

$$f(t) = 1 - exp \left\{ \frac{-2\pi G^2 a}{b^2} \left(\frac{e^{bt}}{b} - \frac{bt^2}{2} - \frac{1}{b} - t \right) \right\} \qquad [4]$$

The values of a and b, from Eq. 3, and the value of G may be substituted in Eq. 4 and a calculated isothermal recrystallization curve obtained, which may be compared

with that measured (Fig. 3). The agreement is fair; sources of error originate in the assumption that the rate of nucleation may be expressed by Eq. 3, in the variableness
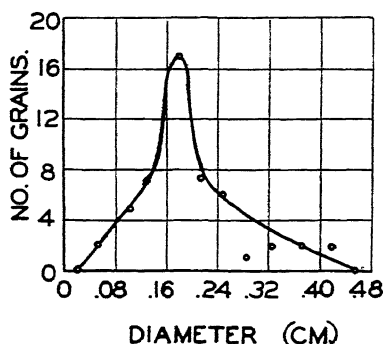
FIG. 10.—DISTRIBUTION OF GRAIN SIZE IN SAMPLE 40 PER CENT RECRYSTALLIZED (120 MINUTES).

of measured N, and in the assumption used in deriving Eq. 4 that each composite nodule (Fig. 6) constitutes a single grain, whereas each part of the composite grains was counted in determining N. A small variation in N sufficient to give $a = 18 \times 10^{-4}$ and $b = 1.3 \times 10^{-4}$ would give a very close agreement between the calculated and the experimental curves.

For gathering data concerning the effect of the many variables on the rate of nucleation, the simplifying assumption may be made that N does not vary with time. For this case the reaction equation becomes (see Appendix):

$$f(t) = 1 - exp \left\{ \frac{-\pi G^2 N t^3}{3} \right\} \qquad [5]$$

If the reaction curve is measured and G determined, N may be calculated. This will yield an average value of N, which should suffice for purposes of comparison.

The values of N listed were obtained on samples recrystallized immediately after cold deformation, for it was found that storage at room temperature induced recovery, lowering N appreciably. A typical example showed the number of grains per

square centimeter of the sample (as in Fig. 8) upon recrystallization for 30 min. was 5.5 when recrystallization was performed immediately after cold-working and

analytical methods given in the appendix, and to Miss M. Ferguson, of the Westinghouse Research Laboratories, for the preparation of the photomicrographs.
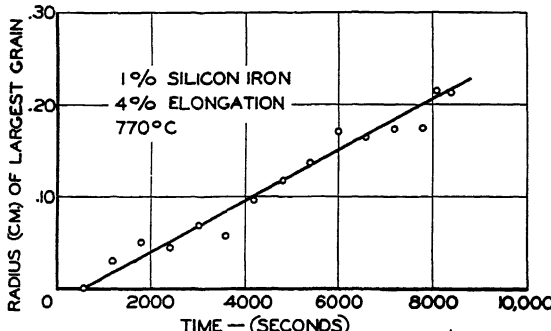
FIG. 11.—RADIUS OF LARGEST GRAINS AS FUNCTION OF TIME.

1.6 when 30 days had been allowed to elapse between cold-working and recrystallization. Apparently recovery[13] decreases N in this material.

SUMMARY

1. Methods are given by which the rate of nucleation and the rate of growth during recrystallization may be determined, and by which the isothermal recrystallization curve may be calculated from the rate of nucleation and the rate of growth.

2. These methods are applied to the recrystallization of silicon ferrite with 1 per cent Si at 770°C. after 4 per cent deformation by elongation in tension.

3. The rate of nucleation is found to increase with time, probably passing through a maximum; the rate of growth remains unchanged with time.

4. Recrystallization affords an isothermal reaction curve similar to those of other processes of nucleation and growth.

5. Recovery preceding recrystallization decreases the rate of nucleation in silicon ferrite.

ACKNOWLEDGMENT

The authors are very much indebted to Dr. W. A. Johnson for the derivation of the

APPENDIX

This is a modification of the analytical method for general nucleation given earlier[5] to apply to "two-dimensional" reaction in sheets where the diameter of the reacted nodule is many times the thickness of the sheets, and where an exponential variation of N with t is assumed.

The area of circle A_1, the nucleus of which formed at time T, is, at some later time, t:

$$A_1 = \pi G^2 (t - T)^2$$

where G is the rate of growth. Differentiating to obtain the rate of change of A with t,

$$dA_1 = 2\pi G^2 (t - T)\, dt$$

The effective increase in area is:

$$dA_2 = dA_1 u(t)$$
$$= 2\pi G^2 (t - T) u(t)\, dt$$

The number of nuclei formed in a short time dT, at some time T, is:

$$dn = a e^{bT}\, dT$$

and the total increase in area of all circles due to such nuclei is

$$dA_3 = dA_2\, dn$$

therefore:

$$dA_3 = 2\pi G^2 a e^{bT} u(t)\, dt(t - T)\, dT$$

and

$$\frac{dA_3}{dt} = 2\pi G^2 a e^{bT} u(t)(t - T)\, dT$$

The total effective rate of growth of all circles nucleated from $T = 0$ to $T = t$ is:

$$\frac{dA_4}{dt} = 2\pi G^2 a u(t) \int_0^t e^{bT}(t - T)\, dT$$

$$= 2\pi G^2 a u(t) \left(\frac{e^{bt}}{b^2} - \frac{t}{b} - \frac{1}{b^2}\right)$$

The fraction transformed is $1 - u(t)$, or the rate is:

$$\frac{-du(t)}{dt}$$

Thus

$$\frac{-du(t)}{dt} = 2\pi G^2 a \left(\frac{e^{bt}}{b^2} - \frac{t}{b} - \frac{1}{b^2}\right) u(t)$$

which becomes:

$$-\ln u(t) = \frac{2\pi G^2 a}{b^2} \left(\frac{e^{bt}}{b} - \frac{bt^2}{2} - t\right) + C$$

From the condition that $u(t) = 1$ when $t = 0$, C is found to be $-\frac{1}{b}$

Then

$$u(t) = e^{-\frac{2\pi G^2 a}{b^2}\left(\frac{e^{bt}}{b} - \frac{bt^2}{2} - t - \frac{1}{b}\right)}$$

And since the fraction transformed is $1 - u(t)$, the expression becomes:

$$f(t) = 1 - e^{-\frac{2\pi G^2 a}{b^2}\left(\frac{e^{bt}}{b} - \frac{bt^2}{2} - t - \frac{1}{b}\right)}$$

The derivation of the reaction equation for constant N and G is given below; the several steps will be made obvious by comparison with the preceding derivation:

$$A_1 = \pi G^2 (t - T)^2$$
$$dA_1 = 2\pi G^2 (t - T)\, dt$$
$$dA_2 = 2\pi G^2 (t - T)u(t)\, dt$$
$$du = N\, dT$$
$$dA_3 = dA_2\, dn$$
$$dA_3 = 2\pi G^2 N u(t)\, dt\, (t - T)\, dT$$
$$\frac{dA_3}{dt} = 2\pi G^2 N u(t)(t - T)\, dT$$
$$\frac{dA_4}{dt} = 2\pi G^2 N u(t) \int_0^t (t - T)\, dT$$
$$-\frac{du(t)}{dt} = 2\pi G^2 N \left(t^2 - \frac{t^2}{2}\right) u(t)$$

$$-\ln u(t) = 2\pi G^2 N \left(\frac{t^3}{3} - \frac{t^3}{6}\right) + C$$

$$u(t) = e^{-\frac{\pi G^2 N}{3} t^3}$$

$$f(t) = 1 - e^{-\frac{\pi G^2 N}{3} t^3}$$

REFERENCES

1. J. Czochralski: Moderne Metallkunde. Berlin, 1924. Julius Springer.
2. R. F. Mehl: Recrystallization. Metals Handbook, 1939. Amer. Soc. for Metals.
3. R. F. Mehl: The Structure and the Rate of Formation of Pearlite. Campbell Memorial Lecture, October 1941. Amer. Soc. for Metals.
4. R. F. Mehl: Physics of Hardenability. Symposium.
5. W. A. Johnson and R. F. Mehl: Reaction Kinetics in Processes of Nucleation and Growth. Trans. A.I.M.E. (1939) 135, 416.
6. H. Hanemann: Über Rekristallisation. Ber. Wertstoffaussch Eisenhüttenleute No. 84.
7. E. Piwowarsky: Allgemeine Metallkunde. Berlin, 1934. Borntraeger.
8. M. Polanyi and E. Schmid: Ztsch. Physik (1925) 32, 684.
9. H. Hanemann: Stahl und Eisen (1927) 47, 481.
10. A. E. van Arkel and M. S. van Bruggen: Ztsch. Physik (1927) 42, 795; (1928) 51, 520.
11. A. E. van Arkel and J. J. A. Ploos van Amstel: Ztsch. Physik (1928) 51, 534.
12. R. Karnop and G. Sachs: Ztsch. Physik (1930) 60, 464.
13. M. O. Kornfeld and W. Pawlow: Phys. Ztsch. Sowjetunion (1934) 6, 74, 537.
14. M. O. Kornfeld: Phys. Ztsch. Sowjetunion (1934) 6, 170.
15. M. O. Kornfeld and F. Sawizki: Phys. Ztsch. (1934) 35, 647.
16. M. O. Kornfeld and F. Sawizki: Phys. Ztsch. Sowjetunion (1935) 8, 528.
17. M. O. Kornfeld and A. Schamarin: Phys. Ztsch. Sowjetunion (1935) 7, 432.
18. M. O. Kornfeld and W. Pawlow: Phys. Ztsch. Sowjetunion (1937) 12, 301.
19. M. O. Kornfeld and A. Schamarin: Phys. Ztsch. Sowjetunion (1937) 11, 302.
20. J. A. Collins and C. H. Mathewson: Trans. A.I.M.E. (1940) 137, 150.
21. V. I. Ivernova: Zadodskaya Labortoriya (U.S.S.R.) (1939) 2, 187.
22. G. Masing and H. Staunau: Ztsch. Metallkunde (1941) 33, 74.
23. E. Schmid and W. Boas: "Kristallplastizitat, 226. Berlin, 1935. Julius Springer.
24. J. Czochralski: Jnl. Met. Erz. (1916) 13, 381.
25. M. O. Kornfeld: Phys. Ztsch. Sowjetunion (1933) 4, 668.
26. F. C. Hull, R. A. Colton and R. F. Mehl: Rate of Nucleation and Rate of Growth of Pearlite. This volume, page 185.
27. R. F. Mehl: Discussion. Trans. A.I.M.E. (1940) 137, 168.

DISCUSSION

(A. B. Greninger presiding)

S. E. MADDIGAN,* Waterbury, Conn.—One
of the major problems in a recrystallization study is the choice of a sampling method. Unfortunately, it seems that most sampling methods are subject to criticism. A statistical

* Research Physicist, Chase Brass and Copper Co.

method like that used here would seem to be preferable usually to that of following the course of a single sample through repeated anneals. One of the objections to the latter method is that the observed reactions occur on an air-metal interface where conditions undoubtedly are different from those in the body of the metal. This objection can also be raised in the present work.

The grain size used was small compared with the sheet thickness, so that nucleation might be considered as random. However, as the authors themselves point out, nucleation occurred first at the sheet surface, indicating that conditions at the air-metal interface were widely different from those in the metal body. This is to be expected, since not only do we have the additional interface term in the free energy expression, but also the strain energy is different at the sheet surface because of the lack of restraint in one direction during the stretching. Furthermore, according to Koehler,[28] dislocations tend to be drawn to the specimen surface and this presumably would affect the nucleation rate. As a result of these factors the nucleation rate determined here might be considerably different from that for the body of the metal.

The question of an incubation period is one that would merit considerable further study. As the authors point out, the positive intercept on the time axis in Fig. 11 may be due to difficulties in observations. However, it is possible that there is an actual delay as observed in some phase changes such as the phenomenon of supercooling. In the latter case, during freezing the phase with higher free energy seems to develop a metastable state until such time as statistical fluctuation or some other cause provides the activation energy to produce the transition at some single point. This seems to act as a trigger mechanism to start the reaction in other parts of the system. From the academic standpoint at least, this is a question that needs to be investigated.

In distinguishing between new grains and unrecrystallized matrix it is advisable to have either a very small initial grain size, as used here, or a sufficiently large initial grain size so that the new grains can be identified by their smallness compared with the old. This latter method would be preferable in studying the early stages of the reaction. However, there

[28] Koehler: *Phys. Rev.* (1941) **60**, 397.

would be still an initial time period when the best microscope could not detect new grains. This problem would seem to be worthy of the electron microscope. It should be mentioned in passing that if the whole curve in Fig. 11 needs to be shifted because of observational error, the same applies to Fig. 8. This might lead to a better agreement between calculated and experimental values.

The lowering of N by recovery is fundamentally important to the theory of recrystallization. The whole subject of nucleation centers and of recovery is largely speculative, and deserves to be reconsidered at frequent intervals. From recent papers on dislocation theory, internal friction, etc., one is led to the possibility that dislocations are responsible not only for work-hardening but also for nucleation in recrystallization. Koehler has indicated the possible existence of a more or less regular lattice of dislocations of about 100 Å. spacing superimposed on the finer lattice of the metal atoms. Perhaps the units of this dislocation lattice act as nuclei; the lack of complete regularity would cause some cells to be more probable as nuclei than others. Perhaps, on the other hand, the motion of dislocations caused by annealing is the mechanism that starts growth of the nuclei. At any rate, evidence exists that processes that cause a decrease in the number of dislocations also cause a decrease in the nucleation rate.

P. A. BECK,* Reading, Pa.—For the first time, accurate measurements have been made to determine the rate of nucleation during recrystallization as a function of time. The most interesting and most astonishing result of this work is that the rate of nucleation monotonously increases with time. This is all the more surprising because a decrease in the number of nuclei by recovery at room temperature was established by the authors. The fact that the rate of nucleation actually increases with time must be the result of some other effect, perhaps a particular distribution of the incubation periods. I hope that the authors may be induced to give us their thought on this subject.

It would be extremely interesting to have such rate of nucleation and rate of growth

* Metallurgist, The Beryllium Corporation of Pennsylvania.

curves established by the method developed by the authors for varying conditions of temperature and deformation. Such exact data will give, for the first time, a deeper insight into the

FIG. 12.

causes of the variation of grain size with recrystallization temperature. It is to be hoped that the authors will be able to extend their studies in this direction.

It is interesting to see that the phenomenon of selective recrystallization along the Lüders' lines occurs with 1 per cent silicon ferrite. This phenomenon was first found with tin and described in a short publication in 1929 (Beck: *Ztsch. fur Physik*). (See Fig. 12.)

There is here a question that requires further clarification. It is stated in the paper that a maximum in the grain-size distribution curve (Fig. 10) should correspond to a maximum in the true rate of nucleation N versus time curve (Fig. 9). According to the grain-size distribution curve, after 7200 sec. of recrystallization the grain size with highest frequency was 0.18 cm. With the value of the rate of linear growth given by the authors, $G = 27 \times 10^{-6}$ cm. per sec. (Fig. 11), the age of these most frequent grains can be calculated to about 3300 sec. This places their date of birth at 3900 sec. after the start of recrystallization. It is readily seen in Fig. 9 that N has no maximum at 3900 sec. As a matter of fact, N has no maximum at all as far as the data go. Fortunately, there is really no need to expect a maximum in Fig. 9. Instead of with N, the grain-size distribution curve should be properly compared with the *uncorrected* rate of nucleation. This is obvious if we consider that the decrease in the rate of formation of recrystallized grains toward the end of the process (toward the small diameters in Fig. 10), which is due to the decrease of unrecrystallized area, finds expression only in the uncorrected rate of nucleation curve.

Fig. 8 gives the total number of recrystallized grains per square centimeter. The slope of

this curve gives the uncorrected rate of nucleation. The maximum of the grain-size distribution curve should correspond to the maximum of this slope. However, the maximum of the slope of the curve in Fig. 8 lies around 6000 sec. instead of at 3900 sec., as could be expected from Fig. 10. To make these considerations somewhat more quantitative, compare the grains of maximum frequency with those half their size. The latter grains, of 0.09 cm. diameter, are only one third as numerous as the 0.18-cm. grains, according to the grain-size distribution curve (Fig. 10). Their date of birth can be calculated to 4550 sec. after the start of recrystallization and, according to the higher slope of the curve in Fig. 8 at this point, they should be roughly 50 per cent more numerous than the grains of 0.18-cm. diameter. Here then is a contradiction worth some attention. Possibly Fig. 10 relates only to a single specimen and does not represent true average conditions, as does Fig. 8. In this case its significance is doubtful, and it should be replaced by a curve giving the average grain-size distribution in all seven or nine samples of identical treatment. Such a curve might achieve better agreement with Fig. 8.

J. K. STANLEY AND R. F. MEHL (authors' reply).—Dr. Maddigan raises the point that the observed reactions in the thin material employed (which might be considered a two-dimensional system) occur on the air-metal interface, and that the results undoubtedly would be different in the body of a "three-dimensional" metal. We are aware of this limitation in the results, but the two-dimensional model was accepted because the recrystallization of thin sheet is a matter of considerable commercial importance; the mathematical methods used are limited to this special case. The work is continuing, with comparable experiments under way on thick samples, both

of iron-silicon alloys and of high-purity aluminum.

The incubation period observed is puzzling in many ways. It was noted by Kornfeld, though we have distrusted his measured values because he employed small samples and may have missed the first recrystallized grain, thus obtaining values too high. In the past we have been skeptical of the reality of the induction period in this and generally in polyphase reactions, but this now seems unwarranted in view of recent results, including the present and those on the formation of pearlite from austenite. It now appears to us that both the induction period and the increase in the rate of nucleation with time must be an inherent characteristic of such nucleation and growth processes, and that any valid theory would include both. While such a theory might now be devised, it appears to us that the sounder approach would be first to develop a considerable body of experimental data. Such work should succeed in defining the relationship between recovery and rate of nucleation, a matter now in a sorry state. Both Dr. Maddigan and Dr. Beck have commented on this.

Dr. Beck has read into the data of Fig. 10 a significance we did not intend. Fig. 10 was introduced primarily to indicate in a qualitative manner that the nucleation curve must have gone through a maximum as indicated in Fig. 8, and secondarily to show the kind of distribution curve of grain size we found experimentally. Fig. 10 by itself without supporting evidence does not prove the inconstancy of the rate of nucleation, for even with a constant rate of nucleation a maximum in the grain-size distribution curve is found.[5]

One of the causes of difficulty is that in samples treated identically the maximum as in Fig. 10 occurs at different times and is of different magnitude. That this might be the case can be inferred from the variability in Table 2. For an accurate grain-size distribution curve, an average for all samples must be statistically derived. With such a wide spread in the data, a rigorous treatment is hardly justified. The specimen used for preparing Fig. 10 is only one of over 200 studied. Another difficulty in assaying the data is the effect of impingement of the growing grains in the matrix, which again varies in the several samples. The mathematical treatment of this impingement effect is extremely difficult, and since no attempt was made experimentally to study this phenomenon, we are at a loss on how to analyze a grain-size distribution curve that will lead to the correlation that Dr. Beck says must exist.

Carbides in Low-chromium Steel

By Walter Crafts,* Member A.I.M.E. and C. M. Offenhauer*

(New York Meeting, February 1942)

In the course of study of the heat-treatment of low-alloy steels, the behavior of alloy carbides at subcritical temperatures was found to vary from that indicated by published investigations. In order to establish the ranges of formation of carbides in low-chromium steels, a series of steels containing up to 0.60 per cent carbon and 7.5 per cent chromium has been investigated with respect to the type of carbide formed after quenching and tempering at subcritical temperatures. The types of carbide formed as products of austenite transformation to pearlitic and pseudomartensitic structures have also been determined.

There have been numerous investigations of the carbides in chromium steels and diagrams of the iron-chromium-carbon system.[1] Westgren, Phragmén and Negresco[2] identified the following carbides in chromium steels:

Cementite............ Fe_3C (containing up to about 15 per cent Cr)

Trigonal carbide...... Cr_7C_3 (containing up to about 55 per cent Fe)

Cubic carbide........ Cr_4C (or $Cr_{23}C_6$) (containing up to about 25 per cent Fe)

Orthorhombic carbide . Cr_3C_2 (containing only a few per cent Fe)

The most complete information on the iron-chromium-carbon system was supplied by Tofaute, Sponheuer and Bennek[3] and by Tofaute, Küttner and Büttinghaus.[4] By

means of dilatometric and microscopic studies, sections of the diagram were established. This diagram showed the presence of the special carbide Cr_7C_3 in steels containing about 2.5 per cent to 12 per cent chromium in low-carbon steels and from about 5 to 20 per cent chromium in 1 per cent carbon alloys from A_1 to room temperature.

The present investigation has shown that a carbide inversion from Fe_3C to Cr_7C_3 occurs in chromium steels containing more than about 1 per cent chromium after hardening and tempering at subcritical temperatures above about 500°C. The type of carbide observed to be more stable in quenched and tempered specimens was also found to be produced by direct austenite transformation in corresponding ranges of temperature and composition.

Experimental Procedure

The steels used in these experiments were made in magnesia-lined crucibles in high-frequency furnaces and were poured into 2-in. ingots. The ingots were forged into 1-in. round bars, and all heat-treatments were conducted on specimens of this section size. Sections of the bar stock 8 in. long were hardened in air, oil or water, depending on the composition, after heating to a temperature sufficiently high to dissolve the carbides. The low-carbon and low-chromium steels were not entirely martensitic after quenching, and contained some ferrite and pseudomartensite. No pearlite was observed in the microstructures after quenching. The quenched bars were cut into

275

sections and tempered at the indicated temperatures. After air cooling, small specimens were cut from the bars for microscopic and X-ray studies.
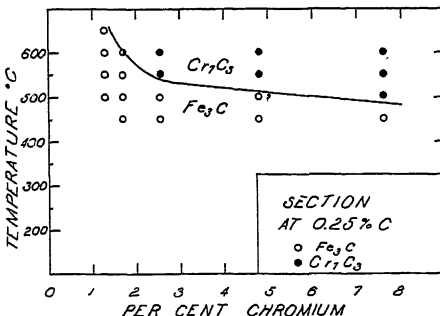
FIG. 1.—CARBIDES IN QUENCHED AND TEMPERED 0.10 PER CENT CARBON STEELS.

The specimens for X-ray examination were completely descaled and subjected to carbide separation in an electrolytic cell consisting of a 5 per cent HCl solution and a platinum cathode. A voltage of approximately 1.5 volts was maintained across the cell for a period of from 8 to 24 hr., depending on the composition. At the conclusion of the separation, the carbides were collected and washed by decantation with successive washes of water, alcohol, and ether. The residues were allowed to dry in air and then formed into a small wedge-shaped specimen. The X-ray camera was of the Debye-Scherrer type using unfiltered cobalt radiation. The X-ray patterns obtained were checked against standard patterns, and data obtained from published work.[2]

It should be noted that certain limitations are involved in the process of separation as conducted in this investigation. The more cathodic materials tend to be emphasized at the expense of the more soluble components. In addition, it is possible that some components may be masked because of volume considerations. Phases other than carbides, such as metal, oxides, sulphides and nitrides, were observed in some cases but have not been reported

because they did not appear to be pertinent to the carbide investigation. All of the residues were not analyzed chemically, and the terms "Fe_3C" and "Cr_7C_3" are used
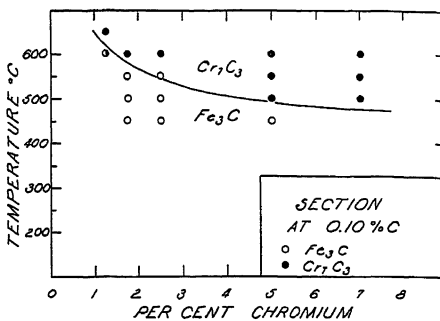
FIG. 2.—CARBIDES IN QUENCHED AND TEMPERED 0.25 PER CENT CARBON STEELS.

to express the crystal structure rather than the exact chemical composition.

In order to determine a suitable period for tempering, steel No. 14 was tempered for various time intervals at 600°C. The amount of conversion is shown in Table 1.

TABLE 1.—Amounts of Conversion

Tempering Period, Hr.	Hardness, R_C	X-ray Structure
1	34	No pattern
3	32	Fe_3C
6	29	Cr_7C_3, small Fe_3C
12	27	Cr_7C_3, trace Fe_3C
24	26	Cr_7C_3, doubtful trace Fe_3C
64	24	Cr_7C_3

In addition, several representative specimens were tempered for both 24-hr. and 64-hr. periods. The longer tempering period did not produce significant changes except in steels of borderline compositions. In order to be assured of more nearly complete conversion of carbides, the specimens were tempered for 64 hours.

RESULTS OF TESTS

The results of the X-ray study of the quenched and tempered specimens are presented in Table 2 and Figs. 1 to 4. After tempering at 500° to 600°C. the carbide in the steels containing more than 1

TABLE 2.—*Composition, Heat-treatment and X-ray Data*

Heat No.	Composition, Per Cent				Quench		Tempering	X-ray Structure
	C	Mn	Si	Cr	Temperature, Deg. C.	Medium	Temperature, Deg. C.	
1	0.06	0.67	0.20	1.26	925	Water	600	Fe_3C, Cr_7C_3
							650	Cr_7C_3
2	0.15	0.43	0.24	1.73	925	Water	450	Fe_3C
							500	Fe_3C
							550	Fe_3C
							600	Cr_7C_3
3	0.14	0.42	0.19	2.51	925	Water	450	Fe_3C
							500	Fe_3C
							550	Fe_3C
							600	Cr_7C_3 tr. Fe_3C?
4	0.05	0.51	0.20	3.48	925	Water	450	Fe_3C
							500	Cr_7C_3 poor pattern
							550	Cr_7C_3
							600	Cr_7C_3
5	0.11	0.51	0.27	4.99	1050	Air	450	Fe_3C
							500	Cr_7C_3 tr. Fe_3C
							550	Cr_7C_3
							600	Cr_7C_3
6	0.09	0.43	0.23	7.53	925	Air	450	No pattern
							500	Cr_7C_3
							550	Cr_7C_3
							600	Cr_7C_3
7	0.28	0.55	0.26	1.31	925	Water	500	Fe_3C
							550	Fe_3C
							600	Fe_3C
							650	Fe_3C
8	0.26	0.42	0.28	1.70	925	Oil	450	Fe_3C
							500	Fe_3C
							550	Fe_3C
							600	Fe_3C, Cr_7C_3
9	0.27	0.48	0.31	2.54	925	Oil	450	Fe_3C
							500	Fe_3C, Cr_7C_3 ? poor pattern
							550	Cr_7C_3 tr. Fe_3C ?
							600	Cr_7C_3
10	0.29	0.49	0.27	4.80	1000	Air	450	Fe_3C
							500	Fe_3C ? poor pattern
							550	Cr_7C_3
							600	Cr_7C_3
11	0.26	0.49	0.28	7.60	1000	Air	450	Fe_3C
							500	Cr_7C_3
							550	Cr_7C_3
							600	Cr_7C_3
12	0.41	0.50	0.22	1.30	925	Oil	500	Fe_3C
							550	Fe_3C
							600	Fe_3C
							650	Fe_3C
13	0.36	0.44	0.29	1.77	925	Oil	450	Fe_3C
							500	Fe_3C
							550	Fe_3C
							600	Cr_7C_3, Fe_3C
14	0.40	0.52	0.27	2.56	925	Oil	450	Fe_3C
							500	Fe_3C
							550	Cr_7C_3 diffuse
							600	Cr_7C_3
15	0.40	0.54	0.27	5.15	1050	Air	450	Fe_3C
							500	Cr_7C_3 ? poor pattern
							550	Cr_7C_3
							600	Cr_7C_3
16	0.40	0.56	0.26	7.51	1050	Air	450	Fe_3C
							500	Cr_7C_3 poor pattern
							550	Cr_7C_3
							600	Cr_7C_3
17	0.60	0.55	0.20	1.74	1000	Oil	450	Fe_3C
							500	Fe_3C
							550	Fe_3C
							600	Fe_3C
18	0.62	0.49	0.30	2.47	925	Oil	450	Fe_3C
							500	Fe_3C
							550	Fe_3C
							600	Fe_3C
19	0.60	0.40	0.30	5.13	1050	Air	450	Fe_3C
							500	Cr_7C_3, Fe_3C
							550	Cr_7C_3 tr. Fe_3C
							600	Cr_7C_3
20	0.65	0.50	0.22	7.54	1110	Air	450	Fe_3C
							500	Cr_7C_3 Weak
							550	Cr_7C_3
							600	Cr_7C_3

to 3 per cent chromium was found to be of the Cr_7C_3 type. After tempering at 450°C. the carbide was of the Fe_3C type. From this it is apparent, contrary to the
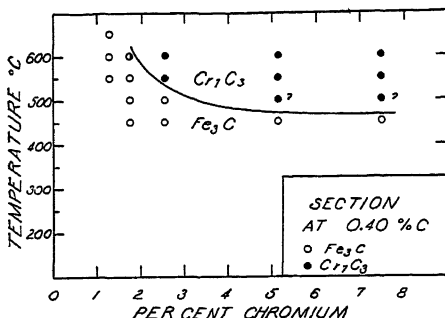
FIG. 3.—CARBIDES IN QUENCHED AND TEMPERED 0.40 PER CENT CARBON STEELS.

prediction of Tofaute, Küttner and Büttinghaus,[4] that the form of the carbide depends on the tempering temperature. The transition temperature range below which Fe_3C is formed and above which Cr_7C_3 is formed, is just below 500°C. for the higher chromium contents and becomes higher as the chromium content is lowered. The precise position of the lines dividing the carbide fields is open to some question, as the diffraction patterns near the mixed fields were relatively weak and diffuse as compared with the other patterns. This condition is thought to reflect the somewhat disorganized state of the carbides during the process of transformation. For this reason the boundaries of the mixed carbide field were not established.

The ranges of inversion with respect to chromium and carbon at 600°C. are illustrated in Fig. 5. The effect of carbon in increasing the range of Fe_3C is in substantial agreement with the work of Westgren, Phragmén and Negresco.[2]

Chemical analyses were determined on residues of steel No. 14 (0.40 per cent C, 2.56 per cent Cr), which approach closely the limit of the Cr_7C_3 range. The chemical composition and X-ray structures of the residues are shown in Table 3.

Considering that the 550°C. product is probably a mixture or a transition structure, these results confirm the solubilities given by Westgren, Phragmén, and Ne-
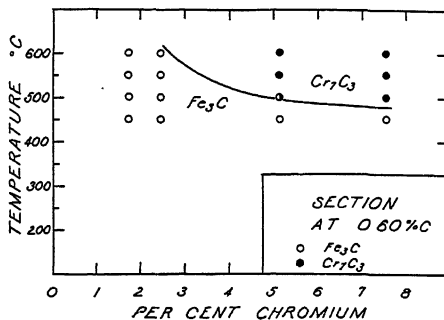
FIG. 4.—CARBIDES IN QUENCHED AND TEMPERED 0.60 PER CENT CARBON STEELS.

gresco[2] of 15 per cent Cr in Fe_3C and 55 per cent Fe in Cr_7C_3. It is of interest that
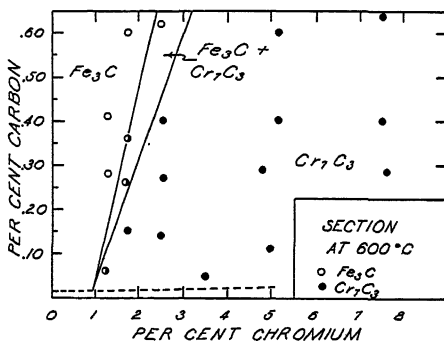
FIG. 5.—CARBIDES IN STEELS QUENCHED AND TEMPERED AT 600°C.

from these analyses it may be calculated that in the sample tempered at 600°C. to

TABLE 3.—*Chemical Composition and Structure*

Tempering Temperature, Deg. C.	X-ray Structure	Fe, Per Cent	Cr, Per Cent	Equivalent to
500	Fe_3C	59.2	12.4	Fe_3C containing 16 per cent Cr
550	Cr_7C_3 (diffuse)	58.1	19.6	Cr_7C_3 containing 68 per cent Fe
600	Cr_7C_3	50.3	29.6	Cr_7C_3 containing 57.5 per cent Fe

form Cr_7C_3 the carbide contained 1.46 per cent and the ferrite 1.10 per cent chromium.

The microstructure of the specimens as the tempering temperature was increased from 450° to 600°C., as shown in Figs. 6 to 9. However, it was not concluded
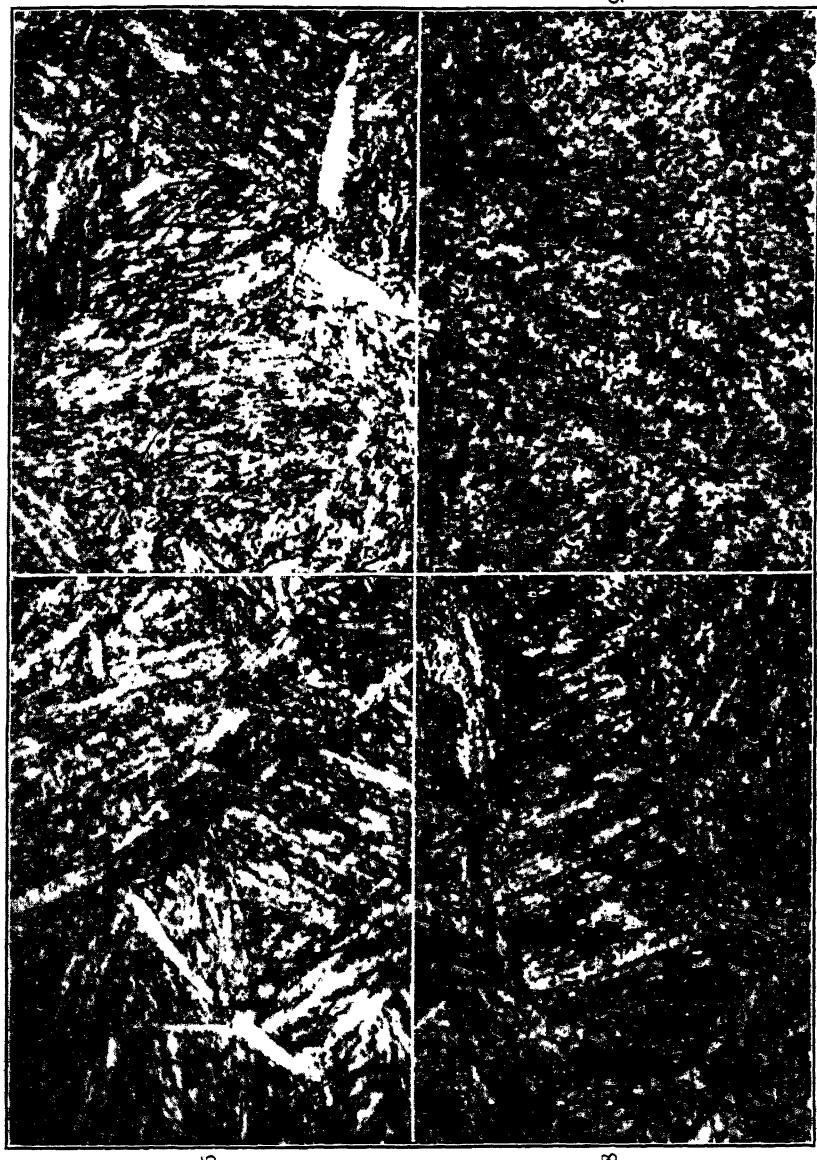
FIG. 6.—STEEL NO. 14 QUENCHED AND TEMPERED AT 450°C. FOR 64 HOURS. × 1000.
FIG. 7.—STEEL NO. 14 QUENCHED AND TEMPERED AT 500°C. FOR 64 HOURS. × 1000.
FIG. 8.—STEEL NO. 14 QUENCHED AND TEMPERED AT 550°C. FOR 64 HOURS. × 1000.
FIG. 9.—STEEL NO. 14 QUENCHED AND TEMPERED AT 600°C. FOR 64 HOURS. × 1000.

changed from a tempered structure showing the markings of the original martensite to an almost completely patternless precipitation of carbides in most of the specimens that this microstructural change was due to the inversion of the carbides, since many of the higher chromium steels retained their acicular appearance above the temperature

at which the inversion occurred and the low-chromium alloys tended to lose the acicular appearance without any change in the type of carbide.

500°C. appeared to be Cr_7C_3, the formation of this carbide instead of cementite was anticipated in the transformation of austenite at these temperatures. In order to deter-
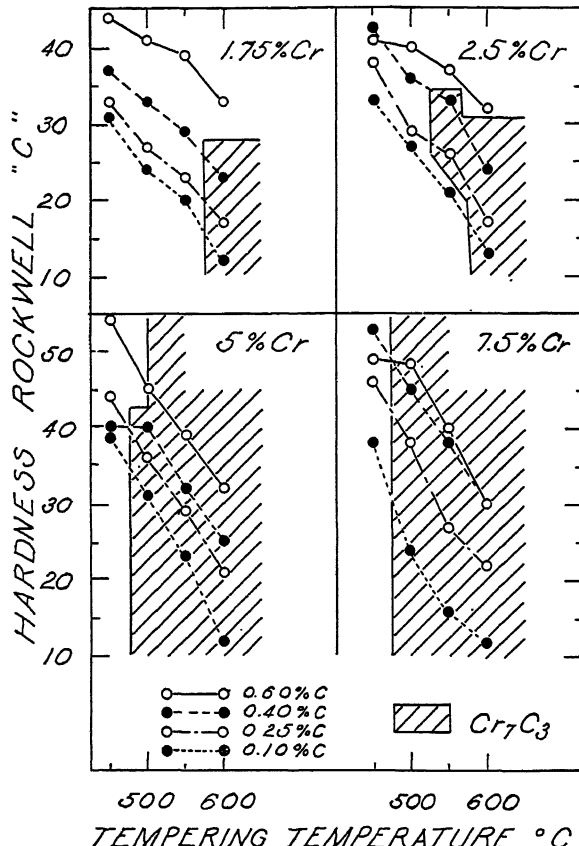
FIG. 10.—HARDNESS OF CHROMIUM STEELS QUENCHED AND TEMPERED FOR 64 HOURS.

The hardness of the specimens tempered for 64 hr. is shown in Fig. 10. Although the gradation to lower hardness with higher tempering temperatures was not always regular, the deviations were of a minor order and did not indicate that the form of the carbide had a significant effect on hardness.

AUSTENITE TRANSFORMATION

Inasmuch as the more stable form of the carbide at subcritical temperatures above

mine whether this was true, steels were transformed isothermally. After heating to dissolve the carbides, a steel containing 0.48 per cent carbon and 3.5 per cent chromium was transformed completely at 650°C. in 500 sec. Another steel containing 0.40 per cent carbon and 5.15 per cent chromium was completely transformed at 600°C. in 24 hr. X-ray diffraction patterns of residues from both steels revealed that the carbides were in the form of Cr_7C_3. It appeared, therefore, that the austenite transformed with the production of primary

Cr_7C_3. The microstructures resulting from the transformation are shown in Fig. 11.

In order to determine the type of carbide formed from austenite transformation at

to electrolytic extraction and X-ray analysis of the carbides. In both cases the carbides were found to be Fe_3C. In higher chromium steels—for example, in a normal-
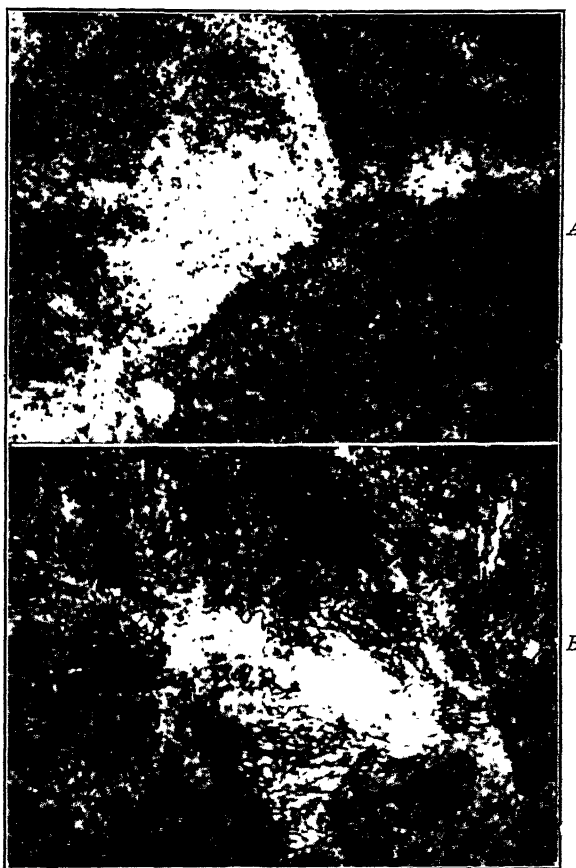
FIG. 11.—ISOTHERMAL TRANSFORMATION STRUCTURES.
A. 0.48 per cent C, 3.5 per cent Cr. 500 sec. at 650°C. × 1500.
B. 0.40 per cent C, 5.15 per cent Cr. 24 hr. at 600°C. × 1000.

temperatures below 500°C., chromium steels were heat-treated to produce pseudomartensite by transformation in the range of 300° to 450°C. on continuous cooling. Steels containing 0.33 per cent carbon, 2 per cent chromium, and 0.27 per cent carbon, 3.05 per cent chromium, were normalized. The samples were examined microscopically to verify the pseudomartensitic character of the microstructure and were submitted

ized 0.17 per cent carbon, 5.04 per cent chromium steel—diffuse patterns of the Fe_3C type have been found.

The limits of composition and temperature within which Cr_7C_3 is produced in the transformation of austenite remain to be determined precisely. It has been found, however, that in specific cases the type of carbide produced by direct transformation was consistent with the type of carbide

found to be more stable after quenching and tempering. The range of greater stability of Cr_7C_3, therefore, seems to be essentially the same whether it is formed from austenite or martensite. Thus it would appear that the tendency toward the formation of Cr_7C_3 may influence the hardening as well as the tempering process and may be closely related to the greater stability of the austenite in ranges in which the alloy carbide is more stable than cementite. This tendency may explain the sluggish formation of pearlite and the pronounced shelf illustrated by Davenport[5] at about 500°C. in the S-curve of chromium steels.

CONCLUSIONS

It cannot be emphasized too strongly that the electrolytic extraction and X-ray examination can only demonstrate the presence—not conclusively prove the absence—of a constituent. However, with this limitation, the study of carbides in low-chromium steels has suggested the following conclusions.

Chromium carbide (Cr_7C_3) is formed at subcritical temperatures above about 500°C. in chromium steels containing from about 1 to more than 7.5 per cent chromium. Within this range Cr_7C_3 may be

formed either directly from austenite or by tempering of martensitic and cementitic structures, and the tendency toward formation of Cr_7C_3 may be related to the stability of austenite above the lower nose of the S-curve. When formed below about 500°C. the carbide was found to be in the form of Fe_3C at all chromium contents. It may be concluded therefore that in these low-chromium steels the form of the carbide is controlled by the temperature of transformation of austenite or tempering of martensite.

ACKNOWLEDGMENTS

REFERENCES

1. A. B. Kinzel and W. Crafts: The Alloys of Iron and Chromium, I—Low-chromium Alloys. New York, 1937. McGraw-Hill Book Co., Inc.
2. A. Westgren, G. Phragmén and T. Negresco: *Jnl. Iron and Steel Inst.* (1928) 117, 383–400.
3. W. Tofaute, A. Sponheuer and H. Bennek: *Archiv Eisenhüttenwesen* (1934–1935) 8, 499–506.
4. W. Tofaute, C. Küttner and A. Büttinghaus: *Archiv Eisenhüttenwesen* 1936 9, 606–616.
5. E. S. Davenport: *Trans. Amer. Soc. Metals* (1939) 27, 837–886.

The S-curve of a Chromium-nickel Steel

By Blake M. Loring,* Junior Member A.I.M.E.

RECENTLY the S-curves for 30 to 40 alloy steels have been published.[1,2] These steels show individual characteristics, which make each additional S-curve of great interest. There are important differences in the mechanism of the transformation process, the type of transformation product, and the influence of alloying elements. Steels of the same general alloy composition may possess such variable characteristics with regard to the length of time of isothermal transformation that an S-curve for each heat of steel may be desirable.

In the present work the isothermal transformation of a steel having the following composition and grain size was studied: 0.29 per cent carbon; 0.21 manganese; 0.026 phosphorus; 0.017 sulphur; 0.056 silicon; 1.45 chromium; 3.25 nickel; austenite grain size, 7.

The progress of the isothermal transformation was followed by several different methods, including hardness measurements, dilatometer observations, and examinations of the microstructure. It was not expected that these methods would be in precise agreement.[3] Accordingly, the changes in microstructure and hardness were given additional weight in determining the initial stage of transformation and the dilatometer measurements were relied on in estimating the completion of the process. The beginning of transformation was indicated by 1 per cent of transformation

products and the end of transformation by about 99 per cent. The reproducibility of the various methods in the ranges of highest sensitivity was checked by several observations at each time and temperature.

The steel used in this investigation was annealed for 24 hr. at 925°C. Macroetching revealed no serious segregation. The specimens for the metallographic and hardness investigations were 1¼ by ½ by ⅛ in. Wires attached to the samples were used for handling, instead of tongs, to avoid chilling.

The specimens were heated at 845°C. for ½ hr. and quenched into constant-temperature salt baths held at various temperatures from 205° to 650°C. The time required to transfer the specimens was found to be about 1½ sec., and nearly 5 sec. more was required for them to come to the temperature of the bath. After various lengths of time in the constant-temperature baths the specimens were quenched in water at 21°C. The specimens were cut in half for the metallographic examination, to provide a surface free from decarburization. To determine the beginning and end of the transformation the percentage of transformation determined metallographically and by hardness was plotted against time. A planimeter was used in the metallographic determination.

The hardness and metallographic determinations made at room temperature were confirmed reasonably well by dilatometer measurements taken during the process of transformation at the various temperatures. Two dilatometers were used to

secure the more direct information. For high temperatures a quartz dilatometer gave best results and for low temperatures a quenching dilatometer based on the relief, or the tempering of a tetragonal phase. The dilatometer observations were checked several times on more than one specimen.
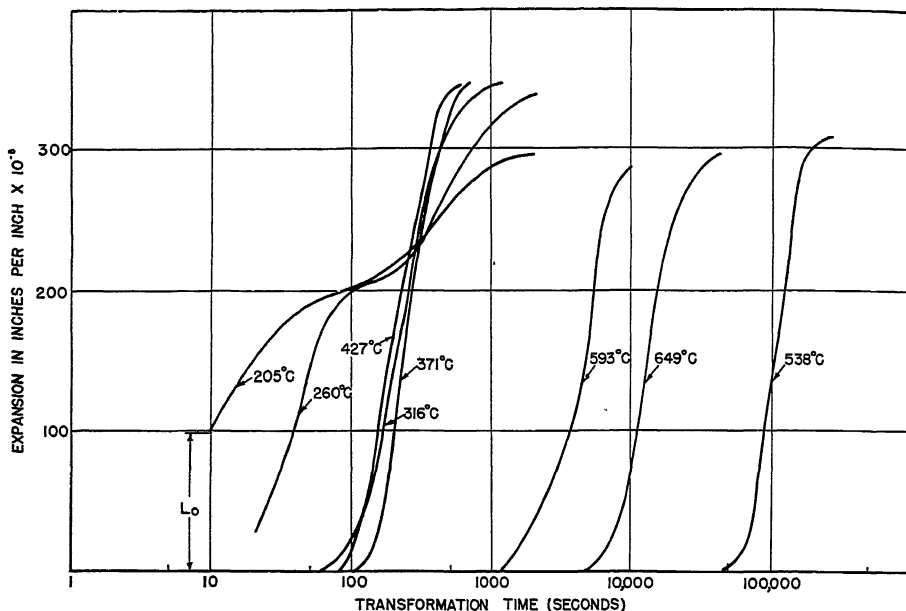
FIG. 1.—EFFECT OF TEMPERATURE ON EXPANSION.

original design of Bain and Davenport was preferred.[4] Both dilatometers could be read to ±0.00001 inches.

The greater expansion at low temperatures shown in Fig. 1 is due to the difference in coefficients of expansion of the austenite and ferrite. This is most noticeable when the dilatometer curves at low temperatures are compared as a group with those at the high temperatures. However, the total observed expansion at 205°C. was possibly 50 per cent of the actual expansion due to the large part of the transformation that took place while the specimen was being quenched to the holding temperature. The curve for 205°C., therefore, has been displaced upward by an arbitrary amount and then shows that comparable irregularities occur in the expansion at 205°C. and at 260°C. The effect might be ascribed either to a two-stage isothermal reaction, stress

A comparison of the results indicated that the maximum difference in the beginning of transformation as measured by different methods amounted to about 10 per cent of the total holding time. The S-curve in Fig. 2 was drawn by giving more weight to the results and methods having greater sensitivity in the respective stages of the transformation process. The ferrite line was determined solely by metallographic observation, since sufficient amounts did not precipitate to give significant changes by the dilatometric or hardness measurements. The delayed transformation at 483° to 540°C. is characteristic of steels containing chromium. After one million seconds at 510°C. the steel was still not completely transformed. This fact is indicated by the dotted lines in the curve marked "transformation ends." In the acicular region of the S-curve below 483°C.

the relatively short time for transformation can be ascribed to low carbon content.

at constant temperature. That the transformation may be in two stages is indicated
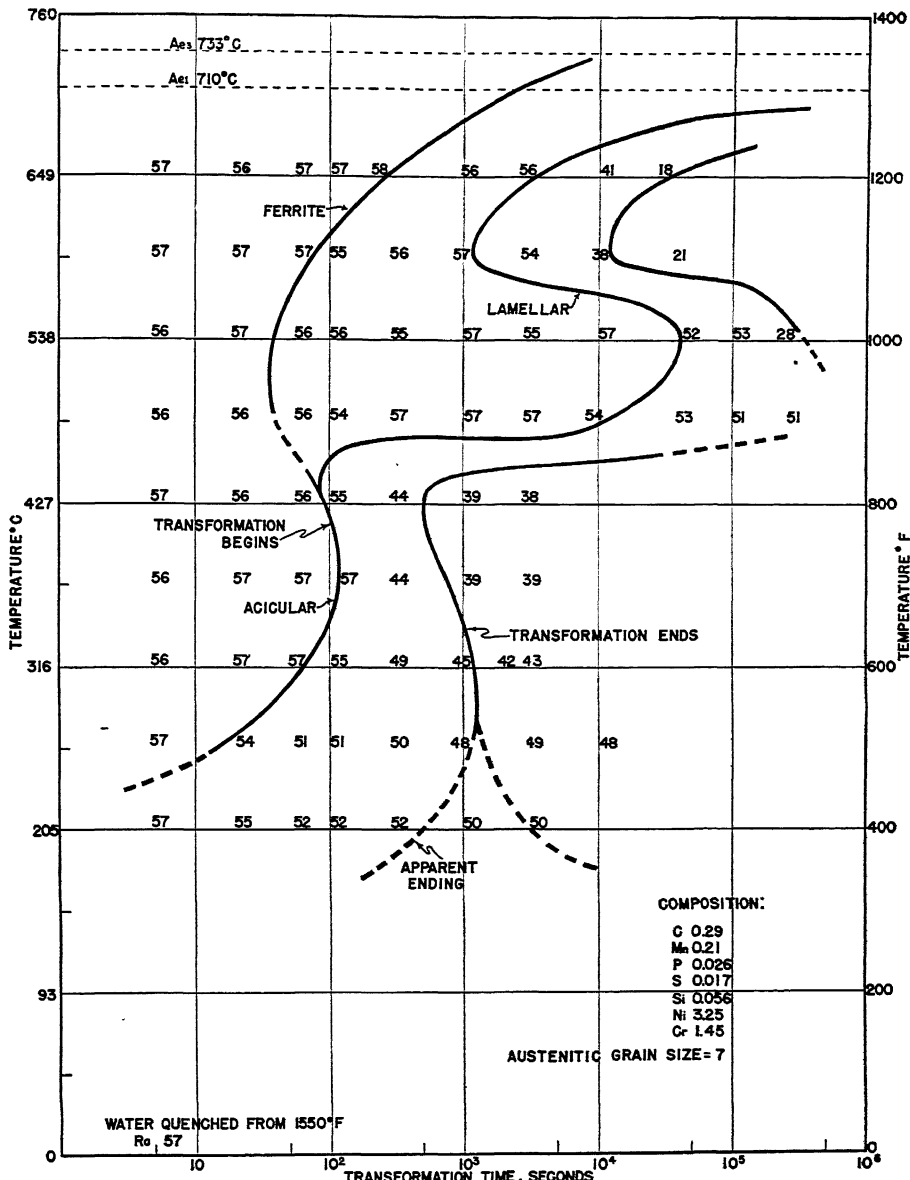
FIG. 2.—TRANSFORMATION DETERMINED METALLOGRAPHICALLY AND BY HARDNESS.

At lower temperatures in this region the transformation tends to take place much faster during quenching and more slowly

by the split, dotted line for "transformation ends."

After the S-curve had been completed,

an attempt was made to estimate the maximum thickness in which this chromium-nickel steel could be austempered to uniform hardness. Beginning with small

similarly treated was uniformly 48 Rockwell C, it is believed that a thickness of 1⅛ in. of this alloy is on the borderline of being truly austempered with the treat-
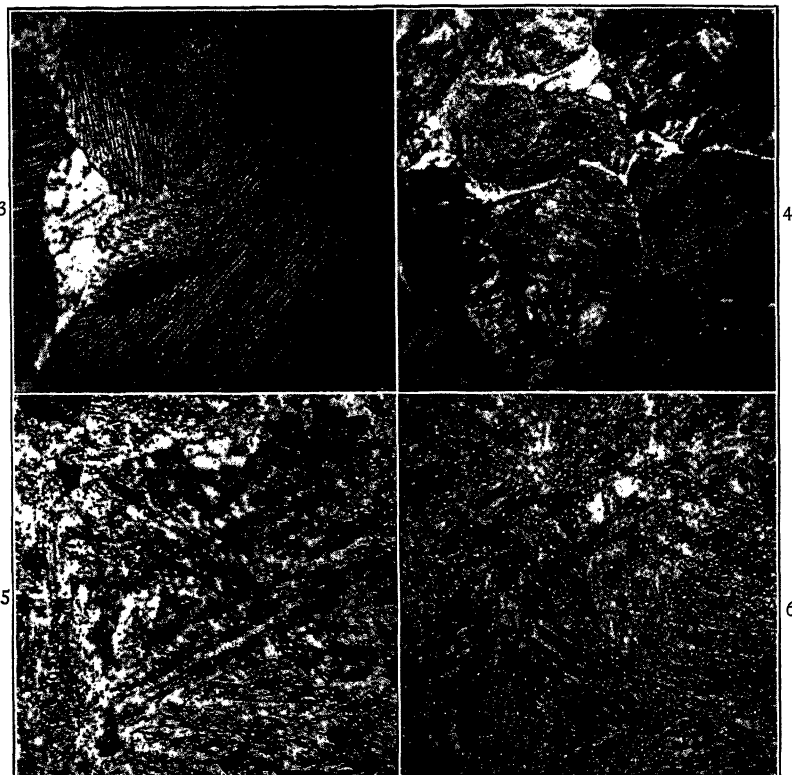
FIGS. 3–6.—REPRESENTATIVE MICROSTRUCTURES. × 1000.
Fig. 3. Transformation complete after 20,000 sec. at 595°C.
Fig. 4. Beginning of transformation, 1200 sec. at 595°C.
Fig. 5. The X constituent, 427°C.
Fig. 6. Bainite; end of transformation at 315°C.
    Etchant 20 c.c. 5 per cent Nital, 20 c.c. 4 per cent Picral, 60 c.c. 95 per cent alcohol. Etching time, 10 to 15 seconds.

samples, the same size as those used in constructing the S-curve, it was found that the hardness predicted from the S-curve could be checked within one point Rockwell C. Successively larger sizes of samples increased the variation in hardness by small amounts. A steel block 1⅛ by 2 by 3 in. when austempered for ½ hr. at 260°C. yielded a hardness of 47 Rockwell C at the surface and 46 Rockwell C at the center. Since the hardness of small samples

ment at 260°C. The hardness of an austempered part, of course, should be uniform from surface to core.

    Some representative microstructures are shown in Figs. 3 to 6. Fig. 3 illustrates a fully transformed specimen austempered at 595°C. for 20,000 sec. One ferrite grain appears at the left surrounded by grains made up entirely of lamellae of pearlite. The lamellae produced by austempering are unusually parallel and free from distor-

tion. Fig. 4 illustrates a specimen that had been austempered at the same temperature, 595°C., for 1200 sec. The isothermal transformation product consists of only a small amount of ferrite at the grain boundaries. Inside the ferrite network will be seen the martensite, which developed on quenching the residual untransformed austenite. Figs. 5 and 6 show the transformation products that formed at lower temperatures of austempering; Fig. 5, the X constituent produced by austempering at 427°C. (a temperature that borders both the lamellar and acicular regions of the S-curve for this chromium-nickel steel) and Fig. 6, a bainite structure typical of the transformations at 260° and 315°C. Even in the acicular region of the S-curve the austempered samples had minute amounts of free ferrite, as shown in Fig. 6.

SUMMARY

1. An S-curve has been made for a chromium-nickel steel of the oil-hardening type. An extremely slow rate of reaction for the lamellar transformation was found at 510°C.

2. The transformation was studied by several methods, including hardness measurements, dilatometer observations, and examination of the microstructure. The dilatometer observations gave evidence of what has been called a two-stage reaction in the low-temperature transformation of austenite. More attention should be given to this region of the S-curve.

ACKNOWLEDGMENTS

The author wishes to thank Dr. Francis M. Walters, Jr., for many suggestions, and the Navy Department for permission for the publication. The photomicrographs were taken through the courtesy of Mr. George A. Ellinger, at the National Bureau of Standards.

REFERENCES

1. E. S. Davenport: Isothermal Transformation in Steels. *Trans. Amer. Soc. Metals* (1939) **27**, 837.

2. R. M. Parks and A. J. Herzig: Hardenability of Molybdenum S.A.E. Steels. *Metals and Alloys* (1940) **11**, 6.
3. H. A. Smith: Reactions in the Solid State. *Trans. A.I.M.E.* (1935) **116**, 342.
4. E. S. Davenport and E. C. Bain: Transformation of Austenite at Constant Subcritical Temperatures. *Trans. A.I.M.E.* (1930) **90**, 117.

DISCUSSION

(L. S. Bergen presiding)

R. A. GRANGE,* Kearny, N. J.—We also have investigated the isothermal transformation behavior of a steel having the same nominal composition as that discussed by Mr. Loring. In the more important respects, our data confirm his and the differences observed may, for the most part, be attributed to the probable variation between one heat of steel and another, even though they be of essentially the same nominal composition.

Mr. Loring has chosen 1 per cent and 99 per cent of transformation at each temperature level as a basis for plotting his beginning and ending curves, respectively. He is justified in this, of course, but it may be well to point out that in an alloy steel of this type, particularly if it is segregated or "banded," the time required for the last 1 per cent of austenite to transform at certain temperature levels may be out of all proportion to that anticipated from extrapolation of an isothermal reaction curve. The effect of such behavior is to destroy the parallelism of the lines that would represent, on a graph of log time versus transformation temperature, 99 per cent and true 100 per cent completion of the transformation. One may argue that only 1 per cent of untransformed austenite is of no practical importance, but this is not true if, as usually occurs in a banded steel, the 1 per cent of untransformed austenite exists in more or less continuous bands running parallel to the principal direction of rolling or forging. If such a condition exists in the steel, 1 per cent of untransformed austenite—which on cooling to room temperature transforms to hard, brittle martensite—assumes an importance with respect to resultant mechanical properties out of all proportion to its relatively small total volume. Because of such behavior in many commercial alloy steels, it has been our usual custom, in plotting the isothermal

* Research Laboratory, U. S. Steel Corporation.

transformation diagram, to base the beginning and ending lines on a definite measurable trace of transformation product and austenite (martensite at room temperature), respectively. In determining the beginning and ending of transformation on this basis, it is our experience that microscopic observations are more reliable than dilatometric or hardness measurements.

Another point pertains to Mr. Loring's photomicrographs showing the character of the transformation product at each of several temperature levels. It is not often wise to base opinion upon a single micrograph, but, in view of the excellence of Mr. Loring's Fig. 5 and our own experience with a steel of similar composition, it is believed that the structure at 427°C. is essentially a relatively high-temperature form of bainite with perhaps 10 per cent of martensite; in the past, we have chosen to designate as the X constituent the product formed at slightly higher temperature levels, 482°C. or thereabouts, in the chromium-nickel steel. Mr. Loring observed free ferrite in the bainite formed as low as 315°C. (Fig. 6); in our experience, we have never found free ferrite grains, at least of this order of magnitude, associated with such "low-temperature" bainite when the

transformation was all strictly isothermal. It is suggested that Mr. Loring reexamine the 315°C. structure to make certain that the light-etching areas shown in Fig. 6 are actually ferrite rather than martensite.

B. M. LORING (author's reply).—It is gratifying to learn that the S-curve determined by Mr. Grange and his associates is in essential agreement with that presented.

The differences in interpretation of the X constituent shown in Fig. 5 are primarily a matter of definition. The specimen from which this photomicrograph was taken had a Widmanstätten type of structure, which has been associated with the X constituent in a previous publication.[1] The identification of the X constituent in Fig. 5 was based on its crystallographic genesis, which was similar to the process at somewhat more elevated temperature.

On reconsideration of the structure in Fig. 6, it is believed that Mr. Grange is quite justified in questioning the production of free ferrite during the isothermal transformation at 315°C. Since the acicular products are platelike as well as needlelike, it is probable that the white areas may be due to etching-orientation relationships.

Structural Diagrams of Nickel Irons and Steels

By J. T. Eash* and N. B. Pilling,* Members A.I.M.E.

(New York Meeting, February 1942)

As a group, the alloys of iron, nickel and carbon are, in application, one of the most versatile of the ferrous alloy family, and while many investigations have been made of their properties and structure only a few attempts have been made to show the microstructural relation over a wide range of composition. It is necessary at once to be clear about the kind of structural relation with which we are concerned. The equilibrium diagram provides quantitative data regarding structural make-up and its variation with temperature, but equilibrium structures often are far different from the technologically significant ones. This is particularly true of steels and cast irons, and some of the most important components of their structure may have no place in the diagram of equilibrium. The fugitive phases that result from transformation are dealt with in a highly detailed and descriptive manner in the S-curves originated by Bain. The present effort lies in a still different field, which is to portray the relation between sweeping changes in composition and in resultant structure, under controlled but nonequilibrium conditions of thermal treatment.

The Guillet[1] diagram presented in 1903 was the initial attempt at such a correlation and frequent references to this diagram can be found in the literature even though later work has shown it to require considerable modification.

Kase[2] published in 1925 a diagram that was based upon observations of furnace-cooled melts. At low carbon contents this diagram agreed fairly well with experience in showing pearlite to exist in alloys containing up to 6 per cent nickel, and completely austenitic steels at 24 to 28 per cent nickel. At high carbon contents, however, irons were indicated as being martensitic at around 2 per cent nickel and austenitic at 12 per cent nickel; these interpretations are open to serious question.

Based upon experience with steels and cast iron, Wickenden[3] suggested a diagram that agreed fairly well with Kase's in the steel range but which presented a wide departure from it in the higher-carbon, high-nickel regions. In its broad picture, the Wickenden diagram is an approach to "practical" structures.

Reference may be made at this point to the efforts of Marsh[5] to construct an iron-nickel-carbon equilibrium diagram by the coordination of scattered data, which are described at length in the monograph cited.

None of these preceding attempts has appeared to meet the need for an exposition of the structural sequence that is encountered in traversing the nickel-steel nickel-cast-iron range under what might be called ordinary departures from equilibrium.

Experimental Conditions

Since the intent has been to establish structures developed under arbitrary conditions, experimental details have perhaps more than usual importance. Three of these conditions should particularly be noticed: (1) the material was cast and not subjected

to other heat or working treatment; (2) the section size was the standard 1.2 in. diameter arbitration bar; (3) the compositions all include small but uniform sulphur, phosphorus and manganese contents. The study was made at three levels of silicon content, to span completely the steel and cast-iron fields.

The melting stock used in making the alloys consisted of Armco iron, electro-nickel and chill-cast pig iron low in silicon, sulphur and phosphorus. The melts were made in an induction furnace and subsequently divided into three portions containing 0.25, 1.5 and 3.0 per cent Si. After the low-silicon castings were poured, the silicon content of the bath was increased to the succeeding desired level and held for 15 min. to eliminate any inoculating effect on the graphite. Each tap was poured into a dry sand core producing a bar of 1.2-in. diameter and 6 in. long and a green-sand mold making a 4 by 5 by 1-in. chill block chilled on the 1 × 5-in. face.

The heating and pouring temperatures were varied according to the carbon contents and maintained at levels that were practical for producing castings so that the structures would be typical of normal melting procedures. Specific temperatures are listed in Table 1. Heating temperature has an important effect on chill and graphite structure, so in the carbon range of 1 to 3 per cent, which spans the range of white irons to irons having flake graphite, it was held constant at 2850°F. Variations in pouring temperature used from the average of 2700°F. for the gray irons have little effect on structure and chill.

The phosphorus content of the alloys was 0.02 to 0.03 per cent. The sulphur was held at 0.05 to 0.065 per cent to ensure typical cast-iron structures; extremely low-sulphur irons have abnormal graphite structures. The manganese content was 0.35 to 0.40 per cent.

Microspecimens were taken from the middles of the bars and the structure was recorded at a depth halfway between the surface and center. A consistent point of observation was necessary because some of the borderline compositions varied in structure across the section.

TABLE 1.—*Heating and Pouring Temperatures*

Carbon, Per Cent	Heating Temperature, Deg. F.	Pouring Temperature, Deg. F.
0.05	2950	2950
0.50	2900	2900
1.00	2850	2850
1.50	2850	2800
2.00	2850	2750
2.50	2850	2700
3.00	2850	2650
4.00	2700	2650

MICROSTRUCTURES

Details of composition of all melts and of their microconstituents are given in Table 2. The matrix structures over the entire range of compositions consisted of four major classes—pearlite with its component parts, ferrite and carbide; bainite; martensite, and austenite. Two kinds of graphite were distinguished, primary flake graphite, formed directly from the melt, and secondary graphite, resulting from the decomposition of cementite in the solid state. Photomicrographs typical of the structures are shown in Figs. 1 to 18.

The pearlite structures are common and need no further explanation.

The intermediate transformation products, all of which have been classified as bainite, were most variable in appearance, as is to be expected when the broad temperature range of formation is considered. Figs. 5 and 6 were typical of bainite structures in castings with less than 2 per cent carbon while Fig. 7 is an example of graphitic cast irons on the low nickel side of the bainite-containing fields. The structure given in Fig. 8 was found only in 0.25 per cent silicon irons containing 1.5 to 2 per cent carbon and 10 to 18 per cent nickel. The plate constituent was high in carbide, as indicated by a sodium picrate

Fig. 1.—0.85 C, 0.25 Si. Pearlite + carbide and graphite in grain boundary.
Fig. 2.—3.0 TC, 0.25 Si. Pearlite + carbide.
Fig. 3.—2.5 TC, 3 Si, 3 Ni. Pearlite + flake graphite.
Fig. 4.—4 TC, 1.5 Si. Pearlite + ferrite + flake graphite.
Fig. 5.—0.05 C, 0.25 Si, 4 Ni. Ferrite + Bainite.
Fig. 6.—0.86 C, 0.25 Si, 6 Ni. Bainite + austenite + carbide in boundary.
Fig. 5 etched with 50:50 Nital Picral; others etched with 2 per cent Nital. × 500.

Fig. 7.—4 C, 0.25 Si, 6 Ni. Bainite + austenite + flake graphite.
Fig. 8.—2 TC, 0.25 Si, 10 Ni. Bainite + austenite + carbide.
Fig. 9.—2.5 TC, 0.25 Si, 10 Ni. Bainite + austenite + flake graphite.
Fig. 10.—3.70 TC, 1.5 Si, 15 Ni. Bainite + austenite + flake graphite.
Fig. 11.—2 C, 1.5 Si, 6 Ni. Carbide + secondary graphite + martensite + pearlite + austenite + bainite + austenite.
Fig. 12.—0.40 TC, 1.5 Si, 8 Ni. Martensite + trace of ferrite in boundary.
Etched with 2 per cent Nital. × 500.
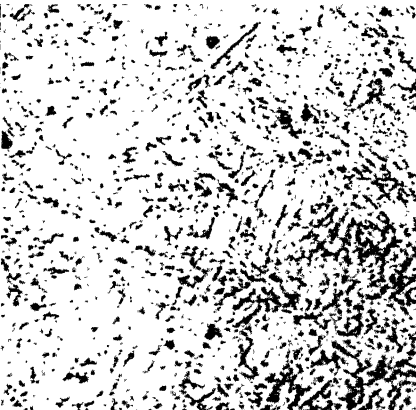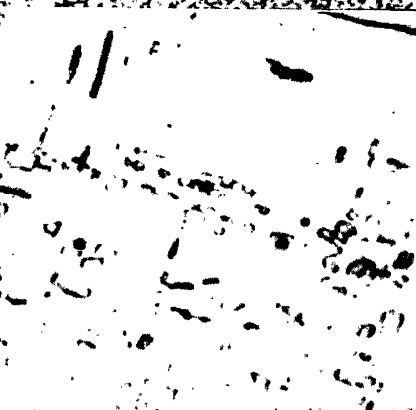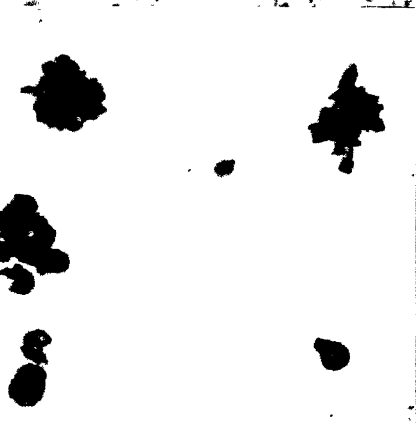
Fig. 13.—2.5 TC, 3 Si, 10 Ni. Martensite + austenite + flake graphite.
Fig. 14.—0.05 C, 0.25 Si, 20 Ni. Martensite.
Fig. 15.—0.05 C, 0.25 Si, 25 Ni. Martensite + austenite.
Fig. 16.—0.05 C, 0.25 Si, 25 Ni. Martensite + austenite.
Fig. 17.—2 TC, 1.5 Si, 18 Ni. Austenite + secondary graphite.
Fig. 18.—1 C, 1.5 Si, 25 Ni. Austenite + secondary graphite.
Figs. 14–16 etched with 50:50 Nital Picral; others etched with 2 per cent Nital.
All × 500 except Fig. 16, which is × 2000.

carbide etch, and was found only in graphite-free areas. The bainite shown in Fig. 9 was found only in this one casting. Fig. 10 was typical of all the high-carbon

of cooling rate and segregation, as indicated by observations following heating and forging treatments.

Secondary-graphite structures in austen-
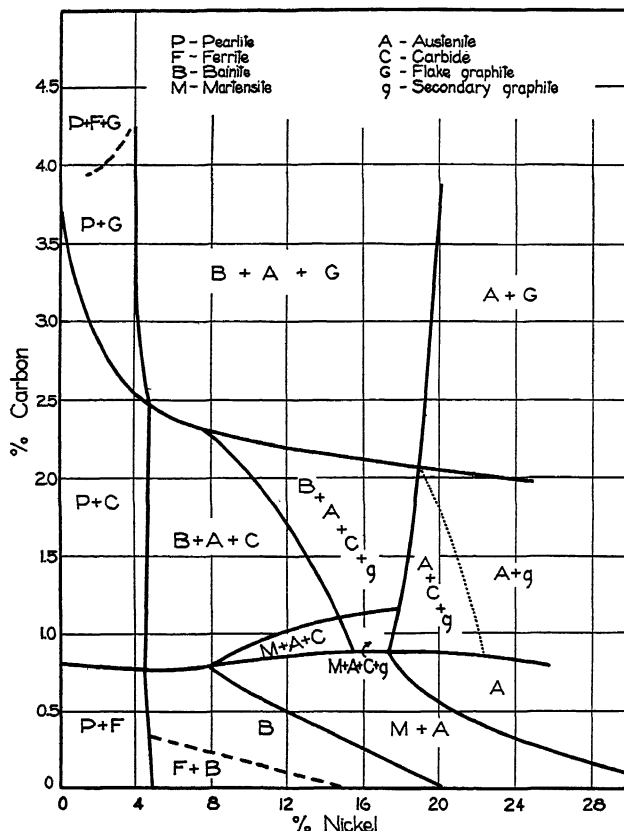
FIG. 19.—STRUCTURAL DIAGRAM OF NICKEL IRONS AND STEELS CONTAINING 0.25 PER CENT SILICON. 1.2-INCH DIAMETER DRY SAND CASTINGS.

high-nickel alloys in the austenite-bainite fields.

Martensitic structures containing appreciable carbon are shown in Figs. 12 and 13 while Figs. 14 and 15 are typical of very low-carbon high-nickel contents. The Widmannstätten precipitate in the latter consisted of numerous small cubes (Fig. 16). The form of the precipitate was a function

ite are illustrated in Figs. 17 and 18, and both types of graphite result from the decomposition of cementite in the solid state.[4] The former is frequently referred to as "dendritic" graphite and is a cause of low strength in cast iron. The nodular type was found only in castings containing 1 to 1.5 per cent carbon and above 12 per cent nickel.

STRUCTURAL DIAGRAMS

The structural diagrams for the three silicon levels based upon these interpreta-

structure and in conjunction with nickel had a strong austenitizing effect. Among the intermediate-nickel steels, those with greater amounts of carbon in solution
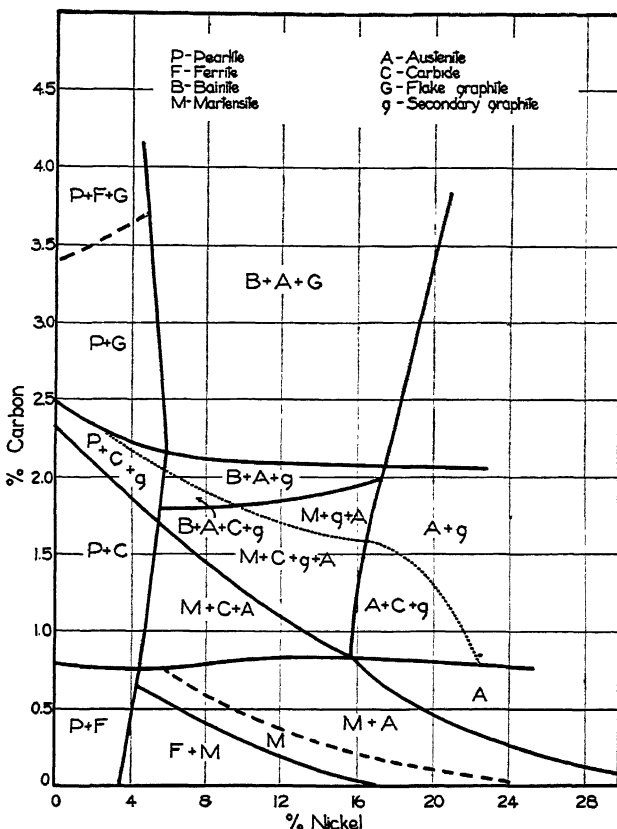
FIG. 20.—STRUCTURAL DIAGRAM OF NICKEL IRONS AND STEELS CONTAINING 1.5 PER CENT SILICON. 1.2-INCH DIAMETER DRY SAND CASTINGS.

tions are given in Figs. 19–21. It should be recognized that the field boundaries do not represent sharp steps from one phase or group of phases to another, but instead narrow transition zones where the bound phases are coexistent.

Considering the influence of the three main alloying elements, it is evident that the amount of carbon in solid solution had a profound influence upon the matrix

became martensitic while with low-solution carbon they were apt to contain bainite.

The excess carbon phase, carbide or graphite, exerted its influence on the structure indirectly as it affected the carbon in solution. In the presence of carbide, austenite or low-temperature decomposition products were observed while in graphitic alloys a higher-temperature decomposition product tended to form because of the

carbon depletion of the surrounding austenite.

A very good example of the influence of field, suppress the formation of bainite and increase the quantity of martensite in the acicular compositions.
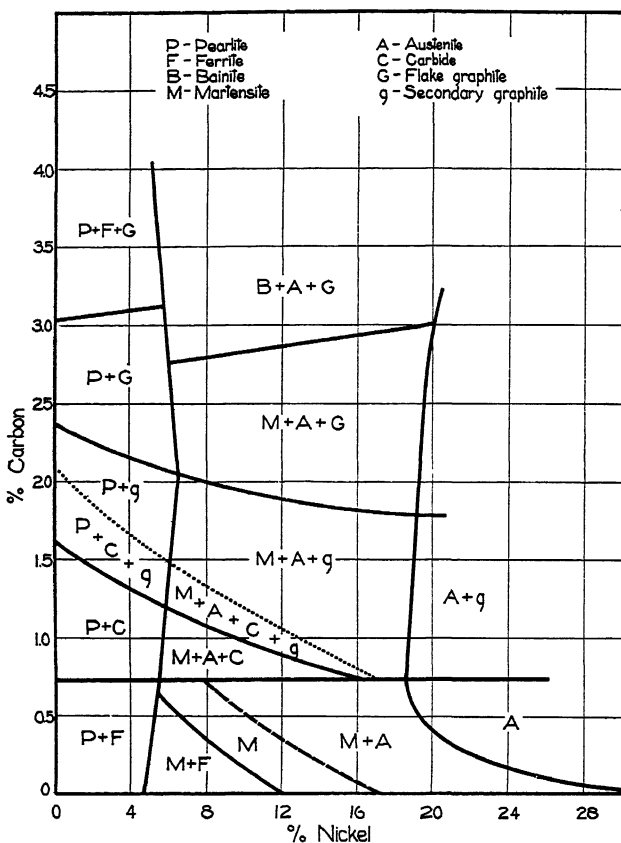
FIG. 21.—STRUCTURAL DIAGRAM OF NICKEL IRONS AND STEELS CONTAINING 3 PER CENT SILICON. 1.2-INCH DIAMETER DRY SAND CASTINGS.

graphite and excess carbide on the matrix structure in the same specimen was found in the mottled iron shown in Fig. 11. In the carbide areas, martensite and austenite were found. Immediately surrounding the graphite were small areas of pearlite, which in turn were surrounded by bainite and austenite.

The predominant effects of silicon, aside from its graphitizing influence, were to broaden slightly the domain of the pearlitic

CHILL DEPTH

The relation between composition and a limiting chill depth of 0.5 in. is given in Fig. 22.

It is evident that silicon and nickel were effective graphitizers, but they differed in the extent of their action. Silicon promoted primary graphitization and decomposition of excess and eutectoid carbide resulting in free ferrite in pearlitic cast irons; nickel

TABLE 2.—*Nickel Steels and Cast Irons*

Alloy No.	Composition, Per Cent — Total C	Si	Ni	Brinell Hardness No.	Chill Depth, In. — White	Total	Ferrite	Pearlite	Bainite	Martensite	Austenite	Carbide	Primary Graphite	Secondary Graphite	Magnetism[d]
						0.25 PER CENT SILICON CASTINGS									
1	(0.05)[d]	0.08	4.10	131			/[b]	/							M
2	0.03	0.23	4.04	126			/	/							M
3	0.02	0.27	6.04	148			/	/							M
4	(0.03)	0.22	8.23	182			/		/						M
5	(0.05)	0.28	10.19	228			/		/						M
6	(0.05)	0.18	20.36	302					/						M
7	(0.05)	0.22	25.12	265							/	/			M
8	(0.05)	0.27	30.01	115							/	/			MM
9	0.45	0.07	8.11	530				/	/						M
10	0.51	0.34	8.04	560					/						M
11	0.47	0.04	12.12	481					/			/			M
12	0.51	0.09	18.04	167							/	/			MM
13	0.42	0.06	25.05	119								/			NM
14	0.85	0.23		240	4			/				/		x	M
15	0.98	0.25	2.07	297	4			/				/		x	M
16	0.89	0.17	4.16	310	4			/		x[c]		/		x	M
17	0.86	0.20	6.06	448	4				/			/		x	M
18	0.85	0.22	10.05	255	4					/		/			M
19	0.88	0.20	12.13	179	4					/		/			MM
20	0.98	0.28	15.32	149	4						x	/		x	SM
21	0.95	0.23	18.01	137	4							/	/	x	NM
22	0.88	0.22	(20)	153	4						x	/		x	NM
23	0.90	0.24	25.23	170	4							/		x	MM
24	1.48	0.29	12.22	225	4				/			/	/		SM
25	1.33	0.30	18.17	202	4				x			/		x	NM
26	2.09	0.24		335	4			/				/	/		M
27	1.97	0.24	2.11	378	4			/				/	/		M
28	1.91	0.25	4.04	405	4			/				/	/		M
29	1.92	0.26	6.05	518	4				/			/	/		M
30	1.95	0.23	10.12	313	4				/			/	/		MM
31	1.84	0.23	15.13	240	4				/			/	/	/	SM
32	1.85	0.26	17.98	240	1.0	4			x			/	/	/	SM
33	1.97	0.25	19.75	134	0.35	1.30						/		/	
34	2.37	0.27	1.09	417	4			/				/			M
35	2.43	0.34	3.03	477	4			/				/			M
36	2.49	0.33	9.90	286	0.55	2.12			/			/	/		M
37	2.49	0.32	17.94	145	0.41	0.67			x			/	/		SM
38	3.03	0.38		422	4			/				/	/		M
39	2.95	0.34	2.06	467	4			/				/	/		M
40	3.00	0.32	4.06	255	1.72	4			x			/	/		M
41	2.97	0.41	10.14	254	0.37	0.90			/			/	/		M
42	2.95	0.27	17.90	126	0.26	0.54			/			/	/		SM
43	3.98	0.18		481	4			/				/	/		M
44	4.10	0.29	2.01	157	0.80	1.45	/	/					/		M
45	4.07	0.31	4.00	155	0.40	0.63		/	/				/		M
46	3.88	0.27	6.12	214	0.33	0.68			/				/		M
47	3.84	0.31	10.04	255	0.18	0.26			/			/	/		M
48	3.78	0.31	14.95	149	0.02	0.02			/			/	/		M
49	3.73	0.31	18.00	99	0	0			x			/	/		MM
50	3.42	0.25	20.12	107	0	0			x			/	/		NM

TABLE 2.—(*Continued*)

Alloy No.	Total C	Si	Ni	Brinell Hardness No.	White	Total	Ferrite	Pearlite	Bainite	Martensite	Austenite	Carbide	Primary Graphite	Secondary Graphite	Magnetism[d]
	Composition, Per Cent				Chill Depth, In.		Microconstituents								
1.5 PER CENT SILICON-IRON-NICKEL CASTINGS															
51	(0.05)	1.37	4.12	176			/			/					M
52	(0.05)	1.34	6.05	193			/			/					M
53	0.04	1.52	8.21	256			/			/					M
54	(0.05)	1.48	10.12	290			/			/					M
55	(0.05)	1.36	20.20	323						/					M
56	(0.05)	1.42	24.85	258						/					M
57	(0.05)	1.40	29.91	120						/	/				MM
58	0.40	1.35	8.06	498			x			/					M
59	0.45	1.24	12.09	454						/	/				M
60	0.49	0.78	18.00	183						/	/				MM
61	0.30	1.37	25.10	124							/				NM
62	0.82	1.54		287	4			/							M
63	0.80	1.61	2.11	324	4			/							M
64	0.90	1.52	4.18	387	4			/	x					x	M
65	0.84	1.49	6.08	488	4			/						x	M
66	0.84	1.48	(10)	321	4					/	/				M
67	0.90	1.50	12.07	239	4					/	/				MM
68	0.93	1.64	15.20	168	4					x	/			x	SM
69	0.97	1.49	18.00	163	4						/	x		/	NM
70	0.89	1.57	19.98	170	4						/	x		/	NM
71	1.02	1.52	25.06	159	4						/			/	NM
72	1.42	1.60	12.25	286	4					/	/	/		/	MM
73	1.42	1.60	18.17	208	0.85	4					/	/		/	VSM
74	2.05	1.55		368	4			/				/			M
75	2.00	1.50	2.09	418	4			/				/			M
76	1.95	1.52	4.05	444	4			/				/		x	M
77	1.81	1.55	6.16	447	0.50	3.55				/	/			/	M
78	1.84	1.52	10.08	418	0.16	1.25				/	/			/	M
79	1.92	1.52	15.03	248	0.14	0.93				/	/			/	MM
80	1.93	1.50	17.96	163	0.45	0.92					/			/	SM
81	1.96	1.55	19.85	134	0.13	0.78					/			/	NM
82	2.44	1.45	(1)	292	0.95	4.0		/					/		M
83	2.46	1.47	(3)	273	0.11	0.95		/					/		M
84	2.54	1.52	(10)	342	0.10	0.31			/		/		/		
85	2.58	1.52	(18)	129	0.09	0.32			x		/		/		VSM
86	3.08	1.47		237	0.45	1.20		/					/		M
87	3.14	1.49	(2)	240	0.13	0.60		/					/		M
88	3.13	1.48	(4)	252	0.13	0.29		/	x				/		M
89	2.92	1.54	9.90	302	0.01	0.05				/			/		M
90	2.96	1.57	(18)	129	0.16	0.29				/			/		MM
91	3.95	1.36		136	0.18	0.47	/	/					/		M
92	4.03	1.45	2.01	138	0	0.01	/	/					/		M
93	3.97	1.54	4.00	148	0	0	x	/					/		M
94	3.62	1.57	(6)	256	0	0		x		/			/		M
95	3.53	1.62	(10)	255	0	0				/			/		M
96	3.70	1.59	(15)	163	0	0				/	/		/		MM
97	3.50	1.61	(18)	112	0	0				/	/		/		MM
98	3.60	1.64	17.5	118	0	0				/	/		/		MM
99	3.29	1.48	20.12	95	0	0				x	/		/		SM

TABLE 2.—(Continued)

Alloy No.	Composition, Per Cent			Brinell Hardness No.	Chill Depth, In.		Microconstituents								Magnetism[d]
	Total C	Si	Ni		White	Total	Ferrite	Pearlite	Bainite	Martensite	Austenite	Carbide	Primary Graphite	Secondary Graphite	
3 PER CENT SILICON-IRON-NICKEL CASTINGS															
100	0.06	2.94	4.12	237			/	x							M
101	(0.05)	3.18	5.95	260			/			x					M
102	0.03	2.75	8.06	311			/			/					M
103	0.05	3.02	10.10	359			/			/					M
104	0.05	2.72	20.25	340			/			/					M
105	0.04	2.84	24.64	228						/					MM
106	0.04	2.68	29.98	133						/	/				SM
107	0.35	2.97	8.10	541			x			/					M
108	0.41	2.66	12.06	477						/	/				M
109	0.45	2.73	17.94	218						/	/				MM
110	0.20	3.04	25.09	121							/				NM
111	0.82	3.25		323	4			/							M
112	0.90	3.30	2.11	371	4			/							M
113	0.91	3.11	4.18	390	4			/							M
114	0.82	3.01	6.02	524	4		x			/		/			M
115	0.84	3.03	10.00	393	4					/	/	/			M
116	0.93	2.93	12.05	297	4					/	/			/	M
117	0.93	1.70	15.22	251	4					/	/			/	MM
118	0.96	2.87	17.97	202	4					/	/			/	SM
119	0.93	3.18	20.11	137	4						/			/	NM
120	1.04	3.05	24.90	146	4						/			/	NM
121	1.37	2.98	12.06	385	0.43	4				/	/	/		/	M
122	1.40	3.11	18.03	202						/	/			/	MM
123	2.00	3.24		298	0.62	4	x	/				/		/	M
124	2.01	2.98	2.09	274	0.22	2.03	x	/						/	M
125	1.97	3.05	4.06	345	0.50	2.00		/						/	M
126	2.03	3.11	6.09	317	0.32	1.61		/	/					/	M
127	2.00	2.96	10.01	418	0.17	0.73				/	/		/		M
128	1.92	2.86	15.00	319	0.20	1.00				/	/		/		MM
129	1.92	2.99	17.84	228	0.43	0.75				/	/		/		MM
130	1.98	3.04	20.03	156	0.40	1.13					/		/		VSM
131	2.47	2.86	(1)	269	0.16	0.51		/					/		M
132	2.47	2.90	(3)	274	0.21	0.43		/					/		M
133	2.52	3.05	9.76	364	0.13	0.19				/	/		/		M
134	2.70	2.99	(18)	129	0.07	0.14				/	/		/		SM
135	3.13	2.92		218	0.11	0.18	x	/					/		M
136	3.18	3.00	2.05	205	0.07	0.10	x	/					/		M
137	3.14	2.99	4.02	237	0.05	0.09	/	/					/		M
138	2.86	2.98	9.84	290	0	0.05			/	/	/		/		M
139	2.94	3.01	(18)	107	0.26	0.26			/	/	/		/		MM
140	2.88	3.13	4.10	268	0.10	0.22		/					/		M
141	2.66	3.12		223	0.29	0.83	x	/					/		M
142	3.01	3.12	2.02	234	0.10	0.18	x	/					/		M
143	3.54	3.17	3.90	228	0.09	0.14		/					/		M
144	3.88	2.76		95	0	0.03	/	/					/		M
145	3.85	2.92	2.01	108	0	0	/	/					/		M
146	3.86	2.94	3.98	149	0	0	/	/					/		M
147	3.53	3.05	(6)	245	0	0			/		/		/		M
148	3.50	3.11	(10)	273	0	0			/		/		/		MM
149	3.42	2.92	(15)	202	0	0			/		/		/		MM
150	3.27	3.08	(18)	117	0	0			/	/	/		/		MM
151	3.28	3.18	17.4	135	0	0			/	/	/		/		MM
152	3.16	3.04	(20)	101	0	0			/	x	/		/		SM

a ( ) = calculated composition.
b / = microconstituent present.
c x = trace of microconstituent.
d Magnetism determined by large Alnico magnet:
    M = magnetic.
    MM = moderately magnetic.
    SM = slightly magnetic.
    VSM = very slightly magnetic.
    NM = nonmagnetic.

promoted graphite formation but had the opposite effect on the pearlite and tended to refine and stabilize it.
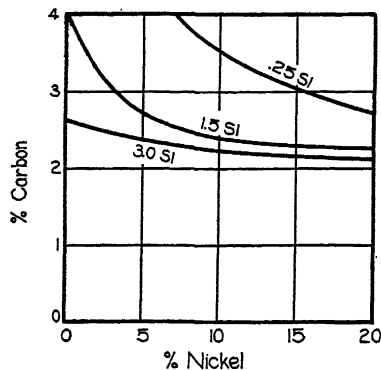
FIG.   22.—COMPOSITIONS   HAVING   0.5-INCH
TOTAL CHILL.

SUMMARY

Structural diagrams have been presented for cast nickel steels and cast irons at 0.25, 1.5 and 3 per cent silicon levels and containing up to 4 per cent carbon and 30 per cent nickel.

REFERENCES

1. L. Guillet: *Compt. rend.* Acad. Sci., Paris (1903) 136, 1319–1321.
2. T. Kase: *Sci. Rept.* Tohoku Imp. Univ. (1925) [1] 14, 173.
3. T. H. Wickenden: Metals Handbook. Amer. Soc. Metals (1939) 577.
4. J. T. Eash: Amer. Foundrymen's Assn. *Preprint* No. 41-9.
5. J. S. Marsh: Alloys of Iron and Nickel, 1, 56. Engineering Foundation, 1938.

Rapid Tension Tests Using the Two-load Method

By A. V. de Forest* and C. W. Mac Gregor,* Members A.I.M.E., and A. R. Anderson*

(Philadelphia Meeting, October 1941)

One of the important problems in the design of structures and machine parts subjected to rapidly applied loads is the determination of the strength and ductility of the material itself under such conditions. Realizing the need for such information, many investigations have been carried out in the past. Most of these experiments have been made using notched bars in bending either with the Charpy or Izod impact machine. While yielding valuable data on the effect of notches in the energy absorption of the material and on the condition of heat-treatment, this form of test does not lend itself readily to a determination of fundamental stress-strain relations. For this and other reasons, more attention has been paid recently to the tension impact test. An extensive literature already exists on the subject and only those investigations somewhat closely related to the present paper will be mentioned. For a more comprehensive list, the reader is referred to the Symposium on Impact Testing of the A.S.T.M., 1938. The work of Mann,[1] Clark and Dätwyler,[2] Nádai and Manjoine,[3] Winlock and Leiter,[4] Deutler,[5] and Brinkmann,[6] however, deserves especial mention.

In most of the previous investigations on the subject, when stress-strain relations were obtained under high rates of loading, it was the common procedure to determine stresses based on the original area and strains based on the original length. Stress-strain curves were then constructed by plotting $S_0 = \dfrac{P}{A_0}$ as a function of $\epsilon_0 = \dfrac{\Delta L_0}{L_0}$, where A_0 and L_0 refer to the original area and gauge length, respectively. At present there exists a paucity of true stress-strain data in the impact problem. The advantages of constructing so-called true stress-strain curves in order to reveal the fundamental physical properties of the material for the tension test were discussed recently by one of the authors.[7,8] It was shown that the true physical behavior of the material in the tension test could best be represented by plotting the average true stress, $S = \dfrac{P}{A}$ as a function of $\epsilon = q' = \log \dfrac{A_0}{A} = \log \dfrac{L}{L_0}$, where $P, A, L, S, \epsilon,$ and q' refer to the load, the cross-sectioned area while the load P is applied, the actual gauge length, the average true stress, the true strain and true reduction in area, respectively. Besides giving a better physical representation, the method has certain additional advantages in that the stress-strain curve so plotted becomes a straight line from the maximum load point to fracture. The construction of such curves, however, while comparatively simple for the slow rates of loading customarily used in the tension test, presents certain difficulties for tensile impact in that both loads and diameters are required throughout the test. The continuous measurement of test-piece diameters to fracture under impact conditions offers considerable experimental difficulty. In order to make it feasible to

[1] References are at the end of the paper.

obtain true stress-strain data from initial yielding to fracture in the tensile impact problem, a two-load method was suggested some time ago.[9]

a straight line from this point tangent to the $\frac{P_{max}}{A}$ vs. q' curve at its point of inflection. It can be shown and checked experi-
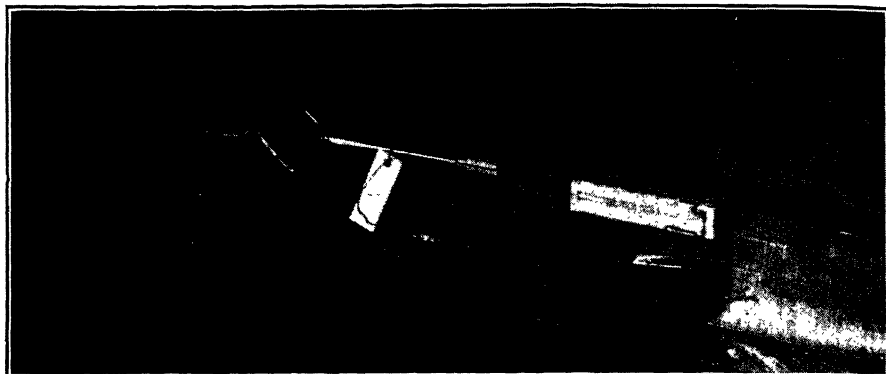
FIG. 1.—TENSILE SPECIMEN IN IZOD MACHINE.

Briefly, this method consists in the scribing of a properly tapered tensile specimen by means of a diamond tool with fine circumferential scratches at different axial locations, measuring the diameters of the bar at these locations before and after the test, noting only the maximum and fracture loads during the test, and constructing the true stress-strain curve. In order to construct the final curve, a preliminary curve of $\frac{P_{max}}{A}$ vs. q' is first obtained by dividing the maximum load by the final areas measured along the bar all the way up to the fractured cross section and plotting each of these values as a function of the corresponding q'. The curve so constructed represents the actual $S - q'$ or $S - \epsilon$ curve from initial yielding to the maximum load, the remaining portion of the $\frac{P_{max}}{A}$ vs. q' curve merely serving as an aid in constructing the rest of the true stress-strain curve from the maximum load point to fracture. This portion is obtained by dividing the fracture load by the fractured area, plotting this with its corresponding q' value on the figure, and drawing

mentally that the curve so constructed represents the true $S - q'$ curve for the material. The method is complete in that it determines the true stress-strain curve from initial yielding to fracture. It lends itself particularly well to the impact problem, since the maximum and fracture loads are readily obtained, and it eliminates the necessity of measuring strains during impact.

It is, therefore, the intention in the paper to discuss the application of this latter method to rapid tension or tensile impact experiments in the velocity range 0 to 11.5 ft. per sec. as obtained on the Izod tensile impact machine. It is intended to carry out further experiments at higher rates of loading in the future, therefore the following discussion is in the nature of a progress report.

EQUIPMENT

The rapid tension or impact experiments were carried out on a converted Izod impact machine. Fig. 1 shows a test specimen in the machine with the tup in position to be struck by the pendulum. The dy-

namic loads were measured by the metalectric strain gauges mounted on the individual specimens. The test specimens used had a curved tapered portion with a minimum
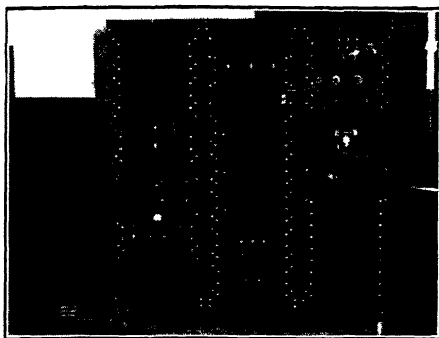
FIG. 2.—OSCILLOGRAPH AND CAMERA.

diameter of 0.2 in. and a radius of curvature of 8 in. Shoulders on each end having a uniform diameter of 0.350 in. joined the curved tapered portion. The strain gauge was mounted on the shoulder at one end of the specimen. The reason for using one end of the specimen as a weighbar instead of providing a separate load-measuring element will be discussed later on.

The wire strain gauge used in the tensile impact tests is based on the change in resistance of a length of resistance wire one mil in diameter cemented directly to paper insulation, which in turn is cemented to the surface of the specimen. The wire is distributed over the circumference in such a way that bending stresses are not measured; only the average longitudinal strain. Gauges of this type show no hysteresis between resistance change and elongation to within 0.1 per cent and are also free of creep under constant load. Tests up to 30,000 cycles per second have not indicated any change due to speed effect, and as nearly as could be ascertained, no change in modulus was discovered; although no especial efforts were made to measure such a possible change to closer than 1 per cent.

Suitable wire for the resistance gauges should have high strain sensitivity and for

static use a low temperature coefficient of resistance, matching approximately the coefficient of expansion of the metal to be tested. For dynamic use, a wire of higher
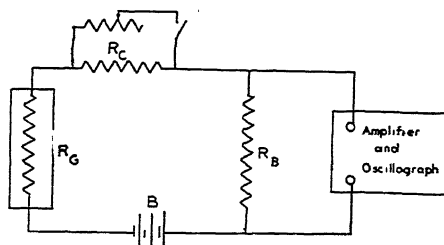
FIG. 3.—CIRCUIT DIAGRAM USED WITH DYNAMIC STRAIN GAUGE.
R_G = gauge resistance.
R_C = calibration resistance.
R_B = ballast resistance.
B = battery.

strain sensitivity may be used, when changes in temperature during a single cycle are not anticipated. These gauges were used with the permission of the Baldwin Southwark Co. The use of wire gauges in conjunction with high-speed oscillographs has been described in a recent paper by one of the authors.[10]

The change in electrical resistance of the gauge due to load changes introduced a signal to the amplifiers and a cathode-ray oscillograph where the spot deflection was recorded on a moving film. A photograph of the oscillograph is shown in Fig. 2. The circuit used is indicated in Fig. 3.

At the outset, a weighbar was built into the Izod machine as shown in Fig. 1, and it was intended to use this as the load-measuring device into which the specimens were screwed, as was followed by Clark and Dätwyler.[2] It was soon found, however, that the weighbar so constructed introduced excessive vibration due to trapped longitudinal waves. This objection was overcome by mounting the resistance gauge on the shoulder of the specimen. Fig. 4 shows an oscillogram in which the behavior of a gauge mounted (1) on the specimen and (2) on the weighbar of the machine are compared. By mounting the gauge on the

specimen the excessive vibration is materially reduced.

The use of a new weighbar for each specimen has of course certain disadvan-

were tested for each material, varying from two test pieces for the S.A.E. 1045 steel to eight for the S.A.E. 1112.

Essentially the same procedure was
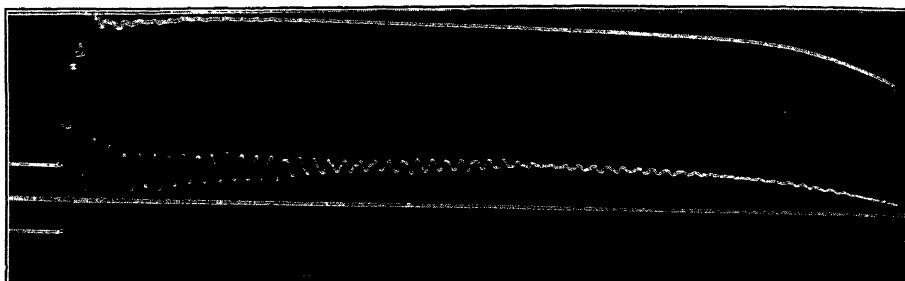
FIG. 4.—COMPARISON OF LOAD-TIME DIAGRAMS OBTAINED WITH GAUGE MOUNTED ON SPECIMEN (UPPER CURVE) AND WITH GAUGE MOUNTED ON WEIGHBAR OF FIG. I (LOWER CURVE). S.A.E.1020 STEEL.

tages in that a separate weighbar calibration had to be made for each specimen. This was done in a manner similar to that used by Clark and Dätwyler by loading each specimen statically, during which the change in resistance for a given load was determined. The spot deflection of the oscillograph was also noted for a sudden change in resistance. These two tests were then sufficient to determine the load per millimeter deflection of the light spot of the oscillograph. A further calibration of the oscillograph was made as a check by means of the momentum relations involved in the pendulum system.

TABLE I.—*Materials Tested*

MATERIAL	HEAT-TREATMENT
S.A.E. 1112 steel....	Annealed 1 hr. at 1650°F. and slowly cooled
S.A.E. 1045 steel....	Annealed 1 hr. at 1450°F. and slowly cooled
S.A.E. 3140 steel....	Hot-rolled, tested as received
Brass (62Cu, 35Zn, 3Pb) ½ hard.	Annealed 1 hr. at 785°F. and slowly cooled

TEST PROCEDURE

Four different materials were tested in the conditions shown in Table 1. Slow static tension tests were made on each in a 60,000-lb. Southwark-Emery testing machine, using the low 2400-lb. range for all materials except the S.A.E. 3140, in which case the 12,000-lb. range was needed. For the tensile impact tests, several specimens

followed as discussed previously for the static tension tests once the load-time curve was obtained from the oscillogram. The maximum and fracture loads were obtained from the latter, the diameters before and after the test were measured along the bar by means of a special dial gauge and clamp attached to a lathe comparator, and the true stress-strain curves constructed by the two-load method. Typical oscillograms are shown for each material in Fig. 5.

DISCUSSION OF RESULTS

The average true stress-strain curves so constructed are shown in Figs. 6, 7, 8 and 9. In most cases the individual test points are indicated for each material. For the S.A.E. 1112 some dispersion of data was present near fracture and for this reason the various points for each material were plotted as obtained for each test bar and an average $S - \epsilon$ or $S - q'$ curve was constructed. Figs. 6 to 9 show that in each case the true stress-strain curve as obtained on the Izod machine lies above that received in the static test, the difference between the two curves continuously increasing to fracture. As might be expected from previous results, the brass shows the greatest speed effect and the S.A.E. 3140 the least.

FIG. 5.—TYPICAL OSCILLOGRAMS.
a. S.A.E.1112. Specimen 2E. Maximum load, 2320 lb. Time, 0.00425 seconds.
b. S.A.E.1045. Specimen 1C. Maximum load, 2910 lb. Time, 0.00226 seconds.
c. S.A.E.3140. Specimen 4E. Maximum load, 4720 lb. Time, 0.0034 seconds.
d. Brass. Specimen 6. Maximum load, 2120 lb. Time, 0.0045 seconds.

The numerical effects of the speed of testing are perhaps best indicated by Table 2. The static tests for the different materials were carried through at somewhat different speeds, the time of test varying from 15 min. for one of the S.A.E. 3140 specimens to 40 min. for the S.A.E.

importance, since the basic static speed ratios may be varied by as much as 10:1 without a noticeable effect on the material properties. It is the intention by these tests to show only the general effect on true stress-strain properties if one passes from a static test to a rapid tension or tensile

TABLE 2.—*Summary of Test Results*

Material	Test Piece No.	Average True Strain Rate (Sec.$^{-1}$)	Speed Ratio $\dfrac{v}{v_0}$	True Stress at Maximum Load, Lb. per Sq. In.	True Stress at Fracture, Lb. per Sq. In.	True Fracture Strain $q_b' = \epsilon_b$	Ratio of q_b' to Static Value	Ratio True Stress at Maximum Load to Static Value	Ratio True Fracture Stress to Static Value
S.A.E. 1112 annealed.	2G, 2J	903 × 10^{-6}	1.0	81,400	124,500	0.9481			
	2A	482	5.34 × 10^5	98,000	153,000	0.9632	1.015	1.29	1.230
	2B	410	4.54 × 10^5	98,000	127,200	0.9222	0.974	1.20	1.022
	2C	388	4.30 × 10^5	97,000	144,000	0.9302	0.983	1.19	1.157
	2D	384	4.25 × 10^5	90,000	136,000	0.9420	0.994	1.105	1.092
	2E	223	2.47 × 10^5	93,000	151,700	0.9497	1.000	1.142	1.218
	2F	230	2.55 × 10^5	89,000	138,800	0.8981	0.948	1.092	1.115
	2H	206	2.28 × 10^5	89,000	125,200	0.8755	0.924	1.092	1.005
	2I	222	2.46 × 10^5	90,000	141,000	0.900	0.950	1.106	1.132
Average 2A-2I....			3.52 × 10^5				0.974	1.140	1.121
S.A.E. 1045 annealed.	1J	335 × 10^{-6}	1.0	104,200	144,800	0.8043			
	1C	358	10.69 × 10^5	115,000	165,500	0.8109	1.001	1.102	1.142
	1H	222	6.61 × 10^5	108,000	157,000	0.8545	1.06	1.036	1.085
Average 1C-1H...			8.65 × 10^5				1.031	1.069	1.113
S.A.E. 3140 hot-rolled.	4M, 4I	387 × 10^{-6}	1.0	158,000	215,000	0.5800			
	4F	224 × 10^{-3}	5.79 × 10^2	158,000	236,000	0.6281	1.083	1.00	1.100
	4H	156 × 10^{-3}	4.06 × 10^2	156,000	233,000	0.6238	1.072	0.987	1.085
	4A	410	10.6 × 10^5	180,000	254,500	0.6355	1.097	1.140	1.183
	4B	457	11.8 × 10^5	180,000	257,500	0.6866	1.184	1.140	1.195
	4C	470	12.2 × 10^5	180,000	254,300	0.6811	1.172	1.140	1.180
	4D	185	4.78 × 10^5	170,000	232,500	0.6168	1.062	1.075	1.080
	4E	186	4.78 × 10^5	170,000	226,500	0.6323	1.090	1.075	1.050
	4G	178	4.60 × 10^5	170,000	228,200	0.6152	1.060	1.075	1.060
Average 4A-4G...			8.12 × 10^5				1.102	1.080	1.116
Brass, annealed...	4	422 × 10^{-6}	1.0	74,500	97,000	0.6840			
	6	186	4.42 × 10^5	85,000	144,000	0.8374	1.226	1.140	1.485
	7	188	4.46 × 10^5	86,000	134,200	0.8374	1.226	1.154	1.388
	9	196	4.66 × 10^5	86,000	130,600	0.8520	1.247	1.154	1.345
Average 6-9......			4.51 × 10^5				1.233	1.149	1.406

1045 steel. The dynamic tests varied from an average time value of 0.00245 sec. for the S.A.E. 3140 to 0.00443 sec. for the annealed brass. Hence, the actual numerical speed ratios given in Table 2 varied from 3.52 × 10^5 for the S.A.E. 1112 to 8.65 × 10^5 for the S.A.E. 1045 steel. The speed ratio $\dfrac{v}{v_0}$ in Table 2 refers to the ratio of the average true strain velocity in impact to the static value. The difference in these ratios is probably of no great physical

impact test as carried out on the Izod machine where the striking velocity is of the order of 11.5 ft. per second.

Table 2 further shows that a speed ratio of 3.52 × 10^5 produces an average increase of 14.0 per cent in the true stress at the maximum load and 12.1 per cent in the true stress at fracture for the S.A.E. 1112, while the average true strain $q' = \epsilon$ at fracture is 2.6 per cent less at the high speed. The S.A.E. 1045 steel showed an increase of 6.9 per cent and 11.3 per cent

in the true stress corresponding to the maximum load and to the fracture loads,

respectively, for a speed ratio of 8.65 × 10⁵, while at the same time the true
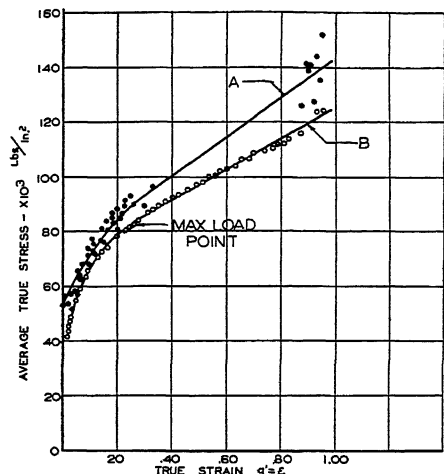
FIG. 6.—TRUE STRESS-STRAIN CURVES FOR S.A.E.1112 CONSTRUCTED BY TWO-LOAD METHOD (CURVE A).

Curve A average for specimens 2A, 2B, 2C, 2D, 2E, 2F, 2I and 2H; average true strain rate, 318 per second.

Curve B average for specimens 2G and 2J; average true strain rate, 903 × 10⁻⁶ per second.
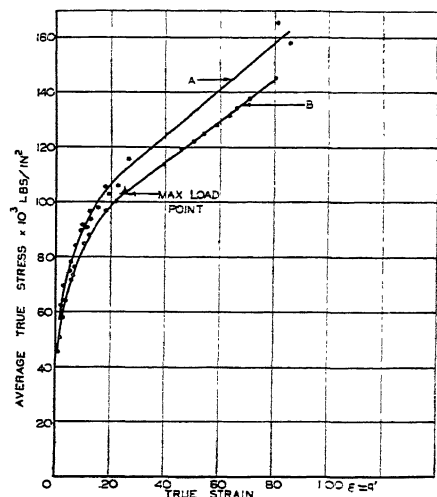
FIG. 8.—TRUE STRESS-STRAIN CURVES FOR S.A.E. 1045 BY TWO-LOAD METHOD (CURVE A).

Curve A average for specimens 1C and 1H. Average true strain rate, 290 per second.

Curve B for specimen 1J. Average true strain rate, 335 × 10⁻⁶ per second.

FIG. 7.—TRUE STRESS-STRAIN CURVES FOR S.A.E.3140 BY TWO-LOAD METHOD (CURVES A AND B).

Curve A average for specimens 4A, 4B, 4C, 4D, 4E and 4G. Average true strain rate, 314 per second.

Curve B average for 4F and 4H. Average true strain rate, 190 × 10⁻³ per second.

Curve C average for 4M and 4I. Average true strain rate, 367 × 10⁻⁶ per second.
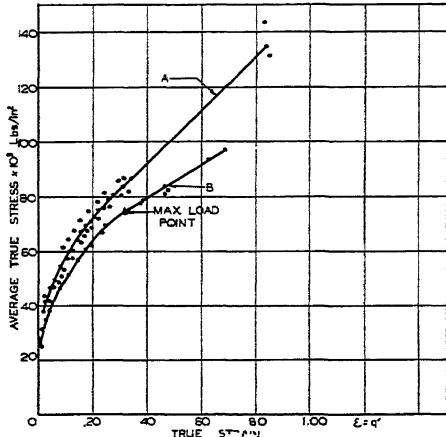
FIG. 9.—TRUE STRESS-STRAIN CURVES FOR BRASS CONSTRUCTED BY TWO-LOAD METHOD (CURVE A).

Curve A average for specimens 6, 7 and 9. Average true strain rate, 190 per second.

Curve B for specimen 4. Average true strain rate, 422 × 10⁻⁶ per second.

strain at fracture $q' = \epsilon$, increased 3.1 per cent. The S.A.E. 3140 indicated an increase of 8 per cent and 11.6 per cent in the true stresses corresponding to the maximum and fracture loads, respectively, for a speed ratio of 8.12×10^5, while the true strain at fracture increased 10.2 per cent. A somewhat greater effect of the speed of testing is shown by the brass where a speed ratio of 4.51×10^5 increased the true stresses corresponding to maximum and fracture loads by 14.9 and 40.6 per cent, respectively, and the true fracture strain by 23.3 per cent.*

---

* In comparing these results with those reported by other investigators, it should be noted that the strain velocities included herein are the average true strain velocities where

$$v = \frac{d\epsilon}{dt} = \frac{d\epsilon_0/dt}{1 + \epsilon_0}.$$

In this equation $\epsilon = \log A_0/A$ and $\epsilon_0 = \Delta L_0/L_0$, both values holding for the bottom of the necked-down region. It is obvious, since the true strain ϵ at fracture measured in the bottom of the necked-down region is larger than the over-all ϵ_0 in 2 in., that this definition results in larger numerical strain velocities.

In using tapered specimens such as those in the paper, it should also be noted that owing to the variation in areas along the bar, the true strain rates also vary along the axis. At any position along the bar the true strain rate is

$$v = -\frac{1}{A} \times \frac{dA}{dt}$$

Specimens may, however, be properly tapered so that the true strain rates will not vary more than 100:1 for any load. Where creep phenomena do not enter, as in short-time tests of the type discussed, such a variation of strain rate along the bar is of no practical importance. It has been shown earlier[9] that true stress-strain curves constructed by the two-load method on tapered specimens were identical with those obtained by measuring the diameter throughout the test at the smallest cross section or by using a uniform bar of a different diameter. If the variation in strain rates along the bar had an important effect, such a check would not be possible. Also, since only rather small effects have been observed herein for speed ratios of a million to one, the variations of true strain rate along the bar itself would produce effects of only a second order importance.

It is felt, moreover, that fundamentally the use of the true strain velocity in the necked-down region has the same basic advantages over the ordinary strain velocity measured in

In common with the results of Nadai and Manjoine,[3] Mann,[1] Clark and Dätwyler,[2] and others, it was found that the general effect of increasing the speeds of testing was in most cases to increase the fracture strains and the stresses at the maximum loads, although true stresses and strains were reported herein. For the latter reason, and since the same materials were not tested by them, a direct comparison of the results reported with those contained in Table 2 does not seem feasible. A comparison of previously reported data does indicate in general, however, that the results reported in this paper appear to be of the expected order of magnitude.

SUMMARY

Experiments are described in which the effects of the speed of testing on the true stress-strain properties of four different materials were investigated by the two-load method. Both slow static tension tests and low-velocity Izod impact tension tests were conducted. True stress-strain curves were reported for each material.

The summary of test data in Table 2 indicates for all of the materials tested, which included S.A.E. 1112, 1045, and 3140 steels and a brass, that the true stresses corresponding to the maximum load increased from 6.9 to 14.9 per cent, the true stresses at fracture increased from 11.3 to 40.6 per cent, and with the exception of the S.A.E. 1112 the true fracture strains increased from 3.1 to 23.3 per cent for the different materials when tested under low-velocity impact conditions as compared with their static tension values.

---

a 2-in. gauge length, throughout which the strain is nonuniform, as the true strain ϵ has over the strain ϵ_0 where the latter is defined for a 2-in. gauge length. In reporting test results, this quantity also has more physical significance than the striking velocity which is often reported in feet per second. Two different materials may have been tested with the same striking velocity and yet have widely different true strain rates.

ACKNOWLEDGMENT

REFERENCES

1. H. C. Mann: High Velocity Tension-Impact Tests. *Proc. Amer. Soc. Test. Mat.* (1936) 36, pt. II, 85–97.
2. D. S. Clark and G. Dätwyler: Stress-Strain Relations under Tension Impact Loading. *Proc. Amer. Soc. Test. Mat.* (1938) 38, pt. II.
3. A. Nádai and M. Manjoine: High-Speed Tension Tests at Elevated Temperatures. *Proc. Amer. Soc. Test. Mat.* (1940) 40, 822–837. Also Parts II and III, *Jnl. Applied Mechanics* (June 1941) 8, A77–A91.
4. J. Winlock and R. W. E. Leiter: Some Factors Affecting the Plastic Deformation of Sheet and Strip Steel and Their Relation to the Deep Drawing Properties. *Trans. Amer. Soc. Metals* (1937) 25 (1), 163–184.
5. H. Deutler: Experimentelle Untersuchungen uber die Abhangigkeit der Zugspannungen von der Verformungsgeschwindigkeit. *Phys. Ztsch.* (1932) 33, 247–259.
6. H. Brinkmann: Zerreissversuche mit hohen Geschwindigkeiten. Dissertation, Technische Hochschule, Hannover, 1933.
7. C. W. MacGregor: Relations between Stress and Reduction in Area for Tensile Tests of Metals, Also, Differential Area Relations in the Plastic State for Uniaxial Stress, Stephen Timoshenko, 60th Anniversary Vol., The Macmillan Co., New York.
8. C. W. MacGregor: The Tension Test, *Proc. Amer. Soc. Test. Mat.* (1940) 40, 508–534.
9. C. W. MacGregor: A Two-load Method of Determining the Average True Stress-strain Curve in Tension. *Jnl. Applied Mechanics* (1939) 6 (4), A156–158.
10. A. V. de Forest: Some Complexities of Impact Strength. *Trans. A.I.M.E.* (1941) 145, 13.

DISCUSSION

(R. M. Bozorth presiding)

R. M. BOZORTH,* New York, N. Y.—I noticed in the last slide that there is just one material for which the strain at fracture was less on the rapid test. Is there any significance to be attached to that?

C. W. MACGREGOR (author's reply).—The fact that one of the materials had a slightly smaller strain at fracture for the rapid test as compared with the slow test merely indicates that this material is rather insensitive to velocity effects in the range studied. The small decrease may have been due to slight differences in the material.

R. M. BOZORTH.—That 3 per cent was then an experimental or natural variation.

One more thing: How does the speed of test compare with the speed of elastic wave in the material? Is the time of test comparable with the time it takes the wave to go the length of the specimen? What is the order of magnitude?

C. W. MACGREGOR.—The time of test is relatively large compared with the natural period of vibration of the weighbar-specimen system. If we compare the time of test with the time per half cycle for the traveling wave, we find that it is at least 60 times greater. This fact makes the weighbar system fairly reliable in measuring loads.

During the time of test the elastic wave would travel approximately 30 ft. or more, which indicates that the load at any instant is, for all practical purposes, the same over all portions of the specimen.

A. V. DE FOREST.—This is one experiment in the direction of trying to find out more about the so-called speed effect. It has not yielded any spectacular results. On the other hand, maybe there are not any spectacular results. We would like to know. In due course we are going to have higher speeds and then we will be able to extend the speed range.

One of the difficulties that comes into the higher rates of loading is this. There are traveling waves through the specimen: therefore the stress is not distributed uniformly along the length. Therefore also, the stress at the measuring point, wherever that is, is not an accurate measure of the stress at some other point.

We have very crudely attempted some higher-speed loadings and found that the mechanisms that are normally in use for the higher speeds lead to very large elastic oscillation during the whole course of the test. Those have to be handled in some way. At least they must be measured and estimated before we draw too many conclusions.

This two-load method and the test specimen looks as though it were a pleasant approach to some of the difficult problems of the measurement, especially at higher temperatures.

V. N. KRIVOBOK,* Burbank, Calif.—Why is it called a two-load method?

* Research Physicist, Bell Telephone Laboratories.

* Lockheed Aircraft Corporation.

A. V. DE FOREST.—The ordinary method is a uniform diameter and the measurement of changing loads. In this method we use a tapered specimen of varied diameter and we need to measure only the maximum load to construct most of the diagrams, and the final breaking load to construct the portion of the diagram after the necking has started to take place. So that by measuring only two loads we can construct the diagram from the shape of the specimen after the failure, instead of the ordinary diagram where many loads are measured. In this case we have only two loads measured on the varying diameter test measurement.

(S. L. Hoyt presiding)

V. N. KRIVOBOK.—The work you have done seems to me very important. I hope that you will be able to pursue it and publish more and more of it.

I should like to make one suggestion: If I understood correctly, you have measured the changes in the diameter of the conical sample. Have you made attempts to measure the local elongation between the two marks you put on the center?

C. W. MAC GREGOR.—We have made measurements of both the axial strains between small scratches for very short gauge lengths and have compared these with the axial strains determined from diameter measurements. The results of these particular tests are included in a previous publication.[8] It was shown there that the true axial strain defined by $\sum = \log \dfrac{L}{L_o}$ is equal to that obtained by diameter measurements and defined as $\sum = q^1 = \log \dfrac{A_o}{A}$.

V. N. KRIVOBOK.—It is most interesting because in the last six months there has been brought to light, at least in my opinion, the importance of the so-called minute or local elongation. I cannot possibly overemphasize the importance of that local elongation. I simply see no sense at all in talking in elongations in 2 in. In a process such as sheet drawing, the matter of local elongation is so important that it spells literally the success or the complete failure of the attempted drawing.

And more work could be done on the effect, for example, of load application, the effect of stretch on the distribution of local elongation, and so forth, and it would indeed be most useful to the sheet-drawing industry.

A. V. DE FOREST.—Might I ask if Dr. Krivobok feels like telling us something of his local measurements? I know that he has some very interesting methods, which have been used in his plant.

V. N. KRIVOBOK.—If you will ask me more specifically what you have in mind, I will be glad to tell you what I know.

A. V. DE FOREST.—Your method of putting a reference grading on the surface in order to be able to measure these local elongations.

V. N. KRIVOBOK.—We use a photographic method. I would be very happy to send you detailed description rather than do it now, for the simple reason that I do not remember the exact details. That is the job of a younger man who does it. We are able, however, to put by means of a photographic method the lines which when magnified 100 times give the thickness of the line of less than $\frac{1}{100}$ in., so that the measurements can be made quite accurately.

The other thing we found out is that the different materials would differ considerably in relation to the local elongation available in the metal, even though the general over-all elongation would be so close together that no intelligent engineer would say that they are different at all.

For aluminum alloys, we were able to find out, for example, that 24-S alloy in the SO condition will have a local elongation of 130 per cent. In the hardened condition we can obtain elongations far in excess of anything that has heretofore been published.

We also found out that it is literally impossible, of course, from the commercial point of view to receive the material always alike, in properties and characteristics. For certain very important deep-drawing operations, we suggest materials in which local elongations are of certain minimum value. Criteria can be established that the metal will not be formable at all if the local elongation is below a certain figure. We simply put that aside and use it for some other less difficult operation.

We realize fully that we cannot ask for nor expect to receive, in these struggling troublesome days, materials that are absolutely alike in their properties. There the question of the selection and control of some intangible, which was unknown to us before, becomes, in practice, very important.

Technical Cohesive Strength and Yield Strength of Metals

By D. J. McAdam, Jr.,* Member A.I.M.E.

In a recent survey of the literature, the author has found evidence incompatible with prevalent views regarding the technical cohesive strength and yield strength of metals. Some of the evidence regarding the technical cohesive strength was presented in a previous paper,[21] and views were presented that are believed to be in better accord with the evidence. In that paper, it was shown that the technical cohesion limit (contrary to prevalent views) varies with the combination of principal stresses,† and that the influence of plastic deformation on the technical cohesive strength is not in accordance with prevalent views. In this paper, consideration will be given to both the technical cohesion limit and the yield stress as affected by the combination of principal stresses. Evidence will be presented that the variations of the yield stress and the technical cohesion limit with the combination of principal stresses are not in accordance with prevalent views. Consideration will also be given to ductility and work-hardening capacity, which depend on the initial difference between the technical cohesion limit and the yield stress.

By the "technical cohesion limit" is meant the mean stress at actual or poten-

tial* fracture. An example of a technical cohesion limit is the "true" breaking stress of a tension-test specimen, the breaking load divided by the sectional area at fracture. The cohesion limit thus obtained for a ductile metal, however, has been greatly altered by the plastic deformation. It is important to consider the cohesion limit of the metal prior to this deformation, and the variation of the cohesive strength with plastic deformation. The relation between the cohesion limit and the corresponding flow stress† determines the ductility of a metal and the energy that it will absorb before fracture.

In this paper, as in the previous paper,[21] tensile stresses will be viewed as positive and compressive stresses as negative. The algebraically greatest principal stress will be designated S_1, the least principal stress will be designated S_3, and the intermediate principal stress will be designated S_2. In the previous paper, attention was confined to stress combinations with two of the principal stresses equal (with the intermediate principal stress S_2 equal either to S_3 or S_1). In this paper, consideration will also be given to the effect of stress combinations with all three principal stresses unequal. In the earlier sections of the paper (pp. 311 to 324), attention will be confined to stress combinations with

† Any stress system can be resolved into three principal stresses normal to three mutually perpendicular planes on which there is no shearing stress.

* Because plastic deformation increases the cohesive strength, the initial cohesion limit sometimes can be only estimated, not actually attained.

† By "flow stress" is meant the yield stress based on the corresponding sectional area, not on the original area.

S_2 equal to S_3; in the sixth section (pp. 325 to 326), the view will be broadened to include stress combinations with S_2 equal to S_1; and in the last three sections (pp. 326 to 335) the view will be further broadened to include stress combinations with no two principal stresses equal.

Fig. 1 shows three typical stress combinations with no two principal stresses equal. The arithmetical value of each principal stress is represented qualitatively by the length of the arrow. Arrows pointing away from the cube indicate tensile stresses; arrows pointing toward the cube indicate compressive stresses.

Stress combinations with two of the principal stresses equal would be produced by subjecting a cylinder to various combinations of axial stress and uniform radial stress. (The uniform radial stress is equivalent to two equal mutually perpendicular principal stresses.) Typical stress systems with two principal stresses equal are illustrated in Figs. 2 and 3. Fig. 2 shows four typical stress combinations with S_2 equal to S_3. In such combinations, the greatest principal stress is in the axial direction, and the stress combination tends to cause either absolute or relative increase in length.* Fig. 2B represents a specimen subjected to longitudinal tension and to a smaller radial tension in the notched section. With an unnotched specimen, such a stress system cannot readily be obtained experimentally. When a notched cylindrical specimen is subjected to longitudinal tension, however, the minimum section is under radial tension. The ratio of S_3 to S_1 increases with the depth and sharpness of the notch, but cannot become actually equal to 1.0. Stress systems qualitatively similar to that shown in Fig. 2C are produced during the cold-drawing of round rod or wire.

Fig. 3 shows four typical stress combinations with S_2 equal to S_1. Such a combina-tion tends to cause either absolute or relative decrease in length. This type of deformation can be caused by uniform radial tension (Fig. 3A). Axial compression of a cylinder causes a stress combination of the type illustrated in Fig. 3C, except that the greatest principal stress (radial) is zero.

In the following pages, consideration will be given to the influence of stress combinations of the types illustrated in Figs. 1, 2, and 3 on the technical cohesion limit and on the yield stress. The distinction between these three types, therefore, should be kept in mind. In studying the variation of the cohesion limit with the combination of principal stresses, attention will be confined almost entirely (as in the previous paper) to the cohesion limit at actual or potential rupture.* Some attention, however, will be given to the relation between the cohesion limits for rupture and shear.

When two of the principal stresses are kept equal, the influence of the combination of principal stresses on the technical cohesion limit and on the yield stress can be expressed in terms of axial stress and radial stress (Figs. 2 and 3). The influence of such stress combinations, therefore, can be represented quantitatively by two-dimensional diagrams. Two-dimensional diagrams, consequently, were used in the previous paper[21] and are used in the earlier part of this paper (pp. 311 to 325). Removal of the restriction that two of the principal stresses are equal, however, makes it necessary to use three-dimensional diagrams. A study of the complete three-dimensional relationship is given in the last three sections of this paper (pp. 326 to 335). The three-dimensional diagrams are derived by exact geometrical methods from two-dimensional diagrams. As the curves in the two-dimensional diagrams

---

* By "relative" increase in length is meant an increase in the ratio of length to diameter.

* The term "rupture" is used to designate fracture by separation as distinguished from a shearing fracture.

can be considered only qualitatively correct, however, the three-dimensional diagrams are presented as merely qualitative pictures of the influence of the combination of principal stresses on the technical cohesion limit and yield stress. Nevertheless, they reveal important relations between these two strength indices, and the influence of these relations on strength, ductility and work-hardening capacity. It is hoped that they will stimulate investigation that will result in the construction of more accurate diagrams.

STRENGTH AND DUCTILITY OF NOTCHED CYLINDRICAL SPECIMENS AS AFFECTED BY RATIO OF S_3 TO S_1

Variation of S_3/S_1 with Depth and Sharpness of Notch

When a notched cylindrical specimen is subjected to longitudinal tension, the stress combination induced is of the type illustrated by Fig. 2B. The minimum section is under longitudinal and radial tensile stresses. The intermediate principal stress S_2 and the least principal stress S_3 are equal. Any such stress combination, consequently, may be expressed in terms of two variables, S_3 and S_1.

The ratio of S_3 to S_1 increases with the depth and sharpness of the notch. The quantitative relationship between S_3/S_1 and the depth and sharpness of the notch was investigated by Kuntze[10-18] by means of elastic stress-strain measurements on cylindrical specimens with sharp V-notches. The root radius ranged between about 0.1 and 0.15 mm. Kuntze found that S_3/S_1 is proportional to a function of the notch depth, according to the equation

$$S_3/S_1 = C(D^2 - d^2)/D^2 \qquad [1]$$

In this equation, d and D represent the minimum and maximum diameters, respectively, of the cylindrical notched

specimen, and C is a constant depending on the notch angle. If d^2/D^2 be designated by k, the equation becomes

$$S_3/S_1 = C(1 - k) \qquad [2]$$

The ratio of S_3 to S_1 was also found to be linearly related to the notch angle according to the equation

$$C = (180 - \omega)/180 \qquad [3]$$

In this equation, ω represents the notch angle in degrees. Combination of equations 2 and 3 gives

$$S_3/S_1 = (1 - k)(180 - \omega)/180 \qquad [4]$$

For zero notch angle, $S_3/S_1 = (1 - k.)$ For a value approaching zero of both ω and k, S_3 becomes equal to S_1. Such a system $(S_2 = S_3 = S_1)$ will be termed (after Kuntze) "polarsymmetric stress."

The ultimate tensile strength (based on the minimum section) of a notched specimen was also found by Kuntze to be linearly related to $(1 - k)(180 - \omega)/180$, the same expression that is given in Eq. 4. This expression was found to be proportional to the difference between the tensile strength of the notched specimen and that of an unnotched specimen. The ultimate tensile strength thus was found to be linearly related to S_3/S_1.

This relationship is the basis of Kuntze's method of determining the technical cohesion limit by extrapolation, using results of tension testing of specimens with various notches. He thus obtains a value representing the breaking stress under polarsymmetric tension. Under such a stress system there is no shearing stress, hence there can be no plastic deformation. Under sufficiently high polarsymmetric stress, the most ductile metal would fracture without plastic deformation. The stress causing such a fracture, therefore, is a technical cohesion limit of unaltered metal. As no method has been found for direct measurement of this stress, it can

be determined only by extrapolation from results of tension tests of notched specimens.

The tensile strength used in Kuntze's method of extrapolation is not the breaking stress, but is the ultimate stress, the stress when the load reaches a maximum. The method of linear extrapolation cannot be applied when the tension test of a notched specimen gives a "premature" fracture; that is, fracture while the tensile load is increasing. At premature fracture the stress concentration due to the notch causes the mean stress to be less than the actual local stress at the origin of fracture. The estimated mean stresses, consequently, do not give a linear relation with $(1 - k)$ $(180 - \omega)/180$, and may give a decidedly curvilinear relationship.

Ultimate Tensile Strength as Affected by Ratio of S_3 to S_1

In the previous paper,[21] various diagrams are used to represent the variation of the strength and ductility of specimens with a constant notch angle. Abscissas in those diagrams represent values of $1 - k$. In Figs. 4, 5 and 6 herewith, however, abscissas represent values of $(1 - k)$ $(180 - \omega)/180$. According to Eq. 4, therefore, each graph shows the influence of both the depth and the sharpness of the notch, and abscissas represent values of S_3/S_1. The indicated values for the ultimate tensile strength (Figs. 4, 5 and 6) are based on the initial minimum sectional area, not on the sectional area when the load reaches a maximum.

Figs. 4 and 5 show results of experiments by Kuntze with notches having a constant angle (60°) but different depths. Fig. 4 shows results obtained with a moderately ductile steel (M); Fig. 5 shows results obtained with brittle steels (R and R_D). Steel R_D was produced by plastic extension of a cylindrical bar of steel R until the cross section had been decreased 4 per cent; steel R_D then was at the beginning

of local contraction. From bars of steels R and R_D, notched and unnotched specimens were then prepared for tension test. Even unnotched specimens of these steels showed very little ductility. The decrease of sectional area at fracture was only 6 per cent for steel R[18] and only 2 per cent for steel R_D (Fig. 5).

As shown in Fig. 2 of the previous paper,[21] notched specimens of steel R gave "premature" fractures. The greater the size of the notched specimen, the greater was the tendency to premature fracture.* With the smallest of the notched specimens, however, fracture occurred only a short time before the load reached a maximum; the results obtained with these specimens are designated in Fig. 5 as fractures. With the unnotched specimen, the load actually reached a maximum; the corresponding point in Fig. 5 therefore represents the ultimate tensile strength. Although the ductility of steel R_D had been nearly exhausted by the prior plastic extension, the notched specimens did not fracture until after the load had reached a maximum.† With the ductile steel M, no premature fractures were obtained.

Fig. 6 is based on experiments by Ludwik and Scheu[20] with mild steel specimens having V-notches all of the same depth, but with different angles. The dimensions of the specimens are given in the insert sketch in Fig. 6. The value of S_3/S_1 corresponding to each of these specimens has been calculated by the use of Eq. 4, and these values have been plotted as abscissas in Fig. 6.

The ultimate strength values for steels M and R_D evidently are linearly related to S_3/S_1, at least within the range of

---

* Much, if not all, of this apparent size effect was due to difference in stress concentration.[21]

† Experiments by Kuntze with various metals have shown that the tendency to premature fracture is decreased by plastic extension (prior to the formation of a notch) to the beginning of local contraction.

values of S_3/S_1 covered by the investigation (Figs. 4 and 5). Because of the prematurity of the fractures obtained with steel R, however, the broken line traversing the points representing fractures is slightly curved. If values of the ultimate strength could have been obtained, the line traversing the corresponding points probably would be straight, like the lines obtained with steels M and R_D, and as indicated by the continuous line for steel R in Fig. 5. To determine values of the technical cohesion limit in accordance with Kuntze's method of extrapolation, the straight lines in Figs. 4 and 5 have been extended to abscissa 1.0. The ordinates of the points T_1 thus obtained represent values of the technical cohesion limit under polarsymmetric tension. As will be shown, however, Kuntze's view that the technical cohesive strength of a metal can be represented by a single stress value is incorrect. As in the previous paper,[21] the technical cohesion limit under polarsymmetric tension will be termed the "disrupture stress," a term used by Bridgman.[5]

In Fig. 6, the line representing the variation of the ultimate tensile strength with S_3/S_1 is slightly curved, thus differing from the lines obtained with constant notch angle and varying notch depth (Figs. 4 and 5). The shape of the line in Fig. 6 casts some doubt on the linear extrapolation represented by Eq. 3. Because the curvature of this line apparently decreases as the line extends to the right, however, the error involved in linear extrapolation to zero notch angle may not be great, unless the extrapolation is based entirely on results obtained with large notch angles. The disruptive stress for steel N, however, may be slightly less than the value represented by the ordinate at point T_1.

Yield Stress and Ductility as Affected by Ratio of S_3 to S_1

Two different indices are used in Figs. 4 and 5 to represent the yield strength; they are distinguished by the indicated percentage of plastic deformation. The 0.002 per cent yield stress is more nearly an index of elastic strength than of yield strength. With increase in S_3/S_1, the 0.002 per cent yield stress decreases to a minimum and then increases (Figs. 4 and 5). The initial descent of these curves is due to increasing stress concentration at the root of the notch. The 0.6 per cent yield stress, however, rises continuously with increase in S_3/S_1. A large part of the stress concentration, therefore, evidently is removed by the 0.6 per cent plastic deformation. The curves for the 0.6 per cent yield stress thus reveal qualitatively the influence of S_3/S_1 on the yield stress. The continuous increase of the yield stress with S_3/S_1 is due to a continuous increase in the ratio of the longitudinal tensile stress to the shearing stress.*

A line representing the variation of the yield strength of the brittle steel R_D with S_3/S_1 (Fig. 5) would be just below the line representing the variation of the ultimate strength. At abscissa 1.0, the curves for yield, ultimate strength and fracture converge to the point (T_1) representing the disruptive stress. Under polarsymmetric tension, fracture would occur without plastic deformation.

As illustrated by the upper diagrams in Figs. 4, 5 and 6, the ductility at first decreases rapidly with increase in S_3/S_1. As shown in Figs. 4 and 5, the ductility again increases with increase of S_3/S_1 beyond about 0.33. The final trend of the ductility, however, must be downward, and the ductility must become zero when S_3/S_1 becomes 1.0. It seems probable that this intermediate increase of ductility is associated with the deformation gradients in the notched specimens. If uniform radial tensile stress could be applied to unnotched cylindrical specimens, the curves of ductility probably would be of the form

---

* The shearing stress is equal to $(S_1 - S_3)/2$.

indicated by the broken lines. The curves probably would descend first at a decreasing rate and then at an increasing rate. It is not impossible, however, that the influence of S_3/S_1 is as indicated by the solid curves. (See footnote on page 331.)

Breaking Stress as Affected by Ratio of S_3 to S_1

The values of the breaking stress* indicated in Figs. 4, 5 and 6 are all less, usually much less, than the corresponding values of the disruptive stress. And yet these values, with the exception of those representing premature fracture of steel R (Fig. 5), were obtained after sufficient plastic extension to permit the tensile load to traverse a maximum. Stress concentration, therefore, was virtually absent, and the values of the breaking stress must be viewed as technical cohesion limits. Moreover, the fact that these measured cohesion limits are all lower than the corresponding disruptive stresses obtained by extrapolation cannot be attributed to an influence of plastic deformation on the measured cohesion limits. The best evidence for this is found in Fig. 5. The ductility of steel R_D was so slight that the corresponding values for the 0.6 per cent yield stress, ultimate stress, and breaking stress are very close together. The idea that the slight plastic deformation is the reason for the differences between the disruptive stress and the measured breaking stresses appears incredible. The simplest and most plausible assumption is that the technical cohesion limit varies with S_3/S_1, and that a line representing this variation of the cohesion limit for the brittle steel R_D would differ little from the line representing the variation of the ultimate tensile strength.

For the ductile steels M and N (Figs. 4 and 6), the curves of variation of the

---

* The indicated values are "true" stresses, based on the sectional area at fracture.

breaking stress with S_3/S_1 are considerably above the corresponding curves of variation of the ultimate tensile stress. The plastic deformation during the local contraction of each of these specimens evidently has caused an increase in the corresponding technical cohesion limit. Nevertheless, the directly determined breaking stresses are all less than the disruptive stress. (The influence of plastic deformation on the technical cohesive strength is discussed on pages 320 to 323.)

VARIATION OF TECHNICAL COHESION LIMIT, YIELD STRESS, AND ULTIMATE STRESS WITH COMBINATION OF PRINCIPAL STRESSES, WHEN THE LEAST TWO OF THE PRINCIPAL STRESSES ARE KEPT EQUAL

Influence of Combination of Principal Stresses on Technical Cohesion Limit of Brittle Metal

When two of the principal stresses are kept equal, any stress combinations may be expressed in terms of only two variables, the axial stress and the radial stress. In Figs. 7 and 8, ordinates represent axial stresses and abscissas represent radial stresses. Abscissas in these figures thus differ from abscissas (S_3/S_1) in Figs. 4, 5 and 6. The range of stress combinations that may be represented is much greater in a diagram of the type shown in Figs. 7 and 8 than in a diagram of the type shown in Figs. 4, 5 and 6. In a diagram of the type shown in Figs. 7 and 8, it is possible to represent not only the stress combinations typified by Fig. 2B, but also all the stress combinations typified in Figs. 2 and 3. In Figs. 7 and 8, attention is confined to stress combinations typified by Fig. 2, combinations with S_2 equal to S_3.

Line H in Figs. 7 and 8, making an angle of 45° with the axes of coordinates, is the locus of all points representing polarsymmetric stress. The field included in the 45° angle between this line and the axis of

ordinates is the only part of such a diagram that corresponds to a diagram of the type shown in Figs. 4, 5 and 6. All the evidence contained in Figs. 4, 5 and 6, has been reproduced in this field of Figs. 7 and 8.

A study of the influence of the combination of principal stresses should begin with a brittle metal. The influence of plastic deformation, a variable affecting the technical cohesion limit, is thus minimized. First consideration, therefore, will be given to the diagrams representing the brittle steels R and R_D (Fig. 7). Because two of the curves correspond to the relationship represented by the two straight sloping lines in Fig. 5, these two curves represent a linear relation between S_3/S_1 and the ultimate tensile strength, the relation assumed in Kuntze's method of determining the disruptive stress by extrapolation (p. 323). The curve representing breaking stresses for steel R_D is only slightly above the curve representing ultimate tensile strengths. Because specimens of steel R broke a little prematurely, however, the points representing fractures of these specimens are a little below the corresponding curve.

The radiating broken lines in Fig. 7 represent typical constant values of S_3/S_1. The intersections of these lines with curves R and R_D represent corresponding values of the technical cohesion limit. The evidence indicates that the technical cohesion limit increases with increase of S_3/S_1 between zero and 1.0, and that the disruptive stress (T_1) is the highest value of the technical cohesion limit.

A diagram intended to represent qualitatively the variation of the technical cohesion limit with S_3/S_1 was presented by Bridgman,[5] based on results of compression tests of various types.* Within the field of

positive values of S_3/S_1, where his diagram has no experimental basis, his curve traverses a maximum before reaching point T_1, thus implying that the disruptive stress is not the highest value of S_1. The experimental evidence in Fig. 7, however, gives no warrant for such a construction, and indicates that S_1 increases continuously from T_0 to T_1.

In the previous paper,[21] the curve of technical cohesion limits is drawn so that it has a horizontal tangent at T_1. If the locus of fractures of steel R_D is straight as represented in Fig. 5, however, the corresponding curve in Fig. 7 would not become horizontal at T_1 (see appendix A).

The extension of the curves in Fig. 7 into the field of negative values of S_3/S_1 is based on compression tests by Bridgman.[2-5] Cylindrical specimens of various materials were subjected to hydrostatic pressure on the cylindrical surface, while the ends of the specimens were subjected only to atmospheric pressure. When the hydrostatic pressure reached a certain value, depending on the material, the specimen fractured transversely as if it had been broken by longitudinal tension. Ductile metals contracted locally before fracture, but brittle materials broke with clean, exactly transverse fracture. Fracture of a brittle material thus occurred with practically no stress normal to the plane of fracture. Such fractures are represented in Fig. 7 by points T_{c2}. The horizontal positions of these points are determined approximately in accordance with the fact[4] that the radial compressive stress at the fracture of a brittle specimen of steel is somewhat greater than the breaking stress under unidirectional tension (T_0).

With extension of the curves into the region representing both axial and radial compression (Fig. 2D), the divergence of the curves from line H (Fig. 7) becomes

---

* In this diagram, abscissas do not represent radial stresses, as in Fig. 7, but represent radial stresses multiplied by $\sqrt{2}$; the locus of polar-symmetric stresses thus makes an angle of 54°

44' with the axis of ordinates. This arrangement was made in order to present a sectional view of a three-dimensional diagram.

gradually less rapid. The radial compressive stress here is arithmetically greater (though algebraically less) than the axial compressive stress. As pointed out by Bridgman,[5] experiments by Richart, Brandtzaeg, and Brown[25] with cylindrical specimens of concrete (under such conditions) gave transverse fractures. Throughout its entire length, therefore, a curve of the type shown in Fig. 7 evidently is the locus of points representing transverse fractures, similar to those produced by an ordinary tension test.

As Bridgman[5] has pointed out, any combination of principal stresses (represented by a point on a curve of this type) may be resolved into a polarsymmetric stress plus a unidirectional (axial) stress. The axial stress is represented by the vertical distance from the given point to line H, and the intersection of this vertical line with line H represents the polarsymmetric stress.

Influence of Combination of Principal Stresses on Ultimate Stress and Yield Stress of Ductile Metal

The curves of variation of the ultimate stress (Figs. 7 and 8), because of their derivation from corresponding straight lines in Figs. 4, 5 and 6, must be similar in form to the curves of technical cohesion of brittle metals (Fig. 7), and must extend to T_1. The extension of these curves into the field of negative values of S_3/S_1 is based on the previously mentioned results of radial compression tests by Bridgman.[2–5] The ultimate radial compressive stress on a ductile metal is slightly greater than the corresponding value of the ultimate stress under unidirectional tension.

A curve of variation of the 0.6 per cent yield stress, throughout its entire length, must be inside the corresponding curve of variation of the ultimate stress, and must intersect line H at T_1. The curves of variation of the yield stress, consequently, are similar in form to the curves of tech-

nical cohesive strength of a brittle metal. For the brittle steel R_D (Fig. 7), the curves representing the technical cohesion limit, ultimate stress, and yield stress practically coincide throughout their entire length. For a ductile steel (Fig. 8), the three curves evidently do not coincide except at T_1. The evidence (Figs. 4 and 8), moreover, appears to indicate that they do not become mutually tangent at T_1.

According to either the theory of constant maximum shearing stress or the theory of constant maximum shearing energy, the locus of yield stresses (in a diagram of this type) would be a straight line parallel to line H. The evidence in Figs. 7 and 8, therefore, is not in accordance with prevalent theory regarding either the technical cohesion limit or the yield stress.

Influence of Combination of Principal Stresses on Technical Cohesion Limit of Ductile Metal

The curves of variation of the technical cohesion limit for ductile steels M and N (Fig. 8) are very different from the curves for the brittle steels R and R_D (Fig. 7). The complex form of the curve for a ductile steel is due to the influence of two variables, S_3/S_1 and plastic deformation, on the technical cohesion limit. If the radial and axial stresses could be applied to an unnotched specimen, the locus of fracture for a ductile metal probably would diverge continuously from the curve of yield stresses with decrease of S_3/S_1 below 1.0, and thus would differ somewhat from the locus curves in Fig. 8.

INFLUENCE OF PLASTIC EXTENSION ON TECHNICAL COHESIVE STRENGTH OF METALS WHEN S_2 IS EQUAL TO S_3

Locus of Fractures

The locus of fractures in Fig. 8 is affected by the combination of principal stresses and by the varying plastic extension.

Other views of the locus of fractures for ductile and brittle steels are shown in Figs. 9 and 10. Ordinates represent values of the axial stress S_1; abscissas represent percentages of decrease in the sectional area due to plastic deformation. The locus of fractures starts at an ordinate representing the estimated disruptive stress, and traverses the points representing actual fractures of notched and unnotched specimens. The stresses and deformations represented by these points are the same as those represented by the corresponding points in Figs. 7 and 8. The decimal adjacent to each of these points in Figs. 9 and 10 indicates the value of S_3/S_1.

According to prevalent views, which are based on publications by Kuntze,[10–18] the influence of plastic deformation on the technical cohesive strength of a metal may be represented by a single curve, such as curve C in Fig. 9. This curve rises to a maximum, and then descends at an increasing rate until it intersects the continuously rising curve of flow stress F at a point P representing fracture. Curve F represents the variation of the flow stress with slow plastic deformation of an initially unnotched specimen. Between H (representing the beginning of local contraction) and P, the course of this curve is influenced by the notch effect of the increasing local contraction. The rise of S_3/S_1 from zero, owing to the increasing notch effect, causes the curve of flow stress to diverge at H from the curve F_0, which represents qualitatively the way the flow stress would vary if it could be kept unidirectional.

An increase in S_3/S_1 by the use of a notched specimen would elevate the entire curve of flow stress, but (according to the prevalent view) would not affect the curve of technical cohesion. With increase in S_3/S_1, therefore, the curve of flow stress would move successively to the positions represented by curves $F_{0.2}$, $F_{0.3}$ and $F_{0.4}$,[*]

[*] The subscripts indicate the corresponding values of S_3/S_1.

and the intersection with C would move successively to points $P_{0.2}$, $P_{0.3}$ and $P_{0.4}$. With further increase of S_3/S_1, the intersection would move upward to the summit of curve C and would then descend to the origin, the point representing the initial (single) cohesion limit of the metal.

The locus of actual fractures of a ductile steel (Fig. 9), however, is very different from curve C. With increase in S_3/S_1, the point representing fracture moves rapidly to the left from point P, descends to a minimum, then ascends, probably traverses a maximum, and approaches the point representing the initial disruptive stress. At P, the locus of fractures makes *only a small angle* with the curve of flow stress, an angle differing by more than 90° from the angle between the curve of flow stress and Kuntze's curve C. Whereas curve C predicts an initial rapid rise of the breaking stress with increase in S_3/S_1, the breaking stress actually *decreases* slightly and the ductility decreases very rapidly. As illustrated by diagram A of Fig. 10, a qualitatively similar locus of fracture is obtained with the moderately ductile steel M. With steels having only slight ductility (B and C), however, the locus of fractures does not traverse a minimum but ascends rapidly with increase of S_3/S_1, and probably traverses a maximum before reaching zero abscissa. As shown in the previous paper,[21] such a locus of fractures is not explainable in terms of prevalent views of the technical cohesive strength of metals.

The evidence leads directly to the surmise that the course of the locus of fractures is not due to the variation of a single cohesion limit with plastic extension. The cohesive strength of a metal (see p. 316) cannot be represented by a single stress value, but comprises an infinite number of values corresponding to the infinite number of possible combinations of the principal stresses. As any of these cohesion limits is affected by plastic deformation, the locus of fractures repre-

sents the influence of two variables, S_3/S_1 and plastic deformation, on the breaking stress. When a metal has little ductility, the influence of the variable plastic deformation is small in comparison with the influence of the variable S_3/S_1 (Fig. 10C). When a metal has considerable ductility, both variables have marked effect on the locus of fractures and thus cause the complex forms shown in Figs. 9 and 10A.

The locus of fractures obtained by the use of notched specimens is affected by minor variables such as the nonuniformity of deformation of a notched specimen.[21] In the absence of the distorting effect of these minor variables, the ductility probably would increase continuously with decrease in S_3/S_1, as indicated by the dotted curves in Fig. 10. A similar qualitative allowance for undesired variables has been made in drawing idealized curves of ductility in Figs. 4 and 5.

With extension beyond point P' (Figs. 9 and 10), the locus of fractures enters the field of negative values of S_3/S_1. In this field, the locus of fractures of the brittle steel R_D (Fig. 10C) continues its steep descent. The curve for steel R (Fig. 10B), if extended further, possibly would continue its rapid decrease of slope but probably would not traverse a minimum as does the curve for the more ductile steel M (Fig. 10A). The curves for the ductile steels M and N (Figs. 9 and 10A), after rising from the minimum, must eventually traverse a maximum and then turn rapidly downward. This final downward course is due to the eventual exhaustion of the ductility; the final course then is that of the curve for a brittle metal. For a few very ductile metals, however, it is possible that the locus of fractures does not take this final downward course, but rises from the minimum at a gradually decreasing rate. Such a metal would not fracture when S_3/S_1 is negative.

Influence of Plastic Extension on Specific Technical Cohesion Limits

As the technical cohesive strength of a metal cannot be represented by a single stress value, any specific cohesion limit must be referred to the corresponding combination of principal stresses. When $S_2 = S_3$, any cohesion limit may be designated with reference to the corresponding value of S_3/S_1. As the cohesion limits for unidirectional and polarsymmetric tension have been designated T_0 and T_1, respectively, the cohesion limit corresponding to any other value of S_3/S_1 will be designated by T with this value as a subscript.

A locus of fractures of the type shown in Figs. 9 and 10 represents cohesion limits corresponding to an infinite number of values of S_3/S_1. Any point on a locus of fractures could be made the terminus of a curve representing the influence of plastic extension on the cohesion limit corresponding to a single value of S_3/S_1. A complete view of the variation of the cohesive strength of a metal with plastic extension would comprise a series of curves, each representing a typical value of S_3/S_1. Each diagram in Fig. 10 contains a series of such curves, and thus gives a qualitative picture of the influence of plastic extension on the technical cohesive strength of a metal.

The available evidence[21] is incompatible with the prevalent view that plastic extension, above a certain amount, decreases the cohesive strength of a metal.* The evidence indicates that any curve representing a single cohesion limit rises continuously at a decreasing rate. It thus resembles qualitatively a curve of flow stress (corresponding to a single value of S_3/S_1). The greater the rate of work-

---

* The curve of variation of T_0 (Fig. 10A), for example, must enter the small angle between curves L and F_0 and intersect these curves at P'. There is no opportunity for a final descent of curve T_0.

hardening, the more rapid is the initial rise of each curve of either flow stress or cohesion. A curve of flow stress, however, rises more rapidly than the corresponding curve of cohesion. Although these two curves may be far apart at the origins, they converge and eventually intersect at a small angle, at a point representing fracture. This relation is illustrated by the T_0 and F_0 curves in diagrams A and B of Fig. 10. Four other pairs of curves of flow stress and cohesion are shown in diagram A. Each of these pairs, however, has been drawn so as to intersect at the idealized locus of fractures. Similar curves of cohesion could be drawn in Fig. 9 to correspond with the F_0, $F_{0.2}$, $F_{0.3}$, and $F_{0.4}$ curves.*

The origins of the cohesion curves of each series represent the cohesion limits of unaltered metal. The ordinates of the origins have been made approximately proportional to the corresponding cohesion limits of a brittle metal, as obtained from a diagram of the type shown in Fig. 7. The method of locating the approximate origins of the curves of cohesion is discussed in the previous paper.[21]

A diagram of the type shown in Figs. 9 and 10 has a disadvantage when it is extended to high percentages of decrease of sectional area. A small change of abscissa here represents a large change in plastic deformation. This is illustrated by Fig. 11, which is derived from diagram A of Fig. 12, to be discussed later. In Fig. 11, abscissas represent "effective extensions," which indicate a value of $(A_0/A - 1) \times 100$ per cent, in which A_0 and A represent the initial and current sectional areas, respectively. In a diagram of the type shown in Fig. 11, each curve representing flow stress or cohesion (for a specific value of S_2/S_1) rises continuously at a decreasing rate. When S_2/S_1 is low enough to permit con-

siderable extension before fracture, the curves eventually become nearly horizontal (curves T_0 and F_0). Because these curves converge so gradually and meet at such a small angle, the ductility is greatly affected by a small change of S_2/S_1, or of any other factor (such as temperature or velocity of deformation) that has a differential effect on the two curves.

Influence of Prior Plastic Extension on Entire Diagram Representing Technical Cohesive Strength of Metals

A complete picture of the influence of plastic extension on the technical cohesive strength of a metal comprises a series of curves, each representing the influence of plastic extension on the technical cohesion limit corresponding to a specific value of S_2/S_1. Consideration will now be given to the influence of *prior* plastic extension on such a series and on the locus of fractures.

In diagram A of Fig. 12 are curves representing the influence of plastic extension on various technical cohesion limits of a ductile steel. This diagram, derived from data presented by Kuntze,[18] is essentially the same as diagram A of Fig. 3 of the previous paper. The relatively low initial value of T_1 and the form of the locus of fractures (L) indicate that this metal had received practically no *prior* plastic deformation. Diagrams B to E of Fig. 12 do not represent additional experimental data, but are derived solely from diagram A. They represent results that would be expected when the same metal has been plastically deformed the indicated amounts prior to the determination of these diagrams. In diagram B, for example, the ordinates at the *origins* of the T and F curves are the same as the ordinates of the corresponding curves in diagram A at 20 per cent decrease in sectional area. The course of each of the curves in diagram B is derived from the corresponding curve of diagram A by making the necessary adjustment of abscissas.

---

* Each curve of cohesion has been drawn so that its approach to the corresponding curve of flow stress is continuous.

Comparison of the five locus curves in Fig. 12 shows that *prior* plastic extension has little effect on the locus of fractures at P', but does elevate this curve at and near the origin. The greater the amount of prior plastic deformation, the greater is the elevation of the origin and of much of this curve. With sufficient prior plastic extension, the locus of fractures becomes nearly vertical (diagram E).*

From the ordinates at zero abscissa in each of the diagrams in Fig. 12, it would be possible to construct a curve of the type shown in Fig. 7. A comparison of such diagrams would give another picture of the influence of prior plastic extension on the technical cohesive strength. The comparison would show that the chief effect of the prior plastic extension is not on the form but on the size of a diagram of this type.

The influence of prior plastic extension on this type of diagram is illustrated in Fig. 13. These diagrams, although they are based on the corresponding diagrams of Fig. 8, are intended as merely qualitative pictures of the influence of prior plastic extension on the technical cohesive strength. Diagram A represents a very ductile steel and diagram B a steel whose inherent ductility is somewhat less, either because of prior plastic deformation or because of a higher carbon content. Curves T represent the initial cohesive strength of these steels, the strength prior to plastic deformation. Curves T' represent the cohesive strength of the metal in the most severely cold-worked state. Curve T', consequently is the uppermost of an infinite number of possible curves of the same type. Curve L represents the locus of fractures, whose complex form is due

to the simultaneous influence of the combination of principal stresses and the plastic deformation occurring between the yield stress and fracture. The locus of fractures is similar in form to the locus of fractures in Figs. 9 and 10A. Each curve traverses a maximum near the point designated T_1, each curve has a minimum at a point representing a value of about 0.2 for S_3/S_1, and each curve turns rapidly downward as it enters the field of negative values of S_3/S_1. In Fig. 13, however, the locus curve joins curve T', and thus does not become nearly vertical as does the locus curve in a diagram of the type shown in Figs. 9 and 10.

Through any point on the locus of fractures, it is possible to draw a curve, similar to curves T and T', to represent the corresponding technical cohesive strength of the metal. The greater the distance between such a curve and curve T, the greater is the amount of work-hardening represented by the intersection of the curve with the locus of fractures; the greater, therefore, is the work-hardening capacity under that combination of the principal stresses.

For the ductile steels represented in Fig. 13, the maximum ductility and work-hardening evidently can be obtained only by plastic deformation within the field of negative values of S_3/S_1. Such plastic deformation could be obtained by radial hydrostatic compression (with or without various amounts of axial tension) as in the previously described investigations made by Bridgman.[2-5] If the stresses be thus applied gradually, with a constant negative value of S_3/S_1, the point representing the stress system would move upward along the corresponding radiating line (Fig. 13). When the point rises above the curve representing the yield stresses (Fig. 13B), the point representing the technical cohesion limit moves upward from curve T, because of the influence of the plastic deformation. In such an experi-

* The locus curves in Fig. 12 are drawn in accordance with the assumption represented by the idealized locus curves (broken lines) in Fig. 10. It is not impossible, however, that these curves should be similar to the solid locus curves in Fig. 10. (See footnote on page 331.)

ment, however, the whole specimen cannot be work-hardened to the degree represented by the corresponding point on curve T'. When the stresses reach the values represented by the ultimate strength (Fig. 13), the specimen contracts locally and fractures. Only in the small region near the surface of fracture, therefore, would the degree of work-hardening correspond to a point on curve T'. By cold-drawing or by cold-rolling, however, the stresses are not applied to the whole specimen simultaneously, and are not distributed automatically. They are applied locally as the specimen is moved past the surfaces through which the stresses are applied. An entire specimen thus may be work-hardened far beyond the "ultimate strength," and the technical cohesive strength may thus be raised to the upper limit (curve T').

Relation between Volume Stress and Maximum Shearing Stress at Yield and at Fracture

The influence of prior plastic extension, and of the combination of principal stresses, on the technical cohesive strength may be represented by diagrams of still another type. These diagrams show the relation between the volume stress and the maximum shearing stress at fracture and at yield.

Any stress system may be resolved into two components, a polarsymmetric stress that causes pure volume strain and a combination of pure shearing stresses, which causes distortion but no change of volume. The volume strain is $(S_1 + S_2 + S_3)/3K$. In this expression, K is the bulk-modulus of elasticity. The volume strain, therefore, is the same as if the stress system were replaced by a polar-symmetric stress equal to the average of the three principal stresses. This stress will be called the volume stress. When $S_2 = S_3$, the volume stress is $(S_1 + 2S_3)/3$. The maximum shearing stress is $(S_1 - S_3)/2$.

By a simple graphical method, it is possible to determine the volume stress and the maximum shearing stress corresponding to any point on one of the curves in Figs. 7, 8 and 13. This graphical method is based on the relationship represented by the dotted line G in each of these diagrams. Any point on line G represents a combination of principal stresses that would cause pure shear. The intersection of this line with a locus of fractures represents fracture under pure shear, and the intersection of the same line with line H represents the corresponding value of the volume stress (zero). Similarly correlated points, moreover, could be obtained by drawing any line parallel to line G. The intersection of such a line with a locus of fractures would represent a combination of the principal stresses at fracture, and the intersection with line H would represent the corresponding volume stress. The maximum shearing stress is proportional to the length of this line between the locus of fractures and line H, but is measured by one and one-half times the corresponding abscissa range. By the use of a series of lines drawn parallel to line G, therefore, it is possible to derive from any of the curves in Figs. 7 and 13 a curve of variation of the maximum shearing stress with the volume stress. Curves of this type are shown in Fig. 14.

The curve in diagram A of Fig. 14 is derived from the locus of fractures of steel R_D in Fig. 7; the two other diagrams in Fig. 14 are derived from those in Fig. 13. The abscissa of any point on a curve in Fig. 14 represents a value of the volume stress, and the ordinate represents the corresponding value of the shearing stress. For convenient correlation with the curves in Figs. 7 and 13, the sloping broken lines have been inserted in Fig. 14 to represent constant values of S_1.

First consideration, in a study of Fig. 14, should be given to the curve representing a brittle steel (diagram A), because this curve is unaffected by plastic deformation. With decrease of the volume stress below the value corresponding to the disruptive stress (T_1), the shearing stress rises from zero. The rise is at a decreasing rate, and is nearly all completed between T_1 and T_0. A curve representing yield of this brittle steel would almost coincide with the curve representing fracture. The curve representing yield of a ductile metal (Fig. 14B), moreover, is similar in form.*

The diagrams representing ductile steels in Fig. 14 are similar in form to the corresponding diagrams in Fig. 13. With decrease in S_3/S_1 below the value corresponding to T_1, the locus of fractures departs from curve T and approaches curve T' (appendix B). The most rapid departure from curve T, in Fig. 14 as in Fig. 13, is in the region near the boundary between the fields of positive and negative values of S_3/S_1. The locus of fractures in Fig. 14, however, has no minimum; the shearing stress rises continuously† with decrease in the volume stress (with decrease in S_3/S_1). The variation of the work-hardening capacity with the volume stress (with S_3/S_1) evidently is better represented by a curve of variation of the maximum shearing stress (Fig. 14) than

by a curve of variation of the greatest principal stress (Fig. 13).

Other Variables Having Differential Effect on Curves of Flow Stress and Cohesion

Any variable, other than S_3/S_1, that has a differential effect on the curves of flow stress and cohesion would influence an entire diagram such as those in Figs. 9 and 10. A variable that tends to raise a curve of flow stress more than the corresponding curve of cohesion would tend to move the entire locus of fractures to the left. Such a differential effect is produced by a fall of temperature or by an increase in the velocity of deformation. The differential effect accounts for the great influence of temperature on the impact resistance of steels. Velocity of deformation, according to prevalent views, has no appreciable effect on the technical cohesion limit; increase in the velocity of deformation, however, tends to increase the flow stress. The acuteness of the angle between the corresponding curves of flow stress and cohesion (Fig. 11) accounts for the fact that even a very slight differential influence of velocity of deformation may greatly affect the ductility and total work.

Fatigue fracture of a metal begins when the local plastic deformation is sufficient to raise the local yield stress to equality with the corresponding cohesion limit. The local plastic deformation at a fatigue fracture, like the plastic deformation at an ordinary tensile fracture, depends on the combination of principal stresses, the temperature, and the velocity of deformation. The fact that a brittle fracture may be obtained by fatigue of a ductile metal is more readily explainable with reference to a pair of curves intersecting at a small angle (Fig. 11) than with reference to the prevalent views of the relation between the curves of flow stress and cohesion.

---

* The tangent to the curve in the upper diagram of Fig. 14 was constructed on the assumption that the tangent to the corresponding curve in Fig. 7 becomes horizontal at T_1. If it does not become horizontal (see p. 317), the slope of the tangent in Fig. 14 should be slightly less. As the volume stress does not reach a maximum (in the mathematical sense) at T_1 but is still increasing rapidly, it is not surprising to find that the tangent to the corresponding curve in Fig. 14 is far from vertical.

† The rise of the shearing stress would be continuous even if the curve in diagram B of Fig. 14 were derived from the distorted curve of fractures in Fig. 8B. This is revealed by a comparison of the lengths of the dotted lines in Fig. 8B between the curve of fractures and line H.

TECHNICAL COHESIVE STRENGTH OF BRITTLE METAL WHEN ANY TWO OF PRINCIPAL STRESSES ARE EQUAL

In the previous sections, attention has been confined to stress combinations with the least two principal stresses equal to ($S_2 = S_3 < S_1$). The view will now be broadened to include stress combinations with the greatest two principal stresses equal ($S_2 = S_1 > S_3$). (Typical stress combinations of this kind are illustrated in Fig. 3.) Fig. 15 represents the complete two-dimensional view of the influence of the combination of principal stresses when any two of the principal stresses are equal. This figure is of the same type that is shown in Fig. 7, and curve A of Fig. 15 is identical with curve R_D of Fig. 7. This curve represents the influence of the combination of principal stresses when S_2 is kept equal to S_3. Curves R, R' and R'' represent three assumptions regarding the influence of the combination of principal stresses when S_2 is kept equal to S_1. For curve A, values of S_1 are represented by ordinates; for curves R, R' and R'', values of S_1 evidently are represented by abscissas.

Point T_R on each curve represents an assumption as to rupture under radial tension (Fig. 3A). Point T_C represents rupture under unidirectional compression. To the right of T_R, each curve represents stress systems of the type shown in Fig. 3B; between T_R and T_C, each curve represents stress systems of the type shown in Fig. 3C; to the left of T_C, each curve represents stress systems of the type shown in Fig. 3D.

The correct quantitative relation between curve A and the corresponding curve on the opposite side of line H is not known. Bridgman[5] says that the unidirectional compressive stress (T_C) at fracture is considerably greater than the compressive stress corresponding to T_{C2}. There is much evidence, moreover, that the stress is considerably greater at rupture under

unidirectional compression (T_C) than at rupture under unidirectional tension, (T_0). In constructing a curve to represent the influence of the combination of principal stresses when S_2 is equal to S_1, therefore, it is necessary to make an assumption as to the relation between this curve and curve A. Curves R, R' and R'' are based on three different assumptions with regard to this relationship. It has been found most convenient to express this relationship in terms of the shearing stresses at rupture.[6]

Line G in Fig. 15 is the locus of all points representing pure shearing stress. The intersection of G with a curve of the diagram represents fracture under pure shear, and the intersection with line H represents (by its coordinates) the corresponding value of the volume stress (p. 323). The distance along G between the curve and H is proportional to the maximum shearing stress. Other correlated values of the volume stress and the maximum shearing stress at fracture may be obtained from the broken lines parallel to G. Curves R, R' and R'' represent three assumptions as to the ratio between the maximum shearing stress (Q_R) when S_2 is equal to S_1 and the maximum shearing stress (Q_A) when S_2 is equal to S_3. For each curve, Q_R/Q_A is assumed to be invariant with the volume stress (S_v). The values of Q_R/Q_A for curves R, R' and R'' are 2.0, 1.5, and 1.0, respectively. Although Q_R/Q_A possibly is not invariant, the assumption that it is invariant will not invalidate the qualitative picture of the influence of the combination of principal stresses on the technical cohesion limit.

Curves R, R' and R'', therefore, have been so drawn that the distances of the curves from H (parallel to G) are 2.0, 1.5, and 1.0 times as great as the corresponding distances from H to A. The correct value for Q_R/Q_A probably is not greater than 2.0 nor less than about 1.5. When Q_R/Q_A is 2.0 (Fig. 15), T_C/T_{C2} is also 2.0. The assumption that Q_R/Q_A is 2.0 (as shown

on pages 328 to 330) leads to the simplest form of the derived three-dimensional diagram.

THREE-DIMENSIONAL DIAGRAMS REPRESENTING TECHNICAL COHESIVE STRENGTH OF BRITTLE METAL

Three-dimensional Diagram with Coordinates Representing Principal Stresses

Removal of the restriction that at least two of the principal stresses are equal makes it necessary to represent the technical cohesive strength of a metal by a three-dimensional diagram. A complete three-dimensional diagram (with rectangular coordinates) has three equivalent, mutually perpendicular, axes of unidirectional stress, three equivalent planes representing zero value of one of the principal stresses, and three equivalent planes (120° apart) representing stress combinations with two of the principal stresses equal. The surface of the diagram represents all possible combinations of the principal stresses at the technical cohesion limit; there are generally six equivalent points for any stress combination. The locus of polarsymmetric stresses makes equal angles with the directions of the three principal stresses and is symmetrically situated with reference to the three equivalent axes of unidirectional stress. As the locus of polarsymmetric stresses is an axis of symmetry of the three-dimensional diagram, the form of the diagram may be clearly revealed by two views: (1) a view of a section containing the axis of symmetry, and (2) a (top) view in the direction of this axis. A vertical section of such a diagram is represented by diagram B of Fig. 16 and a top view is represented by diagram C.

Diagram B is derived from diagram A, which is of the type shown in Fig. 15 and which contains reproductions of curves A and R of that figure. Diagrams A and

B, therefore, are two representations of the influence of stress combinations with two of the principal stresses equal. Diagram A is a two-dimensional representation of the relation between axial and radial stresses* at fracture; diagram B is a section of a three-dimensional diagram. In diagram A, as in Fig. 15, the locus of polarsymmetric stresses (H) makes an angle of 45° with the directions of axial and radial stresses. In a three-dimensional diagram, however, the angle between the locus of polarsymmetric stresses and the directions of each of the principal stresses is $\tan^{-1}\sqrt{2}$, about 54° 44'. In the sectional view shown in diagram B, consequently, the locus of polarsymmetric stresses (H_B) makes an angle of 54° 44' with the axis of ordinates, the line extending through T_0 and T_C.

The tilting of the locus of polarsymmetric stresses from the position represented by line H to the position represented by line H_B involves multiplication of the abscissas by $\sqrt{2}$, with no change of the corresponding ordinates. Any point on a curve of diagram B may be similarly derived from the corresponding point on a curve of diagram A. Ordinates in each diagram represent values of one of the principal stresses at fracture. Abscissas in diagram B, however, do not represent values of a principal stress. Two of the principal stresses are in directions making angles of 45° with the plane of diagram B. (This relation is illustrated in another sectional view, shown in Fig. 17, to be discussed later). Abscissas in diagram B, therefore, are $\sqrt{2}$ times the corresponding principal stresses.

Because of this relation between corresponding abscissas in diagrams A and

---

* The terms "axial stress" and "radial stress" in Fig. 16 apply only to diagram A, not to diagram B. In discussing the relation between A and B, coordinates in the direction designated as axial will be called ordinates, and coordinates in the direction designated as radial will be called abscissas.

B, the line representing pure shear is tilted from the position represented by line G to that represented by line G_B. Line G_B thus becomes perpendicular to the locus of polarsymmetric stresses H_B. Moreover, any other line representing constant volume stress, such as the lines parallel to G in Fig. 15, would become *perpendicular to* H_B, the axis of symmetry of the three-dimensional diagram. Perpendicular distances between H_B and curves A_B and R_B, therefore, are proportional to the corresponding values of the maximum shearing stress. The measure of the shearing stress, however, is $\frac{1}{4}\sqrt{6}$ times the perpendicular distance (in terms of the ordinate scale used for diagram B).

In a three-dimensional diagram, there are three sections representing stress combinations with at least two of the principal stresses equal. These sections pass through the axis of symmetry and are 120° apart. In the top view (diagram C), therefore, these sections appear as three lines radiating from the axis of symmetry. These lines are cut by contour lines, each corresponding to the indicated value of the volume stress. For a constant volume stress, three pairs of points may be established on a contour of diagram C, each pair corresponding to a position of the vertical section (diagram B). The distances from the axis to the points of each pair are equal to the corresponding perpendicular distances from H_B to curves A_B and R_B in diagram B. The distribution of the six points on a contour is such as to establish approximately the form of the entire contour. As the six points are at the vertices and the middles of the sides of an equilateral triangle, the simplest and most plausible assumption is that the entire contour is an equilateral triangle (when Q_R/Q_A is 2.0).

The number adjacent to each contour in diagram C indicates the corresponding value of the volume stress, which is indicated also on line H_B of diagram B. The size of the triangular cross section

of the three-dimensional diagram decreases with increase in the volume stress; the diagram thus tapers nonlinearly to the point (T_1) representing the disruptive stress. All points derived from curve A_B of diagram B are on the sloping sides of the three-dimensional diagram, on the radial lines designated $S_2 = S_3$. These points represent fracture when the relative extension is in only one direction and the fracture is axial. Two such stress systems are represented by the indicated points (diagram C) derived from T_0 and T_{C2} of diagram B. All points derived from curve R_B are on the sloping edges of the three-dimensional diagram. These points represent fracture when $S_2 = S_1$; that is, when the relative extension is equal in two directions (uniform relative radial extension) and the fracture is of the "rending" type. Two such stress systems are represented by the indicated points (diagram C) derived from T_R and T_C of diagram B. The sharp edges of the diagram evidently imply that the rending type of fracture is sensitive to slight variations of the intermediate principal stress (S_2).

Fig. 17 represents the stress combinations at fracture when one of the principal stresses is zero. The section here shown, therefore, is one of three identical sections, each including two of the axes of unidirectional stress. One of these sections is perpendicular to the plane of diagram B of Fig. 16, and passes through the axis of abscissas, the line extending through T_{C2} and T_R.* This line of intersection is represented by the broken line in Fig. 17. Attention will now be confined to the three-cornered figure representing fracture; the oval figure representing yield will be considered later (see pp. 332 to 333). The diagram for fracture differs in one respect from a diagram presented by Bridgman.[5]

---

* The other two principal planes make angles of 45° with the plane of diagram B and intersect this diagram at the line extending through T_0 and T_C.

Bridgman's diagram has corners at T_C as sharp as in Fig. 17, but the boundary is curved continuously at T_R. The discontinuity at T_C in Bridgman's diagram is based on reasoning as to the effect of superposing either a slight tensile or a slight compressive stress perpendicular to the direction of the previously unidirectional compressive stress. The latter stress, according to this reasoning, would be lowered by either of such superposed stresses. Similar reasoning, however, would suggest a discontinuity at T_R (and also at T_1 in Fig. 16B). As shown in Fig. 16C, moreover, both T_R and T_C are on the sharp edges of the three-dimensional diagram. The available evidence, therefore, indicates that the diagram in Fig. 17, like that in Fig. 16C, is three-cornered.

A three-dimensional diagram based on the assumption that Q_R/Q_A is 1.5 would be derived from curves A and R' of Fig. 15, by using the method that was used in deriving diagram B from diagram A of Fig. 16. The top view of such a diagram is shown in Fig. 18A. In each contour line of this figure, the radial distance from the axis of symmetry to the middle of a side is the same as in the corresponding contour line of Fig. 16C, but the radial distance to a vertex is three-fourths as great as in Fig. 16C. In view of the theoretical evidence (mentioned in connection with Fig. 17) that the boundary has vertices at points representing stress combinations with S_2 equal to S_1, the boundaries in Fig. 18A have been drawn with such vertices. This diagram, therefore, differs from diagram C of Fig. 16 only in the curvature of the sides and the sharpness of the vertices. The qualitative significance of each diagram is the same.

If Q_R/Q_A were 1.0, the three-dimensional diagram would be derived from curves A and R'' of Fig. 15 and the contours would be circles. Such a diagram would be identical in form with the three-dimensional diagram representing yield (p. 333). It

is improbable that the technical cohesive strength of any metal would be represented by a diagram of this form.

Stresses Represented by Contour Line of Three-dimensional Diagram

Consideration must now be given to the stresses represented by a point on a contour of the three-dimensional diagram. When the point is either at a vertex or at the middle of a side of a contour, two of the principal stresses are equal, and all three stresses may be estimated in terms of the radial distance from the point to the axis of symmetry ($S_1 - S_3$ is measured by $\frac{1}{2}\sqrt{6}$ times the radial distance). When the point under consideration is neither at the vertex nor at the middle of the side of a contour, however, S_2 has a value intermediate between S_1 and S_3, and the stresses generally cannot be expressed in terms of a single distance, but may be estimated in terms of two distances measured parallel to coordinate lines such as those shown in Figs. 16C and 18A. This use of the coordinate lines is based on the stress relationship illustrated by diagram B of Fig. 18.

In this diagram, the equilateral triangle with vertices M represents a contour of a three-dimensional diagram ($Q_R/Q_A = 2.0$) with the axis of symmetry at O. The rest of the surface of the three-dimensional diagram, however, is not shown, but has been replaced by three sides of a cube with a corner at O; the contour thus is in an octahedral plane of this cube. The three axes of unidirectional stress are assumed to be perpendicular to the sides of the cube and to intersect these sides at points A. The broken lines extending through points A parallel to the edges of the cube, therefore, are intersections of the sides of the cube with the principal planes passing through the (invisible) origin of stress coordinates. Each of the three sides of the cube, consequently, represents the same constant value of S_1.

Six points on a contour line generally are equivalent. This is illustrated by points P in Fig. 18B. When S_2 is equal to either S_3 or S_1, however, there are only three equivalent points. The three principal stresses corresponding to point P evidently are represented by the lengths of the indicated lines. In the absence of a knowledge of S_1 (or of one of the other principal stresses), the three principal stresses could not be determined directly from the position of P on the contour line, but the differences between the three principal stresses could be determined. The stress differences $S_1 - S_3$ and $S_1 - S_2$ are indicated in the diagram; evidently they are represented by the lengths of lines PC and PB, respectively (along the cube surface). The stress difference $S_2 - S_3$ is represented by the length of the line PD.* These principal stress differences are twice the corresponding shearing stresses.

The significance of the distances PC, PB and PD would be unchanged if the contour were actually curved as in Fig. 18A. Six equivalent points on such a contour would still determine an imaginary triangular section, and this section (together with the volume stress) would determine a cube such as that represented in Fig. 18B. By means of coordinate lines of the type shown in Fig. 16C and 18A, therefore, it is possible to estimate the three principal stress differences corresponding to any point on a contour line.† (The indicated coordinate scales in these two diagrams represent stress differences, not shearing stresses.)

When the volume stress corresponding to a contour line is known, an estimate can be made of the three principal stresses corresponding to any point on the contour.

* The projections of lines PB, PC and PD on the octahedral plane are proportional to the lengths of these lines on the cube side. The ratio of a projection to a line on the cube side is $\sqrt{\frac{2}{3}}$.

† Only two of these stress differences are independent.

This calculation involves the use of three simultaneous equations:

$$S_1 + S_2 + S_3 = 3S_v$$
$$S_1 - S_3 = a$$
$$S_1 - S_2 = b$$

The quantities a and b are measured by the lengths of the lines PC and PB, and S_v represents the volume stress.

Relation between Volume Stress and Greatest Principal Stress at Fracture

When a contour is triangular, it represents not only a constant volume stress but also a constant value of S_1 (Fig. 18B). When a contour has curved sides (Fig. 18A), however, it represents a variable value of S_1. At the middles of the sides of a curved contour, S_1 is at a maximum; at the corners of the contour, S_1 is at a minimum.

The variation of S_1 as S_2 increases from equality with S_3 to equality with S_1 is represented qualitatively by the diagrams in Fig. 19. Diagram A of this figure is derived from Fig. 16C, and diagram B is derived from Fig. 18A. Each of the closed curves in Fig. 19 is derived from one of the contour lines in either Fig. 16C or Fig. 18A; it represents the indicated value of the volume stress S_v. Radial distances represent values of $S_1 - S_v$. The three radiating lines 120° apart in each diagram of Fig. 19 represent stress combinations with S_2 equal to S_1; points 60° from these radiating lines represent stress combinations with S_2 equal to S_3.

When the contour lines in the three-dimensional diagram are triangles (Fig. 16C), the curves in the derived diagram (Fig. 19A) are circles. When the contour lines in the three-dimensional diagram are curved (Fig. 18A), the curves in the derived diagram (Fig. 19B) are at variable radial distance from the axis of symmetry. Each curve thus shows the variation of $S_1 - S_v$ as S_2 increases from equality

with S_3 to equality with S_1. As each curve represents a constant value of S_v, it shows qualitatively the variation of S_1. No quantitative significance need be given to the angle of rotation in the diagrams of Fig. 19.

If the three-dimensional diagram has triangular contours (Fig. 16C), therefore, the criterion for technical cohesive strength can be expressed in terms of only two variables—the volume stress and the greatest principal stress. If the three-dimensional diagram has curved contours (Fig. 18A), the criterion for fracture cannot be expressed in terms of only two variables. According to prevalent views, the three-dimensional diagram representing technical cohesive strength consists of three sides of a cube intersecting at a corner, and the criterion for fracture can be expressed in terms of only one variable, the greatest principal stress.[24]

THREE-DIMENSIONAL DIAGRAMS REPRESENTING TECHNICAL COHESIVE STRENGTH AND YIELD STRENGTH OF DUCTILE METAL

Three-dimensional Diagram Representing Influence of Combination of Principal Stresses on Technical Cohesion Limit of Ductile Steel

A three-dimensional diagram representing the initial technical cohesive strength of a ductile metal probably is similar in form to the diagram representing the technical cohesive strength of a brittle metal. Except at the point representing the disruptive stress (T_1), however, a diagram representing the technical cohesive strength of a ductile metal is outside the diagram representing yield, and thus is not a locus of fractures. Any stress combination except polarsymmetric stress, if of sufficient magnitude, would cause plastic deformation, and thus would increase the *size* of the three-dimensional diagram representing the technical cohesive strength. This relationship has been dis-

cussed in connection with the two-dimensional diagrams in Fig. 13. In each of those diagrams, however, the field below the locus of polarsymmetric stresses (H) has been omitted. Consideration will now be given to a complete two-dimensional diagram of this type and to the corresponding three-dimensional diagram.

Diagram A of Fig. 20 is a complete two-dimensional diagram of the same type as that shown in Fig. 13. Curves A and R of Fig. 20A represent the initial technical cohesive strength of a ductile steel. Curve R is so related to curve A that Q_R/Q_A is 2.0. Curves Y_A and Y_R represent the initial yield strength. They have been drawn equidistant from H, distances being measured in a direction parallel to the locus of pure shearing stresses (G). For these curves, therefore, Q_R/Q_A is 1.0. Evidence in support of this ratio will be discussed later (p. 332). That the ratio is at least approximately correct is shown by the fact that yield stresses in tension and compression generally are the same. For reasons previously given, the diagrams for initial yield strength and technical cohesive strength are drawn so as to coincide at the point representing the disruptive stress (T_1).

When the initial yield stress is exceeded (under any stress combination), the plastic deformation increases both the yield strength and the technical cohesive strength, and thus increases the size of the corresponding diagrams. The two curves representing yield strength and the two curves representing the technical cohesive strength, consequently, would move outward from their initial positions, and the point representing the disruptive stress would move upward along H (Fig. 20A). The increase in size of the diagram representing yield, however, would be more rapid than the increase of the diagram representing the technical cohesive strength. If S_2 be kept equal to S_3, continued plastic deformation of most metals

eventually exhausts the ductility, even if S_3/S_1 has a high negative value as in the cold-drawing or cold-rolling of rod or wire. The diagram representing yield then makes contact with the diagram representing the technical cohesive strength, and both diagrams have reached their maximum size under that stress combination. The technical cohesive strength of the metal in that state is represented in Fig. 20A by curves A' and R'.

The locus of fractures (L) joins curve A', and continues downward along this curve.* The cohesive strength represented by curve A' cannot be reached (because of prior fracture) when S_3/S_1 is greater than the value corresponding to the point of first contact of curve L with A'. The significance of curve L has already been discussed in connection with Fig. 13.

For any point on curve L, there is a point on curve L_R representing the corresponding cohesion limit when S_2 is equal to S_1. The ratio of the distances of any two such correlated points from line H evidently is the same as the assumed ratio ($Q_R/Q_A = 2.0$) for any pair of correlated points on curves A and R or on curves A' and R'. Curve L_R is a locus of cohesion limits but is not a locus of fractures. This is illustrated by the relative positions of curves L_R and L_Y. Curve L_Y is a locus of yield stresses corresponding to curve L. Under the combination of stresses represented by any point on curve L, the yield stress has been raised to equality with the technical cohesion limit. Curve L, therefore, is a locus of both yield stresses and breaking stresses. For every point on curve L, consequently, there is a point (on the opposite side of line H) representing the

corresponding yield stress when S_2 is equal to S_1. Correlated points on curves L and L_Y are equidistant, in direction parallel to line G, from line H. Before the cohesion limit represented by any point on curve L_R (except point T_1) could be reached, the yield stress (represented by the corresponding point on curve L_Y) evidently would be exceeded, the metal would be plastically deformed, and both yield strength and cohesive strength would increase. An initially ductile metal that is at the point of fracture when S_2 is equal to S_3, therefore, would not be at the point of fracture if S_2 were increased to equality with S_1.

A complete top view of the three-dimensional diagram could be derived from diagram A, after first constructing a vertical section of the type of diagram B of Fig. 16. Because the complete top view would be too complex, however, such a view has not been constructed, but a cross section of the three-dimensional diagram, on a reduced scale, is shown in Fig. 20B. The section here shown is at a volume stress of minus 100,000 lb. per sq. in., the section represented by line E in diagram A.

The equilateral triangle T and the circle Y represent the initial technical cohesive strength and yield strength, respectively. The triangular form of the contour T is due to the assumption that Q_R/Q_A is 2.0, the same assumption that is made in Fig. 16C. Because curves Y_A and Y_R in diagram A of Fig. 20A are equidistant from line H (in direction parallel to line G), six derived points in diagram B are on the circumference of a circle. The simplest and most plausible assumption, therefore, is that the three-dimensional diagram representing the initial yield strength has circular contours. This assumption, moreover, is based on considerable experimental evidence.

With plastic deformation, both the circle and triangle increase in size. The

---

* The observed variation of the ductility with S_3/S_1 (Figs. 4, 5, 6 and 10) suggests that the first contact of the three-dimensional diagrams for yield and technical cohesive strength may be at a single point between T_0 and T_1. This relationship, however, may be due merely to the deformation gradients in the notched specimens.

rate of increase, however, is more rapid for the circle than for the triangle, and eventually contact is made at the three points representing equality between S_2 and S_3. The state of the metal then is represented by circle Y' and triangle T'. The metal is now at the point of fracture when S_2 is equal to S_3, but is not at the point of fracture when S_2 is greater than S_3; when S_2 is greater than S_3, the metal can be deformed plastically, and both the yield strength and cohesive strength can be increased. The circle representing yield continues to increase more rapidly than the triangle representing the technical cohesive strength, and the six points of contact move from the middles of the sides of the triangle toward the vertices.

The movement of the points of contact toward the vertices, however, is at a decreasing rate, because of the decrease in the rate of work-hardening of the metal with plastic deformation. When a metal is very ductile, therefore, the points of contact never reach, and may never get near, the vertices. A very ductile metal, consequently, does not fail by rupture when the volume stress is low and when S_2 is equal or nearly equal to S_1. Evidence for this may be found in the behavior of ductile metals under unidirectional compression. In such a test, the metal can be flattened out indefinitely with no sign of fracture, provided that the edge of the specimen is kept sufficiently smooth during the flattening. If the edge is allowed to become notched (especially with the root of the notch in the axial direction), the actual local stress combination may depart far enough from unidirectional compression to permit the formation and extension of cracks. Even when the inherent ductility is only slight, it is difficult to determine a definite point of fracture under unidirectional compression.

The reason for the practically unlimited deformability of a ductile metal under unidirectional compression is illustrated

qualitatively by the diagram in Fig. 21, which is of the same type as Fig. 11. In this diagram, ordinates represent values of $S_1 - S_3$ and abscissas represent effective extensions. Little quantitative significance, however, should be given to the scales of coordinates in this diagram.

Curves T_{C2} and F_{C2} represent the influence of plastic deformation on the technical cohesion limit and on the flow stress under radial compression ($S_2 = S_3$ and $S_1 = 0$). Before plastic deformation, as illustrated by the origins of these curves, the flow stress is considerably below the corresponding technical cohesion limit. With plastic deformation, both curves rise at a decreasing rate. The curve of flow stress, however, rises more rapidly than the curve of cohesion limits, and the curves eventually intersect at a point representing fracture.

Under unidirectional compression of the same metal ($S_2 = S_1 > S_3$), however, the relation between the curves of flow stress and cohesion would be very different from that represented by curves F_{C2} and T_{C2}. Although the curve of flow stress would be unchanged, the curve of technical cohesion would be much higher than curve T_{C2}. When Q_R/Q_A is 1.5, the variation of the technical cohesion limit would be represented by curve T_C. When Q_R/Q_A is 2.0, the curve of technical cohesion would be still higher. Because of the approach of curves F_{C2} and T_C to a nearly horizontal direction, curve F_{C2} probably never would intersect curve T_C, even if curve T_C were lowered considerably on the assumption that Q_R/Q_A is less than 1.5. When the metal is ductile, therefore the sharp edge of the three-dimensional diagram is a locus of technical cohesion limits, but is not a locus of actual failures by rupture.

Three-dimensional Diagram Representing Yield Strength

As indicated in diagrams A and B of Fig. 20, the three-dimensional diagram

representing yield has a circular cross section, and tapers nonlinearly to the point (T_1) representing the disruptive stress. The radius of the cross section thus decreases with increase in the volume stress. The significance of the radius may be understood by a reconsideration of Fig. 18B. The radial distance r from the axis of symmetry to point P in this figure is the length of the projection of line OP on the contour plane MMM. In discussing this diagram, a distinction must be made between the length of a line along a side of the cube and the length of its projection. This distinction will be made by enclosing in parentheses the letters representing projections.

It can be shown that r is related to the projections of the lines representing two of the principal stress differences according to the equation

$$r^2 = (PB)^2 + (PD)^2 + (PB)(PD)$$

As the ratio of any such projection to the corresponding line on the surface of the cube is $\sqrt{2/3}$, the equation may be written

$$\tfrac{3}{2}r^2 = (S_1 - S_2)^2 + (S_2 - S_3)^2 + (S_1 - S_2)(S_2 - S_3)$$

This may be changed to

$$3r^2 = (S_1 - S_2)^2 + (S_2 - S_3)^2 + (S_1 - S_3)^2$$

The relationship represented by this equation evidently applies not only to the radial distance of point P in Fig. 18B but also to the radial distance of a point on any contour line, such as a circular contour representing yield (Fig. 20B). A circular contour, consequently, represents a constant value of the sum of the squares of the three principal stress differences.

In this respect, therefore, the circular cross section of the three-dimensional diagram is in accordance with the von Mises,[22] Hencky,[6,7,8] Huber[9] theory of constant maximum shear energy, which has received support by Lode,[19] Nadai,[24]

Taylor and Quinney,[25] and other investigators. (The constancy of the maximum shear energy, however, probably should be viewed merely as a fortuitous consequence of the circularity of the cross section.) According to the prevalent view, however, the cross section is invariant with the volume stress; this implies that the three-dimensional diagram representing yield is a circular cylinder, whose axis is the locus of polarsymmetric stresses.[7,19] There is little doubt that the correct diagram has a circular cross section, and that it is nearly cylindrical except in the part representing triaxial tension. With increase in the volume stress, however, the cross section evidently contracts at an increasing rate until it vanishes at the point representing the disruptive stress (T_1).*

Some Speculations about Three-dimensional Diagram for Shearing Fracture, and about Criteria for Yield and Fracture

Under some stress combinations, it is possible for a metal to fracture at lower stresses than those represented by a point on one of the previously discussed three-dimensional diagrams. Such a fracture, however, is not by rupture but by shear. At rupture, the shearing stress is much greater, possibly 100 per cent greater, when S_2 is equal to S_1 than when S_2 is equal to S_3 (Fig. 16C). When S_2 is equal or nearly equal to S_1, therefore, a metal may fail by shearing fracture rather than by rupture, unless the resistance to shearing fracture is relatively high. A shearing fracture when S_2 is equal to S_1, consequently, does not imply that the three-cornered contour of the three-dimensional diagram representing rupture is incorrect, but merely implies that the corners of the contour are cut by the boundary of a diagram representing shearing fracture.

---

* Because of this contraction, the oblique section representing yield in Fig. 17 is not quite elliptical, as it would be if the three-dimensional diagram were a circular cylinder.

If the criterion for shearing fracture (at constant volume stress) is a constant value of the greatest principal shearing stress, the three-dimensional diagram representing resistance to shearing fracture would have a regular hexagonal contour. Each contour would be similar in orientation to the regular hexagons formed by the coordinate lines in Fig. 20B. If, however, the criterion is the same for shearing fracture as for yield, the contour would be circular. In either case, each contour of the diagram for resistance to shearing fracture might intersect the corresponding contour of the diagram for technical cohesive strength at six points between the middles of the three sides and the three vertices. This relationship is illustrated qualitatively by contour W drawn as a regular hexagon in Fig. 20B.

When the two diagrams for any material are so related, the material would fail by rupture when S_2 is not too much greater than S_3, but would either fail by a shearing fracture, or not fail at all (because of growth of the diagram) when S_2 is nearly equal to S_1. For some materials, the diagram for resistance to shearing fracture probably is outside the diagram for technical cohesive strength. Such a material would fail only by rupture. The diagrams representing resistance to shearing fracture, technical cohesive strength, and yield strength, for any material, probably coincide at the disruptive stress (T_1).

An experimental investigation of a section of the three-dimensional diagram is discussed in Appendix C as an illustration of the difficulties involved and of the care that should be taken in planning the investigation and in drawing conclusions.

If the three-dimensional diagram representing the technical cohesive strength has a triangular contour, the criterion for rupture is a function of the volume stress and the greatest principal stress. The incorrectness of the prevalent view as to the criterion for rupture would then consist

only in neglect of the influence of the volume stress. The defect in the prevalent view thus may be similar to the defect in the prevalent view as to the criterion for yield. It is possible, however, that the sides of the contours of the diagram for technical cohesive strength are curved or become curved with increase in the volume stress. In that case, the criterion for rupture would be a function of more than two variables.

Bridgman[4,5] has made the interesting suggestion, attributed also to Born,[1] that rupture occurs at the limit of stability of the atomic grouping, and that this limit is reached long before the atoms are separated so far that the cohesive force is at a maximum. The existence of such a limit of stability, according to Bridgman, might account for the generally great discrepancy between the technically determined stresses at fracture and the theoretical cohesive forces. Possibly this suggestion could be extended to apply also to yield.

Although it has been found convenient in this paper to confine attention to the variation of the technical cohesion limit and yield point with the combination of principal stresses, there are certain advantages in viewing these limits as functions of the principal strains.

RELATION BETWEEN SOME INDICES OF STRENGTH OF BRITTLE MATERIALS AND FORM OF THREE-DIMENSIONAL DIAGRAM REPRESENTING TECHNICAL COHESIVE STRENGTH

The form of the three-dimensional diagram representing the technical cohesive strength of a brittle material could be determined approximately if information were available as to the values of T_0, T_G and T_{G2}. As illustrated in Fig. 15, a knowledge of the stress values represented by T_0 and T_{G2} would determine approximately the course of curve A between these two points, and would determine roughly the probable course of the curve between

T_0 and T_1. A knowledge of T_C and T_{C2} moreover, would determine approximately the ratio of Q_R to Q_A, and thus would determine with sufficient accuracy the relation between curve A and the curve of variation of the technical cohesion limit when S_2 is equal to S_1. When T_C/T_{C2} is 2.0, Q_R/Q_A is also 2.0. Even if T_C/T_{C2} is only 1.5, T_C/T_{C2} would be approximately equal to Q_R/Q_A. A knowledge of T_0, T_{C2} and T_C, consequently, could be used in establishing with considerable accuracy the entire three-dimensional diagram, although the accuracy would be considerably greater if T_R also were known.

At present, practically no quantitative information is available as to values of T_{C2} for brittle materials. When T_0 and T_C are known, however, little error probably would be involved in constructing the diagram on the assumption that T_C/T_{C2} is 2.0.

The fact that T_{C2}/T_0 is (arithmetically) greater than 1.0^5 implies that T_C/T_0 is greater than T_C/T_{C2} (Fig. 15). When T_C/T_{C2} is 2.0, therefore, T_C/T_0 is greater than 2.0. For steel, T_{C2}/T_0 probably is not much greater than 1.0, and hence T_C/T_0 is not much greater than 2.0. For some brittle materials, however, T_C/T_0 is much greater than 2.0. For cast iron, the ratio is more than 4.0. For glass, the ratio is said to range between 9 and 18. Although the correct values for glass may be somewhat less than these recorded values, there is no doubt that the ratio of T_C to T_0 is rather high. Such materials as cast iron and glass, moreover, differ in another important respect from steel; they have relatively low tensile strength. The ratio T_C/T_0 is higher and the tensile strength is lower for these materials than for steel.

That the association of low tensile strength with a high value of T_C/T_0 may be not uncommon is suggested by a study of the diagram for steel (Fig. 15). If the origin of coordinates be moved upward along line H to the position now representing a polarsymmetric stress of 200,000 lb. per sq. in., the ratio T_C/T_0 would become about 5, and T_0 and T_C would have approximately the values for cast iron. The ratio T_{C2}/T_0, moreover, would be nearly 3 and T_1/T_0 would be only about 1.16, whereas the corresponding ratios for steel are about 1.17 and 2.1 (Fig. 15). This relationship suggests that a high ratio of T_C to T_0 may generally be associated with a high ratio of T_{C2} to T_0 and a low ratio of T_1 to T_0.

The experimental investigation of the ratios needed for determining a three-dimensional diagram is not easy. Determination of T_C for a brittle material may not be possible because of failure by shearing fracture before a true value of T_C could be attained. Nevertheless, even the determination of the stress at shearing fracture would show that T_C has a higher value. Another reason for the difficulty in determining T_C is that the state of stress, which is represented by a point on the sharp edge of the three-dimensional diagram, is unstable. A slight departure from this state would cause failure at a much lower stress. For these reasons, experimentally determined values of T_C tend to be too low. Nevertheless, a thorough investigation of the relation between T_{C2}, T_C and T_0 for brittle materials probably would give qualitatively correct information about the forms of the corresponding diagram representing the technical cohesive strength. The greatest need is for more information about ratios of T_{C2} to T_0.

SUMMARY

1. The technical cohesive strength of a metal cannot be represented by a single stress value, but comprises an infinite number of stress values (cohesion limits) corresponding to the infinite number of possible combinations of the principal stresses.

2. Plastic deformation increases the technical cohesive strength continuously up to the point of fracture. The influence of plastic deformation on the cohesive strength cannot be represented by a single curve, but may be represented by a series of curves, each corresponding to a single value of S_3/S_1. Both the flow stress and the cohesion limit increase continuously with plastic deformation, but the flow stress increases more rapidly than the corresponding cohesion limit. Rupture occurs when the two curves intersect.

3. The three-dimensional diagram representing the technical cohesive strength of a metal has a three-cornered contour, in a plane perpendicular to the locus of polar-symmetric stresses, and tapers nonlinearly to a point. The three-dimensional diagram representing the yield strength has a circular contour and tapers nonlinearly to the same point. For a ductile metal, the diagram representing yield strength is inside the other diagram.

4. With plastic deformation, the diagram representing yield enlarges more rapidly than the other diagram. Eventually the diagram representing yield strength touches the sides of the diagram representing cohesive strength. Rupture then occurs if S_2 is equal to S_3. If S_2 is greater than S_3, rupture would not occur until after additional plastic deformation. If S_2 is equal to S_1, and if S_3/S_1 is algebraically small, there is no attainable limit to the plastic deformation that a very ductile metal will endure without rupture.

5. Some speculations are made about the form of the three-dimensional diagram representing resistance to shearing fracture, and its relation to the diagrams representing rupture and yield. Some speculations are also made about the criteria for fracture and yield.

6. There is need for determination of the values of T_C, T_{C2}, T_0 and T_R for various brittle materials. These values could be used to establish the forms of the three-dimensional diagrams representing technical cohesive strength. The information thus obtained would be applicable also to a study of the qualitative forms of the three-dimensional diagrams for ductile metals.

APPENDIX

A.—If the nearly linear variation of the breaking stress of the brittle steel R_D (indicated in Fig. 5) is correct, the curve of technical cohesion limits does not become horizontal at T_1. If S_1 and S_3 represent the stresses at any point on the straight graph for steel R_D (Fig. 5), and if this graph be viewed as the hypotenuse of a right triangle, the following equation is obtained, based on similarity of triangles:

$$(S_1 - T_0)/(T_1 - T_0) = S_3/S_1 \quad [5]$$

The tangent of slope at any point on the curve would be

$$dS_1/dS_3 = (T_1 - T_0)/(2S_1 - T_0) \quad [6]$$

When $S_1 = T_1$,

$$dS_1/dS_3 = (T_1 - T_0)/(2T_1 - T_0) \quad [7]$$

If T_1/T_0 be designated by n, Eq. 7 becomes

$$dS_1/dS_3 = (n - 1)/(2n - 1) \quad [8]$$

The tangent at T_1 evidently would not be horizontal unless n were 1.0. The tangent of slope at T_1 increases with increase in n. It is $\frac{1}{3}$ when n is 2, the approximate value for the steels represented in Fig. 7.

As illustrated by Fig. 6, however, the relation between S_1 and S_3/S_1 possibly is not exactly linear, and the final slope of the curve in a diagram of the type shown in Fig. 7 may be somewhat less than in accordance with Eq. 8. Nevertheless, there is some doubt that the slope finally becomes zero.

B.—The variation in the rapidity of the departure of the locus of fractures from curve T in Fig. 14 may be attributed to the influence of two oppositely varying

factors, one of which is the rate of divergence of curve T from the curve of yield stresses (Fig. 14B). This divergence probably is most rapid at first, and decreases with decrease in the volume stress (decrease of S_3/S_1). The other factor is associated with the slope of the curves of flow stress and cohesion in a diagram of the type shown in Fig. 10A, and with the angle between these curves at their intersection. With decrease of S_3/S_1, as shown in Fig. 10A, these curves become less steep and the angle between them becomes smaller. For the same differential lowering of the origins of the curves, therefore, the effect on the ductility increases as S_3/S_1 decreases. This factor evidently becomes dominant in the region of most rapid departure of the locus of fractures from curve T.

C.—Siebel and Maier[26] investigated the strength and ductility exhibited by thin-walled tubing of ductile steels and of brass under various combinations of longitudinal and circumferential tension, the circumferential stress being induced by internal hydrostatic pressure. They report that the ductility was at a minimum when the longitudinal and circumferential stresses were equal, and that the strength was generally no greater under this stress combination than under unidirectional tension. Their methods of estimating the ductility of these failed tubes, however, is not made clear. In the presence of circumferential tension, the tubes failed by local one-sided bulging followed by yawning fracture. The stress gradient and deformation gradient thus induced would make it difficult, if not impossible, to estimate the true stress and plastic deformation at fracture, and also would make the local stress combination different from the estimated combination.

Close scrutiny of their illustrations casts doubt on the view that the ductility was least when the longitudinal and circumferential stresses were equal. As would be expected, the ductility was less under pure circumferential tension than under pure longitudinal tension. Such a relationship is due not only to a difference in the properties of the metal when tested in the two directions, but also to the fact that essentially the ductility in the two directions was obtained with two different specimens, different in shape and in cross section. The investigation by Siebel and Maier[26] and a somewhat similar investigation by Siebel and Kopf[27] lead to some definite conclusions as to the relation between the longitudinal and circumferential strength and ductility of tubing, but give no conclusive evidence that the ductility is at a minimum when the longitudinal and circumferential stresses are equal. The several reasons advanced by these investigators to account for such a minimum will not stand close analysis. Moreover, there is no apparent reason for a smaller ductility when S_2 is equal to S_1 than when S_2 is equal to S_3.

Reffrences

1. M. Born and M. Goppert-Mayer: Handbuch der Physik, 24, Ed. 2, pt. 2, 623–790.
2. P. W. Bridgman: Breaking Tests under Hydrostatic Pressure, and Conditions of Rupture. *Phil. Mag.* (July 1912) 24, 63–80.
3. P. W. Bridgman: Theoretically Interesting Aspects of High-pressure Phenomena. *Reviews of Modern Physics* (1935) 7, 1–35.
4. P. W. Bridgman: Reflections on Rupture. *Jnl. Applied Physics* (1938) 9, 517–528.
5. P. W. Bridgman: Considerations on Rupture under Triaxial Stress. *Mech. Eng.* (Feb. 1939) 61, 107–111.
6. H. Hencky: Zur theorie plastischer Deformationen und der hierdurch im Material hervorgerufenen Nachspannungen. *Zisch. angew Math. und Mech.* (1924) 4, 323–334.
7. H. Hencky: Zur theorie plastischer Verformung und der hierdurch gerufenen Nebenspannungen. *Proc. Int. Cong. Applied Mech.*, Delft, 1924, 312–316.
8. H. Hencky: Über das Wesens der plastischer Verformung: *Zisch. Ver. deut. Ing.* (1925) 69, 695.
9. M. J. Huber: Discussion of ref. 7.
10. W. Kuntze: Der Bruch gekerbten Zugproben. *Archiv Eisenhüttenwesen* (1928–1929) 2, 109–111.
11. W. Kuntze: Fragen der technischen Kohäsion. *Zisch. Metallkunde* (1930) 22, 264–268.
12. W. Kuntze: Kerbzahigkeit und statische Kenziffern. *Mitt. Mat. Prüf. Anstalten* (1930) 14, 27–35.
13. W. Kuntze: Zur Deutung und Bewertung der Bruchdehnung bei Metallen. *Mitt. Mat. Prüf. Anstalten* (1930) 14, 61–71.
14. W. Kuntze: Zur Deutung und Bewertung der Bruchdehnung bei Metallen. *Zisch. Metallkunde* (1930) 22, 14–22.

15. W. Kuntze: Über die Kerbgefahr. *Mitt.* Mat. Prüf. Anstalten (1930) 14, 71–77.
16. W. Kuntze: Fragen der technischen Kohäsion. *Mitt.* Mat. Prüf. Anstalten (1930) 14, 85–91.
17. W. Kuntze: Struktur, Festigkeit, Stetigkeit. *Mitt.* Mat. Prüf. Anstalten (1930) 17, 48–52.
18. W. Kuntze: Kohäsionsfestigkeit. *Mitt.* Mat. Prüf. Anstalten (1932) 20, 1–61.
19. W. Lode: Der Einfluss der mittleren Hauptspannung auf das Fliessen der Metalle. *Forschungsarbeiten*, Ver. deut. Ing. (1928) 303.
20. P. Ludwik and R. Scheu: Über Kerbwirkugen bei Flusseisen. *Stahl und Eisen* (1923) 43, 999–1001.
21. D. J. McAdam, Jr.: The Technical Cohesive Strength of Metals. *Trans.* Amer. Soc. Mech. Engrs. (1941) 63; *Jnl. of Applied Mechanics* (Dec. 1941) 8, A-155-165.
22. R. von Mises: Mechanik der festen Körper im plastisch deformablen Zustand. Göttinger Nachrichten, 1913.
23. C. Mohr: Welche Umstände bedingen die Elastizitätsgrenze und den Bruch eines Materials. *Ztsch.* Ver. deut. Ing. (1900) 44, 1524–1530, 1572–1577.
24. A Nadai: Theories of Strength. *Trans.* Amer. Soc. Mech. Engrs. (1930) 55, APM 55-15, 111–129.
25. F. E. Richart, A. Bromttzaeg and R. L. Brown: Univ. Illinois Eng. Expt. Sta. *Bull.* 185 (1928).
26. E. Siebel and A. Maier: *Ztsch.* Ver. deut. Ing. (1933) 77, 1345–1349.
27. E. Siebel and E. Kopf: *Ztsch. Metallkunde* (1934) 26, 169–172.
28. G. I. Taylor and H. Quinney: The Plastic Distortion of Metals. *Phil. Trans.* Roy. Soc. (1930) 230-A, 323–362.
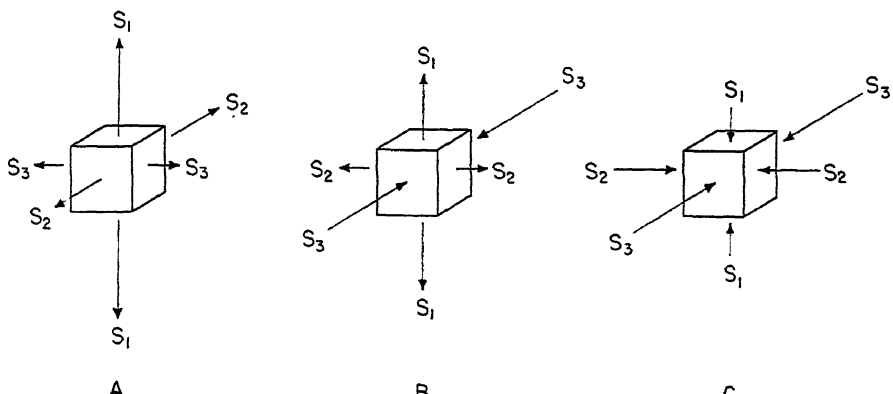
FIG. 1.—STRESS COMBINATIONS WITH NO TWO PRINCIPAL STRESSES EQUAL.
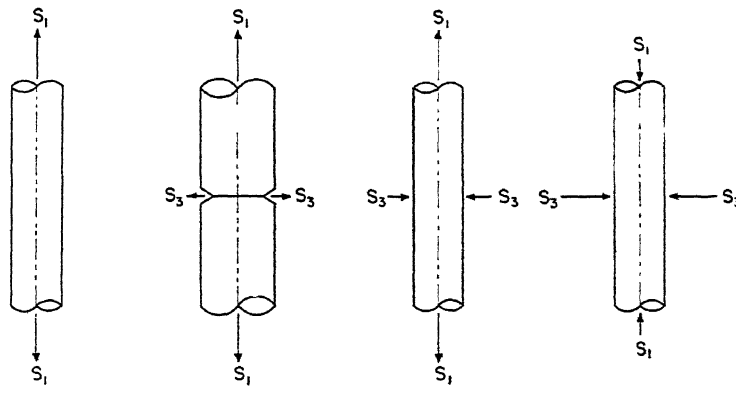
FIG. 2.—TYPICAL STRESS COMBINATIONS WITH S_2 EQUAL TO S_3 $(S_2 = S_3 < S_1)$.
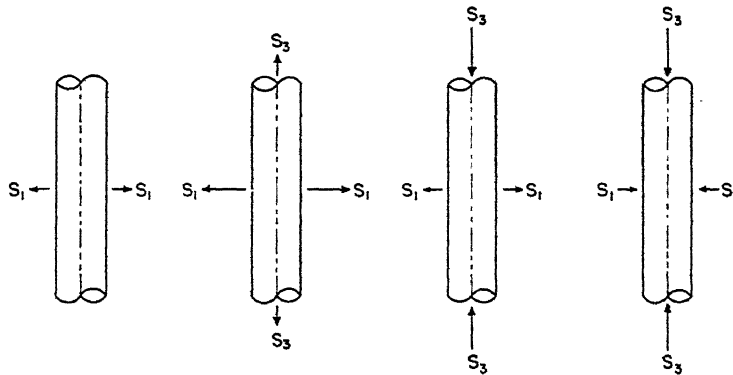
FIG. 3.—TYPICAL STRESS COMBINATIONS WITH S_3 EQUAL TO S_1 $(S_2 = S_1 > S_2)$.
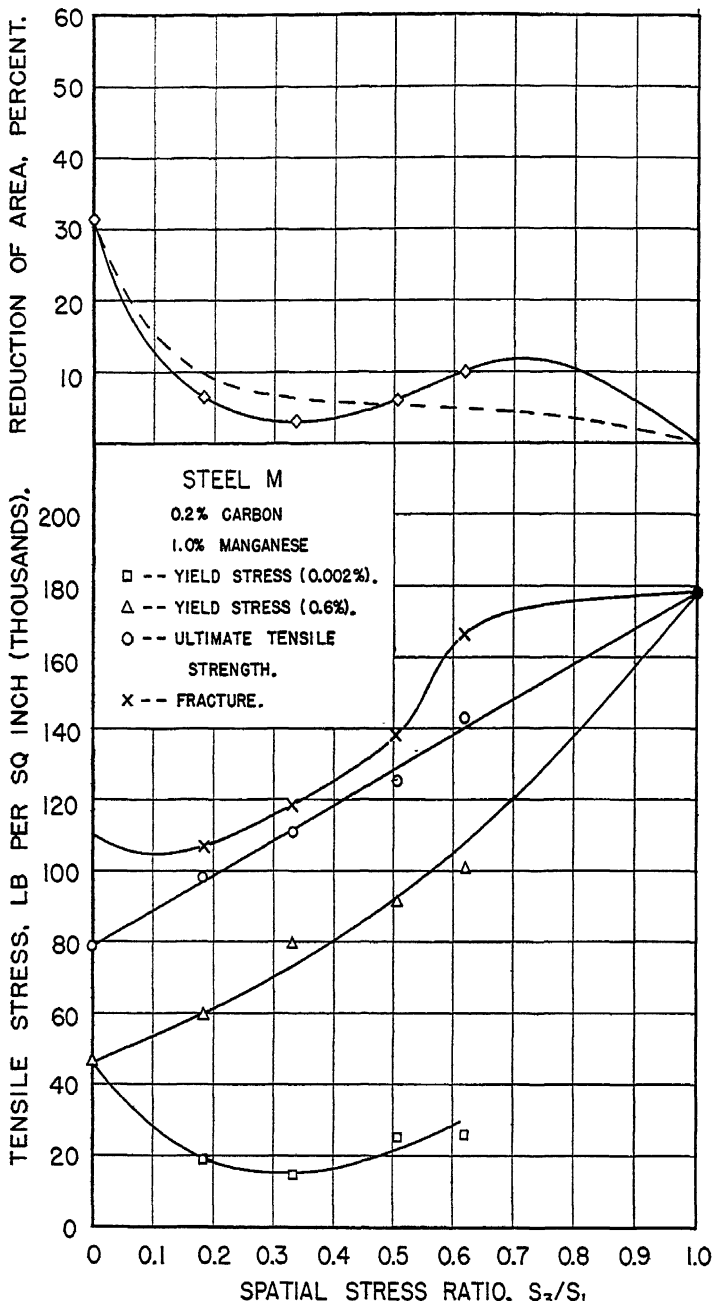
FIG. 4.—INFLUENCE OF SPATIAL STRESS RATIO S_3/S_1 ON ULTIMATE TENSILE STRENGTH, YIELD STRESS, BREAKING STRESS, AND DUCTILITY; LOW-CARBON STEEL.
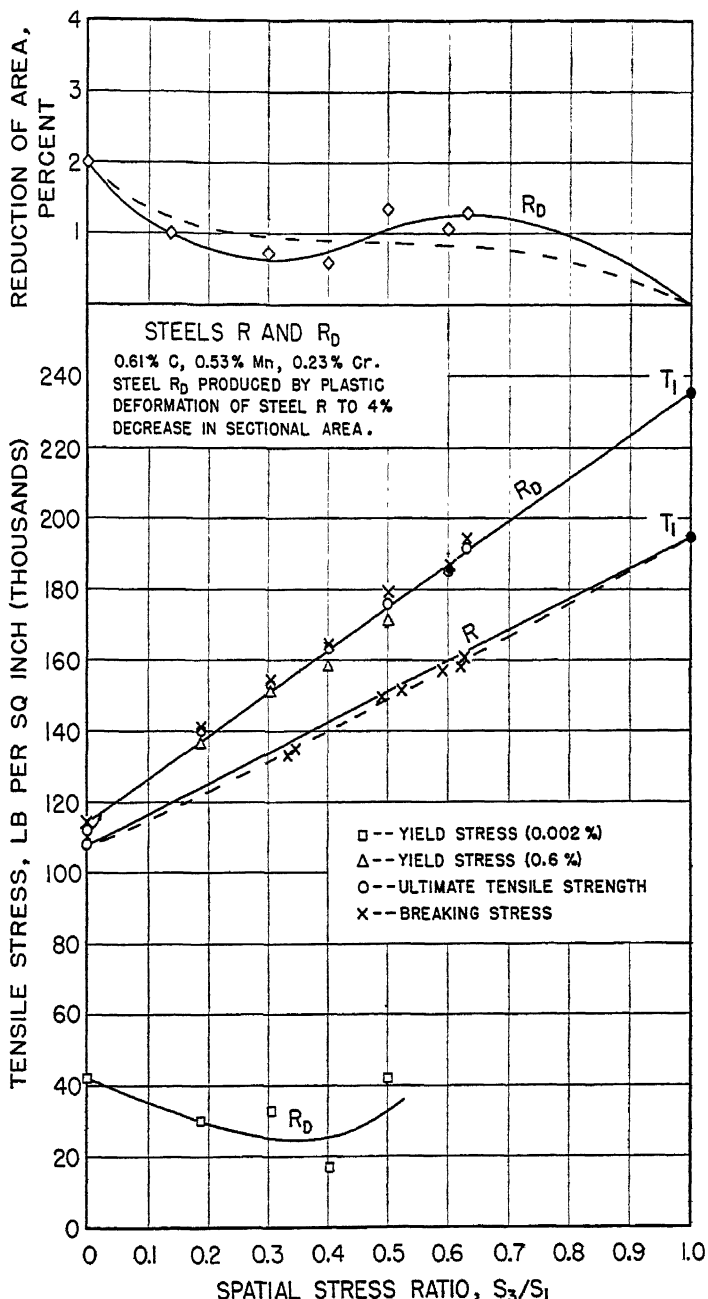
FIG. 5.—INFLUENCE OF SPATIAL STRESS RATIO S_3/S_1 ON ULTIMATE TENSILE STRENGTH, YIELD STRESS, BREAKING STRESS, AND DUCTILITY; HIGH-CARBON STEELS.
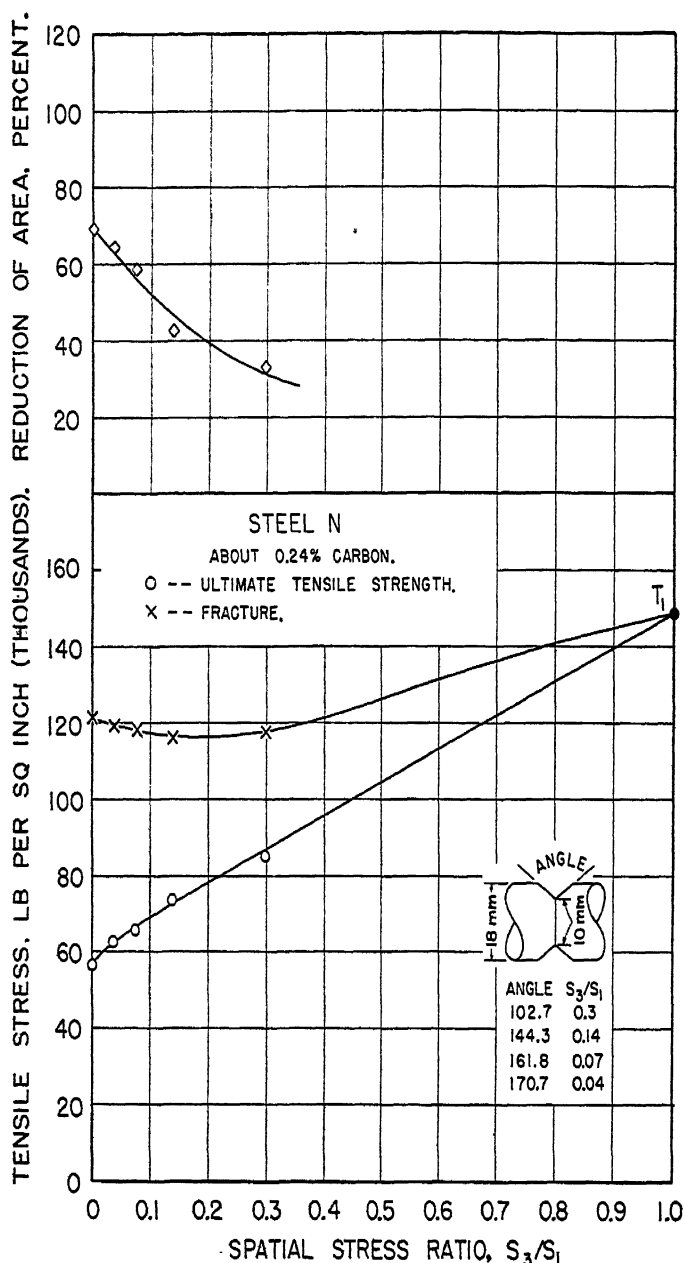
FIG. 6.—INFLUENCE OF SPATIAL STRESS RATIO S_3/S_1 ON YIELD STRESS, ULTIMATE TENSILE STRENGTH, BREAKING STRESS, AND DUCTILITY, LOW-CARBON STEEL.
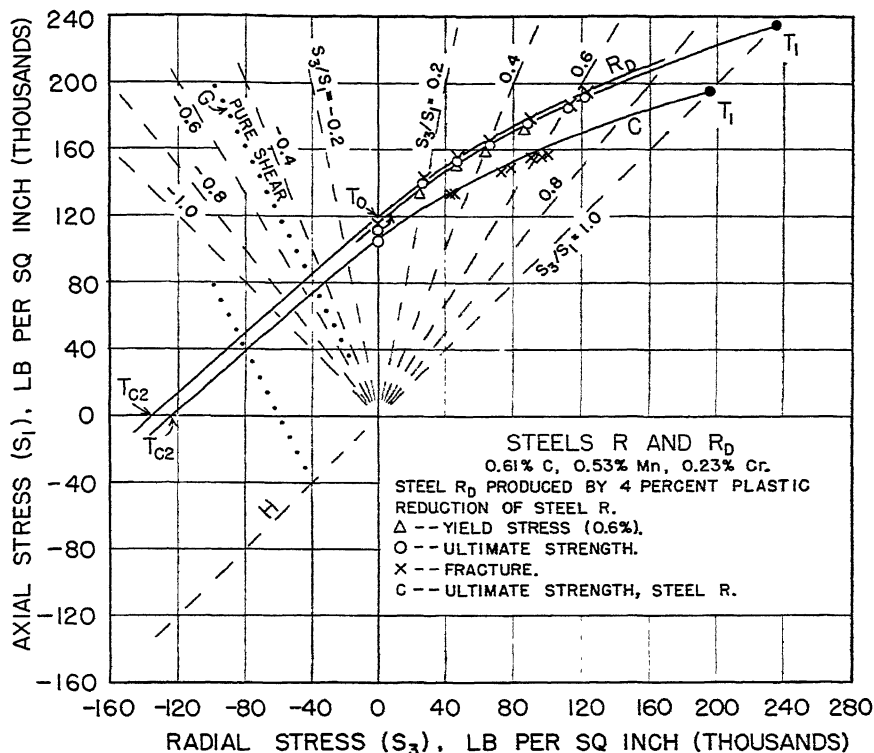
FIG. 7.—TWO-DIMENSIONAL DIAGRAMS REPRESENTING TECHNICAL COHESIVE STRENGTH, ULTIMATE STRENGTH, AND YIELD STRENGTH OF BRITTLE STEELS ($S_2 = S_3$).
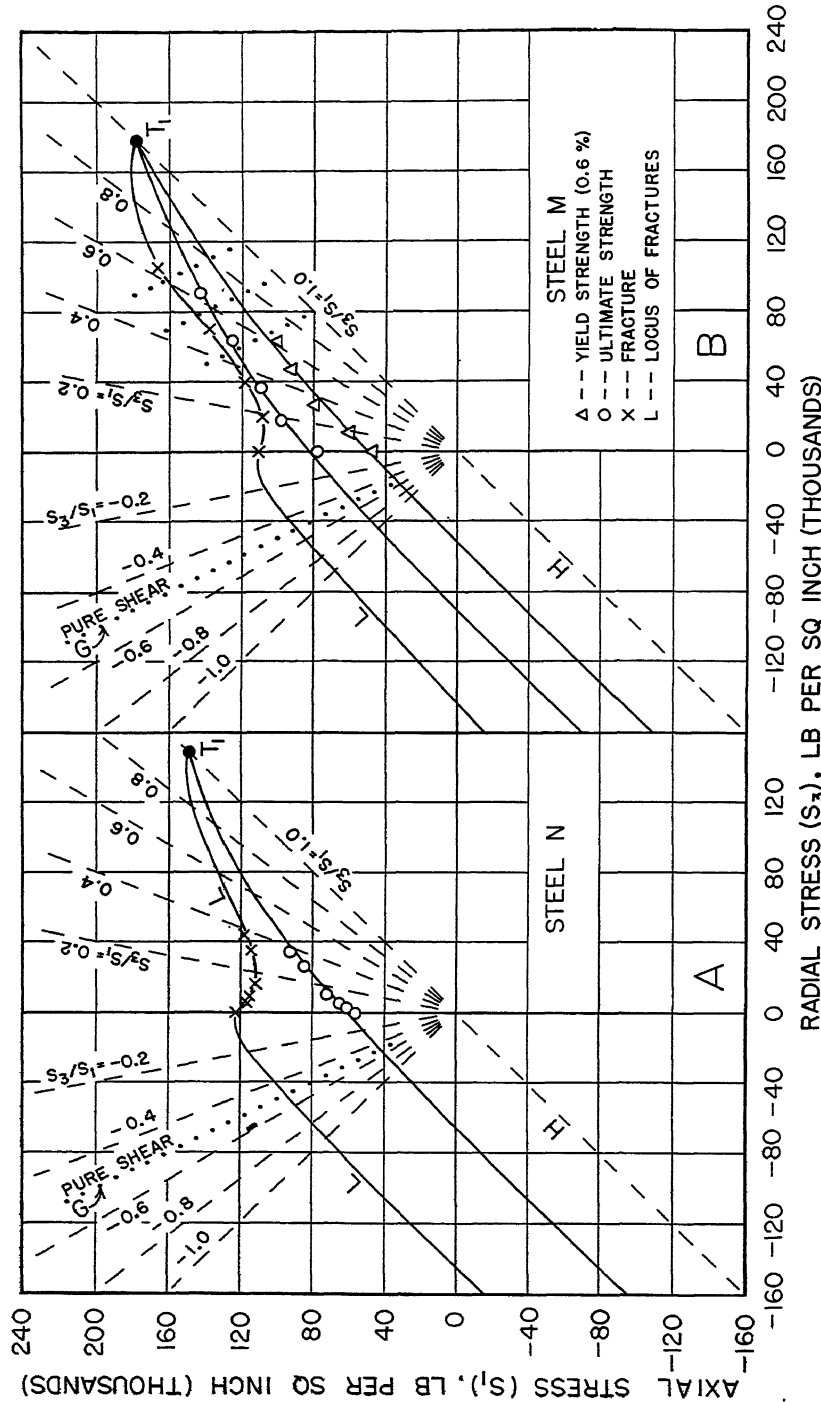
FIG. 8.—TWO-DIMENSIONAL DIAGRAMS REPRESENTING TECHNICAL COHESIVE STRENGTH, ULTIMATE STRENGTH, AND YIELD STRENGTH OF DUCTILE STEELS ($S_2 = S_3$).
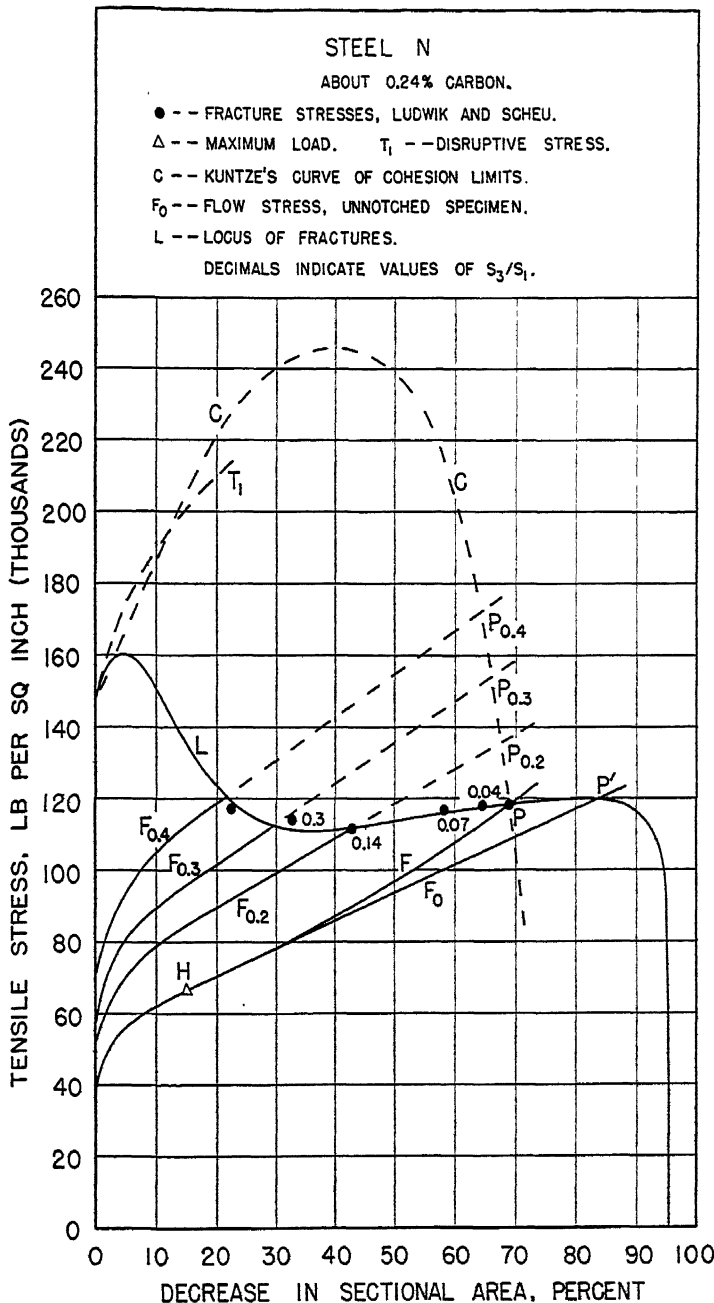
FIG. 9.—VARIATION OF TECHNICAL COHESION LIMIT WITH S_3/S_1 AND WITH PLASTIC DEFORMATION $(S_2 = S_3)$.
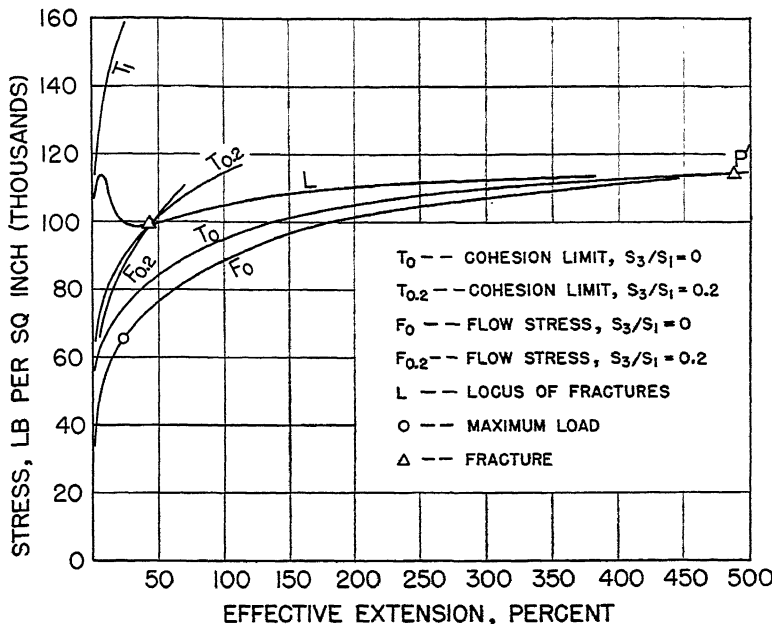
FIG. 11 —INFLUENCE OF PLASTIC EXTENSION ON TECHNICAL COHESIVE STRENGTH OF ANNEALED LOW-CARBON STEEL $(S_2 = S_3)$.
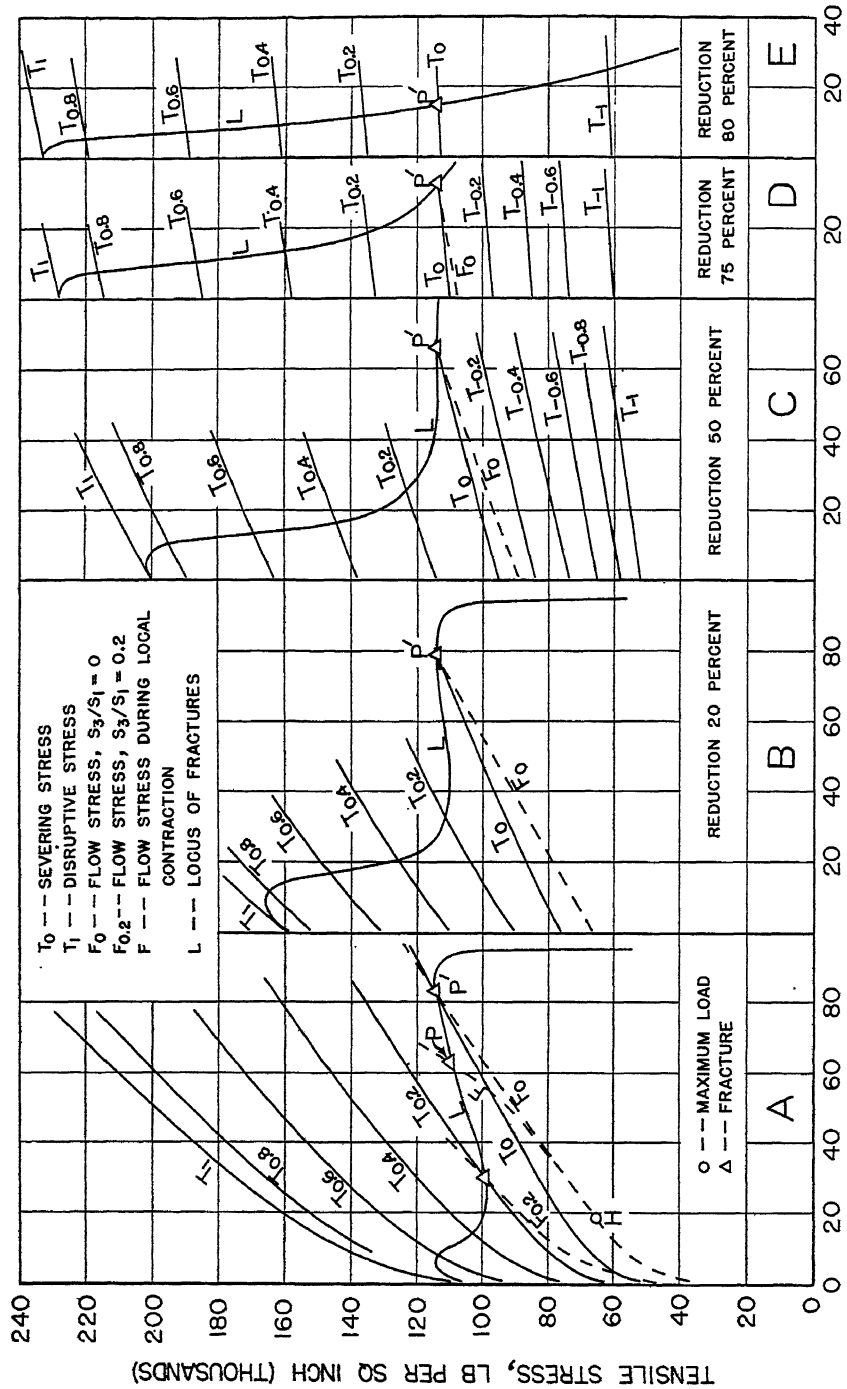
FIG. 12.—INFLUENCE OF PRIOR PLASTIC EXTENSION ON TECHNICAL COHESIVE STRENGTH OF DUCTILE STEEL ($S_2 = S_3$).
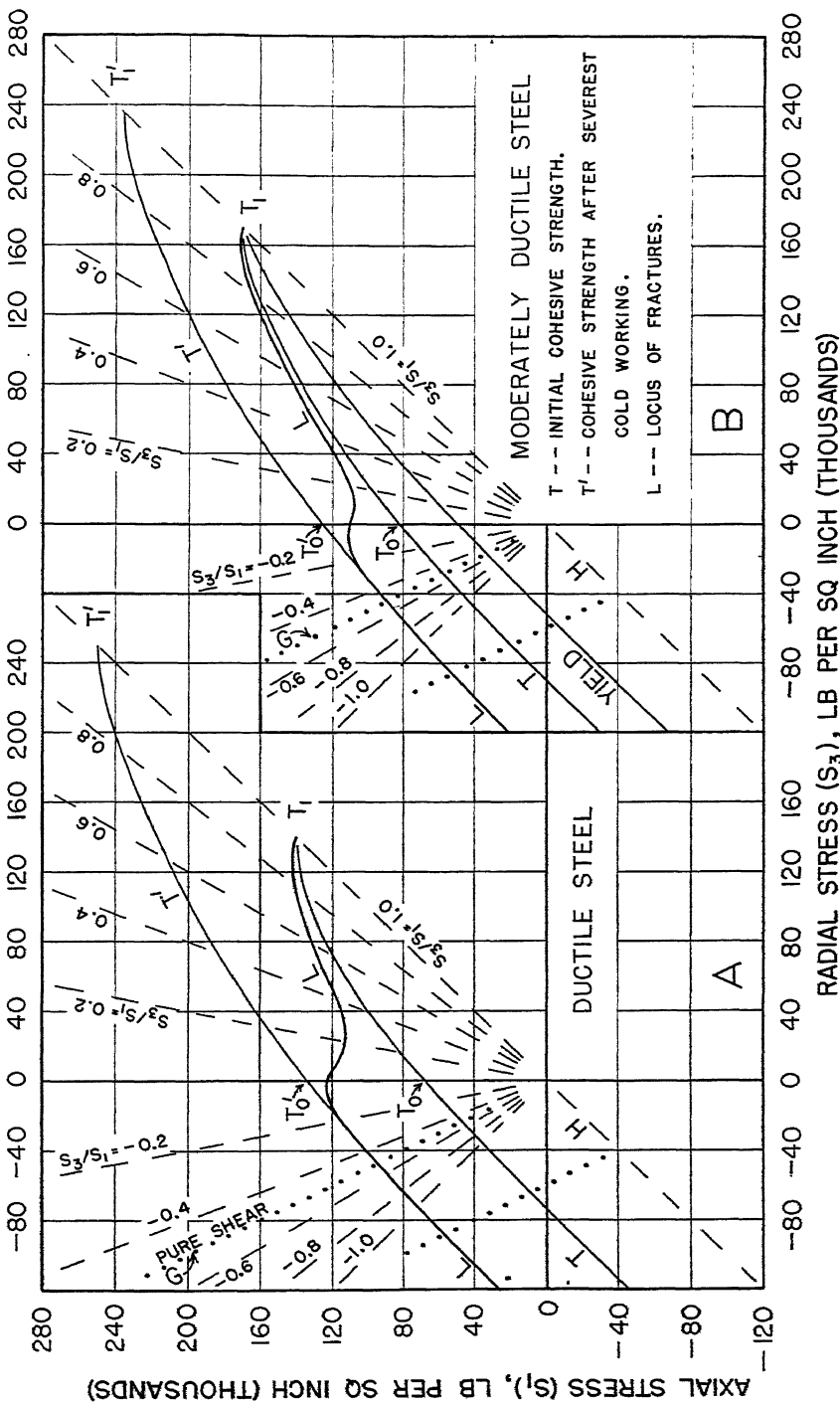
FIG. 13.—TWO-DIMENSIONAL DIAGRAMS REPRESENTING TECHNICAL COHESIVE STRENGTH AND YIELD STRENGTH OF DUCTILE STEELS ($S_2 = S_3$).
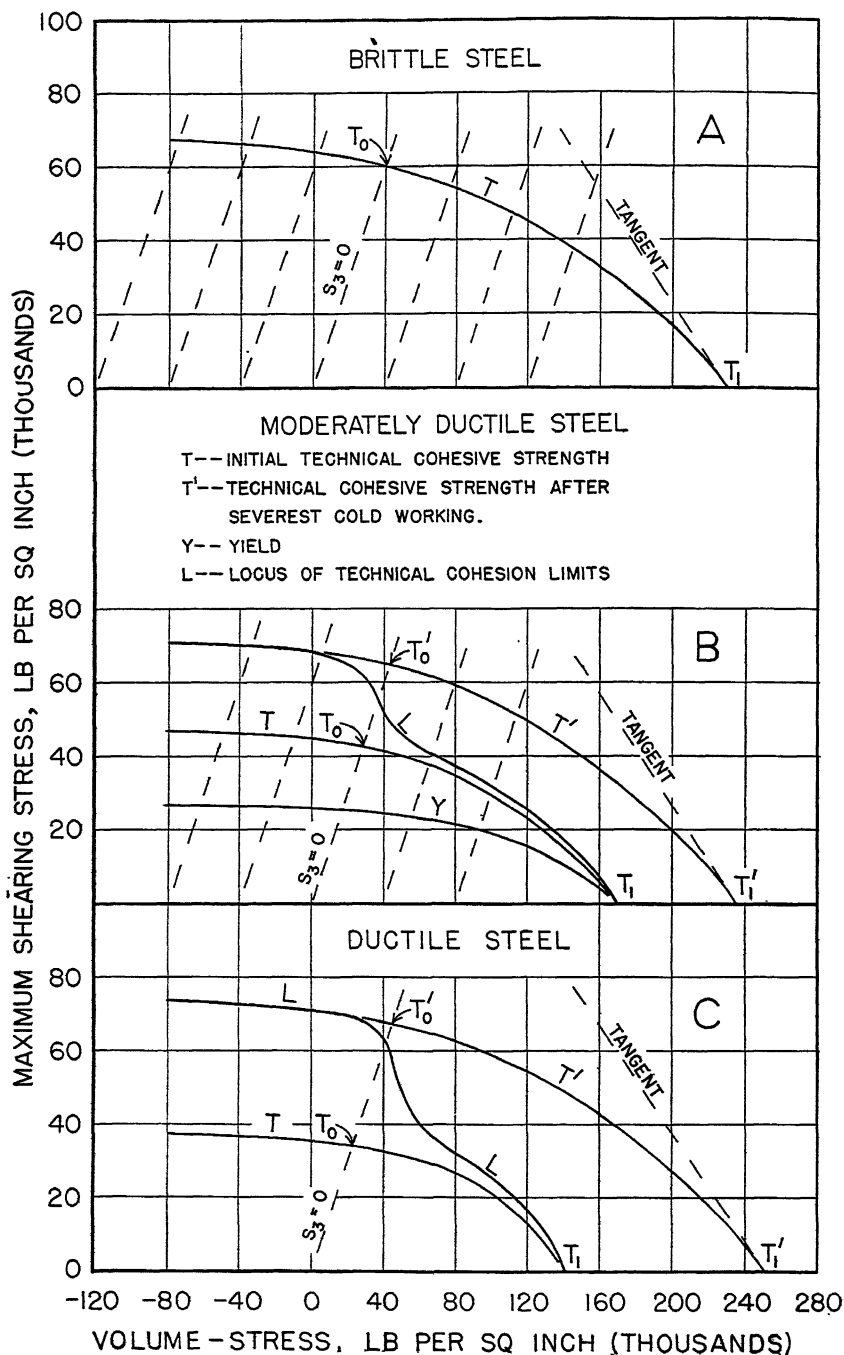
FIG. 14.—VARIATION OF MAXIMUM SHEARING STRESS WITH VOLUME STRESS AT YIELD AND AT RUPTURE ($S_2 = S_3$).

CURVE A REPRESENTS SEVERING FRACTURE $(S_2 = S_3)$.
CURVES R, R', AND R'' REPRESENT THREE ASSUMPTIONS
REGARDING RENDING FRACTURE $(S_2 = S_1)$.
FOR CURVES R, R', AND R'' THE RATIOS OF Q_R TO Q_A ARE
2.0, 1.5, AND 1.0 RESPECTIVELY.
T_0--SEVERING STRESS. T_1--DISRUPTIVE STRESS $(S_1 = S_2 = S_3)$
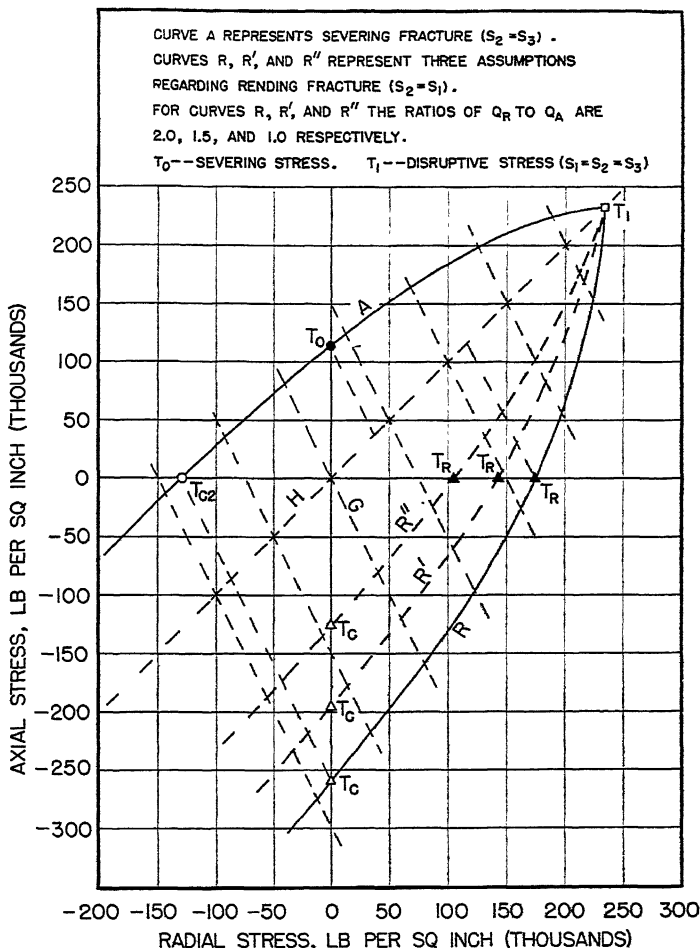
FIG. 15.—TWO-DIMENSIONAL DIAGRAMS REPRESENTING RELATION BETWEEN AXIAL AND RADIAL STRESSES AT TECHNICAL COHESIVE LIMIT OF BRITTLE STEEL. TWO PRINCIPAL STRESSES EQUAL.
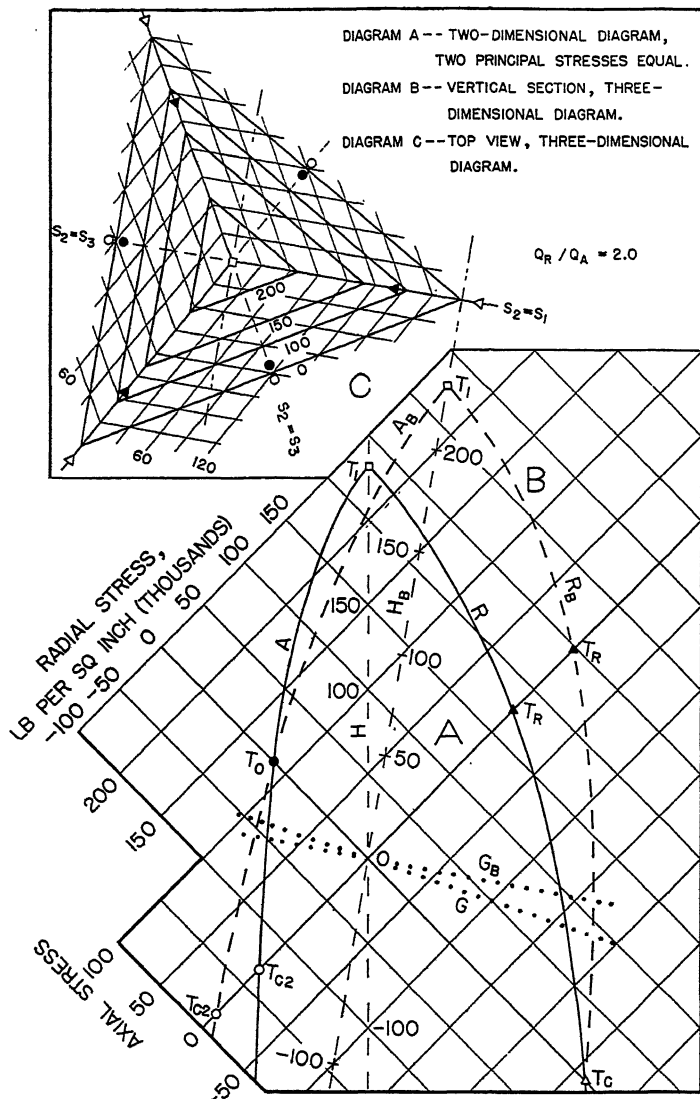
FIG. 16.—TOP VIEW AND VERTICAL SECTION OF THREE-DIMENSIONAL DIAGRAM REPRESENTING TECHNICAL COHESIVE STRENGTH OF BRITTLE STEEL.
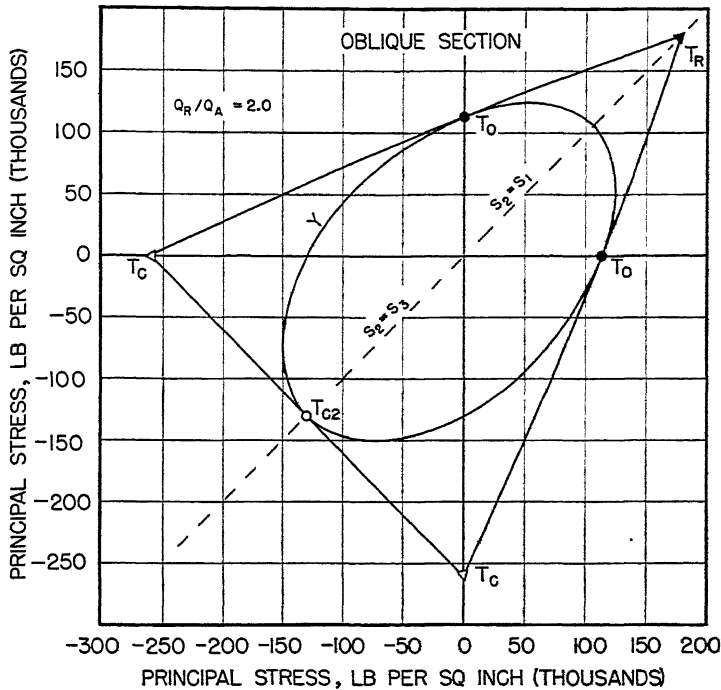
FIG. 17.—OBLIQUE SECTION OF THREE-DIMENSIONAL DIAGRAM REPRESENTING TECHNICAL COHESIVE STRENGTH OF BRITTLE STEEL. SECTION AT ZERO VALUE OF ONE OF THE PRINCIPAL STRESSES.

FIG. 18.—(A) TOP VIEW OF THREE-DIMENSIONAL DIAGRAM REPRESENTING TECHNICAL COHESIVE STRENGTH OF BRITTLE STEEL; (B) QUANTITATIVE SIGNIFICANCE OF POINT ON SURFACE OF THREE-DIMENSIONAL DIAGRAM.
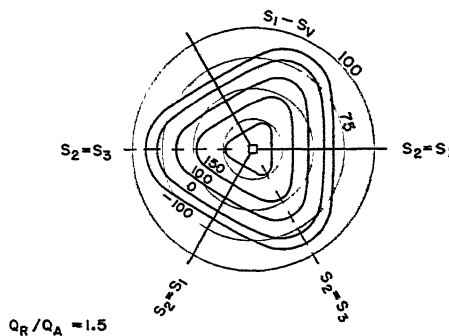
FIG. 19.—VARIATION OF GREATEST PRINCIPAL STRESS WITH COMBINATION OF PRINCIPAL STRESSES AT TECHNICAL COHESION LIMIT OF BRITTLE STEEL.
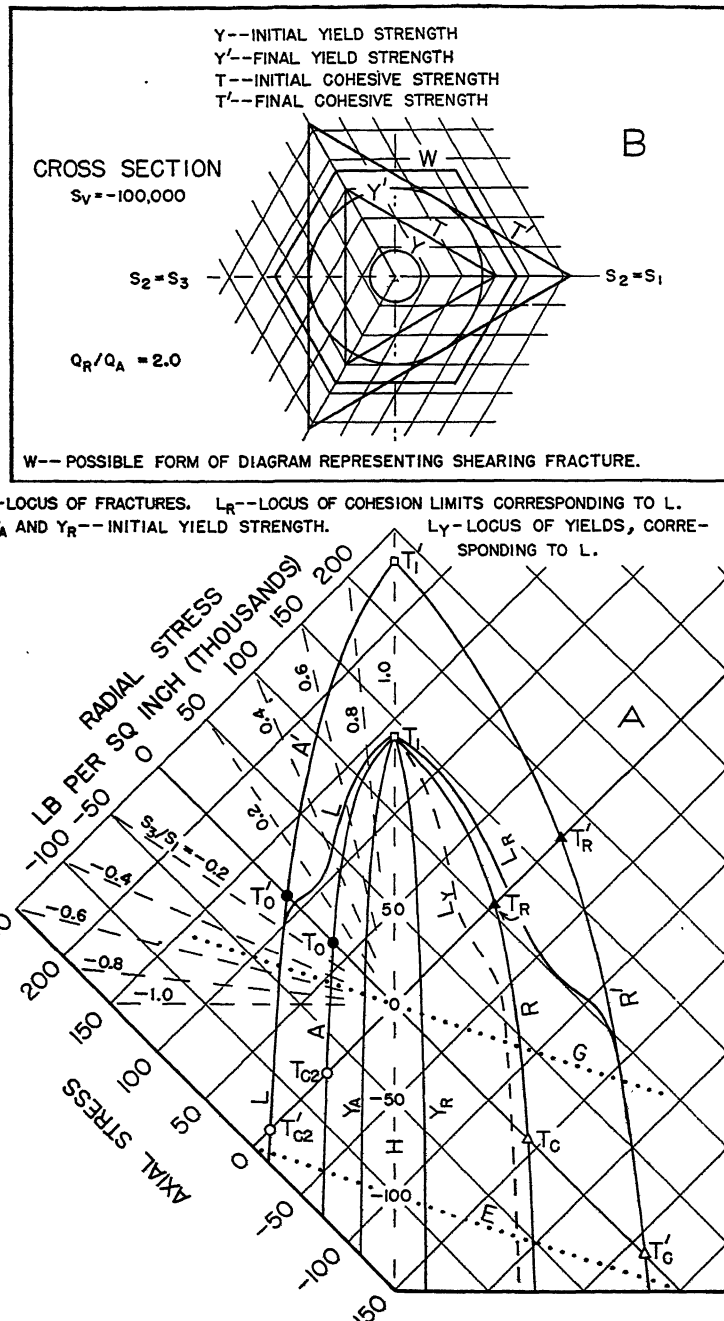
FIG. 20.—COMPLETE TWO-DIMENSIONAL DIAGRAM AND CROSS SECTION OF THREE-DIMENSIONAL DIAGRAM REPRESENTING TECHNICAL COHESIVE STRENGTH AND YIELD STRENGTH OF DUCTILE STEEL.
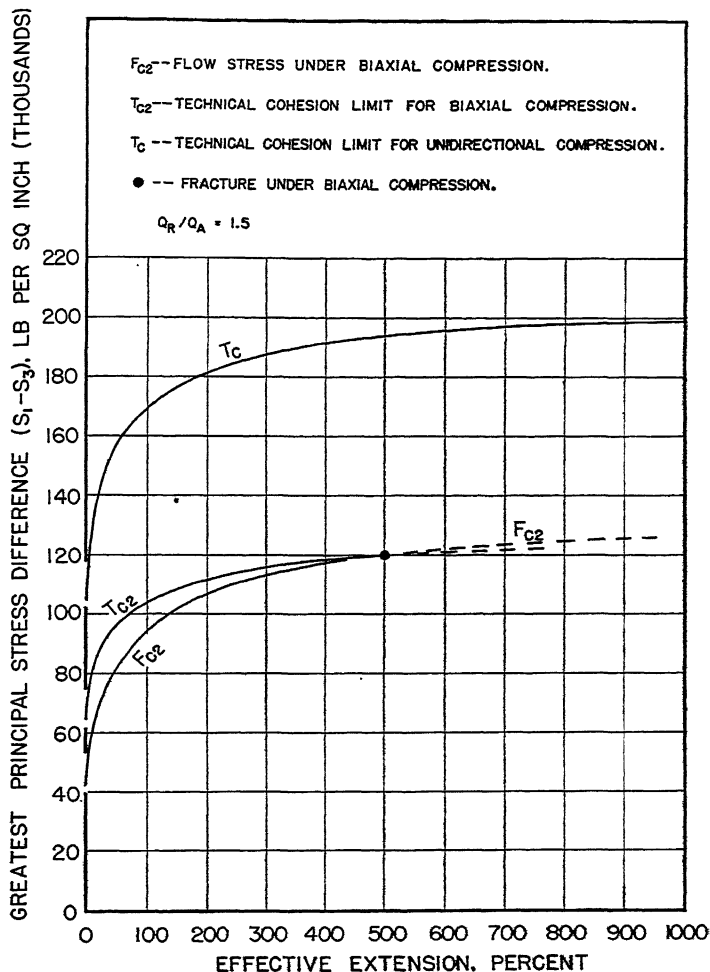
FIG. 21 —INFLUENCE OF PLASTIC DEFORMATION ON FLOW STRESS AND TECHNICAL COHESIVE LIMIT, WHEN S_2 IS EQUAL TO S_3 AND WHEN S_2 IS EQUAL TO S_1.

Precision in Creep Testing

By J. A. Fellows,* Earnshaw Cook* and H. S. Avery,* Members A.I.M.E.

The increased use of heat-resistant alloys (26 per cent Cr, 12 per cent Ni; 16 per cent Cr, 35 per cent Ni; 12 per cent Cr, 60 per cent Ni; etc.) in recent years has been accompanied by continued demands by the consumer for improvement in properties. The manufacturers of these materials, of necessity, have resorted to more critical studies of the basic causes of variations in fundamental properties. To keep pace with the need for augmented information, previous techniques of investigation have been refined and new test methods and instruments created. It is the purpose of this paper to describe the apparatus, experimental technique and precision of measurement that were employed in the exploration of properties of heat-resistant alloys presented in a companion paper.† The detailed precautions in experimental procedure essential for attainment of accurate and comparable data at elevated temperatures cannot be too highly emphasized.

The Creep Test

Since the fundamental concepts of creep testing have been recognized for the past 20 years, present interest is restricted to refinements in equipment and experimental procedure.

The creep-test laboratory constructed for the American Brake Shoe and Foundry Co. is designed to permit 1000-hr. tests in the temperature range of 1200° to 2200°F. with a choice of applied stress extending from 50 to 50,000 lb. per sq. in. in increments of 50 lb. per sq. in. To simplify the calculation of weight combinations, the loading beams (Fig. 1) are provided with counterweights to eliminate the tare. The precision of the knife-edges (10:1 ratio) is such that a 10-gram weight placed on the upper specimen grip will be exactly balanced by a 1-gram weight attached to the loading shackle. Check of the loading weights proved the maximum error to be 0.06 per cent. Axial alignment is provided by crossed knife-edges in the grip seats.

The furnaces are similar in design to those of Crane and Company, Battelle Memorial Institute, and the U.S. Steel Corporation. An 80 per cent Pt, 20 per cent Rh No. 19 B. and S. gauge wire is used as the heating element. The details of construction are shown in the radiograph reproduced in Fig. 2. The windings are held in place on an alundum tube with alundum cement; the distribution of turns is adjusted to give a maximum temperature gradient of ±1°F. over a 4-in. gauge length (Fig. 3). To avoid sharp temperature differentials at the ends of the test section, the length of the furnace is four times the gauge length. Sixteen-inch coupons are used to reduce the temperature of the threaded joints and thus to facilitate removal from the grips. Thermal losses are minimized by refractory insulators cut to shape and surrounded by diatomaceous earth. The taps

visible in Fig. 2 permit the precise adjustment of temperature uniformity required *for each test* by a judicious use of shunts. This is necessary because of the variation

rubber-insulated, lead-sheathed cables were sunk 32 ft. underground. Protection against moisture has been provided by seamless steel tubing, welded and pressure-tested to
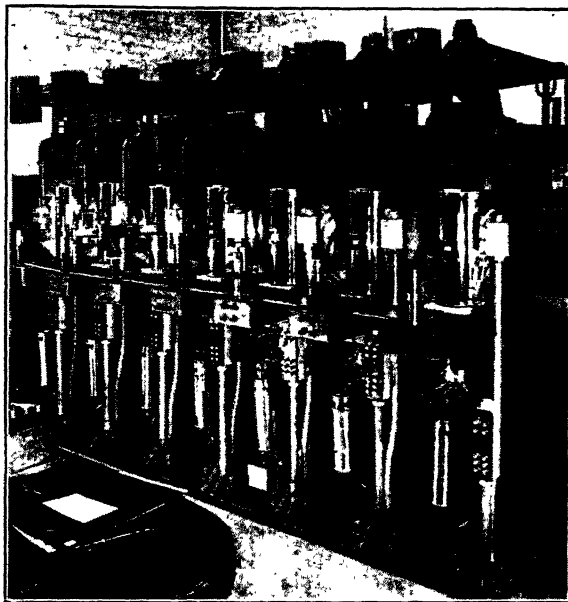
FIG. 1.—CREEP-TEST UNITS.

in heat losses from one test to another through the ends of the furnace and through the threaded joints to the grips.

The furnace temperature is controlled by a potentiometric pyrometer (Fig. 4) operating from a thermocouple attached to the gauge length. The instrument is of the photoelectric type (C. J. Tagliabue Mfg. Co.) equipped with a proportioning device to provide rapid response and to eliminate any dead zone at the control point. A continuous register of control temperature is supplied by a multiple-point recording pyrometer.

Earth temperature is used as the reference point for control to eliminate the nuisance of maintaining ice bottles. An oil bath would be an alternative but is considered less reliable because of possible relay failures. Extension leads encased in

ensure gastightness, which is enclosed in an outer steel casing sealed at the bottom with concrete and asphalt, as are all openings at the ground level.

With this extremely satisfactory arrangement, the total change of the cold-junction temperature (Fig. 5) during the year is within 1.5°F. as measured by an iron-constantan thermocouple included for the purpose. It is interesting to note that the temperature of the thermocouple well lags approximately six months behind that at the surface.

Although approximate room-temperature control is obtained by a thermostatically operated exhaust fan, variations resulting from drastic weather changes were found to affect both the batteries of the pyrometers and the resistivity of their constantan slide wires. Accordingly the batteries were en-

closed in an insulated box and the slide wires have been replaced by duplicates wound with manganin. Figs. 6 and 7 illustrate the precision of control over short and
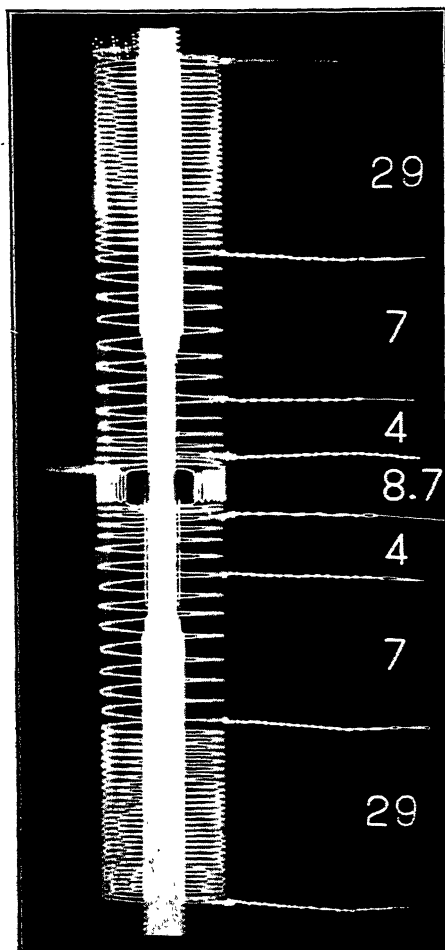
FIG. 2.—RADIOGRAPH SHOWING FURNACE CONSTRUCTION.
Numerals indicate number of turns of wire in various locations.

long periods, respectively. The small fluctuation evident in Fig. 6 is considered preferable to a smoother regulation associated with control from the winding where the mean *specimen* temperature might drift independently of the pyrometer.

The importance of close temperature control in testing austenitic alloys deserves special emphasis. The data in Table 1 were

TABLE 1.—*Effect of Cyclic Temperature Variations upon Creep Rate*

Chemical Analysis, Per Cent					
C	Mn	Si	Ni	Cr	N
0.32	0.46	0.45	11.5	25.9	0.16

Bar No.	Stress, Lb. per Sq. In.	Temperature, Deg. F.	Duration of Test, Hr.	Elongation, Per Cent in 1,000 Hr.	Type of Test
A	3,000	1800	530[a]	3.9	Std.
B	3,000	1800	221[b]	26.0	20° Cycle

[a] Specimen broke.
[b] Test discontinued. Bar had 4.5 per cent residual elongation.

TABLE 2.—*Influence of Temperature upon Limiting Creep Strength*
ALLOYS CONTAINING 26 PER CENT CR AND 12 PER CENT NI

Temperature Deg. F.	Limiting Creep Stress for 0.1 Per Cent Elongation in 1,000 Hr., Lb. per Sq. In.		
	Heat A	Heat B	Heat C
1390	3,200	6,150	8,000
1400	3,100	5,950	7,800
1410	3,020	5,750	7,600
1590	1,810	3,300	4,800
1600	1,750	3,200	4,700
1610	1,700	3,100	4,600
1790	1,030	1,800	2,950
1800	1,000	1,750	2,870
1810	970	1,680	2,800
1990	370	840	
2000	340	790	
2010	300	750	

obtained by varying the temperature of the second test approximately ± 10°F. The length of cycle was roughly 7 min. Both bars were cast from the same heat and were tested at the same *mean* temperature. This sixfold increase in rate is much greater than would have resulted from a test run at 1810°F., the upper limit of the oscillation, as substantiated by the data in Table 2, from the curves in Fig. 8. These values indicate a deviation in limiting creep

strength of 3 to 4 per cent for a 10°F. increase in *constant* temperature while the use of the creep rate of bar B, Table 1, would have caused a 25 per cent error in estimated strength.

Because of the high temperature involved, Pt:Pt-10 per cent Rh thermocouples have been adopted and a precision potentiometer is employed for measurements. Thermocouples were calibrated by
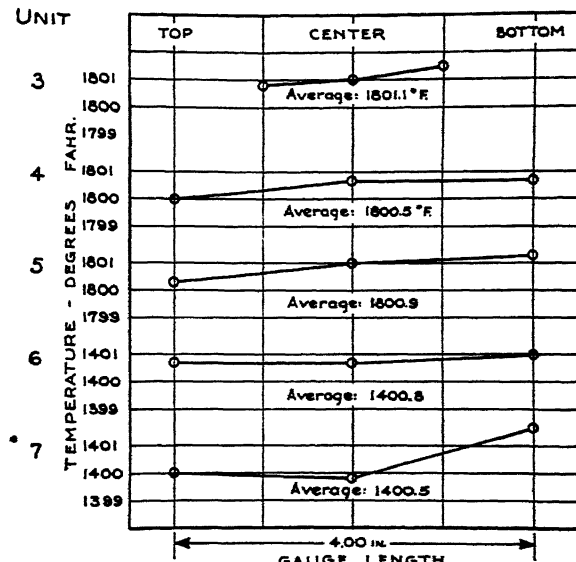
FIG. 3.—REPRESENTATIVE THERMAL GRADIENTS ALONG TEST-BAR GAUGE LENGTHS.

Further evidence of the sensitivity of these alloys to thermal control is offered in Fig. 9. The break in this creep curve was occasioned by a 10-min. power interruption. Since the test was performed at the Massachusetts Institute of Technology, no auxiliary power supply was available. The resultant drop in temperature was sufficient to have altered permanently the rate of flow.

For these reasons every precaution is taken to maintain constant temperature. As an added safeguard two electrical circuits connected through an automatic throw-over panel ensure continuous power in the event of failure of the normal supply. An induction regulator, made necessary by the electrical demands of the adjacent plant, maintains the line voltage within a ±1 per cent variation.

freezing-point determinations. The validity of the derived charts was subsequently verified by a U.S. Bureau of Standards certification of master couples submitted for the purpose. In all temperature measurements Thermos bottles containing ice and distilled water provide the reference temperature.

The chief difficulty is encountered, not in primary calibration, but in *maintaining constant* calibration. Oxides of chromium and iron volatilized from the test bar condense upon the thermocouple leads and cause serious contamination. This has no effect upon temperature observations whenever the contaminated sections are situated in a *uniform* temperature zone, but where sharp thermal gradients exist errors as high as 27°F. have been detected. To avoid this situation, gastight alundum protection

tubing has been secured.* The hot-junction end is sealed with alundum cement fired to 2700°F. About ½ in. of thermocouple wire projects through the seal. The tubes are

The thermocouples are attached to the specimen by spot welding to establish good thermal contact. This has no detectable effect upon the calibration. In general, five
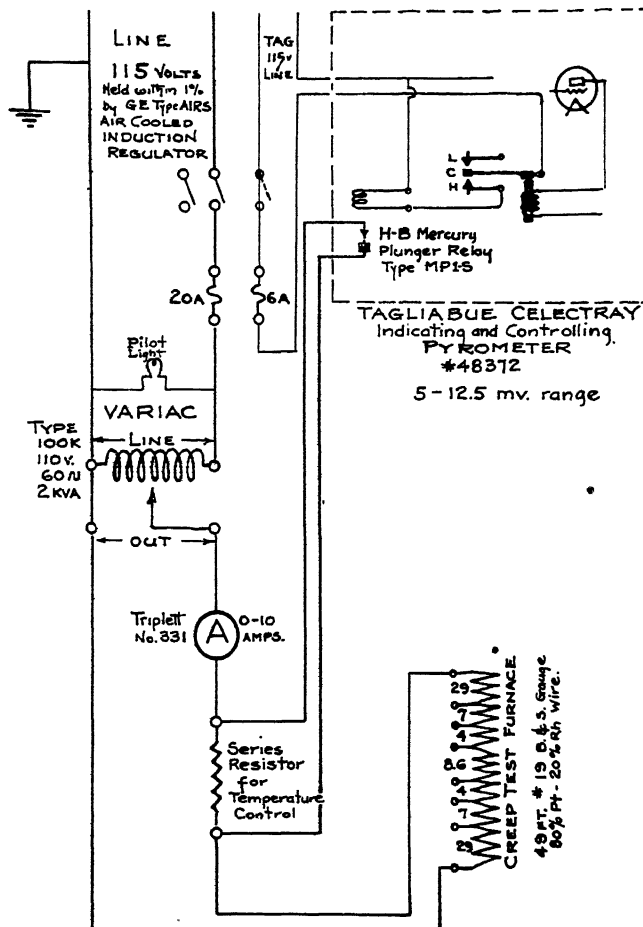
FIG. 4.—CIRCUIT DIAGRAM OF FURNACE CONTROL.

long enough to extend beyond the furnace. While the short exposed hot junctions are subject to contamination, they are entirely within the uniform temperature zone of the gauge length, and have little opportunity for causing erroneous readings. It is thus possible to renew each couple by breaking the seal, cutting back the leads, fusing a new bead and resealing.

* Norton Company, Worcester, Mass.

thermocouples per specimen have been spaced one inch apart along the gauge length. Initial readings are taken with all five couples to ensure the desired thermal uniformity. Thereafter only top, middle, and bottom couples are utilized in daily observations.

Working couples are checked before and after each test by comparison with a secondary standard. This in turn is tested

periodically against the master thermo-couple. A special furnace has been constructed for these comparisons, which possesses both a uniform zone and a gra-

3. Inherent ease in observation because of the V-notch reference marks. A cross hair can be centered most accurately in an illuminated wedge of this type.
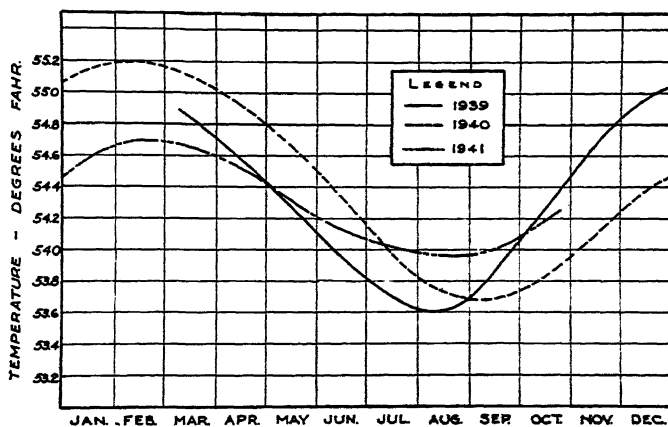
FIG. 5.—VARIATIONS IN COLD-JUNCTION WELL TEMPERATURE.

dient equivalent to that in the creep furnaces between the gauge length and the end. The occasion for the latter detail will be discussed in a subsequent section.

Measurements of elongation are accomplished by means of a telescope sighted on 90 per cent Pt-10 per cent Rh extensometers spot-welded to each side of the gauge

4. Independence of inevitable surface blackening by oxide deposits. Observation by reflected light becomes difficult at these temperatures in tests of long duration.

The telescope (Fig. 12) follows the design adopted by the Creep Laboratory of the U.S. Steel Corporation, with a modified mount. Original calibration was performed
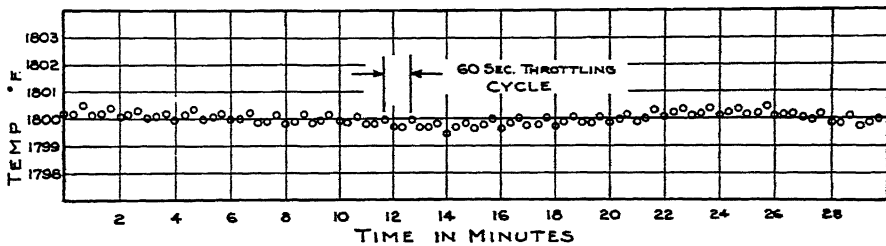
FIG. 6.—SHORT-TIME FLUCTUATIONS IN CONTROL TEMPERATURE.

length (Figs. 10 and 11). Viewed against a light background this method has the following advantages:

1. Rigid attachment to specimen with no discernible effect of spot welding upon flow.

2. Definite gauge length unconfused by presence of fillets between points of attachment.

with the aid of a stage micrometer. One drum division of the filar micrometer eyepiece is equal to 0.00000978 in. per inch for a 4-in. gauge. Cross-hair settings upon the extensometers permit a daily determination of flow in the specimen. The general precision of measurements is demonstrated in the elongation curve of Fig. 13. Calculation of the human error in observations, of the
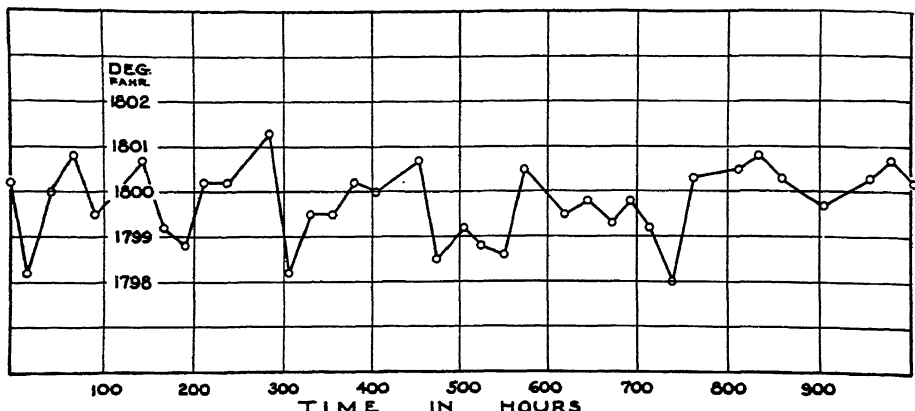
FIG. 7.—LONG-TIME FLUCTUATIONS IN CONTROL TEMPERATURE.
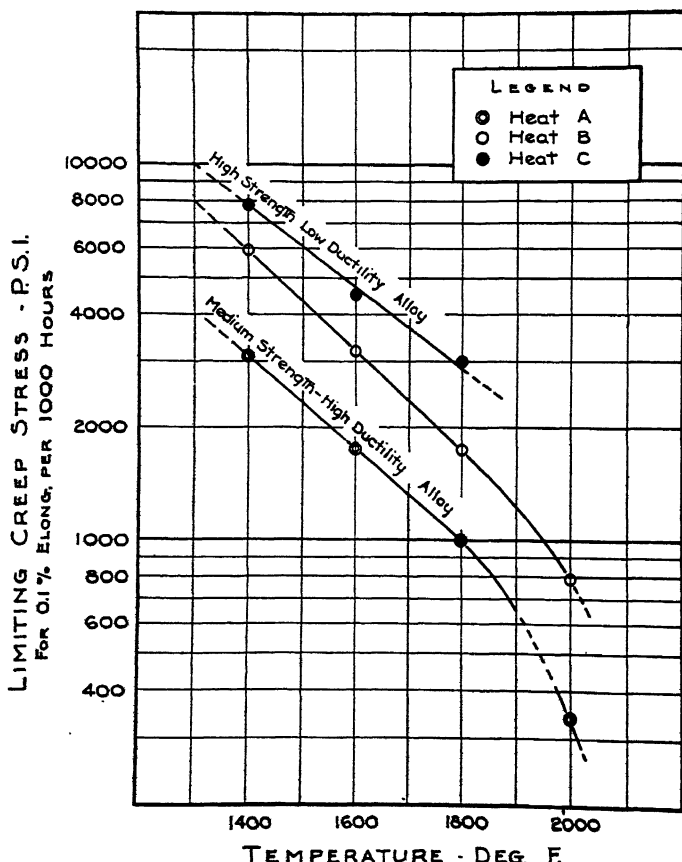
FIG. 8.—LIMITING CREEP STRENGTH VS. TEMPERATURE FOR THREE ALLOY COMPOSITIONS.

mechanical uncertainty of the filar eye-piece, and of the thermal expansion of the coupon for 1°F. deviation, indicates a *possible* variation (*when none of these factors*

time and effort necessary to establish the range of properties of selected analyses. This involved not only the determination of time to failure at various loads and tem-
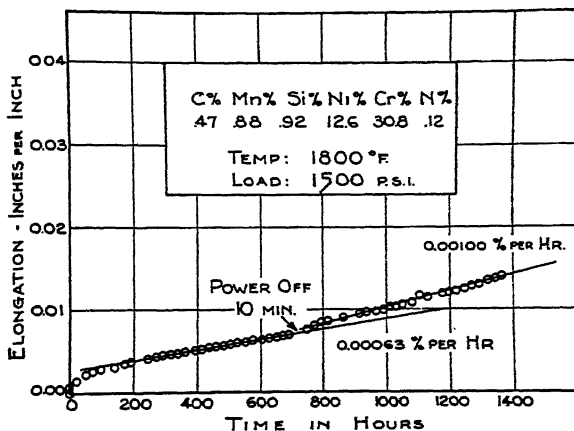
FIG. 9.—EFFECT OF TEMPERATURE INTERRUPTION ON RATE OF CREEP.

are mutually compensating) of ±0.000026 in. per inch, or approximately 2.5 times the precision of plotting on the usual scale.

The interpretation of time-elongation data conforms with conventional practice. The slope of the secondary or straight-line portion of the elongation curve is estimated for each side of the test bar and averaged. This value is then plotted on logarithmic paper against the applied stress. Two or more of these tests make possible an appraisal of the limiting creep strength usually expressed for these alloys as the stress producing a creep rate of 1.0 per cent in 10,000 hr. A rate of 0.0001 per cent per hour is, however, a more precise statement than the customary extrapolation. Representative alignment of data is shown in Fig. 14.

STRESS-STRAIN-RUPTURE TEST

The work of White, Clark and Wilson[77,79] with stress-rupture tests suggested a means for accelerating exploratory investigations of new alloys as well as for curtailing the

peratures but, in addition, the measurement of the secondary rate of uniform elongation for constant stress. By definition and technique, this then becomes an abbreviated creep test. The necessary prerequisite to a useful application of this principle was. evidence that strain rate bears the same relationship to stress in short-time tests as in creep tests. It was foreseen that, *if* this could be established, the test would have a threefold value:

1. Experimental analyses could be ranked according to strength by comparison of deformation rates under a standard load and temperature. Enormous savings in time would be gained over performing the same survey by creep testing.

2. A reasonably accurate estimate of limiting creep strength would be possible from the results of two rapid tests at different loads. This would permit selection of a stress for a creep test whose rate of elongation would be so close to the critical value (0.0001 per cent per hour) as to make further long-time tests unnecessary.

3. Correlation of rupture times for short and long-time creep tests would allow an

[77] See bibliography at end of paper.

appraisal of *maximum* attainable life in service.

A preliminary investigation was made in 1938 using a Baldwin-Southwark tensile

FIG. 10.—SCHEMATIC REPRESENTATION OF CREEP-TEST EXTENSOMETER.

machine and a tensile-test furnace. The test specimens were selected from materials of known creep strength. Constant load was maintained by manual adjustment of the needle valves and elongation was measured

with the aid of a dial gauge actuated by the tensile-machine cross heads. A plot of the elongation rates with the available creep values against the respective loads pro-

FIG. 11.—EXTENSOMETERS ATTACHED TO CREEP-TEST BAR.

duced a log-log plot in which all points fell on or very near a straight line.* It was de-

---

* It is not suggested that this relationship can be extrapolated with assurance to the low rates of deformation involved in turbine de-

cided, therefore, to incorporate this test in the Creep Laboratory as a standard procedure. Two of the seven units illustrated in Fig. 1 are devoted to this work.

Since in most respects the equipment provided for the S.S.R. tests (stress-strain-rupture tests) is identical with that previously described for creep testing, attention will be restricted to the modifications necessary. A gear mechanism is employed for adjusting the lower grip anchorage to prevent the loading beam from reaching its stop before failure occurs. For much the same reason the gauge length is limited to 2 in. Standard tensile-test specimens with internal grips are possible in these short tests. The furnace differs only in the design of the heating element to compensate for the greater heat flow through the heavy grips.

In the measurement of temperature, unprotected thermocouples are used: the

voltage developed in the stress-strain-rupture furnaces.

Time to failure is recorded by a clock set in motion at the instant of load application.
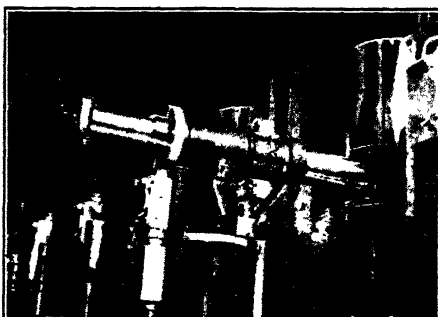
FIG. 12.—TELESCOPE FOR ELONGATION MEASUREMENTS.

At rupture the drop of the beam interrupts the power supply for the clock, the furnace, the controlling pyrometer and for the elongation recorder (described below).
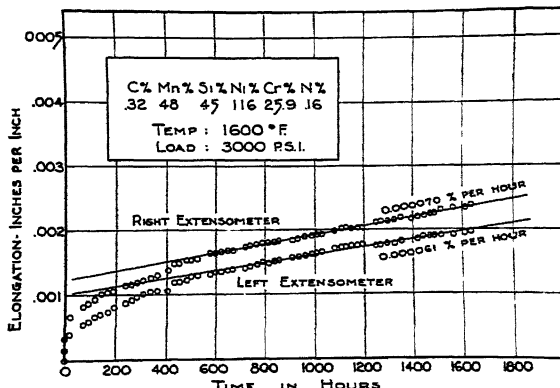
FIG. 13.—TYPICAL TIME-ELONGATION CURVE.

space available between the grips and the furnace wall is insufficient to admit the larger sealed tubes. It is for this reason that the calibration furnace contains a zone of equivalent thermal gradient. Because each exposure to contamination is short and recalibrations are frequent, use of this zone achieves a satisfactory check of the milli-

Elongation is measured by three means. The first is a selected spot check with the telescope sighted on extensometers as in the creep test. This ensures fundamental accuracy. Both of the other two methods make use of the motion of the upper grip seat. In one case a dial gauge mounted on the frame registers its travel; in the other this movement is automatically recorded by a special instrument built for the purpose. Comparison of recorder and dial-

sign. J. J. Kanter and E. A. Sticha have recently indicated a departure from a straight line in this region.[30]

gauge readings with telescope observations has proved the amount of flow occurring in grips and threads to be negligible.

The recorder consists of a recording-

technique has been reported* for the positive identification of minute quantities by the use of Elmore's magnetic suspension under the microscope.
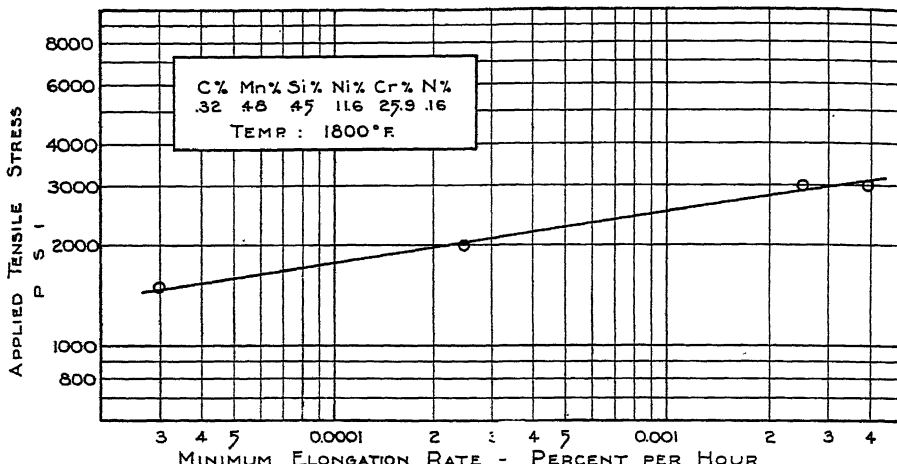
FIG. 14.—LOG-LOG PLOT OF STRESS VS. STRAIN RATE.

pyrometer chassis, chart, pen, and chart drive combined with the Selsyn motors, relays, clutch, and other equipment normally supplied with a Peters stress-strain recorder. Fig. 15 illustrates the Selsyn motor unit with the S.S.R. frame. Since the total elongation in a test is far beyond that registered by one passage of the pen across the chart, limit switches are employed to reverse the direction of travel after reaching each extremity. A portion of an elongation record is reproduced in Fig. 16. The correlation of stress-strain-rupture and creep-test data is illustrated in Fig. 17, which is derived from tests from duplicate heats. The curve for fracture time versus stress is extrapolated to indicate its possible use in forecasting *maximum* attainable service life at that temperature.

MAGNETIC PERMEABILITY

The occurrence of a ferromagnetic phase in the so-called austenitic alloys has long been realized. Ferrite frequently is present in such degree as to be readily detectable with a hand magnet. Furthermore, a

These, however, are qualitative methods. The need for a quantitative evaluation of the influence of ferrite was soon realized in the study of heat-resistant alloy properties. In 1936 an instrument was secured for the measurement of magnetic permeability of samples of convenient sizes. Since the creep-test coupons used at that time had a 2-in. gauge length,† a specimen of 1 by $\frac{1}{4}$-in. diameter was selected. This made available a permeability sample wherever fracture occurred along the test section.

The instrument is capable of determining permeabilities from 1.000 to 300 ($H = 24$). The smallest interval that can be measured is 0.003, although this quantity is reproducible. A sample for which $\mu = 1.003$ was tested at M.I.T. and ascribed a value of $\mu = 1.0025$, indicating the error to be small in this range. A further check by the U.S. Bureau of Standards at an approximate figure of $\mu = 4.0$ revealed that the absolute

---

* H. S. Avery, V. O. Homerberg and E. Cook: Metallographic Identification of Ferromagnetic Phases. *Metals and Alloys* (Nov., 1939) 10, 353–355.

† Creep testing was conducted at M.I.T. prior to construction of the Company laboratory.

values of the constants supplied with the instrument are inaccurate, since a 25 per cent discrepancy was disclosed. Because of recent interest in magnetic permeability,

FIG. 15.—SELSYN MICROMETER SCREW-CONTACT ASSEMBLY ON S.S.R. TEST FRAME.

the derivation of the constants is being checked to permit interchange of values

with other laboratories. For intralaboratory comparisons, however, the instrument has been entirely consistent and has proved to be a valuable research tool. The wiring
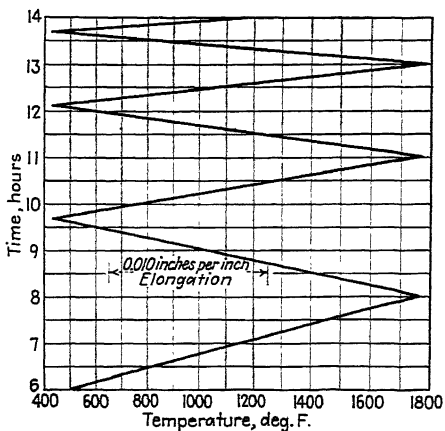
FIG. 16.—REPRODUCTION OF A PORTION OF A TIME-STRAIN RECORD.

diagram of the apparatus is presented in Fig. 18.

As an example of its use, the trend of strength with ferromagnetism is illustrated by the data quoted in Table 3.

It is evident that increased permeability is accompanied by increased flow and decreased strength. A quantitative development of this method of attack will be reported in the companion paper (page 373, this volume), to which this discussion serves as a prologue.

SUMMARY

The apparatus, techniques and precision of a high-temperature creep-test laboratory

TABLE 3.—*Magnetic Permeability vs. Elongation after 210 Hours Creep*
DATA DERIVED FROM CREEP TESTS AT 1800°F. AND 1500 LB. PER SQ. INCH

Specimen No.	Chemical Analysis, Per Cent							Magnetic Permeability	Elongation at 210 Hr., Per Cent in 2 In.
	C	Mn	Si	Ni	Cr	N			
A	0.32	0.85	1.23	11.3	25.4	0.16	V 1.05	1.000	0.02
B	0.35	0.66	0.44	12.5	27.8	0.29		1.171	0.07
C	0.30	1.62	1.28	12.5	28.2	0.09	W 0.51	1.636	0.23
D	0.47	0.69	0.70	12.6	32.1	0.09		1.663	0.40
E	0.25	0.96	0.50	12.1	27.7	0.11	Cu 1.22	3.37	1.63

have been discussed. A type of accelerated creep test and its advantages in a comprehensive program of research have been reported. The possibilities of magnetic test-

an adequate approach to accurate and comparable creep testing at elevated temperatures of nickel-chromium alloys requires meticulous experimental techniques
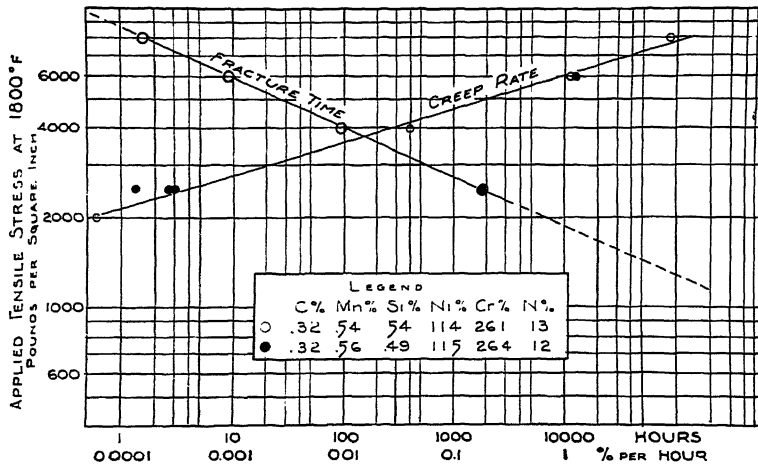
FIG. 17.—CORRELATION OF CREEP AND S.S.R. DATA.
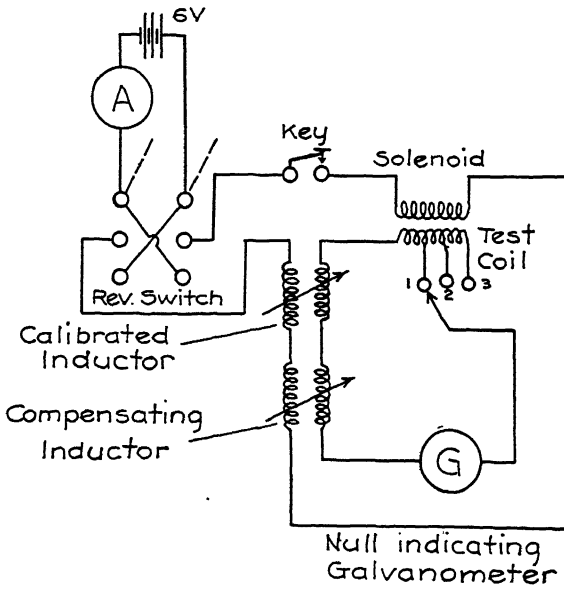
FIG. 18.—ELECTRICAL CIRCUITS OF PERMEAMETER.

ing in studying creep strength have been suggested and a brief description has been given of the instrument employed.

In conclusion, it is again emphasized that

with special attention to: (1) precision of elongation measurements well within overall experimental error; (2) precision of thermocouple calibration and special pre-

cautions in temperature measurements; (3) precision of temperature control within a maximum allowable cycle of ±0.5°F. and within a desirable maximum variation about the control point of ±1.5°F.

ACKNOWLEDGMENT

The most sincere appreciation is extended to Prof. F. H. Norton, for his cooperation and assistance with this program, and to the American Brake Shoe and Foundry Co. for permission to publish these researches.

BIBLIOGRAPHY

Development of Creep-test Methods and Equipment
1922–1926

1. J. H. S. Dickenson: Some Experiments on the Flow of Steels at a Red Heat, with a Note on the Scaling of Heated Steels. *Jnl. Iron and Steel Inst.* (1922) 106, 103–154.
2. F. C. Lea: Effect of Low and High Temperatures on Materials. *Proc. Inst. Mech. Engrs.* (1924) 2, 1053–1096.
3. V. T. Malcolm: Methods of Testing at Various Temperatures. *Proc. Amer. Soc. Test. Mat.* (1924) 24, II, 15–55.
4. J. Cournot and K. Sasagawa: Contribution à l'Etude de la Viscosité des Alliages à Température Elevée. *Rev. Mét.* (1925) 22, 753–763.
5. H. J. French and W. A. Tucker: Flow in a Low-Carbon Steel at Various Temperatures. Nat. Bur. Stds. *Tech. Paper* 296 (1925).
6. T. M. Jasper: Typical Static and Fatigue Tests on Steel at Elevated Temperatures. *Proc. Amer. Soc. Test. Mat.* (1925) 25, II, 27–52.
7. V. T. Malcolm: Metallurgical Developments in the Valve and Fitting Industry. *Jnl. Amer. Soc. Mech. Engrs.* (1925) 47, 1141.
8. L. W. Spring and J. J. Kanter: Accuracy in High Temperature Testing of Materials. *Power* (1925) 62, 325.
9. H. J. French: Methods of Test in Relation to Flow in Steels at Various Temperatures. *Proc. Amer. Soc. Test. Mat.* (1926) 26, II, 7.
10. A. E. White and C. L. Clark: Properties of Boiler Tubing at Elevated Temperatures Determined by Expansion Tests. *Trans. Amer. Soc. Mech. Engrs.* (1926) 48, 1075–1093.

1927–1929

11. A. McCance: Properties of Steel at High Super-Heat Temperatures. *Trans. Liverpool Eng. Soc.* (1927) 48, pp. 205–240.
12. P. G. McVetty and N. L. Mochel: Tensile Properties of Stainless Iron and Other Alloys at Elevated Temperatures. *Trans. Amer. Soc. Steel Treat.* (1927) 11, 73–100.
13. A. Pomp and A. Dahmen: Development of a Shortened Test Method for the Determination of the Creep Limit of Steel at High Temperatures. *Mitt. K.-W.-I. Eisenforschung* (1927) 9, 33–52.
14. L. W. Spring, J. W. Maack and J. J. Kanter: Testing Flow in Metals at Various Temperatures. *Power* (1927) 65, 205–208.
15. E. Honegger: Long Duration Tensile Tests on Metals at High Temperatures. *Brown Boveri Rev.* (1928) 15, 315–320.
16. J. J. Kanter and L. W. Spring: Long Time or "Flow" Tests of Carbon Steels at Various Temperatures with Particular Reference to Stresses Below Proportional Limit. *Proc. Amer. Soc. Test. Mat.* (1928) 80.
17. F. Korber: Ermittlung der Dauerstandfestigkeit von Stahl bei erhöhten Temperaturen. *Ztsch. Metallkunde* (1928) 20, 45–50.

18. G. D. Bagley: A Machine for Making Creep Tests at High Temperatures. *Trans. Amer. Soc. Mech. Engrs.* (1929) 51 (1) FSP-51-38, 259–261.
19. A. G. Lobley and C. L. Betts: The Creep of 80:20 Nickel-Chromium Alloy at High Temperatures. *Jnl. Inst. Metals* (1929) 42, 157–179.
20. F. H. Norton: Creep of Steels at High Temperatures. New York, 1929. McGraw-Hill Book Co

1930–1931

21. J. J. Kanter and L. W. Spring: Some Long Time Tension Tests of Steels at Elevated Temperatures. *Amer. Soc. Test. Mat.* (1930) 30, pt. 1, 110–132.
22. W. Rohn: Determination of the Creep Limit. Publication in Honor of the 70th Birthday of Wilhelm Heraeus 1930, pp. 80–96, pub. by G. M. Alberti's Hofbuchhandlung, Bruno Claus, Langstrasse 47, Hanau, Germany.
23. A. E. White, C. L. Clark and L. Thomassen: An Apparatus for the Determination of Creep at Elevated Temperatures. *Trans. Amer. Soc. Mech. Engrs.* (1930) 52 (1) FSP-52-40.
24. H. J. French, W. Kahlbaum and A. A. Peterson: Flow Characteristics of Special Fe-Ni-Cr Alloys and Some Steels at Elevated Temperatures. *Nat. Bur. Stds. Jnl. of Research* (July 1930) 5, 125–183. Also *Trans. Amer. Soc. Mech. Engrs.* (1931) FSP-53-9-97.
25. J. Galibourg: Les caracteristiques mécaniques des métaux à chaud. *Sci. et Ind.* (1931) 15, 455–462.
26. F. H. Norton and J. B. Romer: New Creep Testing Apparatus at the Massachusetts Institute of Technology. *Proc. Amer. Soc. Test. Mat.* (1931) 31, I, 129.
27. G. Ranque and P. Henry: Sur la détermination des caracteristiques d'allongement visqueax des métaux à chaud. *Génie Civil* (1931) 99, 630–631; *Compt. rend.* (1931) 193, 1061–1063.
28. D. A. Roberts and R. L. Dowdell: A Photographic Creep Testing Apparatus. *Metals and Alloys* (1931) 2 (6), 349–351.
29. H. J. Tapsell: Creep of Metals. New York, 1931. Oxford Univ. Press.

1932–1933

30. W. Barr and W. E. Bardgett: An Accelerated Test for the Determination of the Limiting Creep Stress of Metals. *Engineering* (March 4, 1932) 133, 293–294; *Iron and Coal Tr. Rev.* (Feb. 26, 1932) 124, 354–355.
31. F. P. Coffin and T. H. Swisher: Flow of Steels at Elevated Temperatures. *Trans. Amer. Soc. Mech. Engrs.* (1932) 54, Applied Mech., 59–68.
32. J. Galibourg: Les métaux aux temperatures elevées. Int. Assn. for Test. Mat., Zurich Meeting 1931 (1932) 1, 134–142.
33. W. H. Hatfield, G. Stanfield, J. Woolman and N. B. McGregor: Apparatus for Long Period Temperature-Stress Tests on Metals. *Jnl. Sci. Instr.* (1932) 9, 150–153.
34. A. Pomp and W. Enders: Accelerated Method for Determining Creep Limit. *Instruments* (1932) 5 (7), 166–168.
35. W. Rohn: Apparat zur Bestimmung von Kriechgeschwindigkeit und Kriechfestigkeit. Int. Assn. for Test. Mat., Zurich Meeting, 1931 (1932) 1, 183–186.
36. R. G. Batson and J. H. Hyde: Mechanical Testing. New York, 1933. Dutton.
37. P. L. Everett: Creep of Metals in Shear at High Temperatures. *Physics* (1933) 4 (3), 119–121.
38. F. B. Foley: Characteristics of Steel at Elevated Temperatures. *Refiner and Natural Gas Mfg.* (1933) 12, 180–183.
39. H. W. Gillett and H. C. Cross: Obtaining Reliable Values for Creep at High Temperatures. *Metals and Alloys* (1933) 4, 91–98, 104.
40. H. Juretzek and F. Sauerwald: Experiments to Establish the Conception of the Creep Limit. *Ztsch. Physik* (1933) 83, 483–491.
41. F. H. Norton and J. A. Fellows: A New Device for Creep Testing. *Metal Progress* (1933) 24 (4), 41–43.
42. E. L. Robinson: Metals at High Temperature-Test Procedure and Analysis of Test Data.

Trans. Amer. Soc. Mech. Engrs. (1933) 55, APM-55-17.

43. A. Shimidzu: Process of the Creep of Metals and Its Progress. *Jnl.* Soc. Mech. Engrs. Tokyo (1933) 36, 7–11.

44. W. A. Tucker and S. E. Sinclair: Creep and Structural Stability of Ni-Cr-Fe Alloys at 1600°F. Nat. Bur. Stds. *Jnl. of Research* (1933) 10, 851–862.

45. A. E. White and C. L. Clark: Creep Characteristics of Metals at Elevated Temperatures. *Trans.* Amer. Soc. Steel Treat. (1933) 21, 1–16.

1934–1935

46. H. C. Cross: High Temperature Tensile, Creep, and Fatigue Properties of Cast and Wrought High and Low Carbon 18 Cr, 8 Ni Type Steel from Split Heats. *Trans.* Amer. Soc. Mech. Engrs. (1934) 56, 533–553.

47. H. Dustin: Belgian Research Committee on the Behavior of Metals at Elevated Temperatures. *Jnl.* Iron and Steel Inst. (1934) 130, 127–151.

48. F. Korber: Strength Properties of Steels at High Temperatures. 3rd Congress on Industrial Heating, Oct. 14–17, 1933. *Rev. de Mét., Mem.* (1934) 31, 359–368.

49. H. Montgomery and J. W. Bolton: Furnaces for Elevated Temperature Tests. *Metals and Alloys* (1934) 5, 127–128.

50. I. Musatti and A. Reggiori: Apparatus for Tests at Raised Temperatures and the Creep Strength of Some Steels. 3rd Congress on Industrial Heating, Oct. 14–17, 1933. *Rev. de Mét., Mem.* (1934) 31, 421–438.

51. G. Ranque and P. Henry: The Method of Thermal Autostabilization and Its Use in the Study of Some Heat-Resisting Steels. 3rd Congress on Industrial Heating, Oct. 14–17, 1933. *Rev. de Mét., Mem.* (1934) 31, 248–265; *Aciers Spéciaux* (1934) 9, 176–195.

52. H. J. Tapsell and L. E. Prosser: High Sensitivity Creep Testing Equipment at the National Physical Laboratory. *Engineering* (Feb. 23, 1934) 137, 212–215.

53. P. H. Clark and E. L. Robinson: An Automatic Creep Test Furnace-Guide. *Metals and Alloys* (1935) 6, 46–49.

54. E. A. Davis: Measurement of Creep of Metals. *Instruments* (1935) 8 (5), 128–129, 132.

1936–1937

55. P. Chevenard: Alloys with High Tensile Strength and Resistance to Corrosion at Elevated Temperatures. *Chaleur et Ind.* (1936) 17, 125–137.

56. J. J. Curan and F. H. Morehead: A Direct-Load Creep Test Machine. *Proc.* Amer. Soc. Test. Mat. (1936) 36, II, 161–169.

57. A. Grunert and W. Rohn: Obtaining Time-Deformation Curves with W. Rohn's Creep Testing Apparatus, (Aufnahme von Zeit-Dehnung-Kurven mit dem Kriechgrenzengerat von W. Rohn.) *Archiv Eisenhuttenw.* (1936) 10, 67–68.

58. L. Ya. Liberman and G. N. Buistrov: Machine for Testing Creep of Steel. Zavodskaya Lab. (1936) 5, 341–344.

59. N. A. Shaposhnikov: An Accelerated Creep-Test Method. Zavodskaya Lab. (1936) 5, 630–637.

60. F. Bollenrath, W. Bungardt and Others: Furnaces for Making Atmospheric Creep Tests. *Archiv Eisenhuttenw.* (1937) 10, 555–562.

61. R. Ludwig and H. Wustl: Short-Time Tests for Determining "safe stress" of Steel Under Continuous Loading, and a Method for Evaluating Time-Yield Curves. *Proc.* Int. Assn. Test. Mat. (1937) 9–12.

62. P. G. McVetty: Equipment for Creep Tests at Elevated Temperatures. *Proc.* Amer. Soc. Test. Mat. (1937) 37, II, 235–257.

63. A. Pomp: Testing the Behavior of Metals under Mechanical Loading at High Temperature. *Proc.* Int. Assn. Test. Mat. (1937) 12–15.

64. E. L. Robinson: A Relaxation Test on 0.35 Carbon Steel K20. *Trans.* Amer. Soc. Mech. Engrs. (1937) 59, 451–452.

65. L. Wizenez: Measuring Accuracy of Martens' Mirror Extensometer in Creep Tests. *Archiv Eisenhuttenw.* (1937) 11, 189–194.

1938–1941

66. C. R. Austin and N. D. Nickol: Comparison of the Tensile Deformation Characteristics of Alloys at Elevated Temperatures. *Jnl.* Iron and Steel Inst. (1938) 137, 177–217.

67. A. M. Borzdyka: New Apparatus for Testing Metal Creep by the Torsion Method. Zavodskaya Lab. (1938) 7, 62–71.

68. W. H. Hatfield: Heat Resisting Steels. *Engineering* (1938) 145, 372–374, 455–457; cf. *Chem. Absts.* 32, 5360⁵; *Jnl.* Inst. Fuel (1938) 11, 245–304, 440–450.

69. A. Krisch: Determination of Creep Strength by Different Methods. *Archiv Eisenhuttenw.* (1938) 12, 199–206.

70. G. Lindh: Measurement of the Creep Limit of Steel. *Jernkontorets Ann.* (1938) 122, 185–214.

71. W. Marx: New Testing Machine for Determination of Creep at Elevated Temperatures. *Tech. Zentralblatt prakt. Metallbearbeit.* (1938) 48, 64–67.

72. R. F. Miller, R. F. Campbell, R. H. Aborn and E. C. Wright: Influence of Heat Treatment on Creep of Carbon-Molybdenum and Chromium-Molybdenum-Silicon Steel. *Trans.* Amer. Soc. Metals (1938) 26, 81–101.

73. F. H. Norton: Report of Joint Committee on Effect of Temperature on Properties of Metals. Creep Tests of Tubular Members Subjected to Internal Pressure. *Proc.* Amer. Soc. Test. Mat. (1938) 38, I, 118–120.

74. W. C. Stewart: High-Temperature Properties for Some Alloys of Particular Interest to the Navy. *Jnl.* Amer. Soc. Naval Engrs. (1938) 50, 107–132.

75. H. Esser and S. Eckardt: Experiments with a New Creep Testing Apparatus on the Course of Time-Elongation Curves of Different Steels. *Archiv Eisenhuttenw.* (1939) 13, 209–222.

76. W. E. Trumpler, Jr.: Relaxation of Metals at High Temperatures. *Jnl. Applied Physics* (1941) 12, 248–253.

Stress-rupture Testing

77. A. E. White, C. L. Clark and R. L. Wilson: The Fracture of Carbon Steels at Elevated Temperatures. *Trans.* Amer. Soc. Metals (1937) 25, 863–888.

78. R. H. Thielemann and E. R. Parker: Fracture of Steels at Elevated Temperatures After Prolonged Loading. *Trans.* A.I.M.E. (1939) 135, 559–582.

79. A. E. White, C. L. Clark and R. L. Wilson: The Rupture Strength of Steels at Elevated Temperatures. *Trans.* Amer. Soc. Metals (1939) 26, 52–80.

80. J. J. Kanter and E. A. Sticha: Creep Rates from Tests of Short Duration. *Trans.* Amer. Soc. Metals (1940) 28, 257–271.

81. E. R. Parker: Development of Alloys for Use at Temperatures above 1000°F. *Trans.* Amer. Soc. Metals (1940) 28, 797–807.

82. R. H. Thielemann: Some Effects of Composition and Heat Treatment on the High Temperature Rupture Properties of Ferrous Alloys. *Proc.* Amer. Soc. Test. Mat. (1940) 40, 788–804.

83. R. H. Thielemann: Correlation of High Temperature Creep and Rupture Test Results. *Trans.* Amer. Soc. Metals (1941) 29, 355–369

Engineering Properties of Heat-resistant Alloys

By Howard S. Avery,* Earnshaw Cook,* and J. A. Fellows,* Members A.I.M.E.

Heat-resistant alloys of the higher nickel and chromium ranges have been empirically developed through the practical experience of the past two decades to a position of significant industrial importance. Few quantitative metallurgical data have been published, however, that could be related directly to engineering specifications and design.

Inadequate information led to the inauguration, in 1934, of a research directed toward a better understanding of the properties and performance of these steels at temperatures between 1400° and 2000°F. Investigation was concentrated upon the 26 per cent Cr:12 per cent Ni type, which owes its extensive application to an excellent combination of economy, strength and surface stability at elevated temperatures. The requirements of the oil-refining industry have been prominent in influencing the scope and evolution of the program.

Creep strength at the maximum allowable deformation ranges has been employed to evaluate the merits of these alloys. Permissible elongation rates vary from 1.0 per cent in one million hours for turbine blades to 1.0 per cent in ten thousand hours for tube supports and heating-furnace equipment. Throughout this paper, the limiting creep stress (L.C.S.) for a given temperature has been defined as the stress that will produce a uniform elongation rate (stage II) of one per cent in ten thousand hours as *extrapolated* from rates per hour for tests of less than two thousand hours duration.

Certain current specifications require a minimum L.C.S. of 1600 lb. per sq. in. at 1800°F., of 3600 lb. per sq. in. at 1400°F., and include a tensile acceptance test at room temperature, after aging for 24 hr. at 1400°F., as a measure of embrittlement in service. An elongation of 4 per cent is considered satisfactory for general use, while a minimum of 9 per cent is prescribed on occasion. Many differences of opinion concerning the properties and performance of these alloys appear to result from their sensitivity to unappreciated variations of chemical analyses which, for example, may change their L.C.S. from 3500 to 350 lb. per sq. in. at 1800°F.

Within broad chemical limits, it is possible to balance the six or more important elements present to attain desirable properties with a number of different combinations. One method for adjusting the composition has been described under the sponsorship of the Alloy Casting Institute,[1] in which, by maintaining a substantially austenitic* alloy, optimum creep strength and minimum tendency to embrittle after aging are expected. Unless, however, the limits are undesirably close, it has not been possible to ensure a moderate range of strength and of ductility by any chemical specification alone. There is a definite need

[1] References are at the end of the paper.
* A condition defined by the A.C.I. as the composition balance obtained by a calculated "ratio factor" [RF = (Cr + 3(Si − 1) − 16C) ÷ Ni] of less than "1.7." The omission of nitrogen and other considerations restrict the validity of the formula.

for practical acceptance tests that can be used to reject unsuitable material and that will permit manufacture within a practical composition range.

and, if failure does not take place, plastic deformation will rapidly decrease the stress. Creep at high rates will then continue until: (1) the stresses are relieved by transfer of
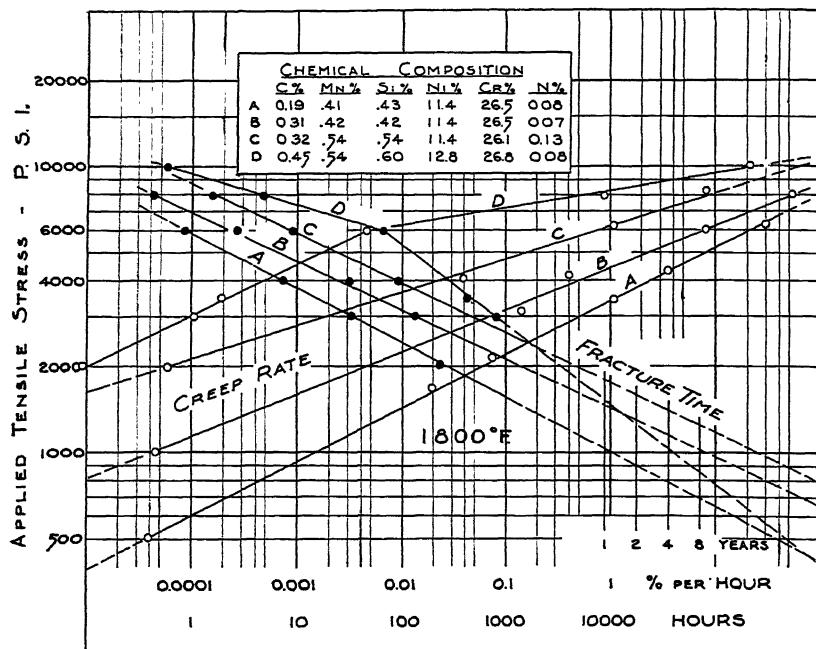
FIG. 1.—CREEP AND RUPTURE CHARACTERISTICS AT 1800°F. OF TYPICAL ALLOYS CONTAINING 26 PER CENT CHROMIUM AND 12 PER CENT NICKEL.

BASIC CONSIDERATIONS

Elastic properties have little application to high-temperature design. Instead, the plastic or creep properties are employed.[2] In the following discussion, resistance to deformation under constant load has been utilized as a basis for comparing the high-temperature strength of different alloys. The creep-testing techniques are described in a companion paper.[3] Elevated-temperature tensile tests, of which many are available,[1,4,5] differ from most service conditions in that they indicate behavior under stresses rapidly and continuously increasing to fracture, while industrial applications ordinarily involve lower, more constant stresses. With drastic overloading in service, accelerated elongation will result

load to adjacent structural units, or (2) stresses have fallen to safe working levels or (3) fracture occurs at some stress below the nominal yield strength. In service, the combination of circumstances that would simulate the tensile test is so rare, and the mechanical properties thus obtained so difficult to interpret, that no attempt to correlate such data with creep information has been made in this research.

Techniques that depend on the uncertain creep rates in stage I, such as Hatfield's time-yield test[6] or the German Industrial Tentative Standard (DVM A-117)[7] have similarly been neglected, since the continuously changing rates of stage I are not considered to furnish dependable data. The creep rates reported herein are those

of the minimum rate, or stage II period,[3] for both long-term creep and short-time stress-strain-rupture tests.

In using the minimum-rate data, how-

Rupture tests frequently have been made on the ferritic alloys employed for lower-temperature service, and the logarithmic nature of the plot has been well
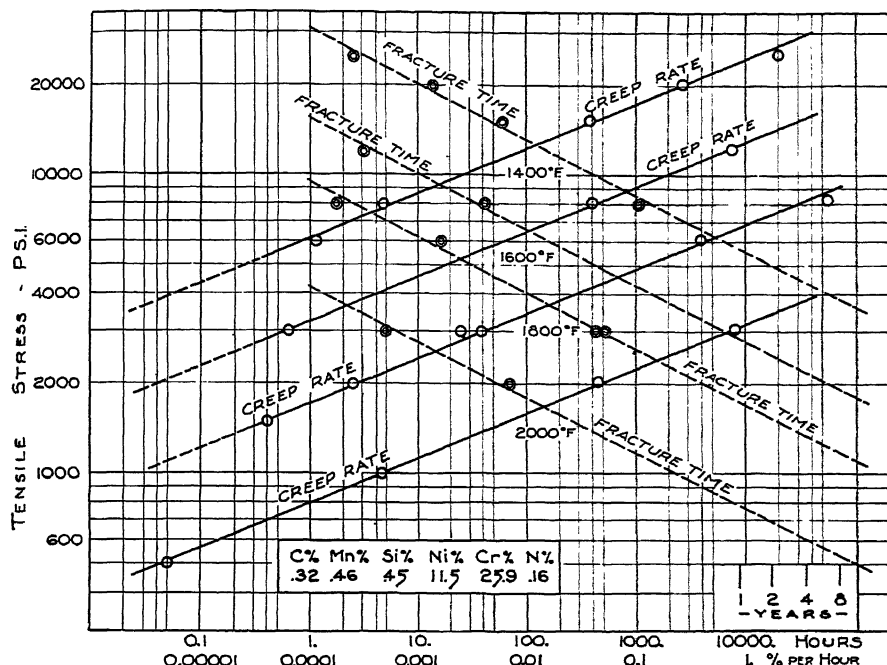
FIG. 2.—CREEP AND RUPTURE CHARACTERISTICS FROM 1400°F. TO 2000°F. FOR AN ALLOY CONTAINING 26 PER CENT CHROMIUM AND 12 PER CENT NICKEL.

ever, the considerable creep that occurs before and after this period should not be disregarded. There is danger in assuming that an extrapolated L.C.S. for 1 per cent elongation in 10,000 hr. can necessarily be sustained for that length of time without structural damage. The cumulative effect of stages I, II, and III can be obtained by creep tests continued to rupture, and may be expressed as life in hours. In a manner similar to the use of creep rates for determining limiting creep stress, the data may be extrapolated to a "maximum life expectancy." This term may be defined as the intercept of a time-to-fracture plot with a given stress coordinate as shown in Fig. 1.

established. The fracture-time behavior reported by several authors[8,9] has been confirmed for cast austenitic alloys at 1800°F. Stress-rupture tests are a valuable adjunct to creep tests and are especially useful for the selection of design stresses when plotted on the same graph, as in Figs. 1 and 2, if their limitations are understood. It is important to realize that, except for overloads that cause fracture within a few hundred hours, they represent extrapolation to durations of time for which few or no data are available. The term "maximum life expectancy" is probably justified, but there is no assurance that fracture will not occur at shorter times than are indicated by the extrapolation.

Since there is no evidence that life will exceed the indicated time, it is obviously unwise to employ stresses that the graph predicts will cause fracture *within* the intended service life, as may be done if creep-strength values alone are available. While these stress-rupture data thus permit the avoidance of definitely unsafe design loads, they do not always permit the estimation of safe maximum stresses.

The discontinuity of the fracture-time plot of the high-strength alloy of Fig. 1 demonstrates the need for caution. It is quite possible that similar slope changes might be found for more ductile alloys if the tests were continued for several years. Despite this limitation, the fracture plots permit illuminating comparisons of different alloys.

A combination of creep and fracture-time data at four temperatures can be arranged as in Fig. 2 to facilitate calculations for design. This is the result of comprehensive tests on one commercial foundry heat. The chemical composition has been established by more than 70 duplicate determinations as well as by analysis of a composite sample from 18 castings. Data after aging are given in Table 9, item 9A, and ductility under various conditions in Tables 5 and 6. This is a nonmagnetic, substantially austenitic alloy; the L.C.S. value of 1750 lb. per sq. in. at 1800°F. is conservative for such material (Fig. 12). In the application of the chart in Fig. 2 at 1800°F., for example, the intersection of the creep-rate curve with the 0.0001 per cent per hour coordinate indicates an L.C.S. of 1750 lb. per sq. in. Following the 1750-lb. per sq. in. stress coordinate to its intersection with the 1800°F. fracture-time graph suggests that fracture may occur in about 10,000 hr. (1.15 years) for this load. Unless these extrapolations can be shown to be unreliable, it is evident that designing for so short a life would not be considered good engineering practice. At 50 per cent of the L.C.S., a maximum life of more than

8 years is indicated for any selected temperature. In addition, safety factors should be included to compensate for the difference between the soundness of commercial castings and of laboratory test bars.

While unsatisfactory performance will result either from structural damage or from excessive flow, moderate deformation can be tolerated in most furnace construction. Succeeding information suggests that strength and ductility are inverse properties: the higher the L.C.S., the less the supportable elongation becomes. Designing to prevent premature failure with lower stresses is of more importance than the questionable economy of resorting to high creep strengths in the lighter, less homogeneous sections more difficult to produce in the foundry.

As previously reported,[3,12] these creep rates are valid and comparable only for nonfluctuating temperatures, and may be considerably accelerated by cycles of plus and minus 10°F. at 1800°F., for example, or by 48-hr. cycles covering the range between room temperature and 1800°F. This phenomenon is sometimes associated with the spheroidization and agglomeration of dispersed carbide particles.[12,13] It is not known whether cyclic heating adversely affects life as it does creep resistance. While fundamental research requires exact nonvarying temperature control, few industrial applications attain this precise regulation. Careful investigation of cyclic heating is an important subject for further research in the laboratory and in the field.

Thus far, strength has been described in terms of creep resistance and of useful life. The inverse property of ductility is more difficult to correlate with service performance. Ductility measurements from a variety of tests in current use are subject to the limitation that their magnitude is a function of the laboratory procedure as well as of characteristics of the material. Elongation to fracture at temperature

under constant load is of interest, as is the residual ductility after a period under stress at high temperature. Short-time, elevated-temperature tensile tests usually exhibit considerably greater plasticity than constant-load stress-rupture tests

FIG. 3.—FINE CARBIDE DISPERSION AND MASSIVE CARBIDE IN AUSTENITE MATRIX. X 2000.

Etchant: hot alkaline potassium ferricyanide. Analysis: C, 0.49 per cent; Mn, 1.08; Si, 0.74; Ni, 12.5; Cr, 27.0; N, 0.12. L.C.S. at 1800°F., 3500 lb. per sq. inch.

of moderate duration, while long-term creep tests to fracture are characterized by surprisingly low total elongation. This decreased ductility associated with long test periods has also been reported[8,9] for lower temperatures.

Elongation after aging without stress, as employed in current acceptance tests, permits a comparison of precipitation-hardening tendencies. As shown later, however, estimates of elevated-temperature ductility or of residual ductility after stressing at service temperatures are

frequently unreliable when based on room-temperature properties after aging.

METALLOGRAPHY

The cast 26 per cent Cr:12 per cent Ni alloys are austenitic, but carbides, ferrite,

FIG. 4.—SIGMA* MASSES (LIGHT GRAY; SOMETIMES CRACKED) AND COMPLEX CARBIDES (DARK GRAY) IN AUSTENITE MATRIX. X 500.

Etchant: 1:1 HCl, followed by hot alkaline potassium ferricyanide. Analysis: C, 0.28 per cent; Mn, 1.08; Si, 0.88; Ni, 12.2; Cr, 26.3; N, 0.12; Mo, 1.58.

History: Creep-tested 668 hr. under 1750 lb. per sq. in. at 1800°F. (creep rate: 0.00135 per cent per hour) followed by room-temperature tensile test (66,200 lb. per sq. in. tensile strength and 3.0 per cent elongation).

the brittle nonmagnetic sigma phase, a lamellar aggregate that resembles pearlite and nonmetallic inclusions also appear under certain conditions. Dendritic segre-

* The sigma phase is at first unattacked by 1:1 HCl, and frequently appears white and shining in a slightly darker austenite matrix. Further etching stains sigma a light brown and reveals previously invisible scratches. These, together with freedom from coloration by hot alkaline potassium ferricyanide, distinguish it from carbides. If ferrite occurs in the same specimen it usually is drastically attacked by 1:1 HCl before staining of the sigma occurs.

gation is usually present and sharply differentiates cast from wrought alloys. Finely precipitated carbides (Fig. 3) characterize the high-strength alloys and

tion, is weak and brittle as illustrated in Fig. 4. If elements like chromium and silicon are undesirably high, in proportion to the austenite stabilizers like nickel,

FIG. 5.—LAMELLAR STRUCTURE OCCURRING IN ALLOY CONTAINING 0.20 PER CENT NITROGEN, 0.39 PER CENT CARBON, 26 PER CENT CHROMIUM AND 12 PER CENT NICKEL. Creep-tested at 1800°F. Etchant: hot alkaline potassium ferricyanide. a, × 100; b, × 500.
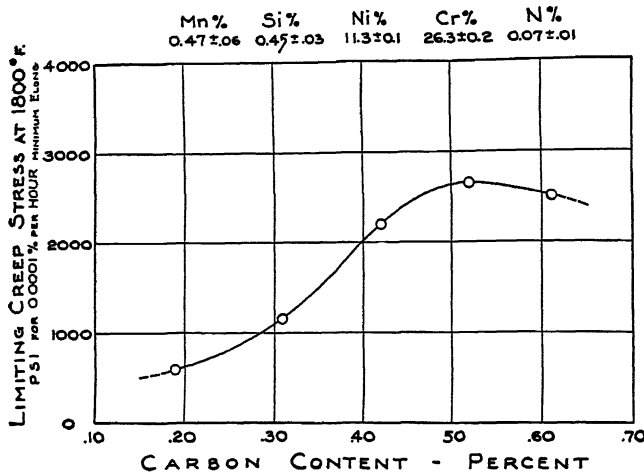
FIG. 6.—LIMITING CREEP STRESS AT 1800°F. VS. CARBON CONTENT.

massive carbide is found in nearly all heat-resistant compositions.

At elevated temperatures, ferrite is weak but very ductile. Its ferromagnetic nature permits quantitative estimation by magnetic analysis. Ferrite is not necessarily detrimental to performance, since under some circumstances the attendant ductility is known to be beneficial. In contrast, the undesirable sigma phase, probably induced by chromium segrega-

sigma may develop readily near 1600°F. Such alloys usually are quite ferritic at higher temperatures. Thus a limitation of ferrite content above 1800°F. may also restrict occurrence of sigma at 1600°F. or below, provided unusual sigma stabilizers, such as molybdenum (Fig. 4), are not present. Embrittlement resulting from small amounts of sigma, however, may be no more serious than that associated with carbide precipitation in the compositions

from which sigma has been excluded by more complete austenite stabilization.

The lamellar constituent (Fig. 5), which is nonmagnetic (and hence not pearlite), function of carbon content up to a maximum, as illustrated in Fig. 6. This change in tendency corresponds with the appearance of continuous networks of carbide

TABLE 1.—*Effects of Carbon on Heat-resistant Alloys Containing 26.3 Per Cent Chromium and 11.3 Per Cent Nickel*

Alloy No	Chemical Analysis, Per Cent						L.C.S. 1800°F., 0.0001 Per Cent per Hr., (1 Per Cent per 10,000 Hr.), Lb. per Sq. In.	Room-temperature Properties after Aging 1400°F. 24 Hr., F.C.		Elevated-temperature Ductility at 1400°F., 20,000 Lb. per Sq. In., Elongation, Per Cent in 2 In.
	C	Mn	Si	Ni	Cr	N		Tensile Strength, Lb. per Sq. In.	Elongation, Per Cent in 2 In.	
1A	0.19	0.41	0.43	11.4	26.5	0.08	600	83,000	30.0	26.5
1B	0.31	0.42	0.42	11.4	26.5	0.07	1,150	86,000	25.0	20.0
1C	0.42	0.45	0.45	11.3	26.1	0.06	2,200	89,000	12.5	9.5
1D	0.52	0.53	0.47	11.4	26.4	0.07	2,650	95,750	4.0	2.5
1E	0.61	0.51	0.48	11.4	26.3	0.07	2,500	93,900	2.8	1.5

Alloy No.	C, Per Cent	Creep Characteristics at 1800°F.			Residual Properties, Room Temperature		
		Load, Lb. per Sq. In.	Duration, Hr.	Minimum Rate, Per Cent per Hr.	Tensile Strength, Lb. per Sq. In.	Elongation, Per Cent	Permeability (H = 24)
1A	0.19	500	1,995	0.000040	81,500	27.0	2.83
1B	0.31	1,000	1,342	0.000043	81,500	15.0	1.81
1C	0.42	2,000	1,244	0.000047	73,500	6.0	1.20
1D	0.52	3,000	950	0.00016	Broke in creep test		1.00
1E	0.61	3,000	783	0.00026	Broke in creep test		1.00

seems to be associated with high nitrogen levels. For some compositions containing more than 0.20 per cent nitrogen, an unexpectedly high creep rate has been noted. It is possible that the lamellae comprise a weaker aggregate than the usual fine dispersions. Until this is clarified, nitrogen contents above 0.20 per cent cannot be employed with assurance.

Inclusions may be developed by certain phases of furnace or foundry practice. Their effect and detection is described later under aging tests (Table 10 and Fig. 8).

EFFECTS OF COMPOSITION

From 0.20 to 0.40 per cent carbon, creep strength is approximately doubled by an increment of 0.10 per cent, while ductility is simultaneously lowered (Table 1). The L.C.S. at 1800°F. seems to be a direct at the grain boundaries. Diminished strength after passing an optimum composition may be characteristic when the alloy is "overbalanced" by unnecessary amounts of austenite-stabilizing elements such as carbon, nitrogen, or nickel. In several unreported experiments, a peak in strength has appeared individually for these three elements.

Ferrite-forming elements, such as chromium, silicon, tungsten, or molybdenum, can be employed to increase ductility at the expense of strength if they do not lead to excessive sigma development.[10] Opposing these trends are the strengthening effects of nickel, nitrogen, and carbon. Several examples of the interactions of the various elements are shown in Table 2, where an increase of 0.10 per cent C or 0.07 per cent N serves to reduce ductility

and to double creep strength, and where a slight change in the nickel-chromium ratio is sufficient to restore the previous balance despite higher nitrogen. The range of properties that may be possible between the extremes of a narrow chemical specification is shown in Table 3. Variations in carbon, nickel, chromium and nitrogen account for the difference, which in practice might be greater because of the effects

TABLE 2.—*Sensitivity to Chemical Composition of Heat-resistant Alloys Containing 26 Per Cent Chromium and 11 Per Cent Nickel*

Alloy No.	Chemical Analysis, Per Cent						L.C.S. at 1800°F., 0.0001 Per Cent per Hr. (1 Per Cent per 10,000 Hr.), Lb. per Sq. In.	Elevated-temperature Stress-strain-rupture Tests, 20,000 Lb. per Sq. In. at 1400°F.		
	C	Mn	Si	Ni	Cr	N		Life, Hr.	Rate, Per Cent per Hr.	Elongation, Per Cent in 2 In.
2A	0.31	0.42	0.42	11.4	26.5	0.07	1,150	2.6	5.09	20.0
2B	0.42	0.45	0.45	11.3	26.1	0.06	2,200	10.3	0.65	9.5
2C	0.32	0.54	0.54	11.4	26.1	0.13	2,100	8.3	0.71	8.5
2D	0.31	0.51	0.53	10.6	26.8	0.14	1,160	6.9	1.45	15.5

TABLE 3.—*Variations that May Occur within Narrow Specification Limits on Molybdenum Alloy Containing 26 Per Cent Chromium and 12 Per Cent Nickel*

Alloy No.	Chemical Analysis, Per Cent							Ratio[a] Factor	As Cast	
	C	Mn	Si	Ni	Cr	N	Mo		Tensile Strength, Lb. per Sq. In.	Elongation in 2 In., Per Cent
Spec.	$\frac{0.31}{0.37}$	0.50	0.50	$\frac{10.5}{12.0}$	$\frac{25.5}{27.0}$	$\frac{0.16}{0.20}$	1.00			
3A	0.31	0.48	0.55	10.8	27.1	0.16	1.05	2.05	92,500	22.5
3B	0.33	0.47	0.51	11.4	26.3	0.19	1.01	1.84	91,000	23.5
3C	0.37	0.47	0.58	12.0	25.4	0.19	1.01	1.62	92,500	19.5

Alloy No.	C, Per Cent	L.C.S. 1800°F., 0.0001 Per Cent per Hr., (1 Per Cent per 10,000 Hr.), Lb. per Sq. In.	Room-temperature Properties after Aging 1400°F., 24 Hr., Furnace Cool		Elevated-temperature Stress-strain-rupture Tests, 1400°F., 20,000 Lb. per Sq. In.		
			Tensile Strength, Lb. per Sq. In.	Elongation, Per Cent in 2 In.	Life, Hr.	Rate, Per Cent per Hr.	Elongation, Per Cent in 2 In.
3A	0.31	830	95,750	20.8	11.6	1.01	16.0
3B	0.33		96,250	14.5	17.0	0.26	6.0
3C	0.37	2,200	102,400	8.3	25.4	0.04	1.5

Alloy No.	C, Per Cent	Creep Characteristics at 1800°F.				Room-temperature Residual Properties		
		Stress, Lb. per Sq. In.	Duration, Hr.	Rate, Per Cent per Hr.	Elongation, Per Cent	Tensile Stress, Lb. per Sq. In.	Elongation, Per Cent in 2 In.	Permeability H = 24
3A	0.31	2,000	290	0.0118	3.8	74,500	7.0	2.125
3C	0.37	2,000	1,115	0.000055	0.12	80,500	3.0	1.003

[a] Ratio factor[1] $= \dfrac{Cr - 16C}{Ni}$

of other elements. This evident sensitivity to apparently minor alloy changes should not be interpreted to mean that acceptable mechanical properties cannot be maintained in the foundry with adequate technical control.

ing various conditions of high-temperature corrosion.

STRENGTH VS. DUCTILITY

There are differences of opinion concerning the relative importance of strength
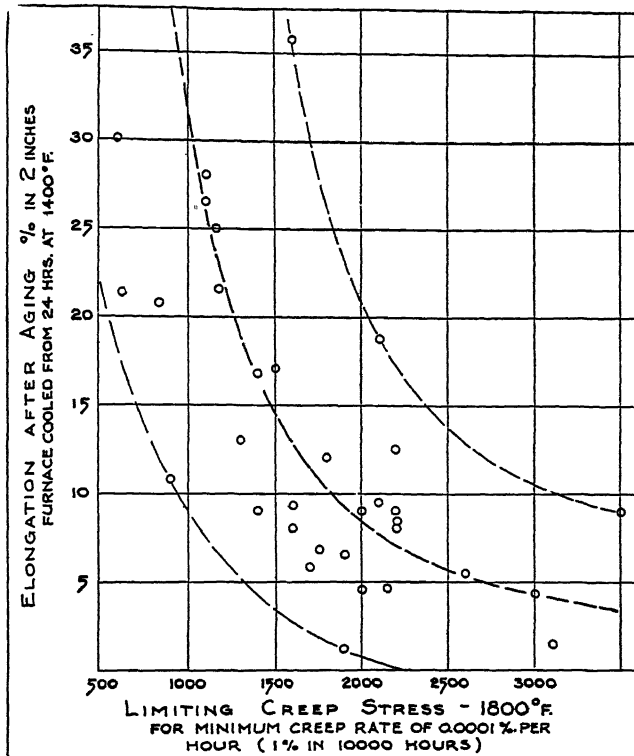
FIG. 7.—INVERSE RELATIONSHIP OF CREEP STRENGTH AND DUCTILITY AFTER AGING.

In balancing compositions of the 26 per cent Cr:12 per cent Ni type to obtain maximum strength and minimum sigma embrittlement, higher nickel and lower chromium contents are logical. Surface stability in hot gases may require high chromium levels while in the presence of sulphur attack the lowest practicable nickel percentage is desirable. Present knowledge of limiting chromium and nickel contents is qualitative. There is a definite need for further delineation of the maximum nickel and the minimum chromium concentrations necessary for resist-

and ductility in the performance of heat-resistant alloys. It has been postulated that a ductile material will relieve overloads by plastic flow. Conversely, it is thought that sufficient strength obviates the need for stress relief by deformation. By comparing the behavior of several alloys, whose stress-strain-rupture characteristics are shown in Fig. 1, the relation of strength and ductility becomes clearer. These compositions are arranged in Table 4 in order of increasing strength and decreasing ductility. The life expectancy of the more ductile alloys appears to be

greater when all are stressed to produce the same creep rate, but, with the same load, the strong analyses have a longer probable life unless a break in the fracture-time plot appears (Fig. 1).

mum L.C.S. at 1800°F. of 1600 lb. per sq. in. is required as certain specifications intend, only C (2100 lb. per sq. in.) and D (3000 lb. per sq. in.) are acceptable. The extreme sensitivity to compositional varia-

TABLE 4.—*Life Expectancy versus Creep Rates and Stress at 1800°F.*[a]

Alloy No.	Chemical Analysis, Per Cent						L.C.S. 1800°F., Lb. per Sq. In.	Design Stress,[b] 1800°F., Lb. per Sq. In.	Elevated-temperature Elongation, 1400°F., 20,000 Lb. per Sq. In., Per Cent in 2 In.
	C	Mn	Si	Ni	Cr	N			
A	0.19	0.41	0.43	11.4	26.5	0.08	600	300	26.5
B	0.31	0.42	0.42	11.4	26.5	0.07	1,150	575	20.0
C	0.32	0.54	0.54	11.4	26.1	0.13	2,100	1,050	8.5
D	0.45	0.54	0.60	12.8	26.8	0.08	3,000	[c] 1,500	1.5

Alloy No.	Stress at 1800°F., Lb. per Sq. In., for Maximum Life of			Maximum Life at 1800°F. for	
	10,000 Hr.	2 Years	8 Years	L.C.S., Hr.	Design Stress,[b] Hr.
A	1,000	900	680	140,000	5,000,000
B	1,450	1,300	1,000	32,000	1,900,000
C	1,750	1,600	1,250	3,200	200,000
D	1,500	1,300	850	816	10,000

Alloy No.	Constant Stress at 1800°F.			Constant Minimum Creep Rate at 1800°F.		
	Stress,[b] Lb. per Sq. In.	Creep Rate, Per Cent per 10,000 Hr.	Maximum Life, Hr.	Stress, Lb. per Sq. In.	Creep Rate, Per Cent per 10,000 Hr.	Maximum Life, Hr.
A	800	5.0	30,000	380	0.1	1,000,000
B	800	0.1	300,000	800	0.1	300,000
C	800	0.00023	1,000,000	1,600	0.1	15,000
D	800	0.0006	80,000	2,000	0.1	3,500

[a] The extrapolated time values shown here should not be considered suitable for engineering calculations. They are tabulated only for purposes of comparison.
[b] Design stress = maximum recommended tensile working stress. The design stress for 1600 lb. per sq. in. L.C.S. material is 800 lb. per sq. in., which is a current specification level.

With conservative design stresses, suitable for the weakest composition, all of the alloys illustrated may be expected to give satisfactory service at 1800°F. An optimum combination of moderate ductility and reasonably high strength might be that of item C in Table 4. This alloy is *substantially*, but not completely, austenitic, since minor amounts of ferrite appear at some temperatures. Alloys similar to B, C, and D have been satisfactory in field installations involving approximately constant temperatures and good design. If a mini-

tions indicates, however, that alloys like B (1150 lb. per sq. in.), are passed without question because the present acceptance test, which has an inverse correlation with creep strength (Fig. 7), places a premium on ductility. Nevertheless, the life expectancy of the B type at the actual working stress of the specification is probably satisfactory and service failures may not result. Insistence upon a ductility specification for acceptance tests implies its importance in design. Until clarified by more specific engineering knowledge,

neither the limits, the inherent type, nor even the method for ductility determination can be selected with assurance.

DUCTILITY

If ductility is an asset, the technique of its measurement is important. The nearest laboratory approach to uniform-temperature service conditions involves creep tests continued to fracture. Here the total elongation seems closely related to the deformation rate for constant temperature with various loads (Table 5) and for constant stress at various temperatures (Table 6). In each instance, the low elongation rates of the longer tests are associated with low total elongation at fracture. This is in agreement with observations[8,12] upon ferritic steels at lower temperatures.

TABLE 5.—*Effect of Various Loads at Constant Temperature on Deformation Rate and Ductility of Creep Tests Continued to Fracture*

Heat No.	Chemical Analysis, Per Cent					
	C	Mn	Si	Ni	Cr	N
CH518ª	0.32	0.46	0.45	11.5	25.9	0.16

Temperature, Deg. F.	Stress, Lb. per Sq. In.	Duration, Hr.	Minimum Creep Rate, Per Cent per Hr.	Total Elongation, Per Cent
1800	8,000	1.7	5.7	21.9
1800	6,000	16.6	0.4	12.2
1800	3,000	530	0.0039	6.0
1800	3,000	440	0.0025	4.0
1400	25,000	2.5	1.99	7.8
1400	20,000	13.9	0.26	5.5
1400	15,000	60.3	0.038	3.0
1400	8,000	1,070	0.00047	1.0

ª See also Fig. 2.

With stress, time, temperature and composition as variables affecting ductility, selection of a suitable reference test is difficult. A practical method for comparing elongation at constant temperature and stress utilizes stress-strain-rupture tests

as reported in Tables 1, 2, 3, 9 and 11. While time is still a variable, these tests more closely approximate service conditions under excessive loads than any other rapid technique. At 1400°F. (Tables 3, 11), embrittlement of austenitic alloys is developed more effectively than by aging tests.

TABLE 6.—*Effect of Temperature at Constant Load on Ductility of Creep Tests Continued to Fracture*

Heat No.	Chemical Analysis, Per Cent					
	C	Mn	Si	Ni	Cr	N
CH518ª	0.32	0.46	0.45	11.5	25.9	0.16

Temperature, Deg. F.	Stress, Lb. per Sq. In.	Duration, Hr.	Minimum Creep Rate, Per Cent per Hr.	Total Elongation, Per Cent
2000	3,000	6	0.81	20.0
1800	3,000	530	0.0039	6.0
1800	3,000	440	0.0025	4.0
1800	8,000	1.7	5.7	21.9
1600	8,000	41.4	0.04	4.0
1400	8,000	1,070	0.00047	1.0

ª See also Fig. 2.

Brittle failures sometimes occur at room temperature while installations that have operated for extended periods between 1400°F. and 2000°F. are being repaired. As a result, residual ductility, which corresponds to the room-temperature tensile properties of an unfractured specimen after creep testing, has been specified as a desirable characteristic. In an attempt to ensure such ductility, the tensile acceptance test after aging at 1400°F. or 1600°F. has often been employed. There is a general correlation of such tests with residual ductility after creep testing when both tests are responding to precipitation-hardening as in Table 1. It is important to realize, however, that this apparent similarity is invalidated if low residual ductility is the result of structural damage

from overstressing, which, rather than embrittlement as such, is probably the cause of many service failures observed at room temperature. An example is shown

and the residual elongation of 11.5 per cent seems characteristic, since two other tests under loads of 1000 and 2000 lb. per sq. in. exhibited similar values of 10 per cent and

TABLE 7.—*Relationship of Stress and Residual Ductility*
Chemical Composition, Per Cent

C	Mn	Si	Ni	Cr	N	W
0.29	1.16	1.02	12.2	26.6	0.12	0.55

Aging Treatment			Room-temperature Properties after Aging			
Temperature, Deg. F.	Time, Hr.	Cooling	Yield Strength, Lb. per Sq. In.	Tensile Strength, Lb. per Sq. In.	Elongation, Per Cent in 2 In.	Reduction of Area, Per Cent
1400	24	Fce.	41,500	91,750	30.0	34.5
1400	24	Fce.	39,500	91,000	23.0	32.5

Creep Test Conditions				Residual Properties at Room Temperature			
Temperature, Deg. F.	Stress, Lb. per Sq. In.	Duration, Hr.	Rate, Per Cent per Hr.	Tensile Strength, Lb. per Sq. In.	Elongation, Per Cent in 2 In.	Reduction of Area, Per Cent	Hardness, B.H.N.
1800	1,000	983	0.00008	87,000	16.5	30.0	192
1800	1,650	1,007	0.00045	55,200	1.5	1.0	192

in Table 7, where an alloy with excellent ductility after aging and after creep testing at 1000 lb. per sq. in. shows a serious loss in residual ductility from overloading at 1650 lb. per sq. in. This effect has been observed repeatedly in conjunction with specimens that show evidence of intergranular oxidation on the fracture faces.

The residual ductility at room temperature decreases with increasing *load* for approximately constant time at 1800°F., as illustrated in Table 7, and diminishes also with increasing *time* under constant load, as shown in Table 8. With stresses from 4000 to 8000 lb. per sq. in., fracture occurs quickly and the total elongation is high. At 2500 lb. per sq. in. there is a drop from 37 per cent elongation as cast to 15 per cent after 24 hr. at 1800°F. This is probably indicative of carbide precipitation in stage I. After 186 hr. at 2500 lb. per sq. in., the next test was in stage II,

11 per cent when terminated in stage II after 1095 hr. The elongation of 4.5 per cent after 600 hr. under 2500 lb. per sq. in. (in stage III) is considered representative of structural damage, which, by slowly increasing, resulted in fracture of a companion bar after 1897 hr. It seems probable that residual ductility rapidly disappears if stage III is induced and continued in these steels by overloading above 1400°F. The specification of high elongation after aging is no insurance of residual ductility or of freedom from failure under this condition. The limiting creep strength of the material *in relation to the selection of working stresses* is of paramount importance in design.

An aging test employed as an index of precipitation-hardening may be misleading if the formation of an embrittling constituent such as sigma is sluggish. In Table 9 are shown two alloys that differ in silicon

TABLE 8.—*Effect of Stress and Time on Ductility*

| Alloy No. | Chemical Analysis, Per Cent | | | | | | Ratio Factor |
	C	Mn	Si	Ni	Cr	N	
8A	0.32	0.54	0.54	11.4	26.1	0.13	1.84
8B	0.33	0.56	0.49	11.5	26.4	0.12	1.85

| Alloy No. | 1800°F. Creep-test Data | | | | Room-temperature Residual Properties | | |
	Stress, Lb. per Sq. In.	Duration, Hr.	Rate (II), Per Cent per Hr.	Elongation, Per Cent in 2 In.	Tensile Strength, Lb. per Sq. In.	Elongation, Per Cent in 2 In.	Reduction of Area, Per Cent
8B	As cast				91,250	37.0	41.6
8A	8,000	1.6	8.8	27.0		Broke in creep test	
8B	6,000	9.3	1.2	21.0		Broke in creep test	
8A	6,000	9.2	1.1	24.5		Broke in creep test	
8A	4,000	96.4	0.04	11.0		Broke in creep test	
8B	2,500	24	a		90,000	15.0	16.5
8B	2,500	186	0.0004	0.1	88,000	11.5	13.4
8B	2,500	600	0.00027	0.2	71,500	4.5	9.6
8B	2,500	1,897	0.00014	1.0		Broke in creep test	
8A	2,000	1,095	0.00006	0.1	79,500	10.0	7.7
8A	1,000	1,095	0.00001	0.05	83,500	11.0	11.5

a Obviously in stage I (0.0024 per cent per hour) at end of 24 hours.

TABLE 9.—*Relative Embrittlement in Short and Long-time Tests*

| Alloy No. | Chemical Analysis, Per Cent | | | | | | Ratio[a] Factor |
	C	Mn	Si	Ni	Cr	N	
9A	0.32	0.46	0.45	11.5	25.9	0.16	1.82
9B	0.29	0.53	1.56	11.5	26.3	0.15	2.03

| Alloy No. | Si, Per Cent | L.C.S. 1400° F. 0.0001 Per Cent per Hr. (1 Per Cent per 10,000 Hr.), Lb. per Sq. In. | Room-temperature Properties after Aging, 1400°F., 24 Hr., F.C. | | Elevated-temperature Stress-strain-rupture Tests, 1400°F., 20,000 Lb. per Sq. In. | | |
			Tensile Strength, Lb. per Sq. In.	Elongation, Per Cent in 2 In.	Life, Hr.	Rate, Per Cent per Hr.	Elongation, Per Cent in 2 In.
9A	0.45	5,950	87,625	6.8	13.9	0.26	5.5
9B	1.56	4,300	93,750	19.8	22.3	0.63	23.5

| Alloy No. | Si, Per Cent | Creep Characteristics at 1400°F. | | | | Room-temperature Residual Properties | |
		Stress, Lb. per Sq. In.	Duration, Hr.	Rate, Per Cent per Hr.	Elongation, Per Cent in 2 In.	Tensile Strength, Lb. per Sq. In.	Elongation, Per Cent in 2 In.
9A	0.45	6,000	1,150	0.00012	0.19	70,500	3.0
9B	1.56	4,000	1,033	0.00007	0.12	81,250	2.0

a Ratio factor: $\dfrac{Cr + 3(Si - 1.0) - 16C}{Ni}$

content; that with the higher silicon is much more ductile than the other in short-time tests but after more than 1000 hr. under stress* at 1400°F. the residual

inherently defective metal by tensile tests after aging. Defects tend to lower both tensile strength and ductility, as is demonstrated in Table 10. This effect is attributed

TABLE 10.—*Acceptance-test Properties of Unsatisfactory and Satisfactory Alloys Containing 26 Per Cent Chromium and 12 Per Cent Nickel*

Alloy No.	Description	Chemical Analysis,[a] Per Cent					
		C	Mn	Si	Ni	Cr	N
10A	Before remelting	0.27	0.55	0.45	11.4	26.8	0.13
10B	After remelting	0.30	0.55	0.57	11.1	26.2	0.14

Alloy No.	Description	Room-temperature Properties after Aging, 1400°F., 24 Hr., Furnace Cool			
		Yield Strength, Lb. per Sq. In.	Tensile Strength, Lb. per Sq. In.	Elongation, Per Cent in 2 In.	Reduction of Area, Per Cent
10A	{ Unsatisfactory { Before remelting	42,500 38,850	78,350 69,750	6.5 7.0	5.0 11.0
10B	{ Satisfactory { After remelting	41,900 42,450	93,700 92,900	20.5 18.0	24.0 21.5
	} Satisfactory { After remelting		94,500 94,500	23.5 19.5	24.6 21.7

[a] Average of determinations in two laboratories. The remelt (alloy 10B) consisted of 98 per cent orignal material from 10A and 2 per cent of alloy additions to compensate melting losses.

elongations of the two are about equal. This pronounced drop in elongation for the higher silicon analysis is attributed to the formation of the sigma phase.

Since precipitation of carbides, as contrasted with sigma, is usually rapid, the elongation after aging for 24 hr. provides useful information in such cases. Referring again to Table 1, it appears that a minimum elongation of 4 per cent would reject alloys that are "overbalanced," such as those which fall to the right of the peak in the plot of L.C.S. versus composition (Fig. 6). The utility of this procedure probably is confined to the substantially austenitic alloys.

Beyond the functions described, some importance is attached to the detection of

to nonmetallic inclusions of the type illustrated in Fig. 8. Normal elongation may vary over a wide range: unless the characteristic values are known, a low figure accompanied by high tensile strength may indicate strong rather than defective material (Fig. 7). Since the tensile-strength level is less variable with composition and structure, it is suggested that a minimum of 80,000 lb. per sq. in. after furnace cooling from 24 hr. at 1400°F. is a better criterion for sound metal than is elongation.

With its ability to evaluate carbide precipitation, to indicate the presence of serious inclusions and to reject badly overbalanced compositions, there is considerable justification for an acceptance test after aging. Unfortunately, when used alone, it tends to place a premium upon weaker alloys. As shown in Fig. 7, the inverse correlation is not sufficiently reliable, however, to permit the use of low ductility as a measure of high creep strength. Some

* Both of the creep tests were discontinued in stage II, to avoid complications from structural damage. The lower load on the 1.56 per cent Si material was necessary to prevent appearance of stage III during the time period used.

estimate of load-carrying ability is needed as a primary acceptance test.

appear. Plastic flow will rapidly reduce severe stresses to the vicinity of a pseudo
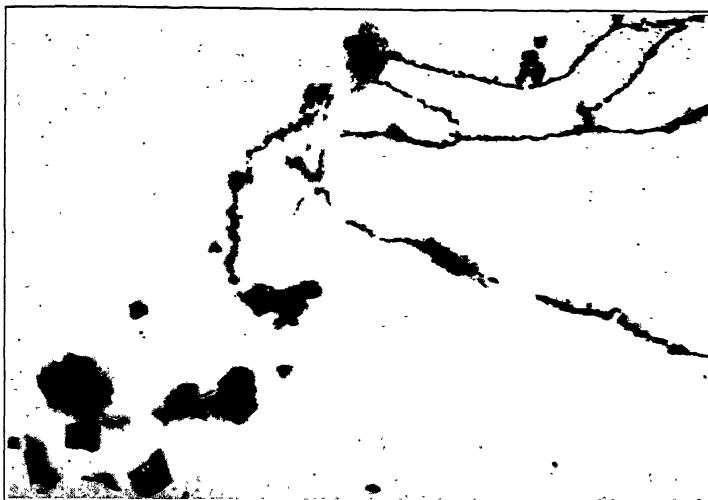
FIG. 8.—OXIDE INCLUSIONS IN ALLOY CONTAINING 26 PER CENT CHROMIUM AND 12 PER CENT NICKEL. UNETCHED. X 300.
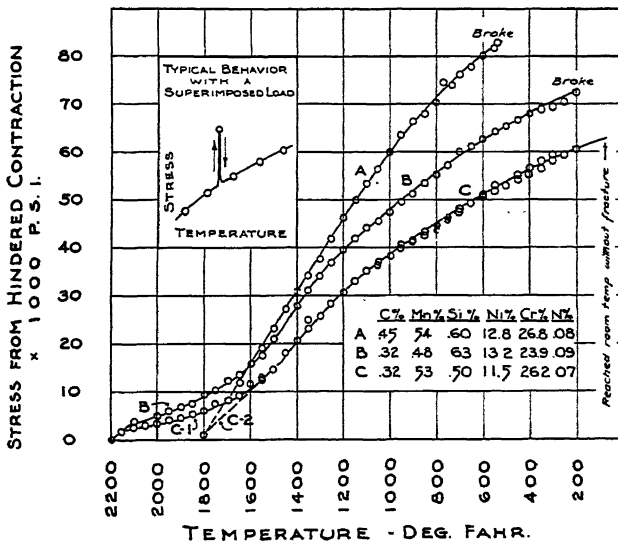
FIG. 9.—STRESSES RESULTING FROM HINDERED THERMAL CONTRACTION.

THERMAL STRESSES

If thermal contraction of these alloys is hindered, either by fixed anchorages or by the rigidity of a casting subjected to differential cooling, serious stresses will

"yield strength." Thereafter, or for stresses below this, stress relief is very slow and is dependent upon the creep characteristics of the material. The limits for rapid stress relief at various temperatures have been

determined experimentally with three alloys.

By heating a specimen (16 by ⅞-in. diameter with 1 by 0.505-in. gauge length) to high temperature in a tensile machine, applying a small load to remove any slack in the system and then slowly cooling the test bar, the unrelieved stress characteristic of each temperature appears on the load indicator of the machine.[a] These data are plotted in Fig. 9. In parallel experiments it was found, by arresting cooling at some temperature and by applying an additional load, that within a few minutes the increased stresses were reduced by flow to values corresponding to the temperatures shown in Fig. 9, but stress decrease thereafter was scarcely perceptible. Further changes, of course, could have been measured by more precise methods.

Interpretation of these data suggests that the more ductile alloys are less susceptible to fracture from thermal causes and, because of their lower strength, they intrinsically develop lower thermal stresses than do materials of higher strength. It follows that hindered contraction or temperature gradients are inherently more dangerous to the high-strength materials. Weaker, ductile compositions thus have a definite field of usefulness because, in appropriate sections, they can replace lighter castings of high strength to provide a greater factor of safety for installations where excessive thermal stresses cannot be avoided in design.

A flexible specification should permit choice between *strong* alloys that may be most economical under well-controlled and precisely known service conditions and weaker, more *ductile* material for struc-

[a] Elastic deflection of the lower crosshead, as measured by a dial gauge, was compensated, but flexing of the upper crosshead undoubtedly permitted some stress relief not reflected by elongation of the specimen. Except for the first few values, this does not affect the indicated stress.

tures where accidental or unavoidable thermal stresses may become a serious factor, and where the possibility of distortion is preferred to that of actual fracture.

It is significant that the stress-strain-rupture test (Table 11) is able to rank the

TABLE 11.—*Ductility Evaluation by 1400°F. Stress-strain-rupture Test[a]*

Alloy No.	Chemical Analysis, Per Cent						L.C.S., 1800°F., Lb. per Sq. In.
	C	Mn	Si	Ni	Cr	N	
11A	0.45	0.54	0.60	12.8	26.8	0.08	3,000
11B	0.32	0.48	0.63	13.2	23.9	0.09	2,500[b]
11C	0.32	0.53	0.50	11.5	26.2	0.07	1,200[b]

Alloy No.	Elevated-temperature Stress-strain-rupture Test at 1400°F., 20,000 Lb. per Sq. In.			Room-temperature Properties after Aging, 1400°F. 24 Hr., F.C., Elongation, Per Cent in 2 In.
	Life, Hr.	Rate, Per Cent per Hr.	Elongation, Per Cent in 2 In.	
11A	29.5	0.30	1.5	4.3
11B	15.5	0.14	3.5	11.3
11C	2.9	4.9	24.0	28.3

[a] These short times at 1400°F. are considered inadequate for detecting the effect of the sigma phase after long heating. They are especially effective for indicating carbide precipitation.
[b] Approximate value estimated from data on comparable analyses.

three alloys of Fig. 9 in ductility, creep resistance, and length of time for which loads near the range of rapid stress relief can be sustained without failure. Of these factors, ductility appears as the most important for avoiding fracture. It is suggested that compositions that show low elongation in the stress-strain-rupture test will fracture under overloads before plastic flow has reduced the excessive stresses to a safe working level. The most ductile alloy (C, Fig. 9) is typical of compositions with wide industrial application. Not only did test bars C1 and C2 survive the initial hindered contraction tests, but the speci-

men C2 cooled from 1800°F. also endured a second identical test (not shown) from

FIG. 10.—CORRELATION OF SINGLE STRESS-STRAIN-RUPTURE TESTS WITH LIMITING CREEP STRESS FOR THE SAME COMPOSITION.

1800°F. to room temperature without breaking.

STRESS-STRAIN-RUPTURE TESTS

Because they have a definite relation to long-term creep tests (Figs. 1 and 2), because they furnish important information about ductility at service temperatures, and particularly because they present a true picture of behavior under overload, stress-strain-rupture tests have been considered for acceptance testing. Either fracture time or strain rate is an approximate function of limiting creep stress, as appears from the plot of a dozen representative heats in Fig. 10. However, the variations are serious. For example, at 1800°F. and 6000 lb. per sq. in., a life of 10 hr. or a minimum (stage II) strain rate of 1 per cent per hour would indicate a probable L.C.S. at 1800°F. of 1500 lb. per sq. in., but with a possible error of 500 lb. per sq. in. This lack of precise correlation is the result of differences in the slope of plots as typified by Fig. 1. Despite

this objection, the data resulting from this method are believed to be more indicative of probable service performance than any current acceptance test for the Cr-Ni-Fe alloys. A standardized stress-strain-rupture

TABLE 12.—*Magnetic Analysis of Heat-resistant Alloys*

Heat No.	Chemical Analysis, Per Cent					
	C	Mn	Si	Ni	Cr	N
XF37	0.19	0.41	0.43	11.4	26.5	0.08
XF38	0.31	0.42	0.42	11.4	26.5	0.07
XF39	0.42	0.45	0.45	11.3	26.1	0.06
XF51	0.32	0.54	0.54	11.4	26.1	0.13
XH61	0.33	0.56	0.49	11.5	26.4	0.12

Heat No.	L.C.S., 1800°F., Lb. per Sq. In.	Permeability (H = 24)			
		As Cast	After Testing at 1800°F.		After Heat-treatment, 2000°F., 24 Hr., Water Quench
			S.S.R. Tests	Creep Tests	
XF37	600	1.60	1.96	2.83	2.01
XF38	1,150	1.05	1.30	1.81	1.39
XF39	2,200	1.01	1.10	1.20	1.02
XF51	2,100	1.02	1.08	1.15	1.02
XH61	2,150	1.04	1.07	1.12	1.07

test at either 1400°F. and 20,000 lb. per sq. in. or 1800°F. and 6000 lb. per sq. in. might be suggested for this purpose if the

MAGNETIC ANALYSIS

Differences in the strengths of alloys with varying amounts of ferrite (Fig. 11)
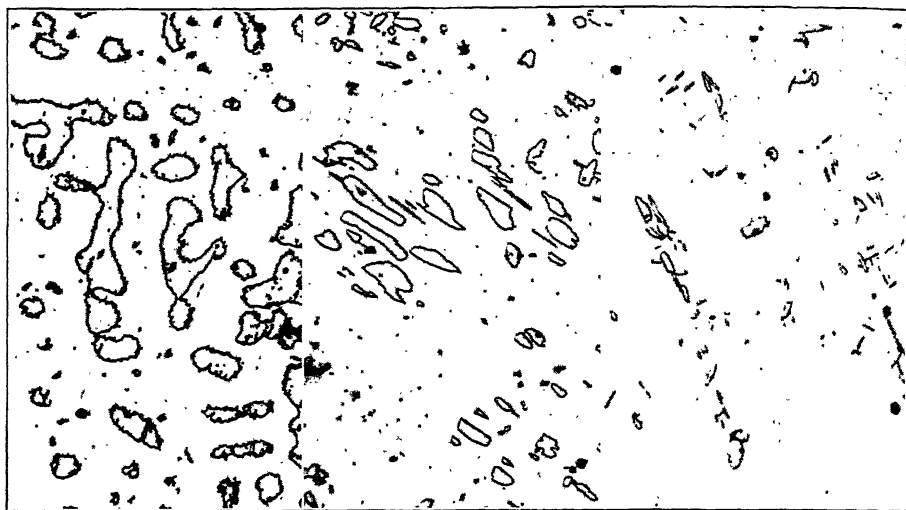
| Alloy 1A, Mu = 2.83 | Alloy 1B, Mu = 1.81 | Alloy 1C, Mu = 1.20 |
| L.C.S. at 1800°F. = 600 lb. per sq. in. | L.C.S. at 1800°F. = 1150 lb. per sq. in. | L.C.S. at 1800°F. = 2200 lb. per sq. in. |

FIG. 11.—FERRITE DISTRIBUTION IN ALLOYS CONTAINING 26.3 PER CENT CHROMIUM AND 11.3 PER CENT NICKEL AFTER CREEP TESTING AT 1800°F. × 135.
Etchant: 1:1 HCl, cold.

necessary precision of testing procedure were not confined to creep laboratory

TABLE 13.—*Effect of Time at Temperature on Permeability*

Heat No.	Chemical Analysis, Per Cent					
	C	Mn	Si	Ni	Cr	N
XH61	0.33	0.56	0.49	11.5	26.4	0.12
XH63	0.32	0.53	0.50	11.5	26.2	0.07

Heat No.	Permeability (H = 24) after Heat-treatment and Water-quenching			
	1800°F., 1 Hr.	1800°F., 24 Hr.	2000°F., 1 Hr.	2000°F., 24 Hr.
XH61	1.003	1.054	1.018	1.066
XH63	1.033	1.180	1.300	1.558

practice, and if magnetic analysis did not offer more interesting possibilities.

suggested that magnetic permeability measurements be used for quantitatively evaluating the extent of this phase. A survey of several heats (Table 12) indicates that ferromagnetism increases with time under stress at 1800°F. and that there is a direct relationship between creep strength and permeability* after creep testing. A plot of L.C.S. at 1800°F. versus permeability for specimens from the gauge lengths of creep bars yields the interesting correlation of Fig. 12. These data are derived from tests employing various stresses sustained for different times.

* The permeability values reported herein are based on the calibration supplied by the manufacturer with a custom-built instrument. They are reproducible, but their accuracy in terms of absolute electromagnetic units has not been fully established. Interlaboratory checking is in progress, and any correction factor found necessary will be made available.

For precise acceptance testing, a uniform reference treatment is necessary since as-cast values (Fig. 14 and Table 12) are not satisfactory. Hence, heating in ferrite-

The point at 800 lb. per sq. in. is at considerable variance with the trend. This heat, with 0.20 per cent C and 0.15 per cent N, is not a commercial composi-
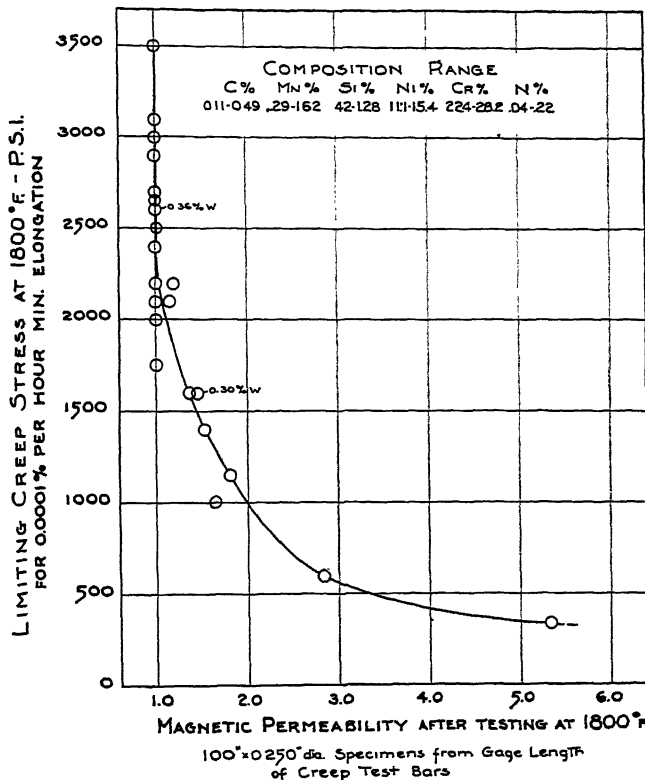
FIG. 12.—CORRELATION OF CREEP STRENGTH AND MAGNETIC PERMEABILITY AFTER CREEP TESTING.

promoting temperature ranges was investigated. Because experiments demonstrated that time at temperature without stress increased permeability (Table 13), a period of 24 hr. was selected. Longer intervals might develop additional ferrite and more closely approximate equilibrium, but would excessively delay foundry production. Since maximum development of ferrite occurs at 2000°F. for a number of compositions (Fig. 13), a treatment at 2000°F. for 24 hr. was established, followed by water quenching to arrest possible transformation during cooling. The relation with creep strength appears in Fig. 14.

tion. It is probable that more evidence will delineate a zone on either side of the plot indicative of the possible error for commercial alloys. Unless this uncertainty becomes greater than the probable error in Fig. 10 for stress-strain-rupture tests, the correlation justifies magnetic acceptance testing in conjunction with tensile tests after aging at 1400°F. for 24 hr. The companion aging test may be quite important for detecting seriously over-balanced compositions at 1.00 permeability where the magnetic test can no longer quantitatively appraise the alloy balance. Magnetic analysis is less expen-
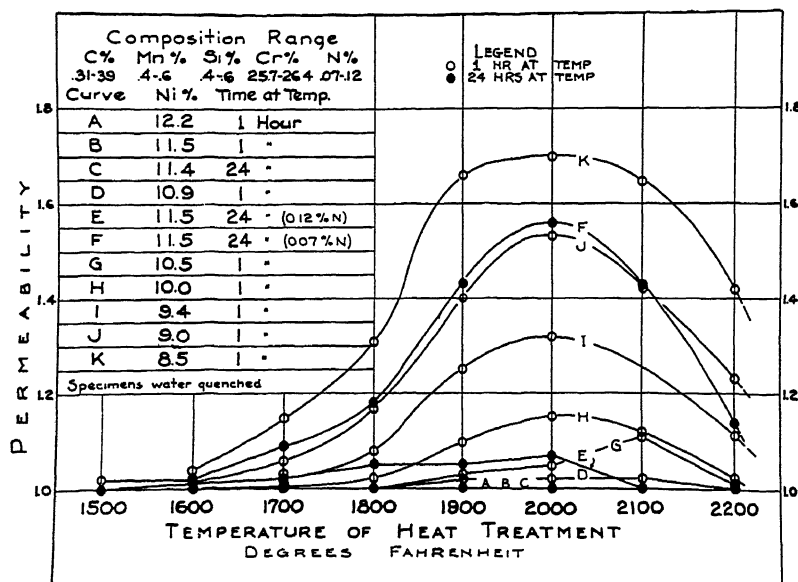
FIG. 13.—EFFECT OF TEMPERATURE ON PERMEABILITY.
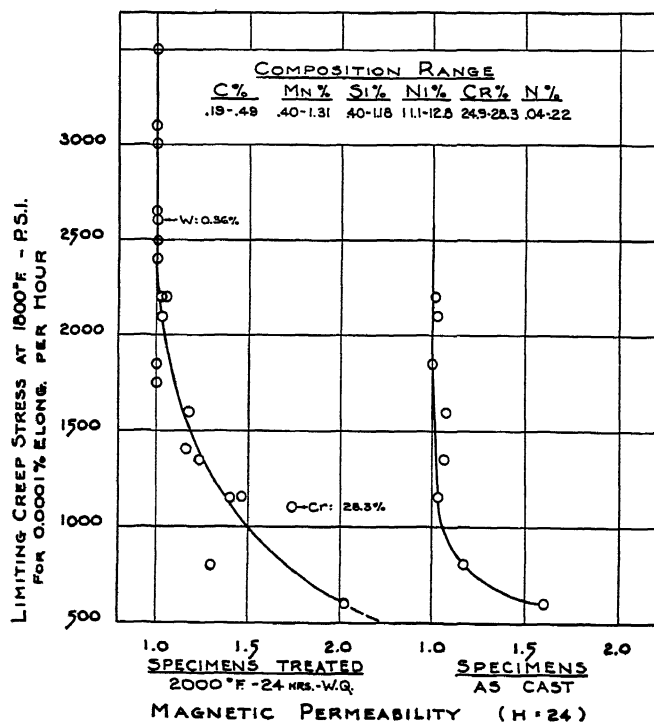
FIG. 14.—CORRELATION OF CREEP STRENGTH WITH PERMEABILITY OF UNSTRESSED SPECIMENS.

sive, less tedious, and less exacting than elevated-temperature acceptance tests. Further, it eliminates heats with excessive amounts of ferrite that may transform to sigma after long exposure at service temperatures. The appearance of this nonmagnetic phase promoted by sigma-forming elements (Cr, Si, Mo[10]) beyond the restricted composition range in Figs. 12 and 14 may seriously disturb the relationship between permeability and creep strength.

From these considerations, it is suggested that a maximum carbon content be established to confine commercial production to the left slope of the curve in Fig. 6, that maxima of 1.75 per cent Si and 28 per cent Cr be used to inhibit development of the embrittling sigma phase, and that the minimum chromium content be established by the degree of oxidation resistance required. Sufficient latitude in nickel (10 to 14 per cent) and nitrogen (up to 0.20 per cent) should be permitted for balancing the composition. Within this broad chemical range some unsatisfactory alloys may be excluded by the tension test after aging at 1400°F. for 24 hr. to detect carbide embrittlement, to identify defective material by a minimum tensile strength of 80,000 lb. per sq. in., and to evaluate the approximate short-term elevated-temperature ductility. A permeability test after 24 hr. at 2000°F. may be employed to estimate limiting creep stress and to eliminate alloys that are below the required strength. The maximum permeability for the required creep strength at 1800°F. may be selected from Fig. 14; the probable maximum, average, and minimum ductility after aging from Fig. 7. The strength at other temperatures may be estimated from Fig. 2. Since magnetic analysis is important in this procedure, data from other laboratories are desirable for establishing its validity and for defining its limitations.

This procedure takes advantage of the current trend toward broader chemical limits and more searching acceptance tests. It should be understood that the method thus far embraces alloys containing only significant percentages of carbon, nickel, chromium, silicon and nitrogen. Other elements probably can be included in this approach but it is essential that the interrelation of creep strength and permeability be separately determined for each special chemical specification.

SUMMARY

In general, hypothetical explanations of the data in this paper have been avoided. Comparisons, correlations, and trends have been indicated, but the positive designation of an optimum alloy depends upon particularized individual requirements. The following observations are believed significant in the industrial utilization of the cast 26 per cent Cr:12 per cent Ni heat-resistant alloys.

1. The metallographic constituents, ferrite, sigma, complex carbides, a lamellar aggregate, and nonmetallic inclusions, modify the properties of these nominally austenitic alloys.

2. These alloys are extremely sensitive to variations of chemical composition.

3. Quantitative information concerning the effects of oxidation and sulphidation at elevated temperatures is urgently required to establish optimum alloy balances for the several service conditions.

4. Any practical restrictions of chemical specifications alone will result in a wide range of properties.

5. The acceleration of creep rates by appreciable temperature fluctuations should be recognized in engineering, in creep laboratory procedures and in future research.

6. Strength and ductility at elevated temperature are inverse qualities and a choice should be made between them, based on service analysis.

7. Ductility values are considerably affected by the technique of measurement.

Total elongation at fracture under constant load and constant temperature seems to be the best rapid measure of comparative ductility.

8. Tensile tests after brief aging are useful for identifying alloys that embrittle rapidly, and for detecting defective material. They are not reliable indices of residual ductility after exposure to stress at high temperature.

9. Elongation after aging has an inverse correlation with creep strength, and should not be used alone to evaluate the merit of material for high-temperature service.

10. Structural damage resulting from overstressing may be the cause of low residual ductility or of failure. It should be distinguished from embrittlement by precipitation-hardening.

11. Strong alloys are more susceptible to failure under overloading from hindered thermal contraction than are very ductile compositions.

12. Stress-strain-rupture tests provide a measure of elevated-temperature strength, ductility and life before fracture under overload.

13. The amount of ferrite developed with or without stress at elevated temperatures is an inverse function of creep strength.

14. Ferrite promoted by 24 hr. at 2000°F. makes possible the use of magnetic analysis for predicting probable creep strength.

15. Data useful in design calculations have been presented.

ACKNOWLEDGMENTS

REFERENCES

1. J. T. Gow and O. E. Harder: Balancing the Composition of Cast 25 % Cr-12 % Ni Type Alloys. Amer. Soc. Metals Preprint No. 21 (1941).
2. H. W. Gillett: Some Things We Don't Know about the Creep of Metals. *Trans.* A.I.M.E. (1939) **135,** 15–58.
3. J. A. Fellows, Earnshaw Cook and H. S. Avery: Precision in Creep Testing. This volume, page 358.
4. A.S.T.M.-A.S.M.E.: Symposium on Effect of Temperature on the Properties of Metals. 1932.
5. R. J. Wilcox: Notes on 29-9 Alloy. *Metal Progress* (May 1935) 49.
6. W. H. Hatfield: Heat Resisting Steels. Inst. of Fuels, London, Preprint (1938).
7. A. Pomp and A. Krisch: Problem of Creep Resistance of High-temperature-strength Steels at 600°, 700°, and 800°C. *Mitt.* K. W. Inst. fur Eisenforschung (1930) **12** (9), 137–149.
8. R. H. Thielemann: Correlation of High Temperature Creep and Rupture Test Results. *Trans.* Amer. Soc. Metals (1941) **29,** 355–372.
9. A. E. White, C. L. Clark and R. L. Wilson: The Fracture of Carbon Steels at Elevated Temperatures. *Trans.* Amer. Soc. Metals (1937) **25,** 863–888.
10. R. Franks, W. O, Binder and C. R. Bishop: The Effect of Molybdenum and Columbium on the Structure, Physical Properties, and Corrosion Resistance of Austenitic Stainless Steels. *Trans.* Amer. Soc. Metals (1941) **29,** 35–84.
11. A. E. White, C. L. Clark and R. L. Wilson: Influence of Time at 1000°F. on the Characteristics of Carbon Steels. *Trans.* Amer. Soc. Test. Mat. (1936) **36,** 139–160.
12. H. S. Avery: Discussion of The Cyclic Heating Acceleration of Strain Rates, by Brophy and Furman. Amer. Soc. Metals, Oct. 1941 Meeting.
13. E. R. Parker: The Development of Alloys for Use at Temperatures above 1000°F. *Trans.* Amer. Soc. Metals (1940) **28,** 797–810.

DISCUSSION

(A. V. de Forest presiding)

O. E. HARDER,[*] Columbus, Ohio.—This paper is an unusually valuable contribution to the all too meager engineering data on heat-resistant alloys. I am in sympathy with the method of approach and in agreement with most of the deductions and comments. There are, however, a few points on which some comments seem to be in order; not to disagree with the authors so much as to avoid the possibility of the reader drawing wrong or unwarranted conclusions.

On page 5, last paragraph of first column, it needs to be remembered that loss of ductility on aging may also result from the transformation of ferrite to the sigma phase in alloys that are not wholly austenitic. Also, in the first paragraph in the second column, the statement

[*] Assistant Director, Battelle Memorial Institute.

that the "cast 26 per cent Cr; 12 per cent Ni alloys are austenitic" seems open to question because, as the authors indicate later, they may be strongly ferritic. "Austenitic" might be

Illustrative of alloys of only about 0.31 per cent carbon, which have good L.C.S. values, certain alloys reported by Gow and Harder[1] may be mentioned (Table 14). It is obvious

TABLE 14.—*Alloys Reported by Gow and Harder*[1]

Alloy No.	Chemical Composition, Per Cent						Ratio Factor	L.C.S. at 1800°F.
	C	N	Cr	Ni	Si	Mn		
AS1	0.33	0.032	24.18	12.36	0.83	0.96	1.54	2000+
AS2	0.33	0.087	24.57	12.48	0.84	0.97	1.54	2000+
AS4	0.31	0.150	25.30	11.97	0.91	0.99	1.70	2000+
AU2	0.30	0.086	22.95	12.66	0.87	0.78	1.43	2000+

justified if it means the greater amount of the structure is austenite. In fact, Fig. 4 shows an alloy of these chromium and nickel contents but which evidently contains some 10 to 20 per cent of a phase other than austenite. Incidentally, considering the molybdenum as equivalent to four times as much chromium, this alloy has a calculated ratio factor of 2.38.

It seems a pity that no use was made of the ratio factor in discussing Fig. 6 and the data in Table 1. Admittedly there are limitations to the applications of the calculated ratio factors, and variations in nitrogen is one of them, but in these alloys (1A to 1E, Table 1) the nitrogen contents are essentially the same and quite close to the nitrogen contents in the alloys used by Gow and Harder to develop the ratio factor.

Calculations for the ratio factors for the alloys in Table 1 and Fig. 6 give values of 2.06, 1.89, 1.71, 1.58 and 1.45 for 1A, 1B, 1C, 1D and 1E, respectively. Thus it is clearly indicated that 1A is strongly ferritic; 1B is moderately ferritic; 1C is most likely substantially austenitic; while 1D and 1E are austenitic. Thus by holding chromium and nickel constant and increasing the carbon content in this series of alloys, the structure has been changed from strongly ferritic to wholly austenitic and this relation has not been brought out adequately in this paper.

The data show that alloy 1B has a much lower L.C.S. than alloy 1D, and it might be inferred that an alloy of only 0.31 per cent carbon cannot be made to have an L.C.S. value equivalent to that of alloy 1D, or even 1C. However, had the nickel content of alloy 1B been increased from 11.3 to 12.67 per cent, its ratio factor would have been 1.7; thus producing a wholly austenitic alloy.

that the four alloys listed, with carbon contents in the range of 0.30 to 0.33, but of balanced composition so that they are wholly austenitic, have very different L.C.S. values at 1800°F. as compared with alloy 1B in Table 1.

The authors discuss the subject of "overbalanced" compositions resulting from the addition of unnecessary amounts of austenite-stabilizing elements and suggest that this may cause a loss of creep strength. Alloy AU2 (Table 14) is decidedly "overbalanced" because of the relatively high percentage of nickel compared with the chromium content, and yet the limiting creep strength does not seem to have been materially affected.

On the other hand, "overbalancing" by adding excess of carbon, as in alloy 1E, may well result in loss of creep strength at 1800°F. Gow and Harder noted that alloys AS1, AS2, AS4, AU2, with carbon contents of 0.33, 0.33, 0.31 and 0.30 per cent, respectively, had higher creep strengths at 1800°F. than alloys AD and AE, with carbon contents of 0.41 and 0.44 per cent, respectively. This relation appears to be reversed at 1400°F., however.

Under Effects of Composition, the authors say that "from 0.20 to 0.40 per cent carbon, the creep strength is approximately doubled by an increment of 0.10 per cent." This is clearly indicated by the curve of Fig. 6. However, as mentioned above, with the chromium and nickel ratios kept constant, increasing the carbon in the range of 0.20 to 0.40 per cent changes the structure of the alloy from one that contained a large amount of ferrite (or sigma) to one that was substantially austenitic, and the data shown in Fig. 6 reflect more the effect of change of structure—that is, the relative amount of ferrite and austenite—than the

effect of carbon content on an alloy that has the same type of structure; for example, one that is wholly austenitic.

Harder and Gow when dealing with wholly austenitic alloys found that the limiting creep strength of alloys containing 0.30 to 0.33 per cent carbon was as good at 1800°F. as for alloys containing 0.41 to 0.44 per cent carbon, if not better. It is not seen that any harmful effect results from slightly "overbalancing" alloys by the use of increased amounts of nickel, although the cost would be increased. Gow and Harder have indicated that in wholly austenitic alloys the elongation at room temperature, after aging 48 hr. at 1600°F., is a function of the carbon plus one-half the nitrogen (C + $\frac{1}{2}$N), while the elongation at 1800°F. is a function of the carbon plus two and one-half times the nitrogen (C + 2$\frac{1}{2}$N). An alloy such as 1E, with a carbon content of 0.61 per cent, would be off the scale shown by Gow and Harder for the elongation after aging 48 hr. at 1600°F.

To summarize, increasing the carbon content of heat-resisting alloys is only one of the possible means of balancing the composition so as to make the alloys wholly austenitic or to decrease the content of ferrite, and if the ratio of chromium to nickel is high, excessive amounts of carbon may be required, and, as a result, alloys of low ductility will be obtained. Obviously, decreasing the ratio of chromium to nickel is another effective way of balancing the composition of the alloys and this means is usable without employing an excessive amount of carbon, so that the ductility would be drastically reduced and no harmful effects on the properties of the alloys are seen from slightly "overbalancing" the composition by the addition of nickel.

In calculating the ratio factors in Table 3, it seems likely that, instead of using the ratio factor as the authors did, a better picture would have been obtained had consideration been given to the molybdenum content and molybdenum calculated as the equivalent of four times as much chromium. This would indicate that all of the alloys are more strongly ferritic, and it is suggested that alloy 3C, with a ratio factor of 1.96, calculated on this basis, was essentially nonmagnetic after the creep test because it contained a substantial amount of the sigma phase, which is nonmagnetic.

The authors' correlation of limiting creep stress at 1800°F. with magnetic permeability, after testing at 1800°F., as shown in Fig. 12, and a similar correlation using specimens that have been heated 24 hr. at 2000°F. and quenched in water, seem to be valuable relations, which deserve continued study as a relatively convenient method of appraising heat-resistant alloys of this type.

P. H. DIKE,* Philadelphia, Pa.—The authors are to be commended for a comprehensive and careful study of the properties of a chromium-nickel-iron group of alloys. To the writer the correlation found between creep strength and magnetic permeability is the most significant and important contribution presented in the paper, since his interests happen to take that direction. The fact that a simple, quickly made measurement of permeability on a sample from a melt gives an index to the behavior of the melt under stress at high temperature offers a most inviting means of escaping the necessity for time-consuming and difficult measurements of creep.

The alloys under consideration are almost nonmagnetic, in spite of containing over 60 per cent of iron, and owe this property to the fact that the formation of ferrite is discouraged in the presence of the particular nonferrous elements combined with the iron. It should be strongly emphasized that the method is applicable, as far as our present knowledge goes, only to a narrow range of heat-resistant alloys. Its validity for other alloys cannot be assumed, and can be established only by such experimentation as has been carried out by the authors. It would be valuable to have information on the range of compositions of these alloys for which the permeability tests give reliable information as to creep strength.

A. B. BAGSAR,† Marcus Hook, Pa.—The oil-refining industry has been an important user of castings of this alloy for tube supports in cracking furnaces, and similar applications. In its early stages of development, the castings made of this general type of alloy usually contained 1 per cent or more of carbon. Although many of these high-carbon castings have given good service, a large number of them have

* Assistant Director of Research, Leeds & Northrup Co.
† Metallurgical Division, Sun Oil Co.

failed by cracking, because of their inherent brittle character and their inability to withstand thermal shock. Better serviceability has been obtained by reducing the carbon content.

to be austenitic by the magnetic permeability test? If this is so, the magnetic permeability test would have a questionable value.

As suggested by the authors, it would appear
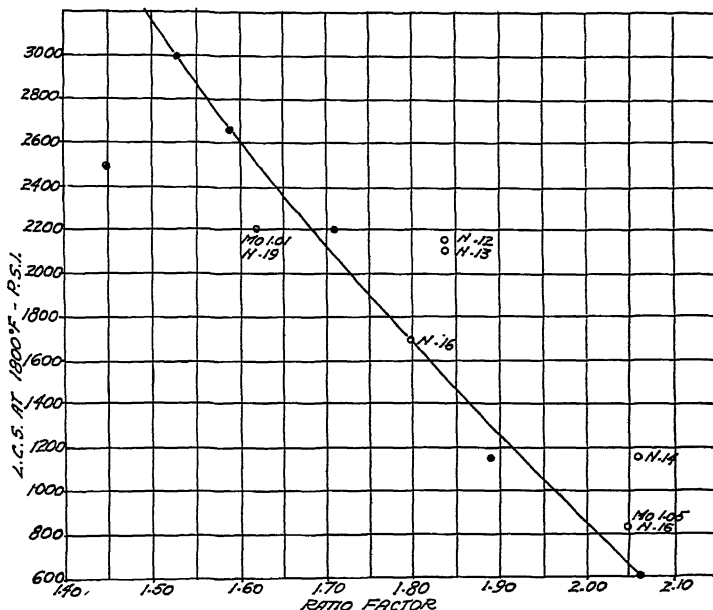
FIG. 15.—RATIO FACTORS PLOTTED AGAINST L.C.S. AT 1800°F.

The castings now generally used in the oil refineries contain 0.25 to 0.35 per cent carbon, possess a fair degree of ductility, and in most part are not wholly or permanently austenitic alloy castings.

The data presented in this paper seem to indicate that the magnetic permeability test could be advantageously used for differentiating between austenitic and ferritic types of alloy after aging for 24 hr. at 2000°F. and water quenching. I do not believe that this test alone is sufficient for predicting serviceability, since an alloy showing low magnetic permeability may have extremely objectionable high-temperature properties due to an unsuspected content of impurities such as tin or lead, the presence of which would not be detected by the permeability test. Another objectionable feature of the magnetic test consists in its dependence on the preliminary aging at 2000°F. Would it be possible to obtain structural changes in an alloy of this type by prolonged heating and stressing at 1400° or 1600°F. under service conditions, which was initially shown

essential to resort to a high-temperature short-time tensile test, or, better still, to a stress-rupture test, for arriving at a more dependable evaluation of high-temperature serviceability of a given alloy of this type.

F. B. FOLEY,[*] Nicetown, Philadelphia, Pa.— According to Gow and Harder, the ratio factor seems to be an indication of the limiting creep stress that may be expected. The present paper reports actual limiting creep stresses (for a rate of 0.1 per cent per 1000 hr.) at 1800°F. for 12 different heats, of which six may be considered normal from the point of view that neither molybdenum nor nitrogen in excess of 0.09 per cent is present in them. The other six contain higher nitrogen and two contain molybdenum also. The ratio factors either appear in the paper or may easily be figured from the composition given. Plotted against the L.C.S. at 1800°F., they present the excellent correlation shown in Fig. 15, in which heats

* Superintendent, Research Department, The Midvale Company.

having special additions are so marked. The creep value of only one of the normal heats lies more than 100 lb. per sq. in. off a smooth curve. This is a much better correlation than is found by plotting carbon instead of the ratio factor against the L.C.S.

The authors, however, make rainbow chasing of the search after high creep strengths. One may have high creep strength, but if it is taken advantage of fully in design one may expect his casting to fail in short order. Designers generally have not asked for over 1600 lb. per sq. in. L.C.S. at 1800°F. and have used half this value (800 lb. per sq. in.) in designing. Seldom has failure occurred, and perhaps the reason for this appears in the authors' Fig. 1 and Table 4, from which the following data are taken:

Alloy	L.C.S. at 1800°F.	Time to Rupture under Applied Load of 800 Lb. per Sq. In.	
		Hours	Years
A	600	35,000	4
B	1150	300,000	34
C	2100	1,000,000	114
D	3000	100,000	11

By using a design stress of 800 lb. per sq. in., it does not appear that there was any grave risk of failure as long as there was a limiting creep strength of from 1100 to 3000 lb. per sq. in. Even were the L.C.S. as low as 600 lb. per sq. in., the casting might be expected to last four years. The paper shows in Table 4 what would happen if half the actual L.C.S. value were used as a design stress. According to it, the higher the L.C.S., the lower the life expectancy. All of this is, of course, based on a considerable amount of extrapolation.

Since there are no indications that any reasonable return in hours of service can be expected from pushing this alloy to higher creep strengths, it seems that designers may well content themselves with adhering to their present 800 lb. per sq. in. figure and rest safe in the use of 25-12 with a ratio factor between say 1.60 and 1.95 and a magnetic permeability not exceeding say 2.0.

The authors are to be commended for the unusual degree of precision with which they conduct their work, and which gives to their results a degree of reliability not always to be depended upon in high-temperature studies of this type.

H. S. AVERY (author's reply).—In condensing the mass of data available into a paper of reasonable length, discussion of many subjects, such as Dr. Harder's "ratio factor," was drastically curtailed. The omission is not serious, as Harder and Gow's extended treatise[1] is readily available, and should be studied by all who attempt to evaluate these alloys.

Since the so-called "austenitic alloys" seldom contain *only* the single-phase austenite, it is our recommendation that the word "austenitic" be considered as an adjective indicating the major portion of the structure to be the gamma phase. In this sense it may be used regardless of whether the steel contains small amounts of *excess carbides*, *sigma* or *ferrite*. The term "ferritic alloys" should be reserved for those steels whose predominant phase is ferrite and whose magnetic permeabilities are several hundred times the values encountered for the high chromium-nickel compositions.

The "ratio factor" provides a means for deducing the magnetic behavior of compositions, placing them in two classes. The approach in our work has been a direct measurement of magnetism to integrate the effect of all the elements present, which includes those like nitrogen that have not been satisfactorily included in the ratio factor. It has the added advantage that it permits the *quantitative* evaluation of the partially ferritic alloys (whose ratio factors are above 1.7) with greater precision, we believe, than is possible by single stress-rupture or hot tensile tests. As Dr. Bagsar points out, a large portion of current production contains ferrite.

The balancing of intended compositions with chromium and nickel, as suggested, is quite practicable, if oxidation and sulphidation resistance can be assured. It has been restricted in the past by specifications that set 12 per cent nickel as a maximum. Manufacturers are reluctant to jeopardize oxidation resistance by reducing chromium. Further, the demand for 9.0 per cent elongation after aging at 1400°F. curtails the employment of wholly austenitic alloys. Some will meet this arbitrary test, but many will range between 4.0 and 9.0 per cent elongation even when austenitized with nickel instead of carbon.

The proposal that molybdenum be included in the calculations of the ratio factor for Table 3 neglects nitrogen. In this series the ferrite-forming tendency of molybdenum is substantially balanced by the austenite-former nitrogen, and the ratio-factor values are approximately correct. Otherwise a substantially austenitic balance for heat 3C probably would not be evident. If sigma (which does not appear in the microstructure after creep-testing at 1800°F.) were present as suggested, the L.C.S. should be appreciably lower, as in Fig. 4.

We agree with Dr. Dike that the composition brackets in Fig. 14 cover a practical manufacturing range for only one alloy type. Additional evidence is being obtained as fast as pertinent creep tests can be made. Already it appears that the nickel range can be expanded without difficulty, and two points may be added to Fig. 14, as follows: 1200 lb. per sq. in. with permeability = 1.66 (2.22 per cent Si) and 1550 lb. per sq. in. with permeability = 1.15 (1.56 per cent Si).

The early failures in oil-refinery castings mentioned by Dr. Bagsar are readily explained by the effects of carbon shown in Table 1 and Fig. 6. Similarly, in Fig. 9, there is experimental justification for the present high ductility trend. Here a word of caution is desirable. There are engineers who insist on combinations of high ductility and high creep strength. The former is measured in an acceptance test but the latter is taken on faith. It is suggested that single heats that show very favorable combinations of these properties are exceptional (as typified by the upper line in Fig. 7) and that the median line in the figure is a truer picture of the average performance of melts in foundry production, even under close technical control.

Dr. Bagsar's question about structural changes at 1400°F. or 1600°F. for an alloy shown to be nonmagnetic after aging at 2000°F. is best answered by Tables 5 and 6 and Fig. 2. The residual elongations (room temperature) of four unfractured creep tests in Fig. 2 were 10 per cent (2000°F.), 7 per cent (1800°F.), 4 per cent (1600°F.) and 3 per cent (1400°F.). These are typical of ferrite-free alloys containing 26 per cent Cr and 12 per cent Ni. We have found no evidence that structural changes other than carbide precipitation and agglomeration take place below 2000°F. for normal compositions of this type. If the validated and recommended chemical ranges are followed, there is little to fear from this source.

For partially ferritic analyses the situation is complicated. Some alloys are reasonably stable: 1A and 1B in Fig. 1 have residual elongations of 12 and 8 per cent, respectively, after creep-testing for 1000 hr. at 1400°F., for example; others, as Dr. Harder has stressed, embrittle markedly from sigma development (see Table 9, alloy 9B). The magnetic test is not intended to indicate phase changes that may occur at various temperatures, even though for nonmagnetic alloys it gives considerable assurance of freedom from sigma development. It is recommended for the estimation of long-term load-carrying ability and should be supplemented by another test if structural changes are suspected.

Alloys containing 26 per cent Cr and 12 per cent Ni perform best above 1600°F. Most of their undesirable features appear at or below this temperature. If a maximum service temperature of 1600°F. is assured for a given application, lower chromium content may be desirable. Sigma embrittlement would thereby be minimized. This type of substitution has been avoided because of design complications, but it may be forced on industry by wartime scarcity of metals.

Dr. Bagsar implies that we favor elevated-temperature acceptance tests. Ideally, these are logical requirements. Practically, even the best (the stress-strain-rupture type) is quite expensive and must be surrounded by so many precautions to ensure reliability that we do not recommend its use for production heats. Consider the difficulties an inspector would have in detecting the errors due to thermocouple contamination or defective pyrometers. On the other hand, the inspector could evaluate the specimens from a week's melting in five minutes with a permeameter and then check the instrument with standard specimens that can be carried in a vest pocket.

We have encountered no failures from tin or lead, perhaps because in production our raw materials are carefully checked and controlled. If their presence is suspected, they may be easily determined in the routine analysis of each melt.

Mr. Foley's ratio-factor plot is a useful supplement. It emphasizes the strengthening

effect of nitrogen and confirms the approximate nitrogen-molybdenum balance for heat 3C. For years we have used a similar formula (that includes nitrogen) to estimate creep strength from composition. Unfortunately, the effect of nitrogen varies in a way that discourages its inclusion in mathematical expressions.

At a 0.09 per cent nitrogen level the "ratio factor" is reasonably valid. However, we have found that in foundry production, when none is intentionally added and no definite steps to control it are taken, nitrogen will range between 0.08 to 0.18 per cent and 63 per cent of the heats will be from 0.11 to 0.14 per cent nitrogen with basic arc melting. With this variation, the neglect of nitrogen may be as serious as a corresponding disregard of carbon.

The remarks on design are very pertinent. Some present and past commercial production ranges as high as 1.7 permeability and down to or below 800 lb. per sq. in. L.C.S. at 1800°F. Despite this, the installations are considered satisfactory, probably because of the low working stresses.

Mechanical Properties of Iron-manganese Alloys

By F. M. Walters, Jr.,* Member, I. R. Kramer* and B. M. Loring,* Junior Members A.I.M.E.

No observations on the mechanical properties of iron-manganese alloys have been published since pure manganese became readily available, either distilled manganese or electrolytic manganese. The purpose of this investigation was to determine whether iron-manganese alloys are essentially brittle, as reported by Hadfield,[1] or whether the lack of ductility observed was due to impurities in the alloys that he studied.

EXPERIMENTAL METHODS

The alloys were melted in a 100-lb. high-frequency induction furnace with a magnesia crucible, using ingot iron and electrolytic manganese. The heats were split, the first giving six 18-lb. ingots and the second three. Each successive heat was higher in manganese and about 0.3 per cent silicon

TABLE 1.—*Chemical Composition of Alloys*[a]
PER CENT

Alloy	Mn	C	Si	S
A	3.74	0.04	0.12	0.021
B	6.66	0.04	0.11	0.019
H	8.80	0.03	0.05	0.016
C	9.60	0.03	0.09	0.019
J	11.54	0.03	0.08	0.014
D	12.93	0.03	0.08	0.016
K	14.04	0.03	0.06	0.012
E	16.29	0.03	0.07	0.013
F	20.51	0.03	0.07	0.013
G	20.70	0.02	0.01	0.017

[a] Phosphorus less than 0.001 per cent.

was added as ferrosilicon. The alloys forged without difficulty and were given a 90 per

cent reduction to ¾-in. rounds. The chemical analysis of the alloys is given in Table 1.

The forged rods were homogenized for
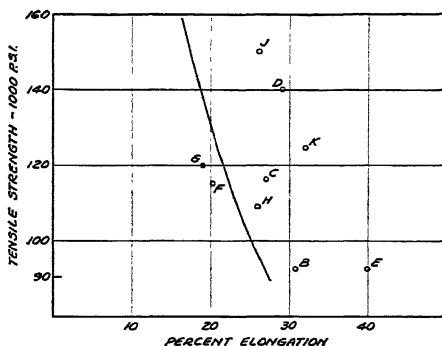
FIG. 1.—CURVE RELATING TENSILE STRENGTH AND ELONGATION.
Drawn from data of Janitzky and Baeyertz.

24 hr. at 1150°C. (2100°F.) and air-cooled. The alloys were tested in two conditions of heat-treatment: (1) as normalized from 870°C. (1600°F.) and (2) normalized from 870°C. and tempered for 1 hr. at 540°C. (1000°F.) and air-cooled.

The tensile specimens were 0.505 in. in diameter with a 2-in. gauge length, and the impact specimens were V-notch Charpy. The proportional limit and yield strength were taken from the stress-strain diagrams drawn by a Peters recorder. The data obtained from the tensile test and the hardness measurements are given in Table 2. Specimens that were normalized are designated by *N*; those that were normalized and tempered by *T*. Alloy G was tempered after forging (D).

DISCUSSION OF RESULTS

The mechanical properties of the iron-manganese alloys are not unexpected when their constitution is considered.[2] Up to 10 per cent Mn, the austenite transforms to ferrite, but at a progressively lower temperature as the manganese is increased the series of alloys is shown by those in this range.

The effect of the tempering at 540°C. was to raise the ductility and lower the tensile strength in the 6.66 and 9.60 per cent Mn alloys, but both the ductility and the strength of the 12.93 per cent alloy were increased by tempering.

TABLE 2.—*Mechanical Properties of Alloys*

Alloy	Mn, Per Cent	Proportional Limit, Lb. per Sq. In.	Yield Strength, 0.2 Per Cent	Tensile Strength, Lb. per Sq. In.	Elonga-tion, Per Cent	Reduction in Area, Per Cent	Hardness Rc	Brinell Hardness No.
A-N	3.74	63,000	75,000	84,500	27.3	72.5	16	163
A-N		63,700	78,000	84,500	27.1	78.0		
A-T		49,500	63,500	72,000	32.0	80.0	14	159
B-N	6.66	90,000	117,000	120,000	14.0	51.7	20	241
B-N		90,000	115,000	120,000	12.5	50.0		
B-T		63,000	82,800	92,000	25.0	62.3	18	187
H-T	8.80	90,000	103,500	110,000	25	74.5	22	235
H-T		81,000	97,500	106,000	27	73.7		
C-N	9.60	97,500	126,000	138,000	16.4	62.1	28	266
C-N		97,500	126,000	137,500	3.1	7.7		
C-T		70,500	102,000	116,500	27	70.1	20	235
J-N	11.54	52,500	87,500	146,500	18.0	47.9	30	277
J-T		43,900	98,900	150,000	25.0	65.4	34	302
J-T		46,800	96,600	150,000	27.0	66.8		
D-N	12.93	88,500	105,000	125,000	6.3	14.1	28	262
D-T		33,000	71,250	140,000	29.0	70.4	29	285
K-N	14.04	36,500	53,200	117,000	25.0	69.4	20	229
K-T		24,300	58,800	124,500	32.0	71.8	21	212
K-T		24,300	56,700	124,500	32.0	69.5		
E N	16.29	31,500	43,500	89,500	32.0	38.2	16	217
E N		34,500	45,000	90,000	28.1	37.3		
E T		31,600	52,500	92,000	40.0	59.0	17	210
F-N	20.51	33,000	45,000	104,000	12.5	14.8	20	217
F-N		34,500	45,000	109,300	15.6	15.2		
F-T		20,600	51,800	111,500	20.0	27.2	20	217
G-D				116,000	19.0	28.0	22	212
G-D				127,500	20.0	29.2	22	217
G-T				120,000	18.0	24.8	21	207

and the fine ferritic grain size and strain resulting from the low-temperature transformation give increased strength and decreased ductility in the normalized condition. Above 14 per cent Mn, the austenite transforms partly to the hexagonal close-packed phase, epsilon, and the alloys show the low elastic limit and high ductility characteristic of austenitic alloys. Between 10 and 14 per cent Mn both ferrite and epsilon are formed by the decomposition of the austenite, and the highest strength of

Since the temperature of the transformations of the binary iron-manganese alloys and the completeness of the transformations have been found to be little affected by the rate of cooling,[2] air cooling was the only rate employed for these experiments. It is believed that the results obtained would not have been materially different if other cooling rates had been used.

Instead of being brittle, most of the iron-manganese alloys actually are more ductile than S.A.E. steels of the same tensile

strength. Fig. 1 shows a curve relating tensile strength and elongation, which was drawn from the data of Janitzky and Baeyertz,[3] together with these values for the iron-manganese alloys. No reason has

TABLE 3.—*Charpy Impact, V-notch*

Alloy	Mn, Per Cent	Normalized[a]	Normalized and Tempered
A	3.74	22, 8[a] 19[c]	156, 154
B	6.66	5, 7	85, 89
C	9.60	6, 8	70
D	12.93	34, 38	71, 75, 80
K	14.04		120, 127
E	16.29	191, 197	127, 149, 112
F	20.51	78,[b] 87	72, 69

[a] All made at 21°C. (70°F.) except as noted.
[b] Tested at 3.5°C.
[c] Tested at 100°C.

been found for the low elongation shown by alloys F and G. Alloys of this composition (20 per cent Mn) have substantially the same constitution as the 16 per cent alloy; that is, in both about one third of the gamma has transformed to epsilon.

The brittleness of Hadfield's alloys[1] was probably due to their fairly high carbon and phosphorus content (0.06 to 0.15 and 0.044 to 0.070 per cent). Furthermore, his heat-treatments (as forged, annealed, and water-quenched) did not include tem-

pering, which has been found to be necessary to develop the best ductility in some of the alloys.

REFERENCES

1. R. A. Hadfield: Alloys of Iron and Manganese containing Low Carbon. *Jnl.* Iron and Steel Inst. (1927) 115, 297–374.
2. F. M. Walters, Jr., and C. Wells: The Constitution of the Binary Alloys of Iron and Manganese. *Trans.* Amer. Soc. Metals (1935) 23, 727–750.
3. E. J. Janitzky and M. Baeyertz: The Marked Similarity in Tensile Properties of Several Heat Treated S.A.E. Steels. Metals Handbook, 515. Cleveland, Ohio, 1939.

DISCUSSION

(L. S. Bergen presiding)

H. H. Uhlig,[*] Schenectady, N. Y.—I should like to ask the authors whether any qualitative magnetic tests they may have made on their pure alloys checked corresponding properties first reported by R. A. Hadfield for alloys containing carbon.

F. M. Walters (author's reply).—The magnetism of low-carbon iron-manganese alloys depends upon their structure: the alpha phase is ferromagnetic while gamma and epsilon are not. The minimum amount of manganese necessary to make the alloys magnetic depends upon the carbon, since carbon helps to make them austenitic.

* Research Metallurgist, General Electric Co.

The Instability of Low-expansion Iron-nickel-cobalt Alloys

By Irvin R. Kramer,* Junior Member and Francis M. Walters, Jr.,* Member A.I.M.E.

The substitution of cobalt for part of the nickel in Invar was found by P. H. Brace[1] to lower the coefficient of expansion. Scott[1] extended the use of cobalt to alloys of higher inflection temperatures. Such alloys have a larger temperature range of low expansion than those without cobalt, and

TABLE 1.—*Chemical Composition*

Alloy	Per Cent						Other Elements
	Ni	Fe	Co	Si	Mn	Ti	
13	31.3	51.8	16.14	0.27	0.49		
19	27.9	53.6	18.14	0.46			
20	37.2	62.2	0.45	0.53			
21	29.4	53.4	17.1			0.40	
26	27.6	50.1	21.75	0.06	0.49		
29	31.7	52.0	15.37	0.43	0.50		
30	29.2	49.5	20.66	0.24	0.40		
33	29.9	55.5	14.47			0.22	
34	29.1	55.8	14.83			0.22	C, 0.07; V, 0.44
35	28.5	55.7	15.71			0.09	
38	27.4	55.2	16.58			0.28	C, 0.08; V, 0.46
39	29.3	54.1	15.49			0.10	Cu, 1.01
40	28.5	53.8	15.36				Cu, 2.29
41	28.2	54.4	12.53				Cu, 4.87
42	37.2	61.3					C, 0.05

their use up to 400° or 500°C. offers decided advantages in certain applications. However, it has been found that the iron-nickel-cobalt alloys are not stable in this temperature range.

EXPERIMENTAL METHODS

Two methods were used in studying the stability of the low-expansion iron-nickel-cobalt alloys. Dilatometer specimens were held at 480°C. for 9 months and the change in expansion characteristics was deter-

mined. Filings were held for about 2 months at various temperatures and the change in structure was determined by X-ray diffraction.

As shown by Table 1, the alloys studied covered a wide range in nickel plus cobalt content (which determines the inflection

TABLE 2.—*Mean Coefficient of Expansion (20° to 425°C.) after Holding at 480°C. (900°F.) for Times Indicated*

Alloy	Mean Coefficient of Expansion after Holding for			Increase in Length after 7 Months, Per Cent
	Initial	2 Months	9 Months	
13	6.50	6.35	6.62	0.10
19	5.15	5.12	5.25	0.13
20ᵃ	3.10		3.56	0.05
21	4.55	5.25	4.88	0.03
26	6.25	7.10	6.88	0.13
29	6.00	6.25	6.25	0.07
30	7.00	6.75	6.75	0.19
33	4.27	4.59	4.20	0.06
34	4.75	5.10	4.57	0.04
35	4.25		5.50	0.03
38	4.25		5.00	0.07
39	4.62	5.00	5.25	0.10
40	5.52	5.50	5.75	0.10
41	6.50	6.00	6.12	0.09
42ᵃ	2.20		3.02	0.10

ᵃ 20° to 250°C.

temperature) as well as some variation in the ratio of nickel to iron (which controls the temperature of the gamma to alpha transformation). Included also are alloys containing carbon and vanadium, carbon and titanium and three with various amounts of copper. The alloys were melted in a high-frequency induction furnace with a magnesia crucible, using ingot iron, electrolytic nickel and commercial cobalt. Fifteen-pound heats were cast into iron molds after deoxidizing with silicon, or

titanium or both. The ingots were soaked for 24 hr. at 1150°C. and were reduced 90 per cent in forging. To study the expansion characteristics, a dilatometer was

EXPERIMENTAL RESULTS

Most of the alloys studied showed higher coefficients of expansion after 2 and
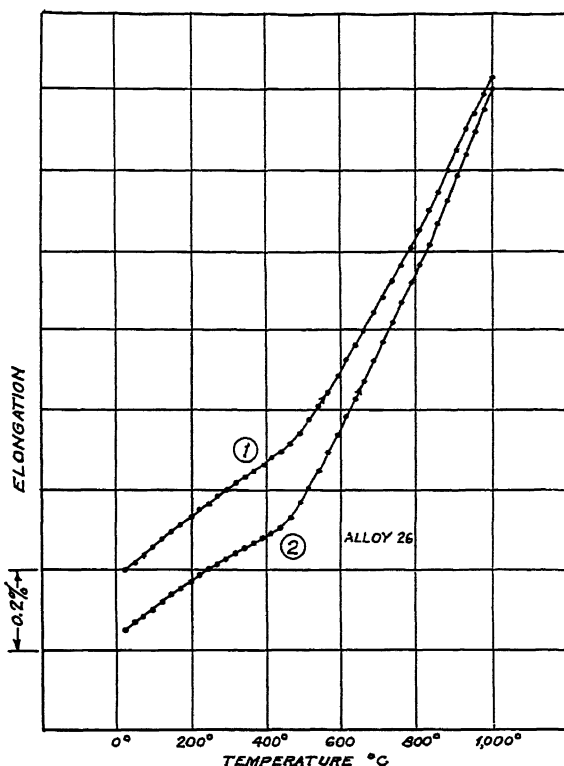
FIG. 1.—BEHAVIOR OF TYPICAL ALLOY (NO. 26).

used similar to that described by Walters and Gensamer.[2] The specimens (1 in. long and ½ in. in diameter) were sealed in evacuated Pyrex tubes before being placed in the furnace, in which they were held first for 2 months and then for an additional 7 months.

The filings for the X-ray studies were passed through a 250-mesh sieve and sealed in Pyrex tubes. No alpha was detected in three alloys which were examined after filing, but before holding at temperature. However, to ensure that the alloys were completely in the gamma state, the filings were heated to 900°C. before holding at temperature.

9 months at 480°C. than they did initially (Table 2), though in some cases the change in coefficient was less than the experimental error ($\pm 0.06 \times 10^{-6}$). That this increase in the coefficient of expansion is due to the formation of alpha is shown by the fact that the alloys were from 0.03 to 0.19 per cent shorter after heating in the dilatometer to 1000°C. than they were initially. Part of the decrease in length occurred in the temperature range of the alpha to gamma transformation for alloys of the same nickel content but without cobalt (500° to 600°C). However, part of the shortening took place at a much higher temperature, 800° to 1000°C. The be-

havior of a typical alloy (No. 26) is shown in Fig. 1, which gives two heating curves, the first after the 9 months holding at 480°C. and the second after heating to 1000°C. The coefficient of expansion has been somewhat lowered by heating to 1000°C., but it is not as low as it was before holding at 480°C.

X-ray examination showed the (110) line due to the alpha phase. This line was faint but in most cases measurable, though not with great precision. The values of the lattice parameter were close to that of iron, as might be expected from the precipitation of a nickel ferrite or of a cobalt ferrite.

Alloys 13, 19, 21, 26 and 30 showed the presence of ferrite after about 2 months at 360°, 425°, 480° and 540°C., as did alloys 20, 28, 33, 34, 35, 39, 41 and 42, which were held at 425°C. only.

DISCUSSION OF RESULTS

Though very little is known of the ternary system, iron-nickel-cobalt, it should be possible to predict something of the behavior of the iron corner from what is known of the binary systems iron-nickel and iron-cobalt. The effect of nickel on iron is to stabilize austenite, to lower the transformation temperature and the rate of transformation. Cobalt, on the other hand, acts to stabilize ferrite and to raise the transformation temperature, but it has very little effect on the transformation rate. Recent work[3,4,5] has confirmed the opinion which many have long held that the gamma phase of iron-nickel alloys is unstable, much beyond the nickel content at which alpha is no longer formed even at slow rates of cooling. Hence it is not unexpected that the low-expansion alloys should be unstable. They contain scarcely enough nickel to depress the gamma to alpha transformation to room temperature in the alloys that contain only iron and nickel (24 to 30 per cent) and their cobalt content (up to 18 per cent) neither stabilizes gamma nor slows down the rate of transformation.

It is difficult to estimate from the expansion curves the amount of alpha that has been formed by holding the low-expansion alloys at temperature. It is likely that 10 to 20 per cent of the alloy has been transformed to alpha. This guess is based on the decrease in length on heating to 1000°C. and on the changes in the coefficient of expansion and of the inflection temperature.

The decrease in the coefficient of expansion of alloy 41 is probably due to the precipitation of part of the 4.9 per cent Cu it contained, since copper in solution has the effect of raising the coefficient of expansion. The decreases in coefficient of expansion shown by alloys 30, 33 and 34 are not so easy to explain. It seems likely that if the gamma changes its nickel and cobalt content when alpha is formed, the relations among the three alloying elements may change in such a way that the net coefficient of expansion is lower in spite of the presence of some alpha, which would tend to raise it.

SUMMARY

It has been shown experimentally that low-expansion iron-nickel-cobalt alloys are unstable in the temperature range 360° to 540°C., that they partially transform to alpha with an increase in length and generally with an increase in the coefficient of expansion.

It may be concluded that these alloys are unsuitable for applications that require long exposures to temperatures of 360° to 540°C.

REFERENCES

1. H. Scott: Expansion Properties of Low-expansion Fe-Ni Alloys. *Trans.* A.I.M.E. (1930) 89, 506–537.
2. F. M. Walters, Jr., and M. Gensamer: A Dilatometric Study of Iron-Manganese Binary Alloys. *Trans.* Amer. Soc. Steel Treat. (1939) 19.
3. E. R. Jette and F. Foote: X-ray Study of Iron-nickel Alloys. *Trans.* A.I.M.E. (1936) 120, 259–276.
4. A. J. Bradly and H. S. Goldschmit: Iron-Rich Nickel-Iron Alloys. *Jnl.* Iron and Steel Inst. (1939) 140, 11–27.
5. E. A. Owens and A. H. Sully: Equilibrium Diagram of Fe-Ni Alloys. *Phil. Mag.* (May 1939) [7] (184).

DISCUSSION

(Cyril Wells presiding)

S. EPSTEIN,* Bethlehem, Pa.—In view of the authors' statement that cobalt neither stabilizes gamma nor slows down the rate of transformation, it would be of interest to know the effect of chromium. This element is like cobalt in not stabilizing gamma but it might have a beneficial effect in slowing down the rate of transformation. Nitrogen is known to have a

* Research and Development Department, Bethlehem Steel Co.

very powerful effect in stabilizing gamma and some way might perhaps be found for incorporating enough of it to make these alloys more stable.

I. R. KRAMER (author's reply).—Although chromium might serve to decrease the gamma decomposition, it has been shown to increase the mean coefficient of expansion markedly and any advantage gained would be counteracted. The influence of nitrogen might prove to be interesting, though its solubility in nickel and cobalt is very low.

Effects of Eight Complex Deoxidizers on Some 0.40 Per Cent Carbon Forging Steels

By George F. Comstock,* Member A.I.M.E.

(New York Meeting, February 1942)

It has been reported recently[1] that the hardenability and toughness of forging steels may be improved appreciably by the use of complex deoxidizers containing titanium, aluminum, and vanadium. In the light of these results, an investigation of similar deoxidizers containing various hardening and grain-refining elements was proposed. These deoxidizers included three manganese-silicon-aluminum-titanium alloys with and without boron and calcium, three titanium-aluminum ferroalloys with vanadium, molybdenum and zirconium, respectively, an aluminum-zirconium ferroalloy, and plain ferroboron. Their approximate compositions are given in Table 1, and the results obtained so far in the investigation of their effects on steel are presented in the later parts of this paper.

steels, which were melted in a small basic-lined induction furnace and cast in the form of 17-lb. ingots about 2.75 in. square. The basic charge for each heat was 10 lb. Armco iron and 6 lb. of clean low-carbon sheet-steel scrap. When melted, this charge was deoxidized with 15 grams of ferrosilicon, then about 500 grams of pig iron was added to give the desired carbon content. After the pig iron was dissolved, nickel

TABLE 1.—*Compositions of Deoxidizers Used*

Designation	Approximate Composition, Per Cent										
	Ti	Al	Zr	V	Mo	B	Ca	Mn	Si	C	Balance (Fe)
Mn-Si-Ti No. 1.........	20.	13.7						24.6	27.6	1.0	13.1
Mn-Si-Ti No. 3.........	18.	14.				1.5		24.	27.	0.75	14.75
Mn-Si-Ti No. 4.........	9.	11.				1.5	1.5	14.	20.	1.2	41.8
Fe-V-Ti..............	15.5	9.		25					4.		46.5
Fe-Zr-Ti.............	22.	21.	5.4			0.13			3.		48.47
Fe-Mo-Ti............	19.7	15.8			36.6				9.5		18.4
Fe-Al-Zr............		24.3	35.6						4.8		35.3
Ferroboron...........		0.77				18.4			0.64	0.39	79.8

loys with and without boron and calcium, three titanium-aluminum ferroalloys with vanadium, molybdenum and zirconium, respectively, an aluminum-zirconium ferroalloy, and plain ferroboron. Their approximate compositions are given in Table 1, and the results obtained so far in the investigation of their effects on steel are presented in the later parts of this paper.

Method of Using Deoxidizers

The deoxidizers listed in Table 1 were used in three series of 0.40 per cent carbon

shot and high-carbon ferrochromium were added if required, and additions of 80 per cent high-carbon ferromanganese and 50 per cent ferrosilicon were made to provide the proper amounts of those elements. Aluminum was added to every heat 2 min. after the silicon, for grain-size control and preliminary deoxidation. One minute later the special deoxidizer was added to the clean bare surface of the molten steel, and 2 min. afterward the steel was poured into the ingot mold, using a hot-top and pipe-preventing compound after pouring to decrease the depth of the shrinkage cavity.

The special deoxidizers were used mostly in the form of about ½ to ¾-in. lumps,

which were thrown into the molten steel so as to be immediately covered, and not stirred very much. When the addition required was less than 9 grams, however, this small amount of special alloy was wrapped, together with a portion of the regular aluminum addition, in thin, clean sheet iron, and added in that form.

KINDS OF STEEL TESTED

The three kinds of steel used for this work were (A) S.A.E. T-1340 (1.8 per cent Mn), (B) 1.15 per cent Mn steel, and (C)

was larger than those of the No. 1 and No. 3 alloys in the first and second ingots, merely because the No. 4 alloy was lower in titanium and aluminum, the intention being to have the total titanium and aluminum additions about equal. The additions of the vanadium and molybdenum alloys were slightly smaller, so as to agree with general practice as reported by commercial users of similar alloys. The ferroboron additions to the Nos. 8 and 9 ingots were designed to give about the same boron content, and about three times this content, respectively,

TABLE 2.—*Deoxidation and Composition of the Steels Used*

Ingot No.	Aluminum Added, Lb. per Net Ton	Special Deoxidizer		Chemical Analysis, Per Cent				
		Designation	Lb. per Net Ton	C	Mn	Si	Ti	B
A-1	0.75	Mn-Si-Ti No. 1	4.0	0.41	1.84	0.27		
A-2	0.75	Mn-Si-Ti No. 3	4.0	0.40	1.75	0.27	0.030	0.005
A-3	0.75	Mn-Si-Ti No. 4	6.25	0.40	1.82	0.26	0.022	0.007
A-4	0.75	Fe-V-Ti	3.0	0.40	1.79	0.14		
A-6	1.0	Fe-Mo-Ti	3.0	0.40	1.80	0.24		
A-7	0.75	Fe-Al-Zr	4.0	0.40	1.87	0.26		
B-1	1.0	Mn-Si-Ti No. 1	4.0	0.40	1.25	0.25	0.030	
B-2	1.0	Mn-Si-Ti No. 3	4.0	0.41	1.19	0.26	0.018	0.001
B-3	1.0	Mn-Si-Ti No. 4	6.25	0.40	1.12	0.26	0.024	0.004
B-4	1.0	Fe-V-Ti	3.0	0.40	1.16	0.32	0.036	
B-5	0.875	Fe-Zr-Ti	3.5	0.40	1.19	0.27	0.032	Trace[a]
B-6	1.0	Fe-Mo-Ti	3.0	0.40	1.19	0.28		
B-7	0.875	Fe-Al-Zr	4.0	0.39	1.12	0.24		
B-8	1.625	Ferroboron	0.5	0.40	1.14	0.31		0.007
B-9	1.625	Ferroboron	2.25	0.41	1.12	0.31		0.018
C-1	1.0	Mn-Si-Ti No. 1	4.0	0.39	0.50	0.24	0.028	
C-2	1.0	Mn-Si-Ti No. 3	4.0	0.40	0.56	0.25	0.024	0.002
C-3	1.0	Mn-Si-Ti No. 4	6.25	0.41	0.54	0.27	0.028	0.004
C-4	1.0	Fe-V-Ti	3.0	0.39	0.49	0.23	0.032	
C-5	0.875	Fe-Zr-Ti	3.5	0.40	0.54	0.25	0.027	Trace[a]
C-6	1.0	Fe-Mo-Ti	3.0	0.38	0.49	0.24		
C-7	0.875	Fe-Al-Zr	4.0	0.39	0.50	0.26		
C-8	1.625	Ferroboron	0.5	0.39	0.55	0.25		0.003
C-9	1.625	Ferroboron	2.25	0.40	0.52	0.29		0.011

[a] Less than 0.001 per cent as estimated with the spectrograph.

S.A.E. 3240 (1.8 per cent Ni and 1 per cent Cr). The carbon contents varied between 0.38 and 0.41 per cent, and the phosphorus and sulphur contents were below 0.04 per cent. The analyses and deoxidation treatments of the individual ingots are reported in Table 2. In each series the ingot numbers correspond in the same way to the deoxidation treatments.

In explanation of the amounts listed in the fourth column of Table 2, it might be noted that the addition of manganese-silicon-titanium No. 4 in the No. 3 ingots

as was derived from the manganese-silicon-titanium alloys 3 and 4. The aluminum addition was increased with the ferroboron, to make up for the virtual absence of aluminum in that alloy.

METHOD OF TESTING STEELS

The ingots were all rolled to 7/8-in. rounds, and the bars were normalized before further treatment. The normalizing temperature was 1600°F. for series A, and 1650°F. for the others. Tensile and Izod impact specimens were rough-machined, hardened and

tempered before final machining or grinding. Hardness tests were also made on many of the test specimens, and the grain sizes were determined at several temperatures.

to one thousandth of the tensile strength, and dividing the sum by five. Tensile-test specimens that broke at the shoulder were rejected, and such tests were repeated. All
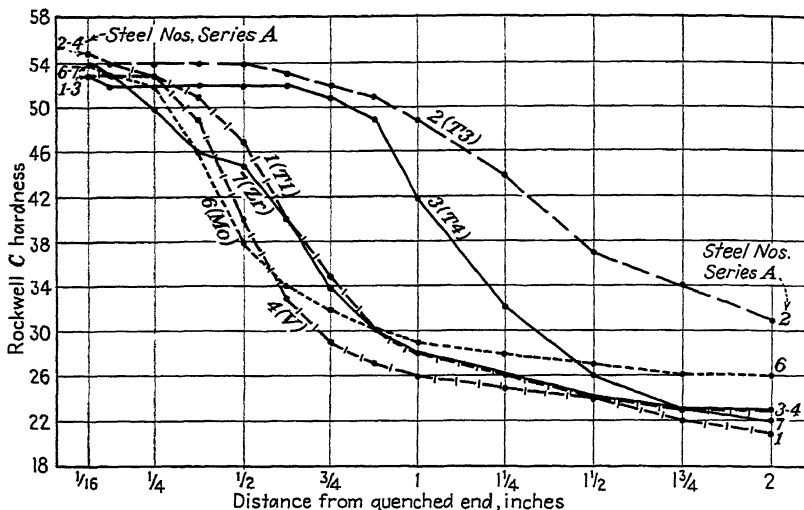
FIG. 1.—HARDNESS DISTRIBUTION ALONG SIDES OF END-QUENCHED SPECIMENS OF SERIES A STEELS CONTAINING 0.40 TO 0.41 PER CENT CARBON, 1.75 TO 1.87 PER CENT MANGANESE AND 0.14 TO 0.27 PER CENT SILICON.

Special Deoxidizer Added

Steel No.	Designation	Special Characteristics	Lb. per Net Ton
1 (T-1)	Mn-Si-Ti No. 1	20 % Ti, no B	4.0
2 (T-3)	Mn-Si-Ti No. 3	18 % Ti, 1.5 % B	4.0
3 (T-4)	Mn-Si-Ti No. 4	9 % Ti, 1.5 % B	6.25
4 (V)	Fe-V-Ti	15.5 % Ti, 25 % V	3.0
6 (Mo)	Fe-Mo-Ti	19.7 % Ti, 36.6 % Mo	3.0
7 (Zr)	Fe-Al-Zr	No Ti, 35.6 % Zr	4.0

tures. The hardenability of each steel was determined on ¾-in. diameter specimens by the end-quench method proposed by Jominy and Boegehold[2] after heating at 1500°F. for series C and 1550°F. for the other steels.

Tables 3, 4 and 5 give the results of the mechanical tests, and the hardenability test results are plotted in Figs. 1, 2 and 3. The merit value reported in connection with the tensile tests is one commonly used in the automobile industry, computed by adding six times the reduction of area

the impact results are averages from three tests each.

DISCUSSION OF MECHANICAL TEST RESULTS

The results in Table 3, obtained from water-quenched specimens drawn at 900° or 950°F., demonstrate the strengthening effects of vanadium in the No. 4 steels and of molybdenum in the No. 6 steels. These results, in general, show about what might be expected from the chemical compositions of the steels. In the manganese series, except for A-2, the steels treated with the manganese-silicon-titanium alloys were

² Jominy and Boegehold: *Trans.* Amer. Soc. Metals (1938) **26,** 574.

slightly superior in merit value to the others, but this did not hold for the nickel-chromium steels. The No. 7 zirconium-treated steels displayed noticeably good

denum, and zirconium-bearing alloys giving comparatively uninteresting results. In the nickel-chromium series, however, steels C-6 and C-7, treated with molybdenum or
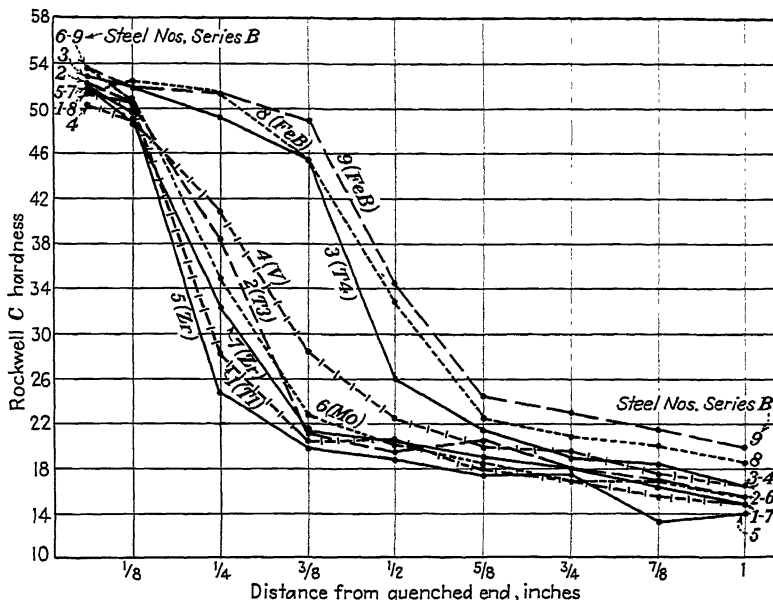
FIG. 2.—HARDNESS DISTRIBUTION ALONG SIDES OF END-QUENCHED SPECIMENS OF SERIES B STEELS CONTAINING 0.39 TO 0.41 PER CENT CARBON, 1.10 TO 1.19 PER CENT MANGANESE, AND 0.24 TO 0.32 PER CENT SILICON.

Special Deoxidizer Added

Steel No.	Designation	Special Characteristics	Lb. per Net Ton
1 (T-1)	Mn-Si-Ti No. 1	20 % Ti, no B	4.0
2 (T-3)	Mn-Si-Ti No. 3	18 % Ti, 1.5 % B	4.0
3 (T-4)	Mn-Si-Ti No. 4	9 % Ti, 1.5 % B	6.25
4 (V)	Fe-V-Ti	15.5 % Ti, 25 % V	3.0
5 (Zr)	Fe-Zr-Ti	22 % Ti, 5.4 % Zr, 0.13 % B	3.5
6 (Mo)	Fe-Mo-Ti	19.7 % Ti, 36.6 % Mo	3.0
7 (Zr)	Fe-Al-Zr	No Ti, 35.6 % Zr	4.0
8 (Fe B)	Ferroboron	No Ti, 18.4 % B	0.5
9 (Fe B)	Ferroboron	No Ti, 18.4 % B	2.25

ductility. The steels treated with ferroboron were not outstanding in this condition of heat-treatment, having comparatively low yield points.

Table 4, giving tensile results after quenching in oil and drawing at 450°F., shows that the highest merit values in both kinds of manganese steel were obtained with the manganese-silicon-titanium alloys or with ferroboron, the vanadium, molyb-

zirconium, exhibited the best combination of properties. Steel C-9, with the highest boron content, was noticeably deficient in ductility.

The impact results in Table 5 reveal a very interesting superiority in toughness in the boron-bearing manganese steels 2, 3 and 8 when drawn at 450°F. In the nickel-chromium series this is less marked, and also at higher drawing temperatures the

improvement fades out in all the series. The molybdenum steel A-6 seems to show an improvement in impact values after tempering at 750° and 900°F., but in the is required to produce a marked improve. ment in hardenability. The vanadium steels, No. 4, showed generally somewhat greater hardenability than those treated
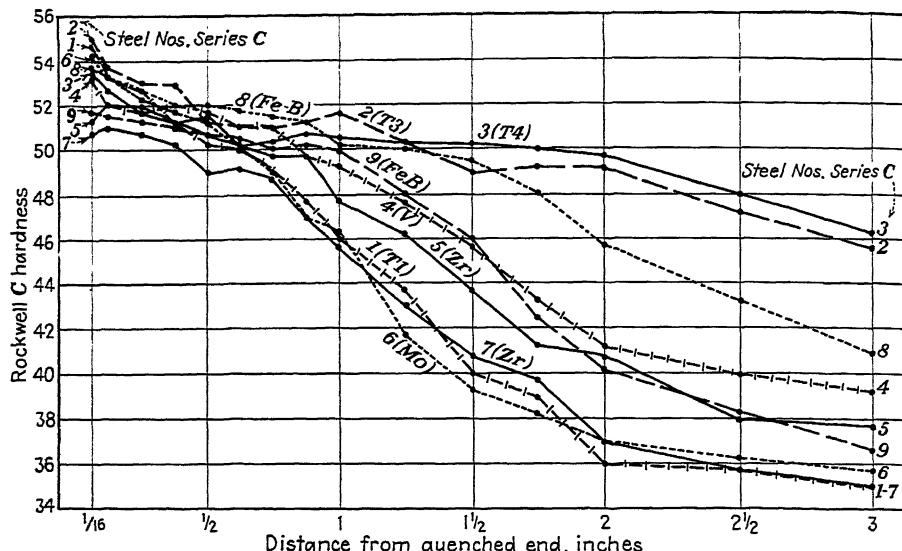
FIG 3.—HARDNESS DISTRIBUTION ALONG SIDES OF END-QUENCHED SPECIMENS OF SERIES C STEELS CONTAINING 0.38 TO 0.41 PER CENT CARBON, 0.49 TO 0.56 PER CENT MANGANESE, 0.23 TO 0.29 PER CENT SILICON, ABOUT 1.8 PER CENT NICKEL, AND ABOUT 1 PER CENT CHROMIUM.

Special Deoxidizer Added

Steel No.	Designation	Special Characteristics	Lb. per Net Ton
1 (T-1)	Mn-Si-Ti No. 1	20 % Ti, no B	4.0
2 (T-3)	Mn-Si-Ti No. 3	18 % Ti, 1.5 % B	4.0
3 (T-4)	Mn-Si-Ti No. 4	9 % Ti, 1.5 % B	6.25
4 (V)	Fe-V-Ti	15.5 % Ti, 25 % V	3.0
5 (Zr)	Fe-Zr-Ti	22 % Ti, 5.4 % Zr, 0.13 % B	3.5
6 (Mo)	Fe-Mo-Ti	19.7 % Ti, 36.6 % Mo	3.0
7 (Zr)	Fe-Al-Zr	No Ti, 35.6 % Zr	4.0
8 (Fe B)	Ferroboron	No Ti, 18.4 % B	0.5
9 (Fe B)	Ferroboron	No Ti, 18.4 % B	2.25

B and C series the molybdenum steels, as well as the high-boron steels, were generally inferior in impact resistance.

The hardenability results as plotted in Figs. 1, 2 and 3 are consistent in demonstrating marked superiority in this respect for the boron-bearing steels, except for steels B-2 and C-9. The analysis of B-2, however, shows comparatively low titanium and boron, indicating that the recovery of the special deoxidizer was poor in this ingot. Evidently more than 0.001 per cent boron

with molybdenum or zirconium, but were decidedly outclassed in this respect by the steels containing boron.

The mechanical tests in general demonstrate that the boron-bearing alloys had better effects on the manganese steels than on the nickel-chromium steels. In the A and B series, steel No. 3 treated with manganese-silicon-titanium alloy No. 4 gave the highest merit value in tension in both conditions of heat-treatment (except for A-1, water-quenched), and was about

equal to the steels treated with ferroboron and above the others in hardenability and resistance to impact. Steel A-2, treated with the other boron-bearing manganese-silicon-titanium alloy, was similarly superior, but B-2, as already noted, suffered from poor recovery of the special deoxidizer addition and was too low in boron.

both merit value and impact resistance after oil quenching. Thus the boron-bearing manganese-silicon-titanium alloys produced about as favorable a combination of general

TABLE 3.—*Tensile and Hardness Tests of Water-quenched and Drawn Specimens*

Ingot No.	Special Deoxidizer	Lb. per Sq. In.		Per Cent		Merit Value	Brinell Hardness Number
		Yield Point	Tensile Strength	Elongation in 2 In.	Reduction of Area		
1.8 PER CENT Mn STEELS, QUENCHED FROM 1550°F., DRAWN AT 900°F.							
A-1	Mn-Si-Ti No. 1	147,000	156,600	17.0	58.8	101.9	321
A-2	Mn-Si-Ti No. 3	146,000	157,500	16.5	51.8	93.7	321
A-3	Mn-Si-Ti No. 4	137,800	150,900	18.0	56.9	98.5	321
A-4	Fe-V-Ti	152,900	160,500	17.0	52.8	95.5	331
A-6	Fe-Mo-Ti	156,900	165,000	16.5	52.5	96.0	341
A-7	Fe-Al-Zr	144,400	154,200	17.5	55.9	97.9	321
1.15 PER CENT Mn STEELS, QUENCHED FROM 1550°F., DRAWN AT 900°F.							
B-1	Mn-Si-Ti No. 1	127,000	138,000	19.0	58.2	97.4	285
B-2	Mn-Si-Ti No. 3	129,500	141,000	19.5	57.8	97.6	302
B-3	Mn-Si-Ti No. 4	128,000	139,800	19.0	58.6	98.3	285
B-4	Fe-V-Ti	143,500	151,600	16.5	54.5	96.5	321
B-5	Fe-Zr-Ti	129,000	140,800	17.0	55.0	94.2	293
B-6	Fe-Mo-Ti	135,000	147,000	17.5	55.0	95.4	302
B-7	Fe-Al-Zr	127,000	139,500	19.0	58.4	98.0	285
B-8	Fe-B (low)	126,000	141,000	18.5	56.9	96.5	285
B-9	Fe-B (high)	124,000	139,300	18.5	54.5	93.3	285
Ni-Cr STEELS, QUENCHED FROM 1500°F., DRAWN AT 950°F.							
C-1	Mn-Si-Ti No. 1	154,500	162,300		(cracked)		321
C-2	Mn-Si-Ti No. 3	153,000	161,800	16.0	51.4	94.0	331
C-3	Mn-Si-Ti No. 4	152,000	161,800	16.5	51.6	94.3	341
C-4	Fe-V-Ti	163,500	170,000	15.5	50.4	94.5	352
C-5	Fe-Zr-Ti	156,500	163,700	16.5	52.8	96.1	341
C-6	Fe-Mo-Ti	161,000	168,000	15.5	50.4	94.1	341
C-7	Fe-Al-Zr	149,500	159,000	17.5	55.5	98.4	331
C-8	Fe-B (low)	146,000	157,600	16.5	50.2	91.8	321
C-9	Fe-B (high)	144,500	156,500	16.5	53.3	95.3	321

In the nickel-chromium series, both the steels treated with boron-bearing manganese-silicon-titanium showed the highest hardenability, and were approximately equal to most of the other steels in tensile and impact properties. The zirconium-treated steel C-7 showed about the best merit value of this series in both conditions of heat-treatment, but its hardenability was low. Steel C-5 showed a good merit value after water quenching, but poor after oil quenching. The steel treated with the larger amount of ferroboron was low in

mechanical properties in these nickel-chromium steels as most of the other deoxidizers, including ferroboron, with appreciably higher hardenability.

MICROSTRUCTURES

The microstructures of many of these specimens were investigated to check the grain sizes. Estimations of the austenite grain size at 1550°F. and at 1750°F. were first attempted by simple normalizing of small specimens at the respective temperatures to produce a ferrite network. This method served well for the manganese steels but not very well for the nickel-chromium steels, since the ferrite network in the latter was very poorly developed.

Holding the nickel-chromium steels at various temperatures between 1300° and 1350°F. during cooling from 1750°F. was tried, without much better success. The ferroboron does not, this difference was compensated for, in the treatment of the steels, by a larger use of shot aluminum with the ferroboron as reported in Table 2.

TABLE 4.—*Tensile Tests of Oil-quenched and Drawn Specimens*

| Ingot No. | Special Deoxidizer | Lb. per Sq. In. | | Per Cent | | Merit Value |
		Yield Point	Tensile Strength	Elongation in 2 In.	Reduction of Area	
1.8 Per Cent Mn Steels, Quenched from 1550°F., Drawn at 450°F.						
A-1	Mn-Si-Ti No. 1	246,000	262,000	9.5	38.1	98.1
A-2	Mn-Si-Ti No. 3	250,000	289,000	8.5	33.7	98.2
A-3	Mn-Si-Ti No. 4	225,000	264,000	10.0	38.9	99.5
A-4	Fe-V-Ti	234,000	254,000	9.0	39.1	97.7
A-6	Fe-Mo-Ti	226,000	249,000	6.5	20.2	74.0
A-7	Fe-Al-Zr	212,000	262,000	10.0	35.0	94.4
1.15 Per Cent Mn Steels, Quenched from 1550°F., Drawn at 450°F.						
B-1	Mn-Si-Ti No. 1	121,200	152,350	10.0	45.7	85.3
B-2	Mn-Si-Ti No. 3	146,700	215,350	9.5	35.4	85.6
B-3	Mn-Si-Ti No. 4	200,000	269,000	12.5	42.5	104.8
B-4	Fe-V-Ti	130,000	207,500	9.5	30.9	78.6
B-5	Fe-Zr-Ti	105,250	144,150	11.5	41.2	77.7
B-6	Fe-Mo-Ti	121,600	152,300	12.0	34.6	72.0
B-7	Fe-Al-Zr	130,900	176,700	3.5	29.6	70.9
B-8	Fe-B (low)	161,900	266,000	9.3	34.7	94.8
B-9	Fe-B (high)	212,700	264,200	9.5	36.2	96.3
Ni-Cr Steels, Quenched from 1500°F., Drawn at 475°F.						
C-1	Mn-Si-Ti No. 1	212,000	247,000	10.8	40.9	98.4
C-2	Mn-Si-Ti No. 3	237,000	262,000	10.3	37.2	97.0
C-3	Mn-Si-Ti No. 4	217,000	262,500	10.3	37.3	97.3
C-4	Fe-V-Ti	230,000	265,000	11.5	37.4	97.9
C-5	Fe-Zr-Ti	223,000	263,500	9.8	33.3	92.6
C-6	Fe-Mo-Ti	232,500	264,000	11.5	42.7	104.0
C-7	Fe-Al-Zr	228,500	261,000	12.5	42.1	102.7
C-8	Fe-B (low)	206,500	252,300	10.5	40.5	99.1
C-9	Fe-B (high)	205,800	258,500	9.5	32.1	90.2

martensite grains could not be developed clearly in these steels after quenching with or without tempering, and finally the McQuaid-Ehn carburizing procedure at 1725°F. was resorted to. Some illustrations of representative grain sizes developed by these methods are presented in the form of photomicrographs (Figs. 4 to 13) and the results of the grain-size estimations are given in Table 6.

Table 6 and the photomicrographs show definitely that the treatment with ferroboron produced coarser-grained steel than treatment with the vanadium, zirconium, or manganese-silicon-titanium alloys. Although the latter contain aluminum and

Thus the coarser grain size when ferroboron was used seems to be due to the boron, rather than to less aluminum. The tendency of boron to coarsen the grain is in evidence to a slight degree in ingots A-3 and B-3 where the boron was added in the form of manganese-silicon-titanium alloy No. 4, but not in ingot C-3, for which the same alloy was used in the nickel-chromium series. In general, it appears that boron can be added in that form or as manganese-silicon-titanium alloy No. 3, to improve the mechanical properties after hardening and drawing at low temperatures, as well as the hardenability, without appreciable loss of the fine-grain characteristics imparted by

aluminum as happens when plain ferro-boron is used.

TRIAL OF ONE ALLOY IN LARGE INGOT

The manganese-silicon-titanium No. 3 alloy was tried in a large ingot, weighing

poured from a heat deoxidized normally with aluminum to produce fine-grained steel. The ingots were rolled to 1¾-in. rounds, and the bars of that size were normalized at 1600°F. The test specimens were rough-machined, quenched in oil

TABLE 5.—*Impact and Hardness Tests of Oil-quenched[a] and Drawn Specimens*

Ingot No.	Special Deoxidizer	Izod Value	Rock-well C	Izod Value	Rock-well C	Izod Value	Rock-well C	Izod Value	Rock-well C
		1.8 PER CENT Mn STEELS, QUENCHED FROM 1550°F.							
Drawn at....................		450°F.		600°F.		750°F.		900°F.[a]	
A-1	Mn-Si-Ti No. 1	8.3	49.9					36.3	32.5
A-2	Mn-Si-Ti No. 3	12.3	50.3	5.0	47.5	5.0	42.5		31.0
A-3	Mn-Si-Ti No. 4	13.3	50.0	6.3	46.8	7.0	41.3	34.7	31.5
A-4	Fe-V-Ti	6.7	49.5	3.7	47.3	5.3	41.5		34.5
A-6	Fe-Mo-Ti	5.7	50.5	4.0	46.5	10.0	42.3	40.7	35.0
A-7	Fe-Al-Zr	7.3	48.9						32.0
		1.15 PER CENT Mn STEELS, QUENCHED FROM 1550°F.							
Drawn at....................		450°F.		600°F.		750°F.		900°F.	
B-1	Mn-Si-Ti No. 1	12.7	43.0	9.3	39.0	34.7	37.7	51.3	29.5
B-2	Mn-Si-Ti No. 3	14.3	50.0	8.7	46.5	27.3	38.7	56.3	30.0
B-3	Mn-Si-Ti No. 4	17.3	46.0	14.7	47.0	24.0	40.0	49.3	31.2
B-4	Fe-V-Ti	11.7	49.7	9.0	46.5	18.7	39.5	41.3	32.7
B-5	Fe-Zr-Ti	10.7	49.0	5.3	45.2	25.0	37.0	50.3	29.0
B-6	Fe-Mo-Ti	10.0	45.5	8.3	45.7	20.0	39.7	48.3	30.5
B-7	Fe-Al-Zr	10.0	42.7	6.3	45.0	22.3	37.5	50.7	28.2
B-8	Fe-B (low)	18.0	48.7	15.3	47.0	20.0	39.0	52.7	30.7
B-9	Fe-B (high)	13.3	44.7	14.0	46.7	15.7	39.0	45.0	30.7
		Ni-Cr STEELS, QUENCHED FROM 1500°F.							
Drawn at....................		475°F.		650°F.		800°F.		950°F.	
C-1	Mn-Si-Ti No. 1	14.0	49.0	13.7	46.2	20.3	40.7	37.0	34.0
C-2	Mn-Si-Ti No. 3	16.7	46.5	14.7	47.0	22.3	41.7	35.7	34.3
C-3	Mn-Si-Ti No. 4	15.0	46.7	15.0	46.7	20.7	41.7	35.3	35.2
C-4	Fe-V-Ti	16.3	49.7	13.3	47.0	20.7	41.7	31.0	36.7
C-5	Fe-Zr-Ti	15.0	49.5	17.0	43.2	22.0	41.5	35.7	35.0
C-6	Fe-Mo-Ti	12.0	46.7	11.7	46.7	12.7	46.0	34.0	36.0
C-7	Fe-Al-Zr	14.3	45.0	12.7	46.7	21.0	40.7	36.7	34.7
C-8	Fe-B (low)	17.7	49.0	14.0	46.2	20.0	41.0	38.7	33.7
C-9	Fe-B (high)	14.0	49.0	12.3	46.5	19.7	41.0	29.3	35.2

[a] The specimens of the A series drawn at 900°F. were quenched in water, and the missing results are omitted because quenching cracks made their value doubtful. Steels A-1 and A-7 were not tested after drawing at 600° or 750°F.

several tons, of 0.38 per cent carbon steel at a mill in the Pittsburgh district. The steel rolled from this ingot was tested, along with steel from an untreated ingot of the same heat for comparison, at the same mill, with the results reported in Table 7. Five pounds of the special deoxidizer per ton was added to the treated ingot, which was

from 1500° to 1550°F., tempered at 450° and 900°F., respectively, and ground to finished size for testing.

The properties of the quenched and drawn specimens, as reported in Table 7, indicate a decidedly increased hardenability for the steel treated with the manganese-silicon-titanium No. 3, with much greater

strength and not appreciably lower reduction of area for the treated steel in that condition of heat-treatment. This agrees

than in any of the laboratory melts, so that a comparison on the basis of ingot size alone is not justified.
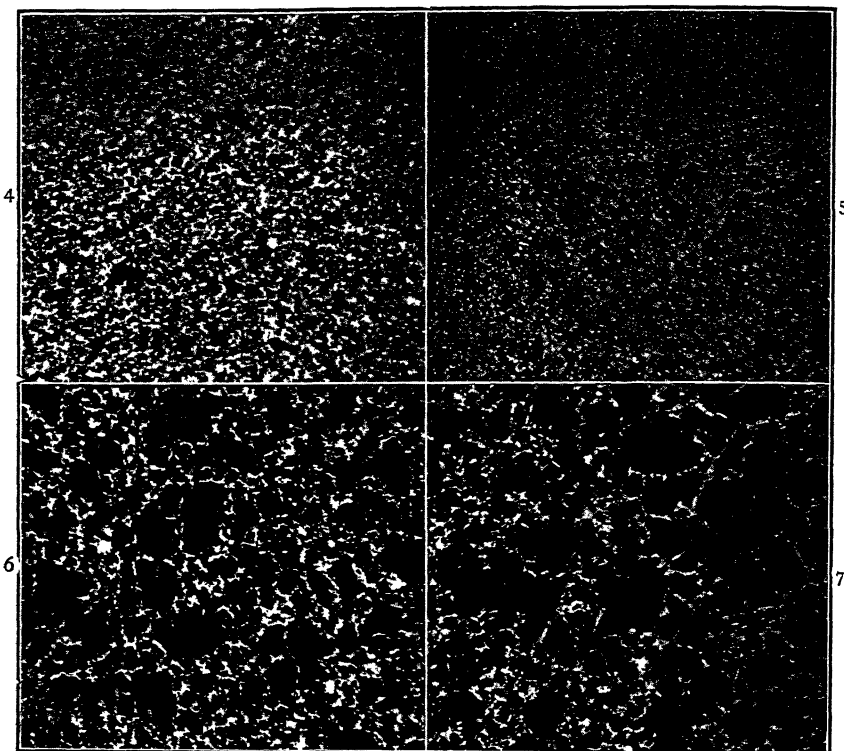
FIG. 4.—STEEL B-3 TREATED WITH MANGANESE-SILICON-TITANIUM NO. 4, SHOWING GRAIN SIZE No. 8.

FIG. 5.—STEEL B-4 TREATED WITH FERRO-VANADIUM-TITANIUM, SHOWING GRAIN SIZE FINER THAN No. 8.

FIG. 6.—STEEL B-8 TREATED WITH SMALLER AMOUNT OF FERROBORON, SHOWING MIXED GRAIN SIZE, ESTIMATED AS 60 PER CENT NO. 5 AND 40 PER CENT NO. 7.

FIG. 7.—STEEL B-9 TREATED WITH LARGER AMOUNT OF FERROBORON, SHOWING MIXED GRAIN SIZE, ESTIMATED AS 80 PER CENT NO. 4 AND 20 PER CENT NO. 7.

All show specimens of the 1.15 per cent Mn steels normalized at 1550°F., etched with Nital and magnified 100 diameters.

with the results obtained from the small, laboratory-size ingots. The elongations after heat-treatment, however, are lower for the special deoxidized steel, as would be expected in view of the greater hardness and much higher yield point. The merit values obtained with the large ingots are noticeably higher than in the 17-lb. ingots, but their manganese contents were lower

CONCLUSIONS

Specific

It must be emphasized that the conclusions that appear below were drawn chiefly from laboratory work with small induction-furnace heats of steel, and require more extensive confirmation in regular practice than is afforded by the
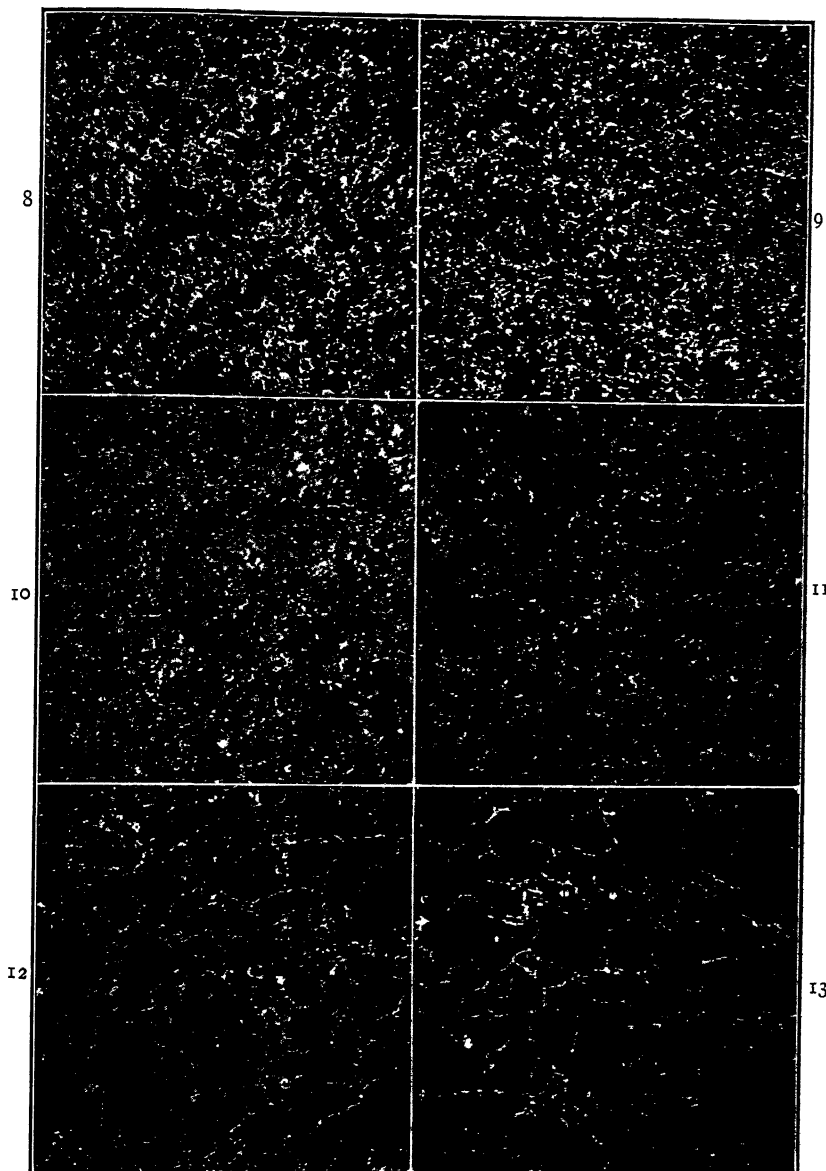
FIG. 8.—STEEL C-1 TREATED WITH MANGANESE-SILICON-TITANIUM NO. 1, GRAIN SIZE NO. 7.
FIG. 9.—STEEL C-2 TREATED WITH MANGANESE-SILICON-TITANIUM NO. 3, GRAIN SIZE NO. 7.
FIG. 10.—STEEL C-3 TREATED WITH MANGANESE-SILICON-TITANIUM NO. 4, GRAIN SIZE NO. 8.
FIG. 11.—STEEL C-4 TREATED WITH FERRO-VANADIUM-TITANIUM, GRAIN SIZE NO. 7 WITH FEW NO. 5.
FIG. 12.—STEEL C-8 TREATED WITH SMALLER AMOUNT OF FERROBORON, GRAIN SIZE NO. 5 TO 6.
FIG. 13.—STEEL C-9 TREATED WITH LARGER AMOUNT OF FERROBORON, GRAIN SIZE NO. 5.
All show hypereutectoid zones of nickel-chromium-steel specimens carburized 7.5 hours at 1725°F. and slowly cooled, etched with Nital and magnified 100 diameters.

single large-scale trial that has been reported. The results of that trial, however, indicate that probably the effects of the "manganese-silicon-titanium" alloys as reported here would not be much different in commercial practice. The specific conclusions also are based on results from the particular quantities of the various additions, as reported in Table 2. No claim is made that different quantities might not give different results; for instance, with larger additions of vanadium or molybdenum the hardenability of steels like No. 4 or No. 6 in each series might very likely be higher. With these limitations understood, the following statements are offered as a summary of the results that have been reported:

TABLE 6.—*Austenitic Grain Sizes of Small Specimens*

Ingot No.	Special Deoxidizer	Normalized 1550°F.	Normalized 1750°F.	McQuaid-Ehn Carburizing Test 1725°F.
		1.8 PER CENT Mn STEELS		
A-1	Mn-Si-Ti No. 1	7	6	
A-2	Mn-Si-Ti No. 3	8	6	
A-3	Mn-Si-Ti No. 4	7	5	
A-4	Fe-V-Ti	7–8	7–8	
		1.15 PER CENT Mn STEELS		
B-1	Mn-Si-Ti No. 1	8	7	
B-2	Mn-Si-Ti No. 3	8	7	
B-3	Mn-Si-Ti No. 4	8	3 (25 %) to 6 (75 %)	
B-4	Fe-V-Ti	9	7	
B-5	Fe-Zr-Ti	8	7	
B-8	Fe-B (low)	5 (60 %) to 7 (40 %)	4–5	
B-9	Fe-B (high)	4 (80 %) to 7 (20 %)	2–4	
		Ni-Cr STEELS		
C-1	Mn-Si-Ti No. 1	10		7
C-2	Mn-Si-Ti No. 3	8		7
C-3	Mn-Si-Ti No. 4	8		8
C-4	Fe-V-Ti	8		7 (few 5)
C-5	Fe-Zr-Ti	10		7
C-8	Fe-B (low)	7		5–6
C-9	Fe-B (high)	7		5

1. The treatment of 0.40 per cent carbon steel containing about 1.15 per cent manganese, or S.A.E. 3240 steel, with ferroboron increased the hardenability, but

TABLE 7.—*Tensile and Hardness Tests of Bars from Large Ingots*

Constituent	Steel Treated with 5 Lb. Mn-Si-Ti No. 3 per Ton	Untreated Steel
CHEMICAL ANALYSIS, PER CENT		
Carbon..........	0.38	0.39
Manganese.......	0.75	0.71
Phosphorus......	0.014	0.014
Sulphur..........	0.016	0.018
Silicon...........	0.20	0.16
Aluminum.......	0.067	0.041
Vanadium........	0.004	0.007
Nitrogen.........	0.004	0.005

SPECIMENS NOT QUENCHED				
Property	As Rolled	Normalized	As Rolled	Normalized
Yield point, lb. per sq. in..........	53,970	50,270	50,180	56,820
Tensile strength, lb. per sq. in....	92,560	83,820	85,870	85,320
Elongation, per cent...........	26.0	29.0	26.0	28.5
Reduction of area, per cent.......	52.2	56.8	52.2	54.7
Brinell hardness number........	179	166	170	163

OIL-QUENCHED SPECIMENS				
Drawn at........	450°F.	900°F.	450°F.	900°F.
Yield point, lb. per sq. in..........	212,300	120,100	78,900	73,700
Tensile strength, lb. per sq. in....	244,300	125,400	105,600	103,900
Elongation, per cent...........	12.5	11.5	21.5	24.0
Reduction of area, per cent.......	51.0	65.7	63.1	63.3
Merit value......	110	103.9	96.8	96.7
Brinell hardness number........	444	241	217	207

tended to coarsen the grain size, giving only mediocre tensile properties after quenching and drawing at 900° to 950°F.

2. Treatment of these steels with complex titanium-aluminum deoxidizers containing vanadium or zirconium gave a fine grain size, but with comparatively low hardenability, and only mediocre tensile and impact properties after quenching and drawing at about 450°F.

3. Treatment of similar steels with "manganese-silicon-titanium" alloys containing boron (also iron and aluminum) gave a fine grain size with practically the same hardenability as after ferroboron treatment, and excellent tensile and impact properties after quenching and tempering at about 450° or 925°F. Similarly superior properties were also found in 1.8 per cent Mn steel.

450°F., the molybdenum alloy did not give as good tensile and impact properties as most of the other additions, but in the nickel-chromium steel drawn at 475°F. it gave the best combination of strength and ductility although with poor impact values.

TABLE 8.—*Summary of Comparative Effects of Deoxidizers on Some Properties of Treated Steels*

| Conclu-sion No. | Deoxidizer Designation | Steel No. | Grain Size | Hardenability | Tensile Properties | | Impact Re-sistance, Oil-quenched, Drawn 450°–650°F. |
					Water-quenched, Drawn 900°–950°F.	Oil-quenched, Drawn 450°–475°F.	
1	Ferroboron	8–9	Coarser	High	Fair	Good	Good
2	Fe-V-Ti	4	Fine	Moderate	High strength	Fair	Fair
2	Fe-Zr-Ti	5	Fine	Moderate or low	Fair	Poor	Fair
3	Mn-Si-Ti No. 3 and No. 4 (containing boron)	2–3	Fine	High	Good	Good	Good
4	Fe-Al-Zr	7	Fine	Low	High ductility	Poor in series B steels; good in others	Fair
5	Fe-Mo-Ti	6		Low	High strength	Good in series C steels; poor in others	Poor
	Mn-Si-Ti No. 1 (no boron)	1	Fine	Low	Series C cracked; good in others	Fair in series B steels; good in others	Fair

4. Treatment of these steels with zirconium (together with aluminum but without titanium) gave comparatively low hardenability, and high ductility after quenching and drawing at 900° to 950°F. Zirconium gave excellent tensile properties in the oil-quenched nickel-chromium steel, and fairly good properties in the 1.8 per cent Mn steel, but not in the 1.15 per cent Mn steel.

5. Treatment of these steels with a molybdenum-titanium-aluminum ferroalloy gave comparatively low hardenability, as with zirconium, but increased the strength after water quenching. The increase, however, was no greater than that derived from the vanadium in the No. 4 steels. In the manganese steels quenched and drawn at

The specific conclusions are presented somewhat more systematically in Table 8, where comparisons can perhaps be more readily grasped.

General

The following general conclusions seem justified from the results reported in this paper:

6. The incorporation of minute amounts of boron in fine-grained 0.40 per cent carbon steels is surprisingly effective in increasing hardenability.

7. The same small boron additions also give good ductility and superior toughness, with high strength, after hardening and drawing at low temperatures, such as 450° or 600°F. When drawn at higher temperatures to hardness values below about 45 Rockwell C, the superiority in toughness of steels so treated over steels similarly treated, but without boron, disappears.

8. The amount of boron that should be present in these 0.40 per cent carbon steels to secure the advantages in hardenability and toughness that have been noted appears to be about 0.002 to 0.007 per cent.

9. To secure a superior combination of strength and ductility, together with high hardenability, in fine-grained steel of this nature, it is advantageous to add the boron in the form of a complex titanium alloy, such as "manganese-silicon-titanium" No. 3 or No. 4, rather than as ferroboron.

ACKNOWLEDGMENTS

Influence of Chromium and Molybdenum on Structure, Hardness and Decarburization of 0.35 Per Cent Carbon Steel

By R. F. Miller,* Member A.I.M.E. and R. F. Campbell*

SIXTEEN steels containing different combinations of chromium and molybdenum, in amounts up to 5 per cent of each element, were examined for microstructure and hardness after air cooling and after furnace cooling from suitable austenitizing temperatures. Diagrams summarizing the structures and hardness resulting from these two cooling rates are presented (Figs. 3, 4, 7).†

Data were also obtained on the influence of these two elements, individually and in combination, on the depth of decarburization observed after furnace cooling (Fig. 8).

COMPOSITION OF MATERIAL

The chemical composition of the steels investigated is given in Table 1. The plain carbon steel was made in a 25-ton Heroult electric-arc furnace, while the alloy steels were made in a 4.5-ton Ajax-Northrup electric induction furnace. The cast ingots were hot-rolled to 1.75-in. bars.

TABLE 1.—*Chemical Composition of Chromium-molybdenum Steels*

Steel	Per Cent Alloy Element, Nominal	Composition, Per Cent						
		C	Mn	P	S	Si	Cr	Mo
A	0 Cr, 0 Mo	0.36	0.39	0.009	0.012	0.23		
B	0.5 Cr, 0 Mo	0.37	0.38	0.022	0.022	0.24	0.56	
C	2 Cr, 0 Mo	0.32	0.45	0.007	0.011	0.28	1.97	
D	3.5 Cr, 0 Mo	0.37	0.48	0.007	0.024	0.26	3.61	
E	0 Cr, 0.5 Mo	0.39	0.42	0.011	0.007	0.20		0.55
F	0 Cr, 2 Mo	0.33	0.41	0.010	0.007	0.20		2.11
G	0 Cr, 5 Mo	0.32	0.37	0.014	0.005	0.27		5.15
H	0.5 Cr, 0.5 Mo	0.32	0.45	0.016	0.018	0.30	0.56	0.56
I	0.5 Cr, 2 Mo	0.33	0.45	0.014	0.007	0.30	0.51	2.01
J	0.5 Cr, 5 Mo	0.34	0.45	0.014	0.004	0.30	0.52	5.02
K	2 Cr, 0.5 Mo	0.35	0.44	0.010	0.010	0.27	2.02	0.52
L	2 Cr, 2 Mo	0.36	0.51	0.012	0.005	0.28	1.89	2.04
M	2 Cr, 5 Mo	0.41	0.39	0.015	0.005	0.25	1.88	5.08
N	5 Cr, 0.5 Mo	0.37	0.45	0.021	0.009	0.29	4.48	0.59
O	5 Cr, 2 Mo	0.38	0.40	0.008	0.005	0.25	4.50	2.03
P	5 Cr, 5 Mo	0.27	0.27	0.011	0.004	0.28	5.16	4.93

AIR-COOLED SERIES

The 1.75-in. bars were forged to flat plates, 0.25 in. thick, from which specimens 0.5 in. wide by 2 in. long were cut. The specimens were pretreated to improve their homogeneity by heating to 1830°F. (1000°C.) for 20 min. and oil-quenching. They were then reheated to 1740°F. (950°C.) for one hour and air-cooled, after
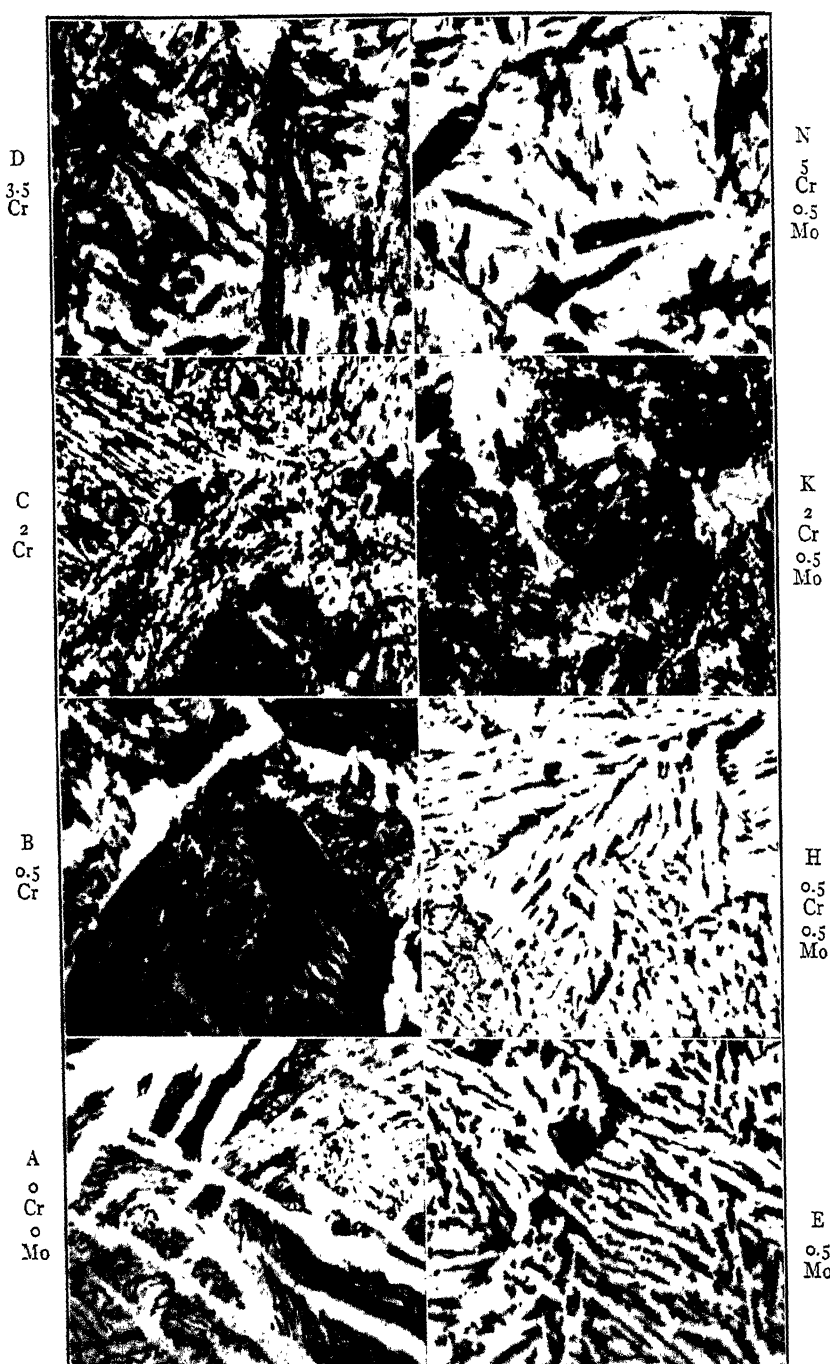
FIG. 1.—CHROMIUM-MOLYBDENUM STEELS AIR-COOLED FROM 1740°F. × 1000.
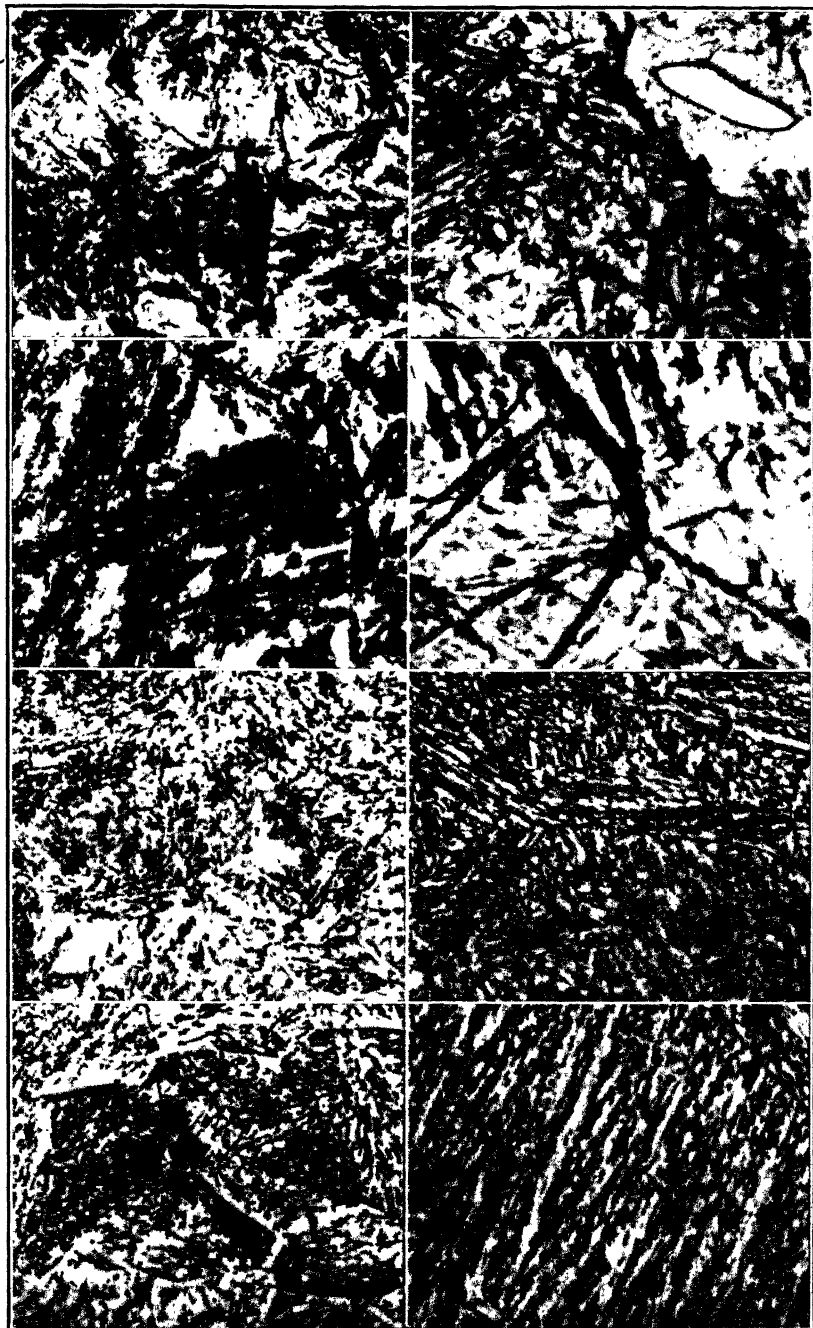
FIG. 2.—CHROMIUM-MOLYBDENUM STEELS AIR-COOLED FROM 1740°F., AND G, J, M AND P AIR-COOLED FROM 2200°F. × 1000.

which they were sectioned midway between the ends, and the microstructure and hardness were determined at the center of the exposed surface. Steels G, J, M and P (con-

0.35 per cent carbon steel, the following differences in structure are seen after air cooling (steels A, B, C, D, Fig. 1). The structure of the plain carbon steel A con-
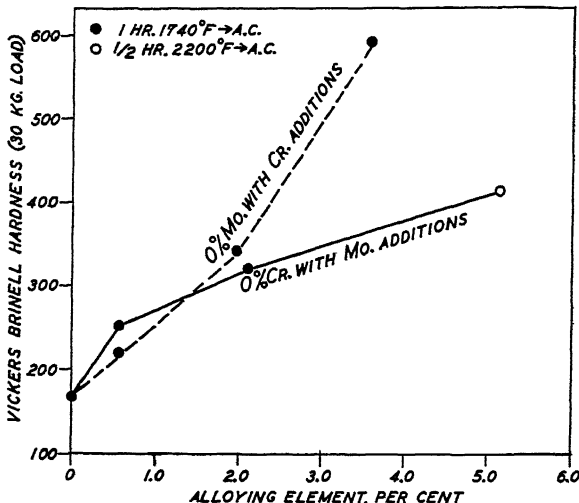
FIG. 3.—EFFECT OF CHROMIUM OR MOLYBDENUM ON HARDNESS OF AIR-COOLED 0.35 PER CENT CARBON STEEL.

taining 5.0 per cent Mo plus 0, 0.5, 2.0 and 5.0 per cent Cr, respectively) were found to contain a large amount of undissolved carbide as cooled from 1740°F. (950°C.). In order to determine the temperature at which the carbides would dissolve completely in austenite within a reasonable length of time, and without serious decarburization, small specimens of these four steels were heated to 1850°F. (1010°C.), 2000°F. (1095°C.), and 2200°F. (1250°C.) and brine-quenched. Microexamination disclosed that these steels must be heated to 2200°F. (1205°C.) for ½ hr. to obtain complete solution of the carbides. This austenitizing treatment was used for steels G, J, M and P in both the air-cooled and the furnace-cooled series.

The microstructures of the 16 steels after air cooling are shown in Figs. 1 and 2. The hardness data are listed in Table 2 and shown graphically in Figs. 3 and 4.

When chromium is added in increasing amount (0.5, 2.0, and 3.5 per cent) to a

sists of Widmanstätten ferrite and pearlite, but in B (0.5 per cent Cr) the pearlite is much finer, there is less ferrite and its distribution is a network outlining the former austenite grains. Addition of 2.0 per cent Cr (steel C) produces a great change from the pearlitic condition; the structure is now an acicular carbide-ferrite aggregate with a small amount of martensite. Further increase of chromium to about 3.5 per cent (steel D) produces an entirely martensitic structure.

On the other hand, when molybdenum is added in increasing amount (0.5, 2.0 and 5.0 per cent) to a 0.35 per cent carbon steel, the following differences in structure are seen after air cooling (steels A, E, F, G, Figs. 1 and 2). Both the plain carbon steel A and steel E, containing 0.5 per cent Mo, have a Widmanstätten structure of ferrite and pearlite, but the structure of E is much finer in character with respect to both the distribution of ferrite and pearlite and the fineness of the pearlite lamellae

than the plain carbon steel A or the 0.5 per cent Cr steel B. The Widmanstätten structure becomes a distinctly acicular pattern of ferrite and carbide accompanied by some martensite in steel F (2.0 per cent Mo); this structure is similar to that produced by the addition of 2.0 per cent Cr (steel C). The structure of steel G (5.0 per cent Mo) consists of ferrite and carbides in a striated pattern, accompanied by a small amount of martensite.

The type of microstructure found after air cooling is related to the effect of chromium and molybdenum on the austenite transformation behavior. Davenport[3] has published isothermal transformation diagrams (S-curves) for steels A (plain carbon), B (0.5 per cent Cr), C (2 per cent Cr), E (0.5 per cent Mo), and F (2 per cent Mo). These diagrams show that the addition of 0.5 per cent Mo retards the transformation rate of austenite in the higher-temperature region (above 1000°F., where pearlite forms) more than does 0.5 per cent Cr. This explains why the structure of B (0.5 per cent Cr) consists of fine pearlite after air cooling (Fig. 1), while steel E (0.5 per cent Mo) has a Widmanstätten structure, which forms over a lower-temperature range. The addition of 2 per cent of either chromium or molybdenum retards the transformation rate still further, and during air cooling the formation of pearlite is prevented in both steel C (2 per cent Cr) and F (2 per cent Mo). The diagrams for these steels containing 2 per cent of either alloying element show that during air cooling they both transform over approximately the same temperature range, and accordingly we find an acicular carbide-ferrite aggregate of similar appearance and hardness in both steels. Isothermal transformation diagrams are not available for the other steels in this series.

Summarizing the effect on the structure when chromium alone is added (steels A, B, C, D) or when molybdenum alone is added (steels A, E, F, G), it can be said that in-creasing the chromium content promotes the formation of martensite, while increasing the molybdenum content results in an acicular carbide-ferrite aggregate accompanied by some martensite. These particular effects are noticeable, but somewhat modified, when both chromium and molybdenum are present in varying amount. In steels containing 0.5 per cent Cr (steels B, H, I, J), the addition of molybdenum facilitates the formation of an acicular carbide-ferrite aggregate in a manner somewhat similar to that observed when molybdenum is added to a steel containing no chromium. On the other hand, in steels C, K, L, M and D, N, O, P, bearing 2.0 and 5.0 per cent Cr, respectively, the influence of chromium in forming martensite predominates and is augmented by the addition of molybdenum.

The influence exerted by chromium in promoting martensite formation, and the effect of molybdenum in forming structures consisting essentially of acicular carbide-ferrite aggregates, is reflected in the hardness of these steels. A comparison of the increase in hardness produced by adding either chromium alone or molybdenum alone is shown in Fig. 3; it appears that 0.5 per cent Mo is slightly more effective than an equal amount of chromium. Approximately the same increase of hardness results from the addition of about 1.5 per cent (interpolated value) of either element, while further additions of chromium are more effective than equal amounts of molybdenum. Figs. 4A and 4B show, respectively, the effect of increasing the amount of chromium or molybdenum in the presence of 0, 0.5, 2.0 and 5.0 per cent of the other element. Increasing the amount of chromium while the molybdenum content remains constant (Fig. 4A) is more effective in raising the hardness than is increasing the molybdenum content in the presence of a fixed amount of chromium (Fig. 4B). This is most apparent in the 5.0 per cent Cr steels where increasing the

molybdenum content has substantially no hardening effect (Fig. 4*B*). Steels M and P do not follow the stated trends exactly, but

per cent C) is considerably lower than the average. It should also be noted that there is some delta ferrite in steel P (Fig. 2),
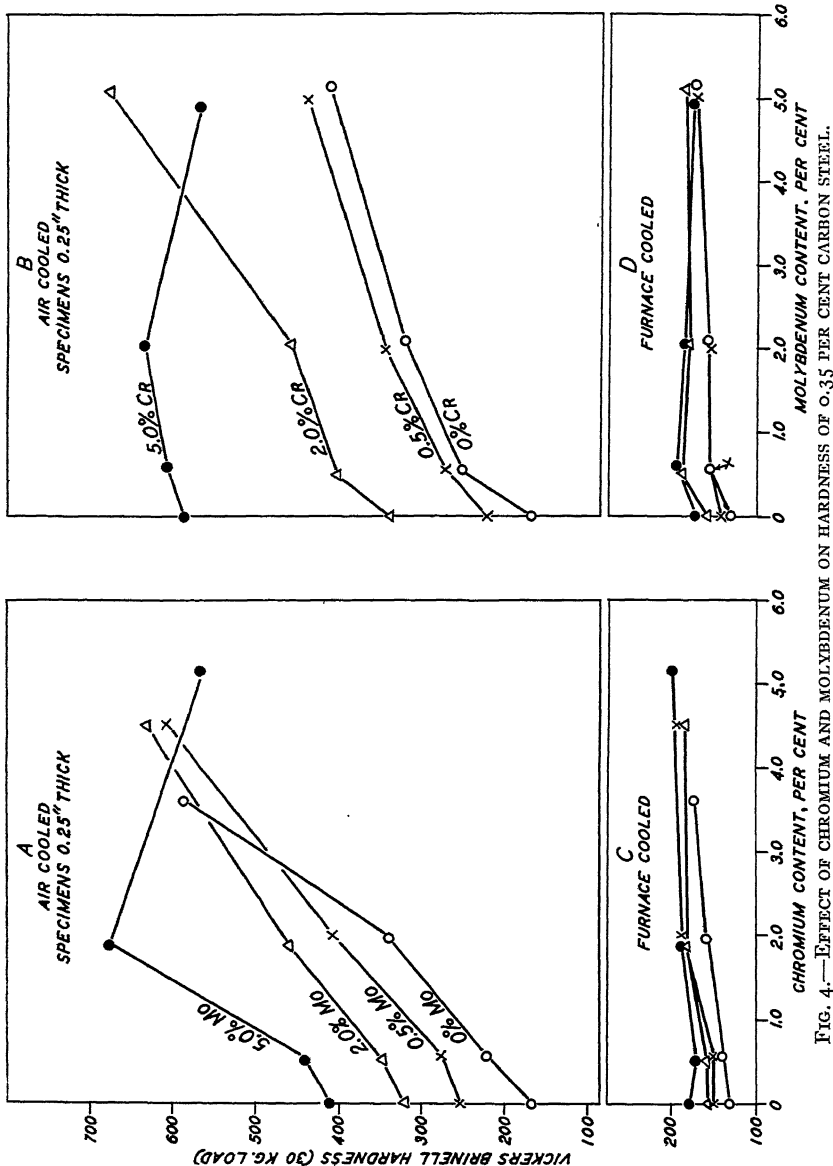
FIG. 4.—EFFECT OF CHROMIUM AND MOLYBDENUM ON HARDNESS OF 0.35 PER CENT CARBON STEEL.

probably this is because the carbon content of steel M (0.41 per cent C) is appreciably higher than that of the other steels, while the carbon content of steel P (0.27

which may decrease the hardness of this material. It may, therefore, be stated that when both chromium and molybdenum are present, chromium is more effective than

molybdenum in increasing the hardness of a steel that has been air-cooled.

FURNACE-COOLED SERIES

Specimens 2 in. long were cut from the 1.75-in. hot-rolled bars and pretreated to improve their homogeneity by heating 1 hr. at 1830°F. (1000°C.) and oil-quenching. The specimens were then reheated to 1740°F. (950°C.) for 1 hr. and furnace-cooled at the controlled rate of 10°F. (5°C.) per hour; except that steels G, J, M and P were heated to 2200°F. (1205°C.) for ½ hr. to dissolve the carbides, cooled to 1740°F. (950°C.) at the normal cooling rate of the furnace and then cooled to room temperature at the controlled rate of 10°F. (5°C.) per hour. When cold, the specimens were sectioned midway between the ends, and the microstructure and hardness were determined on the surface thus exposed, halfway from the center to the edge.

Photomicrographs of the series of furnace-cooled specimens are shown in Figs. 5 and 6. The hardness of these steels is listed in Table 2, and shown graphically in Figs. 4C and 4D.

In the steels A, B, C, D, containing no molybdenum (Fig. 5), the amount of pearl-

TABLE 2.—*Hardness, Vickers Pyramid Number (V.P.N.), with 30-kilogram Load*

Steel	Per Cent Alloy Element, Nominal	V.P.N. Air-cooled Series	V.P.N. Furnace-cooled Series
A	0 Cr, 0 Mo	167	129
B	0.5 Cr, 0 Mo	220	142
C	2 Cr, 0 Mo	341	159
D	3.5 Cr, 0 Mo	588	173
E	0 Cr, 0.5 Mo	254	153
F	0 Cr, 2 Mo	321	158
G	0 Cr, 5 Mo	411	177
H	0.5 Cr, 0.5 Mo	274	150
I	0.5 Cr, 2 Mo	349	157
J	0.5 Cr, 5 Mo	440	170
K	2 Cr, 0.5 Mo	406	188
L	2 Cr, 2 Mo	461	182
M	2 Cr, 5 Mo	679	187
N	5 Cr, 0.5 Mo	608	195
O	5 Cr, 2 Mo	634	185
P	5 Cr, 5 Mo	566	201

ite increases with increasing chromium content from 0 to 3.5 per cent. The same trend is noted in steels E, H, K, N, and F, I, L, O (Figs. 5 and 6), which contain respectively 0.5 per cent and 2.0 per cent Mo with increasing amount of chromium from 0 to 5.0 per cent. Steel K is entirely pearlitic and steel N is hypereutectoid, although this is somewhat obscured by the tendency of the proeutectoid carbide to spheroidize or coalesce. On the other hand, the amount of pearlite does not increase with increasing molybdenum content, as shown by steels A, E, F, G or B, H, I, J, containing no chromium and 0.5 per cent Cr, respectively. A shower precipitate of what may be a complex carbide appears in the ferrite of the 2.0 and 5.0 per cent Mo steels (F, I, L, O and G, J, M, P), and the lamellar distribution of the carbides is substantially absent in steels P (5.0 per cent Cr, 5.0 per cent Mo) and M (2.0 per cent Cr, 5.0 per cent Mo).

These changes of structure are reflected in the changes of hardness shown in Figs. 4C and 4D, which are small compared with the changes encountered in the air-cooled series (Figs. 4A and 4B). The increase in amount of pearlite relative to the amount of ferrite causes a slight increase of hardness with increase of chromium; the addition of 0.5 per cent Mo increases the hardness somewhat, but further additions of molybdenum have no appreciable effect.

SUMMARY DIAGRAMS

The structures resulting from air cooling or furnace cooling are summarized in Figs. 7a and 7b. In both diagrams, the triangular corner bounded by 0 per cent Cr-0 per cent Mo, 2 per cent Cr-0 per cent Mo and 0 per cent Cr-2 per cent Mo is similar in that it contains the basic constituents, ferrite and carbide. With the exception of this corner, the diagram for air-cooled specimens (Fig. 7a) differs from that for furnace-cooled specimens (Fig. 7b) in that martensite is present in the former and not in the latter. It should be noted that
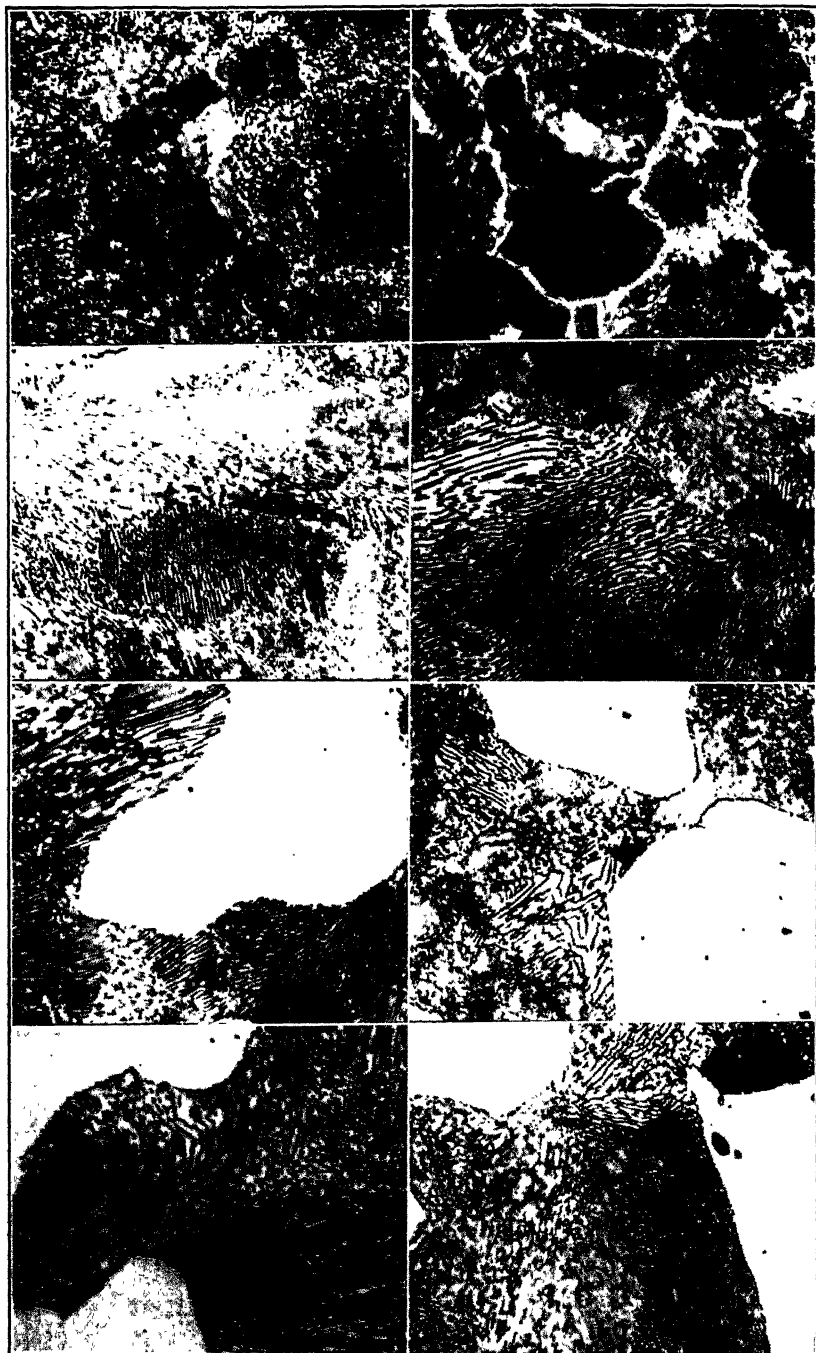
FIG. 5.—CHROMIUM-MOLYBDENUM STEELS FURNACE-COOLED FROM 1740°F. × 500.
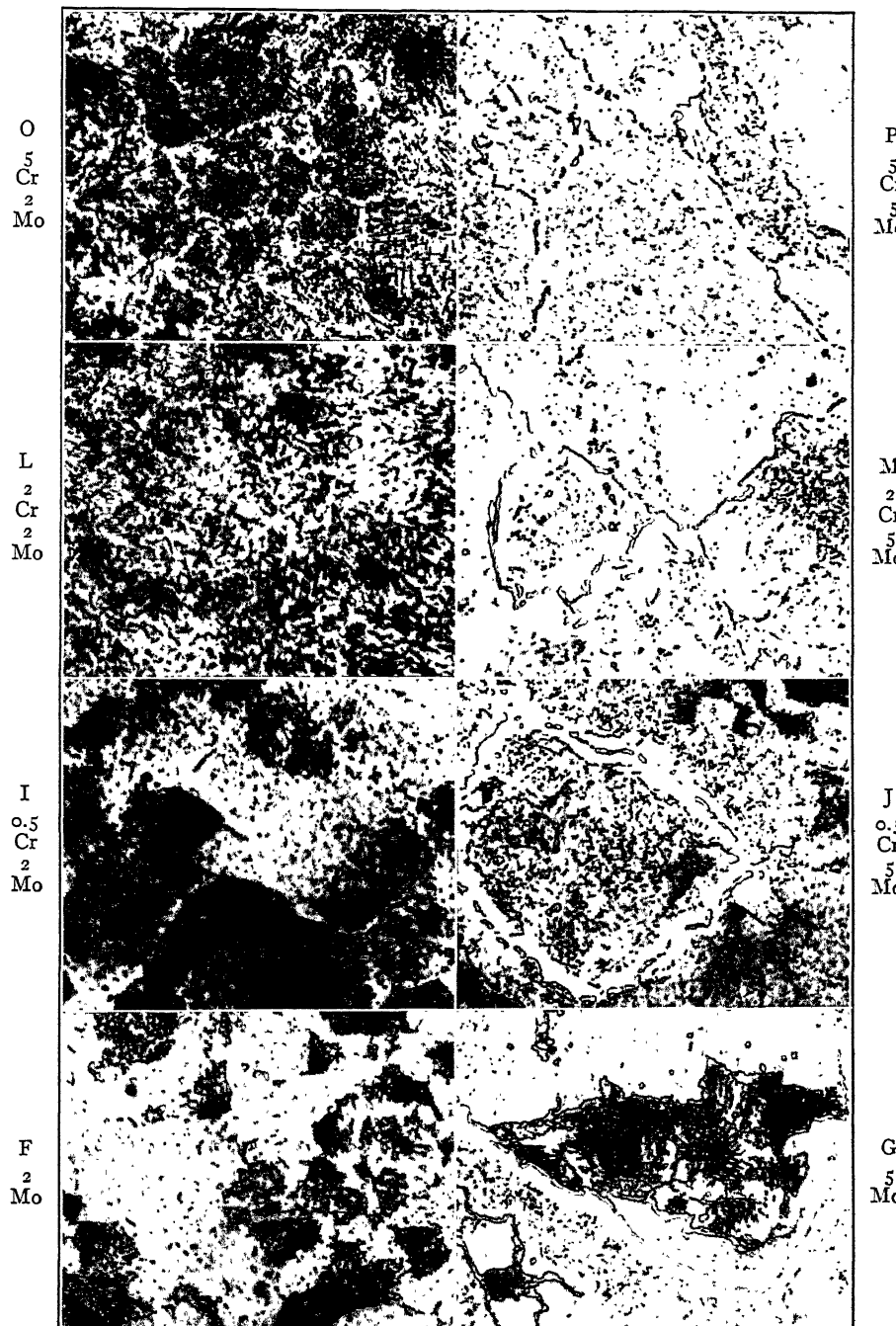
FIG. 6.—CHROMIUM-MOLYBDENUM STEELS FURNACE-COOLED FROM 1740°F., AND G, J, M AND P FURNACE-COOLED FROM 2200°F. × 500.

steel P (5 per cent Cr, 5 per cent Mo) in Fig. 7a has some ferrite, which probably occurs because its carbon content (0.27 per cent C) is low enough to place it in a

and distinguishable from the material in the interior of the specimen. The depth of this decarburized zone was measured with a 0.01-in. rule without the aid of
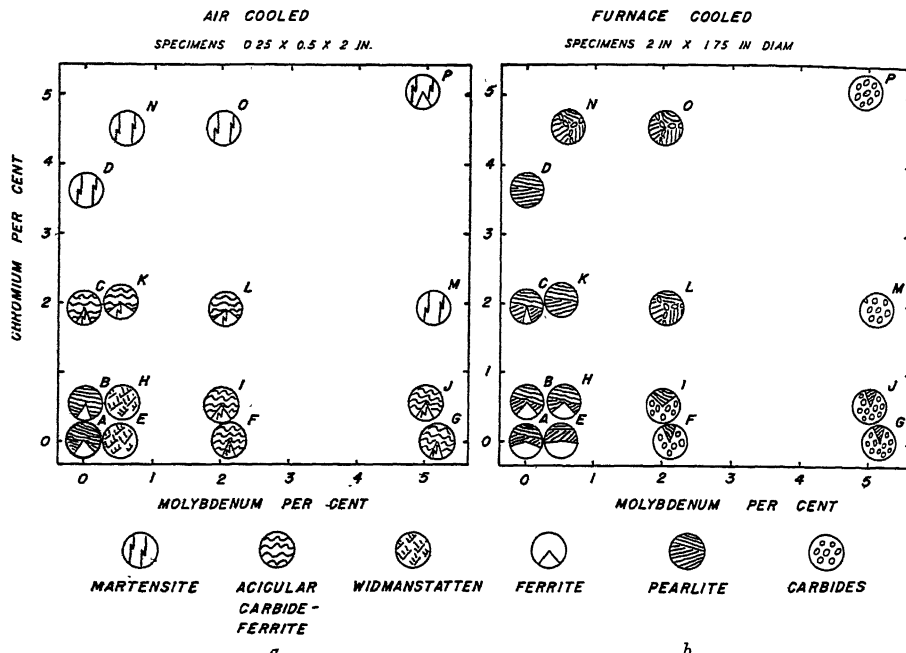
FIG. 7.—SUMMARY OF STRUCTURES AFTER AIR COOLING OR FURNACE COOLING. SPECIMENS COOLED FROM 1740°F. (EXCEPT G, J, M AND P COOLED FROM 2200°F.)

two-phase region of gamma plus delta iron at the austenitizing temperature employed. These diagrams apply only to the austenitizing and cooling conditions stated; changes in these conditions, if sufficiently large, would alter the final microstructure. Further information on constitution diagrams for molybdenum-bearing steels has been published by Blanchard, Parke and Herzig.[4]

DEPTH OF DECARBURIZATION AFTER FURNACE COOLING

The furnace-cooled specimens, 1.75 in. in diameter, which had been cut in half transversely and polished and etched, were examined for decarburization. The decarburized zone in which part or all of the carbon had been lost was clearly visible

a microscope; the results are shown in Fig. 8. It is evident that the amount of decarburization is decreased by chromium but increased by molybdenum, even in the presence of chromium.

It was considered advisable to compare the influence of chromium and molybdenum on the degree of scaling of certain of these steels, since, if there were considerable differences in scaling behavior due to differences in alloy content, the amount of metal lost in the form of scale might be so variable as to render measurements of the decarburized zone unreliable and thus lead to wrong conclusions. Steels A, D, G, P, having maximum difference in composition, were selected for the scaling comparison. After the diameter of the specimens had been measured, they were held 17 hr. at

1740°F. (950°C.) and furnace-cooled to room temperature. The scale was then pickled off and the diameter of the specimens again measured. The results of these

for the scaling measurements; the treatments used in each instance are shown in Table 3.

The chromium-bearing steels D and P
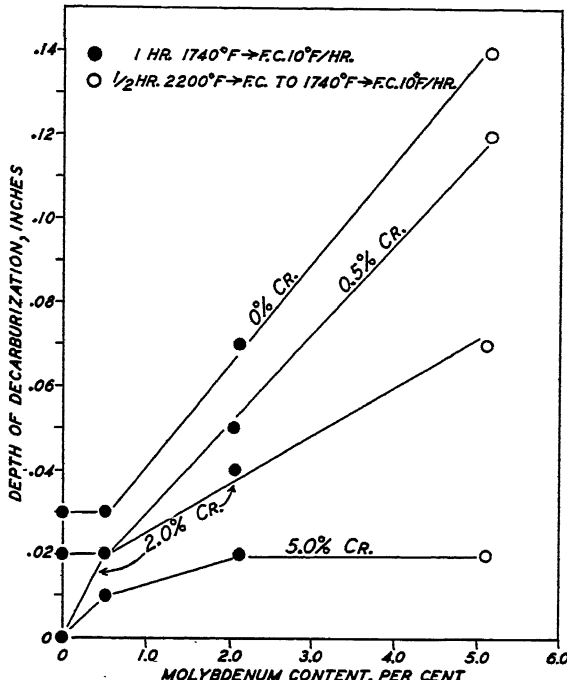
FIG. 8.—EFFECT OF CHROMIUM AND MOLYBDENUM ON DEPTH OF DECARBURIZATION OF 0.35 PER CENT CARBON STEEL.

measurements, in terms of the depth of metal lost by scaling, are shown in Table 3, together with the depth of decarburization of these four steels. It is noteworthy that the scale was more adherent in the molybdenum than in the chromium steels. Attention is also called to the fact that the heat-treatments for the decarburization measurements were not identical with those

show very little less scaling after 17 hr. at 1740°F. than steels A and G, which have no chromium. On the other hand, the same steels show wide differences in their propensity to decarburize (Table 3 and Fig. 8). For example, addition of 3.5 per cent Cr to plain carbon steel decreases the amount of decarburization about 30 times (steels D and A), and addition of 5 per

TABLE 3.—*Metal Lost by Scaling*

Specimen	Per Cent Alloy Element, Nominal	Depth of Metal Lost by Scaling, 17 Hr. at 1740°F., In.	Depth of Decarburization, In.	Treatment Used for Decarburization Measurements
A	0 per cent, Cr, 0 per cent Mo	0.022	0.03	1 hr. 1740°F. → FC
D	3.5 per cent Cr...........................	0.015	0.001	1 hr. 1740°F. → FC
G	5 per cent Mo............................	0.023	0.14	½ hr. 2200°F → FC
P	5 per cent Cr, 5 per cent Mo................	0.016	0.02	½ hr. 2200°F. → FC

cent Cr to steel containing 5 per cent Mo decreases decarburization about 7 times (steels P and G). Therefore, it may be assumed that the loss of metal by scaling has not significantly altered the relative amount of decarburization, and that the trends of Fig. 8 are unaffected by the simultaneous scaling.

CONCLUSIONS

In the air-cooled steels, addition of more than 0.5 per cent Cr changes the pearlitic structure of the plain 0.35 per cent carbon steel to an acicular carbide-ferrite aggregate, and further addition of chromium promotes the formation of martensite. The presence of 0.5 per cent Mo is more effective in forming the acicular structure and increasing the hardness than the presence of 0.5 per cent Cr, but further amounts of chromium are more effective than molybdenum in forming martensite. The first traces of martensite are found in steels containing about 2.0 per cent of either chromium or molybdenum and with this amount of alloy their hardness is about the same. When both elements are present, chromium is more effective than the same amount of molybdenum in forming martensite and increasing the hardness.

In the furnace-cooled series, the amount of proeutectoid ferrite decreases with increasing chromium content, disappearing almost entirely with 3.5 per cent Cr. This change is accompanied by a slight increase of hardness. The addition of 0.5 per cent Mo also causes a slight increase of hardness, but further additions of molybdenum have no appreciable effect.

The depth of decarburization is decreased by chromium and increased by molybdenum even in the presence of chromium.

ACKNOWLEDGMENT

REFERENCES

1. J. L. Gregg: Alloys of Iron and Molybdenum. Alloys of Iron *Monograph.* New York, 1932. McGraw-Hill Book Co.
2. E. C. Bain: Functions of the Alloying Elements in Steel. Amer. Soc. for Metals, 1939.
3. E. S. Davenport: Isothermal Transformation in Steels. *Trans.* Amer. Soc. Metals (1939) 24, 837–886.
4. J. R. Blanchard, R. M. Parke and A. J. Herzig: Constitution Diagrams for Iron-carbon-molybdenum Alloys. *Trans.* Amer. Soc. for Metals (1939) 27, 697–718.

DISCUSSION

(L. S. Bergen presiding)

A. B. BAGSAR,[*] Marcus Hook, Pa.—Did the authors find any peculiarity in the workability of the high-chromium, high-molybdenum steels at elevated temperatures? Can the 5 per cent chromium, 5 per cent molybdenum steel be commercially produced in the form of hot-rolled products and forgings?

M. BAEYERTZ,[†] Chicago, Ill.—Have the authors any data on the oxidation of these steels; that is, did they observe differences in scaling?

R. F. MILLER (author's reply).—As far as we know, the high-chromium, high-molybdenum steels are not produced commercially, and their hot-working characteristics have not been determined.

In reply to Miss Baeyertz: As stated in the paper, measurements were made of the depth of metal lost in specimens A, D, G and P by scaling during 17 hr. at 1740°F. The results of these measurements are shown in Table 3. The specimen containing 5 per cent molybdenum scaled about as much as the plain carbon steel, while the addition of 3.5 or 5.0 per cent chromium decreased the amount of oxidation in plain carbon or molybdenum-bearing steel. We have recently completed, but not as yet released for publication, a series of 1000-hr. oxidation tests on these materials. The new tests were made with equipment that permitted periodic measurement of the gain in weight of the specimens.

---

* Metallurgical Division, Sun Oil Co.
† Carnegie-Illinois Steel Corporation.

INDEX

(NOTE: In this index the names of authors of papers and discussions and of men referred to are printed in SMALL CAPITALS, and the titles of papers in *italics*.)

433

CONTENTS OF VOLUME 147

Transactions A.I.M.E., 1942, Institute of Metals Division

PAPERS